

University of Warwick institutional repository: <http://go.warwick.ac.uk/wrap>

A Thesis Submitted for the Degree of PhD at the University of Warwick

<http://go.warwick.ac.uk/wrap/4045>

This thesis is made available online and is protected by original copyright.

Please scroll down to view the document itself.

Please refer to the repository record for this item for information to help you to cite it. Our policy information is available from the repository home page.

**COMPOSITE BEAMS: RELIABILITY, AND
LONGITUDINAL SHEAR RESISTANCE
WITH PROFILED SHEETING**

by

Dong-jie Huang BEng MSc

A thesis submitted to the University of Warwick

for the degree of

DOCTOR OF PHILOSOPHY

Department of Engineering

University of Warwick

Coventry CV4 7AL

The United Kingdom

January 1994

TO MY WIFE — LIZHENG SU

Abstract

In this thesis, two problems have been studied: one is the reliability of design resistances of composite beams in bending, the other is the longitudinal shear resistances in concrete flanges of composite beams with profiled sheeting.

For the first problem, a general theory is developed based on the concepts of safety-index and second-moment reliability, to analyse the reliability of a design resistance for composite structures. This theory consists of two basic parts: one is the determination of several distinct safety factors for a single resistance function, with respect to the specified safety level; the other is the assessment of safety level, corresponding to given safety factors. Application of this theory is related to the relevant test results. In the scope of Eurocode 4, this theory is particularly used to calibrate safety factors employed for design plastic bending resistances of composite beams. From the calculation based on 122 test results, the reliability of using the Eurocode provisions, including the recommended safety factors and the theoretical models, is judged for bending resistances of beams with full and partial shear connection.

In studying the longitudinal shear resistances in concrete flanges of composite beams with and without profiled sheeting, a simple theory to determine the resistances is established. This theory is based on the “friction-cohesion” and “concrete strut” models for concrete in shear and takes the effect of profiled sheeting into account. Associated with the theoretical work, seven tests on three specimens for investigating the longitudinal shear resistances are reported. From both experimental results and theoretical calculation, the behaviour of the test specimens is studied, and, finally, new design recommendations are made to predict the longitudinal shear resistances of the composite beams.

Contents

Abstract

Acknowledgment

Declaration

Notation

| | | |
|----------|--|-----------|
| 1 | Introduction | 1 |
| 1.1 | Presentation of the problems | 1 |
| 1.2 | Previous research on structural reliability | 5 |
| 1.3 | Previous research on longitudinal shear resistance of composite beams | 7 |
| 1.4 | Layout of the thesis | 9 |
| 2 | Reliability theory for resistances in composite structures | 11 |
| 2.1 | Concepts of second-moment reliability and design resistances . . . | 11 |
| 2.2 | Design resistances of composite structures at given safety levels . | 15 |
| 2.2.1 | Definitions and basic assumptions in the analysis | 15 |
| 2.2.2 | Determination of design resistance in general cases | 19 |
| 2.2.3 | Partial safety factors for design resistances of composite structures | 23 |
| 2.3 | Failure probability corresponding to given safety factors | 31 |
| 2.4 | Summary of the reliability theory | 33 |

| | | |
|----------|--|------------|
| 3 | Investigation of reliability in design bending resistances of composite beams | 35 |
| 3.1 | Applications of test results in analysis | 36 |
| 3.1.1 | Selection of test results | 36 |
| 3.1.2 | Groups of tests | 38 |
| 3.1.3 | Using of non-measured basic variables in test specimens . . | 39 |
| 3.2 | Calibration of partial safety factors for composite beams | 41 |
| 3.2.1 | Full shear connection (Groups A and B) | 41 |
| 3.2.2 | Ductile partial shear connection (Group C) | 44 |
| 3.2.3 | Non-ductile shear connection (Group D) | 49 |
| 3.3 | Calculation of failure probability and model factors by programs . | 54 |
| 4 | Calibration results and discussions | 57 |
| 4.1 | Results of calibration | 57 |
| 4.2 | Reliability assessment of design bending resistances in Eurocode 4 | 82 |
| 4.2.1 | Correlation and variation of the resistances | 82 |
| 4.2.2 | Safety margin underlying the recommended safety factors in Eurocode 4 | 84 |
| 4.2.3 | Applicability of calibration results to Eurocode 4 | 88 |
| 4.3 | Use of reduced γ_a -value | 93 |
| 4.3.1 | Effect of decreasing V_{fy} on calibration | 93 |
| 4.3.2 | Effect of reduction in γ_a on failure probabilities | 96 |
| 5 | Conclusions for reliability of composite beams in bending | 98 |
| 6 | Theory for longitudinal shear resistance of reinforced concrete flanges | 103 |
| 6.1 | The recommendations in Eurocode 4 | 103 |
| 6.2 | Shear resistance with failure of sheeting and reinforcement | 104 |
| 6.2.1 | The basic assumptions | 105 |
| 6.2.2 | Governing equations | 108 |

| | | |
|----------|---|------------|
| 6.2.3 | The effect of the beneficial length | 114 |
| 6.3 | The shear resistance with crushing of concrete | 117 |
| 6.3.1 | Crushing of the concrete struts | 117 |
| 6.3.2 | The maximum effect of sheeting and reinforcement | 119 |
| 6.3.3 | The maximum longitudinal shear resistance | 121 |
| 6.4 | The strength of profiled sheeting | 125 |
| 6.5 | Summary of determining longitudinal shear resistance | 128 |
| 7 | Specimens for testing longitudinal shear resistance | 130 |
| 7.1 | Objective and planning of the tests | 130 |
| 7.2 | Design and fabrication of the specimens | 133 |
| 7.2.1 | Specimen TR1 | 133 |
| 7.2.2 | Specimens TR2T and TR2P | 141 |
| 7.3 | Strengths of materials | 144 |
| 7.4 | Test rig and instrumentation | 148 |
| 7.4.1 | Loading system | 148 |
| 7.4.2 | Measurement of slip and deflexion | 149 |
| 7.4.3 | The strain gauges | 154 |
| 8 | Testing procedure and results | 160 |
| 8.1 | Loading procedure, failure appearance and deformation | 160 |
| 8.1.1 | Tests on specimen TR1 | 162 |
| 8.1.2 | Tests on specimens TR2T and TR2P | 163 |
| 8.2 | Observation of cracks | 169 |
| 8.3 | The forces in steel beams | 175 |
| 9 | Analysis of test results and design recommendations | 179 |
| 9.1 | The cracking load | 179 |
| 9.2 | Performance and failure of the specimens in tests | 184 |
| 9.2.1 | TR2T1 and TR2T2 (shear connection failure) | 185 |
| 9.2.2 | TR2P1 and TR2P2 (longitudinal shear failure) | 186 |

| | | |
|-----------|--|------------|
| 9.2.3 | TR1T, TR1P1 and TR1P2 (punching shear failure) | 190 |
| 9.3 | Longitudinal shear resistances of the specimens | 192 |
| 9.4 | The recommendations for design | 198 |
| 10 | Conclusions for resistances of composite beams to longitudinal shear | 206 |
| | Bibliography | 209 |
| A | Non-central t-distribution and fractile-factors | 216 |
| B | Coefficients of variations of the basic variables | 221 |
| C | Coefficients of variation of resistance functions for composite beams | 223 |
| C.1 | Hogging bending with plastic neutral axis in steel web (group B) . | 223 |
| C.2 | More bending situations of composite beams with full shear connection | 225 |
| C.2.1 | Sagging bending with plastic neutral axis in the steel top flange | 225 |
| C.2.2 | Sagging bending with plastic neutral axis in steel web . . . | 226 |
| C.2.3 | Hogging bending with plastic neutral axis in the steel top flange | 227 |
| C.3 | Beams with ductile partial shear connection (group C) | 228 |
| C.3.1 | Equilibrium method (second neutral axis in the steel top flange) | 228 |
| C.3.2 | Equilibrium method (second neutral axis in steel web) . . | 229 |
| C.3.3 | Linear interpolation (plastic neutral axis for $M_{pl,R}$ in concrete slab) | 231 |
| C.3.4 | Linear interpolation (plastic neutral axis for $M_{pl,R}$ in the top steel flange) | 232 |

| | | |
|----------|---|------------|
| C.3.5 | Linear interpolation (plastic neutral axis for $M_{pl,R}$ in steel web) | 234 |
| D | Computer programs of safety calibration for composite beams | 235 |
| D.1 | Program for composite beams with full shear connection | 235 |
| D.1.1 | Scope of program | 235 |
| D.1.2 | Function of subroutines | 237 |
| D.1.3 | Definition of main variables | 238 |
| D.1.4 | The layout of input file and output file | 239 |
| D.2 | Program for beams with ductile partial shear connection | 241 |
| D.2.1 | Scope of program | 241 |
| D.2.2 | Supervision package <i>rcc</i> | 243 |
| D.2.3 | Package <i>ctc</i> | 244 |
| D.2.4 | Package <i>crb</i> | 247 |
| D.2.5 | Input datafiles for <i>ctc</i> and <i>crb</i> | 252 |
| D.2.6 | Output file after running <i>ctc</i> and <i>crb</i> | 253 |
| D.3 | Program for beams with non-ductile partial shear connection | 256 |
| D.3.1 | Scope of program | 256 |
| D.3.2 | Subroutines and variables in <i>ntc</i> and <i>nrb</i> | 257 |
| D.3.3 | Input files of <i>ntc</i> and <i>nrb</i> | 262 |
| D.3.4 | Output file of <i>ntc</i> and <i>nrb</i> | 264 |
| D.4 | Using <i>ctc</i> and <i>crb</i> for beams with non-ductile shear connection | 265 |
| D.5 | Use of program <i>EP PCB1</i> , source programs and input data files | 266 |

List of Tables

| | | |
|------|--|----|
| 4.1 | Resistances of test specimens in group A | 59 |
| 4.2 | Resistances of test specimens in group B | 60 |
| 4.3 | Resistances of test specimens in group C | 61 |
| 4.4 | Resistances of test specimens in group D (theoretical resistances are predicted from the non-ductile models) | 62 |
| 4.5 | Resistances of test specimens in group D (theoretical resistances are predicted from linear interpolation and the equilibrium method) | 63 |
| 4.5 | (continued) | 64 |
| 4.6 | Mean values of basic variables for samples in group A | 64 |
| 4.7 | Mean values of basic variables for samples in group B | 65 |
| 4.8 | Mean values of basic variables for steel beams and spans for sam- ples in group C | 66 |
| 4.9 | Mean values of basic variables for concrete slabs and shear connec- tors for samples in group C | 67 |
| 4.10 | Mean values of basic variables for steel beams and spans for sam- ples in group D | 68 |
| 4.11 | Mean values of basic variables for concrete slabs and shear connec- tors for samples in group D | 69 |
| 4.12 | Parameters of test correction for groups of beams | 70 |
| 4.13 | Coefficients of variation of resistances in groups A and B | 70 |
| 4.14 | Coefficients of variation of resistances in group C | 71 |

| | | |
|------|--|-----|
| 4.15 | Coefficients of variation of resistances in group D (for non-ductile models) | 72 |
| 4.16 | Coefficients of variation of resistances in group D (for equilibrium method and linear interpolation) | 73 |
| 4.17 | Partial safety factors for beams in groups A and B | 75 |
| 4.18 | Partial safety factors for beams in group C | 76 |
| 4.19 | Partial safety factors for beams in group D (applied to non-ductile models) | 77 |
| 4.20 | Partial safety factors for beams in group D (applied to equilibrium method and linear interpolation) | 78 |
| 4.21 | Group C — failure probabilities and design fractile-factors of design resistances with given safety factors | 79 |
| 4.22 | Group D — failure probabilities and design fractile-factors of design resistances with given safety factors (applying equilibrium method and linear interpolation) | 80 |
| 4.23 | Effect of V_f on safety factors | 96 |
| 4.24 | Effect of change of γ_a on failure probabilities in group C | 97 |
| 7.1 | Size of the steel coupons | 144 |
| 7.2 | Results of coupon test for steel beams | 145 |
| 7.3 | Results of coupon test for sheeting | 145 |
| 7.4 | Strength of concrete in TR1, in N/mm^2 | 147 |
| 7.5 | Concrete strength in specimens TR2T and TR2P, in N/mm^2 | 148 |
| 7.6 | Arrangement of load cells | 149 |
| 7.7 | Use of LVDTs | 154 |
| 8.1 | Predicted bending resistances | 161 |
| 8.2 | The ultimate loads from bending theories and tests | 161 |
| 8.3 | Average width of longitudinal crack in test TR2P1 | 174 |
| 8.4 | The maximum steel force obtained from tests | 178 |

| | | |
|-----|---|-----|
| 9.1 | Load at initial shear crack | 183 |
| 9.2 | Longitudinal shear resistance in each test | 195 |
| 9.3 | Failure load from longitudinal shear resistance | 196 |
| 9.4 | Longitudinal shear resistance from design formulae (kN/m) | 201 |
| A.1 | Factor k_b with $P_f = 0.12\%$ at $\epsilon = 0.75$ | 220 |
| B.1 | Coefficients of variation of basic variables | 222 |

List of Figures

| | | |
|-----|---|----|
| 1.1 | The longitudinal shear in the concrete flange | 3 |
| 1.2 | Cross-section of composite beam with profiled sheeting, and potential surfaces of shear failure | 4 |
| 2.1 | Reliability states of structures | 12 |
| 3.1 | Sagging bending of composite beams with full shear connection, plastic neutral axis in concrete slab | 41 |
| 3.2 | Sagging bending of composite beams with partial partial shear connection, second neutral axis in the steel top flange | 45 |
| 3.3 | Theoretical models for plastic bending resistances of composite beams with ductile partial connection | 46 |
| 3.4 | Theoretical models for plastic bending resistances of composite beams with non-ductile partial connection | 51 |
| 4.1 | Ratio of experimental resistances to the theoretical predictions of beams with full shear connection | 82 |
| 4.2 | Ratio of experimental resistances to the theoretical predictions of beams with partial shear connection | 83 |
| 4.3 | Ratio of experimental resistances to predicted results against concrete density (group C) | 90 |
| 4.4 | Ratio of experimental resistances to predicted results against concrete density (group D) | 91 |

| | | |
|------|---|-----|
| 4.5 | Relationship between calibrated design resistance, r_d , and coefficient of variation of resistance function, V_{R_t} | 94 |
| 6.1 | Calculation pattern of the shear resistance with respect to the failure of reinforcement and sheeting | 109 |
| 6.2 | Variation of $\lambda\beta$ vs α with $\beta = 1.0$ and different n | 115 |
| 6.3 | Variation of $\lambda\beta$ vs α , with $n = 0.15$ and different β | 116 |
| 6.4 | Calculation pattern for shear resistance with respect to crushing of the concrete struts | 118 |
| 6.5 | Variation of \bar{v} against \bar{p} | 123 |
| 6.6 | Error caused by linearization of $v_{R,m}$ | 123 |
| 6.7 | Local failure of sheeting in tension | 125 |
| 6.8 | Local failure of sheeting in shear | 127 |
| 7.1 | Layout of specimen TR1 | 134 |
| 7.2 | Layout of specimen TR2T | 135 |
| 7.3 | Layout of specimen TR2P | 136 |
| 7.4 | Cross-section of the steel beams | 137 |
| 7.5 | ALPHALOK profiled sheet | 138 |
| 7.6 | The joint of steel beams in specimen TR1 | 139 |
| 7.7 | Shear connection in specimen TR1 | 139 |
| 7.8 | Specimen TR1 after stud welding | 140 |
| 7.9 | Edge support of specimen TR1 | 140 |
| 7.10 | Studs in beams TR2T and TR2P | 142 |
| 7.11 | Beam TR2T after stud welding | 143 |
| 7.12 | Beam TR2P after stud welding | 143 |
| 7.13 | The steel coupons | 144 |
| 7.14 | Results of tensile tests on reinforcement | 146 |
| 7.15 | Loading rig in tests on TR1 | 150 |
| 7.16 | Loading rig in tests on TR2T and TR2P | 151 |

| | | |
|------|---|-----|
| 7.17 | Calibration of 50-kN and 100-kN load cells | 151 |
| 7.18 | Calibration of 500-kN and 250-kN load cells | 152 |
| 7.19 | LVDTs used in specimen TR1 | 153 |
| 7.20 | LVDTs used in specimens TR2T and TR2P | 153 |
| 7.21 | LVDTs for measuring slips | 154 |
| 7.22 | Calibration of 50-mm LVDT | 156 |
| 7.23 | Calibration of 100-mm LVDT | 157 |
| 7.24 | Strain gauges in specimen TR1 | 158 |
| 7.25 | Strain gauges in specimens TR2T & TR2P | 159 |
| 8.1 | Deflexion of loaded point in TR1T | 162 |
| 8.2 | Deflexion of loaded points in TR1P1 & TR1P2 | 164 |
| 8.3 | Slip at the tested ends in TR1P1 & TR1P2 | 164 |
| 8.4 | Specimen TR1 in Test TR1P2 | 165 |
| 8.5 | Deflexion of loaded points in TR2T | 166 |
| 8.6 | Slips at the tested ends in TR2T | 166 |
| 8.7 | Deflexions of loaded point in TR2P | 168 |
| 8.8 | Slips at the tested ends in TR2P | 168 |
| 8.9 | Beam TR2P under loading in test TR2P2 | 169 |
| 8.10 | Crack pattern in test TR1T | 170 |
| 8.11 | Crack pattern in test TR1P1 | 170 |
| 8.12 | Crack pattern in test TR1P2 | 171 |
| 8.13 | Crack pattern in test TR2T1 | 171 |
| 8.14 | Crack pattern in test TR2T2 | 172 |
| 8.15 | Crack pattern in test TR2P1 | 172 |
| 8.16 | Crack pattern in test TR2P2 | 173 |
| 8.17 | Steel force measured in test TR1T | 176 |
| 8.18 | Steel force measured in tests TR1P1 & TR1P2 | 176 |
| 8.19 | Steel force measured in tests TR2T1 & TR2T2 | 177 |
| 8.20 | Steel force measured in tests TR2P1 & TR2P2 | 177 |

| | | |
|-----|---|-----|
| 9.1 | Stress state in uncracked concrete | 180 |
| 9.2 | Longitudinal shear force and bending force in concrete | 182 |
| 9.3 | Failure surfaces of longitudinal shear considered for the tests | 183 |
| 9.4 | Finding steel force for test TR1P1 | 192 |
| 9.5 | Bending moment at longitudinal shear failure | 195 |
| 9.6 | Design curve of longitudinal shear resistance (transverse sheeting) | 204 |
| 9.7 | Design curve of longitudinal shear resistance (parallel sheeting, or without sheeting) | 205 |
| A.1 | Fractile-factor and probability of the standard normal distribution | 218 |
| C.1 | Hogging bending of composite beams in full shear connection, plas- tic neutral axis in steel web | 224 |
| C.2 | Sagging bending of composite beams with full shear connection, plastic neutral axis in top steel flange | 225 |
| C.3 | Sagging bending of composite beams with full shear connection, plastic neutral axis in steel web | 226 |
| C.4 | Hogging bending of composite beams with full shear connection, plastic neutral axis in steel top flange | 227 |
| C.5 | Sagging bending of composite beams with ductile partial shear connection, second neutral axis in steel web | 230 |
| D.1 | Steel section considered by program <i>sacb</i> for hogging bending | 236 |

Acknowledgment

I am greatly indebted to my supervisor, Professor R.P. Johnson; without his guidance, advice and encouragement, I would not be able to complete the research works.

The sincerest thanks go to the Steel Construction Institute, Ascot, and ORS Awards Scheme for the financial supports, and State Education Commission, People's Republic of China, for the arrangement of my studying abroad.

My appreciation and gratitude also go to Mr. Collin Bank and his team for their skillful work in preparing the test specimens and assistance to the experiments.

Finally, I would like to thank my parents and the rest of my family, whose care and help are important for me to accomplish this study.

Declaration

I hereby declare that all the investigations presented in this thesis are my own works except where specific reference has been made to the work of others. No part of this thesis has been submitted to any university and other institution for a degree, diploma or the other qualifications.

Notation

| | |
|---------------|---|
| a | distance from centre of a stud to free edge of sheeting |
| A_a | area of cross-section of structural steel |
| A_{cv} | mean area of concrete per unit length along the shear surface |
| A_e, A'_e | sum of the cross-sectional areas of all transverse reinforcement (perpendicular to the beam) per unit length of beam crossing the shear surface |
| $(A_e f_s)_m$ | tensile strength of transverse reinforcement developed at the crushing of concrete struts |
| A_{eb} | involved shear bond area per unit length along beam span |
| A_p | cross-sectional area of profiled sheeting per unit length of the beam |
| A_s | area of longitudinal reinforcement |
| b | r/r_t , called correction term of r_t |
| \bar{b} | mean of b , as called the mean correction of r_t |
| b_0 | average width of hunch |
| b_c | breadth of concrete slab |
| b_{eff} | effective width |
| b_f | width of steel flange |
| b_p | width of the plate attached the bottom steel flange |
| b_s | distance between the potential surfaces of shear failure |
| c | apparent cohesion of concrete |
| d | diameter of stud shank |
| E_a, E_c | Young's modulus of steel and concrete, respectively |
| f_a | steel force per unit length developed within shear span, the maximum stress in steel beam at $M_{a,s}$ |
| $f_{a,max}$ | the maximum value of f_a obtained from tests |
| f_b | shear bond via embossments on webs of profiled sheets to concrete |
| f_c | compressive strength of concrete (cylinder strength of concrete) |
| f_{ct} | tensile strength of concrete |

| | |
|--------------------------------------|--|
| f_{cu} | cube strength of concrete |
| $f_{lg,a}$ | f_a corresponding to v_R |
| f_s, f'_s | yielding strength of the transverse reinforcement |
| f_{ut} | the ultimate tensile strength of a headed stud connector |
| f_y | yield strength of structural steel |
| f_{ya} | the maximum stress in steel beam at the $M_{el,R}$ determined by taking limiting bending stresses as f_y in steel beam and $0.85f_c$ in concrete |
| $f_{y,d}, f_{c,d}, f_{s,d}, P_{R,d}$ | γ_{mp} – altered strengths of f_y, f_c, f_s and P_R , respectively |
| $f_{yk}, f_{ck}, f_{sk}, P_{Rk}$ | characteristic values of f_y, f_c, f_s and P_R , respectively |
| f_{yp} | yield strength of sheeting |
| F | normal force on transverse section of a concrete flange |
| F_0 | normal force on transverse section of flange portion where $Q = 0$ |
| F_a | force in steel beam |
| F_c | longitudinal shear resistance provided by shear connection in the shear span, force in concrete slab |
| $F_{cf}, M_{pl,R}, P_{pl,R}$ | concrete force, the ultimate bending moment (resistance) and ultimate load at plastic state with full shear connection, respectively |
| F_{ck} | normal force on transverse section of concrete slab corresponding to $F_{lg,ck}$ |
| $F_{cp}, M_{pp,R}, P_{pp,R}$ | concrete force, the ultimate bending moment (resistance) and ultimate load at plastic state with partial shear connection, respectively |
| $F_{el}, M_{el,R}, P_{el,R}$ | concrete force, the ultimate bending moment (resistance) and ultimate load at first yielding, respectively |

| | |
|----------------------------------|--|
| F_{lg} | normal force on transverse section of a concrete flange, in the position where the maximum bending moment occurs |
| $F_{lg,ck}$ | F_{lg} at occurrence of the initial shear cracks |
| $F_{tr,t}$, $F_{tr,c}$ | tensile force and compressive force on longitudinal section of concrete flange, respectively |
| h | overall height of stud |
| h_a | overall height of steel section |
| h_c | overall height of concrete slab |
| h_g | distance from the top surface of top steel flange to the centre of area of the steel section |
| h_{na} | depth of plastic neutral axis of the steel section along, measured from top surface of the top steel flange |
| h_t | height of the thinnest part of concrete slab |
| h_p | height of hunch of concrete slab |
| h_s | distance between the center of area of longitudinal reinforcement in the slab to the top surface of top steel flange |
| I_a | inertial moment of a steel cross-section |
| k | reduction factors for strength of shear connectors |
| $k_{ad}, k_{cd}, k_{sd}, k_{vd}$ | fractile-factors corresponding to $f_{y,d}$, $f_{c,d}$, $f_{s,d}$ and $P_{R,d}$, respectively |
| $k_{as}, k_{cs}, k_{ss}, k_{vs}$ | fractile-factors corresponding to f_{yk} , f_{ck} , f_{sk} and P_{Rk} , respectively |
| k_b | design fractile-factor associated with V_δ only |
| k_d | design fractile-factor |
| $k_{d,\infty}$ | design fractile-factor associated with V_{Rt} only |
| k_{md} | unique value taken for k_{ad} , k_{cd} and k_{sd} |

| | |
|-------------|---|
| K | friction factor for concrete shear strength |
| l | shear span under consideration |
| l_m | distance from the section where the steel force is measured to the nearest support |
| L | total span of beam |
| M | bending moment |
| M_{apl} | plastic bending resistance of steel beam along |
| $M_{a,S}$ | bending moment acting on the steel beam due to actions on the steelwork alone, before composite action becomes effective |
| M_c | bending moment on composite section determined by elastic theory and assuming the compressive force in concrete to be F_c |
| M_{max} | the maximum bending moment in the beam |
| n | number of test specimens in a group, eccentricity ratio |
| N | number of shear connectors provided in a shear span |
| N_{at} | tensile force reached in profiled sheets at the pull-out failure |
| N_f | number of shear connectors required in a shear span for full shear |
| N_r | number of shear connectors within one rib |
| P | load |
| P_c | probability of load effects exceeding structural resistances |
| P_{ck} | load corresponding to the initial crack due to longitudinal shear, corresponding to F_{ck} |
| $P_{e,max}$ | the maximum load obtained from tests |
| P_f | probability of structures failing to achieve the design resistances |
| P_{fm} | load corresponding to $f_{a,max}$ |
| $P_{lg,R}$ | the ultimate load corresponding to v_R |
| P_R | strength of shear connectors |
| Q | shear force on transverse section of concrete flange |

| | |
|---------------------------|--|
| Q_0, T | shear force on longitudinal section fo concrete flange |
| r | real structural resistances |
| r_d | design value of a structural resistance |
| r_{ei}, r_{ti} | experimental value and theoretical value of the resistance of test specimen i ($i = 1, \dots, n$) in a group, respectively |
| r_t | theoretical prediction of a structural resistance |
| R, S | linear transformation variables for $\ln r$ and $\ln s$, respectively |
| s | load effects; longitudinal spacing centre-to-centre of groups of studs |
| S_{at} | the maximum shear force sustained by the sheet for per stud |
| S_{cv} | same as A_{cv} , but excluding the rib area |
| t | thickness of sheet |
| t_f | thickness of steel flange |
| t_p | thickness of the plate attached the bottom steel flange |
| t_w | thickness of steel web |
| v_p | general term of contribution to longitudinal shear resistance from profiled sheeting |
| v_{pc} | effect of profiled sheets to v_R controlled by crushing in concrete |
| v_{ps} | strength developed in profiled sheets to longitudinal shear |
| v_{pt}, v'_{pt} | strength developed in profiled sheets to transverse tension |
| $v_{pt,m}$ | tensile strength of transeverse sheeting developed at the cruching of concrete struts |
| v_R | longitudinal shear resistance per unit length |
| v_s | contribution from Q to longitudinal shear resistance in shear span |
| V_δ | coeffecient of variation of the error term δ |
| V_r, V_{r_t} | coeffecient of variation of r and r_t , respectively |
| V_{X_1}, V_{X_2}, \dots | coeffecients of variation of the basic variables |

| | |
|--|---|
| W_a | plastic modulus of a steel cross-section |
| W_c | the density of concrete |
| x | length of the compression zone of concret |
| x_0 | distance between the sections with $Q = 0$ and $M = M_{\max}$ |
| X_1, X_2, \dots | basic variables |
| $\bar{X}_1, \bar{X}_2, \dots$ | mean values of the basiv variables |
| X_{g1}, X_{g2}, \dots | basic variables for geometric dimensions |
| X_{p1}, X_{p2}, \dots | basic variables for material properties |
| \underline{X}_{p0} | material properties other than the strengths |
| y_c | depth of plastic neutral axis, measured from top surface of concrete slab |
| α | reduction factors for strength of shear connectors, $(L - l)/l$ |
| α_r, α_s | sensitive factors on resistance side and load side, respectively |
| β | safety index; parameter used to consider effects of the beneficial length on longitudinal shear resistances |
| $\gamma_a, \gamma_c, \gamma_s, \gamma_v$ | partial safety factors applied to f_y, f_c, f_s and P_R , respectively |
| $\gamma_{ma}, \gamma_{mc}, \gamma_{ms}, \gamma_{mv}$ | material factors for f_y, f_c, f_s and P_R , respectively |
| γ_{md} | model factor |
| γ_{mp} | genereal notation for the material factors |
| δ | b/\bar{b} , called the error terms of r_t |
| ϵ | confidence level imposed on P_f |
| θ | angle between a diagonal crack and a londitudinal shear surface |
| λ | x_0/l , representing the beneficial length |
| μ | reduction factor for f_{ct} in consideration of contribution of the concrete to the transverse tension |

| | |
|---|--|
| $\mu_{\ln r}, \mu_{\ln s}$ | mean values of $\ln r$ and $\ln s$, respectively |
| ρ | correlation coefficient of r_t and r |
| σ_c | compression stress in concrete, developed along a longitudinal surface |
| σ'_c | compression stress in concrete at crushing, developed in concrete struts |
| $\sigma_{c,m}$ | compression stress in concrete at crushing, developed along a longitudinal surface |
| $\sigma_{\ln r}, \sigma_{\ln s}$ | standard deviations of $\ln r$ and $\ln s$, respectively |
| $\sigma_{\ln X_1}, \sigma_{\ln X_2}, \dots$ | standard deviations of $\ln X_1, \ln X_2, \dots$ |
| τ_c | shear strength of concrete |
| $\tau_{c,m}$ | the maximum shear stress in concrete at crushing, developed along a longitudinal surface |
| ϕ_{do} | diameter of weld |
| χ | x/l |

Chapter 1

Introduction

1.1 Presentation of the problems

Composite beams are common structural members in engineering. In designing the bending resistance of these beams, safety factors are normally employed. These safety factors should, at a specific probability level, cover the following random variations:

- the difference between the theoretical model and the real behaviour, and the variation of the geometric dimensions, which may be defined as the model uncertainty;
- the variation of the material strengths, which may be defined as the uncertainty of material strength;
- the variation of the loads, which may be defined as the load uncertainty.

Therefore, it is reasonable to determine safety factors on a probabilistic base.

In design of structures, safety factors are usually set for loads on the structure and structural resistance separately. So these factors are called partial safety factors.

On the resistance side, for each kind of material used in a composite structure, a particular safety factor is normally employed for the design. Therefore, to

determine the bending resistance in a composite beam, several different safety factors would be used within one formula [1], i.e.

- γ_a applied to the steel strength f_y ;
- γ_c applied to the concrete strength f_c ;
- γ_s applied to the reinforcement strength f_s ;
- γ_v applied to the strength of shear connection P_R ;

These partial safety factors should be determined by considering both the model uncertainty and the uncertainty of material strength. Therefore a reliability analysis is needed, in which the following work should be done:

- (1) the calibration of partial safety factors for resistance, with respect to the given safety level (or failure probability);
- (2) the determination of the safety level (or failure probability) of the design resistance, corresponding to given partial safety factors.

Associated with bending, a composite beam must also be designed for resistance to longitudinal shear.

Corresponding to the normal stress on concrete and steel due to bending as shown in Figure 1.1(a), on the transverse cross-section of concrete flange exist the normal force F and shear force Q , as shown in Figure 1.1(b); correspondingly, the forces on the longitudinal surface, F , $F_{tr,c}$ and $F_{tr,t}$ would occur.

Therefore, in order to prevent the possible failure of composite beams caused by such longitudinal shear and in-plane bending, along the critical surfaces as shown in Figure 1.2, sufficient resistance is needed to resist the shear force F and the bending forces $F_{tr,t}$ and $F_{tr,c}$. In practice, the transverse tensile force $F_{tr,t}$ is usually designed to be resisted by the transverse reinforcement, while the concrete is considered to resist F and $F_{tr,c}$.

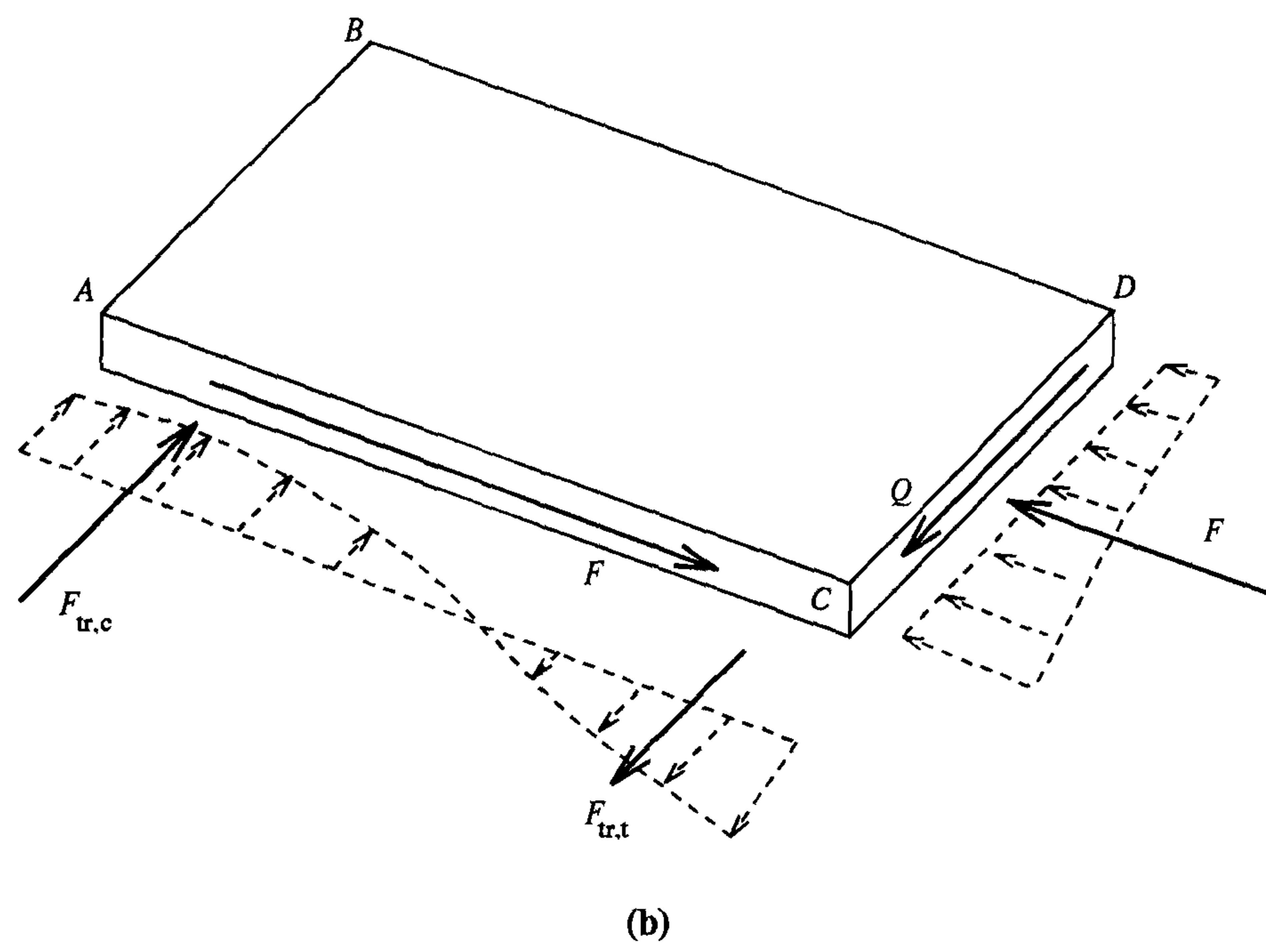
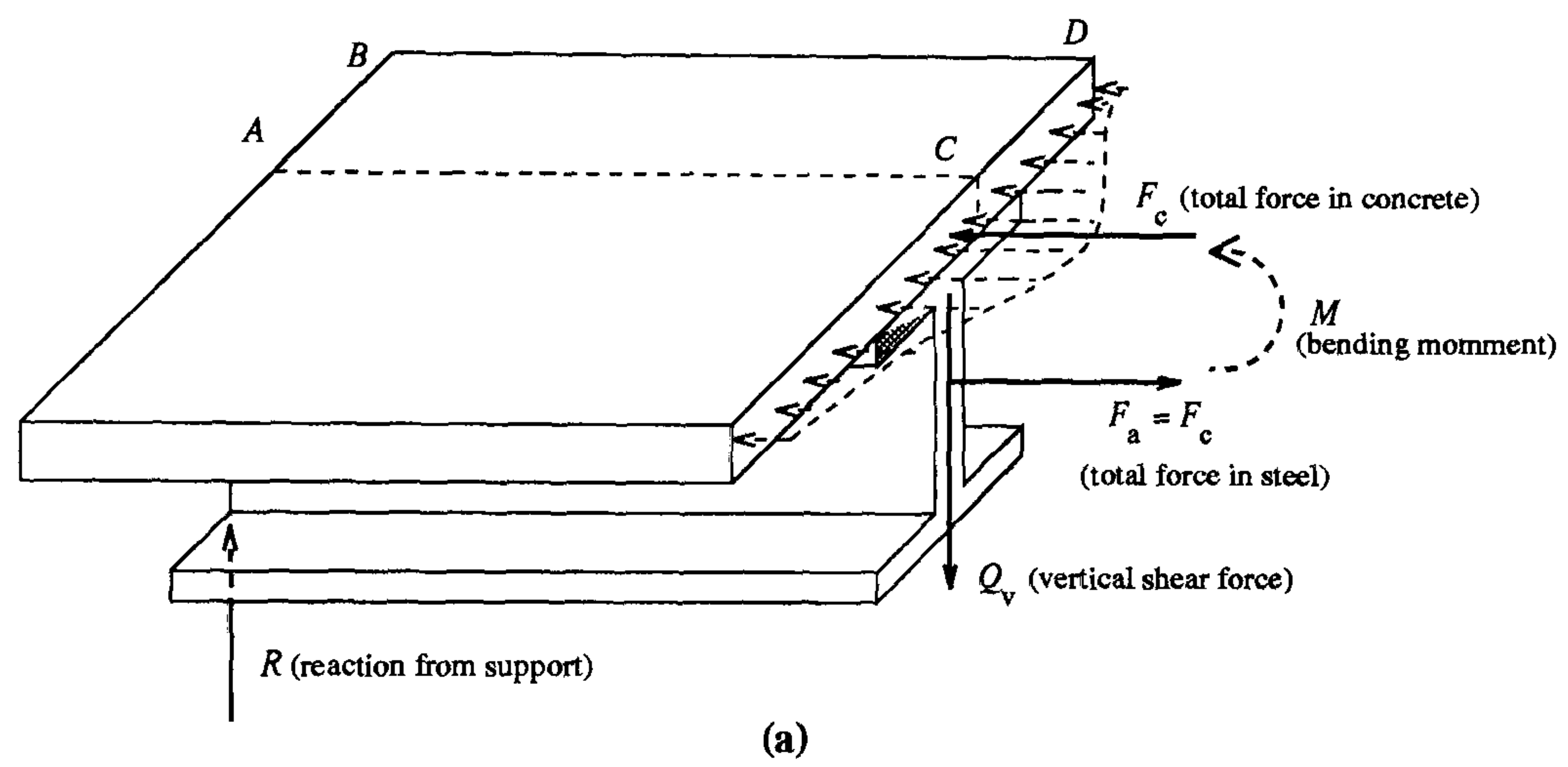
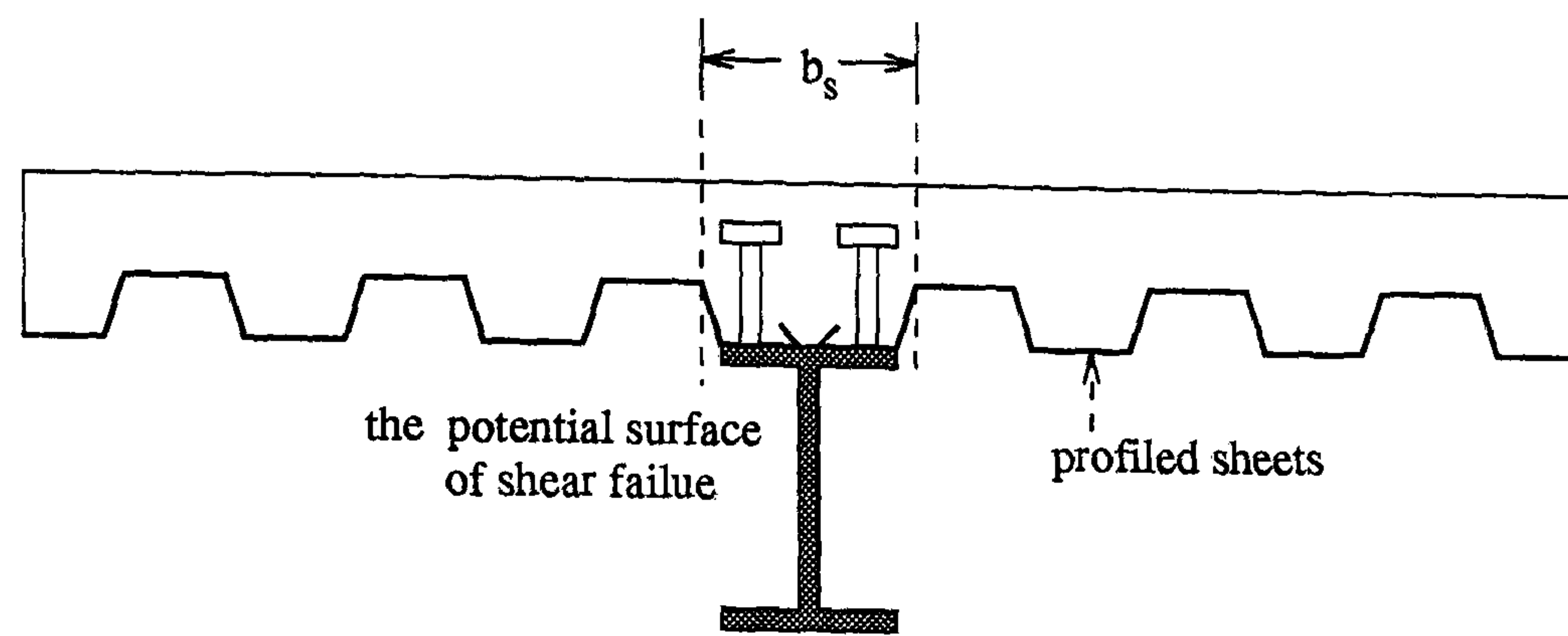
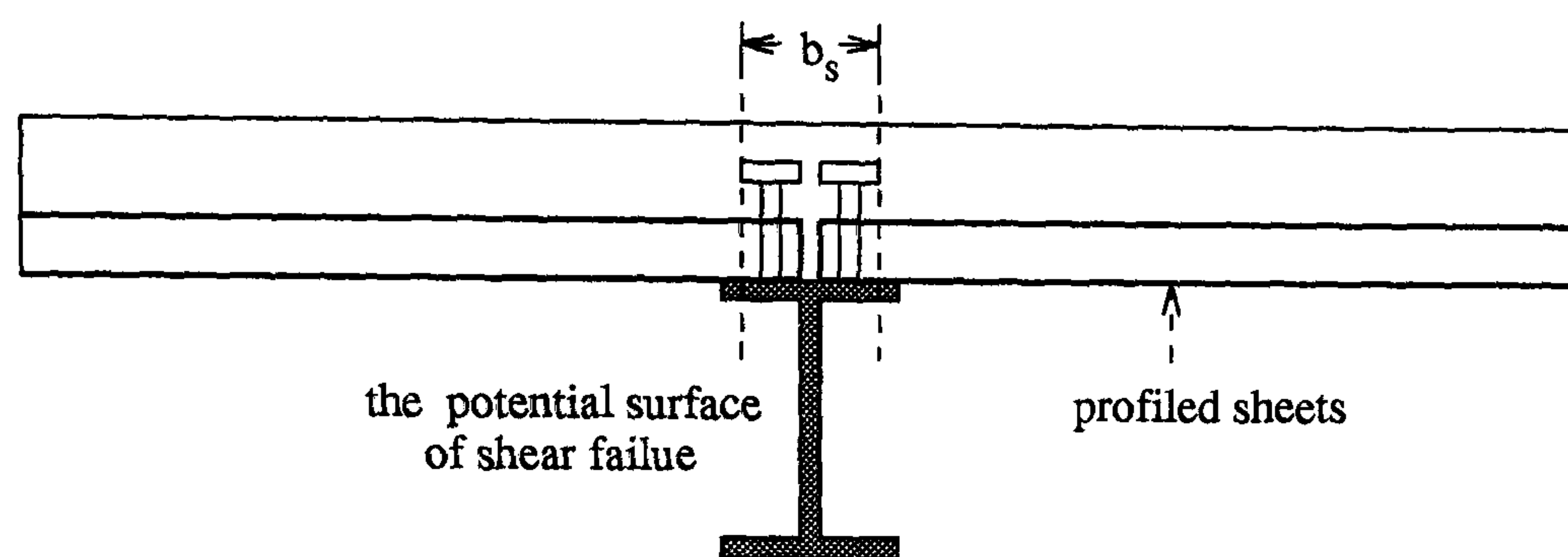


Figure 1.1: The longitudinal shear in the concrete flange



(a) Sheeting parallel to the steel beam



(b) Sheeting transverse to the steel beam

Figure 1.2: Cross-section of composite beam with profiled sheeting, and potential surfaces of shear failure

The flanges of the composite beams may be built up with the profiled sheets. These sheets normally have the shape shown in Figure 1.2. When proper anchorage of the sheeting to the steel beam is used, e.g. when stud shear connectors are welded to the steel beam directly through the sheets [1], the profiled sheets may be expected to help to resist transverse tension $F_{tr,t}$ or the longitudinal shear F , which would lead to stronger longitudinal shear resistance in the composite beams. Therefore, the longitudinal shear resistance of composite beams with profiled sheeting needs to be researched by investigating the following problems:

- (1) the behaviour in longitudinal shear of the composite beams with and without profiled sheeting
- (2) determination of the relative contributions from profiled sheeting, reinforcement and concrete to the longitudinal shear resistance.

1.2 Previous research on structural reliability

As reviewed by Madsen et al [22], the development of structural reliability theory began in the 1920s. Since the 1960s, there has been a rapid growth of academic interest in such theories and a growing acceptance by engineers of probability-based structural design.

In modern safety analysis for structural engineering, the theory called the second-moment reliability method is commonly used, which was originally suggested by Cornell [23,24]. The idea behind this theory was that all uncertainties concerning the structural reliability can be expressed solely in terms of expected values (first moments) and covariances (second moments) of all the variables. In measuring the structural safety, Cornell [24] also defined a safety index. The safety measurement from such an index was then widely accepted in structural reliability analysis, as reviewed below.

To obtain consistent safety measurement for different definitions of the failure function, Hasofer and Lind [25] further studied the safety index and showed that this index can be defined as the distance from the mean of the variable vector to the failure region boundary, measuring the variables in standard-deviation units. It was then shown [22] that safety assessment in structural design from the safety index can be made from a design point.

Applying the concepts of second-moment reliability and safety index, Ang and Cornell [26] further developed the safety-index design formats for assessing structural safety and performance, and presented the formulation of evaluating the uncertainties of resistance and load effect from the variances of the basic variables.

Following the study by Ang and Cornell [26], Ellingwood and Ang [27] illustrated the quantitative analysis of design uncertainties and investigated the effects of uncertainties of basic design variables (geometric properties, material strengths, etc) on reliability of a design.

Based on the safety-index design formats, a series of calibrations have been

carried out to investigate the safety level in design codes [28,29,30,31]. In these works, the safety index was used to obtain the safety margins on load side and the resistance side. On the load side, considering that the effects of different loads were additive, the partial safety factors for different loads were calibrated, while on resistance side, the calibrations usually achieved a single safety factor for the safety margin of the resistance.

In 1988, the Nordic Committee on Building Regulation (NKB) [32] established the guidelines for determining reliability in structural design. A method of partial coefficients, developed from the safety-index theory, was presented there, which divided the partial safety factors into several parts, to consider the uncertainties in material strength, design model for resistance and load effect, geometric dimensions, etc. With this method, the reliability of a design format would be still calibrated by taking one safety factor to represent the total safety margin on the resistance side.

In 1987, a general procedure based on the safety-index theory was developed by Bijlaard et al [33], to make reliability analyses, particularly for structural resistances. This procedure can be directly used to calibrate the design formulae of resistances with one safety factor. According to this procedure, to assess the uncertainties of a predicted resistance, test data for the resistance should be used to find out in terms of statistics the difference between a theoretical model for the resistance and the reality, which was also recommended in JCSS working document [34].

The procedure presented in [33] has been directly applied to calibrate the design resistance of stud connectors in composite structures [35,36], whose formula only employs one safety factor.

As indicated above, for bending resistance in composite beams (and some other resistances), distinct safety factors are currently required within one design formula [1], and these factors also need to be calibrated through a safety analysis, on which, however, few studies have been carried out so far.

1.3 Previous research on longitudinal shear resistance of composite beams

In order to investigate shear transfer behaviour of concrete and the longitudinal shear resistance of a reinforced concrete flange, some researches have been done in the past.

In studying the behaviour of connections in precast concrete buildings, Birkeland and Birkeland [17] and Mast [18] developed a “shear-friction” model to describe shear transfer on a cracked concrete in monolithic concrete. This model suggested that along a crack in concrete, the tension in reinforcement due to slippage and subsequent separation along the crack would cause the concrete on the cracked surface to be subject to compressive stress, and the shear resistance across the crack may be determined as the friction force caused by the yield stress of reinforcement and an appropriate friction factor.

Hofbeck and Mattock et al [2,19] carried out a series of push-off and pull-off tests to investigate shear strength in reinforced concrete with and without a pre-existing crack. They found that the shear-friction hypothesis gave a conservative estimation for shear transfer strength of concrete. Hofbeck et al [2] found from the test results that, within certain upper limit, the shear strength of concrete along an initially cracked surface was as a combination of cohesion and friction effects. A truss model was introduced by Mattock and Hawkins [19] to analyze the shear transfer behaviour of initially uncracked concrete with reinforcement normal to the shear plane. Considering the cohesion effect in concrete, Mattock and Hawkins [19] presented a safe estimation of the maximum shear that, within a certain upper limit, could be transferred across a pre-cracked shear plane in concrete.

The “friction-cohesion” model was used by Regan and Placas [3] to study the longitudinal shear with in-plane bending in flanges of reinforced concrete T beams. Nielsen et al showed in their book [10] that the failure criterion for

concrete may be developed from the “friction-cohesion” concept.

The “shear-friction” approach was recommended by Sen and Chapman [4] for designing composite beams for longitudinal shear. To investigate the longitudinal shear resistance in composite beams with solid slabs, they carried out tests on eleven beams, including four haunched beams whose ribs were higher than the studs.

Based on results of tests on composite beams and shear tests on reinforced slabs, Johnson [11,12,13] studied the effect of transverse reinforcement on longitudinal shear resistance in composite beams with and without transverse bending and made design recommendations for the top and bottom transverse reinforcement in slabs. He suggested from the tests [11] that, in design, the top transverse reinforcement can be allowed to resist both transverse bending and longitudinal shear.

In 1975, Morley and Rajendran [5] presented an approximate plastic theory for the limit state of longitudinal shear in reinforced concrete flanges, where they related the shear strength to the compression strength in concrete by means of Mohr’s circle. Based on an assumed position of the neutral axis in the concrete slab, they also studied the relationship between the effective width in slabs of composite beams and the amount of transverse reinforcement.

Profiled sheets have been used in composite structures for a long time. The bending resistance of composite beams with profiled sheeting has been studied quite comprehensively [9,14,20,21], but little literature can be found on longitudinal shear resistance in such beams. However, a common opinion [1,9] has been formed that the profiled sheets can act as transverse reinforcement to composite beams.

Currently, the design formulae provided in Eurocode 4 [1] for predicting longitudinal shear resistance in composite beams are based on the truss-analogy that was applied to the vertical shear in a reinforced concrete web [7]. According to this code model, longitudinal shear resistance in composite beams is determined

by either yielding of the transverse reinforcement or crushing in the concrete struts. For situations where profiled sheeting is used, the code only allows the transverse sheeting, as shown in Figure 1.2(b), to be considered to contribute to longitudinal shear resistance the same way as transverse reinforcement, when the sheeting meets certain conditions stated in the code.

1.4 Layout of the thesis

In this thesis, work on problems is presented; one is the reliability analysis for resistances of composite beams to bending, aiming at calibrating the different safety factors which are applied in one formula to different materials, as given by Eurocode 4 [1]; the other is the study of longitudinal shear resistances in composite beams with profiled sheeting, to understand the behaviour in longitudinal shear of the composite beams and the effect of profiled sheeting on the resistance to shear.

Chapter 2 to Chapter 5 are devoted to the work of reliability analysis, while Chapter 6 to Chapter 10 present the investigation of longitudinal shear resistance in composite beams.

In Chapter 2, the theory of safety-index and second-moment reliability is briefly described at first, from which the distribution of overall safety margin between the loadings and the resistances can be determined. Then, corresponding to a target safety level, the design resistances of composite structural members is derived in detail, and a method is developed to calibrate distinct safety factors in one design formula for the resistances. In addition, a procedure of obtaining reliability of a design formula for the resistances with the given safety factors is presented. In principle, the theory presented in this chapter can be applied more generally, not just to bending resistances of composite beams only.

Chapter 3 concerns particularly the reliability analysis in bending resistances of composite beams. In this chapter, the principles of selecting the reported

results of bending tests composite beams are presented at first; then, based on the accessible test data, the bending resistances of composite beams are classified into several groups. Subsequently, this chapter deals with the particular problems in assessing the reliability in bending resistances of composite beams, including processing of the test data, treatment of design parameters and algorithm for the calibrations.

In Chapter 4, the calibration results for bending resistances of composite beams are presented at first; then, based on the calibration results, the reliability of bending resistances designed in accordance with Eurocode 4 [1] is discussed.

Conclusions for reliability analysis of composite beams in bending are given in Chapter 5.

Taking the effect of profiled sheeting into account, Chapter 6 presents a theoretical model for determining the longitudinal shear resistances in composite beams. Longitudinal shear resistances in concrete flanges of a composite beam are studied with respect to failure of transverse reinforcement and sheeting at first; then, considering the concrete strength against crushing, the upper limit to such longitudinal shear resistance in concrete flanges is derived. The strength of profiled sheets contributing to the longitudinal shear resistances is also discussed.

Seven tests on three specimens were done for investigating longitudinal shear resistance in composite beams. Chapter 7 reports details of the specimens and planning of the tests.

Chapter 8 describes the test results and test procedures.

In Chapter 9, according to both the theory established in Chapter 6 and the test results, several problems about the behaviour of composite beams in longitudinal shear are discussed, including the load to cause shear cracking in concrete, modes of longitudinal shear failure, the resistances to such failures, etc. Finally, recommendations are made for design of resistances of composite beams to longitudinal shear.

Chapter 10 gives the conclusions of study of the longitudinal shear resistances.

Chapter 2

Reliability theory for resistances in composite structures

2.1 Concepts of second-moment reliability and design resistances

In the limit state design, it is normally required [1,8] that the resistance in a structure should be not smaller than the corresponding load effect. Therefore, the structural reliability for such a design may be classified as [22,26]

$$\begin{cases} r - s > 0 & \text{(acceptable, safe)} \\ r - s = 0 & \text{(critical)} \\ r - s < 0 & \text{(unacceptable, unsafe)} \end{cases} \quad (2.1)$$

where

r is the structural resistance at a limit state;

s is the load effect corresponding to the resistance r .

In structural safety analysis, both r and s are treated as random variables; and, normally, r and s are further assumed to be mutually uncorrelated [22-26]. Expression (2.1) suggests that the reliability state for structural performance can be measured by the random variable $r - s$.

With respect to the physical significance, r and s should be restricted to positive values [22,33], so the safety state shown in (2.1) may be alternatively established in the form [22,26]:

$$\begin{cases} \ln r - \ln s > 0 & \text{(acceptable, safe)} \\ \ln r - \ln s = 0 & \text{(critical)} \\ \ln r - \ln s < 0 & \text{(unacceptable, unsafe)} \end{cases} \quad (2.2)$$

where, $\ln r$ and $\ln s$ are normally regarded as two uncorrelated random variables.

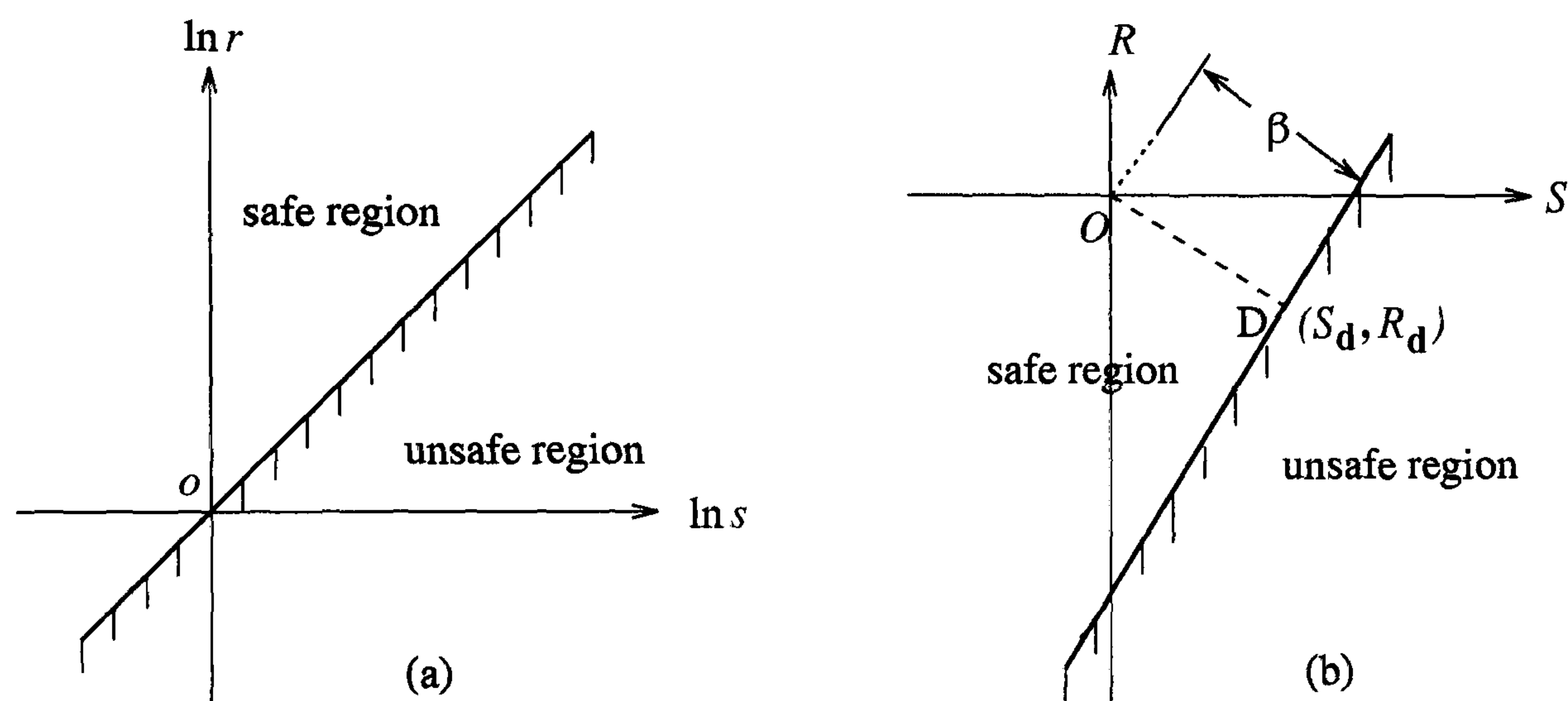


Figure 2.1: Reliability states of structures

The reliability states classified by (2.2) can be shown in Figure 2.1(a) or (b). In Figure 2.1(b), classification (2.2) is expressed in terms of the normalized transformation

$$\begin{cases} S = (\ln s - \mu_{\ln s}) / \sigma_{\ln s} \\ R = (\ln r - \mu_{\ln r}) / \sigma_{\ln r} \end{cases} \quad (2.3)$$

where, $\mu_{\ln s}$ and $\mu_{\ln r}$ are the mean values of $\ln s$ and $\ln r$, respectively;

$\sigma_{\ln s}$ and $\sigma_{\ln r}$ are the standard deviations of $\ln s$ and $\ln r$, respectively.

According to classification (2.2), the probability of failure of a structure, P_c , can be obtained as [22]:

$$P_c = P\{\ln r - \ln s < 0\} \quad (2.4)$$

or, equivalently,

$$P_c = P\left\{\frac{(\ln r - \ln s) - (\mu_{\ln r} - \mu_{\ln s})}{\sqrt{\sigma_{\ln r}^2 + \sigma_{\ln s}^2}} < -\frac{\mu_{\ln r} - \mu_{\ln s}}{\sqrt{\sigma_{\ln r}^2 + \sigma_{\ln s}^2}}\right\} \quad (2.5)$$

where, $P\{\dots\}$ represents the probability of occurrence of events "...".

From their study, Ang and Cornell [26] pointed out that the calculated probability P_c is not very sensitive to the type of the distribution for s and r unless a very low value, e.g. $\leq 10^{-5}$, is required for P_c and, for practical application, they suggested that a log-normal distribution may be assumed to s and r . Therefore, regarding $\ln r$ and $\ln s$ as uncorrelated random variables, the probability P_c can be obtained from equation (2.5) as

$$P_c = \frac{1}{\sqrt{2\pi}} \int_{-\infty}^{-\beta} \exp\left(-\frac{x^2}{2}\right) dx \quad (2.6)$$

where

$$\beta = \frac{\mu_{\ln r} - \mu_{\ln s}}{\sqrt{\sigma_{\ln r}^2 + \sigma_{\ln s}^2}} \quad (2.7)$$

It is seen here that the probability of a structure failing to resist the load effect is governed by the parameter β . This parameter is called the safety index [22-26] which governs P_c , as shown in (2.6). Normally, the safety criteria for modern structural designs are established by prescribing such an index [31-34]. It is shown in Reference [33] that an acceptable safety index is $\beta = 3.8$, which, according to equation (2.6), leads to $P_c = 7.2 \times 10^{-5}$.

Therefore, to reach the safety level specified by a given safety index, the following condition should be satisfied by design work:

$$\frac{\mu_{\ln r} - \mu_{\ln s}}{\sqrt{\sigma_{\ln r}^2 + \sigma_{\ln s}^2}} \geq \beta \quad (2.8)$$

According to the research by Hasofer and Lind [25], in geometry, the safety index β can be measured as the length of line OD marked in Figure 2.1(b) (i.e.

the distance from the origin O to the safe region boundary). Therefore, the point D has been traditionally taken as the design point, from which the design resistance r_d and design load effect s_d can then be determined [22,31-34].

In Figure 2.1(b), the coordinates of point D can be found as

$$\begin{cases} S_d = \alpha_s \beta \\ R_d = -\alpha_r \beta \end{cases} \quad (2.9)$$

where

$$\begin{cases} \alpha_s = \sigma_{\ln s} / \sqrt{\sigma_{\ln s}^2 + \sigma_{\ln r}^2} \\ \alpha_r = \sigma_{\ln r} / \sqrt{\sigma_{\ln s}^2 + \sigma_{\ln r}^2} \end{cases} \quad (2.10)$$

Therefore, according to equations (2.3) and (2.9), the design values of structural resistances, r_d , and load effects, s_d , are obtained as [22,31-34]

$$s_d = \exp(\mu_{\ln s} + \alpha_s \beta \sigma_{\ln s}) \quad (2.11)$$

$$r_d = \exp(\mu_{\ln r} - \alpha_r \beta \sigma_{\ln r}) \quad (2.12)$$

Equations (2.11) and (2.12) show that the target safety margin would eventually be distributed between the resistance and the load effect, and such a distribution would exclusively depend on α_s and α_r . In the literature [22,31-34], α_s and α_r are called the sensitivity factors on the load side and the resistance side, respectively. According to the recommendation given in [34], on the resistance side, the sensitivity factor can be taken as $\alpha_r = 0.8$, which would lead to $\alpha_s = 0.6$ since equation (2.10) implies

$$\alpha_r^2 + \alpha_s^2 = 1 \quad (2.13)$$

In [33], corresponding to $\alpha_r = 0.8$, α_s was taken as 0.7.

Assuming that $\alpha_r = 0.8$ and that r follows a log-normal distribution [26,32,33], the design resistance in (2.12) can further be given as

$$r_d = \bar{r} \exp(-k_d \sigma_{\ln r} - 0.5 \sigma_{\ln r}^2) \quad (2.14)$$

where, \bar{r} is the mean value of r and k_d is the design fractile factor, given by

$$k_d = 0.8\beta \quad (2.15)$$

Noting $P\{r \leq r_d\} = P\{\ln r \leq \ln r_d\}$, it can be shown from the assumption of r following a log-normal distribution that the probability of the structure resistance failing to reach or exceed a specified value r_d given in (2.14) is

$$P_f = \frac{1}{\sqrt{2\pi}} \int_{-\infty}^{-k_d} \exp\left(-\frac{x^2}{2}\right) dx \quad (2.16)$$

Thus, P_f , named the failure probability in this study, can be determined for a given k_d ; taking $k_d = 0.8 \times 3.83.04$, (2.16) gives that $P_f = 0.12\%$.

Obviously, for any specified fractile factor k other than k_d , equations (2.14) and (2.16) can be used to determine the corresponding resistance and failure probability, as long as k_d is replaced by k .

2.2 Design resistances of composite structures at given safety levels

According to the concepts of second-moment reliability introduced above, to obtain a design resistance r_d for a composite structural member, several factors, including the type of distribution of the resistances, the mean value and standard deviation of the resistance, etc. need to be considered. Therefore, a detailed study is needed, to determine the design resistances for composite structures.

2.2.1 Definitions and basic assumptions in the analysis

To determine a resistance for a composite structural member, a theoretical model will be developed, which would usually lead to the resistance to be expressed as a function of structural properties:

$$r_t = g_R(\underline{X}) \quad (2.17)$$

where, r_t denotes the prediction of the structural resistance from the theoretical

model, and

$$\underline{X} = (X_1, X_2, \dots, X_J) \quad (2.18)$$

are the design parameters used in determining r_t , which usually include geometric dimensions of the structural members and the basic material properties. These parameters are regarded as the basic variables in a reliability analysis [33,34]. Considering \underline{X} to be the random variables, the theoretical resistance r_t would be a function of random variables and, therefore, is a random variable as well.

In this study, structural members are classified as belonging to the same *population* if their all basic variables \underline{X} are statistically the same. i.e. the mean value, the standard deviation, the type of distribution, etc. are all the same.

In practice, when a satisfactory quality control is achieved, the values of the basic variables achieved after construction should appear to deviate just around their intended value by design; therefore, the intended values of the basic variables may be regarded as their mean values. According to previous research [31], it can be regarded that the distribution type and the standard deviation or coefficient of variation of the basic variables are invariant in relation to their mean values, provided that the same procedure controlling the fabrication quality is followed. Thus, *all* structural members under the same design can normally be considered to be in the same population.

A *sample* from a population is defined here as *a set of* structural members from the population.

It is realized that practical situations could be more complicated than those in laboratories. However, as a normal case, the actual resistances in a structural member can only be measured by means of laboratory tests. Therefore, the following assumption has to be made

- (1) the test results are the measurement of the real resistances r or, in statistical term, are observations of the random variable r .

Regarding this assumption, it would be ideal that, under the same design, a

large number of specimens can be made for testing the resistances. Unfortunately, the cost of experimental work (say tests on the ultimate bending resistances of composite beams) rarely allows replication of the tests unless the scale of the tests is small (say tests on strength of steel bolts or welded stud connectors [35,36]). A sample, as defined above, taken in tests often consists of quite limited number of specimens (sometimes only one specimen in bending resistance tests) based on which no statistical inference can be reasonably made for the population represented.

As a result, when considering the test data for structural members within one population only, it is in many cases not feasible to analyse the reliability of the resistance for that population. However, if a group of the test specimens is appropriately chosen, for the populations represented by such a group, the ratio

$$b = r/r_t \quad (2.19)$$

may still be treated as a random variable, which may enable the reliability of resistances designed for these populations to be deduced.

In physical sense, it is reasonable to consider that the classification of the test specimens for this study should be related to the structural behaviours of the specimens.

If, based on the well recognized theories (say accepted by the design codes), it is shown that the resistances of a group of specimens from different populations should be predicted by the same resistance function, then it may be considered that all the populations of the structural members represented by this group perform in a similar way, say the same failure mode and same behaviour during functioning.

Therefore, a *group* of n test specimens are in this study defined as a set that has the same resistance function; but may represent up to n populations of structural members of different dimensions and material properties. Thus, the reliability investigation for the structural resistances of all the populations

represented by such a group may be made, if it is assumed that

- (2) for all populations represented in a group of test specimens, the (unknown) random variables r/r_t all have the same probability distribution, which can be estimated from the results from the group, taking the sample size not as one but as n .

Based on this assumption, the statistical properties of r/r_t for a population in a particular group can be estimated from the observations of this variable. Ideally, the observations of r/r_t should be made such that, apart from r being measured, the theoretical resistance r_t is calculated from equation (2.17) using measured values of all the basic variables. However, it is quite usual that measured values of geometric dimensions are not reported for experimental works, so it has to be assumed that

- (3) in calculating r_t to obtain observations of r/r_t , the measured values of the basic variables are used; when the measured geometric properties of a test specimen are unavailable and the variation of these properties are known to be small, the intended values of these variables may be used as the measured values.

The validity of this assumption will be further discussed in Section 3.1.3.

It can be imagined that the variation of ratio r/r_t should mainly depend on the theoretical model adopted, rather than r_t itself obtained from the model, e.g. if the most perfect model were developed, r/r_t would be 1.0 always, irrespective of r_t varying from case to case. So, to simplify the analysis, it is assumed here that

- (4) the random variables r/r_t and r_t are mutually independent.

According to the analysis in the last section, for a structural resistance, it is assumed in this study that

- (5) the structural resistance follows a log-normal distribution.

Moreover, the following common assumption [22,26,33] will also be used in this study:

- (6) there is negligible correlation between the basic variables of the resistance function.

2.2.2 Determination of design resistance in general cases

According to assumption (1) given above, the measured resistance from tests may be regarded as the resistance actually occurred, therefore, for all the populations of structural members represented by a group of n test specimens, the correlation coefficient ρ between the real structural resistance and the resistance predicted from a theoretical model (2.17) can first of all be estimated [33,37], such that

$$\rho = \frac{(n \sum_{i=1}^n r_{ei} r_{ti} - \sum_{i=1}^n r_{ei} \sum_{i=1}^n r_{ti})}{\sqrt{[n \sum_{i=1}^n r_{ei}^2 - (\sum_{i=1}^n r_{ei})^2][n \sum_{i=1}^n r_{ti}^2 - (\sum_{i=1}^n r_{ti})^2]}} \quad (2.20)$$

where, r_{ei} and r_{ti} are the experimental and theoretical values of the resistance in specimen i , ($i = 1, \dots, n$), respectively.

According to assumption (3) above, r_{ti} should in principle be calculated from the measured values of basic variables, but the mean value of a geometric dimension may replace its measured value, if the measurement for this dimension is not made.

In general, an acceptable resistance model can be expected to lead to the predicted resistance r_t and the real resistance r being well correlated, so, normally, a comprehensive reliability analysis for a resistance model would only be valid if the ρ estimated appears sufficiently high.

Following the instruction given in [33], the correlation between r and r_t can be regarded as sufficiently high if $\rho \geq 0.9$.

In order to make reliability analysis for a structural resistance, a new random variable δ , related to b defined in (2.19), for a structural member population is

introduced as follows,

$$\delta = \frac{b}{\bar{b}} = \frac{r/r_t}{\bar{b}} \quad (2.21)$$

where \bar{b} is the mean value of $b(= r/r_t)$. Obviously, the mean of δ , $\bar{\delta}$, is 1.0.

Using equations (2.17) and (2.21), the real resistances r can be expressed as

$$r = \bar{b}\delta g_R(X_1, \dots, X_J) \quad (2.22)$$

Taking the first-order approximation [37] and noticing $\bar{\delta} = 1.0$, the mean of r can be found as

$$\bar{r} = \bar{b}g_R(\bar{X}_1, \dots, \bar{X}_J) \quad (2.23)$$

where, $\bar{X}_1, \dots, \bar{X}_J$ are the mean values of basic variables X_1, \dots, X_J , respectively.

With respect to assumption (4) made above, the coefficient of variation of r is obtained as

$$V_r = \sqrt{V_\delta^2 + V_{r_t}^2} \quad (2.24)$$

where, V_r , V_δ and V_{r_t} are the coefficients of variation of r , δ and r_t , respectively.

Equation (2.23) shows that the mean values of r and r_t are related to each other through the parameter \bar{b} , so \bar{b} can be called mean correction of the theoretical resistance [33]. It follows from the definition of δ (see equation (2.21)) that the parameter V_δ characterizes the extent to which r differs from r_t , so V_δ is called the coefficient of variation of error terms for the theoretical resistance [33].

With respect to assumptions (1) and (2), for a population of structural members among those represented by a group of test specimens, the estimators of \bar{b} and V_δ can be made from the test results of such a group of specimens, i.e.

$$\bar{b} = \frac{1}{n} \sum_{i=1}^n \frac{r_{ei}}{r_{ti}} \quad (2.25)$$

$$V_\delta = \sqrt{\frac{1}{n-1} \sum_{i=1}^n \left[\frac{1}{\bar{b}^2} \left(\frac{r_{ei}}{r_{ti}} \right)^2 - 1 \right]} \quad (2.26)$$

As indicated above, r_{ti} ($i = 1, \dots, n$) is in principle obtained from measured values of the basic variables, so it can be regarded that r_{ti} ($i = 1, \dots, n$) itself is free of the uncertainties. Thus \bar{b} and V_δ found in this way would particularly reflect the difference and relative variation between the real resistance and the theoretical model.

Equation (2.24) shows the variation of the resistance is also affected by V_{rt} , which, as implied by (2.17), depends on the uncertainties in the basic variables. Taking the first-order approximation [37], V_{rt} is obtained as follows,

$$V_{rt} = \frac{1}{g_R(\underline{\bar{X}})} \sqrt{\sum_{i=1}^J V_{X_i}^2 \bar{X}_i^2 \left(\frac{\partial g_R}{\partial X_i}\right)^2 + 2 \sum_{i=1}^{J-1} \sum_{j=i+1}^J V_{X_i} \bar{X}_i V_{X_j} \bar{X}_j \rho_{X_i X_j} \left(\frac{\partial g_R}{\partial X_i} \frac{\partial g_R}{\partial X_j}\right)} \Big|_{\underline{\bar{X}}} \quad (2.27)$$

where $\underline{\bar{X}}$ or \bar{X}_i and \bar{X}_j ($i, j = 1, \dots, J$) are mean values of the basic variables; V_{X_i} and V_{X_j} ($i, j = 1, \dots, J$) are the coefficients of variation of the basic variables;

$\rho_{X_i X_j}$ is the correlation coefficient of X_i and X_j ($i, j = 1, \dots, J$).

Applying assumption (6) made above, it yields that $\rho_{X_i X_j} = 0$ ($i, j = 1, \dots, J$), so equation (2.27) can be simplified to

$$V_{rt} = \frac{1}{g_R(\underline{\bar{X}})} \sqrt{\sum_{i=1}^J [V_{X_i}^2 \bar{X}_i^2 \left(\frac{\partial g_R}{\partial X_i}\right)^2]_{X_i=\bar{X}_i}} \quad (2.28)$$

When V_{rt} and V_δ are determined, the coefficient of variation for the real resistance r , V_r , can be obtained from (2.24). Thus, for the assumed log-normal distribution of r (assumption (5) given above), it yields [37]:

$$\sigma_{\ln r} = \sqrt{\ln(1 + V_r^2)} \approx V_r \quad (2.29)$$

The approximation is valid when V_r is small (say < 0.4).

Hence, for each population of structural members in the group considered, the mean resistance, \bar{r} , can be found from (2.23) and (2.25), and $\sigma_{\ln r}$ from (2.24).

(2.26), (2.28) and (2.29), so equation (2.14) can be used to determine the design resistance according to a given design fractile-factor k_d .

Assuming that $V_r < 0.4$ is the normal situation and specifying the basic variables involved in the resistance function (2.17) as geometric variables, \underline{X}_g , and basic material properties, \underline{X}_p , then according to equation (2.24) and (2.29), r_d can be found as

$$r_d = \bar{b}g_R(\bar{X}_p, \bar{X}_g) \exp\left(-\frac{V_{r_t}^2 k_d + V_\delta^2 k_d}{V_r^2} V_r - 0.5V_r^2\right) \quad (2.30)$$

where, \bar{X}_p and \bar{X}_g represent the mean value of \underline{X}_p and \underline{X}_g , respectively.

It is mentioned in Section 2.1 that the target reliability level may be established as $\beta = 3.8$ (β is the safety index) and $k_d = 0.8 \times 3.8 = 3.04$ [33,34], which, from equation (2.16), leads to the probability of $r < r_d$, P_f , being 0.12%. According to the research reported in [33], the value of $k_d = 3.04$, may be directly used in equation (2.14) if a large number of test results is available and variations of the basic variables, V_{X_1}, \dots, V_{X_J} , are well know.

In many cases, however, the number of specimens in a group under consideration is limited, which, therefore, requires more prudence for using the estimators of \bar{b} and V_δ in equation (2.14) or (2.30). So, in determining the design resistances, the design fractile-factor k_d should be related to the number of test specimens in the group (group size), rather than taken as 3.04 always.

Equation (2.30) suggests that the design fractile-factor may be applied to V_{r_t} and V_δ separately. Accordingly, as suggested in Reference [33], when the acceptable values of V_{X_1}, \dots, V_{X_J} are used and the safety level is given as $P_f = 0.12\%$, the fractile factor k_d associated with V_{r_t} is taken as 3.04; but for V_δ the value of k_d leading to $P_f = 0.12\%$ should be determined based on the group size and a confidence level of 0.75 (see Appendix A).

Hence, the design resistance r_d can normally be determined as

$$r_d = \bar{b}g_R(\bar{X}_p, \bar{X}_g) \exp(-k_d \sigma_{\ln r} - 0.5\sigma_{\ln r}^2) \quad (2.31)$$

where

$$k_d = \frac{3.04V_{rt}^2 + k_b V_\delta^2}{V_r^2} \quad (2.32)$$

In equation (2.32), k_b is a factor corresponding to 0.12% fractile at a confidence level of 0.75, which is determined from the group size n and a non-central t -distribution ignoring the randomness of the basic variables, as shown in Appendix A and Table A.1 there.

2.2.3 Partial safety factors for design resistances of composite structures

Equation (2.30) provides designers with design values of structural resistances, which enables designs to achieve the prescribed safety margin on the resistance side. For prediction of structural resistance in design, the theoretical functions shown in (2.17) are normally used with nominal values of the mean or characteristic values of the basic variables. In order to make the resistance designed in such a way match the values given by equation (2.30), a set of safety factors should also be applied in the resistance function.

As indicated in Chapter 1, in designing resistances for composite structures, distinct partial safety factors are required for the different material strengths [1]. Quite commonly, the material strengths involved in a resistance function (2.17) for composite structures may include yield strength of structural steel, f_y , yield strength of reinforcement, f_s , compressive strength of concrete, f_c and, if any, the strength of shear connection, P_R . Therefore, calibration of the safety factors to these strengths would be of special interest.

It is noted here that strength of shear connection P_R is normally represented by the resistance of a shear connector which should be regarded as a function of several variables, such as compressive strength of concrete, dimensions of studs, etc. [1], and, therefore, is not a basic variable as considered in this study.

However, according to the design code of composite structures [1], the design

format of a resistance function which contains f_y , f_s , f_c and P_R , may be presented as

$$r_d = g_R\left(\frac{f_{yk}}{\gamma_a}, \frac{f_{ck}}{\gamma_c}, \frac{f_{sk}}{\gamma_s}, \frac{P_{Rk}}{\gamma_v}, \bar{X}_{p_0}, \bar{X}_g\right) \quad (2.33)$$

where,

f_{yk} , f_{ck} , f_{sk} and P_{Rk} are the characteristic values of f_y , f_c , f_s and P_R , respectively;

γ_a , γ_c , γ_s , γ_v are the safety factors applied to f_y , f_c , f_s and P_R , respectively.

\bar{X}_{p_0} are the mean values (nominal values) of the other material properties X_{p_0} , say density or Young's modulus, which may be involved in the resistance function;

\bar{X}_g represents the mean values (nominal values) of the geometric dimensions;

Normally, for a material strength f , its characteristic value f_k for design is related to a specifying the probability $P\{f < f_k\}$. According to the reported calibration for Netherlands building codes [31] and statistical analysis for the strength of a single shear connector [33,35,36], the strength f_y , as well as f_c , f_s and P_R , can be assumed to follow a log-normal distribution. Therefore, f_{yk} can be obtained as

$$f_{yk} = \bar{f}_y \exp(-k_{as}\sigma_{\ln f_y} - 0.5\sigma_{\ln f_y}^2) \quad (2.34)$$

where,

k_{as} is the fractile-factor corresponding to probability $P\{f_y < f_{yk}\}$;

\bar{f}_y represents the mean value of f_y

$\sigma_{\ln f_y}$ is found from the coefficient of variation of f_y , V_{f_y} , such that

$$\sigma_{\ln f_y} = \sqrt{\ln(1 + V_{f_y}^2)} \quad (2.35)$$

Similarly, f_{ck} , f_{sk} and P_{Rk} can be given as

$$f_{ck} = \bar{f}_c \exp(-k_{cs} \sigma_{\ln f_c} - 0.5 \sigma_{\ln f_c}^2) \quad (2.36)$$

$$f_{sk} = \bar{f}_s \exp(-k_{ss} \sigma_{\ln f_s} - 0.5 \sigma_{\ln f_s}^2) \quad (2.37)$$

$$P_{Rk} = \bar{P}_R \exp(-k_{vs} \sigma_{\ln P_R} - 0.5 \sigma_{\ln P_R}^2) \quad (2.38)$$

where

$$\sigma_{\ln f_c} = \sqrt{\ln(1 + V_{f_c}^2)} \quad (2.39)$$

$$\sigma_{\ln f_s} = \sqrt{\ln(1 + V_{f_s}^2)} \quad (2.40)$$

$$\sigma_{\ln P_R} = \sqrt{\ln(1 + V_{P_R}^2)} \quad (2.41)$$

In view of the analysis presented in Section 2.2.2, it can be concluded that, as indicated in Section 1.1, a design resistance r_d associated with a specified reliability level (a given failure probability P_f) depends on

- (1) uncertainties in the theoretical model — the difference and relative variation between the real resistance and the the theoretical model, as reflected by \bar{b} and V_δ ;
- (2) uncertainties in the properties of materials used in structural members, as considered in V_{Rt} ;
- (3) uncertainties in the geometric dimensions related to the structural resistance, which is also considered in V_{Rt} .

As considered in Eurocode 2, etc. [8,32,33], the safety factors in a design formula for a resistance can be decomposed with respect to the different types of uncertainty. Since, in design of composite structures, the safety factors are applied to the material strengths, it is considered here that, in equation (2.33), each factor may be regarded as a product

$$\gamma_m = \gamma_{mp} \gamma_{md} \quad (2.42)$$

where,

γ_{mp} is a factor that represents uncertainties of strength in the relevant material, called material factor;

γ_{md} is a factor that represents uncertainties in the theoretical model and the geometric dimensions, called model factor.

Thus, it is obtained from (2.42) that

$$\gamma_a = \gamma_{ma}\gamma_{mda} \quad \gamma_c = \gamma_{mc}\gamma_{mdc} \quad \gamma_s = \gamma_{ms}\gamma_{m ds} \quad \gamma_v = \gamma_{mv}\gamma_{mdv} \quad (2.43)$$

where, γ_{ma} , γ_{mc} , γ_{ms} and γ_{mv} denote the material factors and γ_{mda} , γ_{mdc} , $\gamma_{m ds}$ and γ_{mdv} the model factors.

Since the model factors are introduced here to associate with the uncertainties in the model and the geometric dimensions only, they can be regarded material-independent and, therefore, are taken as a single value, γ_{md} in this study. So, the safety factors presented in (2.43) become

$$\gamma_a = \gamma_{ma}\gamma_{md} \quad \gamma_c = \gamma_{mc}\gamma_{md} \quad \gamma_s = \gamma_{ms}\gamma_{md} \quad \gamma_v = \gamma_{mv}\gamma_{md} \quad (2.44)$$

If applying the material factors only, the material strengths in (2.33) can be first of all altered as

$$f_{y,d} = \frac{f_{yk}}{\gamma_{ma}} \quad f_{c,d} = \frac{f_{ck}}{\gamma_{mc}} \quad f_{s,d} = \frac{f_{sk}}{\gamma_{ms}} \quad P_{R,d} = \frac{P_{Rk}}{\gamma_{mv}} \quad (2.45)$$

Such values, $f_{y,d}$, etc. given by (2.45) are called γ_{mp} -altered strengths here.

Obviously, like the characteristic values of the material strengths, for any specified material factors, the γ_{mp} -altered strengths, $f_{y,d}$, etc. can be related to probabilities $P\{f_y < f_{y,d}\}$, etc., respectively. Furthermore, as the material strengths are assumed to follow log-normal distributions, the γ_{mp} -altered strengths in (2.45), like the characteristic strengths in (2.34) and ((2.36) to (2.38)), can be specified in terms of

$$\begin{cases} f_{y,d} = \bar{f}_y \exp(-k_{ad}\sigma_{\ln f_y} - 0.5\sigma_{\ln f_y}^2) \\ f_{c,d} = \bar{f}_c \exp(-k_{cd}\sigma_{\ln f_c} - 0.5\sigma_{\ln f_c}^2) \\ f_{s,d} = \bar{f}_s \exp(-k_{sd}\sigma_{\ln f_s} - 0.5\sigma_{\ln f_s}^2) \\ P_{R,d} = \bar{P}_R \exp(-k_{vd}\sigma_{\ln P_R} - 0.5\sigma_{\ln P_R}^2) \end{cases} \quad (2.46)$$

where, k_{ad} is a fractile factor corresponding to the probability $P\{f_y < f_{y,d}\}$; similar explanations apply to k_{cd} , k_{sd} and k_{vd} .

According to equations (2.45) and (2.46), the material factors can be expressed as

$$\begin{cases} \gamma_{ma} = \bar{f}_y \exp(-k_{ad}\sigma_{\ln f_y} - 0.5\sigma_{\ln f_y}^2) / f_{yk} \\ \gamma_{mc} = \bar{f}_c \exp(-k_{cd}\sigma_{\ln f_c} - 0.5\sigma_{\ln f_c}^2) / f_{ck} \\ \gamma_{ms} = \bar{f}_s \exp(-k_{sd}\sigma_{\ln f_s} - 0.5\sigma_{\ln f_s}^2) / f_{sk} \\ \gamma_{mv} = \bar{P}_R \exp(-k_{vd}\sigma_{\ln P_R} - 0.5\sigma_{\ln P_R}^2) / f_{Rk} \end{cases} \quad (2.47)$$

or, applying (2.34) and (2.36) to (2.38),

$$\begin{cases} \gamma_{ma} = \exp[(k_{ad} - k_{as})\sigma_{\ln f_y}] \\ \gamma_{mc} = \exp[(k_{cd} - k_{cs})\sigma_{\ln f_c}] \\ \gamma_{ms} = \exp[(k_{sd} - k_{ss})\sigma_{\ln f_s}] \\ \gamma_{mv} = \exp[(k_{vd} - k_{vs})\sigma_{\ln P_R}] \end{cases} \quad (2.48)$$

Normally [33,35,36], for the characteristic (nominal) value of the yield strength of steel, f_{yk} , the fractile-factor k_{as} is taken as 2.0, which corresponds to the probability $P\{f_y < f_{yk}\} = 2.3\%$, while f_{ck} and f_{sk} are related to 5% fractiles and, therefore, $k_{cs} = k_{ss} = 1.64$.

From equation (2.48), it is seen that the material factor for shear connectors, γ_{mv} , is not only related to the parameters k_{vd} and k_{vs} , but also the coefficient of variation of its shear resistance, V_{P_R} , which, as shown in Reference [33,35,36], depends on many factors, such as the type of connectors, the mode of failure, the resistance function adopted, etc. Because of the complicity, this study does not

intend to determine γ_{mv} from (2.48) for general cases.

In composite structures, the most popular shear connectors are the welded headed studs. So, in this study, only this type of shear connectors are considered.

For the welded stud shear connectors, an extensive statistical study of the results of push tests, as well as the safety calibration of the strength formulated in Eurocode 4 [1], has been made [33,35,36]. These works, similar to investigating strength of a material itself, were carried out irrespective of any particular behaviour of the structural members where the shear connectors are used. From such an investigation, Eurocode 4 [1] takes the safety factor for strength of the welded stud shear connectors as $\gamma_v = 1.25$, which should be applied to the characteristic strength as specified in the code [1]. As presented in (2.42), the model factor γ_{md} should be introduced in relation to the behaviours of particular structural members (e.g ultimate plastic bending of composite beams and so on). Since the adoption of $\gamma_v = 1.25$ for P_{Rk} specified in [1] is made on the base independent of the structural resistances related, the value 1.25 may be assumed as the safety factor that does not include γ_{md} (see (2.42) or (2.44)).

Therefore, as discussed in [59], if the strength of the welded stud shear connectors, P_R , and the characteristic value, P_{Rk} , are given in consistency with Eurocode 4 [1], then, for a particular structural resistance (say bending resistance of a composite beam), this study considers that the safety factor γ_v defined in (2.44) can be determined by finding out the model factor γ_{md} and taking

$$\gamma_{mv} = 1.25 \quad (2.49)$$

As presented above, for the material factors γ_{ma} , γ_{mc} and γ_{ms} given in (2.48), k_{as} has been taken as 2.0, and k_{cs} and k_{ss} as 1.64. In order to determine γ_{ma} , γ_{mc} and γ_{ms} , the fractile-factors, k_{ad} , k_{cd} and k_{sd} , are further assumed to have the same value k_{md} , which means that the probabilities $P\{f_y < f_{y,d}\}$, etc. are the same. From (2.44) and (2.48), it is then obtained

$$\frac{\gamma_a}{\gamma_c} = \exp[(k_{md} - 2.00)\sigma_{\ln f_y} - (k_{md} - 1.64)\sigma_{\ln f_c}] \quad (2.50)$$

In Eurocode 4, besides $\gamma_v = 1.25$, γ_a , γ_c and γ_s have been given as 1.10, 1.50 and 1.15, respectively. These values except for $\gamma_c = 1.50$ are to be taken as the objectives of calibration in this study.

As explained in [40,58], for the reliability analysis based on laboratory tests (assumption (1) in Section 2.2.1), the code value γ_c should be regarded as 1.25, rather than 1.50, and the reasons can be presented below.

In the code [1], the factor $\gamma_c (= 1.50)$ “includes about 1.1 for errors in dimensions of cross-sections, particularly in the positions of reinforcing bars, and another 1.1 for variations in the strength of concrete as placed, in excess of those found from laboratory-made test specimens” [40]. Generally, these variations are not relevant to laboratory tests where specimens are carefully fabricated. Therefore, γ_c should be 1.25 ($\approx 1.5/1.1^2$).

Hence, taking the ratio of γ_a to γ_c just as 1.10/1.25, equation (2.50) turns to be

$$\frac{1.10}{1.25} = \exp[(k_{md} - 2.0)\sigma_{\ln f_y} - (k_{md} - 1.64)\sigma_{\ln f_c}] \quad (2.51)$$

Using the coefficients of variation of the design parameters given in the relevant References [31,33,35,36] (see Table B.1 in Appendix B), it can be calculated that

$$\sigma_{\ln f_y} = 0.080 \quad \sigma_{\ln f_c} = 0.149 \quad \sigma_{\ln f_s} = 0.100 \quad (2.52)$$

So, from (2.51) and (2.52), it yields that $k_{md} = 3.07$. This value is quite close to the design fractile-factor $k_d = 3.04$ for resistance, as given in equation (2.32), when a large number of test results are available. Under the condition of $k_{as} = 2.00$ and $k_{cs} = k_{ss} = 1.64$, if it is directly taken that

$$k_{md} = 3.04 \quad (2.53)$$

it can be obtained from equation (2.48) that

$$\begin{cases} \gamma_{\text{ma}} = \exp(1.04\sigma_{\text{ln}f_y}) \\ \gamma_{\text{mc}} = \exp(1.40\sigma_{\text{ln}f_c}) \\ \gamma_{\text{ms}} = \exp(1.40\sigma_{\text{ln}f_s}) \end{cases} \quad (2.54)$$

Substituting (2.52) into (2.54), it yields

$$\gamma_{\text{ma}} = 1.087 \quad \gamma_{\text{mc}} = 1.234 \quad \gamma_{\text{ms}} = 1.150 \quad (2.55)$$

These values are all close to the relevant safety factors proposed in the code [1]. So, if regarding $k_{\text{md}} = 3.04$, it appears that the code values of γ_a , γ_c and γ_s have ratios to one another that are fairly consistent with the assumed coefficients of variation (Table B.1 in Appendix B). Furthermore, according to (2.44), if equation (2.55), as well as (2.49), is used, the reliability underlining the design formula in the code [1] (where $\gamma_a = 1.10$, $\gamma_c = 1.25$, $\gamma_s = 1.15$ and $\gamma_v = 1.25$) can be assessed simply by comparing the calibrated γ_{md} with the value 1.012 ($= 1.10/1.087 \approx 1.25/1.234$).

Therefore, equation (2.54) is chosen in this study to determine the material factors, γ_{ma} , γ_{mc} and γ_{ms} .

Once the material factors are determined, the only unknown for safety factors remains the model factor γ_{md} .

Substituting equation (2.44) into (2.33) and replacing \bar{X}_p in (2.31) with \bar{f}_y , \bar{f}_c , \bar{f}_s , \bar{P}_R and \bar{X}_{p_0} , elimination of r_d from equations (2.33) and (2.31) would give that

$$\begin{aligned} & g_R[f_{yk}/(\gamma_{\text{ma}}\gamma_{\text{md}}), f_{ck}/(\gamma_{\text{mc}}\gamma_{\text{md}}), f_{sk}/(\gamma_{\text{ms}}\gamma_{\text{md}}), P_{Rk}/(\gamma_{\text{mv}}\gamma_{\text{md}}), \bar{X}_{p_0}, \bar{X}_g] \\ & = \bar{b}g_R(\bar{f}_y, \bar{f}_c, \bar{f}_s, \bar{P}_R, \bar{X}_{p_0}, \bar{X}_g) \exp(-k_d\sigma_{\text{ln}r} - 0.5\sigma_{\text{ln}r}^2) \end{aligned} \quad (2.56)$$

Applying (2.49) and (2.54), the model factor γ_{md} can then be found from equation (2.56). When γ_{md} is known, the safety factors, γ_a , γ_c , γ_s and γ_v , can be determined from (2.49), (2.54) and (2.44).

2.3 Failure probability corresponding to given safety factors

Equation (2.16) shows that a fractile-factor for the design resistance can be determined with respect to a specified failure probability P_f , and vice versa. As discussed in Section 2.2.2, the design fractile-factor directly determined from (2.16) (which is taken as 3.04 above), denoted by $k_{d,\infty}$ hereafter, may only be directly applied in equation (2.31), if a large number of test results is available and the acceptable values of coefficients of variation for the basic variables are used; otherwise, the design fractile-factor should be determined from equation (2.32).

In general, it should be considered that the failure probability P_f for the design resistance may have other values, rather than $P_f = 0.12\%$ only. According to the analysis in Section 2.2.2, for any target safety level with a specified P_f , the design fractile-factor k_d should be determined based on the concepts suggested in equation (2.32), i.e.

$$k_d = \frac{k_{d,\infty} V_{rt}^2 + k_b V_\delta^2}{V_r^2} \quad (2.57)$$

where,

the factor $k_{d,\infty}$ is the fractile-factor of the standard normal distribution, determined from the given P_f using equation (2.16);

k_b is the fractile-factor of a non-central t -distribution, determined by the group size n (number of test specimens in the group) and the same P_f at a confidence level of ϵ (ϵ is taken as 0.75 in this study [33]), as shown in Appendix A.

Therefore, the design fractile-factor k_d can be generally regarded as a function of the group size n , the failure probability P_f and the confidence level ϵ imposed on P_f . This function may generally be denoted as

$$k_d = k_d(n, P_f, \epsilon) \quad (2.58)$$

Taking advantage of equations (2.57) or (2.58), an inverse problem in reliability analysis for structural resistance may then be investigated, i.e. to assess the safety levels underlying the design formulae of structural resistances based on given safety factors.

In design of composite structural members, for a design formula of resistance related to yield strength of structural steel, compression strength of concrete, yield strength of reinforcement and strength of the welded stud shear connectors, the code values of the safety factors [1], as discussed above, are in this study regarded as

$$\gamma_a = 1.10 \quad \gamma_c = 1.25 \quad \gamma_s = 1.15 \quad \gamma_v = 1.25 \quad (2.59)$$

Therefore, for resistances of composite structures designed by a formula in form of (2.33), if

- V_δ and \bar{b} can be estimated from tests results of a group of n specimens;
- V_{r_t} has been obtained;

then, using equation (2.56), the design fractile-factor k_d can be inversely found from such known safety factors as given in (2.59). Subsequently, with respect to a specified confidence level ϵ , say $\epsilon = 0.75$ here, the failure probability P_f can be found from equation (2.57) or (2.58). Thus, based on the calculated failure probability P_f , one can judge the reliability underlying a design formula, denoted by (2.33), with the proposed safety factors.

Since, as shown above, equation (2.57) or (2.58) is usually linked with both the standard normal distribution and a non-central t -distribution, these equations are strongly nonlinear in relation to the probability P_f , so some numerical techniques are needed for solving P_f , which will be presented in the next chapter.

2.4 Summary of the reliability theory

A general theory is developed in this chapter to analyse the reliability in design resistances of composite structural members. This analysis is related to the relevant experimental results for the structural resistances.

For a structural resistance r , it is considered that the populations of the structural members represented by the relevant test specimens can be classified into one group, if the theoretical predictions of r , r_t , for these specimens are given by the same resistance function. Within the same group, the random variable r/r_t for all the populations is assumed to follow the same probability distribution.

Therefore, applying the basic assumptions made in Section 2.2.1 to a test group, the correction parameter from test results, \bar{b} and V_δ , can be obtained from equations (2.25) and (2.26), while the correlation coefficient between r and r_t , ρ , is found from (2.20).

The theoretical model is regarded to be sufficiently correlated to the reality if ρ appears not smaller than 0.9.

Knowing \bar{b} and V_δ , further reliability analysis of the resistance can be carried out for the structural member populations covered by the test group. For a population considered, equation (2.28) is developed to calculate the coefficient of variation of r_t , V_{r_t} , while (2.24) and (2.29) to V_r (total coefficient of variation of r) and $\sigma_{\ln r}$, respectively. As a result, the design value of the resistance, r_d , for such a population of structural members can then be determined from equation (2.31), where, corresponding to the specified safety target [33] (i.e. the failure probability, $P_f = P(r < r_d)$, is set as 0.0012), the design fractile-factor k_d is given by equation (2.32).

To calibrate the partial safety factors for the resistance in design, the design resistance r_d from equation (2.31) should be used, and a safety factor applied to a material strength can be splitted into two components: a material factor and a model factor, as shown in equation (2.42).

The design situations where f_y , f_c , f_s and P_R may be involved are particularly

studied. In the study, the shear connectors are considered as the welded stud connectors.

For f_y , f_c , f_s and P_R , the partial safety factors in design, γ_a , γ_c , γ_s and γ_v , are considered to be applied to the characteristic values, f_{yk} , f_{ck} , f_{sk} and P_{Rk} , respectively. For P_R , the value of P_{Rk} will be determined in Section 3.2.2, while the material factor γ_{mv} has been assigned 1.25 (equation (2.49)). For f_y , f_c and f_s , their characteristic values are given in equations (2.34), (2.36) and (2.37), respectively, while the material factors, γ_{ma} , γ_{mc} and γ_{ms} , in (2.54). In the current stage, the fractile-factors for f_{ck} and f_{sk} are taken as $k_{cs} = k_{ss} = 1.64$, and for f_{yk} , $k_{as} = 2.00$.

Accordingly, the model factor γ_{md} can be found from equation (2.56), and, in turn, equation (2.44) is used to determine the partial safety factors, γ_a , γ_c , γ_s and γ_v , for the population of structural member under consideration.

The values of γ_a , γ_c , γ_s and γ_v adopted in Eurocode 4 [1] are regarded by the analysis as those shown in equation (2.59).

According to the theory developed in this chapter, the failure probability P_f underlying a design model with given partial safety factors for a resistance can be inversely found out. To do so, a nonlinear equation as denoted by (2.58) needs to be solved, which, as shown in Appendix A, is related to a non-central t -distribution and the standard normal distribution. Section 3.3 will present a numerical technique (iteration) to solve this problem.

Chapter 3

Investigation of reliability in design bending resistances of composite beams

A reliability theory for resistances in composite structures has been presented in the last chapter. The main purpose of developing such a theory in this study, as implied in Section 1.1, is to calibrate the partial safety factors for design resistance of composite beams in bending within the scope of Eurocode 4 [1].

The bending resistances of composite beams may be considerably affected by buckling of the steel beams, which would prevent development of the plastic moment resistances in the beams. The buckling behaviour of beams is not considered in the current reliability analysis for composite beams in bending. So this study is to check the safety in design of the ultimate plastic bending resistances for beams with compact sections, i.e. beams in class 1 or 2 [1].

It should be also noted here that the beams to be analysed are those with uncased steel beams (so the composite cross-section can be typically shown in Figure 3.1, etc.), and, in theory, the study allows the shapes of the steel sections to be symmetric or asymmetric (i.e. the top flange and the bottom flange may not have the same dimensions). Furthermore, the effect of reinforcement or profiled

sheeting on the sagging bending is ignored in the following studies, and the theory developed is considered to be applicable to the beams with either normal weight concrete or light-weight concrete.

This chapter presents the particular principles and techniques for analysis of the beams. The calibration results and the relevant discussions are given in the next chapter.

3.1 Applications of test results in analysis

3.1.1 Selection of test results

According to the theory in Section 2.2, the determination of design bending resistances for composite beams should be related to the test corrections, \bar{b} and V_δ , and these parameters should be estimated, as shown by equations (2.25) and (2.26), from experimental results that give the resistances concerned.

There is an extensive literature of experimental research on composite beams, but few of these researches were directly related to the problem of plastic bending resistance. This may be because plastic bending of the beams has been regarded as a solved problem for several decades. Based on a wide search, a limited number of test results was found to be sufficiently reliable and suitable for this safety calibration. The reported test results in the following situations are not used in this study:

- (1) the failures were not mainly caused by plastic bending or, for beams with partial shear connection, by shearing of shear connection, but were significantly affected by other factors, such as buckling, high vertical shear, longitudinal splitting, etc. (in these cases, the experimental results would considerably differ from the ultimate plastic bending resistances);
- (2) the measured values of f_y , f_c and f_s are not all available, (as implied by basic assumption (3) in Section 2.2.1, it is important to know the measured

material strengths in a test specimen when these material strengths are used as the basic variables in the resistance functions);

- (3) abnormal conditions occurred in the specimens (e.g, concrete was not cured properly);
- (4) the design of the test specimens violated the detailing rules of Eurocode 4 [1] (as indicated above, this calibration is to be made particularly for the designs following Eurocode 4 in all aspects);
- (5) for beams with partial shear connections, the shear connectors are not headed welded stud connectors (as considered in Section 2.2.3, only the shear connection of headed welded studs are analyzed in this study);
- (6) the reported data were incomplete or suspect, e.g. the measured resistance appeared exceptionally low (say less than 90% of the predicted value), and no information about failure mode was given.

For composite beams with full shear connection, the test results of sagging bending resistance are collected from [41-48], while results in hogging bending are from [42,44,48-50]. From the collected test data, it is found that plastic sagging bending of the specimens mostly occurred with the neutral axis within the concrete slabs, while hogging bending was with the neutral axis within the steel webs.

According to Eurocode 4 [1], when composite beams have partial shear connection, the shear connectors should be classified as “ductile” or “non-ductile” depending on the degree of shear connection, as explained later. For beams with partial shear connection, the test results are obtained from References [51-57], among which the results for beams with “ductile” partial shear connection are collected from [51-53]. All these reported tests were carried out for sagging bending. In Eurocode 4 [1], there are no provisions for partial shear connection in hogging bending, so, for beams with partial shear connection, only sagging bending is studied here.

Most of the references only reported the tests done by the authors (first hand test data for the authors). In Reference [51], besides their own tests, the authors also gave a summary of 58 other tests, most of which were taken from unpublished reports, and these reports were rarely accessible. To make the size of test groups as large as possible, it is decided [59] that these secondary test data are also used for the reliability analysis.

Details of the selected test specimens and the results will be given in the next chapter.

3.1.2 Groups of tests

As discussed in Section 2.2.1, a set of beam specimens that have the same resistance function may be defined as one group, which can represent all the beam populations represented by the beam specimens. With the available test results, analysis of the reliability in bending resistances may be made for the beam populations represented by the following four groups of specimens:

1. **Group A:** sagging bending with full shear connection and the plastic neutral axis in the concrete slab.
2. **Group B:** hogging bending with full shear connection and the plastic neutral axis in the steel web.
3. **Group C:** sagging bending with partial shear connection, where the connectors are “ductile” (as defined by Eurocode 4 [1] and described in Section 3.2.3) and made of headed welded studs.
4. **Group D:** sagging bending with partial shear connection, where the connector are “non-ductile” (as defined in Eurocode 4 [1] and described in Section 3.2.4) and made of headed welded studs.

According to Eurocode 4, the sagging bending resistances of beams with partial shear connection can be either predicted by the equilibrium method (when

shear connectors are “ductile”), or by linear interpolation techniques (when shear connectors are “ductile” or “non-ductile”), as explained in Sections 3.2.2.

According to the equilibrium model [16,59], there are two plastic neutral axes: one is always in the concrete slab and the other, called the second neutral axis, is normally in either the top steel flange or the steel web. For different positions of the second neutral axis, the forms of resistance function of the beams are not fully consistent. However, the precise position of this neutral axis has no influence on the behaviour of the beam. When the interpolation concepts are used, the bending resistances calculated by assuming full shear connection are used. This also results in differences in the resistance function, however, the bending properties subjected to full shear connection are not directly relevant to the behaviour of the beams.

Therefore, for beams with partial shear connections, the difference in resistance function is assumed not to influence the homogeneity of statistical properties of r/r_t defined in (2.19), and groups C and D are as defined above.

3.1.3 Using of non-measured basic variables in test specimens

In many reported beam tests, the geometric properties were not presented with the measured values. It is proposed in References [33,34] that, when some basic variables are not measured, in finding V_δ from equation (2.26), r_{ti} can be calculated with the mean values or intended values of the non-measured variables, but, to determine the design resistance for a population of structural members from equation (2.31) or (2.33), V_δ should be increased to V_D , such that

$$V_D = \sqrt{V_\delta^2 + \frac{1}{g_R^2(\underline{X})} \left(\frac{n-1}{n-2} \right) \sum_{i=1}^{J'} (\bar{X}_i V_{X_i})^2 \left(\frac{\partial g_R}{\partial X_i} \Big|_{X_i=\bar{X}_i} \right)^2} \quad (3.1)$$

where,

X_i ($i = 1, \dots, J'$) are the unmeasured basic variables;

\bar{X}_i and V_{X_i} are the mean value and coefficient of variation of X_i , respectively;

n is the group size;

$g_R(\bar{X})$ is the first-order approximation of the theoretical resistance of the population (see equation (2.23)).

For bending resistances of composite beams represented by the groups defined above, as presented in the next chapter, use of the theoretical models recommended in Eurocode 4 [1] result in high coefficients of correlation between the real resistance r (with the experimental observation r_{ei} from specimen i) and the theoretical resistance r_t (with the calculated value r_{ti} for finding out V_δ , etc.), i.e. $\rho \geq 0.96$ (ρ is found from equation (2.20)), which suggests that the models chosen reflect the reality well. For specimen i , any deviation of an unmeasured geometric dimension X_{gu} from the mean value \bar{X}_{gu} would change the experimental observation r_{ei} of r , rather than r_{ti} from \bar{X}_{gu} . Therefore, for a theoretical model which is highly correlated to the reality (say $\rho \geq 0.90$ [33]), it can be considered that, for a test group of n specimens, values of r_{si}/r_{ti} ($i = 1, \dots, n$) based on measured geometric dimensions would have less scatter than those based on the mean dimensions (intended dimensions).

So, for bending resistance of composite beams where the good models are used, V_δ calculated based on basic assumption (3) (see Section 2.2.1) for a group of tests would actually cover more scatter than that based on all measured basic variables. Thus, the increase of V_δ given in (3.1) is considered over-conservative for analysis of the bending resistances in composite beams, and is not used in this safety calibration.

However, as indicated in [59]: “it is likely that the variation of geometric variables in the test specimens is less than it would be in pan-European practice”, so it is considered that the variation of geometric variables should still be in all cases taken into account when determining V_{r_t} from equation (2.28).

To sum up, if the measured values of the geometric properties are unknown for beam specimens in the groups defined above, the mean values or intended values will be used to calculate r_{ti} (the theoretical value of the resistance in beam specimen i , as defined for equations (2.20), (2.25) and (2.26)) for obtaining V_δ . This V_δ , rather than V_D in (3.1), will be used in (2.33) etc. to make further reliability analyses.

3.2 Calibration of partial safety factors for composite beams

According to the theory presented in Section 2.2, V_δ and \bar{b} can be obtained from the test data for the beams represented by the groups defined above, therefore, the partial safety factors applied to the design bending resistances of the composite beams can also be determined, as explained below.

3.2.1 Full shear connection (Groups A and B)

The theoretical models of Eurocode 4 [1] for plastic bending resistance of beams in groups A and B are well established [61].

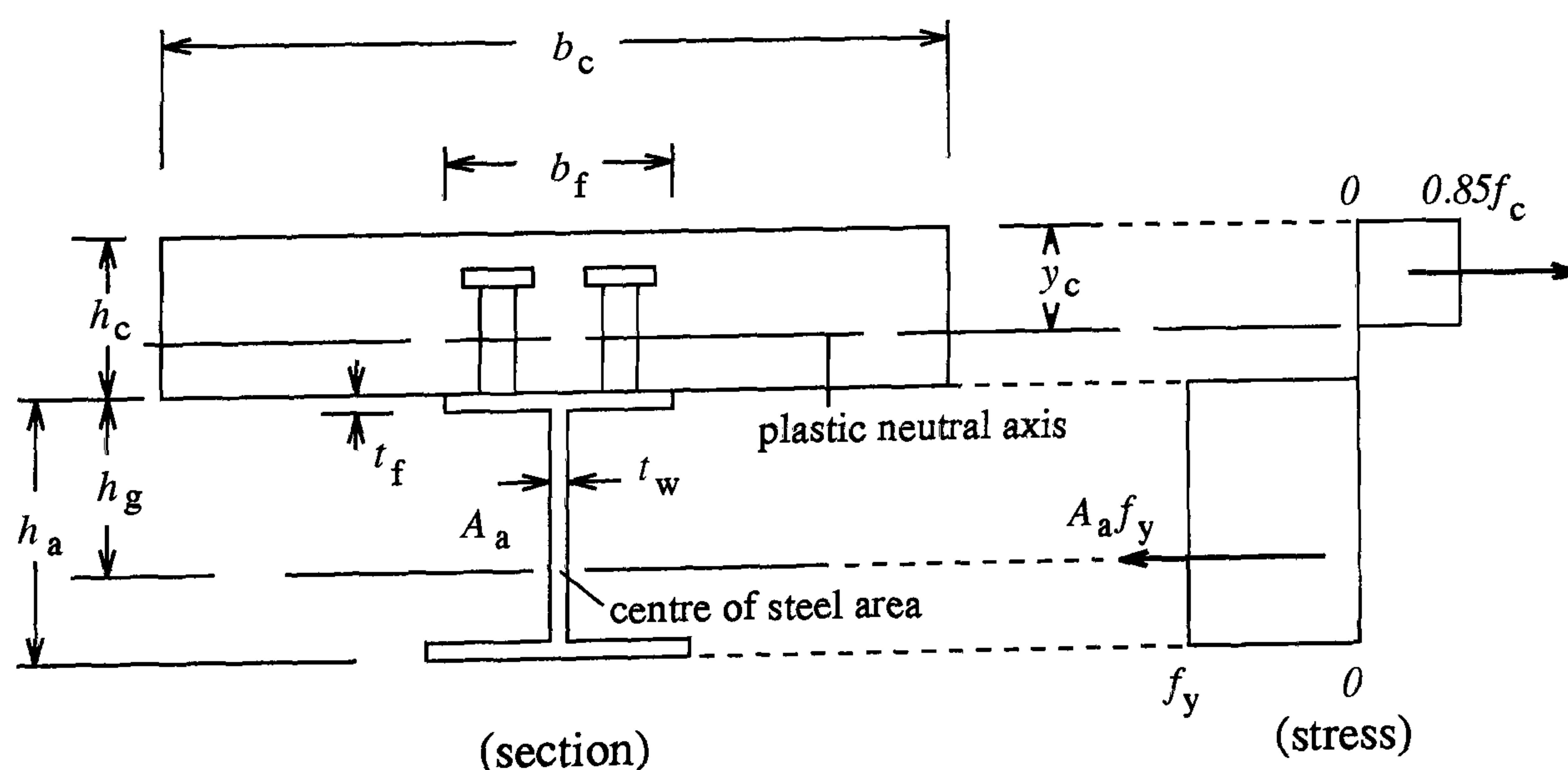


Figure 3.1: Sagging bending of composite beams with full shear connection, plastic neutral axis in concrete slab

For plastic sagging bending with full shear connection, the effect of longitudinal reinforcement can be ignored and, therefore, the resistance function is given as follows [1,61]:

$$r_t = g_R(\underline{X}_p, \underline{X}_g) = A_a f_y (h_g + h_c - \frac{A_a f_y}{1.7 f_c b_c}) \quad (3.2)$$

where, \underline{X}_p and \underline{X}_g specify the basic variables as geometric properties and material properties, respectively, and, as shown in Figure 3.1,

- f_y yield strength of structural steel;
- f_c compression (cylinder) strength of concrete;
- A_a area of steel section;
- h_g distance between the surface of top flange and the centre of steel area;
- h_c overall height of concrete slab;
- b_c breath of concrete slab.

Thus, the coefficient of variation of r_t , V_{r_t} , can be derived from equation (2.28), and is:

$$V_{r_t}^2 = \frac{\bar{r}_1^2}{g_R^2(\bar{X}_p, \bar{X}_g)} [(\bar{r}_2 + \bar{r}_3 + 2\bar{r}_1\bar{r}_4)^2 V_{r_1}^2 + \bar{r}_2^2 V_{r_2}^2 + \bar{r}_3^2 V_{r_3}^2 + (\bar{r}_1\bar{r}_4)^2 V_{r_4}^2] \quad (3.3)$$

where, $g_R(\bar{X}_p, \bar{X}_g)$ is the mean theoretical resistance \bar{r}_t (the first-order approximation [37]):

$$g_R(\bar{X}_p, \bar{X}_g) = \bar{r}_t = \bar{r}_1(\bar{r}_2 + \bar{r}_3 + \bar{r}_1\bar{r}_4) \quad (3.4)$$

and

$$\left. \begin{aligned} \bar{r}_1 &= \bar{A}_a \bar{f}_y & V_{r_1} &= \sqrt{V_{A_a}^2 + V_{f_y}^2} \\ \bar{r}_2 &= \bar{h}_g & V_{r_2} &= V_{h_g} \\ \bar{r}_3 &= \bar{h}_c & V_{r_3} &= V_{h_c} \\ \bar{r}_4 &= -1/(1.7 \bar{f}_c \bar{b}_c) & V_{r_4} &= \sqrt{V_{b_c}^2 + V_{f_c}^2} \end{aligned} \right\} \quad (3.5)$$

From function (3.2), two distinct safety factors, γ_c (for f_c) and γ_a (for f_y), are

needed for the design resistance in plastic sagging bending, so, using equation (2.44), the design format (2.33) can be specified in this case as

$$r_d = \frac{1}{\gamma_{md}} A_a \frac{f_{yk}}{\gamma_{ma}} \left[h_g + h_c - \frac{A_a (f_{yk}/\gamma_{ma})}{1.7 (f_{ck}/\gamma_{mc}) b_c} \right] \quad (3.6)$$

Hence, according to equation (2.56), the model factor γ_{md} for theoretical model (3.2) can be derived as

$$\gamma_{md} = \frac{\bar{A}_a (f_{yk}/\gamma_{ma}) \{ \bar{h}_g + \bar{h}_c - \bar{A}_a (f_{yk}/\gamma_{ma}) / [1.7 (f_{ck}/\gamma_{mc}) \bar{b}_c] \}}{\bar{b} g_R(\bar{X}_p, \bar{X}_g) \exp(-k_d \sigma_{lnr} - 0.5 \sigma_{lnr}^2)} \quad (3.7)$$

where, $g_R(\bar{X}_p, \bar{X}_g)$ is given by (3.4); σ_{lnr} is determined from V_{rt} and V_δ (see equations (2.24) and (2.29)).

As shown in Section 2.2.3, f_{yk} and f_{ck} can be found from (2.34) and (2.36) (with $k_{as} = 2.00$ and $k_{cs} = 1.64$), respectively, and the material factors from (2.54). Therefore, γ_{md} is obtained by substituting equation (2.54) into (3.7), and γ_a and γ_c for beams represented by group A are then determined from (2.44).

It is seen from (3.6) that, for the beams in group A, the design resistance is proportional to the factor $1/\gamma_{md}$, which leads to the simple expression of γ_{md} given in equation (3.7). In fact, it can be shown that, for beams in groups B and C, the similar linear relationship between r_d and $1/\gamma_{md}$ also exists. Therefore, in most situations studied here, the model factor γ_{md} can be explicitly expressed from equation (2.56) as

$$\gamma_{md} = \frac{g_R(f_{yk}/\gamma_{ma}, f_{ck}/\gamma_{mc}, f_{sk}/\gamma_{ms}, P_{Rk}/\gamma_{mv}, \bar{X}_{p0}, \bar{X}_g)}{\bar{b} g_R(\bar{f}_y, \bar{f}_c, \bar{f}_s, \bar{P}_R, \bar{X}_{p0}, \bar{X}_g) \exp(-k_d \sigma_{lnr} - 0.5 \sigma_{lnr}^2)} \quad (3.8)$$

For plastic hogging bending of composite beams with full shear connection, no concrete (tensile) strength is included in prediction of the bending resistance [1,61], so only the yield strengths of structural steel and reinforcement, f_y and f_s , are involved in the resistance function. Therefore, the design resistance of beams in group B only employs γ_s (for f_s) and γ_a (for f_y).

The resistance function $g_R(\underline{X})$ and coefficient of variation, V_{rt} , of beams in

group B are given in Appendix C.

As presented in Section 2.2.3, the characteristic value of f_s is given by equation (2.37) with $k_{ss} = 1.64$ and the material factor γ_{ms} is obtained from (2.54).

The procedure for founding the safety factors (i.e. γ_s and γ_a) for beams in group B is same as that for group A, and is not repeated here.

3.2.2 Ductile partial shear connection (Group C)

In Eurocode 4 [1], where the steel sections are of equal flanges, the shear connectors used in composite beams are defined as “ductile” if the degree of shear connection, N/N_f , satisfies

$$N/N_f \geq \begin{cases} 0.4 & \text{when } L \leq 5 \\ N/N_f \geq 0.25 + 0.03L & \text{when } 5 \leq L \leq 25 \\ N/N_f \geq 1.0 & \text{when } L \geq 25 \end{cases} \quad (3.9)$$

where, L is beam span in metres, N is the number of shear connectors provided in the shear span, and N_f is the number of shear connectors required in the shear span for full shear connection, which can be determined as

$$N_f = \min\{0.85(h_c - h_p)b_c f_c, A_a f_y\} / P_R \quad (3.10)$$

where, P_R is the strength of a shear connector (see Section 2.2.3); the other notations are defined in Figure 3.2.

In this study, parameters L and N are regarded as determinate.

According to the Eurocode 4 [1], strength function P_R , for a headed welded stud connector is given as

$$P_R = 0.8k f_{ut} (\pi d^2 / 4) \quad (3.11)$$

or

$$P_R = 0.29\alpha k d^2 \sqrt{f_c E_c} \quad (3.12)$$

whichever is smaller, where

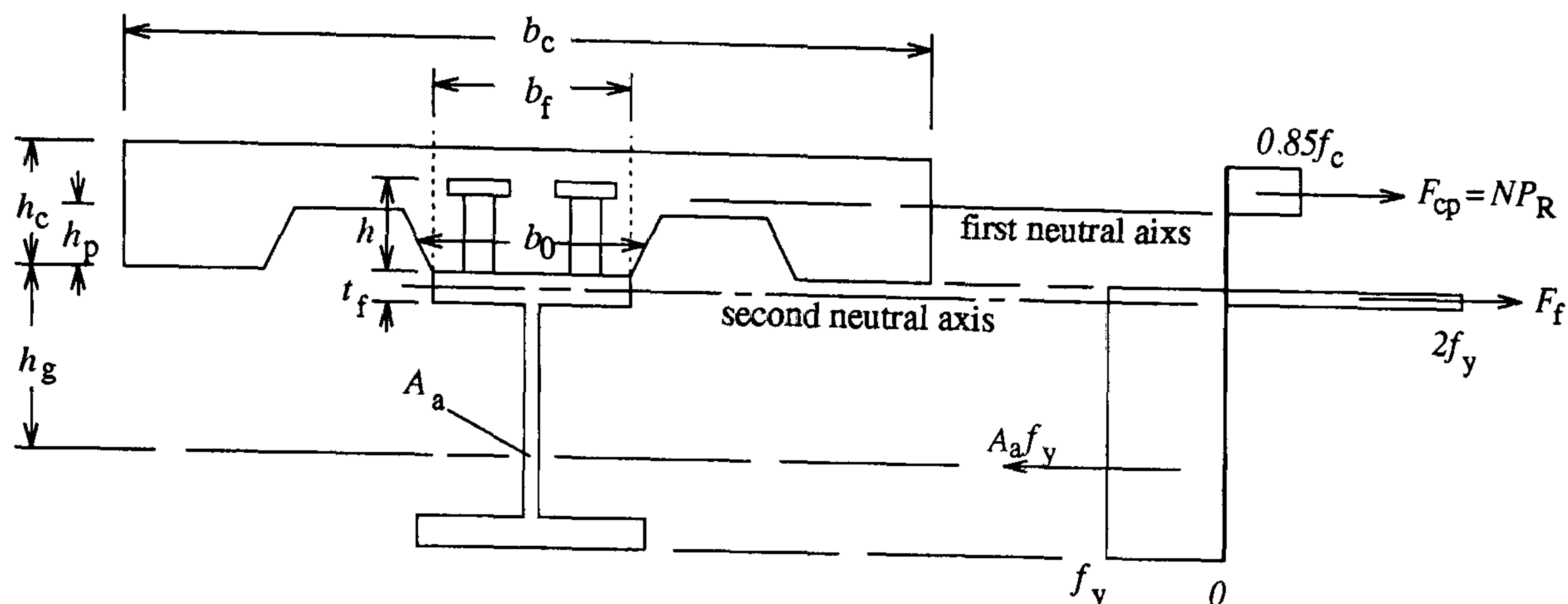


Figure 3.2: Sagging bending of composite beams with partial partial shear connection, second neutral axis in the steel top flange

$$\alpha = \begin{cases} 0.2(h/d + 1) & \text{if } 3 \leq h/d \leq 4 \\ 1 & \text{if } h/d > 4 \end{cases} \quad (3.13)$$

and

f_{ut} is the ultimate tensile strength of a headed stud;

E_c is Young's modulus of concrete;

f_c is the cylinder strength of concrete;

d is the diameter of shank of the stud;

h is the overall height of the stud;

k is the reduction factor for the influence of the ribs of profiled sheeting (in any), as determined below:

for sheeting with ribs parallel to the beam,

$$k = 0.6(b_0/h_p)[(h/h_p) - 1] \leq 1.0 \quad (3.14)$$

for sheeting with ribs transverse to the beam,

$$k = 0.7N_r^{-0.5}(b_0/h_p)[(h/h_p) - 1] \leq 1.0 \quad (3.15)$$

In equations (3.14) and (3.15), N_r stands for the number of stud connectors in one rib, not to exceed two in computations, and the other symbols are defined

in Figure 3.2.

For all the test specimens collected [51-57] for this study, the calculation showed that P_R is always determined by equation (3.12), so the reliability analysis to be carried out is based on equation (3.12), rather than (3.11).

It can be inferred that, in case of the lower P_R being determined from (3.11), use of equation (3.12) would lead to higher theoretical resistance and, therefore, lower \bar{b} (see equation (2.25)); thus, under the condition of little change in V_δ , a conservative (higher) value of γ_{md} (equation (3.8)) would be obtained.

According to the design code [1], the plastic bending resistance of a composite beam with ductile partial shear connection may be predicted in two alternative ways. As shown in Figure 3.3, one of these theoretical models is developed from the equilibrium conditions and can be characterized by curve ABC, while the other method is a conservative simplification: “linear interpolation”, as shown by straight line AC.

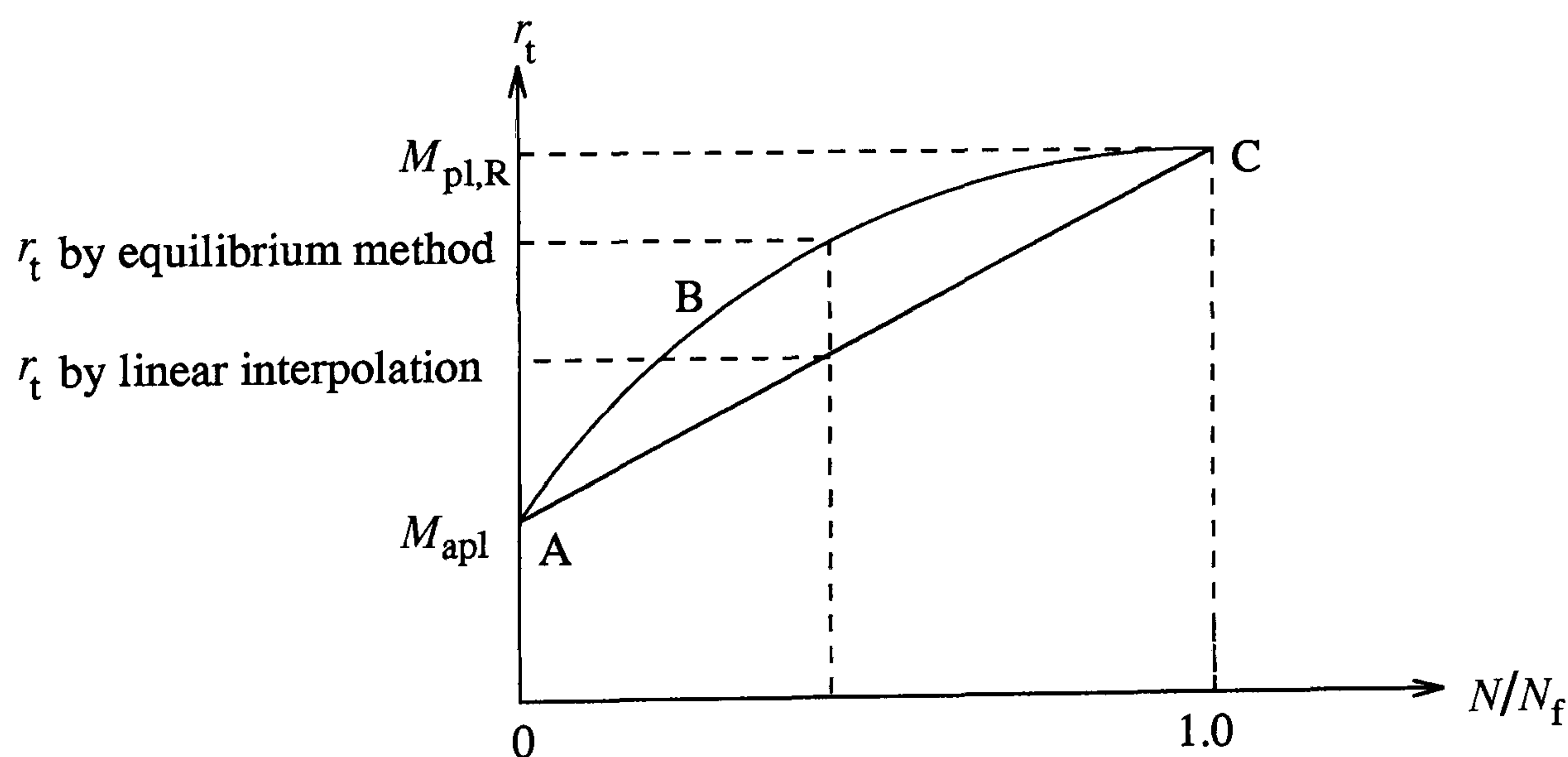


Figure 3.3: Theoretical models for plastic bending resistances of composite beams with ductile partial connection

In Figure 3.3, M_{apl} is the plastic bending resistance of steel beam alone, and $M_{pl,R}$ is the plastic bending resistance of the beam with full shear connection.

The resistance functions from these two models are given in Appendix C.

As implied by equations (3.12) to (3.15), in a resistance function for beams with partial shear connection, the reduction factors, α and k , may be involved.

According to (3.13) to (3.15), α and k are only applied in the equations when beams are built with profiled sheeting, or when short stud connectors (i.e. $h/d < 4$) are used. Normally, the influence on the theoretical resistances from the variation of these reduction factors, if any, is negligible, so, for simplicity, α and k are directly assumed as deterministic parameters in the analysis.

To find P_R from equation (3.12), one needs to know the concrete strength, f_c , as well as the Young's modulus, E_c . As discussed in Section 3.1.1, the results of beam tests are not used for calibration if no measured value of f_c for the specimen is available. In some reported tests, the measured material strengths of the specimens are available, but Young's modulus of concrete was not given. According to the relationship from Eurocodes 2 and 4 [1,4], the mean value of E_c is related to the mean value of f_c as follows,

$$\bar{E}_c = 9500 \bar{f}_c^{\frac{1}{3}} \left(\frac{W_c}{2400} \right)^2 \quad (3.16)$$

where \bar{E}_c and \bar{f}_c are in units of N/mm², and W_c is the density of concrete, in kg/m³ units, which is assumed as a determinate parameter in the analysis.

In this study, it is further considered that the actual value of E_c for a test specimen may be estimated from formula (3.16), with \bar{f}_c replaced by the measured value of f_c . So, when the Young's modulus of concrete is unavailable for a test specimen, this estimation is used to calculate the theoretical resistance for finding \bar{b} and V_δ . This causes an error in the results. Fortunately, the effect of variation of E_c on the theoretical resistance appears to be quite small; with respect to the coefficients of variation in Appendix B, the variance of E_c only causes the theoretical resistance r_t to vary about 1% to 1.5%.

Another problem from the involvement of Young's modulus E_c in the analysis is that, as is well known, this variable is correlated to the strength f_c to some extent. However, no applicable information for such a correlation has been found so far. According to basic assumption (6) in Section 2.2.1, the random variables E_c and f_c are still assumed to be uncorrelated in the analysis. In fact, when f_c and

E_c are considered as fully correlated, i.e. the correlation coefficient, as denoted $\rho_{X_i X_j}$ in equation (2.27), for f_c and E_c becomes 1 instead of 0, the calculation shows that, compared with the analysis based on uncorrelated E_c and f_c , the model factors γ_{md} can typically increased by about 1.5%. Since, the reality is that E_c and f_c is only partly correlated at most, it is concluded that the error in assuming no correlation between E_c and f_c is only of the order of 1%, which is obviously acceptable.

For bending resistances of beams with ductile partial shear connection, the safety calibration is needed for each of two theoretical models shown in Figure 3.3, equilibrium method and linear interpolation. According to the resistance functions developed from the two models, the coefficients of variation, V_{r_i} , can be derived correspondingly, and are listed in Appendix C.

With respect to the relevant test results, both the equilibrium method and linear interpolation are applied to the test specimens, so that the test corrections, \bar{b} and V_δ can be obtained for each of these theoretical models. Then, the partial safety factors (i.e. γ_a , γ_c and γ_v) can be determined in the same way as for the beams in groups A and B.

As presented above, the model factor γ_{md} for beams with ductile partial shear connection (beams in group C) can be found out in closed form (3.8). Here, in determining γ_{md} , the strength of reinforcement f_s need not be considered; f_{yk} , f_{ck} , γ_{ma} and γ_{mc} are same as those used in beams for group A. According to the discussion in Section 2.2.3, for the characteristic strength P_{Rk} specified in Eurocode 4 [1], the material factor γ_{mv} to strength of shear connection is directly taken as 1.25.

According to the code [1], when the strength of shear connectors are dominated by the concrete strength, i.e, determined by equation (3.12), the characteristic strength P_{Rk} is given by the same equation, but with E_c replaced by the mean value \bar{E}_c and f_c with f_{ck} .

Once the model factor γ_{md} is known, the partial safety factors for design

bending resistances of beams in group C can be easily determined from equation (2.44).

3.2.3 Non-ductile shear connection (Group D)

As explained above, the shear connectors used in a beam are regarded in Eurocode 4 as “ductile” when the degree of shear connection for the beam does not violate condition (3.9), otherwise, the shear connectors are classified as “non-ductile”.

For “non-ductile” connectors, the theoretical bending resistance of such a beam, r_t , is related to the longitudinal force provided by the shear connectors by

$$\begin{cases} F_c \geq F_{el}(r_t - M_{a,S}) / (M_{el,R} - M_{a,S}) & (r_t < M_{el,R}) \\ F_c \geq (F_{cf} - F_{el})(r_t - M_{el,R}) / (M_{pl,R} - M_{el,R}) + F_{el} & (M_{el,R} \leq r_t \leq M_{pl,R}) \end{cases} \quad (3.17)$$

where

$M_{el,R}$ is the ultimate elastic bending moment (resistance) of the composite section;

F_{el} is the concrete force at $M_{el,R}$;

$M_{a,S}$ is the bending moment acting on the steel beam due to actions on the steelwork alone, before composite action becomes effective;

$M_{pl,R}$ is the ultimate plastic bending moment (resistance) of the composite section with full shear connection;

F_{cf} is the concrete force at $M_{pl,R}$;

F_c is the longitudinal shear resistance provided by shear connection in the shear span.

As the beams with “ductile partial shear connection” (see Figure 3.2 and C.5), the longitudinal shear resistance F_c is determined by the strength of the shear connectors, P_R , and the number of connectors used in the shear span, N :

$$F_c = NP_R = \frac{N}{N_f}(N_f P_R) \quad (3.18)$$

where P_R for this study is found from equation (3.12).

In calculation, the inequality signs in (3.17) can be replaced by equality signs, so, from (3.17), the theoretical resistance for composite beams with non-ductile partial shear connection is in general written

$$r_t = \begin{cases} (M_{el,R} - M_{a,S})(F_c/F_{el}) + M_{a,S} & (F_c < F_{el}) \\ (M_{pl,R} - M_{el,R})(F_c - F_{el})/(F_{cf} - F_{el}) + M_{el,R} & (F_{el} \leq F_c \leq F_{cf}) \end{cases} \quad (3.19)$$

To generate above resistance functions, besides Young's modulus of concrete, E_c , the modulus of steel, E_a , needs to be known as well. Compared with E_c , even fewer test reports gave the results of measuring E_a . When E_a is not available for the specimens, the analysis simply takes E_a as 210kN/mm^2 , as the effect of variation in E_a , like E_c , is small.

In applying equation (3.17) or (3.19), the design code [1] requires that the construction procedure needs to be taken into account, so that two situations should be distinguished in predicting the resistances: propped construction and unpropped construction.

When a beam is unpropped during construction, the construction load causes a bending moment $M_{a,S}$ in the steel beam alone, in other words, $M_{a,S} \neq 0$. According to the code [1], the elastic bending resistance $M_{el,R}$ should then be determined from

$$M_{el,R} = \frac{f_{ya}}{f_{ca} + f_a}(M_c + M_{a,S}) \quad (3.20)$$

where,

M_c is the bending moment on the composite section determined by elastic theory and assuming the compressive force in concrete to be F_c ;

f_a is the maximum stress in the steel beam at $M_{a,S}$;

f_{ca} is the maximum stress in the steel beam at M_c ;

f_{ya} is the maximum stress in steel beam at $M_{el,R}$ determined by taking the limiting bending stresses as f_y in the steel beam and $0.85f_c$ in concrete;

As the elastic bending resistance $M_{el,R}$ for unpropped construction includes the effect of the construction load, $M_{a,S}$, and this is only related to the steel beam, it is considered that the compressive force F_{el} in the concrete slab is not determined from $M_{el,R}$ by means of general elastic formula; instead, based on the design code [1], this study takes F_{el} as

$$F_{el} = \frac{f_{ya}}{f_{ca} + f_a} F_c \quad (3.21)$$

When propped construction is used, the steel beam during construction would carry negligible load, so it can be assumed that $M_{a,S} = 0$ and (therefore) $f_a = 0$. Consequently, as implied by equations (3.20) and (3.21), determination of $M_{el,R}$ and F_{el} for beams propped during construction becomes normal as usual.

The resistance functions (3.19) for propped construction and unpropped construction can be described by Figure 3.4.

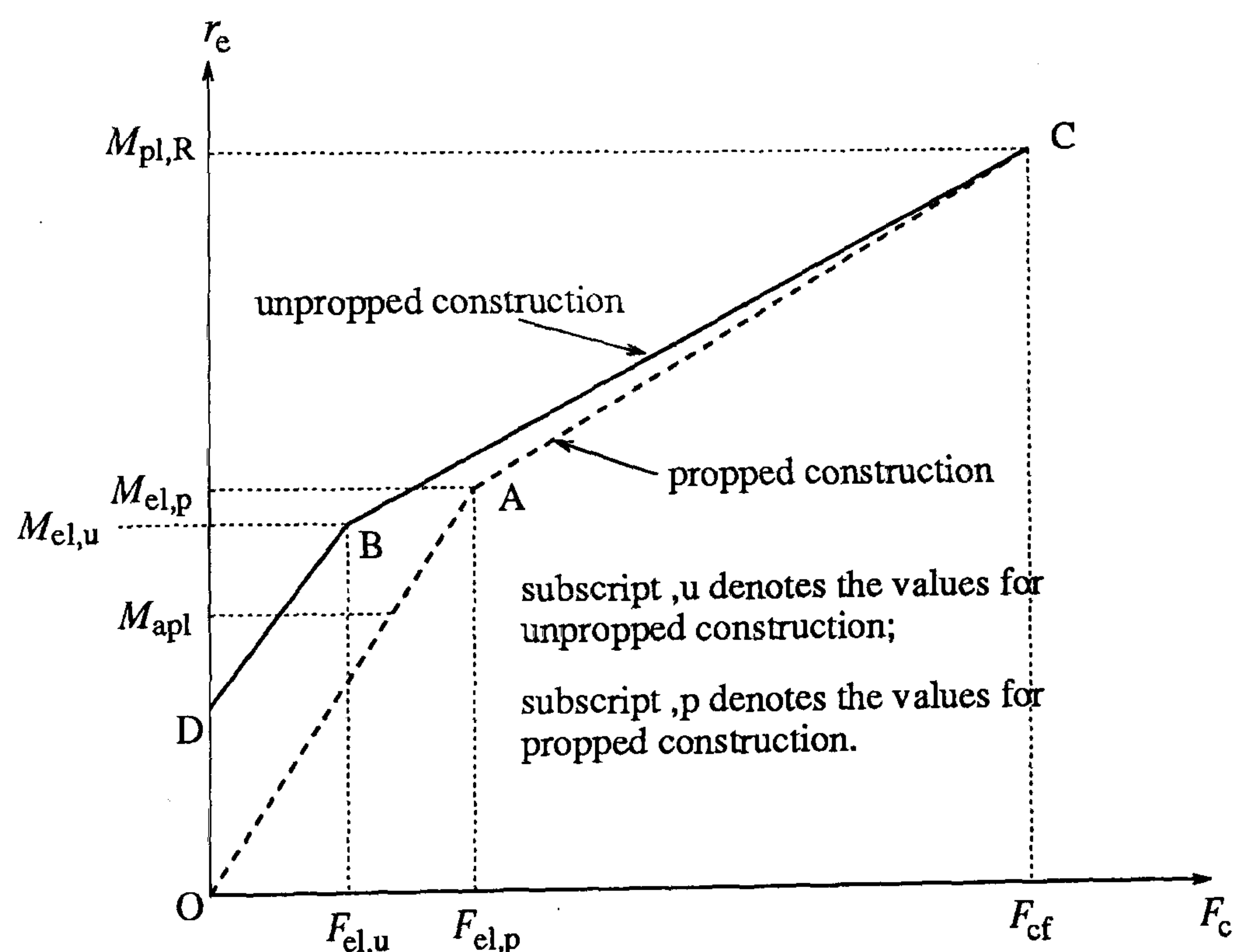


Figure 3.4: Theoretical models for plastic bending resistances of composite beams with non-ductile partial connection

If the beams are constructed unpropped, the steel beams could be subjected to various kinds of construction loads, which can lead to an over-complicated

situation for calculating $M_{a,s}$ and f_a . Nevertheless, it can be recognized that, normally, the construction load is dominated by the self-weight of fresh concrete. So it is assumed for the analysis that

- (1) in determining $M_{a,s}$ and f_a for beams constructed unpropped, the self-weight of the fresh concrete is the only construction load on the steel beam.

Usually, the construction load dominated by the self-weight of fresh concrete, is significantly smaller than the ultimate load to be carried by the beams. Furthermore, in Eurocode 4 [1], no safety factor is specified for $M_{a,s}$ or f_a . Therefore, this study assumes that

- (2) no safety factors are applied to $M_{a,s}$ or f_a .

Since the prediction of bending resistance for beams with non-ductile partial shear connection is not the same for different construction procedures, it would be ideal to know the construction method for each specimen in the tests reported. However, in the test data found so far, it is rarely stated whether the construction was propped or unpropped, which then results in difficulty in calculating the theoretical resistance to obtain the test corrections, \bar{b} and V_δ . From equation (2.31), it is suggested that the lower (conservative) design resistance would be obtained when \bar{b} is decreased. Therefore, considering that the higher the theoretical resistance is taken, the lower the value of \bar{b} which results in, it is assumed that

- (3) in using equations (2.25) and (2.26), between the two predictions, based on propped and unpropped construction, for test specimen i ($i = 1, \dots, n$), the higher of the two calculated resistances is taken as the r_{ti} .

The parameters \bar{b} and V_δ determined according to this assumption are then used to calibrate the design resistances for both propped and unpropped constructions.

As suggested by equation (3.18), F_c is decreased when a lower degree of shear

connection N/N_f is used in a beam. It can be seen from Figure (3.4) that when F_c becomes lower than certain level, the predicted bending resistance, r_t , for the beams becomes even smaller than the plastic bending resistance of steel beam alone, M_{apl} . This means that the theoretical model given by equation (3.19) is not suitable to be used for beams with an exceptionally low degree of shear. In practice, such beams are not used. Thus, the following assumption is made:

- (4) if, from the calculations based on both unpropped and propped construction, the theoretical resistances, r_t , of a test specimen are both lower than M_{apl} , the test specimen is excluded from the safety calibration for design resistance based on (3.19).

The test corrections \bar{b} and V_δ found from assumption (4) will be used to calibrate design resistances for both propped and unpropped construction.

The reliability of using equilibrium method and linear interpolation (as developed for beams with ductile partial shear connection) for the beams with non-ductile shear connection is also studied. When these models are used, the problems covered by the above assumptions do not exist. This enables more test specimens to be included in the analysis.

From the presentation of the theoretical model (3.19), one can realize that it would be too complicated to derive a closed form for the coefficient of variation V_{r_t} for this model. Therefore, for either propped or unpropped construction, equation (2.28) is still used to determine V_t , but the derivative of the value of the resistance function with respect to a basic variable X_i , at point $\underline{X} = \bar{\underline{X}}$, is calculated in the following numerical way:

$$\frac{\partial g_R(\underline{X})}{\partial X_i} \Big|_{\underline{X}=\bar{\underline{X}}} = \frac{g_R[\bar{X}_1, \dots, \bar{X}_{i-1}, \bar{X}_i(1 + \theta), \bar{X}_{i+1}, \dots, \bar{X}_J] - g_R(\bar{\underline{X}})}{\theta \bar{X}_i} \quad (3.22)$$

where θ is a small constant. Calculations by computer show that an appropriate value of θ may be selected between 0.001 to 0.005.

Same as for beams with ductile shear connection (group C), in determining

V_{rt} , reduction factors, α and k , for P_R , beam span L , number of shear connectors, N , and density of concrete, W_c , are treated as deterministic parameters here.

When the relevant parameters, \bar{b} , V_δ , n (number of test specimens in the group) and V_t are all known, the partial safety factors for the beams with non-ductile shear connectors can be calibrated.

According to assumption (2), no safety factors are applied to $M_{a,s}$ and f_a . Thus, when unpropped construction is considered, it can be shown [60] from equations (3.19) to (3.21) that the design resistance is not in general, like beams in the other groups, proportional to $1/\gamma_{md}$, so equation (3.8) cannot be used to determine γ_{md} in this case. Nevertheless, using numerical techniques, there is no difficulty to find the model factor γ_{md} from the general equation (2.56).

If propped construction is considered, $M_{a,s}$ and f_a are considered to be zero, so γ_{md} can be expressed in the form of equation (3.8).

The numerical format of calculating γ_{md} for the beams in group D with unpropped construction is given in the next section.

The other concepts for obtaining the partial safety factors for design resistances of the beams in group D are the same as those applied in group C.

3.3 Calculation of failure probability and model factors by programs

All the calculations for the reliability analysis of the beams in bending are implemented by computer programs. The use of these programs is introduced in Appendix D.

It has been shown in Section 2.3 that with respect to the given partial safety factors, the probability of the real resistances failing to reach the design values, P_f , can be inversely found out, and, therefore, the reliability of the design formulae with these safety factors may be judged from another aspect.

For composite beams represented by the test groups studied here, applying

the code values of the partial safety factors [1] (as listed in equation (2.59) to the characteristic strengths used above (i.e. f_{yk} etc.)), the corresponding design fractile-factor, k_d , underlying the design bending resistances can be found according to equation (2.56). Consequently, as presented in Section 2.3, the failure probability P_f at a given confidence level ϵ can be determined from k_d and the group size n .

However, P_f needs to be found from a nonlinear equation (equation (2.58)). So, in the computer program, an iterative method is employed to calculate P_f from known k_d , ϵ and n .

In order to develop the iteration format, equation (2.57) is re-written

$$k_b = \frac{k_d V_r^2 - k_{d,\infty} V_{rt}^2}{V_\delta^2} \quad (3.23)$$

where, as explained for equation (2.57), $k_{d,\infty}$ is a fractile-factor corresponding to P_f , found from the standard normal distribution; and k_b is a fractile-factor of the non-central t -distribution (Appendix A), determined by P_f at a certain confidence level ϵ and group size n .

Therefore, knowing V_r^2 , V_{rt}^2 , V_δ^2 , k_d and n , for a specified confidence level ϵ (this study takes $\epsilon = 0.75$), the failure probability P_f can be calculated as follows.

1. Guess an initial value for P_f , denoted P'_{f1} (in this study, the initial value is taken as 0.0012)
2. Find $k_{d,\infty}$ from P'_{f1} using the standard normal distribution.
3. Calculate k_b from equation (3.23).
4. Determine a new value of P_f , denoted P_{f1} , from k_b , n and $\epsilon = 0.75$, using tables for the non-central t -distribution [39].
5. Set up a better value for P_f :

$$P'_{f2} = \frac{P_{f1} + P'_{f1}}{2}. \quad (3.24)$$

6. Compare P'_{f2} with P_{f1} . If the two values differ by less than 0.1%, then P_f is determined as P'_{f2} ; otherwise, replace P'_{f1} by P'_{f2} and return to step 2 for the next iteration.

It was found that a satisfactory value for P_f can normally be achieved in fewer than 10 rounds of iteration.

Another numerical technique is used in the computer program to find the model factor γ_{md} for beams in group D with unpropped construction.

As indicated in Section 3.2.3, γ_{md} for the resistance function (3.19) needs to be found from equation (2.56), if the beams are considered to be unpropped during construction. So the computation uses trail and error method as follows.

1. Calculate the right side of equation (2.56); the result is denoted r_d .
2. Guess the range in which γ_{md} lies, $\gamma_{md,l} \leq \gamma_{md} \leq \gamma_{md,u}$, (for this study, $\gamma_{md,l}$ is initially taken as 0.5 and $\gamma_{md,u}$ as 3.0).

3. Calculate

$$\gamma'_{md} = \frac{\gamma_{md,l} + \gamma_{md,u}}{2} \quad (3.25)$$

and take γ_{md} as γ'_{md} to calculate the left side of equation (2.56). The result is denoted r'_d .

4. Compare r'_d with r_d . If $|r'_d - r_d|/r_d \leq 0.01\%$, then γ_{md} is determined as γ'_{md} ; otherwise
 - (a) if $r'_d < r_d$ (which means the assumed value of γ_{md} is too large), then take $\gamma_{md,u}$ as γ'_{md} and return to step 3 for the next iteration;
 - (b) if $r'_d > r_d$ (which means the assumed value of γ_{md} is too small), then take $\gamma_{md,l}$ as γ'_{md} and return to step 3 for the next iteration.

Following this procedure, γ_{md} for resistance function (3.19) can normally be obtained in less than 15 cycles.

Chapter 4

Calibration results and discussions

Following the concepts developed in the last chapter, the safety of designing bending resistances for composite beams, in accordance with Eurocode 4, has been calibrated. As considered in Section 3.1, the calibration has been made based on the test results of composite beams as defined in the four groups. This chapter is to present the calibration results for the beams represented by these test groups. With respect to the results obtained, the reliability underlying the relevant design formulae of Eurocode 4 [1] is also discussed in this chapter.

All the calculations are made by the computer programs. Notes on the using of these programs and all the original input datafiles are given in Appendix D.

4.1 Results of calibration

From the literature study, acceptable test results for the reliability analysis of composite beams have been found from

- 27 specimens for group A;
- 21 specimens for group B;

- 26 specimens for group C;
- 27 specimens for group D when the theoretical model is as given by Eurocode 4 (equation (3.19)), and 48 specimens for the same group when the models provided for beams in group C are used (i.e. the equilibrium method and linear interpolation described in Section 3.2.2).

For the test specimens in each group, the experimental resistances and the theoretical values of r_t calculated according to assumption (3) in Section 2.2.1, denoted r_{ei} and r_{ti} , respectively, are shown in Tables 4.1 to 4.5. The designations of the specimens and sources are also recorded in these tables.

It is treated in the analysis that the specimens with the same intended values of basic variables (i.e. the same design) constitute a sample, which, as shown in Tables 4.1 to 4.5, leads to 14 samples (numbered S1 to S14) from group A, 15 (numbered H1 to H15) from group B, 24 (numbered SD1 to SD24) from group C, and 18 (numbered SN1 to SN18) from group D for the models used in the code [1] (Section 3.2.3) and 38 (numbered CN1 to CN38) from group D for the theoretical models developed [1] for beams in group C.

Tables 4.6 to 4.11 give the mean values of basic variables for all the beam samples except for H15 in group B. For sample H15, the plastic neutral axis of the steel section alone is within the bottom flange. Its ratio t_{ei}/t_{ti} is included in calculating the parameters, \bar{b} , V_δ , etc., but the further reliability analysis for this sample is not made, as the resistance function differs from that for the other samples in hogging bending.

The test specimens collected for all the four groups had the concrete flanges symmetrical about the steel web.

For group A, the test data were obtained in a total of four different research laboratories which locate in two countries: UK and U.S.A. Only one of the specimens was fabricated with profiled steel sheeting and lightweight concrete [41]. Except for those in samples S13 and S14 [48], the sections of specimens were all formed by symmetrical steel sections. The size of the steel bottom flanges of

Table 4.1: Resistances of test specimens in group A

| sample number | Ref. | name of specimen | r_{ti} (kN-m) | r_{ei} (kN-m) | r_{ei}/r_{ti} |
|---------------|-------|------------------|--------------------|--------------------|-----------------|
| S1 | 41 | No.1 | 377.0 | 435.0 | 1.154 |
| S2 | 42 | No.1 | 83.7 | 87.0 | 1.039 |
| S3 | 42 | No.2 | 87.6 | 92.0 | 1.050 |
| S4 | 43 | A1 | 511.1 | 578.0 | 1.131 |
| | | A2 | 528.5 | 604.9 | 1.145 |
| | | A3 | 565.0 | 604.9 | 1.071 |
| | | A4 | 579.2 | 696.3 | 1.202 |
| | | A5 | 572.3 | 638.5 | 1.116 |
| | | C1 | 557.9 | 601.6 | 1.078 |
| | | D1 | 556.6 | 612.9 | 1.101 |
| | | F1 | 583.7 | 653.3 | 1.119 |
| S5 | 43 | T1 | 498.7 | 604.9 | 1.213 |
| | | B1 | 527.5 | 655.3 | 1.242 |
| | | E1 | 610.7 | 697.3 | 1.142 |
| | | U1 | 592.5 | 699.6 | 1.181 |
| | | U2 | 519.2 | 695.6 | 1.340 |
| S6 | 44 | U3 | 522.5 | 680.5 | 1.302 |
| | | CB2 | 38.2 | 46.9 | 1.228 |
| | | CB4 | 37.2 | 40.0 | 1.075 |
| S7 | 45,46 | SS1 | 152.9 | 188.7 | 1.234 |
| S8 | 45,46 | SS2 | 177.3 | 200.0 | 1.128 |
| S9 | 45,46 | SS3 | 203.7 | 216.9 | 1.065 |
| S10 | 45,46 | SS6 | 225.3 | 232.8 | 1.033 |
| S11 | 47 | CB10 | 164.1 | 199.0 | 1.213 |
| S12 | 47 | CB12 | 191.7 | 205.0 | 1.069 |
| S13 | 48 | No.2 | 5517.7 | 6019.8 | 1.091 |
| S14 | 48 | No.3 | 3615.4 | 3618.1 | 1.001 |

Table 4.2: Resistances of test specimens in group B

| sample number | Ref. | name of specimen | r_{ti} (kN-m) | r_{ei} (kN-m) | r_{ei}/r_{ti} |
|---------------|------|------------------|--------------------|--------------------|-----------------|
| H1 | 42 | No.1 | 56.0 | 73.9 | 1.320 |
| | | No.2 | 60.1 | 78.9 | 1.313 |
| H2 | 44 | CB2 | 24.1 | 31.2 | 1.295 |
| | | CB4 | 24.1 | 30.6 | 1.295 |
| H3 | 49 | SC-3S | 683.3 | 697.8 | 1.021 |
| H4 | 49 | SC-4S | 757.6 | 778.3 | 1.027 |
| H5 | 50 | 4A | 185.0 | 217.0 | 1.173 |
| H6 | 50 | 2 | 224.0 | 238.7 | 1.066 |
| | | 5 | 224.0 | 239.1 | 1.067 |
| | | 6 | 224.0 | 244.1 | 1.090 |
| H7 | 50 | 11 | 280.2 | 375.2 | 1.339 |
| H8 | 50 | 12 | 305.0 | 388.7 | 1.274 |
| H9 | 50 | 13 | 313.0 | 393.2 | 1.256 |
| | | 16 | 313.0 | 391.0 | 1.249 |
| | | 17 | 313.0 | 388.7 | 1.242 |
| H10 | 50 | 22 | 253.9 | 323.2 | 1.273 |
| H11 | 50 | 23 | 280.8 | 337.9 | 1.203 |
| H12 | 50 | 24 | 285.0 | 340.1 | 1.193 |
| H13 | 50 | 32 | 240.9 | 271.2 | 1.126 |
| H14 | 50 | 33 | 266.1 | 291.5 | 1.096 |
| H15 | 49 | No.3 | 4110.4 | 4293.5 | 1.045 |

Table 4.3: Resistances of test specimens in group C

| sample number | Ref. | name of specimen | $^1 \frac{N}{N_f}$ | $^2 (\frac{N}{N_f})_l$ | (1) $^3 r_{ti}$ (kN-m) | (2) $^4 r_{ti}$ (kN-m) | (3) r_{ei} (kN-m) | (3)/(1) | (3)/(2) |
|---------------|-------|------------------|--------------------|------------------------|------------------------------|------------------------------|---------------------------|---------|---------|
| SD1 | 51 | IA1R | 0.495 | 0.47 | 753.1 | 832.6 | 826.6 | 1.098 | 0.993 |
| SD2 | 51 | IA5R | 0.465 | 0.43 | 788.8 | 876.5 | 1026.2 | 1.301 | 1.171 |
| SD3 | 51 | IB2 | 0.489 | 0.47 | 617.9 | 697.1 | 682.5 | 1.105 | 0.979 |
| SD4 | 51 | ID1 | 0.495 | 0.47 | 749.0 | 828.3 | 813.3 | 1.086 | 0.982 |
| SD5 | 52 | A1 | 0.705 | 0.41 | 250.1 | 266.6 | 264.7 | 1.058 | 0.993 |
| | | A2 | 0.721 | 0.41 | 254.7 | 270.3 | 276.8 | 1.087 | 1.024 |
| SD6 | 52 | A3 | 0.556 | 0.41 | 227.2 | 248.9 | 257.8 | 1.135 | 1.036 |
| SD7 | 51 | 70-4 | 0.607 | 0.52 | 316.2 | 351.9 | 361.2 | 1.142 | 1.026 |
| SD8 | 51 | 66-11(56) | 0.436 | 0.43 | 112.0 | 128.7 | 147.4 | 1.317 | 1.146 |
| SD9 | 51 | 66-11(W) | 0.769 | 0.43 | 345.1 | 367.1 | 382.0 | 1.107 | 1.041 |
| SD10 | 51 | 64-15(H1) | 0.599 | 0.40 | 267.5 | 290.6 | 330.6 | 1.236 | 1.138 |
| SD11 | 51 | 64-15(E1) | 0.724 | 0.40 | 264.6 | 281.7 | 322.8 | 1.220 | 1.146 |
| SD12 | 51 | 71(EPIC) | 0.517 | 0.40 | 239.9 | 263.8 | 327.1 | 1.364 | 1.240 |
| SD13 | 51 | 68-4(1) | 0.664 | 0.43 | 319.9 | 348.3 | 328.5 | 1.027 | 0.943 |
| SD14 | 51 | 69-1(3) | 0.598 | 0.43 | 304.3 | 335.6 | 341.6 | 1.122 | 1.018 |
| SD15 | 51 | 70-31(A) | 0.708 | 0.42 | 307.3 | 333.0 | 357.6 | 1.164 | 1.074 |
| SD16 | 51 | 67-36CU3 | 0.486 | 0.47 | 219.9 | 246.1 | 270.0 | 1.228 | 1.097 |
| SD17 | 51 | 65-19BS12 | 0.942 | 0.40 | 309.4 | 313.7 | 299.5 | 0.968 | 0.955 |
| SD18 | 51 | 65-19BS11 | 0.938 | 0.40 | 310.0 | 314.6 | 310.2 | 1.001 | 0.986 |
| SD19 | 51 | 76-36CU2 | 0.798 | 0.47 | 293.5 | 306.7 | 317.1 | 1.081 | 1.034 |
| SD20 | 51 | 67-36CU1 | 0.910 | 0.47 | 279.1 | 284.4 | 339.9 | 1.218 | 1.195 |
| SD21 | 51 | TEX-3 | 0.714 | 0.54 | 688.1 | 729.4 | 859.8 | 1.250 | 1.179 |
| SD22 | 51 | 174-75 | 0.730 | 0.57 | 1234.9 | 1315.2 | 1469.5 | 1.190 | 1.117 |
| SD23 | 52,53 | 68-5(2) | 0.640 | 0.52 | 349.3 | 385.0 | 384.7 | 1.101 | 0.999 |
| SD24 | 52 | A4 | 0.639 | 0.41 | 272.2 | 298.9 | 285.5 | 1.049 | 0.955 |
| | | A5 | 0.848 | 0.41 | 322.7 | 334.0 | 314.9 | 0.976 | 0.943 |

¹ actual degree of shear connection;

² the lowest degree of shear connection required for ductile partial shear connection [1];

³ theoretical resistances found from linear interpolation;

⁴ theoretical resistances found from the equilibrium method.

Table 4.4: Resistances of test specimens in group D (theoretical resistances are predicted from the non-ductile models)

| sample number | Ref. | name of specimen | $^1 \frac{N}{N_f}$ | $^2 (\frac{N}{N_f})_l$ | M_{apl} (kN-m) | $^3 r_{ti}$ (kN-m) | r_{ei} (kN-m) | r_{ei}/r_{ti} |
|---------------|------|------------------|--------------------|------------------------|---------------------|-----------------------|--------------------|-----------------|
| SN1 | 51 | ID2 | 0.458 | 0.47 | 470.9 | 614.0 | 698.4 | 1.137 |
| SN2 | 51 | 66-11(42) | 0.328 | 0.43 | 74.4 | 87.8 | 139.0 | 1.583 |
| SN3 | 51 | 67-38 | 0.388 | 0.47 | 209.5 | 263.2 | 410.8 | 1.561 |
| SN4 | 51 | 73(RF) | 0.445 | 0.48 | 201.3 | 302.8 | 415.1 | 1.371 |
| SN5 | 51 | 70-31(D) | 0.370 | 0.42 | 191.9 | 231.8 | 342.7 | 1.478 |
| SN6 | 51 | 70-31(C) | 0.361 | 0.57 | 480.6 | 607.4 | 846.0 | 1.400 |
| SN7 | 51 | 72-12(80) | 0.293 | 0.48 | 382.5 | 402.2 | 574.0 | 1.427 |
| SN8 | 51 | 175-75 | 0.410 | 0.57 | 572.2 | 773.5 | 1071.8 | 1.386 |
| SN9 | 51 | 16-76 | 0.492 | 0.62 | 437.0 | 637.1 | 931.8 | 1.462 |
| SN10 | 56 | IS | 0.530 | 0.55 | 661.7 | 921.6 | 1011.0 | 1.097 |
| SN11 | 57 | 1 | 0.381 | 0.49 | 140.7 | 190.5 | 254.4 | 1.335 |
| SN12 | 57 | 3 | 0.263 | 0.49 | 145.4 | 152.5 | 238.4 | 1.563 |
| SN13 | 51 | TEX-1 | 0.295 | 0.54 | 385.6 | 420.5 | 677.2 | 1.610 |
| | | TEX-6 | 0.309 | 0.54 | 388.1 | 436.4 | 724.9 | 1.661 |
| SN14 | 51 | TEX-2 | 0.533 | 0.54 | 416.4 | 642.5 | 899.1 | 1.399 |
| | | TEX-8 | 0.537 | 0.54 | 405.6 | 629.3 | 867.5 | 1.378 |
| SN15 | 51 | TEX-4 | 0.422 | 0.54 | 374.7 | 523.6 | 752.1 | 1.436 |
| | | TEX-5 | 0.407 | 0.54 | 388.6 | 535.1 | 790.1 | 1.476 |
| | | TEX-7 | 0.446 | 0.54 | 405.2 | 578.8 | 819.6 | 1.416 |
| SN16 | 51 | IR-1-76 | 0.400 | 0.54 | 352.9 | 472.2 | 645.2 | 1.367 |
| | | IR-2-76 | 0.431 | 0.54 | 355.8 | 492.8 | 638.5 | 1.296 |
| SN17 | 51 | HHR-1-76 | 0.324 | 0.54 | 365.4 | 417.2 | 592.6 | 1.420 |
| | | HHR-2-76 | 0.346 | 0.54 | 359.9 | 431.0 | 590.3 | 1.369 |
| | | RF-1-76 | 0.332 | 0.54 | 364.0 | 422.8 | 606.3 | 1.434 |
| | | RF-2-76 | 0.318 | 0.54 | 358.6 | 404.2 | 610.9 | 1.512 |
| SN18 | 3 | BS1 | 0.408 | 0.48 | 449.4 | 545.2 | 710.4 | 1.303 |
| | | BS2 | 0.459 | 0.48 | 436.2 | 617.6 | 715.5 | 1.158 |

¹ actual degree of shear connection;

² the lowest degree of shear connection required for ductile partial shear connection [1];

³ higher value of theoretical resistances from propped and unpropped constructions (assumption (3) in Section 3.2.3).

Table 4.5: Resistances of test specimens in group D (theoretical resistances are predicted from linear interpolation and the equilibrium method)

| sample number | Ref. | name of specimen | $^1 \frac{N}{N_f}$ | $^2 (\frac{N}{N_f})_l$ | (1) $^3 r_{ti}$ (kN-m) | (2) $^4 r_{ti}$ (kN-m) | (3) r_{ei} (kN-m) | (3)/(1) | (3)/(2) |
|---------------|------|------------------|--------------------|------------------------|------------------------------|------------------------------|---------------------------|---------|---------|
| CN1 | 51 | IA2 | 0.331 | 0.47 | 610.1 | 700.0 | 705.0 | 1.156 | 1.007 |
| CN2 | 51 | IA3R | 0.193 | 0.54 | 637.6 | 712.7 | 788.3 | 1.236 | 1.106 |
| CN3 | 51 | IA6R | 0.324 | 0.47 | 778.2 | 898.1 | 945.5 | 1.215 | 1.053 |
| CN4 | 51 | IA7 | 0.207 | 0.54 | 636.5 | 725.1 | 698.8 | 1.098 | 0.964 |
| CN5 | 51 | IB1 | 0.225 | 0.54 | 487.3 | 554.7 | 650.3 | 1.334 | 1.172 |
| CN6 | 51 | IC1 | 0.281 | 0.47 | 588.8 | 680.2 | 690.1 | 1.172 | 1.015 |
| CN7 | 51 | IC2A | 0.086 | 0.54 | 588.7 | 637.1 | 710.9 | 1.208 | 1.116 |
| CN8 | 51 | IC2B | 0.096 | 0.54 | 602.9 | 657.2 | 728.5 | 1.208 | 1.108 |
| CN9 | 51 | IC3 | 0.176 | 0.47 | 669.6 | 757.8 | 782.8 | 1.169 | 1.033 |
| CN10 | 51 | IC4 | 0.142 | 0.54 | 685.7 | 745.3 | 841.7 | 1.227 | 1.129 |
| CN11 | 51 | ID2 | 0.458 | 0.47 | 637.6 | 731.7 | 689.4 | 1.095 | 0.955 |
| CN12 | 51 | ID3 | 0.185 | 0.54 | 719.7 | 810.4 | 846.1 | 1.176 | 1.044 |
| CN13 | 51 | ID4 | 0.229 | 0.54 | 671.0 | 765.7 | 717.7 | 1.070 | 0.937 |
| CN14 | 54 | 1 | 0.228 | 0.52 | 459.6 | 527.6 | 538.5 | 1.172 | 1.021 |
| CN15 | 54 | 2 | 0.244 | 0.52 | 466.3 | 536.3 | 537.6 | 1.153 | 1.002 |
| CN16 | 51 | 66-11(42) | 0.328 | 0.43 | 108.6 | 125.7 | 139.0 | 1.280 | 1.106 |
| CN17 | 51 | 67-38 | 0.388 | 0.47 | 290.8 | 337.6 | 410.8 | 1.413 | 1.217 |
| CN18 | 51 | 72-12(75) | 0.171 | 0.48 | 654.7 | 723.7 | 716.1 | 1.094 | 0.990 |
| CN19 | 51 | 73(RF) | 0.445 | 0.48 | 328.7 | 364.3 | 415.1 | 1.263 | 1.139 |
| CN20 | 51 | 67-11(B1) | 0.184 | 0.40 | 207.0 | 232.6 | 252.3 | 1.219 | 1.085 |
| | | 67-11(B2) | 0.195 | 0.40 | 209.7 | 235.7 | 246.6 | 1.176 | 1.046 |
| CN21 | 51 | 70-31(D) | 0.370 | 0.42 | 252.2 | 292.7 | 342.7 | 1.359 | 1.171 |
| CN22 | 51 | 70-31(C) | 0.361 | 0.57 | 647.4 | 747.7 | 846.6 | 1.308 | 1.132 |
| CN23 | 51 | 69-2(HR) | 0.224 | 0.44 | 145.7 | 162.9 | 175.8 | 1.207 | 1.079 |
| CN24 | 51 | TEX-1 | 0.295 | 0.54 | 515.3 | 591.5 | 677.2 | 1.314 | 1.145 |
| | | TEX-6 | 0.309 | 0.54 | 528.2 | 603.2 | 724.9 | 1.372 | 1.202 |
| CN25 | 51 | TEX-2 | 0.533 | 0.54 | 675.3 | 744.4 | 899.1 | 1.331 | 1.208 |
| | | TEX-8 | 0.537 | 0.54 | 662.7 | 728.2 | 867.5 | 1.309 | 1.191 |
| CN26 | 51 | TEX-4 | 0.422 | 0.54 | 559.6 | 630.4 | 752.1 | 1.344 | 1.193 |
| | | TEX-5 | 0.407 | 0.54 | 572.6 | 647.7 | 790.1 | 1.380 | 1.220 |
| | | TEX-7 | 0.446 | 0.54 | 617.4 | 691.6 | 819.6 | 1.328 | 1.185 |
| CN27 | 51 | IR-1-76 | 0.400 | 0.54 | 506.8 | 574.2 | 645.2 | 1.273 | 1.124 |
| | | IR-2-76 | 0.431 | 0.54 | 524.9 | 589.4 | 638.5 | 1.216 | 1.083 |
| CN28 | 51 | HHR-1-76 | 0.324 | 0.54 | 494.2 | 562.6 | 592.6 | 1.199 | 1.053 |
| | | HHR-2-76 | 0.346 | 0.54 | 496.7 | 563.1 | 590.3 | 1.188 | 1.048 |
| | | RF-1-76 | 0.332 | 0.54 | 496.0 | 563.8 | 606.3 | 1.222 | 1.075 |
| | | RF-2-76 | 0.318 | 0.54 | 483.0 | 549.7 | 610.9 | 1.265 | 1.111 |
| CN29 | 51 | 72-12(80) | 0.293 | 0.48 | 531.3 | 596.7 | 574.0 | 1.080 | 0.962 |
| CN30 | 51 | 75-16 | 0.314 | 0.52 | 472.3 | 537.8 | 547.7 | 1.160 | 1.018 |

Table 4.5: (continued)

| sample number | Ref. | name of specimen | $^1 \frac{N}{N_f}$ | $^2 (\frac{N}{N_f})_l$ | (1) $^3 r_{ti}$ (kN-m) | (2) $^4 r_{ti}$ (kN-m) | (3) r_{ei} (kN-m) | (3)/(1) | (3)/(2) |
|---------------|------|------------------|--------------------|------------------------|------------------------------|------------------------------|---------------------------|---------|---------|
| CN31 | 51 | 175-75 | 0.410 | 0.57 | 833.3 | 961.1 | 1071.8 | 1.286 | 1.115 |
| CN32 | 51 | 16-76 | 0.492 | 0.62 | 667.9 | 760.8 | 931.8 | 1.395 | 1.225 |
| CN33 | 55 | BS1 | 0.408 | 0.48 | 629.4 | 738.2 | 710.4 | 1.129 | 0.962 |
| | | BS2 | 0.459 | 0.48 | 650.5 | 747.9 | 715.5 | 1.100 | 0.957 |
| CN34 | 56 | IS | 0.530 | 0.55 | 961.5 | 1083.0 | 1011.0 | 1.051 | 0.933 |
| CN35 | 57 | 1 | 0.381 | 0.49 | 215.0 | 243.0 | 254.4 | 1.183 | 1.046 |
| CN36 | 57 | 2 | 0.191 | 0.49 | 194.5 | 218.4 | 214.4 | 1.102 | 0.982 |
| CN37 | 57 | 3 | 0.263 | 0.49 | 198.2 | 225.3 | 238.4 | 1.203 | 1.058 |
| CN38 | 57 | 4 | 0.138 | 0.49 | 178.8 | 197.5 | 184.4 | 1.032 | 0.934 |

¹ actual degree of shear connection;

² the lowest degree of shear connection required for ductile partial shear connection [1];

³ theoretical resistances found from linear interpolation;

⁴ theoretical resistances found from the equilibrium method.

Table 4.6: Mean values of basic variables for samples in group A

| sample | A_a mm ² | h_g mm | t_w mm | b_f mm | t_f mm | f_y N/mm ² | h_c mm | h_p mm | b_c mm | f_c N/mm ² |
|--------|--------------------------|------------------|-------------|------------------|----------------|----------------------------|-------------|-------------|-------------|----------------------------|
| S1 | 4750 | 151.9 | 7.2 | 123.5 | 10.7 | 308 | 127 | 51.0 | 1500 | 27.0 |
| S2 | 2270 | 76.0 | 5.8 | 76.2 | 9.6 | 316 | 60.0 | - | 610 | 48.0 |
| S3 | 2270 | 76.0 | 5.8 | 76.2 | 9.6 | 316 | 60.0 | - | 610 | 38.0 |
| S4 | 8390 | 152.4 | 11.0 | 152.4 | 17.8 | 253 | 152 | - | 1219 | 22.1 |
| S5 | 8390 | 152.4 | 11.0 | 152.4 | 17.8 | 253 | 152 | - | 1219 | 30.1 |
| S6 | 1230 | 60.4 | 4.6 | 44.5 | 8.3 | 286 | 76.0 | - | 305 | 24.2 |
| S7 | 3800 | 103.4 | 6.3 | 133.6 | 9.6 | 269 | 127 | - | 254 | 41.0 |
| S8 | 3800 | 103.4 | 6.3 | 133.6 | 9.6 | 269 | 127 | - | 305 | 43.0 |
| S9 | 3800 | 103.4 | 6.3 | 133.6 | 9.6 | 269 | 127 | - | 406 | 32.0 |
| S10 | 3800 | 103.4 | 6.3 | 133.6 | 9.6 | 269 | 127 | - | 616 | 32.0 |
| S11 | 3800 | 103.4 | 6.3 | 133.6 | 9.6 | 282 | 76 | - | 915 | 29.6 |
| S12 | 3800 | 103.4 | 6.3 | 133.6 | 9.6 | 282 | 102 | - | 1220 | 29.6 |
| S13 | 20050 | 706.0 | 6.4 | 254.0 | 12.7 | 336 | 191 | - | 1194 | 41.0 |
| S14 | 14895 | (1054.1) | | (406.4) | (25.4) | | | | | |
| | | 549.2 (847.8) | 4.8 | 203.2 (406.4) | 15.9 (19.1) | 336 | 165 | - | 1168 | 51.0 |

Table 4.7: Mean values of basic variables for samples in group B

| sample | A_s mm ² | f_y N/mm ² | ¹ b_p mm | ² t_p mm | ³ h_a mm | f_s N/mm ² | h_s mm | b_f mm | t_w mm | t_f mm | ⁴ A_a mm ² |
|--------|--------------------------|----------------------------|--------------------------|--------------------------|--------------------------|----------------------------|-------------|-------------|-------------|-------------|---------------------------------------|
| H1 | 594 | 316 | - | - | 152.0 | 316 | 36.3 | 76.2 | 5.8 | 9.6 | 2271 |
| H2 | 222 | 286 | - | - | 120.7 | 428 | 47.0 | 44.5 | 4.6 | 8.3 | 1232 |
| H3 | 1419 | 240 | - | - | 532.7 | 310 | 114.8 | 211.1 | 10.4 | 14.0 | 11325 |
| H4 | 2419 | 240 | - | - | 532.7 | 310 | 99.7 | 211.1 | 10.4 | 14.0 | 11325 |
| H5 | 774 | 319 | 76.2 | 9.5 | 304.8 | 329 | 38.1 | 101.6 | 6.11 | 6.7 | 3859 |
| H6 | 1600 | 320 | 76.2 | 9.5 | 304.8 | 329 | 38.1 | 101.6 | 6.11 | 6.7 | 3859 |
| H7 | 761 | 296 | - | - | 310.9 | 373 | 50.8 | 166.6 | 7.8 | 13.7 | 6832 |
| H8 | 1265 | 296 | - | - | 310.9 | 373 | 50.8 | 166.6 | 7.8 | 13.7 | 6832 |
| H9 | 1600 | 296 | - | - | 310.9 | 373 | 50.8 | 166.6 | 7.8 | 13.7 | 6832 |
| H10 | 516 | 303 | - | - | 307.1 | 341 | 50.8 | 165.6 | 6.7 | 11.8 | 5884 |
| H11 | 1200 | 303 | - | - | 307.1 | 341 | 50.8 | 165.6 | 6.7 | 11.8 | 5884 |
| H12 | 1600 | 303 | - | - | 307.1 | 341 | 50.8 | 165.6 | 6.7 | 11.8 | 5884 |
| H13 | 516 | 351 | - | - | 303.5 | 341 | 50.8 | 165.1 | 6.1 | 10.2 | 5142 |
| H14 | 1032 | 351 | - | - | 303.5 | 341 | 50.8 | 165.1 | 6.1 | 10.2 | 5142 |

¹ breath of the steel plate attached to the bottom flange, as shown in Figure D.1;

² thickness of the attached steel plate, as shown in Figure D.1;

³ height of steel section, excluding t_p , as shown in Figure D.1;

⁴ area of steel section, including cross-section of the attached steel plate (if any).

Table 4.8: Mean values of basic variables for steel beams and spans for samples in group C

| sample | A_a mm ² | h_g, h_{na} mm | t_w mm | b_f mm | t_f mm | f_y N/mm ² | L (span) m |
|--------|--------------------------|---------------------|-------------|-------------|-------------|----------------------------|-----------------|
| SD1 | 7613 | 203.3 | 7.8 | 177.7 | 12.8 | 495.5 | 7.315 |
| SD2 | 8581 | 204.9 | 8.8 | 178.7 | 14.4 | 463.4 | 6.096 |
| SD3 | 10994 | 201.6 | 11.1 | 215.9 | 15.8 | 262.8 | 7.315 |
| SD4 | 7613 | 203.3 | 7.8 | 177.7 | 12.8 | 492.4 | 7.315 |
| SD5 | 4742 | 127.0 | 7.6 | 114.3 | 12.8 | 323.5 | 5.190 |
| SD6 | 4742 | 127.0 | 7.6 | 114.3 | 12.8 | 296.0 | 5.190 |
| SD7 | 4954 | 199.3 | 6.4 | 139.7 | 8.8 | 282.1 | 9.114 |
| SD8 | 2865 | 103.0 | 6.2 | 102.0 | 8.0 | 318.6 | 6.096 |
| SD9 | 5710 | 175.8 | 6.9 | 170.9 | 9.8 | 271.0 | 6.096 |
| SD10 | 5125 | 155.2 | 6.1 | 171.1 | 9.7 | 286.2 | 4.572 |
| SD11 | 5125 | 155.2 | 6.1 | 171.1 | 9.7 | 254.1 | 4.572 |
| SD12 | 5125 | 155.2 | 6.1 | 171.1 | 9.7 | 246.9 | 4.572 |
| SD13 | 5710 | 175.8 | 6.9 | 170.9 | 9.8 | 263.8 | 6.096 |
| SD14 | 5710 | 175.8 | 6.9 | 170.9 | 9.8 | 259.0 | 6.096 |
| SD15 | 5710 | 175.8 | 6.9 | 170.9 | 9.8 | 251.7 | 5.791 |
| SD16 | 5125 | 155.2 | 6.1 | 171.1 | 9.7 | 251.0 | 7.315 |
| SD17 | 5125 | 155.2 | 6.1 | 171.1 | 9.7 | 266.5 | 4.572 |
| SD18 | 5125 | 155.2 | 6.1 | 171.1 | 9.7 | 267.6 | 4.572 |
| SD19 | 5125 | 155.2 | 6.1 | 171.1 | 9.7 | 279.3 | 7.315 |
| SD20 | 5125 | 155.2 | 6.1 | 171.1 | 9.7 | 249.0 | 7.315 |
| SD21 | 9484 | 206.5 | 9.7 | 179.6 | 16.0 | 250.0 | 9.754 |
| SD22 | 11553 | 301.5 | 10.7 | 175.9 | 15.0 | 250.0 | 10.64 |
| SD23 | 4936 | 198.4 | 6.4 | 139.7 | 9.5 | 317.6 | 9.114 |
| SD24 | 4742 | 127.0 | 7.6 | 114.3 | 12.8 | 323.5 | 5.190 |

Table 4.9: Mean values of basic variables for concrete slabs and shear connectors for samples in group C

| Sample | h_c mm | b_c mm | b_0 mm | h_p mm | h mm | d mm | studs in shear span | | | f_c ($\frac{N}{mm^2}$) | E_c ($\frac{kN}{mm^2}$) | W_c ($\frac{kN}{m^3}$) |
|--------|-------------|-------------|-------------|-------------|-----------|-----------|------------------------|------|-----|-------------------------------|--------------------------------|-------------------------------|
| | | | | | | | (1) | (2) | drs | | | |
| SD1 | 101.6 | 1829 | 57.2 | 38.1 | 76.2 | 19.1 | 4 | 10 | T | 23.9 | 16.0 | 18.0 |
| SD2 | 101.6 | 1829 | 76.2 | 38.1 | 76.2 | 19.1 | 4 | 8 | T | 25.6 | 15.0 | 18.5 |
| SD3 | 101.6 | 1829 | 76.2 | 38.1 | 76.2 | 19.1 | 3 | 8 | T | 33.3 | 14.9 | 18.1 |
| SD4 | 101.6 | 1829 | 57.2 | 38.1 | 76.2 | 19.1 | 4 | 10 | T | 23.9 | 14.0 | 18.0 |
| SD5 | 102.0 | 1830 | - | - | 76.0 | 20.0 | 0 | 5 | S | 27.2 | 26.4 | 23.5 |
| SD6 | 102.0 | 1830 | - | - | 76.0 | 20.0 | 0 | 5 | S | 32.3 | 15.2 | 18.0 |
| SD7 | 101.6 | 1778 | 54.1 | 38.1 | 76.2 | 19.1 | 14 | 0 | T | 21.9 | 15.3 | 17.8 |
| SD8 | 101.6 | 1118 | 57.1 | 38.1 | 76.2 | 19.1 | 5 | 0 | T | 23.9 | 25.8 | 22.8 |
| SD9 | 101.6 | 1194 | 57.1 | 38.1 | 76.2 | 19.1 | 13 | 0 | T | 27.8 | 27.1 | 22.8 |
| SD10 | 101.6 | 1219 | 114.3 | 38.1 | 76.2 | 19.1 | 12 | 0 | T | 26.6 | 16.8 | 18.1 |
| SD11 | 101.6 | 1219 | 114.3 | 38.1 | 76.2 | 19.1 | 5 | 4 | T | 27.7 | 17.1 | 18.1 |
| SD11 | 101.6 | 1219 | 114.3 | 38.1 | 76.2 | 19.1 | 5 | 4 | T | 27.7 | 17.1 | 18.1 |
| SD12 | 133.4 | 1524 | 127.0 | 50.8 | 101.6 | 19.1 | 11 | 0 | T | 21.3 | 13.8 | 17.0 |
| SD13 | 101.6 | 1194 | 57.1 | 38.1 | 76.2 | 19.1 | 13 | 0 | T | 30.0 | 17.8 | 18.0 |
| SD14 | 101.6 | 1194 | 57.1 | 38.1 | 76.2 | 19.1 | 13 | 0 | T | 31.7 | 15.4 | 18.0 |
| SD15 | 101.6 | 1219 | 57.1 | 38.1 | 76.2 | 19.1 | 8 | 5 | T | 22.8 | 16.3 | 18.0 |
| SD16 | 88.9 | 1588 | 57.1 | 38.1 | 63.5 | 15.9 | 12 | 3 | T | 22.1 | 25.5 | 23.0 |
| SD17 | 101.6 | 1219 | 57.1 | 33.2 | 76.2 | 19.1 | 14 | 0 | T | 27.6 | 27.5 | 23.0 |
| SD18 | 101.6 | 1219 | 44.5 | 22.4 | 76.2 | 19.1 | 14 | 0 | T | 27.6 | 27.5 | 23.0 |
| SD19 | 88.9 | 1588 | 92.2 | 38.1 | 63.5 | 15.9 | 18 | 0 | T | 29.0 | 27.9 | 23.0 |
| SD20 | 88.9 | 1588 | 127.0 | 38.1 | 63.5 | 15.9 | 10 | 4 | T | 29.7 | 28.1 | 23.0 |
| SD21 | 158.8 | 2438 | 152.4 | 76.2 | 152.4 | 19.1 | 0 | 13 | T | 26.2 | 14.8 | 17.0 |
| SD22 | 228.6 | 2616 | 184.2 | 76.2 | 177.8 | 19.1 | 0 | 5(6) | T | 29.3 | 28.0 | 23 |
| SD23 | 101.6 | 1156 | 57.1 | 38.1 | 76.2 | 19.1 | 14 | 0 | T | 23.5 | 17.1 | 17.0 |
| SD24 | 102.0 | 1830 | - | - | 76.0 | 20.0 | 0 | 7 | S | 27.2 | 26.4 | 23.5 |

Table 4.10: Mean values of basic variables for steel beams and spans for samples in group D

| sample | A_a mm ² | h_g, h_{na} mm | t_w mm | b_f mm | t_f mm | f_y N/mm ² | L (span) m |
|-----------|--------------------------|---------------------|-------------|-------------|-------------|----------------------------|-----------------|
| CN1 | 7612.9 | 203.4 | 7.75 | 177.7 | 12.8 | 411.0 | 7.315 |
| CN2 | 7612.9 | 203.4 | 7.75 | 177.7 | 12.8 | 461.4 | 9.754 |
| CN3 | 8580.6 | 204.9 | 8.76 | 178.7 | 14.4 | 461.0 | 7.315 |
| CN4 | 7612.9 | 203.4 | 7.75 | 177.7 | 12.8 | 445.2 | 9.754 |
| CN5 | 10993.5 | 201.6 | 11.1 | 215.9 | 15.8 | 231.4 | 9.754 |
| CN6 | 7612.9 | 203.4 | 7.75 | 177.7 | 12.8 | 414.1 | 7.315 |
| CN7 | 7612.9 | 203.4 | 7.75 | 177.7 | 12.8 | 459.3 | 9.754 |
| CN8 | 7612.9 | 203.4 | 7.75 | 177.7 | 12.8 | 466.5 | 9.754 |
| CN9 | 7612.9 | 203.4 | 7.75 | 177.7 | 12.8 | 496.2 | 7.315 |
| CN10 | 8580.6 | 204.9 | 8.76 | 178.7 | 14.4 | 459.0 | 9.754 |
| CN11,SN1 | 7612.9 | 203.4 | 7.75 | 177.7 | 12.8 | 400.0 | 7.315 |
| CN12 | 8580.6 | 204.9 | 8.76 | 178.7 | 14.4 | 458.0 | 9.754 |
| CN13 | 7612.9 | 203.4 | 7.75 | 177.7 | 12.8 | 458.6 | 9.754 |
| CN14 | 6717.6 | 201.5 | 7.50 | 177.0 | 10.9 | 359.8 | 9.144 |
| CN15 | 6717.6 | 201.5 | 7.50 | 177.0 | 10.9 | 359.8 | 9.144 |
| CN16,SN2 | 2864.5 | 103.0 | 6.2 | 102.0 | 8.0 | 342.1 | 6.096 |
| CN17,SN3 | 5709.7 | 175.8 | 6.9 | 170.9 | 9.8 | 274.8 | 7.315 |
| CN18 | 10977.7 | 154.8 | 9.10 | 254.3 | 16.3 | 404.5 | 7.620 |
| CN19,SN4 | 5709.7 | 175.8 | 6.9 | 170.9 | 9.8 | 264.1 | 7.620 |
| CN20 | 5125.3 | 155.2 | 6.0 | 171.1 | 9.7 | 269.3 | 4.572 |
| CN21,SN5 | 5709.7 | 175.8 | 6.9 | 170.9 | 9.8 | 251.7 | 5.791 |
| CN22,SN6 | 11354.8 | 231.7 | 10.5 | 191.9 | 17.7 | 241.0 | 10.82 |
| CN23 | 3996.8 | 129.2 | 5.8 | 139.5 | 9.1 | 263.1 | 6.401 |
| CN24,SN13 | 9483.9 | 206.5 | 9.7 | 179.6 | 16.0 | 259.1 | 9.754 |
| CN25,SN14 | 9483.9 | 206.5 | 9.7 | 179.6 | 16.0 | 275.3 | 9.754 |
| CN26,SN15 | 9483.9 | 206.5 | 9.7 | 179.6 | 16.0 | 260.9 | 9.754 |
| CN27,SN16 | 8580.6 | 204.9 | 8.76 | 178.7 | 14.4 | 265.2 | 9.754 |
| CN28,SN17 | 8580.6 | 204.9 | 8.76 | 178.7 | 14.4 | 270.9 | 9.754 |
| CN29,SN7 | 12322.6 | 153.9 | 9.90 | 304.8 | 15.4 | 244.8 | 7.620 |
| CN30 | 7612.9 | 203.4 | 7.75 | 177.7 | 12.8 | 312.1 | 9.1444 |
| CN31,SN8 | 10451.6 | 299.4 | 10.0 | 177.9 | 12.8 | 265.5 | 10.638 |
| CN32,SN9 | 8387.1 | 262.4 | 8.9 | 165.1 | 11.4 | 286.2 | 12.192 |
| CN33,SN18 | 7270.0 | 180.0 | 8.00 | 170.0 | 12.7 | 454.8 | 7.778 |
| CN34,SN10 | 10400.0 | 264.2 | 9.6 | 208.7 | 13.2 | 327.0 | 10.000 |
| CN35,SN11 | 4180.0 | 156.4 | 6.6 | 102.4 | 10.8 | 297.0 | 8.000 |
| CN36 | 4180.0 | 156.4 | 6.6 | 102.4 | 10.8 | 325.0 | 8.000 |
| CN37,SN12 | 4180.0 | 156.4 | 6.6 | 102.4 | 10.8 | 307.0 | 8.000 |
| CN38 | 4180.0 | 156.4 | 6.6 | 102.4 | 10.8 | 317.0 | 8.000 |

Table 4.11: Mean values of basic variables for concrete slabs and shear connectors for samples in group D

| Sample | h_c mm | b_c mm | b_0 mm | h_p mm | h mm | d mm | studs in shear span | | | f_c ($\frac{N}{mm^2}$) | E_c ($\frac{kN}{mm^2}$) | W_c ($\frac{kN}{m^3}$) |
|-------------------------|-------------|-------------|-------------|-------------|-----------|-----------|------------------------|-----|-----|-------------------------------|--------------------------------|-------------------------------|
| | | | | | | | (1) | (2) | drs | | | |
| CN1 | 114.0 | 2032.0 | 76.0 | 51.0 | 88.9 | 19.1 | 4 | 10 | T | 25.6 | 14.96 | 18.5 |
| CN2 | 139.7 | 2438.4 | 114.0 | 76.0 | 114.3 | 19.1 | 0 | 13 | T | 22.4 | 13.72 | 18.1 |
| CN3 | 114.3 | 2032.0 | 101.6 | 50.8 | 88.9 | 19.1 | 0 | 10 | T | 34.0 | 17.38 | 19.8 |
| CN4 | 139.7 | 2438.4 | 152.0 | 76.0 | 114.3 | 19.1 | 4 | 7 | T | 29.0 | 15.79 | 18.8 |
| CN5 | 139.7 | 2438.4 | 114.0 | 76.0 | 114.3 | 19.1 | 1 | 12 | T | 25.9 | 12.48 | 19.3 |
| CN6 | 101.6 | 1828.8 | 57.0 | 38.0 | 76.2 | 19.1 | 11 | 0 | T | 30.0 | 17.17 | 18.3 |
| CN7 | 139.7 | 2438.4 | 114.0 | 76.0 | 114.3 | 19.1 | 5 | 2 | T | 28.5 | 16.65 | 17.8 |
| CN8 | 139.7 | 2438.4 | 114.0 | 76.0 | 114.3 | 19.1 | 2 | 5 | T | 27.5 | 16.45 | 17.8 |
| CN9 | 114.3 | 2032.0 | 102.0 | 51.0 | 88.9 | 19.1 | 9 | 0 | T | 33.4 | 17.24 | 18.5 |
| CN10 | 139.7 | 2438.4 | 152.0 | 76.0 | 114.3 | 19.1 | 0 | 2 | T | 22.4 | 14.41 | 18.7 |
| CN11,SN1 | 101.6 | 1828.8 | 57.0 | 38.0 | 76.2 | 19.1 | 4 | 10 | T | 31.8 | 14.96 | 18.1 |
| CN12 | 139.7 | 2438.4 | 152.0 | 76.0 | 114.3 | 19.1 | 4 | 7 | T | 27.3 | 15.17 | 19.1 |
| CN13 | 139.7 | 2438.4 | 152.0 | 76.0 | 114.3 | 19.1 | 4 | 7 | T | 33.4 | 17.79 | 19.6 |
| CN14 | 141.0 | 2440.0 | 181.5 | 76.0 | 116.0 | 19.0 | 8 | 0 | T | 21.3 | 26.33 | 23.5 |
| CN15 | 141.0 | 2440.0 | 152.5 | 76.0 | 116.0 | 19.0 | 10 | 0 | T | 21.9 | 26.58 | 23.5 |
| CN16,SN2 | 101.6 | 1117.6 | 57.2 | 38.1 | 76.2 | 19.1 | 4 | 0 | T | 22.9 | 25.39 | 22.8 |
| CN17,SN3 | 120.7 | 1473.2 | 152.4 | 44.5 | 88.9 | 19.1 | 0 | 5 | T | 21.4 | 15.47 | 18.0 |
| CN18 | 158.2 | 1828.8 | 184.2 | 76.2 | 114.3 | 19.1 | 0 | 7 | T | 28.0 | 16.92 | 18.0 |
| CN19,SN4 | 158.8 | 2438.4 | 101.6 | 76.2 | 139.7 | 19.1 | 0 | 8 | T | 32.7 | 15.90 | 17.0 |
| CN20 | 139.7 | 1219.2 | 103.1 | 76.2 | 127.0 | 19.1 | 0 | 4 | T | 33.1 | 14.96 | 18.0 |
| CN21,SN5 | 101.6 | 1219.2 | 57.1 | 38.1 | 76.2 | 19.1 | 5 | 9 | T | 22.8 | 16.34 | 18.0 |
| CN22,SN6 | 152.4 | 1828.8 | 143.0 | 76.2 | 127.0 | 19.1 | 16 | 1 | T | 22.8 | 16.34 | 18.0 |
| CN23 | 157.5 | 1270.0 | 66.8 | 76.2 | 127.8 | 19.1 | 6 | 0 | T | 33.1 | 24.07 | 23.0 |
| CN24,SN13 | 158.8 | 2438.4 | 152.4 | 76.2 | 114.3 | 19.1 | 0 | 13 | T | 22.8 | 13.28 | 16.5 |
| CN25,SN14 | 158.8 | 2438.4 | 152.4 | 76.2 | 139.7 | 19.1 | 0 | 13 | T | 27.1 | 14.07 | 16.5 |
| CN26,SN15 | 158.8 | 2438.4 | 152.4 | 76.2 | 127.0 | 19.1 | 0 | 13 | T | 25.1 | 13.38 | 16.3 |
| CN27,SN16 | 139.7 | 2413.0 | 184.2 | 76.2 | 127.0 | 19.1 | 0 | 6 | T | 30.7 | 28.49 | 23.0 |
| CN28,SN17 | 139.7 | 2413.0 | 152.4 | 76.2 | 127.0 | 19.1 | 0 | 6 | T | 30.3 | 27.76 | 22.8 |
| CN29,SN7 | 177.8 | 1828.8 | 184.2 | 76.2 | 114.3 | 19.1 | 1 | 10 | T | 26.6 | 16.64 | 18.0 |
| CN30 | 127.0 | 2209.8 | 152.4 | 76.2 | 114.3 | 19.1 | 12 | 0 | T | 22.7 | 25.77 | 23.0 |
| CN31,SN8 | 158.8 | 2616.2 | 184.2 | 76.2 | 127.0 | 19.1 | 4 | 7 | T | 27.9 | 16.90 | 18.0 |
| CN32,SN9 | 139.7 | 2400.3 | 171.5 | 76.2 | 124.5 | 19.1 | 0 | 10 | T | 23.9 | 26.21 | 23.0 |
| CN33,SN18 | 130.0 | 1500.0 | 114.5 | 51.0 | 100.0 | 19.1 | 13 | 0 | T | 35.3 | 29.85 | 23.0 |
| CN34,SN10 | 120.0 | 2500.0 | 150.0 | 60.0 | 100.0 | 19.0 | 17 | 0 | T | 34.6 | 29.65 | 23.0 |
| CN35, ¹ SN11 | 125.0 | 2000.0 | 150.0 | 50.0 | 100.0 | 19.0 | 5 | 0 | T | 33.6 | 24.3 | 19.5 |
| CN36 | 125.0 | 2000.0 | 150.0 | 50.0 | 100.0 | 19.0 | 3 | 0 | T | 35.2 | 19.3 | 19.5 |
| CN37, ² SN12 | 125.0 | 2000.0 | 150.0 | 50.0 | 100.0 | 19.0 | 4 | 0 | T | 32.0 | 20.3 | 19.5 |
| CN38 | 125.0 | 2000.0 | 150.0 | 50.0 | 100.0 | 19.0 | 2 | 0 | T | 32.0 | 24.0 | 19.5 |

¹ $\bar{E}_a = 207kN/mm^2$ ² $\bar{E}_a = 199kN/mm^2$

Table 4.12: Parameters of test correction for groups of beams

| | | \bar{b} | V_δ | ρ | number of specimens, n | number of laboratories |
|---------|---|-----------|------------|--------|--------------------------|------------------------|
| group A | | 1.139 | 0.074 | 0.999 | 27 | 4 |
| group B | | 1.187 | 0.090 | 0.999 | 21 | 5 |
| group C | using equilibrium method | 1.054 | 0.082 | 0.991 | 26 | 7 |
| | using linear interpolation | 1.140 | 0.091 | 0.991 | | |
| group D | using non-ductile model (Section 3.2.3) | 1.409 | 0.096 | 0.959 | 27 | ≈ 12 |
| | using equilibrium method | 1.076 | 0.080 | 0.970 | 48 | ≈ 12 |
| | using linear interpolation | 1.218 | 0.080 | 0.973 | | |

Table 4.13: Coefficients of variation of resistances in groups A and B

| group A | | | | group B | | | |
|---------|-----------|-------|----------------|---------|-----------|-------|----------------|
| sample | V_{r_t} | V_r | σ_{lnr} | sample | V_{r_t} | V_r | σ_{lnr} |
| S1 | 0.089 | 0.116 | 0.115 | H1 | 0.075 | 0.117 | 0.116 |
| S2 | 0.087 | 0.114 | 0.114 | H2 | 0.072 | 0.115 | 0.115 |
| S3 | 0.086 | 0.114 | 0.113 | H3 | 0.075 | 0.117 | 0.116 |
| S4 | 0.085 | 0.113 | 0.113 | H4 | 0.074 | 0.116 | 0.116 |
| S5 | 0.087 | 0.114 | 0.114 | H5 | 0.072 | 0.115 | 0.115 |
| S6 | 0.085 | 0.113 | 0.113 | H6 | 0.072 | 0.115 | 0.115 |
| S7 | 0.087 | 0.114 | 0.114 | H7 | 0.078 | 0.119 | 0.118 |
| S8 | 0.085 | 0.113 | 0.112 | H8 | 0.077 | 0.118 | 0.118 |
| S9 | 0.085 | 0.113 | 0.112 | H9 | 0.078 | 0.119 | 0.118 |
| S10 | 0.086 | 0.114 | 0.113 | H10 | 0.080 | 0.120 | 0.120 |
| S11 | 0.086 | 0.114 | 0.113 | H11 | 0.077 | 0.118 | 0.118 |
| S12 | 0.088 | 0.115 | 0.115 | H12 | 0.078 | 0.119 | 0.119 |
| S13 | 0.089 | 0.116 | 0.116 | H13 | 0.080 | 0.120 | 0.120 |
| S14 | 0.090 | 0.117 | 0.117 | H14 | 0.077 | 0.118 | 0.118 |

Table 4.14: Coefficients of variation of resistances in group C

| sample | Equilibrium method | | | linear interpolation | | |
|--------|--------------------|-------|----------------|----------------------|-------|----------------|
| | V_{rt} | V_r | σ_{lnr} | V_{rt} | V_r | σ_{lnr} |
| SD1 | 0.075 | 0.111 | 0.111 | 0.080 | 0.121 | 0.121 |
| SD2 | 0.075 | 0.111 | 0.111 | 0.080 | 0.121 | 0.121 |
| SD3 | 0.082 | 0.116 | 0.116 | 0.072 | 0.116 | 0.116 |
| SD4 | 0.075 | 0.111 | 0.111 | 0.080 | 0.121 | 0.121 |
| SD5 | 0.078 | 0.113 | 0.113 | 0.076 | 0.119 | 0.118 |
| SD6 | 0.078 | 0.113 | 0.113 | 0.075 | 0.118 | 0.117 |
| SD7 | 0.081 | 0.115 | 0.115 | 0.074 | 0.117 | 0.117 |
| SD8 | 0.078 | 0.113 | 0.113 | 0.074 | 0.117 | 0.117 |
| SD9 | 0.079 | 0.114 | 0.114 | 0.078 | 0.120 | 0.120 |
| SD10 | 0.079 | 0.114 | 0.114 | 0.073 | 0.117 | 0.116 |
| SD11 | 0.079 | 0.114 | 0.114 | 0.077 | 0.119 | 0.118 |
| SD12 | 0.078 | 0.113 | 0.113 | 0.073 | 0.117 | 0.117 |
| SD13 | 0.080 | 0.114 | 0.114 | 0.075 | 0.118 | 0.118 |
| SD14 | 0.080 | 0.115 | 0.114 | 0.074 | 0.117 | 0.117 |
| SD15 | 0.080 | 0.114 | 0.114 | 0.076 | 0.119 | 0.118 |
| SD16 | 0.082 | 0.115 | 0.115 | 0.072 | 0.116 | 0.116 |
| SD17 | 0.078 | 0.113 | 0.113 | 0.082 | 0.122 | 0.122 |
| SD18 | 0.078 | 0.113 | 0.113 | 0.082 | 0.123 | 0.122 |
| SD19 | 0.079 | 0.114 | 0.113 | 0.077 | 0.119 | 0.119 |
| SD20 | 0.079 | 0.114 | 0.113 | 0.077 | 0.119 | 0.119 |
| SD21 | 0.078 | 0.113 | 0.113 | 0.078 | 0.120 | 0.119 |
| SD22 | 0.078 | 0.113 | 0.113 | 0.080 | 0.121 | 0.121 |
| SD23 | 0.082 | 0.116 | 0.115 | 0.079 | 0.121 | 0.120 |
| SD24 | 0.078 | 0.113 | 0.113 | 0.083 | 0.123 | 0.123 |

Table 4.15: Coefficients of variation of resistances in group D (for non-ductile models)

| sample | propped construction | | | unpropped construction | | |
|--------|----------------------|-------|----------------|------------------------|-------|----------------|
| | V_{Rt} | V_R | σ_{lnr} | V_{Rt} | V_R | σ_{lnr} |
| SN1 | 0.067 | 0.117 | 0.117 | 0.067 | 0.117 | 0.117 |
| SN2 | 0.102 | 0.140 | 0.140 | 0.083 | 0.127 | 0.126 |
| SN3 | 0.117 | 0.151 | 0.151 | 0.103 | 0.140 | 0.140 |
| SN4 | 0.120 | 0.153 | 0.153 | 0.072 | 0.120 | 0.120 |
| SN5 | 0.116 | 0.151 | 0.150 | 0.109 | 0.145 | 0.144 |
| SN6 | 0.116 | 0.151 | 0.150 | 0.097 | 0.136 | 0.136 |
| SN7 | 0.117 | 0.151 | 0.151 | 0.099 | 0.138 | 0.137 |
| SN8 | 0.118 | 0.152 | 0.151 | 0.070 | 0.119 | 0.118 |
| SN9 | 0.119 | 0.153 | 0.152 | 0.071 | 0.119 | 0.119 |
| SN10 | 0.070 | 0.119 | 0.119 | 0.071 | 0.119 | 0.119 |
| SN11 | 0.121 | 0.155 | 0.154 | 0.089 | 0.131 | 0.130 |
| SN12 | 0.121 | 0.154 | 0.153 | 0.080 | 0.125 | 0.125 |
| SN13 | 0.117 | 0.151 | 0.151 | 0.089 | 0.131 | 0.130 |
| SN14 | 0.074 | 0.121 | 0.121 | 0.073 | 0.121 | 0.120 |
| SN15 | 0.117 | 0.152 | 0.151 | 0.070 | 0.119 | 0.119 |
| SN16 | 0.119 | 0.153 | 0.152 | 0.070 | 0.119 | 0.118 |
| SN17 | 0.119 | 0.153 | 0.152 | 0.086 | 0.129 | 0.129 |
| SN18 | 0.119 | 0.153 | 0.152 | 0.108 | 0.145 | 0.144 |

Table 4.16: Coefficients of variation of resistances in group D (for equilibrium method and linear interpolation)

| sample | Equilibrium method | | | linear interpolation | | |
|--------|--------------------|-------|----------------|----------------------|-------|----------------|
| | V_{rt} | V_r | σ_{lnr} | V_{rt} | V_r | σ_{lnr} |
| CN1 | 0.074 | 0.109 | 0.109 | 0.078 | 0.112 | 0.111 |
| CN2 | 0.075 | 0.110 | 0.109 | 0.079 | 0.113 | 0.112 |
| CN3 | 0.074 | 0.109 | 0.109 | 0.078 | 0.112 | 0.111 |
| CN4 | 0.074 | 0.109 | 0.109 | 0.074 | 0.109 | 0.109 |
| CN5 | 0.074 | 0.109 | 0.109 | 0.073 | 0.109 | 0.108 |
| CN6 | 0.075 | 0.110 | 0.109 | 0.079 | 0.113 | 0.112 |
| CN7 | 0.079 | 0.112 | 0.112 | 0.081 | 0.114 | 0.113 |
| CN8 | 0.078 | 0.112 | 0.111 | 0.080 | 0.113 | 0.113 |
| CN9 | 0.076 | 0.110 | 0.110 | 0.081 | 0.114 | 0.113 |
| CN10 | 0.077 | 0.111 | 0.111 | 0.082 | 0.114 | 0.114 |
| CN11 | 0.083 | 0.115 | 0.115 | 0.072 | 0.107 | 0.107 |
| CN12 | 0.075 | 0.110 | 0.109 | 0.079 | 0.113 | 0.112 |
| CN13 | 0.074 | 0.109 | 0.109 | 0.073 | 0.108 | 0.108 |
| CN14 | 0.074 | 0.109 | 0.108 | 0.073 | 0.108 | 0.108 |
| CN15 | 0.073 | 0.109 | 0.108 | 0.073 | 0.108 | 0.108 |
| CN16 | 0.072 | 0.108 | 0.107 | 0.072 | 0.107 | 0.107 |
| CN17 | 0.074 | 0.109 | 0.109 | 0.071 | 0.107 | 0.107 |
| CN18 | 0.076 | 0.110 | 0.110 | 0.079 | 0.112 | 0.112 |
| CN19 | 0.079 | 0.112 | 0.112 | 0.073 | 0.108 | 0.108 |
| CN20 | 0.074 | 0.109 | 0.109 | 0.074 | 0.109 | 0.108 |
| CN21 | 0.075 | 0.109 | 0.109 | 0.071 | 0.107 | 0.107 |
| CN22 | 0.074 | 0.109 | 0.108 | 0.076 | 0.110 | 0.110 |
| CN23 | 0.072 | 0.108 | 0.108 | 0.071 | 0.107 | 0.107 |
| CN24 | 0.073 | 0.108 | 0.108 | 0.071 | 0.107 | 0.107 |
| CN25 | 0.079 | 0.112 | 0.112 | 0.074 | 0.109 | 0.108 |
| CN26 | 0.080 | 0.113 | 0.113 | 0.072 | 0.107 | 0.107 |
| CN27 | 0.081 | 0.114 | 0.114 | 0.071 | 0.107 | 0.107 |
| CN28 | 0.073 | 0.109 | 0.108 | 0.071 | 0.107 | 0.107 |
| CN29 | 0.080 | 0.113 | 0.112 | 0.071 | 0.107 | 0.107 |
| CN30 | 0.074 | 0.109 | 0.109 | 0.077 | 0.111 | 0.111 |
| CN31 | 0.073 | 0.108 | 0.108 | 0.072 | 0.107 | 0.107 |
| CN32 | 0.074 | 0.109 | 0.108 | 0.072 | 0.108 | 0.108 |
| CN33 | 0.081 | 0.114 | 0.113 | 0.072 | 0.108 | 0.107 |
| CN34 | 0.083 | 0.115 | 0.115 | 0.072 | 0.108 | 0.108 |
| CN35 | 0.072 | 0.108 | 0.108 | 0.072 | 0.107 | 0.107 |
| CN36 | 0.073 | 0.108 | 0.108 | 0.073 | 0.108 | 0.108 |
| CN37 | 0.072 | 0.108 | 0.108 | 0.072 | 0.107 | 0.107 |
| CN38 | 0.075 | 0.109 | 0.109 | 0.076 | 0.110 | 0.110 |

samples S13 and S14 (as given in Table 4.6) were larger than the top flanges.

For group B, the tests collected were from five different research laboratories in three different countries: UK, U.S.A and Canada. These specimens are all of solid concrete slabs. It is not found that any of these specimens used lightweight concrete. The steel beam used for the specimen in sample H15 [48] was of larger bottom flange than the top. The rest of the specimens used steel beams with symmetrical sections, but, for beams in samples H5 and H6 [50], a cover plate (with the size given in Table 4.7) was attached to the steel bottom flange.

The reported test data for specimens in samples H5 to H14 did not include the positions of the reinforcement, however, the theoretical values of r_t calculated from the simple plastic theory and measured material strengths have been presented for all the specimens [50]. From the design diagrams shown in [50], the reinforcement should be placed somewhere close to the middle layer of the slab depth. Assuming the reinforcement being just placed in the middle layer of the slab depth, the calculated results only differ from the reported values of r_t by about 2% to 4%. It is then decided that the reported values of r_t , as shown in Table 4.2, are directly used in determining the test corrections, \bar{b} , V_δ , etc., while in the further calculations, the reinforcement for the samples from these specimens is assumed to be placed in the middle layer of concrete slabs.

The test results in group C were obtained from six different laboratories in U.S.A and one in Australia. Fourteen out of all the specimens have lightweight concrete, with density (W_c in Table 4.9) ranging from 17.0 to 18.5 kN/m³. Five specimens have solid slabs [52], and the others have profiled sheeting running transverse to the beam spans. The steel beam used in each of the specimens had a symmetrical section.

The test data for beams with non-ductile shear connectors (group D) were from about twelve different laboratories in four different countries: U.K, U.S.A, Canada and Germany. Most of the specimens have lightweight concrete of density (W_c in Table 4.11) from 16.5 to 19.5 kN/m³. All the specimens were simply

supported and had steel beams of symmetrical section.

Table 4.17: Partial safety factors for beams in groups A and B

| group A | | | | | group B | | | | |
|--------------------|-------|---------------|------------|------------|--------------------|-------|---------------|------------|------------|
| sample | k_d | γ_{md} | γ_a | γ_c | sample | k_d | γ_{md} | γ_a | γ_c |
| S1 | 3.202 | 0.979 | 1.064 | 1.207 | H1 | 3.306 | 0.961 | 1.044 | 1.105 |
| S2 | 3.205 | 0.967 | 1.050 | 1.191 | H2 | 3.313 | 0.952 | 1.035 | 1.095 |
| S3 | 3.208 | 0.955 | 1.038 | 1.177 | H3 | 3.304 | 0.963 | 1.046 | 1.107 |
| S4 | 3.209 | 0.948 | 1.030 | 1.168 | H4 | 3.309 | 0.958 | 1.041 | 1.102 |
| S5 | 3.206 | 0.964 | 1.048 | 1.188 | H5 | 3.313 | 0.954 | 1.037 | 1.097 |
| S6 | 3.210 | 0.928 | 1.009 | 1.144 | H6 | 3.313 | 0.953 | 1.036 | 1.096 |
| S7 | 3.206 | 0.919 | 0.998 | 1.132 | H7 | 3.295 | 0.971 | 1.056 | 1.117 |
| S8 | 3.210 | 0.931 | 1.011 | 1.147 | H8 | 3.299 | 0.968 | 1.052 | 1.113 |
| S9 | 3.210 | 0.930 | 1.010 | 1.146 | H9 | 3.296 | 0.970 | 1.055 | 1.116 |
| S10 | 3.208 | 0.956 | 1.039 | 1.178 | H10 | 3.290 | 0.976 | 1.061 | 1.122 |
| S11 | 3.207 | 0.957 | 1.040 | 1.180 | H11 | 3.299 | 0.968 | 1.052 | 1.114 |
| S12 | 3.203 | 0.975 | 1.060 | 1.202 | H12 | 3.295 | 0.972 | 1.056 | 1.117 |
| S13 | 3.200 | 0.977 | 1.062 | 1.204 | H13 | 3.290 | 0.976 | 1.061 | 1.123 |
| S14 | 3.198 | 0.985 | 1.071 | 1.214 | H14 | 3.299 | 0.968 | 1.052 | 1.113 |
| $\bar{\gamma}$ | | 0.955 | 1.037 | 1.177 | $\bar{\gamma}$ | | 0.965 | 1.049 | 1.110 |
| s.d.(s_γ) | | 0.022 | 0.024 | 0.027 | s.d.(s_γ) | | 0.009 | 0.010 | 0.010 |

In Tables 4.6 to 4.11, the values for material strengths are obtained from the measured results, while the geometric dimensions are generally the intended values in the designs. The entries for t_f and b_f in the tables are dimensions of the steel top flanges. Under the titles h_g , b_f and t_f , the bracketed values of S13 and S14 (their steel beams are not of symmetric sections) in Table 4.6 are the overall height of the steel section, breadth of the steel bottom flange and thickness of the bottom flange, respectively.

In Tables 4.9 and 4.11, most of the values for E_c were calculated from f_c and W_c , using equation (3.16). Furthermore, in these two tables, under “studs in shear span”, the subheadings (1) and (2) give the number of cross-sections where there were one and two studs, respectively. Thus, for example, the beam of sample SD1 (see Table 4.9) would have $4 + 2 \times 10 = 24$ studs in the shear span. Sample SD22 had six cross-sections at which there were three studs, as

Table 4.18: Partial safety factors for beams in group C

| sample | equilibrium method | | | | | linear interpolation | | | | |
|--------------------|--------------------|---------------|------------|------------|------------|----------------------|---------------|------------|------------|------------|
| | k_d | γ_{md} | γ_a | γ_c | γ_v | k_d | γ_{md} | γ_a | γ_c | γ_v |
| SD1 | 3.257 | 1.047 | 1.138 | 1.290 | 1.309 | 3.265 | 1.025 | 1.114 | 1.264 | 1.282 |
| SD2 | 3.258 | 1.047 | 1.137 | 1.290 | 1.308 | 3.266 | 1.025 | 1.113 | 1.262 | 1.281 |
| SD3 | 3.239 | 1.061 | 1.153 | 1.308 | 1.327 | 3.286 | 0.982 | 1.068 | 1.211 | 1.228 |
| SD4 | 3.257 | 1.047 | 1.138 | 1.290 | 1.309 | 3.265 | 1.025 | 1.114 | 1.263 | 1.282 |
| SD5 | 3.250 | 1.036 | 1.126 | 1.277 | 1.295 | 3.275 | 0.959 | 1.042 | 1.182 | 1.199 |
| SD6 | 3.250 | 1.040 | 1.130 | 1.281 | 1.299 | 3.279 | 0.962 | 1.045 | 1.186 | 1.203 |
| SD7 | 3.242 | 1.055 | 1.146 | 1.300 | 1.319 | 3.281 | 0.964 | 1.047 | 1.187 | 1.205 |
| SD8 | 3.249 | 1.027 | 1.116 | 1.266 | 1.284 | 3.281 | 0.958 | 1.041 | 1.180 | 1.197 |
| SD9 | 3.246 | 1.043 | 1.133 | 1.285 | 1.303 | 3.271 | 0.976 | 1.060 | 1.202 | 1.220 |
| SD10 | 3.246 | 1.046 | 1.137 | 1.289 | 1.308 | 3.282 | 0.962 | 1.045 | 1.185 | 1.202 |
| SD11 | 3.249 | 1.040 | 1.130 | 1.281 | 1.300 | 3.274 | 0.960 | 1.043 | 1.182 | 1.199 |
| SD12 | 3.249 | 1.041 | 1.132 | 1.283 | 1.302 | 3.282 | 0.961 | 1.045 | 1.185 | 1.202 |
| SD13 | 3.245 | 1.047 | 1.138 | 1.291 | 1.309 | 3.278 | 0.960 | 1.043 | 1.183 | 1.200 |
| SD14 | 3.244 | 1.051 | 1.142 | 1.295 | 1.313 | 3.282 | 0.962 | 1.046 | 1.186 | 1.203 |
| SD15 | 3.245 | 1.045 | 1.136 | 1.288 | 1.307 | 3.274 | 1.000 | 1.086 | 1.232 | 1.250 |
| SD16 | 3.241 | 1.058 | 1.150 | 1.304 | 1.323 | 3.287 | 0.976 | 1.060 | 1.202 | 1.219 |
| SD17 | 3.250 | 1.031 | 1.121 | 1.271 | 1.289 | 3.260 | 0.960 | 1.043 | 1.183 | 1.200 |
| SD18 | 3.250 | 1.031 | 1.121 | 1.271 | 1.289 | 3.260 | 0.960 | 1.043 | 1.183 | 1.200 |
| SD19 | 3.248 | 1.041 | 1.132 | 1.283 | 1.302 | 3.273 | 0.962 | 1.046 | 1.186 | 1.203 |
| SD20 | 3.248 | 1.041 | 1.132 | 1.283 | 1.302 | 3.273 | 0.962 | 1.046 | 1.186 | 1.203 |
| SD21 | 3.251 | 1.034 | 1.124 | 1.275 | 1.293 | 3.271 | 0.962 | 1.045 | 1.185 | 1.203 |
| SD22 | 3.251 | 1.035 | 1.125 | 1.275 | 1.294 | 3.266 | 0.964 | 1.048 | 1.188 | 1.205 |
| SD23 | 3.240 | 1.056 | 1.148 | 1.302 | 1.320 | 3.267 | 1.020 | 1.108 | 1.256 | 1.274 |
| SD24 | 3.251 | 1.027 | 1.116 | 1.266 | 1.284 | 3.258 | 0.961 | 1.044 | 1.184 | 1.201 |
| $\bar{\gamma}$ | | 1.043 | 1.133 | 1.285 | 1.304 | | 0.976 | 1.060 | 1.202 | 1.219 |
| s.d.(s_γ) | | 0.010 | 0.010 | 0.012 | 0.012 | | 0.024 | 0.026 | 0.030 | 0.030 |

Table 4.19: Partial safety factors for beams in group D (applied to non-ductile models)

| sample | propped construction | | | | | unpropped construction | | | | |
|--------------------|----------------------|---------------|------------|------------|------------|------------------------|---------------|------------|------------|------------|
| | k_d | γ_{md} | γ_a | γ_c | γ_v | k_d | γ_{md} | γ_a | γ_c | γ_v |
| SN1 | 3.302 | 0.796 | 0.865 | 0.981 | 0.996 | 3.303 | 0.798 | 0.867 | 0.983 | 0.998 |
| SN2 | 3.223 | 0.791 | 0.860 | 0.975 | 0.989 | 3.264 | 0.777 | 0.844 | 0.957 | 0.971 |
| SN3 | 3.197 | 0.818 | 0.889 | 1.008 | 1.022 | 3.222 | 0.804 | 0.874 | 0.991 | 1.006 |
| SN4 | 3.193 | 0.823 | 0.894 | 1.014 | 1.028 | 3.289 | 0.766 | 0.832 | 0.943 | 0.957 |
| SN5 | 3.198 | 0.816 | 0.887 | 1.005 | 1.020 | 3.211 | 0.809 | 0.879 | 0.997 | 1.011 |
| SN6 | 3.198 | 0.816 | 0.887 | 1.006 | 1.020 | 3.234 | 0.798 | 0.867 | 0.983 | 0.998 |
| SN7 | 3.197 | 0.818 | 0.889 | 1.008 | 1.022 | 3.229 | 0.802 | 0.871 | 0.988 | 1.002 |
| SN8 | 3.196 | 0.819 | 0.890 | 1.009 | 1.024 | 3.295 | 0.774 | 0.841 | 0.954 | 0.968 |
| SN9 | 3.194 | 0.821 | 0.892 | 1.011 | 1.026 | 3.292 | 0.792 | 0.860 | 0.975 | 0.989 |
| SN10 | 3.293 | 0.795 | 0.864 | 0.980 | 0.994 | 3.293 | 0.794 | 0.863 | 0.978 | 0.992 |
| SN11 | 3.190 | 0.825 | 0.897 | 1.017 | 1.032 | 3.251 | 0.796 | 0.864 | 0.980 | 0.994 |
| SN12 | 3.191 | 0.825 | 0.896 | 1.016 | 1.031 | 3.270 | 0.788 | 0.857 | 0.971 | 0.985 |
| SN13 | 3.197 | 0.818 | 0.889 | 1.008 | 1.022 | 3.249 | 0.793 | 0.861 | 0.977 | 0.991 |
| SN14 | 3.286 | 0.791 | 0.860 | 0.975 | 0.989 | 3.286 | 0.790 | 0.858 | 0.973 | 0.987 |
| SN15 | 3.197 | 0.818 | 0.889 | 1.008 | 1.022 | 3.294 | 0.781 | 0.849 | 0.962 | 0.976 |
| SN16 | 3.194 | 0.821 | 0.892 | 1.012 | 1.026 | 3.295 | 0.766 | 0.832 | 0.944 | 0.958 |
| SN17 | 3.194 | 0.821 | 0.892 | 1.012 | 1.026 | 3.255 | 0.792 | 0.860 | 0.975 | 0.989 |
| SN18 | 3.194 | 0.821 | 0.892 | 1.012 | 1.026 | 3.212 | 0.811 | 0.882 | 1.000 | 1.014 |
| $\bar{\gamma}$ | | 0.814 | 0.884 | 1.002 | 1.018 | | 0.791 | 0.859 | 0.975 | 0.989 |
| s.d.(s_γ) | | 0.014 | 0.015 | 0.018 | 0.018 | | 0.017 | 0.018 | 0.021 | 0.021 |

Table 4.20: Partial safety factors for beams in group D (applied to equilibrium method and linear interpolation)

| sample | equilibrium method | | | | | linear interpolation | | | | |
|--------------------|--------------------|---------------|------------|------------|------------|----------------------|---------------|------------|------------|------------|
| | k_d | γ_{md} | γ_a | γ_c | γ_v | k_d | γ_{md} | γ_a | γ_c | γ_v |
| CN1 | 3.185 | 1.010 | 1.097 | 1.244 | 1.262 | 3.178 | 0.917 | 0.996 | 1.130 | 1.146 |
| CN2 | 3.184 | 1.013 | 1.101 | 1.249 | 1.267 | 3.176 | 0.919 | 0.999 | 1.132 | 1.149 |
| CN3 | 3.185 | 1.009 | 1.097 | 1.244 | 1.262 | 3.179 | 0.916 | 0.996 | 1.129 | 1.145 |
| CN4 | 3.185 | 1.009 | 1.096 | 1.243 | 1.261 | 3.186 | 0.898 | 0.975 | 1.106 | 1.122 |
| CN5 | 3.186 | 1.008 | 1.095 | 1.242 | 1.260 | 3.187 | 0.889 | 0.966 | 1.095 | 1.111 |
| CN6 | 3.184 | 1.012 | 1.100 | 1.247 | 1.265 | 3.176 | 0.921 | 1.001 | 1.135 | 1.152 |
| CN7 | 3.177 | 1.028 | 1.117 | 1.267 | 1.285 | 3.174 | 0.920 | 1.000 | 1.134 | 1.150 |
| CN8 | 3.178 | 1.026 | 1.115 | 1.264 | 1.282 | 3.175 | 0.920 | 1.000 | 1.134 | 1.150 |
| CN9 | 3.183 | 1.016 | 1.104 | 1.252 | 1.270 | 3.174 | 0.918 | 0.998 | 1.132 | 1.148 |
| CN10 | 3.180 | 1.023 | 1.112 | 1.261 | 1.279 | 3.172 | 0.925 | 1.005 | 1.140 | 1.156 |
| CN11 | 3.170 | 1.031 | 1.120 | 1.270 | 1.288 | 3.190 | 0.900 | 0.978 | 1.110 | 1.126 |
| CN12 | 3.184 | 1.013 | 1.100 | 1.248 | 1.266 | 3.176 | 0.918 | 0.998 | 1.132 | 1.148 |
| CN13 | 3.186 | 1.007 | 1.095 | 1.241 | 1.259 | 3.187 | 0.888 | 0.964 | 1.094 | 1.109 |
| CN14 | 3.186 | 1.006 | 1.093 | 1.240 | 1.257 | 3.187 | 0.891 | 0.968 | 1.097 | 1.113 |
| CN15 | 3.187 | 1.005 | 1.092 | 1.238 | 1.256 | 3.188 | 0.886 | 0.963 | 1.092 | 1.108 |
| CN16 | 3.189 | 0.994 | 1.081 | 1.225 | 1.243 | 3.190 | 0.867 | 0.942 | 1.068 | 1.083 |
| CN17 | 3.186 | 1.006 | 1.093 | 1.239 | 1.257 | 3.190 | 0.870 | 0.946 | 1.073 | 1.088 |
| CN18 | 3.182 | 1.017 | 1.105 | 1.253 | 1.271 | 3.178 | 0.914 | 0.993 | 1.126 | 1.142 |
| CN19 | 3.177 | 1.002 | 1.089 | 1.235 | 1.252 | 3.188 | 0.871 | 0.946 | 1.073 | 1.088 |
| CN20 | 3.186 | 1.008 | 1.095 | 1.242 | 1.260 | 3.186 | 0.889 | 0.966 | 1.096 | 1.112 |
| CN21 | 3.184 | 1.010 | 1.097 | 1.244 | 1.262 | 3.190 | 0.898 | 0.976 | 1.106 | 1.122 |
| CN22 | 3.186 | 1.006 | 1.093 | 1.239 | 1.257 | 3.182 | 0.909 | 0.988 | 1.120 | 1.137 |
| CN23 | 3.188 | 0.998 | 1.085 | 1.230 | 1.248 | 3.190 | 0.878 | 0.954 | 1.082 | 1.098 |
| CN24 | 3.187 | 1.002 | 1.089 | 1.235 | 1.253 | 3.190 | 0.877 | 0.953 | 1.081 | 1.096 |
| CN25 | 3.178 | 1.009 | 1.096 | 1.243 | 1.261 | 3.186 | 0.867 | 0.942 | 1.069 | 1.084 |
| CN26 | 3.175 | 1.013 | 1.101 | 1.248 | 1.266 | 3.190 | 0.870 | 0.945 | 1.072 | 1.088 |
| CN27 | 3.174 | 1.014 | 1.102 | 1.249 | 1.267 | 3.190 | 0.873 | 0.949 | 1.076 | 1.092 |
| CN28 | 3.187 | 1.005 | 1.092 | 1.238 | 1.256 | 3.190 | 0.878 | 0.954 | 1.082 | 1.098 |
| CN29 | 3.176 | 1.015 | 1.103 | 1.251 | 1.269 | 3.191 | 0.870 | 0.946 | 1.073 | 1.088 |
| CN30 | 3.186 | 1.007 | 1.095 | 1.241 | 1.259 | 3.180 | 0.912 | 0.991 | 1.124 | 1.140 |
| CN31 | 3.188 | 1.000 | 1.086 | 1.232 | 1.250 | 3.190 | 0.874 | 0.950 | 1.077 | 1.092 |
| CN32 | 3.186 | 1.003 | 1.090 | 1.236 | 1.254 | 3.188 | 0.870 | 0.945 | 1.072 | 1.087 |
| CN33 | 3.174 | 0.990 | 1.076 | 1.220 | 1.237 | 3.189 | 0.889 | 0.966 | 1.096 | 1.111 |
| CN34 | 3.171 | 1.029 | 1.118 | 1.268 | 1.286 | 3.189 | 0.873 | 0.948 | 1.075 | 1.091 |
| CN35 | 3.189 | 0.996 | 1.083 | 1.228 | 1.246 | 3.190 | 0.872 | 0.948 | 1.075 | 1.091 |
| CN36 | 3.187 | 1.004 | 1.091 | 1.238 | 1.256 | 3.187 | 0.889 | 0.967 | 1.096 | 1.112 |
| CN37 | 3.188 | 0.999 | 1.086 | 1.231 | 1.249 | 3.190 | 0.880 | 0.957 | 1.085 | 1.100 |
| CN38 | 3.184 | 1.012 | 1.099 | 1.247 | 1.265 | 3.183 | 0.899 | 0.977 | 1.108 | 1.124 |
| $\bar{\gamma}$ | | 1.010 | 1.097 | 1.244 | 1.262 | | 0.893 | 0.970 | 1.100 | 1.116 |
| s.d.(s_γ) | | 0.009 | 0.010 | 0.011 | 0.012 | | 0.019 | 0.021 | 0.024 | 0.025 |

Table 4.21: Group C — failure probabilities and design fractile-factors of design resistances with given safety factors

| Sample | Equilibrium method | | | | Linear interpolation | | | |
|--------|--------------------|-------------------|-------------------|-------------------|----------------------|-------------------|-------------------|-------------------|
| | $\gamma_a = 1.10$ | | $\gamma_a = 1.05$ | | $\gamma_a = 1.10$ | | $\gamma_a = 1.05$ | |
| | $\gamma_c = 1.25$ | | $\gamma_c = 1.25$ | | $\gamma_c = 1.25$ | | $\gamma_c = 1.25$ | |
| | $\gamma_v = 1.25$ | | $\gamma_v = 1.25$ | | $\gamma_v = 1.25$ | | $\gamma_v = 1.25$ | |
| | k_d | $P_f \times 10^3$ | k_d | $P_f \times 10^3$ | k_d | $P_f \times 10^3$ | k_d | $P_f \times 10^3$ |
| SD1 | 2.934 | 3.14 | 2.597 | 8.03 | 3.134 | 1.84 | 2.792 | 4.84 |
| SD2 | 2.938 | 3.11 | 2.601 | 8.01 | 3.142 | 1.80 | 2.799 | 4.76 |
| SD3 | 2.814 | 4.17 | 2.487 | 9.91 | 3.517 | ≤ 1.2 | 3.175 | 1.74 |
| SD4 | 2.934 | 3.14 | 2.596 | 8.08 | 3.135 | 1.84 | 2.793 | 4.82 |
| SD5 | 3.013 | 2.42 | 2.729 | 5.62 | 3.690 | ≤ 1.2 | 3.481 | ≤ 1.2 |
| SD6 | 3.985 | 2.62 | 2.697 | 6.15 | 3.674 | ≤ 1.2 | 3.449 | ≤ 1.2 |
| SD7 | 2.864 | 3.67 | 2.544 | 8.84 | 3.669 | ≤ 1.2 | 3.429 | ≤ 1.2 |
| SD8 | 3.091 | 1.98 | 2.804 | 4.44 | 3.721 | ≤ 1.2 | 3.495 | ≤ 1.2 |
| SD9 | 2.970 | 2.73 | 2.662 | 6.72 | 3.538 | ≤ 1.2 | 3.237 | 1.36 |
| SD10 | 2.936 | 3.03 | 2.627 | 7.30 | 3.691 | ≤ 1.2 | 3.375 | ≤ 1.2 |
| SD11 | 2.990 | 2.57 | 2.692 | 6.22 | 3.690 | ≤ 1.2 | 3.477 | ≤ 1.2 |
| SD12 | 2.971 | 2.74 | 2.676 | 6.52 | 3.690 | ≤ 1.2 | 3.456 | ≤ 1.2 |
| SD13 | 2.928 | 3.10 | 2.616 | 7.49 | 3.693 | ≤ 1.2 | 3.415 | ≤ 1.2 |
| SD14 | 2.898 | 3.36 | 2.584 | 8.10 | 3.684 | ≤ 1.2 | 3.442 | ≤ 1.2 |
| SD15 | 2.946 | 2.93 | 2.634 | 7.16 | 3.341 | ≤ 1.2 | 3.034 | 2.43 |
| SD16 | 2.838 | 3.90 | 2.515 | 9.39 | 3.578 | ≤ 1.2 | 3.243 | 1.41 |
| SD17 | 3.065 | 2.13 | 2.777 | 4.85 | 3.655 | ≤ 1.2 | 3.479 | ≤ 1.2 |
| SD18 | 3.064 | 2.14 | 2.775 | 4.87 | 3.656 | ≤ 1.2 | 3.480 | ≤ 1.2 |
| SD19 | 2.976 | 2.68 | 2.674 | 6.52 | 3.662 | ≤ 1.2 | 3.446 | ≤ 1.2 |
| SD20 | 2.976 | 2.68 | 2.674 | 6.52 | 3.662 | ≤ 1.2 | 3.446 | ≤ 1.2 |
| SD21 | 3.028 | 2.34 | 2.749 | 5.31 | 3.655 | ≤ 1.2 | 3.455 | ≤ 1.2 |
| SD22 | 3.021 | 2.38 | 2.744 | 5.40 | 3.620 | ≤ 1.2 | 3.435 | ≤ 1.2 |
| SD23 | 2.857 | 3.72 | 2.532 | 9.02 | 3.173 | 1.66 | 2.855 | 3.96 |
| SD24 | 3.092 | 1.99 | 2.827 | 4.13 | 3.637 | ≤ 1.2 | 3.474 | ≤ 1.2 |

Table 4.22: Group D — failure probabilities and design fractile-factors of design resistances with given safety factors (applying equilibrium method and linear interpolation)

| Sample | Equilibrium method | | | | Linear interpolation | | | |
|--------|---|-------------------|---|-------------------|---|-------------------|---|-------------------|
| | $\gamma_a = 1.10$ $\gamma_c = 1.25$ $\gamma_v = 1.25$ | | $\gamma_a = 1.05$ $\gamma_c = 1.25$ $\gamma_v = 1.25$ | | $\gamma_a = 1.10$ $\gamma_c = 1.25$ $\gamma_v = 1.25$ | | $\gamma_a = 1.05$ $\gamma_c = 1.25$ $\gamma_v = 1.25$ | |
| | k_d | $P_f \times 10^3$ | k_d | $P_f \times 10^3$ | k_d | $P_f \times 10^3$ | k_d | $P_f \times 10^3$ |
| CN1 | 3.187 | ≤ 1.20 | 2.851 | 3.33 | 4.043 | ≤ 1.20 | 3.676 | ≤ 1.20 |
| CN2 | 3.152 | 1.37 | 2.809 | 3.72 | 4.020 | ≤ 1.20 | 3.644 | ≤ 1.20 |
| CN3 | 3.189 | ≤ 1.20 | 2.854 | 3.31 | 4.050 | ≤ 1.20 | 3.683 | ≤ 1.20 |
| CN4 | 3.192 | ≤ 1.20 | 2.857 | 3.28 | 4.276 | ≤ 1.20 | 3.894 | ≤ 1.20 |
| CN5 | 3.199 | ≤ 1.20 | 2.866 | 3.20 | 4.372 | ≤ 1.20 | 4.028 | ≤ 1.20 |
| CN6 | 3.165 | 1.31 | 2.825 | 3.58 | 3.994 | ≤ 1.20 | 3.620 | ≤ 1.20 |
| CN7 | 3.023 | 2.00 | 2.661 | 5.76 | 4.007 | ≤ 1.20 | 3.617 | ≤ 1.20 |
| CN8 | 3.045 | 1.88 | 2.686 | 5.37 | 4.010 | ≤ 1.20 | 3.621 | ≤ 1.20 |
| CN9 | 3.132 | 1.46 | 2.785 | 3.94 | 3.971 | ≤ 1.20 | 3.592 | ≤ 1.20 |
| CN10 | 3.067 | 1.77 | 2.710 | 4.99 | 3.953 | ≤ 1.20 | 3.571 | ≤ 1.20 |
| CN11 | 3.000 | 2.08 | 2.769 | 3.98 | 4.251 | ≤ 1.20 | 3.880 | ≤ 1.20 |
| CN12 | 3.160 | 1.33 | 2.819 | 3.63 | 4.027 | ≤ 1.20 | 3.652 | ≤ 1.20 |
| CN13 | 3.206 | ≤ 1.20 | 2.874 | 3.13 | 4.385 | ≤ 1.20 | 4.016 | ≤ 1.20 |
| CN14 | 3.219 | ≤ 1.20 | 2.890 | 2.98 | 4.353 | ≤ 1.20 | 3.974 | ≤ 1.20 |
| CN15 | 3.228 | ≤ 1.20 | 2.901 | 2.87 | 4.399 | ≤ 1.20 | 4.022 | ≤ 1.20 |
| CN16 | 3.322 | ≤ 1.20 | 3.021 | 2.08 | 4.609 | ≤ 1.20 | 4.330 | ≤ 1.20 |
| CN17 | 3.322 | ≤ 1.20 | 2.894 | 2.94 | 4.575 | ≤ 1.20 | 4.273 | ≤ 1.20 |
| CN18 | 3.124 | 1.50 | 2.775 | 4.04 | 4.079 | ≤ 1.20 | 3.706 | ≤ 1.20 |
| CN19 | 3.240 | ≤ 1.20 | 2.942 | 2.47 | 4.547 | ≤ 1.20 | 4.281 | ≤ 1.20 |
| CN20 | 3.200 | ≤ 1.20 | 2.868 | 3.19 | 4.363 | ≤ 1.20 | 4.019 | ≤ 1.20 |
| CN21 | 3.187 | ≤ 1.20 | 2.851 | 3.33 | 4.283 | ≤ 1.20 | 3.909 | ≤ 1.20 |
| CN22 | 3.186 | ≤ 1.20 | 2.896 | 2.92 | 4.127 | ≤ 1.20 | 3.774 | ≤ 1.20 |
| CN23 | 3.285 | ≤ 1.20 | 2.977 | 2.33 | 4.488 | ≤ 1.20 | 4.174 | ≤ 1.20 |
| CN24 | 3.252 | ≤ 1.20 | 2.932 | 2.61 | 4.506 | ≤ 1.20 | 4.190 | ≤ 1.20 |
| CN25 | 3.181 | ≤ 1.20 | 2.880 | 3.00 | 4.574 | ≤ 1.20 | 4.321 | ≤ 1.20 |
| CN26 | 3.143 | 1.37 | 2.833 | 3.42 | 4.569 | ≤ 1.20 | 4.287 | ≤ 1.20 |
| CN27 | 3.137 | 1.39 | 2.822 | 3.51 | 4.539 | ≤ 1.20 | 4.245 | ≤ 1.20 |
| CN28 | 3.228 | ≤ 1.20 | 2.86 | 2.93 | 4.491 | ≤ 1.20 | 4.174 | ≤ 1.20 |
| CN29 | 3.124 | 1.46 | 2.812 | 3.62 | 4.576 | ≤ 1.20 | 4.279 | ≤ 1.20 |
| CN30 | 3.206 | ≤ 1.20 | 2.874 | 3.13 | 4.096 | ≤ 1.20 | 3.734 | ≤ 1.20 |
| CN31 | 3.274 | ≤ 1.20 | 2.964 | 2.39 | 4.531 | ≤ 1.20 | 4.235 | ≤ 1.20 |
| CN32 | 3.243 | ≤ 1.20 | 2.925 | 2.66 | 4.562 | ≤ 1.20 | 4.266 | ≤ 1.20 |
| CN33 | 3.352 | ≤ 1.20 | 3.030 | 1.94 | 4.365 | ≤ 1.20 | 4.012 | ≤ 1.20 |
| CN34 | 3.012 | 2.02 | 2.729 | 4.57 | 4.537 | ≤ 1.20 | 4.236 | ≤ 1.20 |
| CN35 | 3.302 | ≤ 1.20 | 3.001 | 2.19 | 4.542 | ≤ 1.20 | 4.257 | ≤ 1.20 |
| CN36 | 3.231 | ≤ 1.20 | 2.906 | 2.83 | 4.362 | ≤ 1.20 | 4.020 | ≤ 1.20 |
| CN37 | 3.279 | ≤ 1.20 | 2.969 | 2.37 | 4.468 | ≤ 1.20 | 4.148 | ≤ 1.20 |
| CN38 | 3.166 | 1.31 | 2.827 | 3.56 | 4.250 | ≤ 1.20 | 3.892 | ≤ 1.20 |

indicated by (6) in Table 4.11, and five cross-sections of two studs. The heading “drs” means the direction of the rib span (direction of profiled sheeting), and “T” indicates the rib runs transverse to the beam span and “S” means solid slab (i.e. no rib and sheeting).

No reported value of E_a was found from the data of most specimens. So, as considered in Section 3.2.3, $E_a = 210 \text{ kN/mm}^2$ has been assumed in calculation for those specimens and samples in group D.

Using data shown in Tables 4.1 to 4.5, the correlation coefficient ρ , the mean correction \bar{b} and the coefficient of variation V_δ have been calculated for beams represented by each of the test groups, as shown in Table 4.12.

Table 4.13 gives the calculated coefficients of variation, V_{r_t} , for each of the beam samples from test groups A and B, together with V_r and σ_{lnr} . The same coefficients for beams in groups C and D are shown in Tables 4.14 and 4.15. Table 4.16 also presents the coefficients of variation for beams in group D, but the resistance functions used are those originally developed for beams in group C (i.e. the equilibrium method and linear interpolation) [1].

The partial safety factors determined with respect to the target safety margin $P_f = 0.0012$ for the beam samples in each group are presented in Tables 4.17 to 4.20, where, “mean ($\bar{\gamma}$)” means the averaged values of the safety factors for all beam samples in the group, and “s.d. (s_γ)” stands for the standard deviation for the safety factors obtained. The design fractile-factors k_a listed in these tables are those corresponding to the failure probability, $P_f = 0.0012$.

In order to investigate the reliability of the design formulae with the given safety factors and the effect of changes in safety factors, the failure probability, with 75% confidence level, has been calculated for the design resistances of beams with partial shear connection. The equilibrium method and linear interpolation are taken as the investigation objectives. The calculations are made with respect to two conditions: (1) the Eurocode values of safety factors [1] are used: $\gamma_a = 1.10$, $\gamma_c = 1.25$, and $\gamma_v = 1.25$; (2) a smaller value of γ_a is used: $\gamma_a = 1.05$, $\gamma_c = 1.25$,

and $\gamma_v = 1.25$. Tables 4.21 and 4.22 present the obtained results, where the design fractile-factors corresponding to the given safety factors are also shown.

4.2 Reliability assessment of design bending resistances in Eurocode 4

4.2.1 Correlation and variation of the resistances

It can be seen from Tables 4.1 to 4.5 that, for each of the groups, the ratio of the experimental resistances to the predictions made with the measured (in principle) basic variables, denoted r_{ei}/r_{ti} for a specimen, varies within a narrow range. Such variations may be plotted against the experimental bending resistances, as shown in Figures 4.1 and 4.2 (where notation b stands for the ratio r_{ei}/r_{ti}).

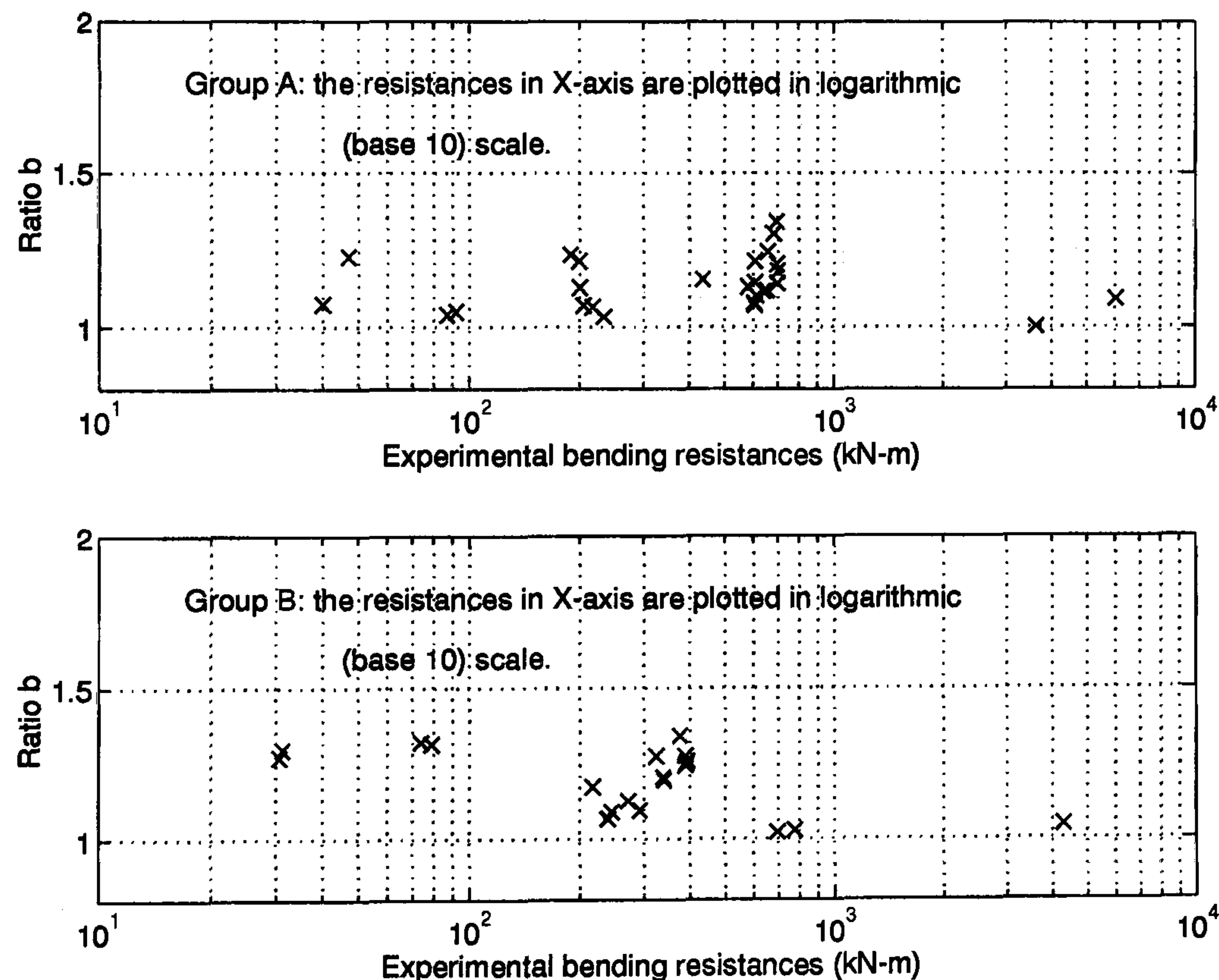


Figure 4.1: Ratio of experimental resistances to the theoretical predictions of beams with full shear connection

As a result, the small variation of r_{ei}/r_{ti} has led to low values of V_δ and high values of ρ for each of the groups, as shown in Table 4.12.

For beams with full shear connection and ductile partial shear connection, i.e.

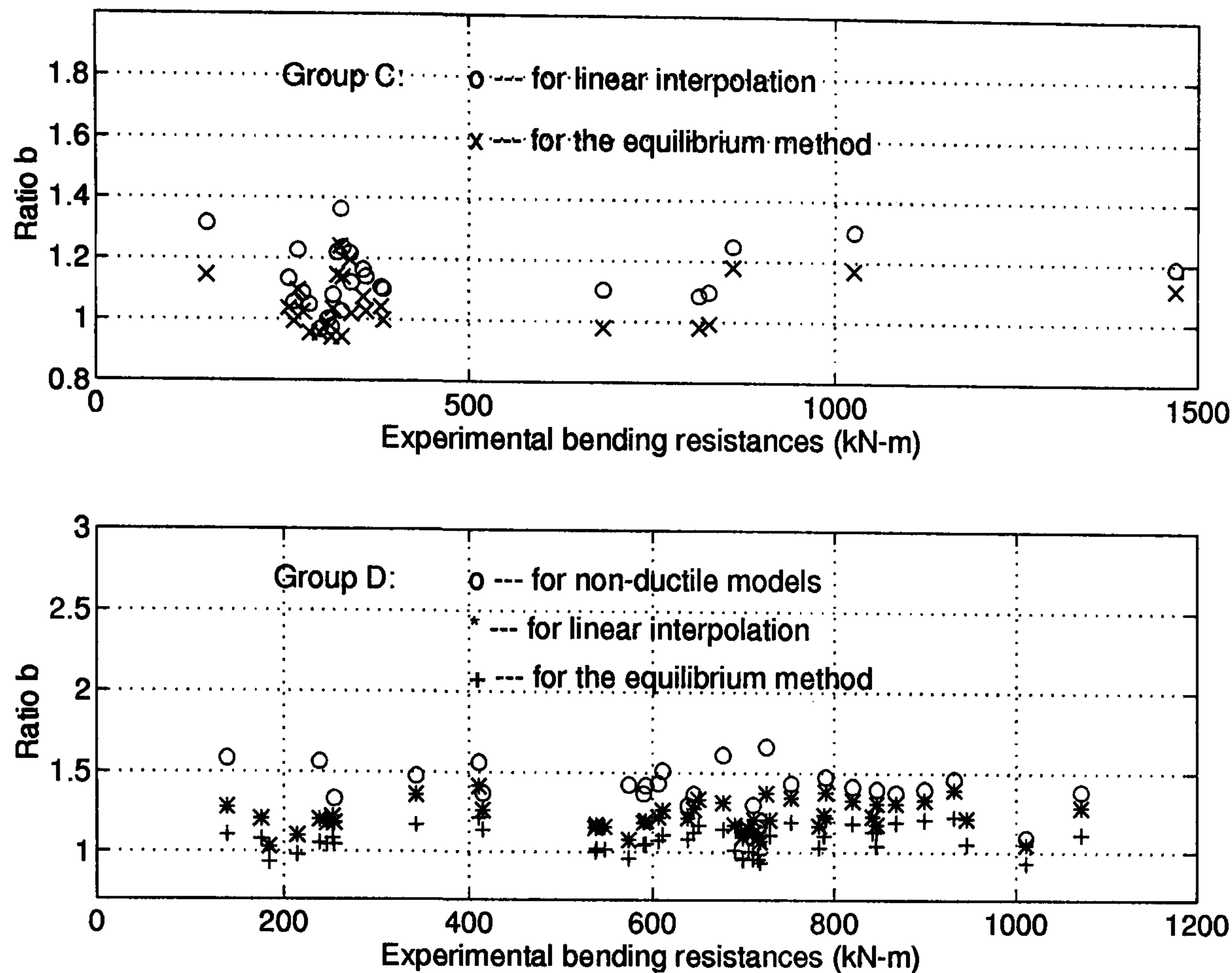


Figure 4.2: Ratio of experimental resistances to the theoretical predictions of beams with partial shear connection

beams in groups A, B and C, the test data shows that the predicted resistances are correlated to the actual resistances to a remarkably high level, all providing $\rho > 0.99$ (Table 4.12), which suggest that the theoretical models adopted by Eurocode 4 [1] for these types of beams are well related to the structural behaviours.

For beams with non-ductile shear connectors (group D), the results in Table 4.12 show that either the ductile models (the equilibrium method and linear interpolation) or non-ductile models (equation (3.19)) can also be judged to correlate to the real resistances satisfactorily, since ρ still ranges from 0.959 to 0.973. However, one may notice that \bar{b} ($= 1.409$) for the non-ductile model is considerably higher than the values for the other models (ranging from 1.054 to 1.218). It is thus expected that the resistance function (3.19) would be verified as being more conservative than the other models.

Being consistent with the small variation of r_{ei}/r_{ti} , all the values of V_{δ} obtained for the test groups are less than 10%, and are regarded to be quite low. This,

from another point of view, implies that the prediction based on the models are fairly proportional to the real resistances. It is interesting to see that the values of V_δ for each group are fairly consistent. The average value of all V_δ presented in Table 4.12 is about 0.085 which differs from the maximum value of V_δ ($= 0.095$) by only 8.5%.

In one word, it is judged that, compared with the accepted criterion ($\rho \geq 0.9$) [33], the Eurocode models for composite beams in bending are sufficiently correlated to the real structural resistances.

From Tables 4.13 to 4.16, one can also see that, except for the non-ductile models (Table 4.16), within the same group, the coefficients of variation of theoretical resistances, V_{R_t} , for the samples appear very consistent. The range of V_{R_t} obtained for the samples in groups A, B and C is summarized as follows,

- $V_{R_t} = 0.085 \sim 0.090$ in group A;
- $V_{R_t} = 0.072 \sim 0.080$ in group B;
- $V_{R_t} = 0.075 \sim 0.082$ and $0.072 \sim 0.083$ in group C for the equilibrium method and linear interpolation, respectively.

Therefore, the representative value of V_{R_t} for these groups may be taken as equal to the averaged value of V_δ , i.e. $V_{R_t} = V_\delta = 0.085$. Thus, from equation (3.24), the representative value of V_R for beams in groups A, B and C may be regarded as 0.120.

4.2.2 Safety margin underlying the recommended safety factors in Eurocode 4

Using coefficients of variation of basic variables given in Appendix B and data in Tables 4.6 to 4.12, the partial safety factors for the beam samples from each test group have been determined with respect to the target safety level: $P_f = 0.0012$, as shown in Tables 4.17 to 4.20. It can be seen from these tables that the safety

factors determined for beams with different dimensions and material strengths appear quite consistent with each other. The variations of the model factors for each group are ranged as follows,

- $\gamma_{\text{md}} = 0.919 \sim 0.985$ in group A (sagging bending with full shear connection);
- $\gamma_{\text{md}} = 0.952 \sim 0.976$ in group B (hogging bending with full shear connection);
- in group C (sagging bending with ductile partial shear connection), $\gamma_{\text{md}} = 1.031 \sim 1.061$ and $0.958 \sim 1.025$ for the equilibrium method and linear interpolation, respectively;
- in group D (sagging bending with non-ductile partial shear connection),
 $\gamma_{\text{md}} = 0.791 \sim 0.825$ and $0.774 \sim 0.809$ for non-ductile models considering propped construction and unpropped construction, respectively;
 $\gamma_{\text{md}} = 0.994 \sim 1.031$ and $0.867 \sim 0.921$ for the equilibrium method and linear interpolation, respectively.

As discussed in Section 2.2.3, corresponding to the safety factors used in Eurocode 4 (see equation (2.59)), the model factor can be generally regarded as 1.012, so, comparing the calibrated γ_{md} with this value, the safety margins provided by the safety factors adopted in this code can be assessed.

Therefore, based on γ_{md} calibrated for the samples from each group, the safety level of using the partial safety factors given in Eurocode 4 for designing bending resistances of composite beams can be judged as follows.

- **Sagging and hogging bending with full shear connection (groups A and B)** Using the safety factors given by code [1], a safety margin greater than that required can be achieved. With respect to the highest value of γ_{md} obtained in the two groups, the code values of the safety factors could be reduced by about 3%;

- **The equilibrium method for beams with ductile partial shear connection (group C)** As can be seen, the highest value of the calibrated γ_{md} appears higher than 1.012 by 4.8%, which means that the safety margin achieved would be smaller than that required. So, application of the equilibrium method to the beams gives $P_f > 0.0012$ and, for this model, the safety factors in the code [1] may need to be increased by about 4.5%. Nevertheless, as introduced in Section 2.1.1, $P_f = 0.0012$ is originally determined from the safety index $\beta = 3.8$ and the sensitivity factor $\alpha_r = 0.8$; according to the discussion in [33], $\beta = 3.8$ can be regarded as an average value defined for all the sub-sets of a resistance, and, for the most unfavourable sub-set, β may be reduced by 0.5. Therefore, taking $\beta = 3.3$, it can be obtained from equations 2.15 and 2.16 that $P_f = 4.15 \times 10^{-3}$. The failure probability P_f corresponding to the given safety factors have been calculated for beam samples from group C, as shown in Table 4.21. It can be seen from Table 4.21 that in using the equilibrium method with safety factors, $\gamma_a = 1.10$ and $\gamma_c = \gamma_v = 1.25$, even the highest value of P_f for the beam samples is only 4.17×10^{-3} (sample SN3). Therefore, the safety factors of Eurocode 4 may be still considered as acceptable when using the equilibrium method for beams in group C.
- **Linear interpolation for beams with ductile partial shear connection (group C)** Based on the code values [1] for the safety factors, the safety obtained from using this model could be lower than the target level, as the highest value (1.025) of the calibrated γ_{md} for this model is higher than 1.012. However, as shown in Table 4.18, the calibration on most of the beam samples leads to a γ_{md} lower than 1.012, and the highest value of the calibrated γ_{md} is only higher than 1.012 by about 1%. In Table 4.21, it is shown that, when the safety factors given in the code [1] are used, only a few of the beams samples in group C have failure probabilities greater than the target value $P_f = 0.0012$ (the highest one is only 0.00184). Hence, it

is concluded that application of linear interpolation with the safety factors given in code [1] can achieve sufficient safety margin.

- **Non-ductile models for beams with non-ductile shear connection (group D)** As expected from the high value of \bar{b} , the calibration of the safety factors shows that, if the safety factors given in the code [1] are used, then the resistance function (3.19) appears over-conservative. Taking the highest value of the calibrated γ_{md} , 0.825, into account and regarding $P_f = 0.0012$ as the target safety level, application of (3.19) to beams in group D would allow the values of safety factors in Eurocode 4 to be decreased by about 20%.
- **Ductile models for beams with non-ductile shear connection (group D)** In order to explore more reasonable models for beams with non-ductile connectors, the equilibrium method and linear interpolation were also calibrated for this type of beams; the results are given in Table 4.20. It is interesting to see that, using the linear interpolation approach, the model factors determined for all the samples appear lower than $\gamma_{\text{md}} = 1.012$, while for the equilibrium method, only a few of the samples obtained γ_{md} slightly higher than 1.012 (the highest one is 1.031, greater than $\gamma_{\text{md}} = 1.012$ by 1.9%). The failure probabilities corresponding to the safety factors specified by the code [1] for these situations are shown in Table 4.22, which shows that only a few of the samples reach a failure probability higher than $P_f = 0.0012$ (the highest one is only $P_f = 0.0021$). Hence, either the equilibrium method or linear interpolation approach may be considered for beams with non-ductile shear connectors.

In summary, it is recognized that, using the Eurocode values for γ_a , γ_c , γ_s and γ_v [1], the resistance functions in the code for beams with full shear connection and ductile partial shear connection (groups A, B and C) are good models, which provide design with sufficient safety margin and appear not over-conservative.

For beams with non-ductile shear connectors, the design based on the models and safety factors recommended by the code would be conservative.

4.2.3 Applicability of calibration results to Eurocode 4

It is obvious that, as shown in Tables 4.1 to 4.11, the data used in the analysis cannot cover the full range of the many relevant situations within the scope of Eurocode 4. Briefly speaking, this calibration only covers the reliability of plastic bending resistances of symmetrical T-composite beams with welded stud shear connection.

In general, the calibration has resulted in favourable comments on the design models of Eurocode 4 for bending resistances of composite beams, but these reliability analyses are based on

- (1) the limited quantity and range of test data;
- (2) the reported values of coefficients of variation for the basic variables (Table B.1), which were based on observations in rather few countries.

Besides the coefficients of variation of the basic variables, the most relevant effects for the calibration of the test data are considered as the size of specimen sections, the degree of shear connection, the beam span and the grade of concrete (i.e. lightweight or normal weight), which are discussed as follows.

Tables 4.1 to 4.5 show that, among the collected test data, few specimens are as large as some composite beams used in practice; taking the experimental results as the measurement, in group A, only two of the 27 sections had measured bending resistances exceeding 800 kN-m, while, in groups B and C, such sections are only counted as one of 21 and five of 26, respectively. For group D, the measured bending resistances range fairly uniformly from 139 kN-m to 1071.8 kN-m, but only two of the 48 sections had the measured bending resistances exceeding 1000 kN-m.

As shown in Figures 4.1 and 4.2, no clear evidence can be statistically drawn so far that larger beams would have r/r_t smaller (where, r and r_t stand for the real resistance and the predicted resistance, respectively), and the calibration would then present less favourable results. However, to assess the reliability for the larger beams, more relevant test data are needed for the analysis, as the larger beams may need to be treated as different sub-sets [33]. In practice, very large composite beams are common in bridge structures, but not for buildings, so, it is considered that the results obtained in this study can normally be applicable to composite beams in buildings.

One can see from Tables 4.3 to 4.5 that the degree of shear connection for beams in groups C and D varies from 0.465 to 0.942 and 0.086 to 0.537, respectively. These ranges are fairly complete for beams with partial shear connection in practice. However, it is realized that few beam specimens in groups C and D had long span (only one specimen in group C and three in group D had the spans longer than 10 m). As considered in the design code [1], when the beam spans become longer, the shear connectors could be less ductile and, in turn, the bending resistances could be less safe. Therefore, although the calibration has suggested conservatism in the method of Eurocode 4 for beams with non-ductile connectors, more experimental results on the beams with longer spans should be studied before the modification is made.

It has been indicated in Section 4.1 that many specimens in groups C and D were made of light-weight concrete. The ratio of the experimental resistances to the predicted results, r_{ei}/r_{ti} , for the specimens has been plotted against density of concrete: figures 4.3 and 4.4 shows the results for the resistance functions adopted in Eurocode 4. From the Figures, for the beams with light-weight concrete (approximately, $W_c \leq 18 \text{ kN/m}^3$), the ratios r_{ei}/r_{ti} seem, in terms of trend, slightly higher than those for beams with normal weight concrete ($W_c \approx 23 \text{ kN/m}^3$). This is perhaps because when light-weight concrete is used, the Young's modulus of concrete becomes lower (equation (2.16) and, from the Eurocode formula (equa-

tion (2.12), the strength of shear connection could be slightly underestimated. However, as shown in the figures, this variation (if any) is far from significant, and it can be still considered that the variation of the ratio r_{ei}/r_{ti} is uniform for specimens over the full range of concrete density.

It has been shown that the resistance functions for plastic bending resistances of beams with full shear connection [1,61] are well established. In these resistance functions (see Section 3.2.1 and Appendix C), the density of concrete is not related to the resistances of the beams with full shear connection (as guided by the codes [1,8], even the compressive strength of concrete need not to be modified when the concrete has light-weight density), therefore, it is considered that, although few test specimens in groups A and B have light-weight concrete, the calibration results are still suitable for the beams with full shear connection and light-weight concrete.

So, in summary, the calibration results are applicable to beams with either light-weight concrete or normal weight concrete.

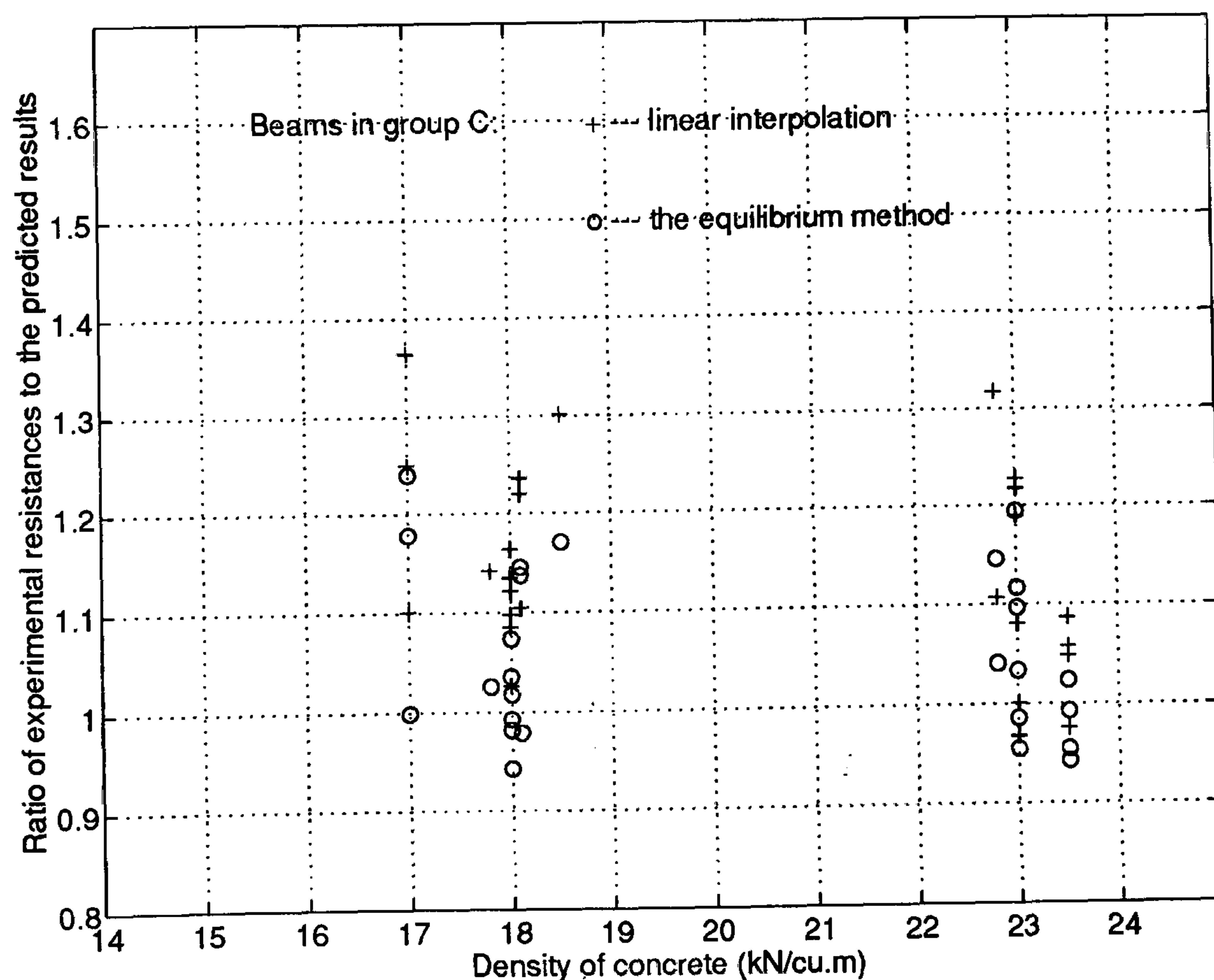


Figure 4.3: Ratio of experimental resistances to predicted results against concrete density (group C)

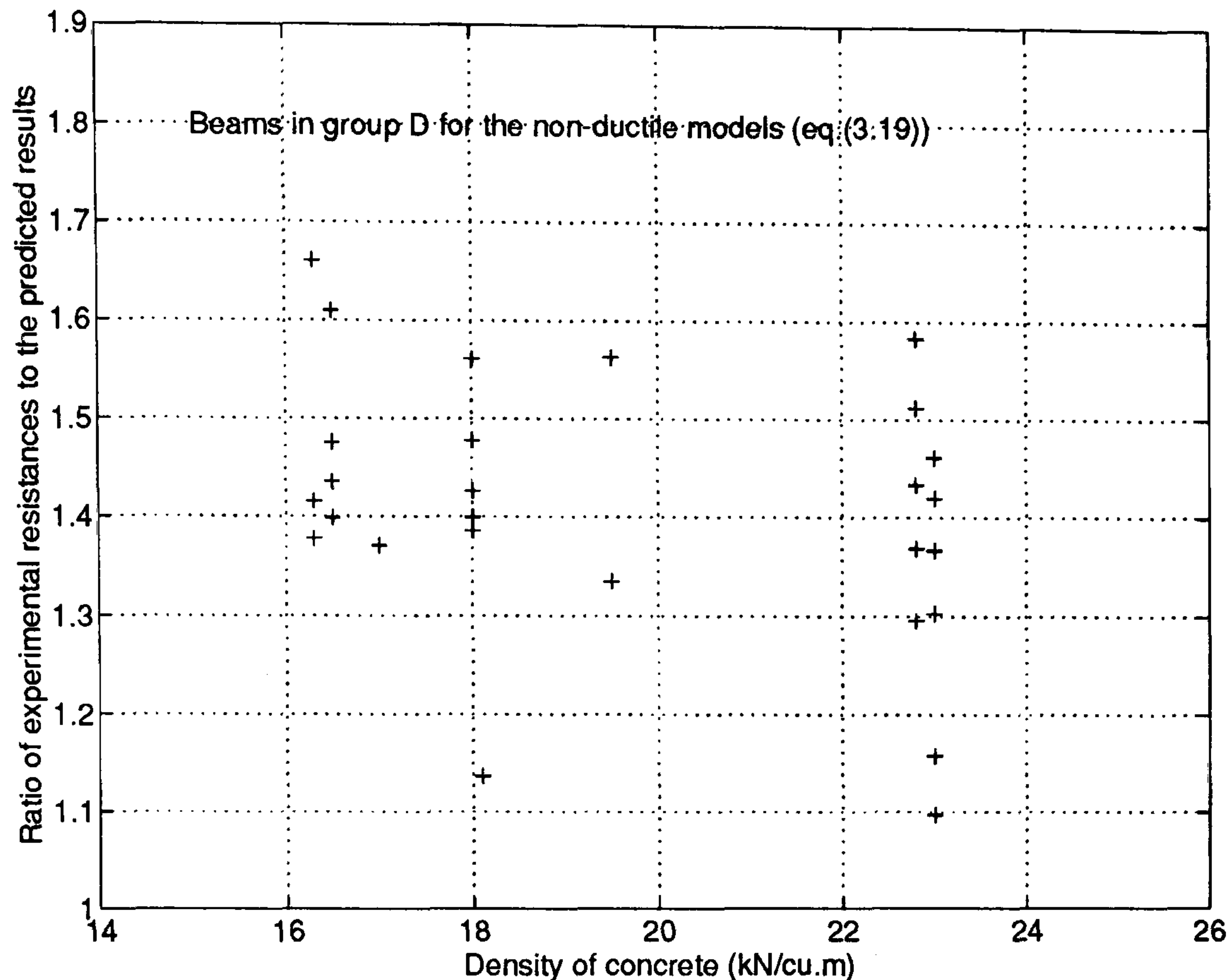


Figure 4.4: Ratio of experimental resistances to predicted results against concrete density (group D)

Most of the specimens in group C and D had profiled sheeting running transverse to the beam span (see Tables 4.9 and 4.11, only three samples from five specimens in group C had solid slabs), so there may be more confidence in applying the calibration results to beams with transverse sheeting. However, in practice, the normal reason of using partial shear connection is probably that the areas for placing studs are limited, while the main cause for such limited area is use of the transverse sheeting. In other words, it is likely that, in practice, most of beams with partial shear connection are those with transverse sheeting. Therefore, it is believed that the calibration made so far for beams in groups C and D is of significance for the common situations.

Apart from the properties of test specimens, another major influence on the calibration results is the evaluation of coefficients of variation for the basic variables. As indicated in Appendix B, it is very difficult to obtain comprehensive data for these parameters; the current analyses have to rely on the reported results given in Table B.1. The calculations show that the major contribution to

V_{r_i} is normally from the coefficients of variation of basic variables for steel beams, including those for the dimensions and strength.

For the linear dimensions of a steel cross-section, the feasibility of using the values given Table B.1 has been checked [62]. However, due to lack of information, it is still difficult to discover the relationship between coefficients of variation for the linear dimensions of a steel cross-section and those for its A_a , W_a , etc.

As an illustration, considering A_a of a rolled steel section, this variable is approximately given by

$$A_a = h_a b_f - (h_a - 2t_f)(b_f - t_w) \quad (4.1)$$

where the notation is as shown in Figure 3.1.

Assuming that h_a , b_f , t_f and t_w are independent random variables with the same coefficient of variation V , then, using equation (2.28), it can be shown for a typical steel section (254 × 146UB31) that $V_{A_a} = 1.031V \approx V$.

If, however, assuming that h_a , b_f , t_f and t_w were all proportional to a single variable Δ of coefficient of variation, V , such that $h_a = \bar{h}_a \Delta$, $b_f = \bar{b}_f \Delta$, $t_f = \bar{t}_f \Delta$ and $t_w = \bar{t}_w \Delta$, then it can be shown that $V_{A_a} = 2V$.

Therefore, if ignoring the other factors (e.g. the fillet between the web and flanges) V_{A_a} could be a value between V and $2V$.

Use of different values of V_{A_a} , V_{W_a} , etc. has considerable effects on the calibration results. For example, if assuming $V = 0.04$ and $V_{A_a} = 2V = 0.08$ and no changes in the other parameters, it can be calculated for beam samples in group A that the highest value of γ_{md} would be increased to 1.035; compared with the highest γ_{md} for group A (0.985) in Table 4.17, this value is greater by 5%, so γ_a could be increased from 1.05 to $1.05 \times 1.05 = 1.10$.

This study adopted $V_{A_a} = V_{W_a} = V_{I_a} = 0.04$ (Table B.1). These values are thought to be well established with respect to many factors, rather than the above simplified situation. Nevertheless, a check of these values should still be made when sufficient information becomes available.

Another important coefficient of variation for a steel beam is V_{f_y} . The effect of

this parameter on calibration results is of particular interests, as studied below.

4.3 Use of reduced γ_a -value

As commented in [40], “some members of CEN chose to use values of γ_a , for structural steel, that differ from the value 1.10 recommended in EC3 and EC4”. Therefore, further study of the effects on calibration of changes in γ_a and in the most relevant coefficient of variation, V_{f_y} , is carried out.

4.3.1 Effect of decreasing V_{f_y} on calibration

In order to reveal the effect of using smaller value for V_{f_y} , the safety factors have been re-calibrated for all the groups of beams, with V_{f_y} reduced from 0.08 to 0.04 while the other parameters are not changed. The averaged values ($\bar{\gamma}$) of safety factors so obtained for samples in groups A, B and C are listed in Table 4.23, corresponding to the title “case (2)”. In the same table, corresponding to the title “case (1)” are the $\bar{\gamma}$ -values presented in Tables 4.17 and 4.18 (which are based on $V_{f_y} = 0.08$).

It is noted here that

- (1) as shown in Tables 4.17 to 4.20, the scatter of the calibrated safety factors in a group is very small, so the averaged values can satisfactorily represent all the results for the beams in the group;
- (2) to simplify the presentation, the following discussion is made using results for groups A, B and C only; the analysis is also applicable to beams in group D.

Comparing the results in “case(2)” with “case(1)”, it is noticed that, based on the same target safety level, $P_f = 0.0012$, the calibrated safety factors are higher when V_{f_y} is decreased. This seems strange, as lower V_{f_y} means less uncertainty in the basic variable f_y and, therefore, the calibration results should be more favourable. Now, further analysis is presented.

First of all it is evident from equations (2.28) that, in absence of other changes, reduction of the coefficient of variation of a basic variable would result in smaller values of V_{rt} and, therefore, σ_{lnr} . For the design resistance determined from equation (2.31), it can be defined

$$w = \frac{r_d}{g_R(\underline{X}_p, \underline{X}_g)} = \bar{b} \exp(-k_d \sigma_{lnr} - 0.5 \sigma_{lnr}^2) \quad (4.2)$$

where σ_{lnr} and k_d are functions of V_{rt} (see equations (2.24), (2.29) and (2.32)).

Thus, using the known test corrections, \bar{b} , V_δ , etc., the variation of w against V_{rt} for beams in groups A, B and C can be shown in Figure 4.5. In this figure, V_{rt} stands for V_{rt} .

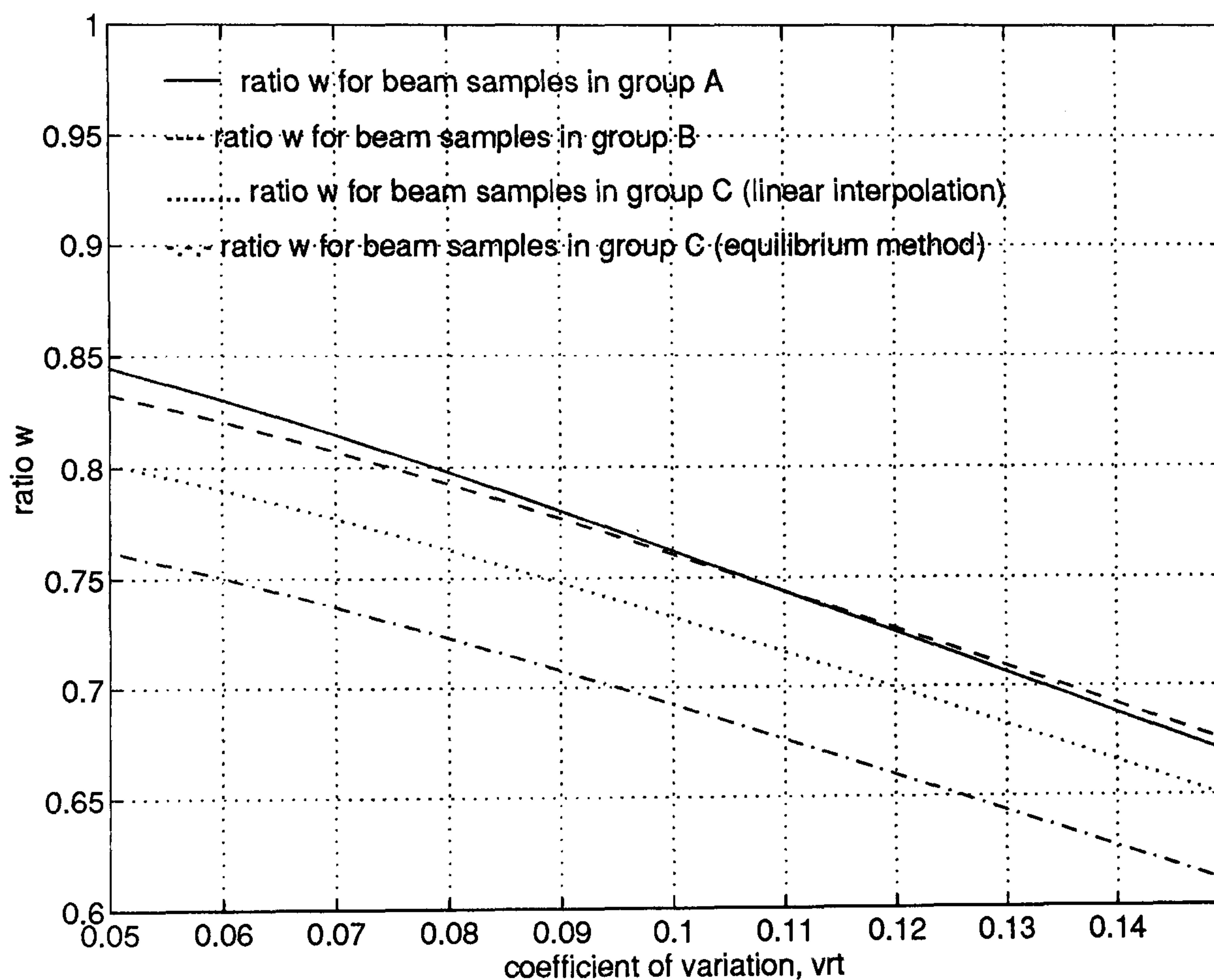


Figure 4.5: Relationship between calibrated design resistance, r_d , and coefficient of variation of resistance function, V_{rt}

Figure 4.5 shows that, when V_{rt} is reduced, using unchanged mean values of the basic variables and the same target safety level, an higher design resistance (but not lower safety factors) can be calibrated from equation (2.31). This confirms that reduction of coefficient of variation of any basic variable does improve

the overall safety margin for the design resistance.

However, since the base of calibration in case (2) is same as that in case (1) except for $V_{f_y} = 0.04$ rather than 0.08, the fractile-factor k_{as} for the characteristic strength of steel, f_{yk} , is 2.00 for both the calibrations. According to equation (2.34), reduction in V_{f_y} would then increase f_{yk} ; with respect to the situations studied here, when V_{f_y} is decreased from 0.08 to 0.04, for the same mean strength \bar{f}_y , f_{yk} would then be increased from $0.85\bar{f}_y$ to $0.92\bar{f}_y$. This would in turn increase the design resistance r_d given in (2.33). Therefore, applying equation (2.56), higher values of the safety factors may be obtained.

The above analysis shows that, if improvement of the quality control in steel production enables a lower value of V_{f_y} to be used and the characteristic strength of f_y is still specified by the old fractile-factor (i.e. $k_{as} = 2.00$ always), then the benefit of using the steel beams with better quality in structural design would be appear in the use of a higher f_{yk} , rather than lower safety factors.

If, however, when V_{f_y} becomes lower than the current accepted value, 0.08, no changes are made to either mean value or characteristic value of f_y , then for $V_{f_y} = 0.04$, f_{yk} is kept as $0.85\bar{f}_y$. Assuming no changes in all the other parameters and still using equations (2.49) and (2.54) to determine the material factors, the safety factors for the beams can be calibrated again; the results for groups A, B and C are shown in Table 4.23, corresponding to the title "case (3)". Now, one can see that, compared with "case (1)" ($V_{f_y} = 0.08$), γ_a is decreased for each group by about 4 ~ 5%, while changes in the other safety factors are negligible, which shows that, in absence of the other alterations, if the mean and characteristic strengths of steel are not changed when the coefficient of variation V_{f_y} is decreased, the favourable effect can be embodied in the adoption of a lower γ_a -value.

Extending the above analysis, it is inferred that, if the coefficient of variation of a material strength is reduced, and the mean and characteristic values of its strength, as well as the other factors, are not changed, then the relevant safety

Table 4.23: Effect of V_{fy} on safety factors

| | group A | | group B | | group C | | | | | |
|---|------------------|------------------|------------------|------------------|--------------------|------------------|------------------|----------------------|------------------|------------------|
| | $\bar{\gamma}_a$ | $\bar{\gamma}_c$ | $\bar{\gamma}_a$ | $\bar{\gamma}_s$ | equilibrium method | | | linear interpolation | | |
| | | | | | $\bar{\gamma}_a$ | $\bar{\gamma}_c$ | $\bar{\gamma}_v$ | $\bar{\gamma}_a$ | $\bar{\gamma}_c$ | $\bar{\gamma}_v$ |
| case (1) $V_{fy} = 0.08$ $f_{yk} = 0.85\bar{f}_y$ | 1.037 | 1.177 | 1.049 | 1.110 | 1.133 | 1.285 | 1.304 | 1.060 | 1.202 | 1.219 |
| case (2) $V_{fy} = 0.04$ $f_{yk} = 0.92\bar{f}_y$ | 1.047 | 1.237 | 1.068 | 1.179 | 1.153 | 1.362 | 1.382 | 1.081 | 1.278 | 1.296 |
| case (3) $V_{fy} = 0.04$ $f_{yk} = 0.85\bar{f}_y$ | 0.982 | 1.161 | 0.999 | 1.102 | 1.084 | 1.281 | 1.300 | 1.022 | 1.208 | 1.220 |

factor can be reduced for the design; however, if an higher characteristic strength of the material is used when its coefficient of variation becomes smaller, use of lower safety factors may reduce the safety.

Table 4.24 shows the maximum and minimum values of failure probabilities of the design resistance obtained for beam samples in group C, based on the given safety factors and the cases studied above. It can be seen that, for “case (2)”, as f_{yk} has been increased to $0.92\bar{f}_y$ ($= \exp\{-2.0 \times 0.04 - 0.5 \times 0.04^2\}\bar{f}_y$), although V_{fy} is 0.04, corresponding to the same safety factors, P_f appears even higher than that associated with $V_{fy} = 0.08$ (“case (1)”). By contrast, for “case (3)”, since the value of f_{yk} is same as that in “case (1)”, the reduction of V_{fy} , as expected, leads to lower P_f than that in “case (1)”.

4.3.2 Effect of reduction in γ_a on failure probabilities

Tables 4.21 and 4.22 show failure probabilities for the equilibrium method and linear interpolation, using different safety factors. It can be seen that, in absence of the other changes, when γ_a is reduced from 1.10 to 1.05, the failure probability P_f underlying the design resistances is considerably increased; applying the equilibrium method to beams in group C (Table 4.21), the maximum failure

Table 4.24: Effect of change of γ_a on failure probabilities in group C

| | Equilibrium method | | | | linear interpolation | | | |
|--|--------------------|--------------|-------------------|--------------|----------------------|---------------|-------------------|--------------|
| | $\gamma_a = 1.10$ | | $\gamma_a = 1.05$ | | $\gamma_a = 1.10$ | | $\gamma_a = 1.05$ | |
| | $\gamma_c = 1.25$ | | $\gamma_c = 1.25$ | | $\gamma_c = 1.25$ | | $\gamma_c = 1.25$ | |
| | $\gamma_v = 1.25$ | | $\gamma_v = 1.25$ | | $\gamma_v = 1.25$ | | $\gamma_v = 1.25$ | |
| | $P_{f,\min}$ | $P_{f,\max}$ | $P_{f,\min}$ | $P_{f,\max}$ | $P_{f,\min}$ | $P_{f,\max}$ | $P_{f,\min}$ | $P_{f,\max}$ |
| case (1) $V_{f_y} = 0.08$ $f_{yk} = 0.85\bar{f}_y$ | 0.0020 | 0.0042 | 0.0041 | 0.0099 | ≤ 0.0012 | 0.0018 | ≤ 0.0012 | 0.0048 |
| case (2) $V_{f_y} = 0.04$ $f_{yk} = 0.92\bar{f}_y$ | 0.0042 | 0.0096 | 0.0095 | 0.0234 | ≤ 0.0012 | 0.0038 | 0.00123 | 0.00107 |
| case (3) $V_{f_y} = 0.04$ $f_{yk} = 0.85\bar{f}_y$ | ≤ 0.0012 | 0.0016 | 0.0022 | 0.0046 | ≤ 0.0012 | ≤ 0.0012 | ≤ 0.0012 | 0.0017 |

probability found for the samples reaches 0.0099 when $\gamma_a = 1.05$ is used. Even for the linear interpolation approach, some samples in group C would have P_f exceeding the acceptable maximum value 4.15×10^{-3} [33].

Therefore, based on the obtained information, including the test data, the coefficients of variation of the basic variables, etc., this study shows that, in absence of the other changes, using $\gamma_a = 1.05$ cannot generally give satisfactory safety margins for the design of composite beams, and is not recommended.

However, if taking the results for “case (3)” given in Table 4.23 into account, acceptance of $\gamma_a = 1.05$ for design may be re-considered. As calculation shows, the most unfavourable sub-set for this calibration is beams in group C (using the equilibrium method), but in “case (3)”, only two samples (SN3 and SN16) have P_f over 4.15×10^{-3} . It can be seen from Table 4.24 that, corresponding to $\gamma_a = 1.05$, $\gamma_c = 1.25$ and $\gamma_v = 1.25$, even the highest failure probability (happened to sample SN3) in “case (3)” has been decreased to a level close to $P_f = 4.15 \times 10^{-3}$.

So, if V_{f_y} can be reduced from the current accepted value 0.08 to 0.04 and no alteration is made on either f_{yk} and \bar{f}_y , then, in absence of the other changes, use of $\gamma_a = 1.05$ with the other unchanged safety factors can generally provide the design of bending resistances of composite beams with satisfactory reliability.

Chapter 5

Conclusions for reliability of composite beams in bending

A reliability investigation has been carried out on purpose to calibrate partial safety factors used in Eurocode 4 for bending resistances in composite beams. Based on the earlier work [23,24,33-36], a general procedure of analyzing the design reliability of structural resistances has been developed, in relation to the test results of the structural resistances (Chapter 2). Following such a procedure, the calibration is made for the safety factors used in designing plastic bending resistances of composite beams in accordance with Eurocode 4 [1] (Chapters 3 and 4). The main conclusions from this study are drawn as follows.

1. The reliability analysis for a structural resistance can be made based on the relevant experimental results. To carry out such an analysis, the relevant test specimens may be classified into the same group if they follow the same resistance function; such a group of n different specimens can be assumed to represent up to n different populations of the structural members, and the ratio of real resistance to the predicted resistance for all the populations of the structural members in the same group may be assumed to have the same probability distribution.

2. To calibrate several different safety factors for a single design formula, a safety factor applied to a material strength can be considered to comprise two factors: a material factor which represents uncertainties of strength of the material, and a model factor which represents uncertainties in the theoretical model and the geometric dimensions of structural members; the feasibility of doing so is confirmed by calculation for the bending resistances of composite beams
3. Determination of safety factors from the specified safety target (i.e. $P_f = 0.0012$) and the inverse study (i.e. finding P_f from given safety factors) have been made for composite beams represented by four test groups:
 - group A — beams in sagging bending with full shear connection and the plastic neutral axis in the concrete slab;
 - group B — beams in hogging bending with full shear connection and the plastic neutral axis in the steel web;
 - group C — beams in sagging bending with “ductile” partial shear connection [1];
 - group D — beams in sagging bending with “non-ductile” partial shear connection [1].
4. Among the available test data (totally, 122 test results have been collected for the four groups), few specimens are as large as some beams used in practice, particularly in bridge structures; at the current stage, the results obtained in this study are considered applicable to the beams used in buildings, rather than bridges. Furthermore, for beams with partial shear connection, there is more confidence to apply the calibration results to the beams with transverse profiled sheeting, a type of beam that has partial shear connection.

-
5. The results obtained based on the collected test data can be used for beams with light-weight concrete or normal weight concrete, and for beams with a degree of shear connection within a wide range (say, $0.10 \leq N/N_f \leq 1.0$).
 6. The calibration is made based on the coefficients of variation of the basic variables taken from publications, which are believed to be well established; however, the illustrative analysis shows that the influence on calibration of changes in some of these coefficients could be considerable, so further check of these values should be made when sufficient information becomes available.
 7. With respect to the target failure probability, $P_f = 0.0012$, for the bending resistance in design to Eurocode 4, it is shown by the calibration that
 - the models used by Eurocode 4 for composite beams represented by these four groups are all highly correlated to the actual bending resistances, particularly for groups A, B and C;
 - for beams with full shear connection (groups A and B), a higher safety level than that required can be reached; in general, the code values of the safety factors could be reduced by about 3%;
 - for beams with “ductile” partial shear connectors (group C), application of the linear interpolation approach provides sufficient safety margin for the design, while when the equilibrium method is used, the safety margin achieved appears lower than that required, and, to match the safety level, $P_f = 0.0012$, the safety factors used in code [1] should be increased by up to about 4.5%. However, if allowing the reduced safety index $\beta = 3.3$ rather than 3.8 [33], the values of safety factors in Eurocode 4 are still acceptable when using the equilibrium method;
 - for beams with “non-ductile” partial shear connectors (group D), use of the model in the code (equation (3.19)) can lead to design safety

considerably higher than the target level. The safety factors for this model could be reduced by about 20%.

8. The calibration suggests that the design methods used in Eurocode 4 to beams in groups A, B and C are good models, but the model in this code for beams in group D is over conservative; it appears from Tables 4.20 and 4.22 that either of the methods for group C may even be safely used for beams in group D; however, as the collected test specimens do not have long span (say $L > 12.5$ m) and the connectors which may be less ductile than the studs, further experimental study is needed before any change is made to the model given in Eurocode 4.
9. On condition of no changes occurring to the other factors, reduction of coefficient of variation of a material strength improves the overall safety margin for the design resistance; but, if this advantage is given to design by adopting an higher characteristic value of the material strength (at constant mean strength) then use of reduced safety factors may reduce the design safety. On the other hand, if no change is made to either the mean strength or characteristic strength, the reliability of using lower safety factors can be justified.
10. In particular, for steel strength f_y , calibration based on available test data shows that,
 - if V_{f_y} is reduced to half the current accepted value, 0.08, but no changes are made to both the mean value and characteristic value of f_y , then for beams in all the groups studied, the code value of γ_a may be reduced from 1.10 to 1.05 while no alteration needs to be made on the other safety factors.
 - however, if all the conditions are not changed, simply reducing γ_a from 1.10 to 1.05 can increase the failure probability P_f considerably. For

example, P_f for beams in group C can then be nearly up to 1%; so, with respect to the current knowledge about the uncertainties in the design parameters, use of such reduced γ_a is not agreed by this study.

Finally, it should be noted that since the test data collected are limited, the range of composite beams covered by Eurocode 4 is much wider than those calibrated in this study; this study has only calibrated the reliability of plastic bending resistances of symmetric T-composite beams with welded stud shear connection, and, even for such type of beams, more design situations as listed in Section C.2 of Appendix C should be studied, when sufficient test data are available.

Chapter 6

Theory for longitudinal shear resistance of reinforced concrete flanges

6.1 The recommendations in Eurocode 4

As indicated in Section 1.1, sufficient longitudinal shear resistance in the flange portion must be achieved in composite beams. Considering that the transverse reinforcement in concrete flanges can strengthen the longitudinal shear resistance in the same way as the stirrups in a concrete web for vertical shear [7], Eurocode 4 [1] suggests the resistance of a potential surface to shear failure to be given by:

$$v_R = 0.625f_{ct}A_{cv} + A_e f_s + v_p \quad (6.1)$$

$$\text{or} \quad v_R = 0.2f_c A_{cv} + v_p/\sqrt{3} \quad (6.2)$$

whichever is smaller, where:

v_R the longitudinal shear resistance per unit length along the shear surface under consideration;

f_{ct} the tensile strength of concrete; for design purpose, it should be taken as characteristic value based on the fractile-factor 0.05;

- f_c the cylinder strength of concrete; in design, the characteristic value f_c should be taken;
- A_{cv} the mean cross-sectional area per unit length of beam of the concrete shear surface under consideration;
- f_s the yield strength of the reinforcement; in design, the characteristic value f_{sk} should be taken;
- A_e the sum of the cross-sectional areas of transverse reinforcement (assumed to be perpendicular to the beam) per unit length of beam crossing the shear surface under consideration, including any reinforcement provided for bending of the slab;
- v_p the contribution of the sheeting, to be considered for situation of sheeting transverse to steel beam only, determined in accordance with the relevant provisions.

In presenting the formulae above, the partial safety factors are not included; f_{ct} and f_c represent the strengths of concrete in normal-weight or lightweight, so the reduction factor η for strength of lightweight concrete does not appear here.

Eurocode 4 also states that A_{cv} should include the rib area when using equation (6.1), but the rib area should be excluded from A_{cv} in using equation (6.2).

According to the truss-model, equation (6.1) is established with respect to the yield of transverse reinforcement and the failure of sheeting due to the transverse tension, while equation (6.2) is based on crushing failure of the concrete struts.

6.2 Shear resistance with failure of sheeting and reinforcement

As shown in Figure 1.1, when the cross-section of composite beam is subjected to a bending moment, the caused normal force F in the concrete flange results in shear force T and the transverse forces, $F_{tr,t}$ and $F_{tr,c}$, on the longitudinal

surface along the flange portion (as represented by region AC in Figure 1.1(b)). The concrete flange is thus subjected to longitudinal shear and in-plane bending simultaneously. The effect of in-plane bending needs to be considered in studying the longitudinal shear resistance.

6.2.1 The basic assumptions

The transverse reinforcement is normally used to resist the transverse tension. With reference to previous research [1,5], the assumptions for describing the behaviour of transverse reinforcement at the stage of longitudinal shear failure may be presented as

- (1) the transverse reinforcement is yielded all along the shear span considered.

Due to the in-plane bending, a part of concrete along the longitudinal surface must be in compression, so assumption (1) actually implies that the yielding region of the transverse reinforcement in tension is partly overlapped by the compression zone for the concrete, which is obviously an idealized picture of the stress distribution. However, the researches reported in [3,5] showed that, by assuming such an overlapping, the prediction of the shear resistance in reinforced concrete flange reasonably agreed with test results. Hence, assumption (1) is also adopted in this analysis.

When profiled sheets are used in the composite beams, the sheeting is normally orientated in a direction either parallel or perpendicular (transverse) to the steel beam, as shown in Figure 1.2. If transverse sheeting is continuous over the steel beam, or discontinuous but anchored by stud shear connectors welded to the steel beam, as shown in Figure 1.2(b), the sheets should be able to develop transverse resistance, and act as transverse reinforcement. Therefore, it is assumed here that

- (2) where transverse sheeting is continuous over the steel beam or anchored by stud shear connectors welded to the steel beam, the profiled sheeting per-

forms as transverse reinforcement and therefore can develop resistance to the transverse tension.

The similar resistance to transverse tension, however, can not be expected from sheets where the sheeting runs parallel to the steel beam. This is because the sheeting in this case is corrugated transversely, as shown in Figure 1.2(a). Nevertheless, if the connection of the parallel sheets to the steel beam is provided by studs welded directly through the sheets, as specified in Eurocode 4 (clause 6.6.3(2)), it can be considered that the profiled sheets, associated with resistance from concrete, and from transverse reinforcement to the transverse tension, can exert resistance directly in longitudinal shear. An assumption is made that

- (3) where parallel sheeting is anchored by stud shear connectors welded to the steel beam, the profiled sheets can develop resistance directly to longitudinal shear.

Where light transverse reinforcement is used, the tensile strength of concrete may have to be considered, otherwise, with respect to the existence of in-plane bending, it is difficult to explain the longitudinal shear resistance where little or no transverse reinforcement is used. Hence, the following assumption is made:

- (4) along the longitudinal surface, the tensile strength of concrete in the transverse tension zone can be considered, to contribute to the resistance to transverse tension.

Since the concrete would normally be cracked if the reinforcement is yielded (assumption 1), this assumption is actually made on a pragmatic base, by which, together with the other assumptions, the complex behaviour of concrete may be considered in predicting the longitudinal shear resistance. Analysis results from a model based on such assumptions needs to be checked against tests.

It has been realized [2,3,19] that, taking account of cracks existing in a concrete shear plan, the suitable relationship between the shear strength and the compressive stress developed in concrete may be described by the “shear-friction

+ cohesion" model, i.e.

$$\tau_c = c + K\sigma_c \quad (6.3)$$

where τ_c — the shear strength of concrete;

c — the apparent cohesion of concrete;

K — the friction factor;

σ_c — the compressive stress developed on the shear surface

From the previous studies [2,3,4], it may be taken that $c = 0.1f_{cu}$ and $K = 1.0$ where f_{cu} is the cube strength of concrete. According to the theory of concrete plasticity [10], when taking $K = 1.0$, then the cohesion c may also be taken as the tensile strength f_{ct} . In fact, f_{ct} may be considered as approximately equal to $0.1f_{cu}$. However, as the concrete tensile strength f_{ct} can vary between $\frac{1}{15}f_{cu}$ and $\frac{1}{8}f_{cu}$, it may be prudent to take the cohesion c as $0.8f_{ct}$, rather than f_{ct} directly. Therefore, it is assumed that

- (5) the shear strength in concrete is related to the compressive stress σ_c and the tensile strength f_{ct} as follows,

$$\tau_c = 0.8f_{ct} + \sigma_c \quad (6.4)$$

The theory presented in [3,4,5] for the longitudinal shear resistance in reinforced concrete flanges assumed that, on the cross-section where the bending moment M , and hence the normal force F on the transverse cross-section of concrete flange (Figure 1.1(b)) reaches the maximum value, the transverse shear force Q , as shown in Figure 1.1(b), is zero. In a non-elastic situation, the validity of this assumption can perhaps only be proved where the loads act on beam symmetrically and the maximum moment merely occurs at middle span. Regarding the more general situation, it is worth exploring what is the effect on the longitudinal shear resistance if the conditions of $Q = 0$ and $M = M_{max}$ do not appear at the same transverse cross-section. In order to produce manageable equations,

only the situation of beam subjected to a concentrated load is to be studied for this problem, and the following assumptions are made:

- (6) along the beam span, the variation of the normal force F on a transverse cross-section of the concrete flange is proportional to the bending moment;
- (7) the eccentricity of normal force F on the sections of $M = M_{\max}$ and $Q = 0$ is proportional to the distance from the section to the nearest support.

6.2.2 Governing equations

With respect to the assumptions made above, the ultimate resistance to longitudinal shear and in-plane bending in a composite beam may be analysed by considering the flange portion shown in Figure 6.1.

Apart from those given above, the following symbols are used here:

- v_{ps} strength developed in the sheets to longitudinal shear, per unit length along beam span;
- v_{pt}, v'_{pt} strength developed in the sheets to transverse tension;
- μ reduction factor for f_{ct} in considering the contribution of concrete to the transverse tension;
- n the eccentricity ratio;
- l the length of shear span under consideration, i.e. the distance from the section with maximum moment to the nearest support;
- L the total span of the beam;
- x the length of the zone of transverse compression in concrete;
- x_0 the distance between the section EG where $Q = 0$ and CD where $M = M_{\max}$, as shown in Figure 6.1.
- Q_0 the shear force on the longitudinal surface region between section CD and EG, as shown in Figure 6.1;

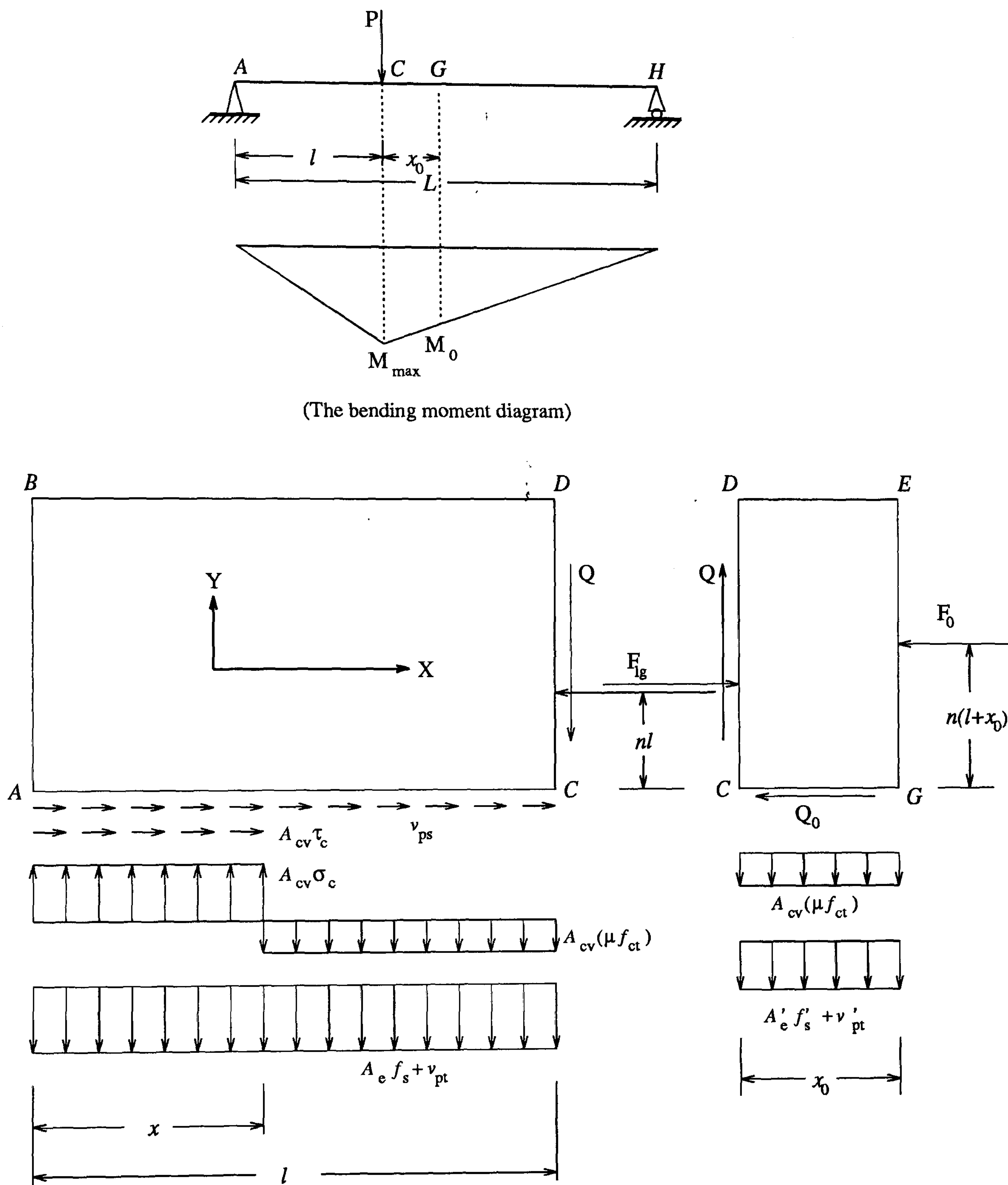


Figure 6.1: Calculation pattern of the shear resistance with respect to the failure of reinforcement and sheeting

- F_0 the normal force on flange portion where $Q = 0$;
- F_{lg} the normal force on flange portion at the section with M_{\max} ;
- P the concentrated load assumed on the beam to study the effect of $Q \neq 0$ on the longitudinal shear resistance.

From Figure 6.1, the equilibrium of part ABDC in direction X and Y leads to

$$lv_{ps} + xA_{cv}\tau_c - F_{lg} = 0 \quad (6.5)$$

$$xA_{cv}\sigma_c - (l-x)A_{cv}(\mu f_{ct}) - l(A_e f_s + v_{pt}) - Q = 0 \quad (6.6)$$

Taking moments about point A,

$$nlF_{lg} + A_{cv}\sigma_c \frac{x^2}{2} - Ql - (A_e f_s + v_{pt}) \frac{l^2}{2} - A_{cv}(\mu f_{ct}) \frac{(l^2 - x^2)}{2} = 0 \quad (6.7)$$

In these equilibrium equations, τ_c can be expressed in terms of f_{ct} and σ_c , as assumed by equation (6.4), f_{ct} , $A_e f_s$ and l refer to the tensile strength of concrete, the property of the reinforcement and the shear span considered, respectively, which can be known in advance for the given beam and load position. For v_{ps} and v_{pt} , it can be evaluated by considering the anchorage strength of sheeting to the stud shear connectors and the shear bond strength of the sheeting to concrete, which will be presented later. Therefore, the unknowns remain F_{lg} , σ_c , x , μ , n and Q .

Taking equilibrium of part CDEG in the Y-direction and rotation about point C,

$$Q - x_0[A_{cv}(\mu f_{ct}) + A'_e f'_s + v'_{pt}] = 0 \quad (6.8)$$

$$n(l+x_0)F_0 - nlF_{lg} - [A_{cv}(\mu f_{ct}) + A'_e f'_s + v'_{pt}]x_0^2/2 = 0 \quad (6.9)$$

According to assumption (6), for the moment distribution of a beam under a concentrated load, as shown in Figure 6.1, F_{lg} and F_0 can be related as follows,

$$F_0 = \frac{L - l - x_0}{L - l} F_{lg} \quad (6.10)$$

Substituting equation ((6.10)) into ((6.9)),

$$F_{lg} x_0 = \frac{[A_{cv}(\mu f_{ct}) + A'_e f'_s + v'_{pt}]}{2n[1 - (l + x_0)/(L - l)]} x_0^2 \quad (6.11)$$

It can be seen that one of the possible solutions for equation (6.11) is that $x_0 = 0$, which would lead to $Q = 0$, as assumed in the previous research [3,4,5]. However, as long as $l \neq L/2$, a non-zero x_0 is also possible for equation (6.11), which results in

$$F_{lg} = \frac{[A_{cv}(\mu f_{ct}) + A'_e f'_s + v'_{pt}]}{2n[1 - (l + x_0)/(L - l)]} x_0 \quad (6.12)$$

According to the explanation for equations (6.5) to (6.9), $A'_e f'_s$, v'_{pt} and L can also be known in advance, so the new unknown appearing in equations (6.8) and (6.12) is x_0 only.

Therefore, by using equations (6.4) to (6.8) and (6.12), F_{lg} , x , σ_c , τ_c , Q and x_0 can be determined by fixing the reduction factor μ for concrete tensile strength and the eccentricity ratio n for F_{lg} . The values of μ and n may have to be assumed, but the determination of these factors should be checked with respect to the tests on longitudinal shear resistance.

Substituting equation (6.4) into (6.5) and eliminating σ_c from equation (6.5) and (6.6), it is obtained that

$$v_R = \mu A_{cv} f_{ct} + A_e f_s + v_{ps} + v_{pt} + v_s + (0.8 - \mu) A_{cv} f_{ct} x/l \quad (6.13)$$

where, $v_s = Q/l$ and $v_R = F_{lg}/l$. It is easy to see that v_R is just the longitudinal shear resistance as defined in Section 6.1.

If it is assumed that $\mu = 0.8$, then equation (6.13) simply appears as

$$v_R = 0.8 A_{cv} f_{ct} + A_e f_s + v_{ps} + v_{pt} + v_s \quad (6.14)$$

This equation implies that, if v_s is ignored and in respect of failure caused by yielding of reinforcement and sheeting, the value 0.8 for μ leads to the longitudinal shear resistance v_R only depending on the concrete tensile strength and the strength from the sheeting and transverse reinforcement. This is consistent with the design method of Eurocode 4, as shown in equation (6.1).

Therefore, the μ is taken as 0.8 in the following analysis.

Since F_{lg} can be replaced by $v_R l$, substituting equation (6.14) into (6.7) and eliminating σ_c by using equation (6.6), the compression zone due to the in-plane bending can be found as

$$\chi = 1 - 2n - \frac{2nv_{ps} - v_s}{0.8f_{ct}A_{cv} + A_e f_s + v_{pt} + v_s} \quad (6.15)$$

where $\chi = x/l$.

Similarly, with $\lambda = x_0/l$, equation (6.8) gives

$$v_s = \lambda(0.8f_{ct}A_{cv} + A'_e f'_s + v'_{pt}) \quad (6.16)$$

From equations (6.14) and (6.16), it can be seen that if x_0 (hence λ) $\neq 0$, the longitudinal shear resistance v_R appears greater when considering v_s . The x_0 ($= \lambda l$) is therefore called the beneficial length to the v_R within the shear span under consideration.

Using $\mu = 0.8$, the following equation can be derived from equations (6.12), (6.14) and (6.16)

$$1 + \lambda\beta - \frac{\beta\lambda}{2n[1 - (1 + \lambda)/\alpha]} = 0 \quad (6.17)$$

where

$$\alpha = (L - l)/l \quad (6.18)$$

$$\beta = \frac{0.8f_{ct}A_{cv} + A'_e f'_s + v'_{pt}}{0.8f_{ct}A_{cv} + A_e f_s + v_{pt} + v_{ps}} \quad (6.19)$$

Solving equation (6.17) for λ ,

$$\lambda = \frac{1}{2\beta} \left[\sqrt{\left(\frac{\alpha\beta}{2n} - \alpha\beta + \beta + 1\right)^2 + 4\beta(\alpha - 1)} - \left(\frac{\alpha\beta}{2n} - \alpha\beta + \beta + 1\right) \right] \quad (6.20)$$

If n is assumed in advance, then λ can be found from equation (6.20), hence v_s can be found from equation (4.16). Knowing v_s and λ , the longitudinal shear resistance v_R can be determined from equation (6.14) and, if necessary, χ can be evaluated from equation (6.15).

The eccentricity factor n may be related to the effective width of the concrete slab b_{eff} . Based on the effective width b_{eff} , n may be found as

$$n = \frac{b_{\text{eff}} - b_s}{4l} \quad (6.21)$$

where b_s is the distance between the potential surfaces of shear failure, as shown in Figure 1.2.

It is realized that b_{eff} depends on many factors, such as the position of the cross section considered, the type of load, the geometry of the beam, etc [6,63]. The rigorous determination of b_{eff} is normally avoided, for simplicity. Eurocode 4 [1] recommends that, for all sections over the whole of beam span, b_{eff} at midspan may be used, and b_{eff} at midspan can be approximately taken as $L/4$. Compared with the tabular determination of b_{eff} given in BS5400 [6,63], the recommendation in Eurocode 4 can considerably overestimate b_{eff} when the cross-section is far away from midspan (say the section under point load at quarter-span).

Therefore, in order to make analysis of longitudinal shear manageable and more reasonable, it is simpler to assume that, wherever the maximum bending moment M_{max} occurs in the beam span, n , rather than b_{eff} , is a constant on the section of $M = M_{\text{max}}$.

If taking b_{eff} as $L/4$ for the section of $M = M_{\text{max}}$ at midspan and ignoring D , n would turn to be $(0.25L/4)/(0.5L) = 0.125$. If considering that the b_{eff} actually changes overall the beam span [6,63], n may appear greater than 0.125 for section of $M = M_{\text{max}}$ off midspan. To develop a simple theory for longitudinal

shear resistance and make analysis safe, a value of n higher than 0.125 would be better. So, in this study, n is assumed as 0.15 for analysing the longitudinal shear resistance. It is realised that adopting $n = 0.15$ is only an assumption and it may be modified if necessary. As recognized [9], the bending capacity of the composite beam is relatively insensitive to the value of effective width of slab. So this study still respects that b_{eff} may be taken as $L/4$ in determining the bending resistances in composite beam, as suggested by Eurocode 4 [1].

6.2.3 The effect of the beneficial length

From equation (6.14), it can be seen that, if by considering the effect of the beneficial length $x_0 (= \lambda l)$, a larger longitudinal shear resistance v_R can be obtained. It is necessary to study the effect from λl .

According to equations (6.16) and (6.19), v_R given in equation (6.14) may be expressed as follows,

$$v_R = (1 + \lambda\beta)(0.8A_{cv}f_{ct} + A_e f_s + v_{pt} + v_{ps}) \quad (6.22)$$

Therefore, the effect of λl is embodied in the term $\lambda\beta$. Using equation (6.20), $\lambda\beta$ can be given as follows,

$$\lambda\beta = \frac{1}{2} \left[\sqrt{\left(\frac{\alpha\beta}{2n} - \alpha\beta + \beta + 1\right)^2 + 4\beta(\alpha - 1)} - \left(\frac{\alpha\beta}{2n} - \alpha\beta + \beta + 1\right) \right] \quad (6.23)$$

In practice, the transverse reinforcement or transverse sheeting is normally arranged such that $A_e f_s + v_{pt} = A'_e f'_s + v'_{pt}$. Furthermore, according to assumption (2) in section 2.2.1, in determining the longitudinal shear resistance with respect to the failure in sheeting and reinforcement, v_{ps} is not considered when transverse sheeting is used, so, for beams with transverse sheeting or reinforcement, it can be taken $\beta = 1.0$. Therefore, for different n , curves of $\lambda\beta$ against α can be drawn, which are presented in Figure 6.2. From Figure 6.2, it is seen that, the larger the value of n , the greater is the beneficial effect, $\lambda\beta$. This is because, in this

model, the determination of the beneficial length x_0 is actually based on the effect of in-plane bending, which is inferred from equation (6.9) where $n \rightarrow 0$ would lead to $\lambda \rightarrow 0$, and the effect of in-plane bending would be more significant as n increases.

The same result can be also obtained when $\beta \neq 1.0$.

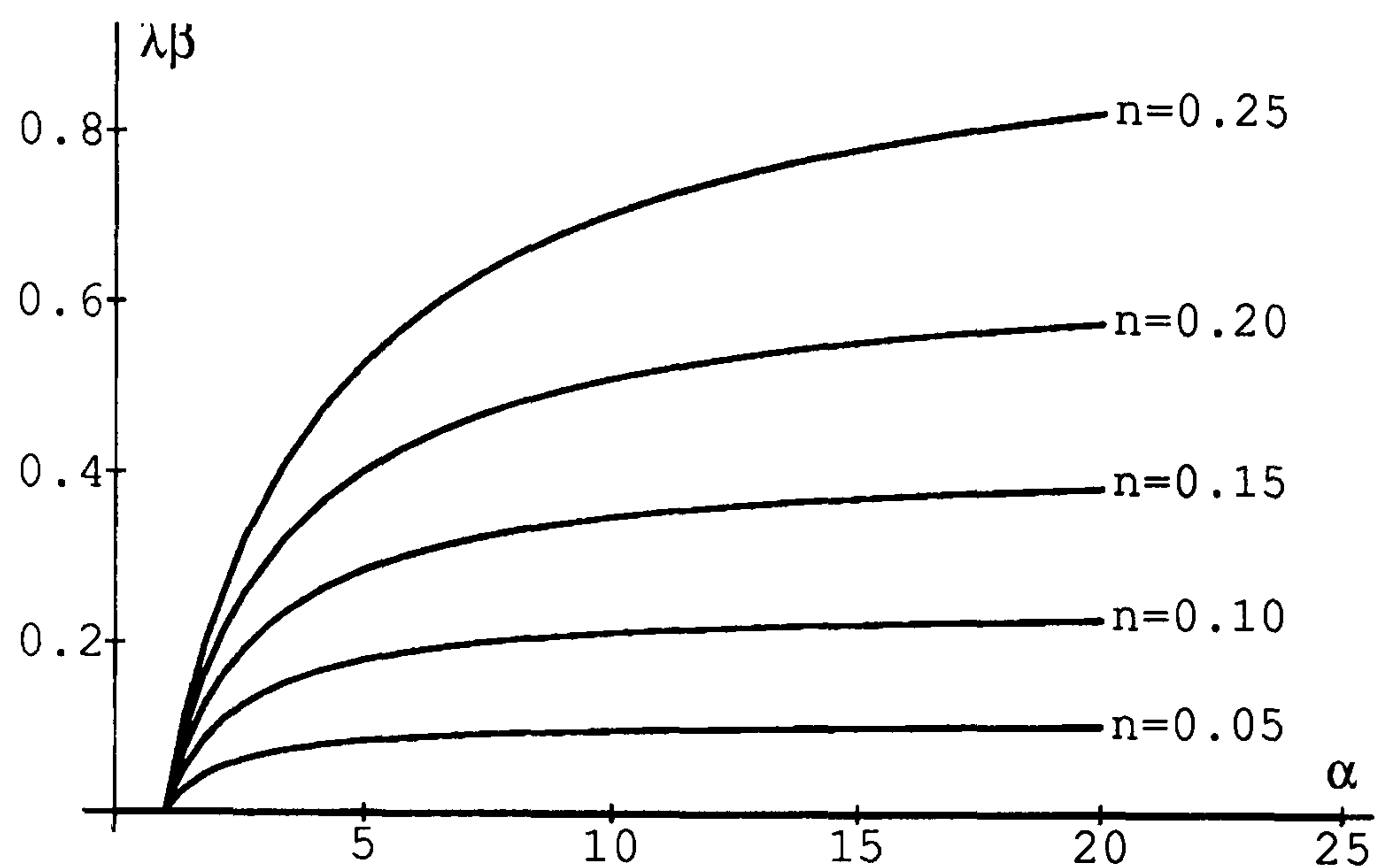


Figure 6.2: Variation of $\lambda\beta$ vs α with $\beta = 1.0$ and different n

Since a larger n would result in a larger v_s , according to equation (6.14) or (6.22); a larger v_R would also be obtained, but there is no evidence to support this. This method of studying the effect of the beneficial length is an approximation, developed by assuming n as constant rather than variable.

For a fixed n , e.g. $n = 0.15$ as assumed in Section 6.2.2, the approach given by equation (6.14) or (6.22) finds v_R in two phases: one determines the contributions within the shear span only, as given by $0.8A_{cv}f_{ct} + A_e f_s + v_{pt} + v_{ps}$, the other assesses the contribution from the beneficial length which is given by $(\lambda\beta)(0.8A_{cv}f_{ct} + A_e f_s + v_{pt} + v_{ps})$.

With a specified n , for different β , another group of curves for $\lambda\beta$ against α can be drawn. Using $n = 0.15$, such a group of curves is presented in Figure 6.3. From this Figure, it can be seen that, $\lambda\beta$ decreases as β gets smaller, but the variation

of β does not affect $\lambda\beta$ much when β is in its normal range $0.5 \sim 1.5$. From the definition of β in equation (6.19), it is known that the smaller β means the weaker strength in region CG, compared with that in shear span AC, and, therefore, the contributions from the beneficial length would appear smaller compared with those from the shear span under consideration. According to equation (6.22), $\lambda\beta$ actually represents the ratio of the contributions from the beneficial length to those from the shear span considered, so $\lambda\beta$ should be decreased if the smaller β appears.

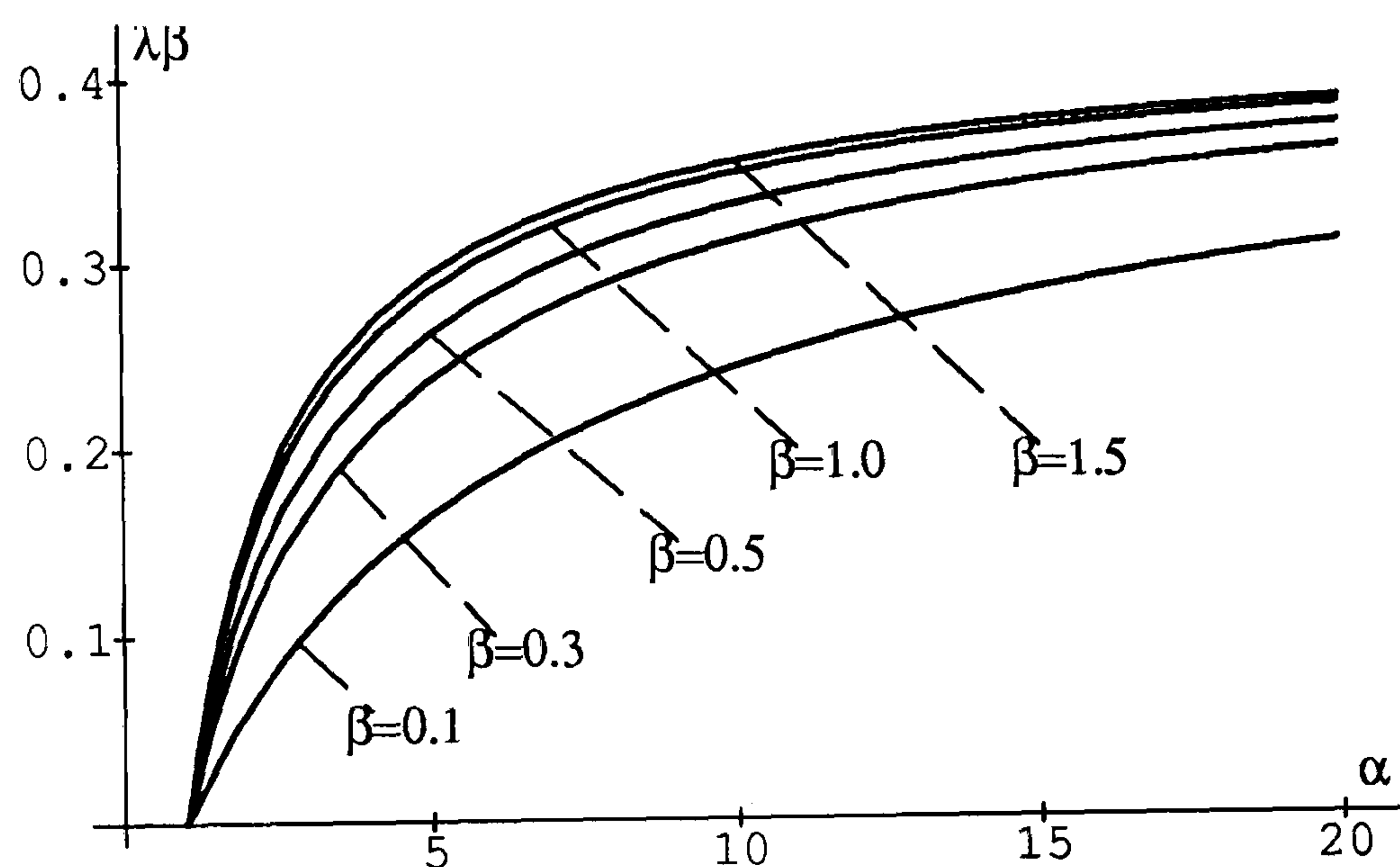


Figure 6.3: Variation of $\lambda\beta$ vs α , with $n = 0.15$ and different β

Equation (6.23) also suggests that, when $\alpha = 1$, $\lambda\beta = 0$, hence $\lambda = 0$. According to equation (6.18), $\alpha = 1$ corresponds to $l = L/2$. Therefore, if a point load P acts at midspan, the cross-section with the maximum moment would, even at the non-elastic state, coincide with that of $Q = 0$. Based on this result, it may be extensively considered that, for the beam under symmetric loading, the ultimate resistance to longitudinal shear may be determined ignoring the effect of Q , as in the previous research [4,5].

6.3 The shear resistance with crushing of concrete

From the analysis presented, the longitudinal shear resistance v_R can be determined with respect to the strengths of sheeting and transverse reinforcement. However, as visualised, when the transverse sheeting or reinforcement is very strong in transverse tension, longitudinal shear failure would not depend on tension failure in transverse sheeting or reinforcement. Instead, it would be caused by crushing of the concrete in the compression zone. Therefore, assumptions (1) and (2) made in Section 6.2.1 are no longer reasonable in this case, and the longitudinal shear resistance v_R should be determined based on the compression strength of concrete.

6.3.1 Crushing of the concrete struts

To obtain the longitudinal shear resistance v_R with respect to the compression strength of concrete, it is necessary to determine the maximum compression stress and shear stress which can be developed in concrete.

It has been understood [1,7] that, under the effect of longitudinal shear, a series of diagonal cracks would occur in the flange. Therefore, it can be idealized that a series of the independent concrete struts are formed as shown in Figure 6.4. In Figure 6.4, the new notation is used as follows:

- $\sigma_{c,m}$ the maximum compression stress in concrete on the longitudinal surface;
- $\tau_{c,m}$ the maximum shear stress in concrete on the longitudinal surface;
- σ'_c the compression stress in a concrete strut at crushing;
- $(A_e f_s)_m$ the tensile strength of transverse reinforcement developed at the crushing of concrete struts;

- $v_{pt,m}$ the tensile strength of transverse sheeting developed at the crushing of concrete struts;
- θ the angle between the diagonal crack (the strut) and the longitudinal shear surface;

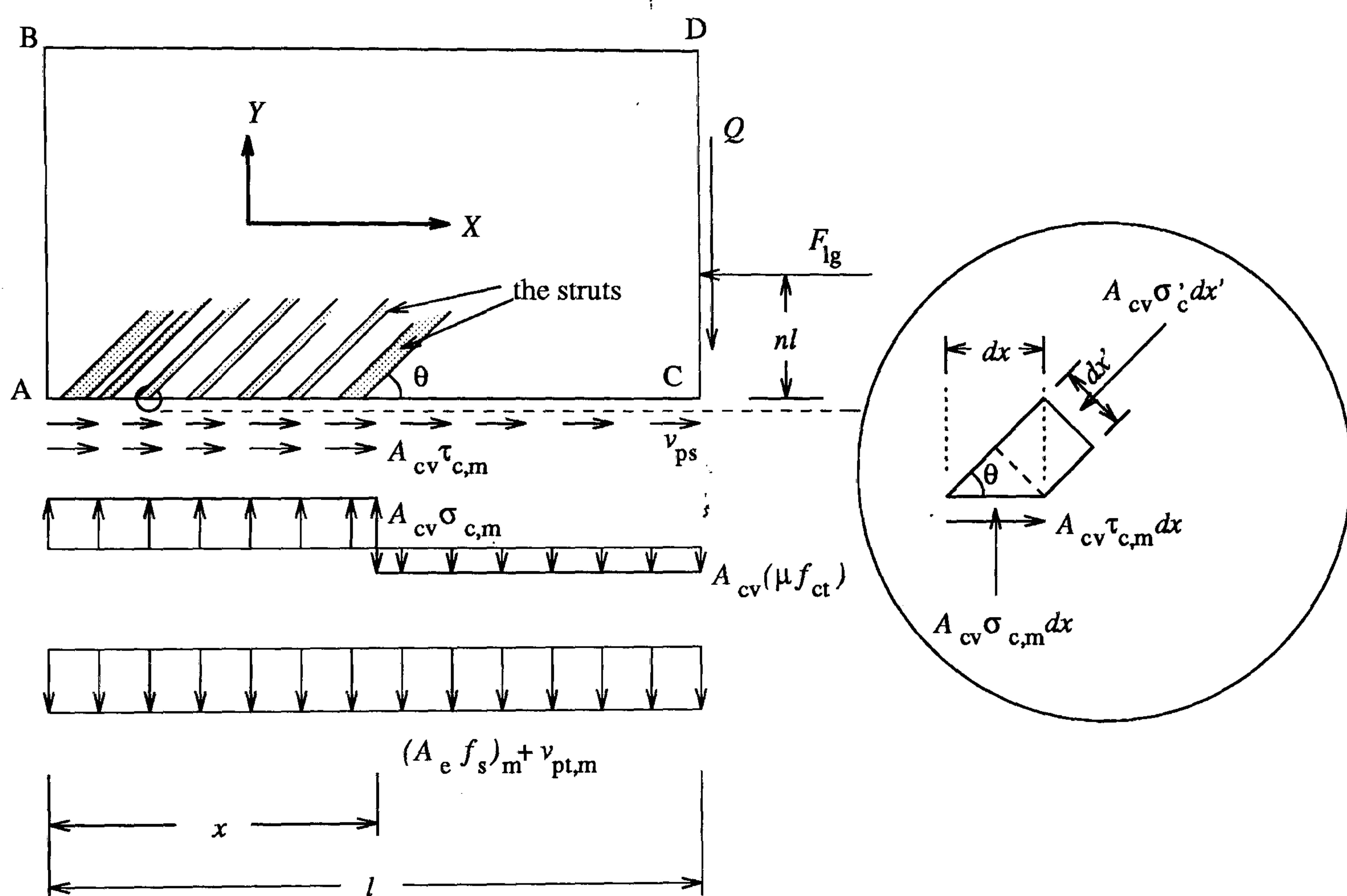


Figure 6.4: Calculation pattern for shear resistance with respect to crushing of the concrete struts

Ignoring the influence from the sheeting and reinforcement, the stress state on the strut element may be as shown in Figure 6.4.

According to the equilibrium of the strut element shown in Figure 6.4, the following equations can be obtained:

$$\begin{cases} \sigma_{c,m} = \sigma'_c \sin^2 \theta \\ \tau_{c,m} = \sigma'_c \sin \theta \cos \theta \end{cases} \quad (6.24)$$

It is assumed that the struts crush when the stress reaches the cylinder

strength f_c , i.e.

$$\sigma'_c = f_c \quad (6.25)$$

So, replacing σ'_c with f_c and $\tau_{c,m}$ with $\sigma_{c,m} + 0.8f_{ct}$ (see equation (6.4)), the following equation can be derived:

$$\sin(2\theta) + \cos(2\theta) = 1 + 1.6\frac{f_{ct}}{f_c} \quad (6.26)$$

From equation (6.26), the direction of the concrete struts at the occurrence of crushing can be obtained.

With the approximation $f_{ct} = 0.1f_{cu}$ and regarding f_c related to f_{cu} as $f_c = 0.8f_{cu}$ [1,8], it is found from equation (6.26) that $\theta = 38.5^\circ$, so the $\sigma_{c,m}$ and $\tau_{c,m}$ can be determined as:

$$\begin{cases} \sigma_{c,m} = 0.310f_{cu} \\ \tau_{c,m} = 0.390f_{cu} \end{cases} \quad (6.27)$$

From equations (6.27), it is concluded that, when σ_c and τ_c on the longitudinal shear surface reach $0.31f_{cu}$ and $0.39f_{cu}$, respectively, crushing of the concrete struts would occur.

6.3.2 The maximum effect of sheeting and reinforcement

The compression zone in concrete has been found by equation (6.15), hence, in order to avoid crushing in the concrete, the concrete stress in this zone should not exceed the value as given by formula (6.27). Therefore, it can be concluded that, only within certain range, increasing strength in sheeting or the transverse reinforcement would effectively enhance the longitudinal shear resistance.

According to equations (6.6) and (6.27), the strength developed in sheeting and reinforcement should satisfy the following condition:

$$(A_e f_s + v_{pt})l + Q + (l - x)A_{cv}(0.8f_{ct}) \leq xA_{cv}(0.310f_{cu}) \quad (6.28)$$

Letting $f_{ct} = 0.1f_{cu}$, this inequality can be re-written as

$$(A_e f_s + v_{pt}) + v_s \leq 0.390 A_{cv} f_{cu} \chi - 0.08 A_{cv} f_{cu} \quad (6.29)$$

where, $v_s = Q/l$ and $\chi = x/l$. Applying equation (6.15), it can then be obtained from condition (6.29) that

$$v_l \leq v \leq v_u \quad (6.30)$$

where

$$v = (A_e f_s + v_{pt}) + v_s \quad (6.31)$$

$$v_l = \{0.39(0.5 - n)[1 - \sqrt{1 + \frac{4(v_s - 2nv_{ps})}{0.39(1 - 2n)^2 A_{cv} f_{cu}}}] - 0.08\} A_{cv} f_{cu} \quad (6.32)$$

$$v_u = \{0.39(0.5 - n)[1 + \sqrt{1 + \frac{4(v_s - 2nv_{ps})}{0.39(1 - 2n)^2 A_{cv} f_{cu}}}] - 0.08\} A_{cv} f_{cu} \quad (6.33)$$

Expressions (6.30) to (6.33) describe the conditions under which the longitudinal shear resistance v_R would depend on the strength of sheeting and reinforcement, as determined by equation (6.14).

Equation (6.32) and (6.33) show that, as v_s increases, v_l and v_u would decrease and increase, respectively, so, the restriction for using equation (6.14) turns to be weaker when taking the effect of the beneficial length into account. Hence, to simplify the analysis, the effect of the beneficial length may be ignored, which makes condition (6.30) stricter and, therefore, safer. Thus, as assumed in section 6.2.2, letting $n = 0.15$, equations (6.32) and (6.33) appear as

$$v_l = [0.137(1 - \sqrt{1 - 6.279 \frac{v_{ps}}{A_{cv} f_{cu}}}) - 0.08] A_{cv} f_{cu} \quad (6.34)$$

$$v_u = [0.137(1 + \sqrt{1 - 6.279 \frac{v_{ps}}{A_{cv} f_{cu}}}) - 0.08] A_{cv} f_{cu} \quad (6.35)$$

If condition (6.30) is broken such that $v > v_u$, then the transverse sheeting or reinforcement would be over strong and v_R would be controlled by the concrete strength in compression. Therefore, for the sheeting and reinforcement within the

shear span, the maximum effect of the transverse tension will be reached when $v = v_u$. Hence, from equations (6.14), (6.31) and (6.35), v_R corresponding to v_u may be found by taking $f_{ct} = 0.1f_{cu}$,

$$v_R = 0.137\left(1 + \sqrt{1 - 6.279\frac{v_{ps}}{A_{cv}f_{cu}}}\right)A_{cv}f_{cu} + v_{ps} \quad (6.36)$$

Equation (6.36) gives the maximum longitudinal shear resistance which could be developed in the beam when controlled by the concrete strength in compression.

It can be shown that, only if

$$v_{ps} \leq 0.130A_{cv}f_{cu} \quad (6.37)$$

the larger v_R can be achieved from equation (6.36) as v_{ps} increases. Furthermore, when $v_{ps} > (1/6.279)A_{cv}f_{cu} (= 0.159A_{cv}f_{cu})$, no solution can be obtained from equation (6.36). These results imply that, when the sheeting appears excessively strong in shear, it is not reasonable to determine v_{ps} based on the failure of sheeting. In fact, if the sheeting is very strong in shear, shear failure in sheeting would not occur at concrete crushing. So, determining v_{ps} , an upper limit should also be established, and this limit may be taken as condition (6.37).

From equation (6.34) or (6.32), it is easy to see that the condition $v_1 \leq v$ appears significant only when $v_{ps} \neq 0$. However, since the determination of v_{ps} should be limited by condition (6.37); using $v_{ps} = 0.130A_{cv}f_{cu}$ would lead to $v_1 = -0.002A_{cv}f_{cu} < 0$. Therefore, the condition $v > v_1$ can actually be satisfied in all cases.

6.3.3 The maximum longitudinal shear resistance

As found above, the maximum longitudinal shear resistance which could be developed in the composite beam depends on compression failure in the concrete. According to equation (6.36) and condition (6.37), this resistance, denoted by $v_{R,m}$, can be found as

$$v_{R,m} = 0.137\left(1 + \sqrt{1 - 6.279\frac{v_{ps}}{A_{cv}f_{cu}}}\right)A_{cv}f_{cu} + v_{ps} \quad (6.38)$$

$$\text{with } v_{ps} \leq 0.130A_{cv}f_{cu}$$

The dimensionless form of equation (6.38)

$$\bar{v} = 0.137\left(1 + \sqrt{1 - 6.279\bar{p}}\right) + \bar{p} \quad (6.39)$$

may be shown by curve ABC in Figure 6.5, where $\bar{v} = v_{R,m}/(A_{cv}f_{cu})$ and $\bar{p} = v_{ps}/(A_{cv}f_{cu})$. Based on this variation, a straight line AC may be used to replace the curve ABC, such that

$$\bar{v} = 0.274 + 0.4\bar{p} \quad (6.40)$$

With respect to line AC, the maximum longitudinal shear resistance $v_{R,m}$ may be determined as follows,

$$v_{R,m} = 0.274A_{cv}f_{cu} + 0.400v_{ps} \quad (6.41)$$

$$\text{with } v_{ps} \leq 0.130A_{cv}f_{cu}$$

Figure 6.6. shows the variation of ratio

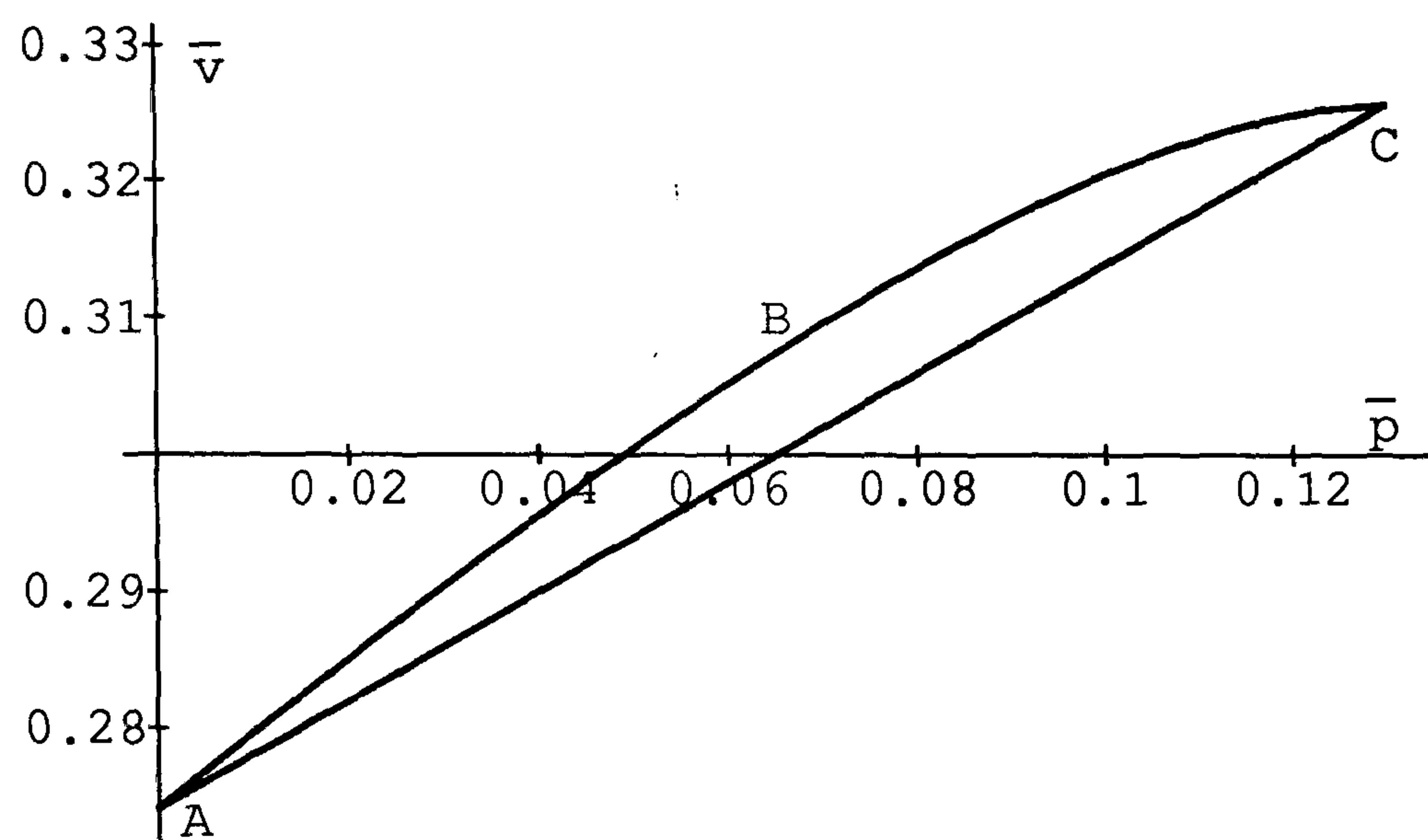
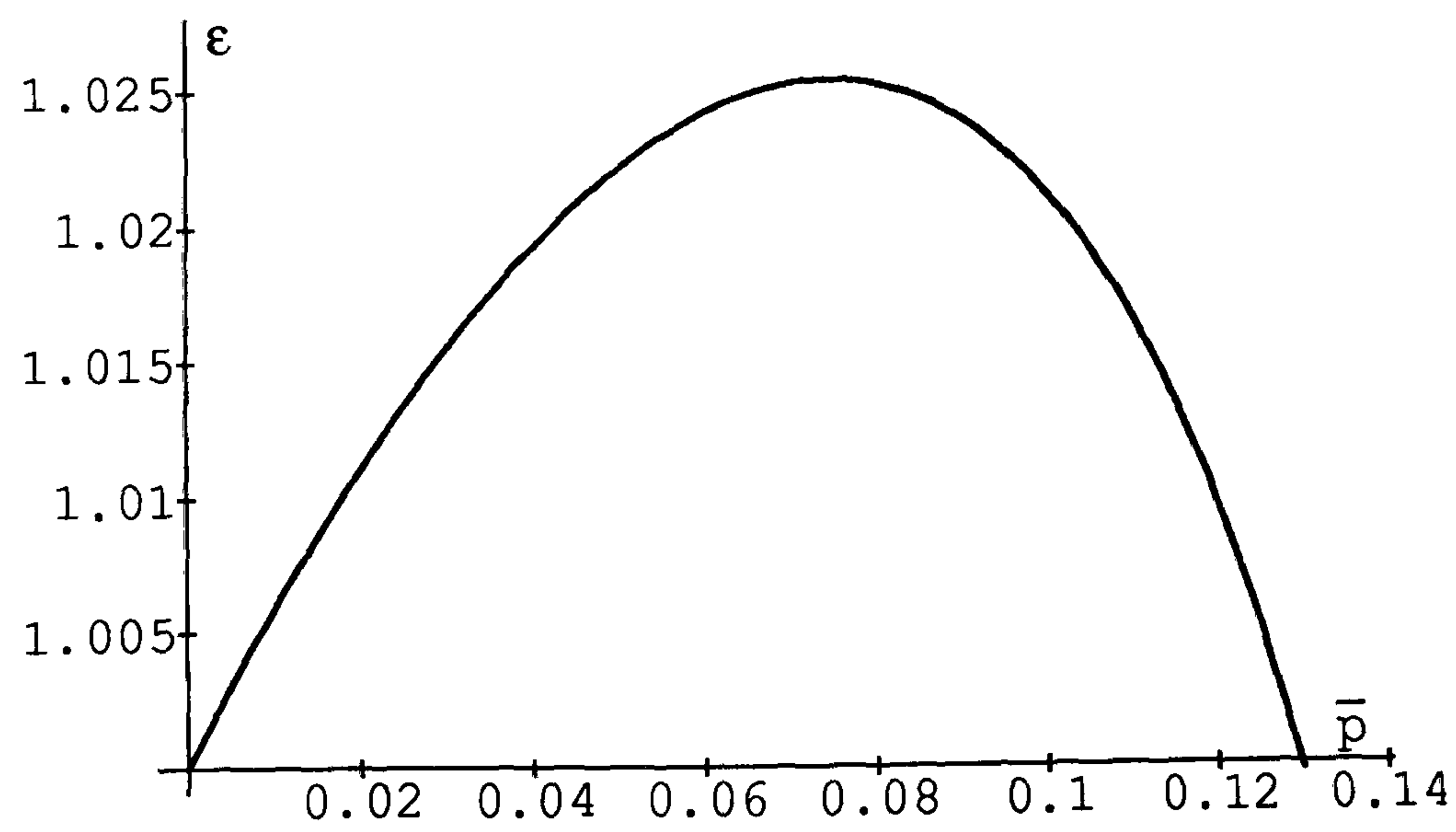
$$\epsilon = \frac{0.137\left(1 + \sqrt{1 - 6.279\bar{p}}\right) + \bar{p}}{0.274 + 0.4\bar{p}} \quad (6.42)$$

which confirms that the error caused by replacing equation (6.38) with (6.41) is negligible.

If considering that $f_{cu} = 0.8f_c$, Equation (6.41) may be expressed as,

$$v_{R,m} = 0.34A_{cv}f_c + 0.40v_{ps} \quad (6.43)$$

$$\text{with } v_{ps} \leq 0.16A_{cv}f_c \quad (6.44)$$

Figure 6.5: Variation of \bar{v} against \bar{p} Figure 6.6: Error caused by linearization of $v_{R,m}$

Where profiled sheeting is used, the concrete slab is usually corrugated, as shown in Figure 1.2. For this reason, it is reasonable that, in considering the crushing of the concrete the weakest part of the slab should be considered. In Eurocode 4, the mean area of concrete A_{cv} excludes the rib effect when the concrete strength in compression dominates the longitudinal shear resistance. Therefore, a further assumption is made here that

- (1) the mean cross-sectional area of the concrete, A_{cv} , should include the rib area when using equation (6.14), but the rib area should be excluded from A_{cv} in applying equation (6.43) and condition (6.44).

According to assumption (2) in section 6.2.1, the transverse sheeting is assumed to resist the transverse tension only, so $v_{ps} = 0$ is taken for the transverse sheeting. However, when the sheeting or reinforcement appears so strong that the tension failure becomes impossible, it may not be appropriate to neglect the v_{ps} for transverse sheeting. Therefore, it is also assumed here that

- (2) In applying equation (6.43), the sheeting, whether parallel or transverse to the steel beam, can develop the shear strength v_{ps} .

These assumptions are not necessary for solid slabs and slabs with parallel sheeting. For a solid slab, no sheeting is used and, therefore, no corrugation needs to be considered. For slab with parallel sheeting, the potential longitudinal surface of shear failure is usually taken as that excluding the rib, as shown in Figure 1.2, so the A_{cv} should not be changed in applying equation (6.14) and (6.43).

For beams with transverse sheeting, on one hand, by using assumption (1), the flange portion shown in Figure 6.1 or 6.4 would be treated as a flat slab with the thickness excluding the rib in using equation (6.43), which makes calculation of $v_{R,m}$ conservative, on the other hand, a higher value of $v_{R,m}$ can be obtained when assumption (2) is applied in equation (6.43). As a result, it may be expected that, by applying these two assumptions together, the errors caused can be partly cancelled.

6.4 The strength of profiled sheeting

As presented in equation (6.14) and (6.43), the profiled sheeting contributes to the longitudinal shear resistance.

If the sheeting is continuous over the steel beam, the tensile strength v_{pt} in transverse sheeting may be directly taken as

$$v_{pt} = A_p f_{yp} \quad (6.45)$$

where A_p is the cross-sectional area of the profiled sheeting per unit length of the beam;

f_{yp} is the yield strength of sheeting.

When sheeting is discontinuous over the steel beam but fixed to the steel beam by welded studs, the tensile strength v_{pt} normally depends on anchorage failure in sheets around the studs, as shown in Figure 6.7.

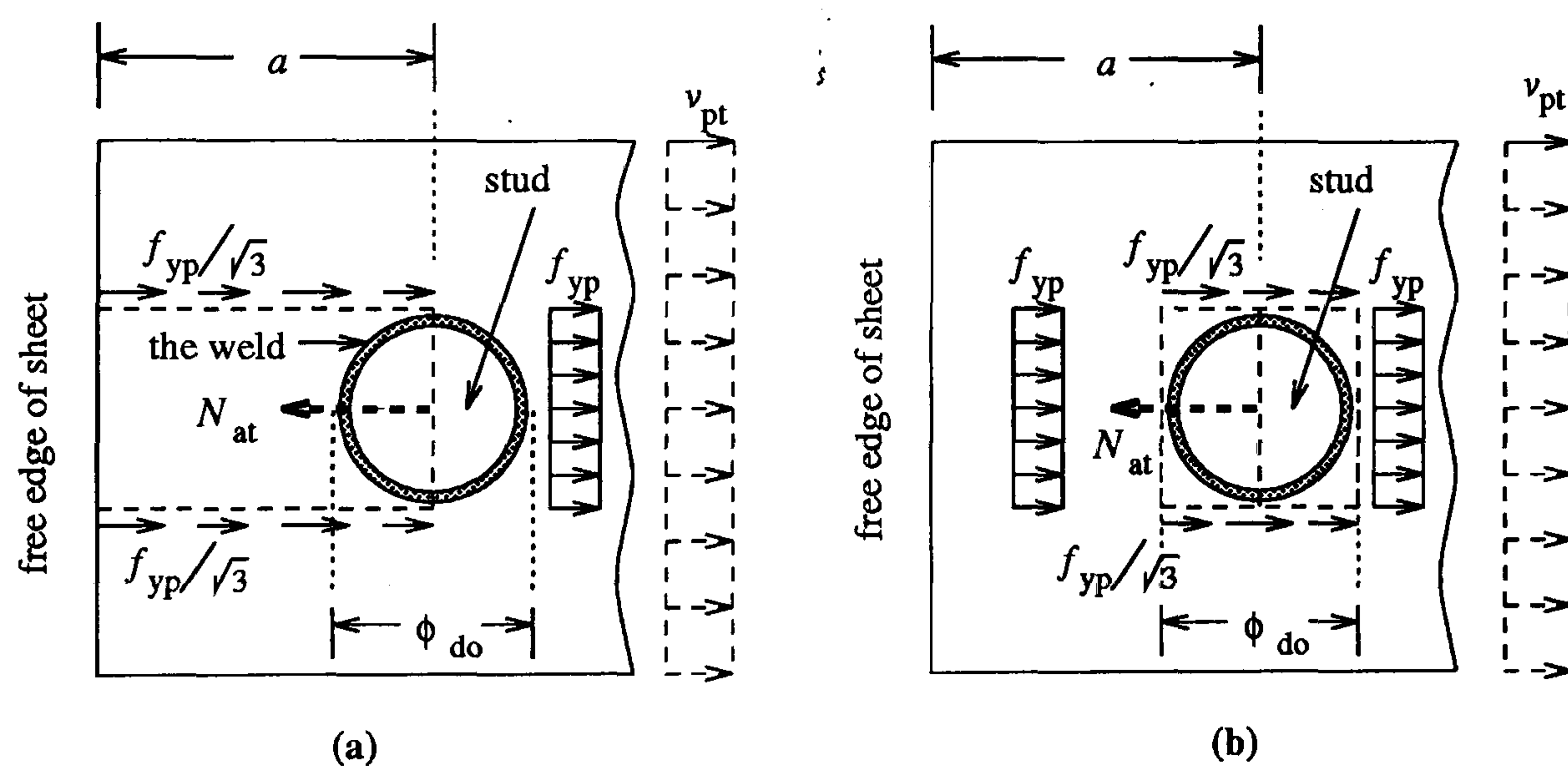


Figure 6.7: Local failure of sheeting in tension

Figure 6.7 shows two possible models for local yielding in the sheeting under the transverse tension. The failure shown in Figure 6.7 (a) assumes the sheeting to be pulled out from the studs. From Figure 6.7 (a), the pull-out strength of the sheet for one stud shear connector can be obtained as

$$N_{at} = (1 + 1.15a/\phi_{do})\phi_{do}t f_{yp} \quad (6.46)$$

where N_{at} is the tensile force reached in the sheet at the local failure;
 ϕ_{do} is diameter of the weld;
 a is the distance from the centre of the stud to the end of the sheeting;
 t is the thickness of sheet.

Figure 6.7 (b) suggests another mode of the local failure in sheeting, which leads to the tensile force developed in sheet for one stud shear connector as

$$N_{at} = 3.15\phi_{do}t f_{yp} \quad (6.47)$$

Eurocode 4 presents a formula the same as equation (6.46) except that the factor $(1 + 1.15a/\phi_{do})$ is simply replaced by $(1.0 + a/\phi_{do})$, which only causes a small difference.

It is also stated in Eurocode 4 that, in determining N_{at} , $(1.0 + a/\phi_{do})$ should not be greater than 4.0, while, according to equation (6.47), this limit seems to be 3.15. Nevertheless, either equation (6.47) or the Eurocode regulation shows the same idea that, when a becomes sufficiently large, it is unsuitable to determine N_{at} by considering pull-out failure in sheets. Because the derivation of equation (6.47) does not consider other effects such as the shear bond of the concrete to sheeting, as a increases, equation (6.47) may give a conservative prediction of N_{at} .

Therefore, the method in Eurocode 4 is adopted to find out v_{pt} , i.e.

$$\begin{aligned} v_{pt} &= (1 + a/\phi_{do})\phi_{do}t f_{yp}/s \\ \text{but } (1.0 + a/\phi_{do}) &\leq 4.0 \end{aligned} \quad (6.48)$$

where s is the longitudinal spacing centre-to-centre of groups of studs.

Since the shear force would be transferred from a flange into the steel beam through the shear connectors, it is reasonable to determine the shear strength of the sheeting v_{ps} by considering local yielding of the sheets around the studs, as

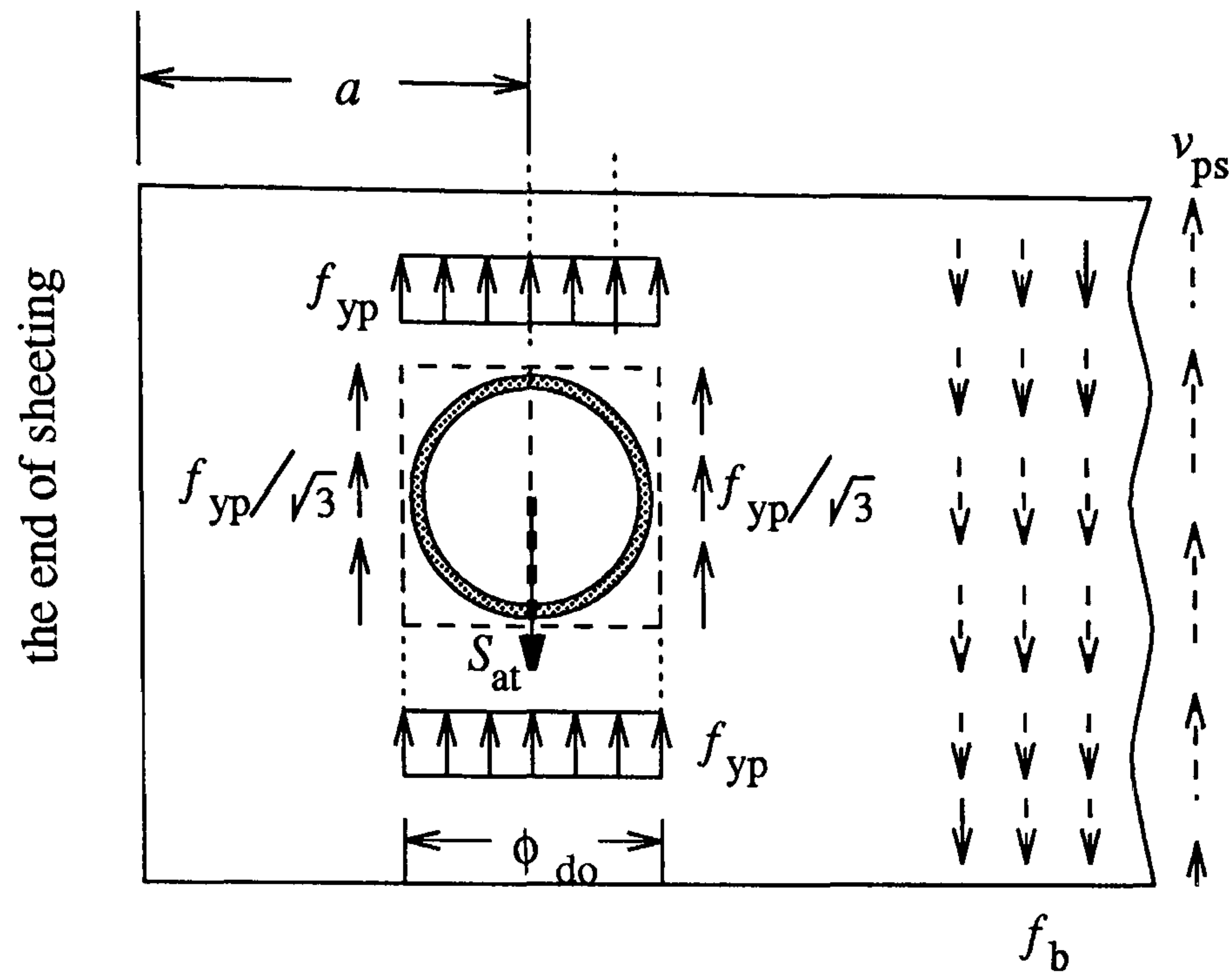


Figure 6.8: Local failure of sheeting in shear

shown in Figure 6.8. From this idealized local failure, it can be obtained that

$$S_{at} = 3.15\phi_{do}t f_{yp} \quad (6.49)$$

where S_{at} is the maximum shear force per stud sustained by the sheet.

Thus, the shear strength v_{ps} along the longitudinal shear surface under consideration can be found from the equilibrium

$$v_{ps}s = S_{at} + f_b A_{eb}s \quad (6.50)$$

where f_b is shear bond stress via the embossments on the sheet web to the concrete [9];

A_{eb} is the involved shear bond area per unit length along the beam.

Therefore, with respect to the limit shown in condition (6.44), v_{ps} may be determined as follows,

$$\begin{aligned} v_{ps} &= 3.15\phi_{do}t f_{yp}/s + f_b A_{eb} \\ \text{but } v_{ps} &\leq 0.16A_{cv}f_c. \end{aligned} \quad (6.51)$$

It should be noted that the shear bond area A_{eb} involved in the calculation depends on the consideration of the potential surface of shear failure. For beams

with transverse sheeting, in finding v_{ps} for the maximum longitudinal shear resistance as given in equation (6.43), it appears that $A_{eb} = 0$. This is because, as shown in Figure 1.2(b), the potential longitudinal surface of the shear failure should be taken as that just beside the studs. For beam with parallel sheeting, as shown in Figure 1.2(a), the determination of v_{ps} may consider that A_{eb} includes the whole web of the sheeting, as the potential longitudinal surface of the shear failure is normally taken as that excluding the rib, which leads to that the part of sheeting between studs and the longitudinal surface would cover sheet web.

6.5 Summary of determining longitudinal shear resistance

An approach of determining the longitudinal shear resistance in composite beams with or without profiled sheeting is presented in this chapter.

Failure of longitudinal shear in composite beam is considered to be caused by two reasons: failure in transverse reinforcement or sheeting or crushing of concrete struts.

Longitudinal shear resistance of composite beam may be determined from equation (6.22) considering failure in transverse reinforcement or sheeting, or equation (6.43) considering crushing of concrete struts, whichever is smaller.

In applying equation (6.22), for composite beams with sheeting transverse to steel beam, $v_{ps} = 0$ and v_{pt} is determined from equation (6.45) (continuous sheeting) or (6.48) (discontinuous sheeting); for composite beams with sheeting parallel to steel beam, $v_{pt} = 0$ and v_{ps} is determined from equation (6.51).

In applying equation (6.43), the contribution of sheets, either transverse or parallel to steel beam, may be taken as v_{ps} found from equation (6.51).

According to the analysis on a beam subjected to concentrated load off midspan, as shown in Figure 6.1, it is shown that, if considering a transverse shear force $Q \neq 0$ (see Figure 6.1), then a certain beneficial length λl can be obtained,

which would in turn to enhance longitudinal shear resistance in the shear span under consideration. This effect $\lambda\beta$ for a beam under a concentrated load may be assessed with respect to equations (6.18), (6.19) and (6.23).

In general, however, determination of effect of the beneficial length λl seems not simple. Since the study shows that existence of such a beneficial length would make a favourable effect to longitudinal shear resistance, such an effect may be ignored in calculating longitudinal shear resistance, which would give a simple and safe result. Therefore, letting $\lambda\beta = 0$, the longitudinal shear resistance may be generally found as

$$v_R = 0.8A_{cv}f_{ct} + A_e f_s + v_{pt} + v_{ps} \quad (6.52)$$

$$v_R = 0.34A_{cv}f_c + 0.40v_{pc} \quad (6.53)$$

whichever is smaller.

To avoid ambiguity in application, equation (6.53) employs a new symbol v_{pc} to replace v_{ps} used in equation (6.43) to represent the effect of sheeting (either transverse or parallel) on v_R controlled by crushing in concrete. Determination of v_{pc} is of course still same as v_{ps} .

It should be noticed that A_{cv} in equation (6.52) and (6.53) includes and excludes the rib area, respectively.

Chapter 7

Specimens for testing

longitudinal shear resistance

In the last chapter, a theoretical model has been presented, by which the longitudinal shear resistance in composite beams with or without profiled sheeting can be predicted. Together with the theoretical study, tests are required to check the theory established here. Furthermore, since the theory suggests that the profiled sheeting can make contribution to the longitudinal shear resistance, tests are needed to examine such effects of profiled sheeting. Therefore, a series of tests have been carried out for this study. This chapter is to present the details of preparing these tests.

7.1 Objective and planning of the tests

For longitudinal shear resistance in composite beams with solid concrete flanges (no sheeting), several studies based on tests have been done by Johnson [11,12,13] and Sen [4]. Therefore, the tests in this study were mainly done on concrete flanges with profiled sheeting. Their objectives were:

- (1) to investigate the effect of profiled sheeting on the behaviour of composite beams in longitudinal shear;

- (2) to reveal failure modes in longitudinal shear of beams with profiled sheeting;
- (3) to check the ultimate resistance to longitudinal shear of concrete flanges with profiled sheeting;
- (4) to examine the theories established for longitudinal shear and, if necessary, to improve the current design method for longitudinal shear resistance in composite beams.

Three test specimens were constructed.

The first specimen, labelled as TR1, was to simulate a part of a floor system in a composite structure. The concrete slab was fabricated with profiled sheeting discontinuous over the steel beams. As shown in Figure 7.1, three tests were originally planned on this specimen, i.e.

- Test TR1T, with loading at point B on the secondary steel beam, to check the longitudinal shear resistance in region AB where profiled sheeting was spanned transverse to the steel beam, and the amount of transverse reinforcement was less than the minimum value given by the code [1];
- Test TR1P1, with loading at point D on the primary steel beam to check the longitudinal shear resistance in region DL where profiled sheeting was spanned parallel to the steel beam, and the amount of transverse reinforcement was less than the minimum value given by the code [1];
- Test TR1P2, the same as test TR1P1 but loading at point C to check the longitudinal shear resistance in region CH where amount of transverse reinforcement just reaches the minimum value given by the code [1].

In order to simulate the practical situation that transverse hogging bending of the concrete flange portion occurs, it was considered that tests TR1P1 and TR1P2 should be carried out so that the longitudinal shear resistance after the occurrence of the longitudinal crack in the slab due to the transverse hogging

bending can be examined. Therefore, in test TR1P1, a small constant load was also arranged at point G to make longitudinal cracks in concrete along the primary steel beam deliberately.

It had been expected that, for each test, the behaviour of specimen TR1 in the concerned region could be treated as that of a composite beam with certain effective width. However, from the tests on specimen TR1, it was found that, due to the occurrence of large deformations before maximum load was reached, a specimen like TR1 would eventually perform as a nonlinear orthotropic plate; as a result, the situation became excessively complicated for studying the longitudinal shear resistance of composite beams. Therefore, it was decided after testing TR1 that the second and third specimens should be made into two isolated composite beams.

As shown in Figure 7.2, the second specimen, labelled as TR2T, was designed as a composite beam with discontinuous transverse sheeting, and two tests were to be conducted on TR2T1:

- Test TR2T1, with loading at point B (Figure 7.2), to examine the longitudinal shear resistance in region AB where the sheeting was placed but no transverse reinforcement was used;
- Test TR2T2, with loading at point C, to examine the longitudinal shear resistance in region CD where light transverse reinforcement (A98) was used but no sheeting was placed.

It was intended to reveal the effect of transverse sheeting by comparing results from tests TR2T1 and TR2T2.

The third specimen, labeled as TR2P, was designed as a composite beam with discontinuous parallel sheeting, as shown in Figure 7.3. Two tests were arranged for this beam:

- Test TR2P1, with loading at point J, to examine the longitudinal shear resistance in region HJ where the sheeting is placed but no transverse re-

inforcement was used;

- Test TR2P2, loading at point K, to examine the longitudinal shear resistance in region KL where the light transverse reinforcement was used but no sheeting was placed.

The effects of parallel sheeting may be investigated by comparing results from tests TR2P1 and TR2P2.

7.2 Design and fabrication of the specimens

7.2.1 Specimen TR1

Specimen TR1 was designed as large as the size of the loading goal-post in the laboratory allowed. The overall dimensions in plan are shown in Figure 7.1

Two rolled steel beams as specified in BS 4: Part 1: 1980 were used:

- secondary beam: Universal beam $203 \times 133 \times 30$ kg/m (see Figure 7.4);
- primary beam: Universal beam $254 \times 146 \times 37$ kg/m (see Figure 7.4);

ALPHALOK profiled sheeting [14] with thickness 0.9 mm was used in this specimen. The dimensions of the sheets are shown in Figure 7.5. In TR1, the sheeting was discontinuous above the steel beams but fixed to them by studs welded directly through. Views 1-1 and 2-2 in Figure 7.1 gives details of the end anchorage for the sheets.

The overall thickness of the concrete slab of TR1 was originally designed as 120 mm. However, measurements made after construction showed that the mean overall thickness of the concrete slab may be taken as 125 mm.

As shown in Figure 7.1, A98 mesh was supplied in areas for test TR1T and test TR1P1, and A142 for test TR1P2. The nominal dimensions of these meshes are shown in Figure 7.3.

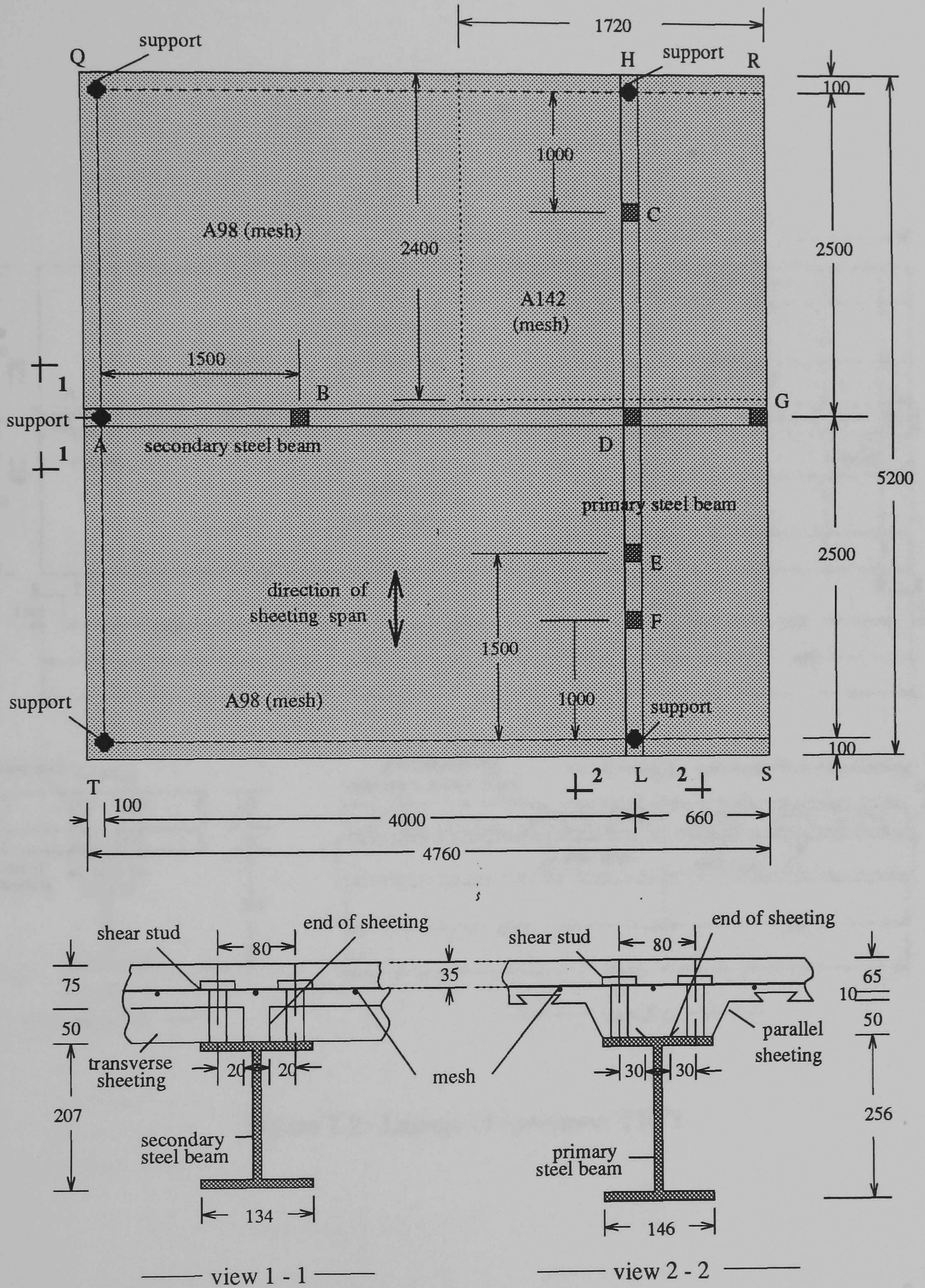


Figure 7.1: Layout of specimen TR1

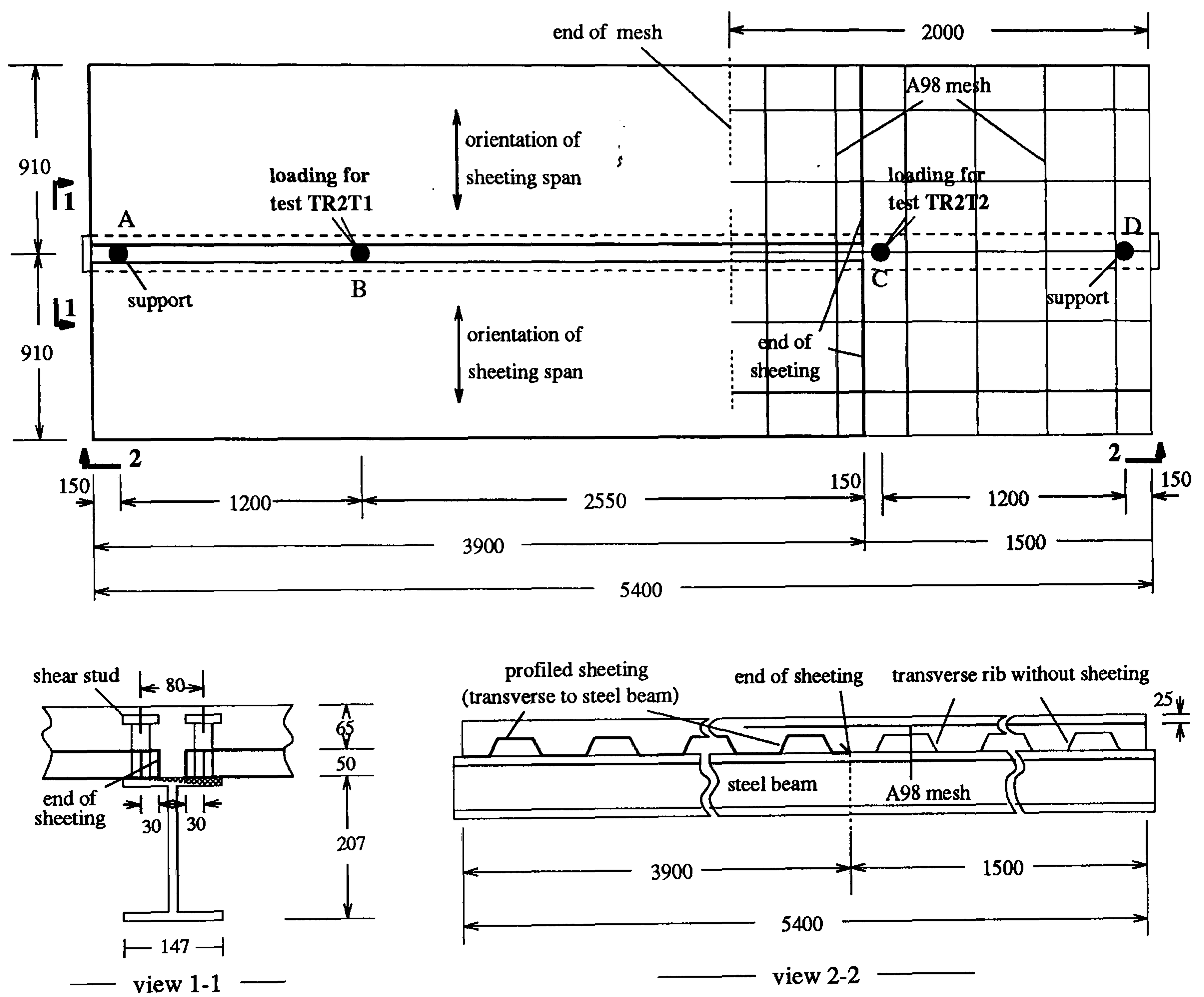


Figure 7.2: Layout of specimen TR2T

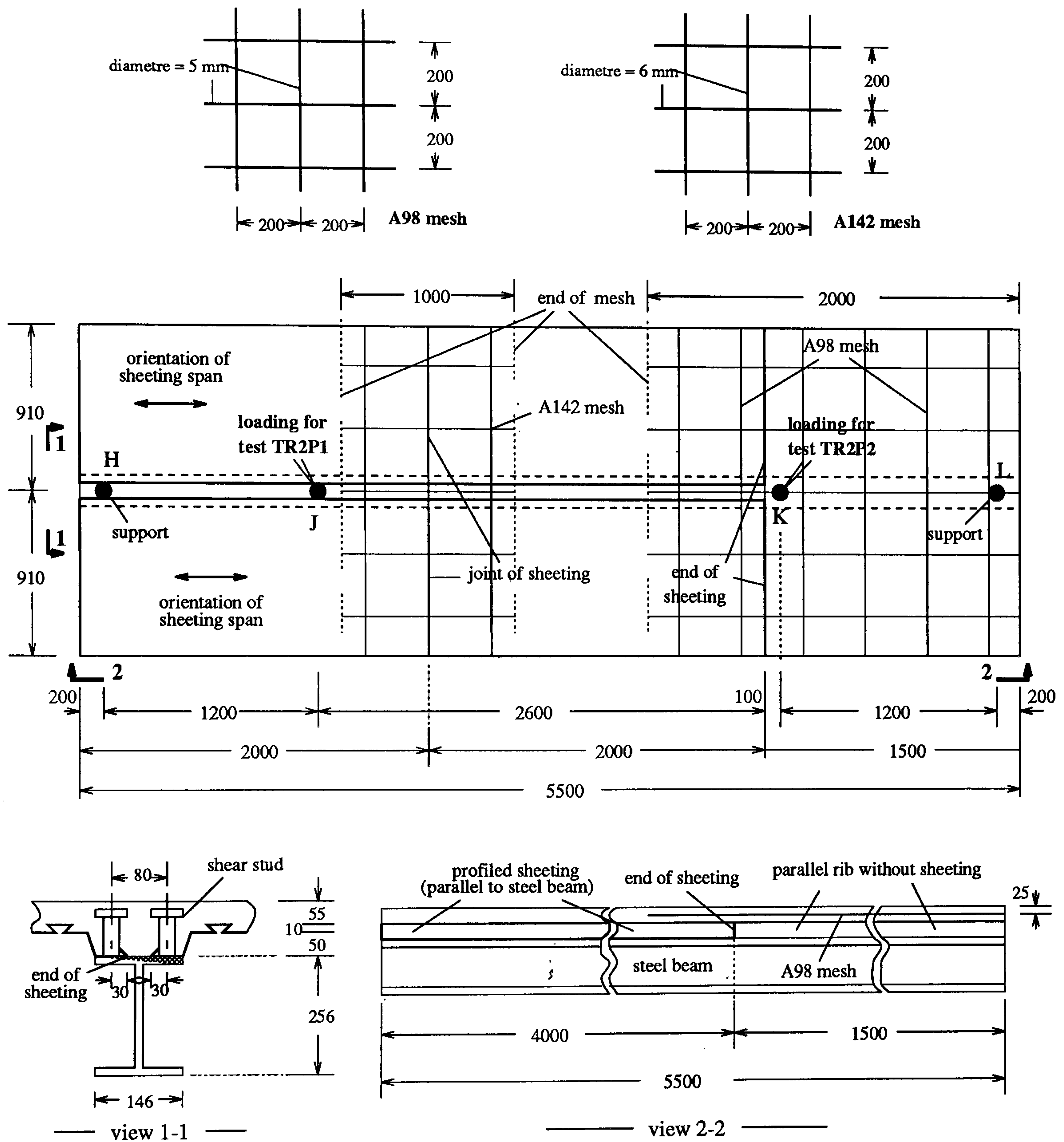


Figure 7.3: Layout of specimen TR2P

According to Eurocode 4 [1], in specimen TR1, the mean area of concrete per unit length along the critical longitudinal shear surface A_{cv} (see Figure 1.2), may be taken as $99000\text{mm}^2/\text{m}$ for test TR1T and $65000\text{mm}^2/\text{m}$ for tests TR1P1 and TR1P2, which leads to the ratio of transverse reinforcement area to concrete area in this specimen as

- test TR1T: $A_e/A_{cv} = 98/99000 = 0.0010$;
- test TR1P1: $A_e/A_{cv} = 98/65000 = 0.0015$;
- test TR1P2: $A_e/A_{cv} = 142/65000 = 0.0022$.

Eurocode 4 requires this ratio to be at least 0.002, so this rule was satisfied only in the region for test TR2P2 (see Figure 7.1).

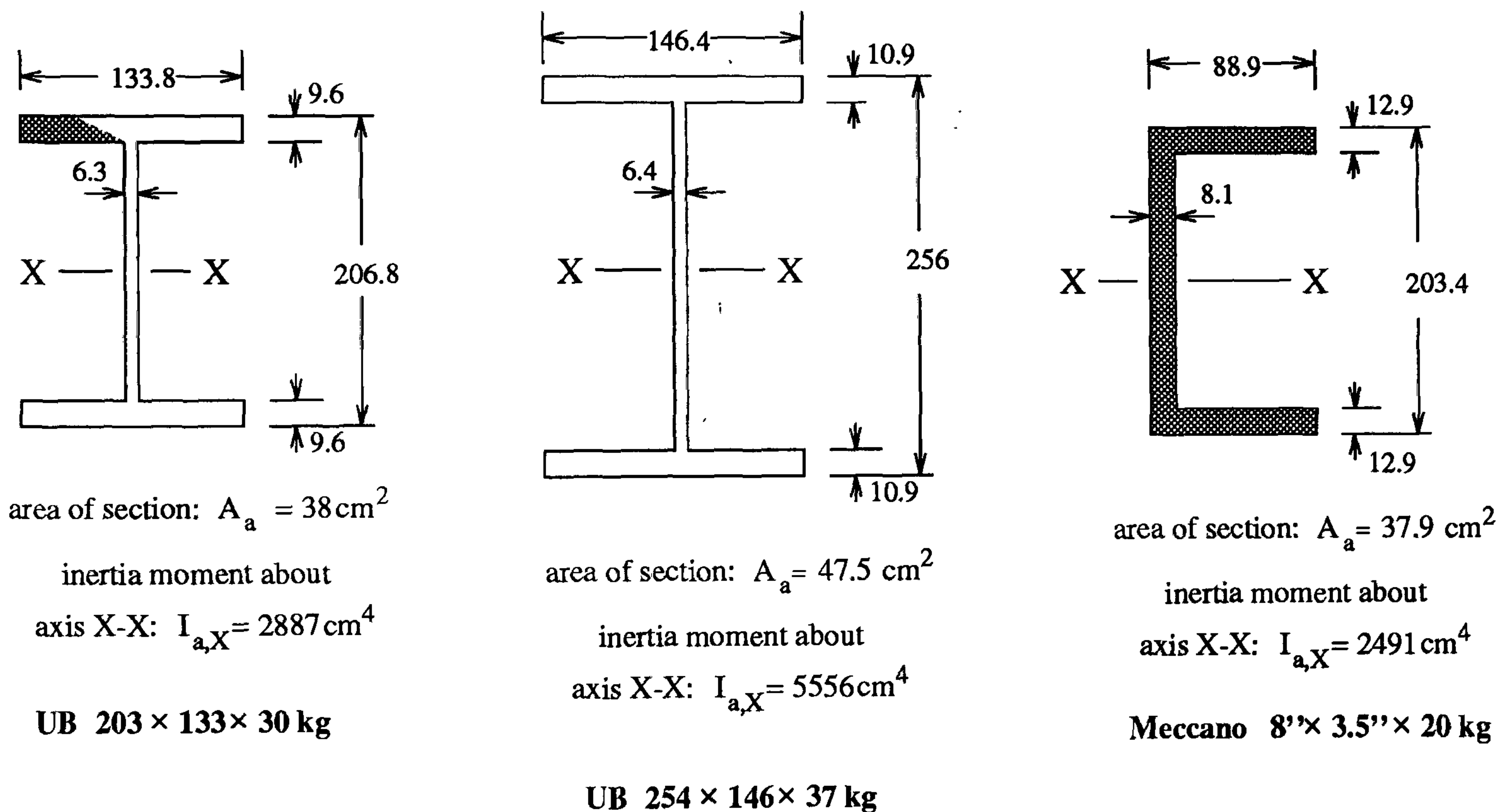


Figure 7.4: Cross-section of the steel beams

The connection of the secondary beam to the primary beam in TR1 was made by M20 grade 8:8 bolts, as shown in Figure 7.6. Because of the clearance between such a bolt and its hole, rotational restraint to the secondary steel beam at D may be ignored and can therefore be assumed to be simply supported at both

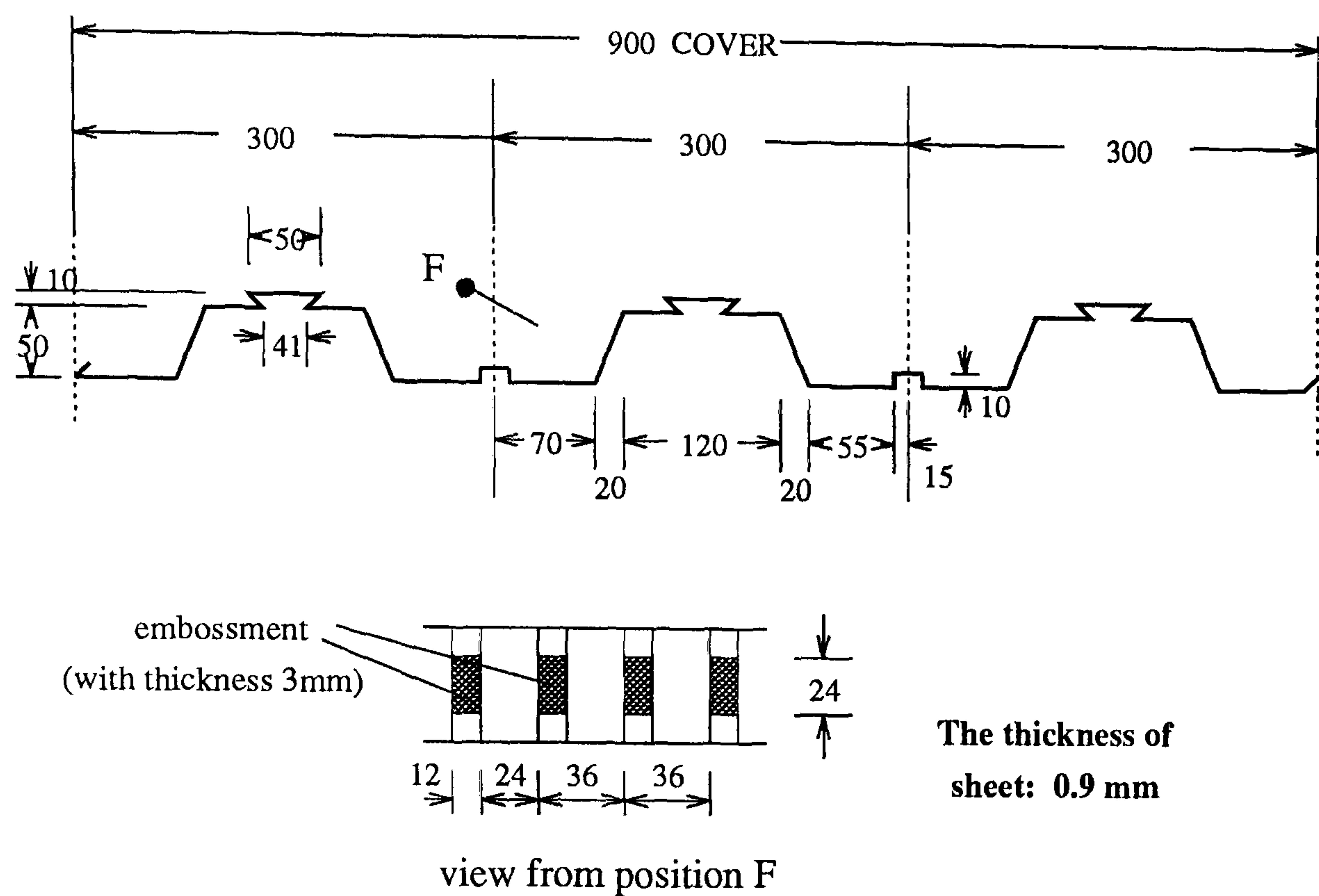


Figure 7.5: ALPHALOK profiled sheet

ends. As shown in Figures 7.1 and 7.6 along length DG, a short steel beam same as the secondary beam was also arranged. This part of steel beam, however, was connected to the primary steel beam with the high friction bolts (M20 8:8 H.S.F.G bolts), as no support was to be supplied at end G.

Figure 7.7 describes the shear connection in TR1. The concrete slab was connected to the steel beams by stud shear connector which were directly welded through the sheets. The studs used were headed studs of size 19×100 . The studs on the primary steel beam was arranged so that, with respect to the loading at D (see Figure 7.1), the full shear connection along the primary beam could be achieved for the ultimate state of plastic bending.

Figure 7.8 shows the specimen just after stud welding.

On edges Q-H-R and T-L-S of the specimen (see Figure 7.1), the concrete slab was supported on the "Meccano" steel channels with section size $8'' \times 3.5''$ shown in Figure 7.4. The concrete slab was attached to the "Meccano" channels at each edge by a single M20 studding of mild steel, as shown in Figure 7.9.

From Figure 7.1, it can be seen that the steel beams and the "Meccano"

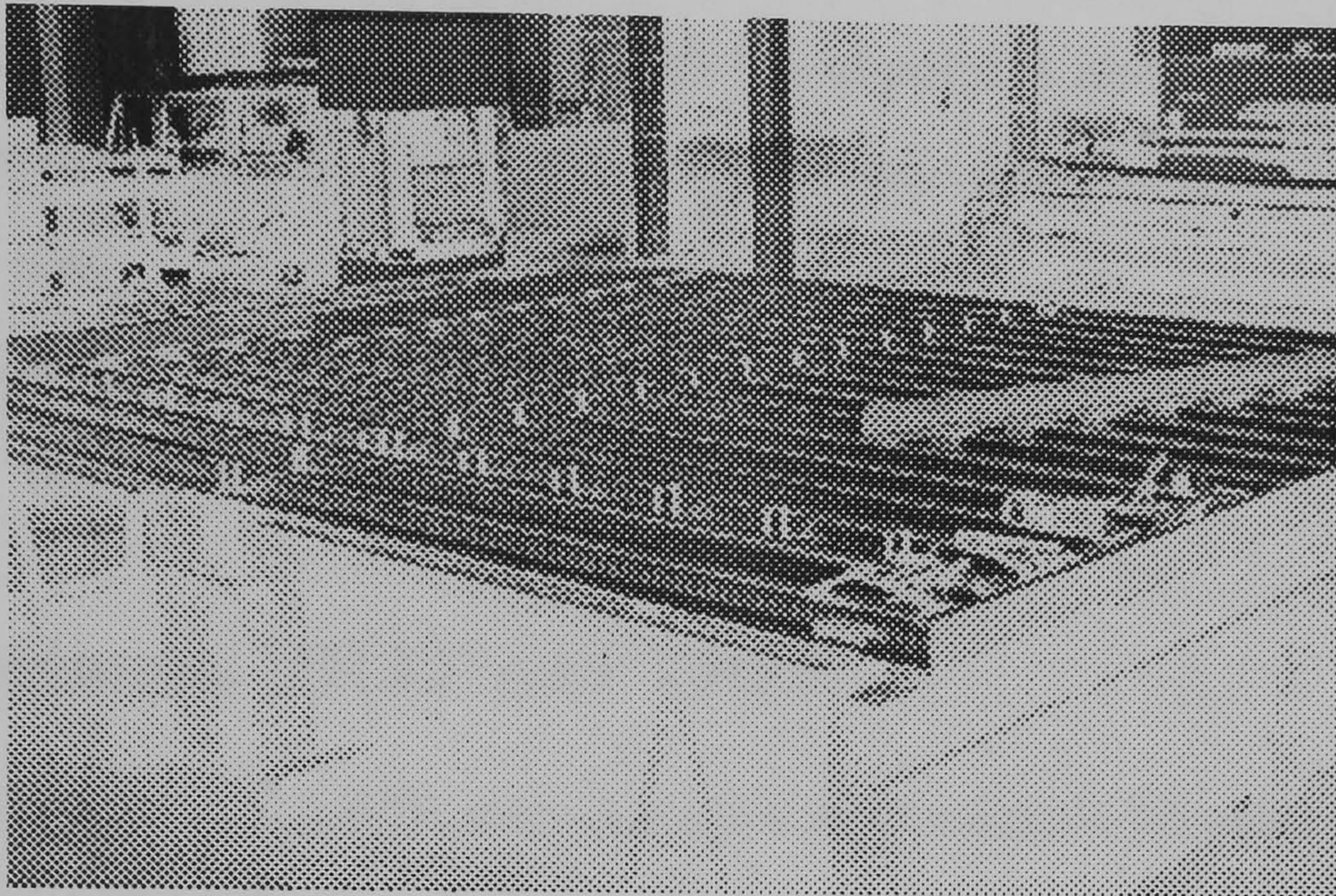


Figure 7.8: Specimen TR1 after stud welding

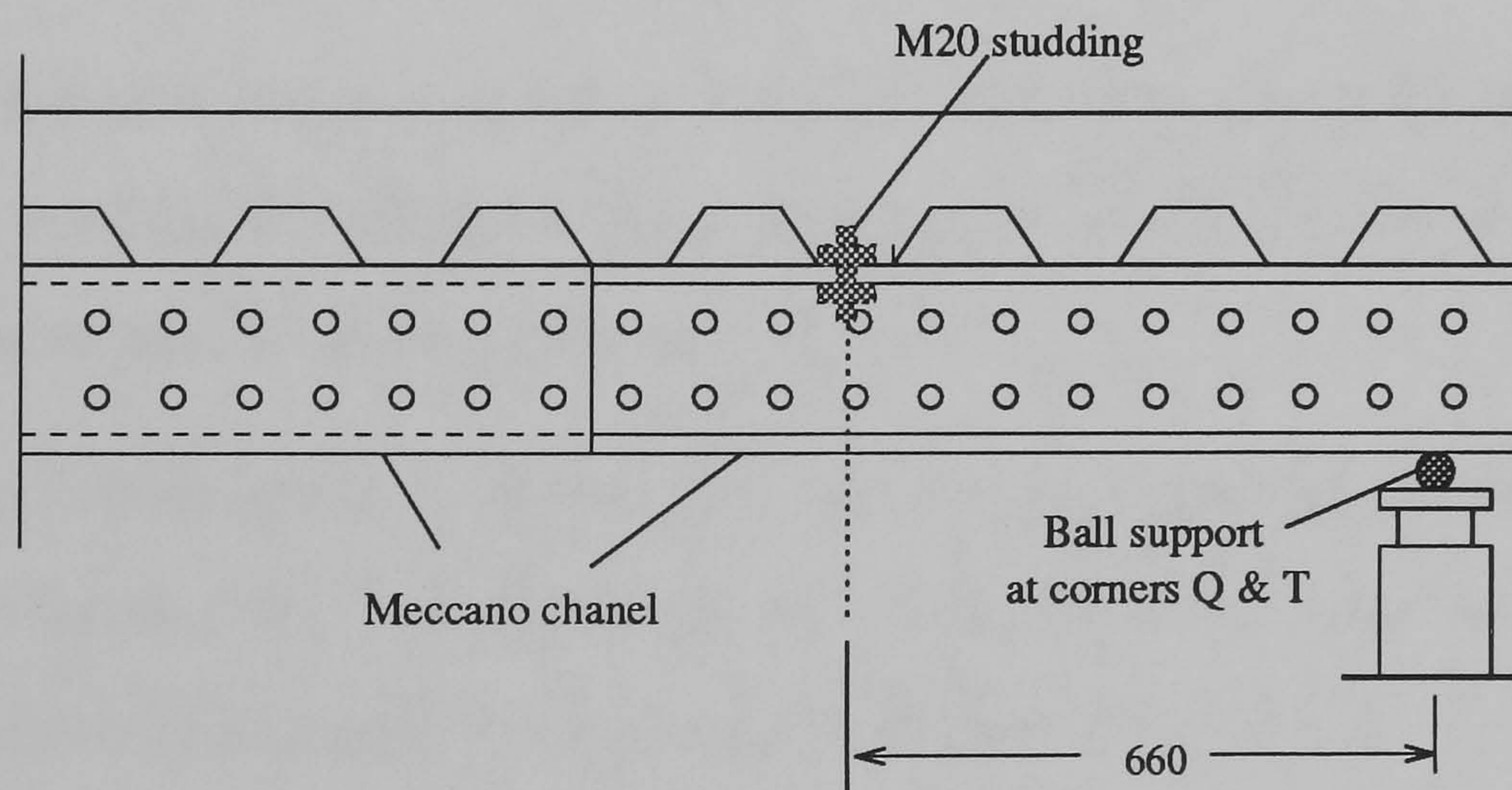


Figure 7.9: Edge support of specimen TR1

channels were supported at five points, A, L, H, Q and T. Ball supports were used at corners Q and T, which provided no restraint in any horizontal direction. Roller supports were used at A, H and L so that the horizontal movements of points H and L along the primary beam and that of point A along secondary beam were free of restraint, which leads to no indeterminate reaction from restraints in the horizontal plan.

In casting the concrete, the additional supports were temporarily used so that specimen TR1 were fully propped during construction.

7.2.2 Specimens TR2T and TR2P

The specimens TR2T and TR2P were designed as the isolated beams with transverse and parallel sheeting, respectively.

Figure 7.2 and Figure 7.3 show the plan and cross section of beams TR2T and TR2P. The basic design points for both beams can be listed below.

- The intended overall thickness of the concrete slab, including the thickness of sheeting, is 110 mm for both beams. Nevertheless, according to measurements made after casting the concrete, the actual overall thickness of the slab for both beams may be taken as 115 mm.
- Two rolled steel beams to BS 4: Part 1: 1980 were used: UB 203 × 133 × 30kg/m for TR2T; UB 254 × 146 × 37kg/m for TR2P. The sections of these steel beams are detailed in Figure 7.4.
- ALPHALOK sheeting as shown in Figure 7.5 was used again for TR2T and TR2P. The sheeting was discontinuous over steel beam but the studs were welded directly through it, as shown in Figure 7.2 and 7.3.
- At one end of each beam, the profiled sheeting was left out but the cross section was kept the same as the parts with sheeting. Thus the sheeting effects can be focused by comparing the results from the tests on the sheeting end and the non-sheeting end.

- In the non-sheeting end of each beam, A98 mesh was supplied, while in the sheeting end, no reinforcement was used. For beam TR2P, A142 mesh was also used in the middle part of beam, as shown in Figure 7.3, to cover the longitudinal joint of the sheeting,
- As presented in Figure 7.10, for beam TR2T, two studs were welded in “staggered pattern” in each trough, including the non-sheeting end; for beam TR2P, to provide full shear connection at the ultimate state of plastic bending, the studs were welded in pairs at 160 mm pitch all along the steel beam. The studs used were headed studs of size 19×100 .

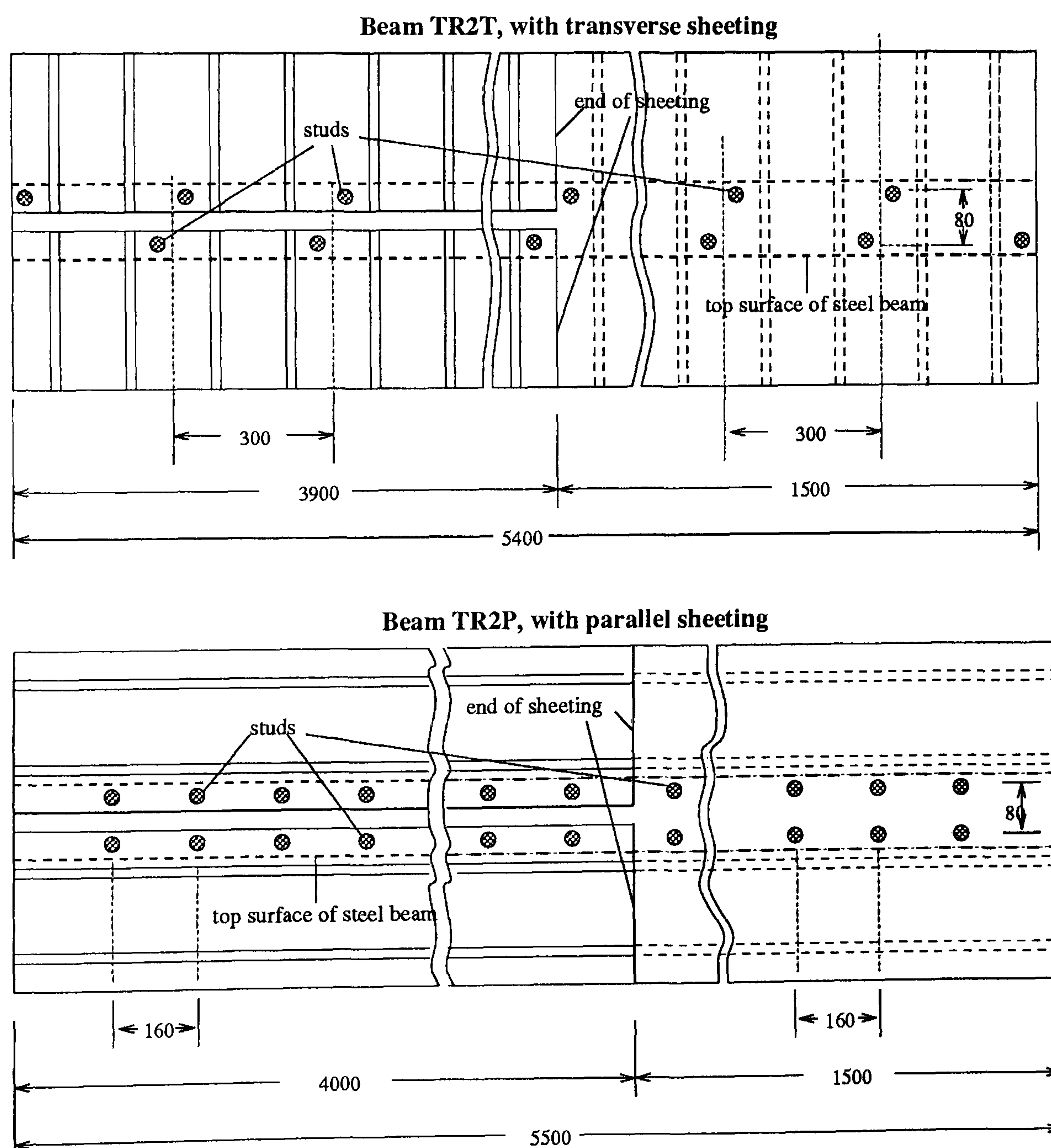


Figure 7.10: Studs in beams TR2T and TR2P

Figure 7.11 and Figure 7.12 show the specimens just after stud welding.

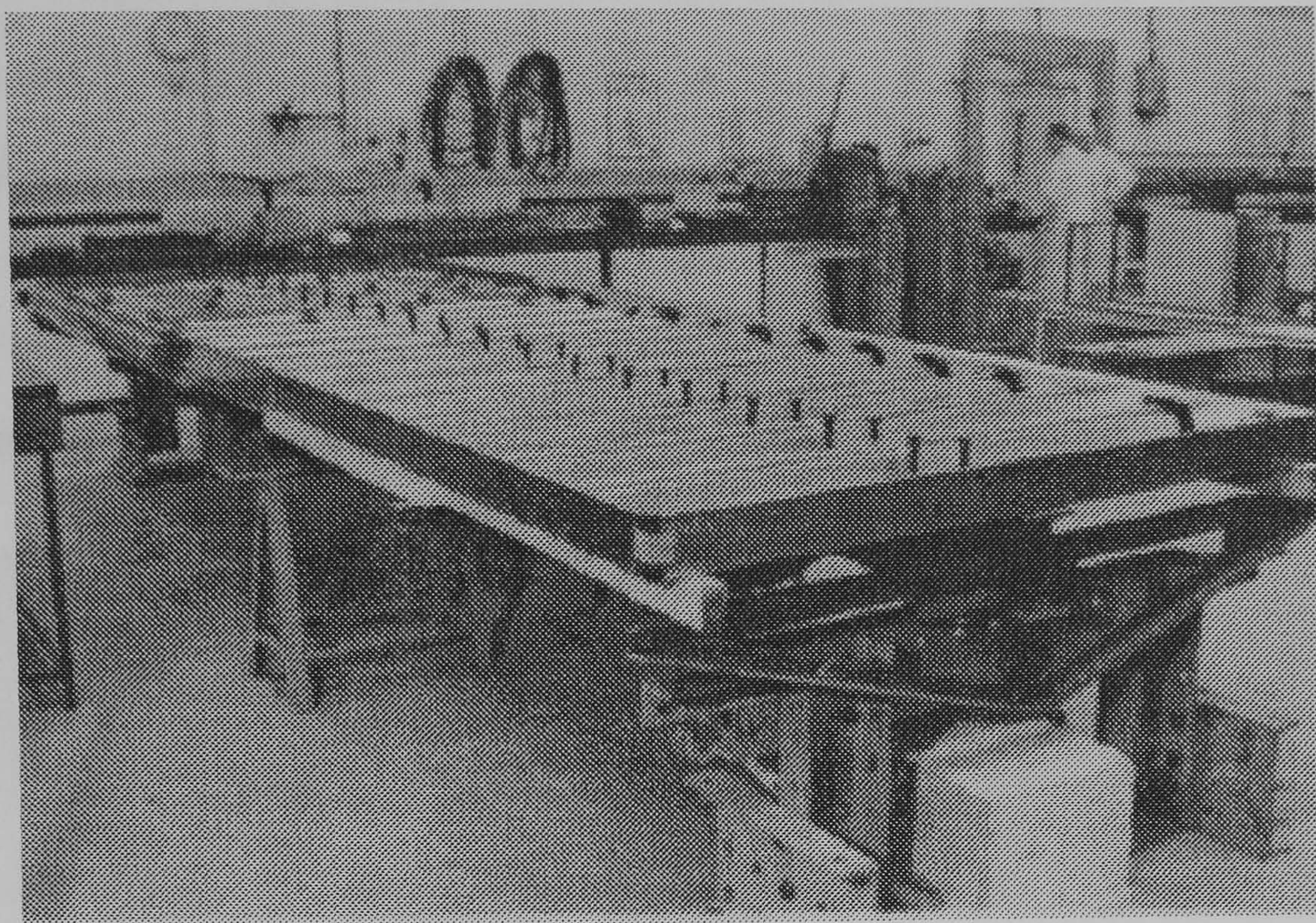


Figure 7.11: Beam TR2T after stud welding

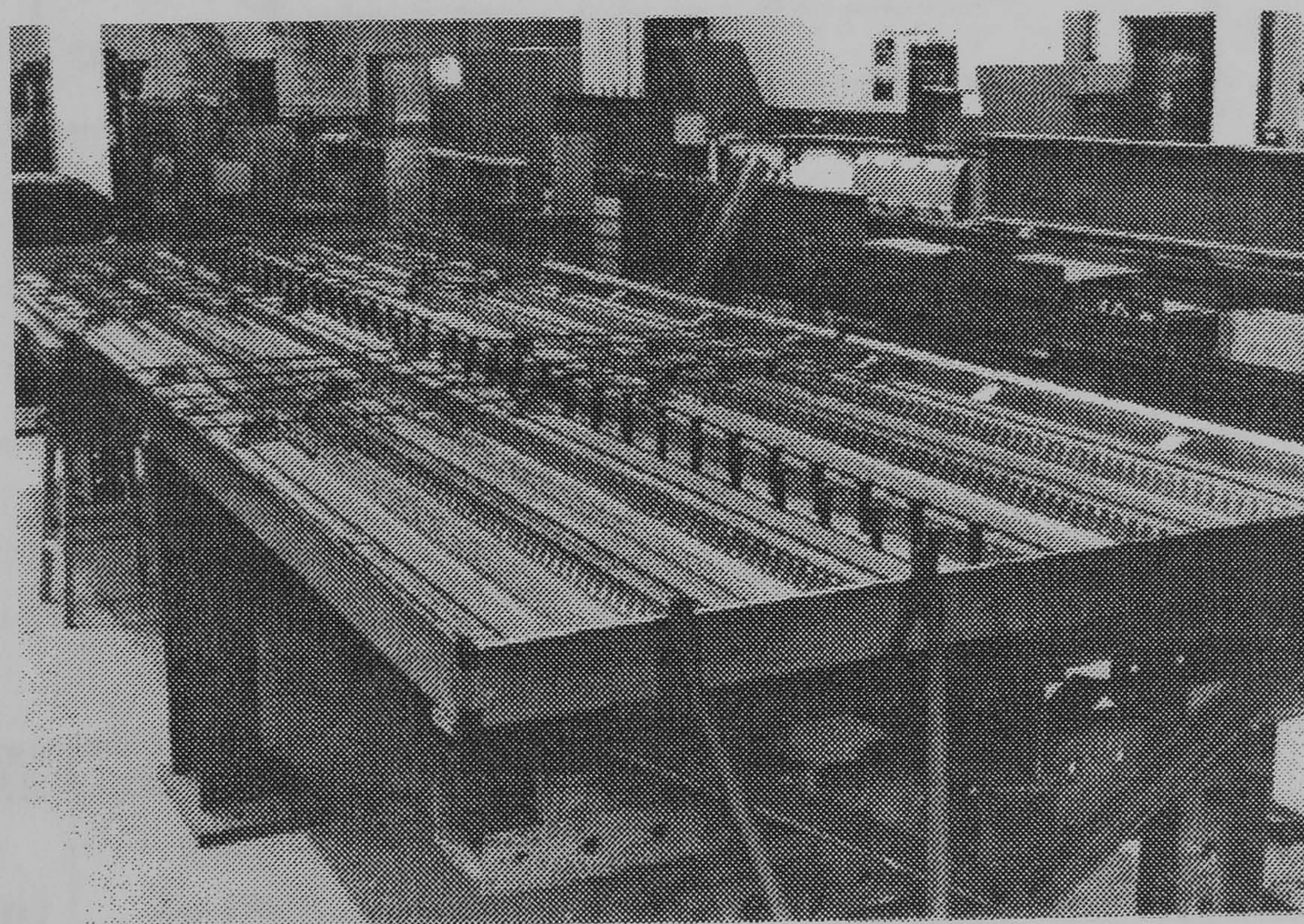


Figure 7.12: Beam TR2P after stud welding

Both beams were simply supported at the ends during tests. Unpropped construction was used for the specimens when casting concrete.

7.3 Strengths of materials

All the steel beams used in tests were of grade 43A to BS4360: 1986. In order to measure the strength and Young's modulus, six coupons were tested for each steel beam, two each from the top flange, bottom flange and web. All the test pieces were prepared in accordance with BS18:1987, as shown in Figure 7.13 and Table 7.1. The measured properties of steel beams are given in Table 7.2, where the following notations are used:

- $f_{y,f}$ yield strength in the steel flange;
- $f_{y,w}$ yield strength in the steel web;
- E_a Young's modulus of the steel;
- f_u ultimate strength in the steel.

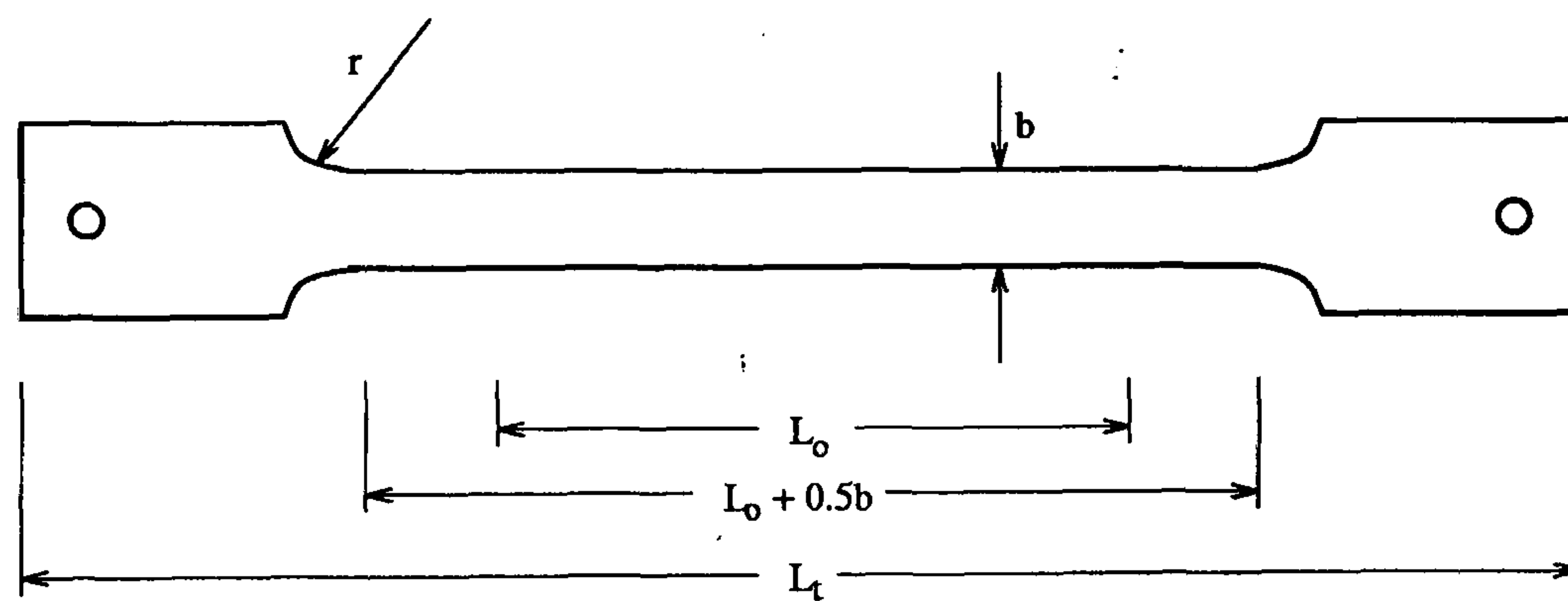


Figure 7.13: The steel coupons

Table 7.1: Size of the steel coupons

| width b (mm) | original gauge length L_o (mm) | transition radius r (mm) | approximate total length L_t (mm) | parallel length $L_o + b/2$ (mm) |
|----------------------|--|----------------------------------|---|--|
| 25 | 100 | 25 | 300 | 115 |

From the results of the coupon tests, the following values may be used as measured properties of the steel beams:

Table 7.2: Results of coupon test for steel beams

| | | UB 203 × 133 × 30 kg/m | | UB 254 × 146 × 37 kg/m | |
|--------------------------------|-------|------------------------|-----------|------------------------|-----------|
| | | In TR1 | In TR2T | In TR1 | In TR2P |
| $f_{y,f}$ N/mm ² | range | 262 - 278 | 267 - 286 | 282 - 291 | 285 - 290 |
| | mean | 271 | 278 | 286 | 287 |
| $f_{y,w}$ N/mm ² | range | 316 - 320 | 301 - 333 | 307 - 322 | 300 - 310 |
| | mean | 318 | 317 | 315 | 305 |
| E_a N/mm ² | range | 195 - 210 | 205 - 219 | 203 - 205 | 186 - 208 |
| | mean | 202 | 211 | 204 | 200 |
| f_u N/mm ² | range | 449 - 508 | 462 - 505 | 457 - 470 | 456 - 474 |
| | mean | 470 | 477 | 461 | 465 |

$$f_{y,f} = 280 \text{ N/mm}^2$$

$$f_{y,w} = 315 \text{ N/mm}^2$$

$$E_a = 205 \text{ kN/mm}^2$$

$$f_u = 468 \text{ N/mm}^2$$

In predicting behaviours of the the specimens, $f_y = 290 \text{ N/mm}^2$ would then be used for whole steel section.

Coupon tests were also done for the profiled sheets used in specimens. Three coupons were cut from bottom face of the sheets. The results of tensile tests on these coupons are given in Table 7.3.

Table 7.3: Results of coupon test for sheeting

| | coupon 1 | coupon 2 | coupon 3 | mean value |
|--|--------------|--------------|--------------|-------------|
| measured size of the cross section (mm) | 0.90 × 20.17 | 0.90 × 20.38 | 0.91 × 20.31 | 0.9 × 20.29 |
| measured yield strength (N/mm ²) | 368 | 390 | 373 | 377 |

According to table 7.3, the measured yield strength of the sheeting may be regarded as

- $f_{yp} = 377 \text{ N/mm}^2$

Three bars with length about 300 mm were cut from each kind of mesh and tensile tests were conducted on these bars. Figure 7.14 shows the measured relationship of stress and strain in these mesh bars. Based the results obtained, the following value was taken in analyses as yield strength of the transverse reinforcement in the specimens.

- $f_s = 600 \text{ N/mm}^2$

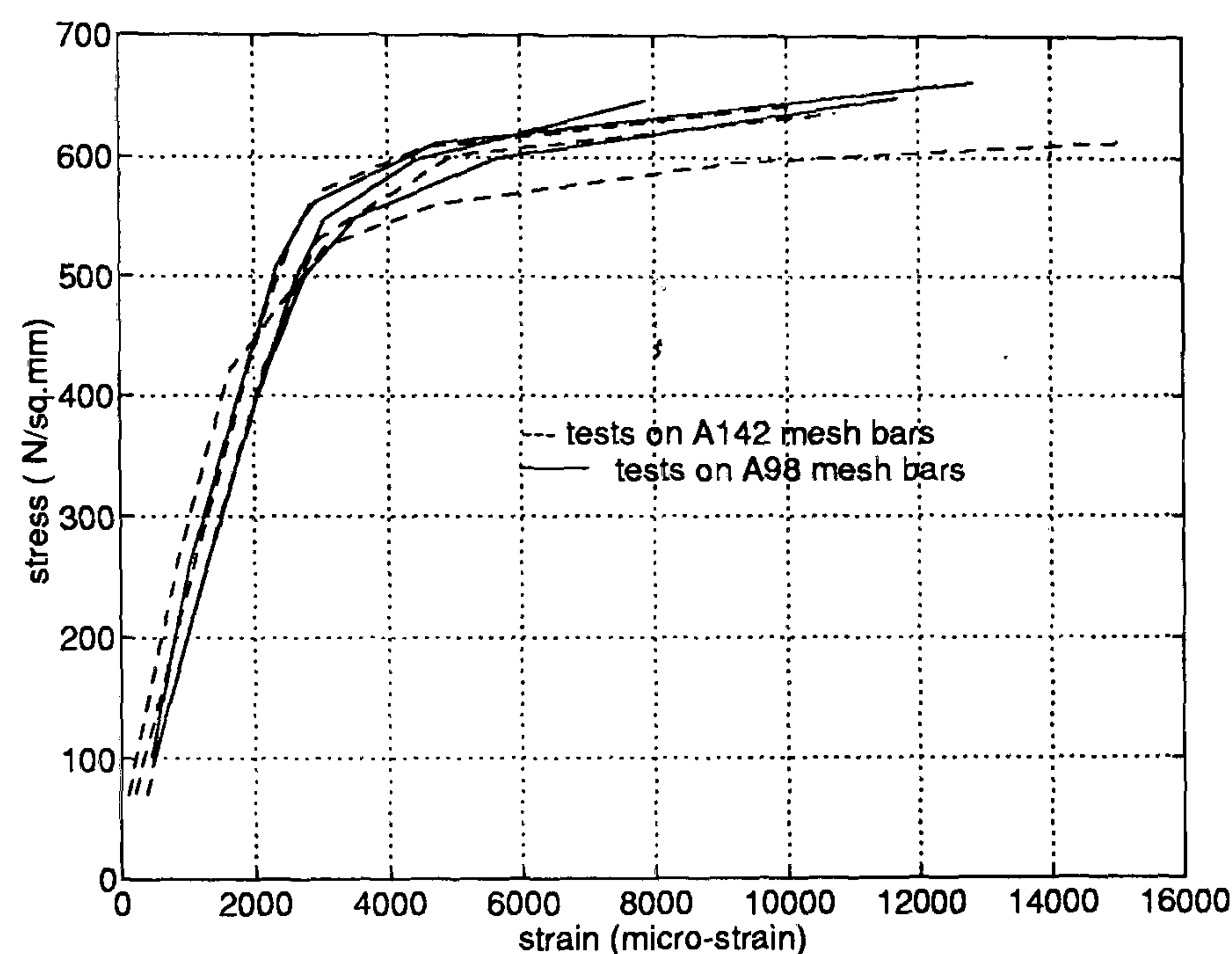


Figure 7.14: Results of tensile tests on reinforcement

Ready-mix concrete was used for all specimens.

In fabricating specimen TR1, the ready-mixed concrete was ordered with the following specifications:

- cube strength at 28 days: 20 N/mm^2 ;
- aggregate size: 10 mm;
- classification: normal weight;
- slump: 50 — 70 mm.

For specimens TR2T and TR2P, the specification for the concrete was as for TR1 except that

- cube strength at 28 days: 15 N/mm²;

Twelve 150 × 150 cubes and six 100 × 200 cylinders were made at the same time as casting specimen TR1.

Specimen TR2T and TR2P were cast at the same time, and twelve 150 × 150 cubes and six 100 × 200 cylinders were made.

The specimens, cubes and cylinders were cured under the same condition: covered by damp cloth for the first 7 days and then exposed in air until the tests were carried out.

The compression strength of concrete was measured by cube tests, in accordance with BS1881: Part 117: 1983; the loading rate was 450 kN/min. The tensile strength of concrete was measured from splitting tests on the cylinders, in accordance with BS1881: Part 116: 1983, with loading rate 56 kN/min. Tables 7.4 and 7.5 show the measured strengths of concrete for TR1, TR2T and TR2P.

Table 7.4: Strength of concrete in TR1, in N/mm²

| age (day) | number of cubes tested | mean of strength | number of cylinders tested | mean of strength | notes |
|-----------------|------------------------|------------------|----------------------------|------------------|-------------------------------|
| 14 (4/8/92) | 2 | 31.2 | – | – | |
| 21 (11/8/92) | 2 | 33.2 | 2 | 3.70 | test TR1T started on 12/8.92 |
| 28 (18/8/92) | 2 | 37.0 | – | – | test TR1P1 started on 19/8/92 |
| 37 (27/8/92) | 3 | 36.0 | 2 | 3.21 | |
| 44 (3/9/92) | 3 | 38.4 | 2 | 3.51 | test TR1P2 started on 2/9/92 |

From the material tests on concrete in specimen TR1, the cube strength of concrete may be taken as $f_{cu} = 33 \text{ N/mm}^2$ for test TR1T and $f_{cu} = 37 \text{ N/mm}^2$ for tests TR1P1 and TR1P2. The results for the tensile strength f_{ct} for concrete in TR1 showed no clear trend, so the mean of all tested values was taken as

Table 7.5: Concrete strength in specimens TR2T and TR2P, in N/mm²

| age (day) | number of cubes tested | mean of strength | number of cylinders tested | mean of strength | notes |
|-----------------|---------------------------|---------------------|-------------------------------|---------------------|------------------------------|
| 7 (10/3/93) | 2 | 13.55 | – | – | |
| 14 (17/3/93) | 2 | 18.13 | 2 | 2.08 | |
| 26 (29/3/93) | 2 | 23.07 | 2 | 2.43 | TR2T1 started on 30/3/93 |
| 47 (19/4/93) | 2 | 23.97 | 2 | 2.67 | |
| 54 (26/4/93) | 2 | 24.46 | - | - | TR2P1 started on this day |
| 57 (29/4/92) | 2 | 25.17 | - | - | |

tensile strength of the concrete: $f_{ct} = 3.5 \text{ N/mm}^2$.

From the measurements shown in Table 7.5, for tests on beam TR2T, the tensile strength and cube strength of concrete may be taken as $f_{ct} = 2.4 \text{ N/mm}^2$ and $f_{cu} = 23 \text{ N/mm}^2$, respectively, while for tests on beam TR2P, $f_{ct} = 2.7 \text{ N/mm}^2$ and $f_{cu} = 25 \text{ N/mm}^2$, respectively.

7.4 Test rig and instrumentation

7.4.1 Loading system

According to the test plan for specimen TR1, TR2T and TR2P, the main load applied in every test would be a concentrated load. The loading point for each test has been shown in Figures 7.1, 7.2 and 7.3.

On specimen TR1, A 500-kN jack was used to apply the test load; during test TR1P1, a 50-kN jack was also used at point G shown in Figure 7.1, to make longitudinal cracks along the primary beam. Figure 7.15 gives the loading system for specimen TR1.

In tests on specimens TR2T and TR2P, the test load was applied by a 500-kN jack and the loading rig is shown in Figures 7.16.

At each support and loading point in each test, a load cell was used to measure the force. With reference to Figures 7.1, 7.2 and 7.3, details of the load cells and their calibration results are given in Table 7.6. All the load cells were calibrated before the tests. The calibration curves of load cell used are shown in Figures 7.17 and 7.18.

Table 7.6: Arrangement of load cells

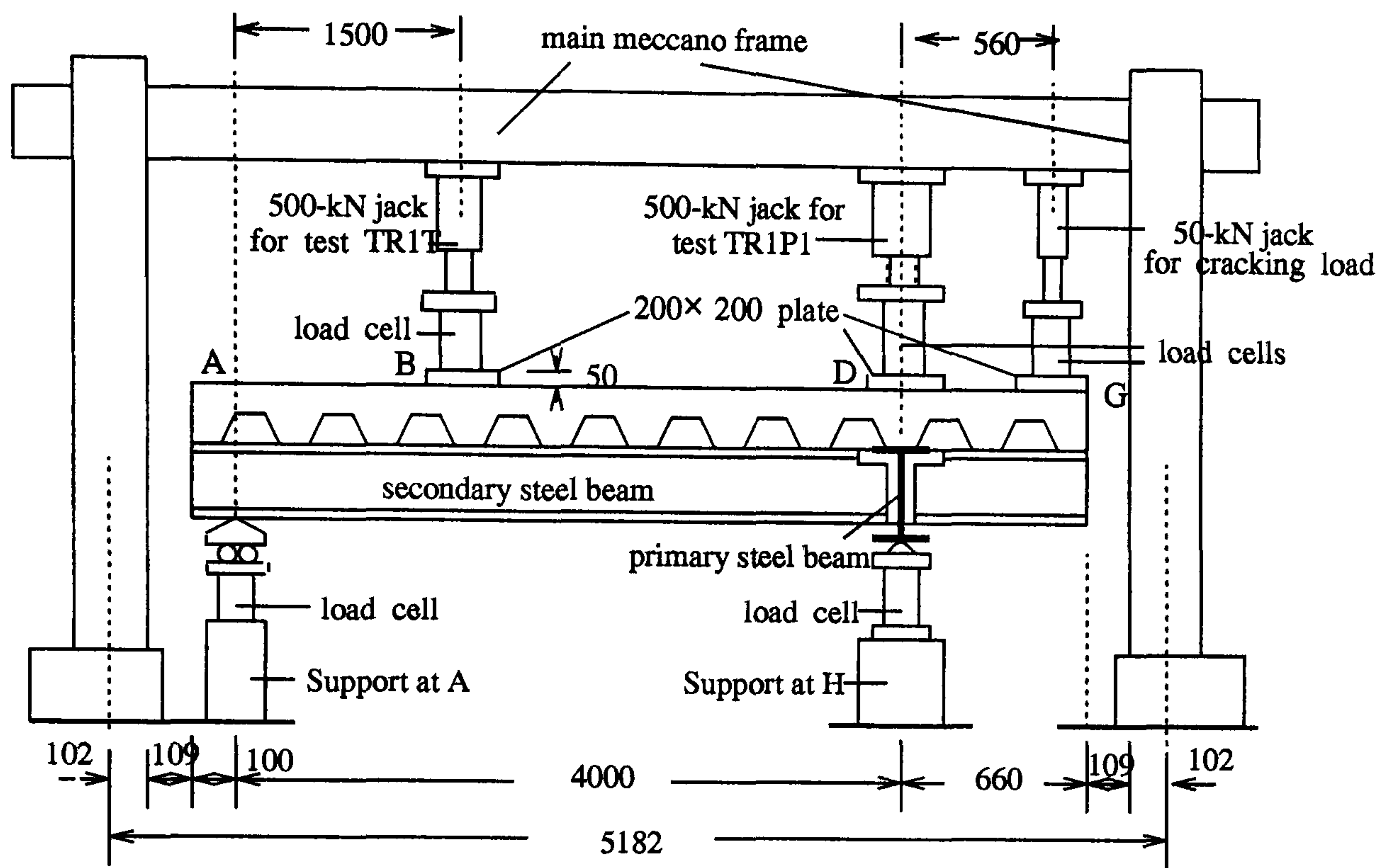
| Load cell No. | Location | Scale range | calibration formula |
|---------------|--|--------------|---------------------------|
| No.2657 | support A in TR1; support A in TR2T; support H in TR2P | 0 - 250 (kN) | $f = 10.37D_{mv} + 1.21$ |
| No.1690 | support H in TR1 | 0 - 500 (kN) | $f = 30.21D_{mv} - 0.74$ |
| No.1837 | support L in TR1; loading points in TR2T & TR2P | 0 - 500 (kN) | $f = 20.91D_{mv} + 18.40$ |
| No.1854 | support D in TR2T; support L in TR2P | 0 - 250 (kN) | $f = 10.35D_{mv} + 21.68$ |
| No.1674 | load at point G in TR1 | 0 - 50 (kN) | $f = 3.02D_{mv} + 0.32$ |
| No.1817 | the rest loading points in TR1 | 0 - 500 (kN) | $f = 41.80D_{mv} + 6.03$ |
| No.12385 | support Q in TR1 | 0 - 100 (kN) | $f = 6.41D_{mv} + 1.10$ |
| No.12386 | support T in TR1 | 0 - 100 (kN) | $f = 6.36D_{mv} + 3.14$ |

In Table 7.6, f denotes the measured force, in units of kN, and D_{mv} the electronic output from the data-logger, in milli-volts.

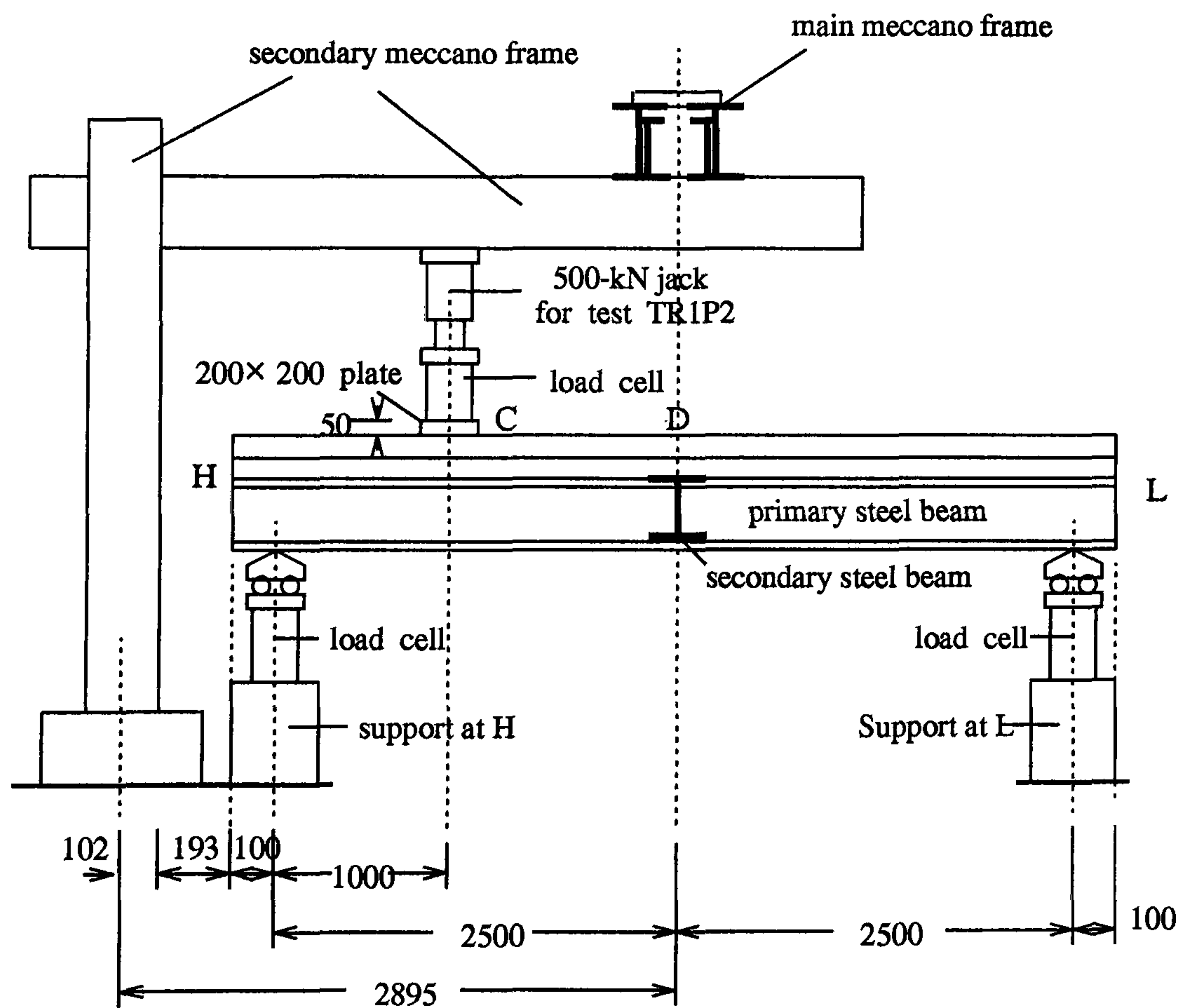
7.4.2 Measurement of slip and deflexion

In the tests, electronic transducers (LVDTs) were used to measure

- the slip between the concrete slab and steel beam at the tested end,
- the deflexion of the loaded point in each test.



(a)



(b)

Figure 7.15: Loading rig in tests on TR1

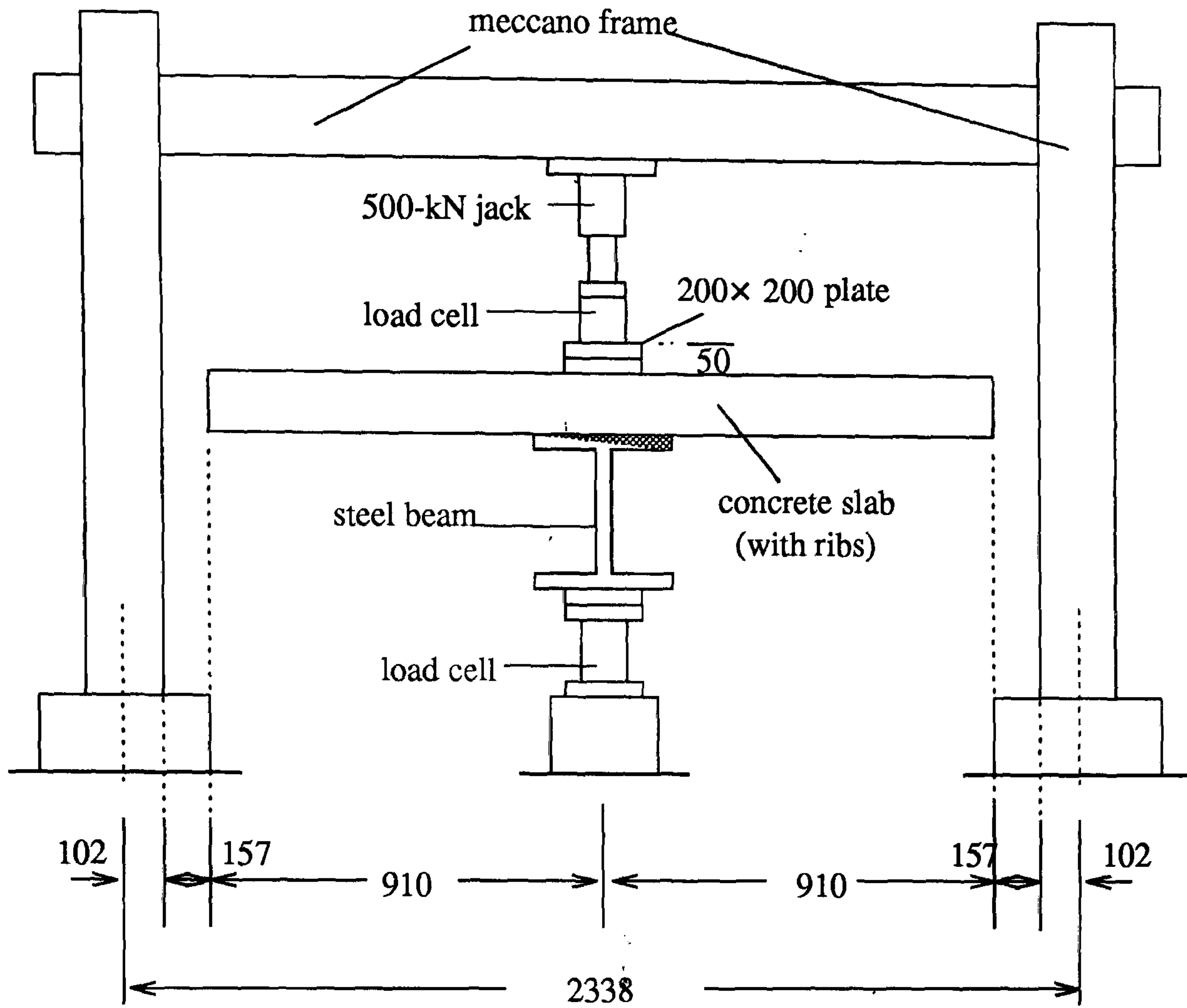


Figure 7.16: Loading rig in tests on TR2T and TR2P

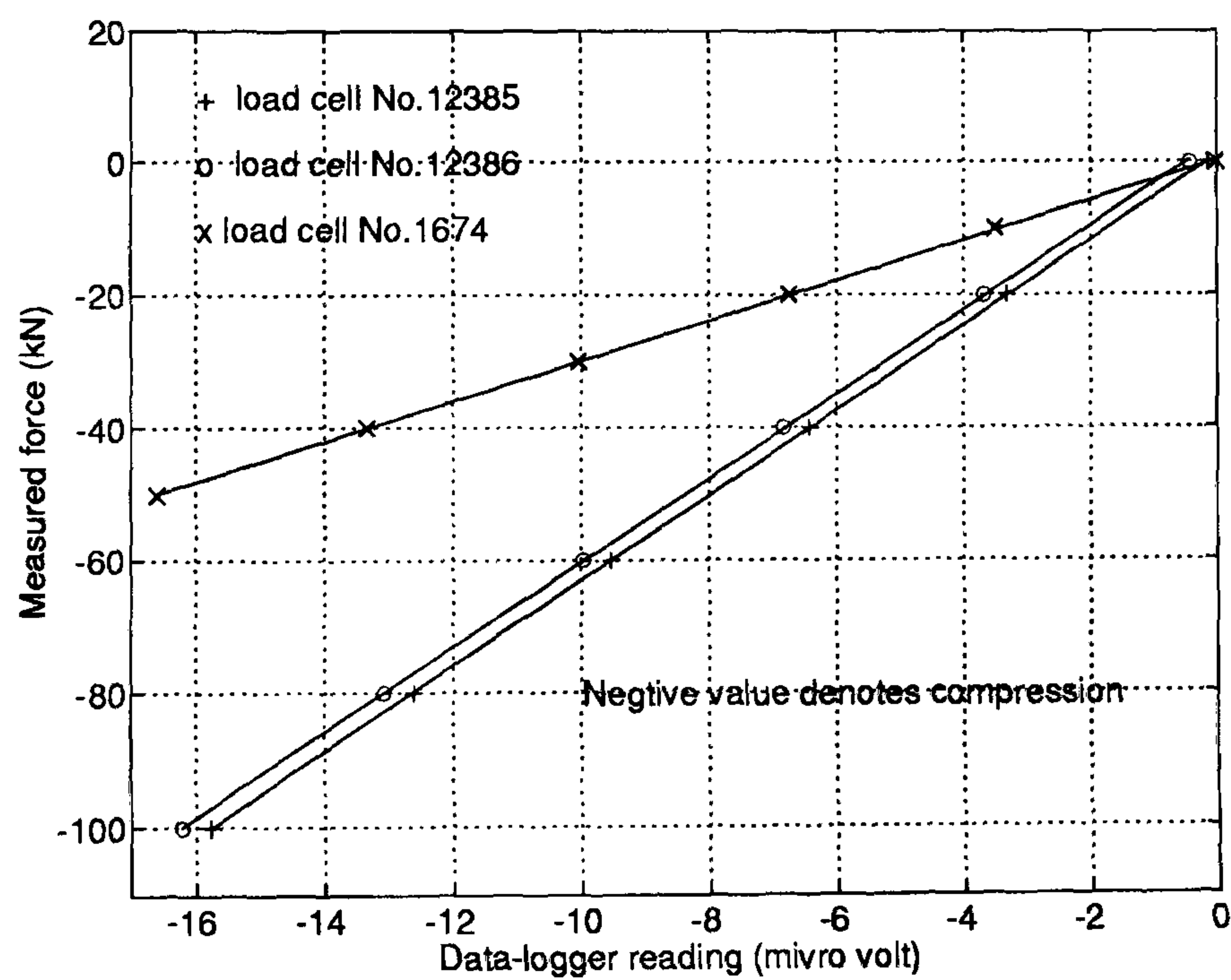


Figure 7.17: Calibration of 50-kN and 100-kN load cells

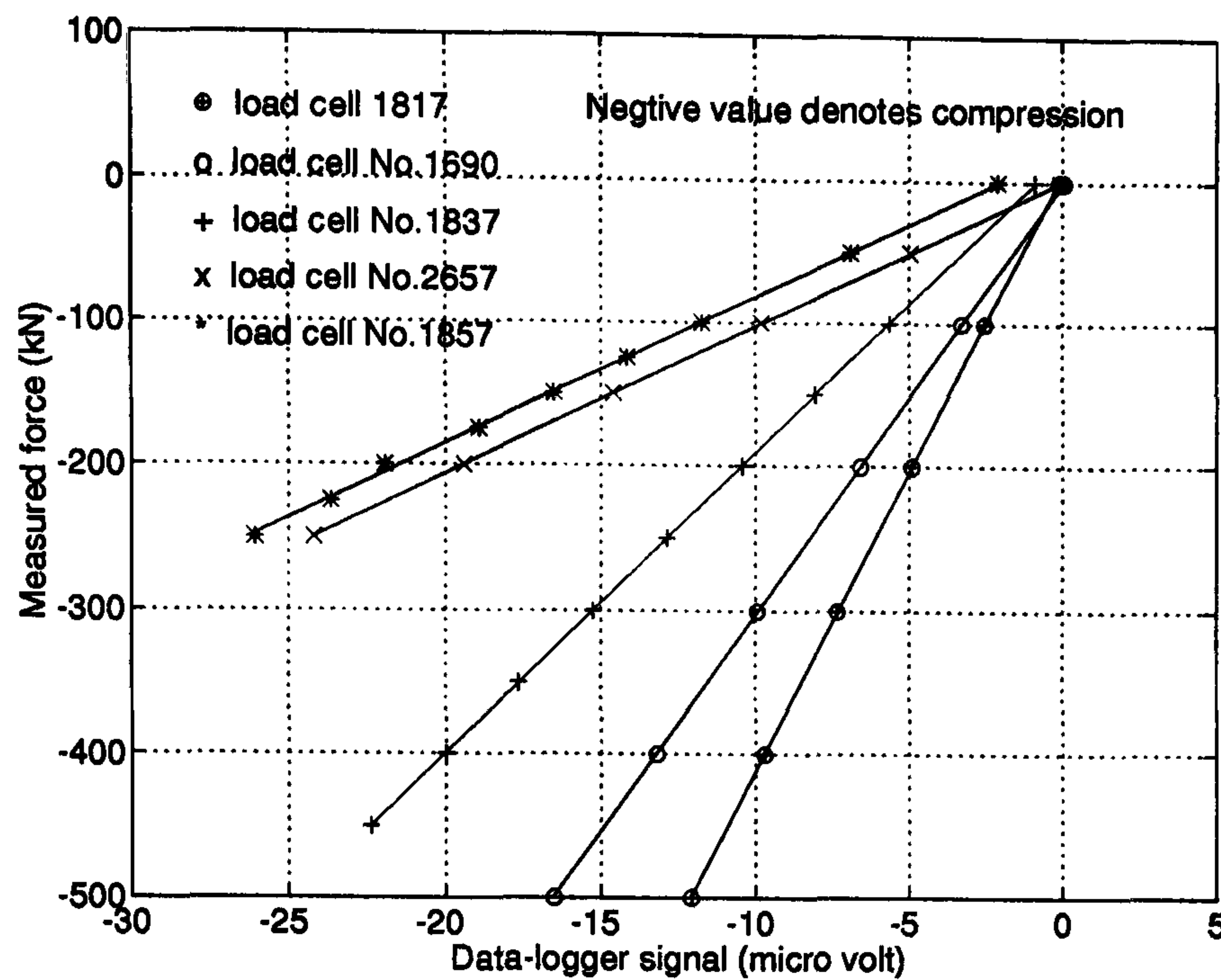


Figure 7.18: Calibration of 500-kN and 250-kN load cells

Figure 7.19 shows use of LVDTs on specimen TR1, while Figure 7.20 gives application of LVDTs in beams TR2T and TR2P.

In test TR1T on TR1, two LVDTs with 50-mm scale range were horizontally fixed to the column of the “Meccano” frame”, as shown in Figure 7.21(a). It was originally considered that the slip at end A of specimen TR1 could be found from the difference of the horizontal movement measured by such two LVDTs. However, it was realized after test TR1T that the slip can not be measured reliably in this way, as relative horizontal movement is caused also by the rotation of the end section. Therefore, the slip at end A in test TR1T can not be reported.

The slips at the tested end in the other tests were measured by one LVDT of 50-mm scale range, as shown in Figure 7.21(b).

The deflexions were monitored by 100-mm LVDTs. Besides the loaded points, the deflexions at midspan were also measured in tests on specimens TR2T and TR2P.

Every LVDT used was calibrated over its full scale range, as shown in Figure 7.22 and 7.23. Table 7.7 gives the calibration results, where Δ denoted the measured displacement, in unit of mm, and ε the electronic output from Data-

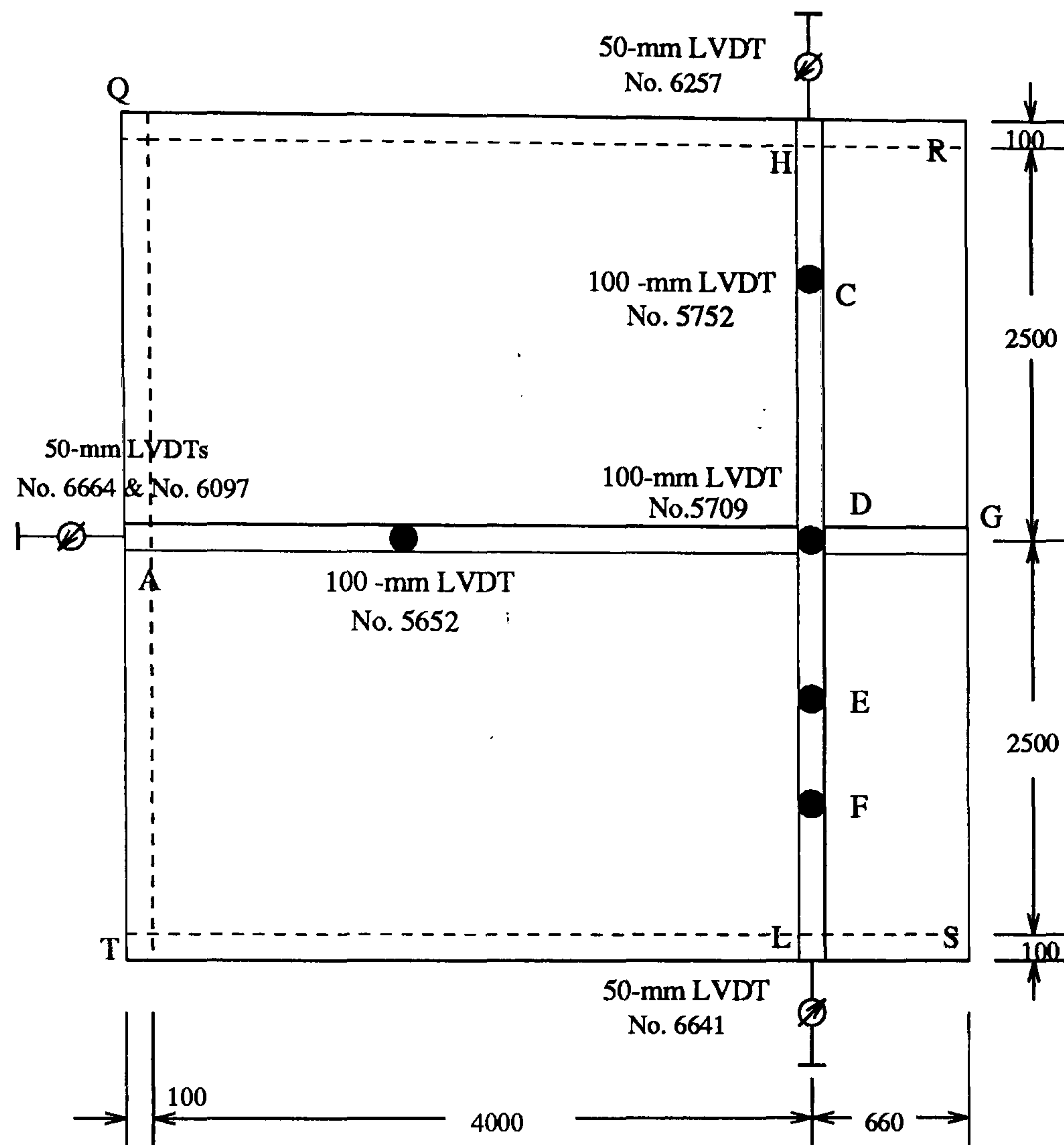


Figure 7.19: LVDTs used in specimen TR1

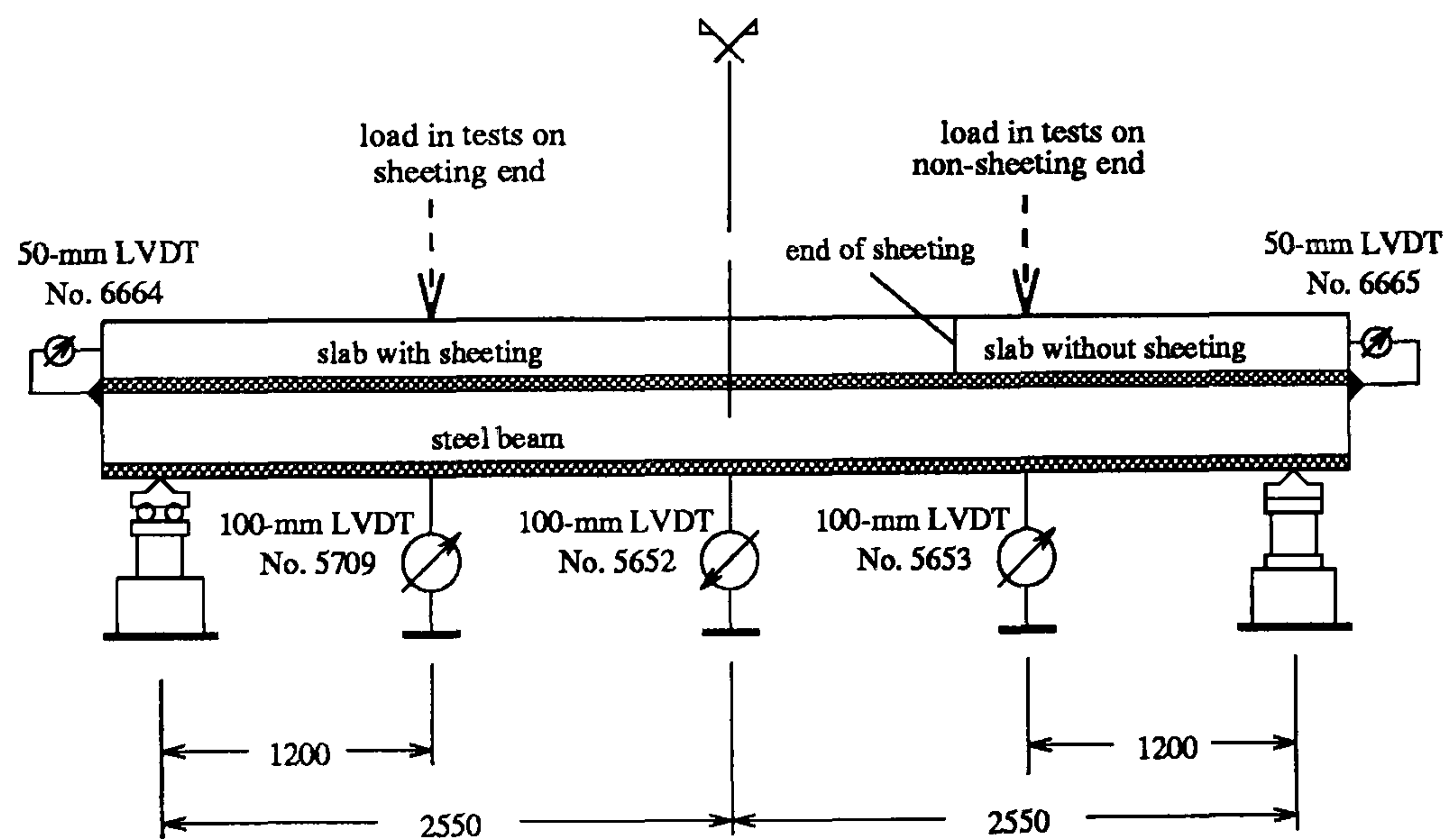


Figure 7.20: LVDTs used in specimens TR2T and TR2P

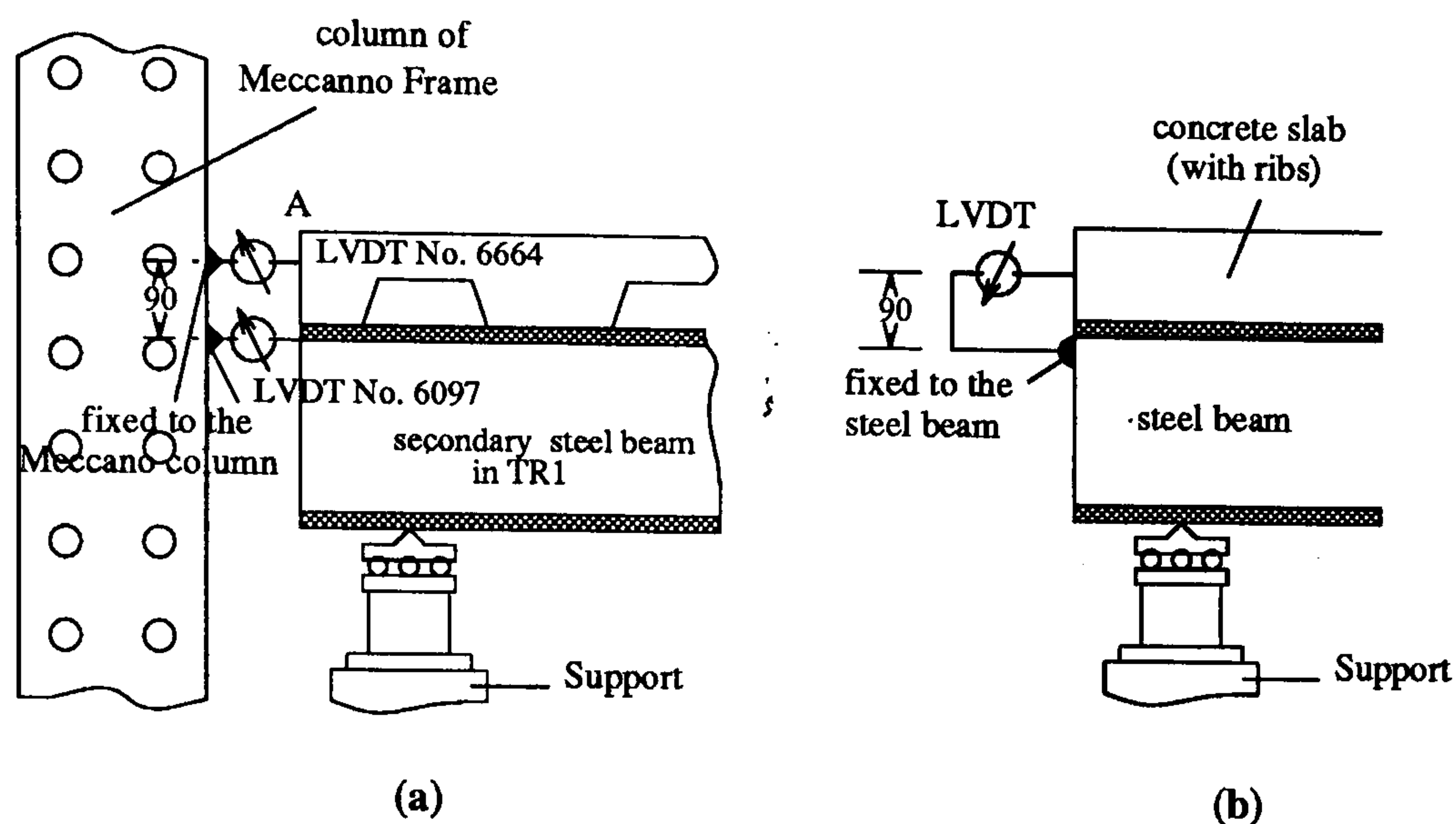


Figure 7.21: LVDTs for measuring slips

logger, given by micro strain.

Table 7.7: Use of LVDTs

| LVDT No. | scale range | calibration formula |
|----------|--------------|---|
| No.6079 | 0 - 50 (mm) | $\Delta = (6.90\varepsilon + 34.90) \times 10^{-3}$ |
| No.6664 | 0 - 50 (mm) | $\Delta = (7.05\varepsilon + 11.27) \times 10^{-3}$ |
| No.6665 | 0 - 50 (mm) | $\Delta = (6.93\varepsilon - 39.21) \times 10^{-3}$ |
| No.6641 | 0 - 50 (mm) | $\Delta = (6.90\varepsilon + 3.9) \times 10^{-3}$ |
| No.6257 | 0 - 50 (mm) | $\Delta = (6.90\varepsilon - 36.5) \times 10^{-3}$ |
| No.5709 | 0 - 100 (mm) | $\Delta = (9.56\varepsilon - 39.35) \times 10^{-3}$ |
| No.5652 | 0 - 100 (mm) | $\Delta = (9.73\varepsilon - 19.35) \times 10^{-3}$ |
| No.5653 | 0 - 100 (mm) | $\Delta = (9.72\varepsilon - 37.42) \times 10^{-3}$ |
| No.5752 | 0 - 100 (mm) | $\Delta = (9.60\varepsilon - 1.80) \times 10^{-3}$ |

7.4.3 The strain gauges

Taking account of the positions where load was to be applied in each test, strain gauges were placed on several sections of each steel beam, so the total force in steel beam F_a shown in Figure 1.1(a) can be obtained, from which the force F on the flange portion as shown in Figure 1.1(b) may in turn be estimated.

The strain gauges were arranged for the tests as shown in Figures 7.24 and 7.25. Because test TR1P2 on TR1 had to be conducted on the same steel beam

as TR1P1, it was not certain before the tests that the failure would occur within region CH, since the primary steel beam might have been weakened within CL by test TR1P1. Therefore, as shown in Figure 7.25, strain gauges, No.101-109 and No.131-139, were as a precaution placed on two sections within length DC.

All the strain gauges were post-yield type YL-10, with gauge length 100 mm and strain limit (10-20)%.

For the tests, some demec gauges were also originally arranged to monitor the strain on the top surface of concrete slab. However, it was found during tests that, in the middle of the tests, the concrete between the measurement points of many demec gauges cracked, so the reading from such demec gauges would be no longer reliable; furthermore, since the concrete slab was measured by demec gauges only along the lines on the top surface, the deformation and stress in concrete slab along the slab width would still remain obscure. Hence, for checking stress distribution in concrete along longitudinal shear surface and effective width of concrete slab etc. the demec readings actually provided little useful information. Therefore, these readings were not reported in this study.

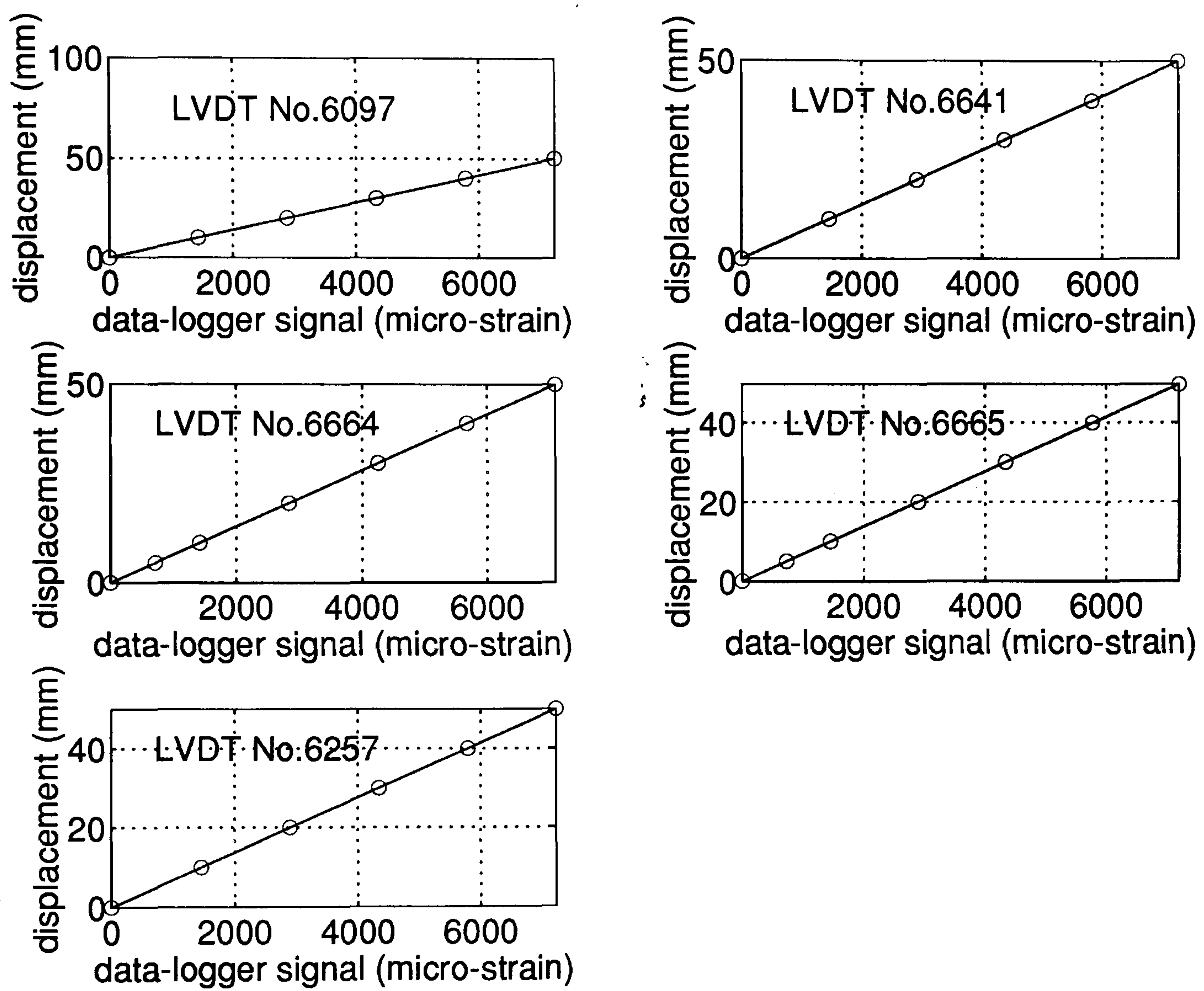


Figure 7.22: Calibration of 50-mm LVDT

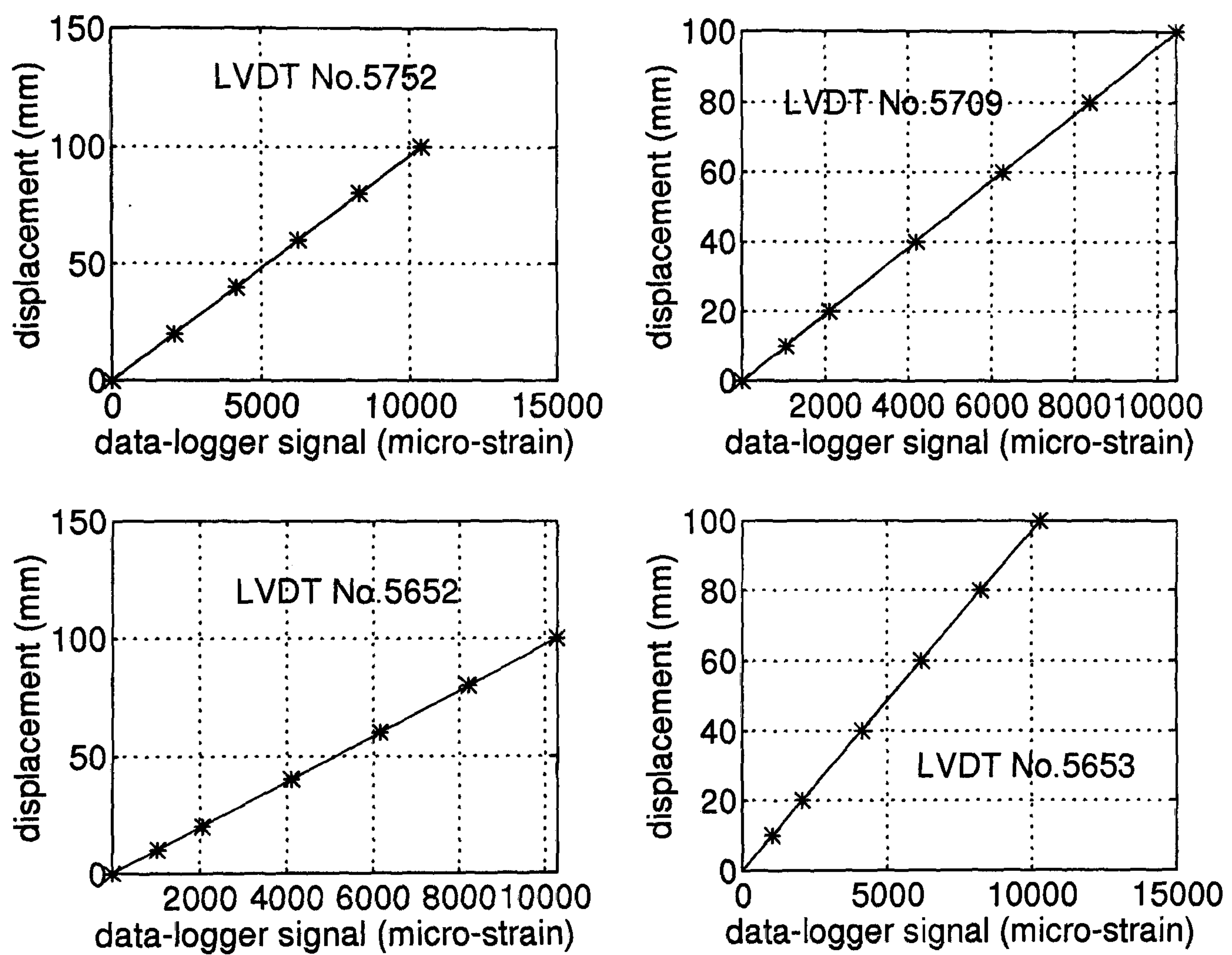
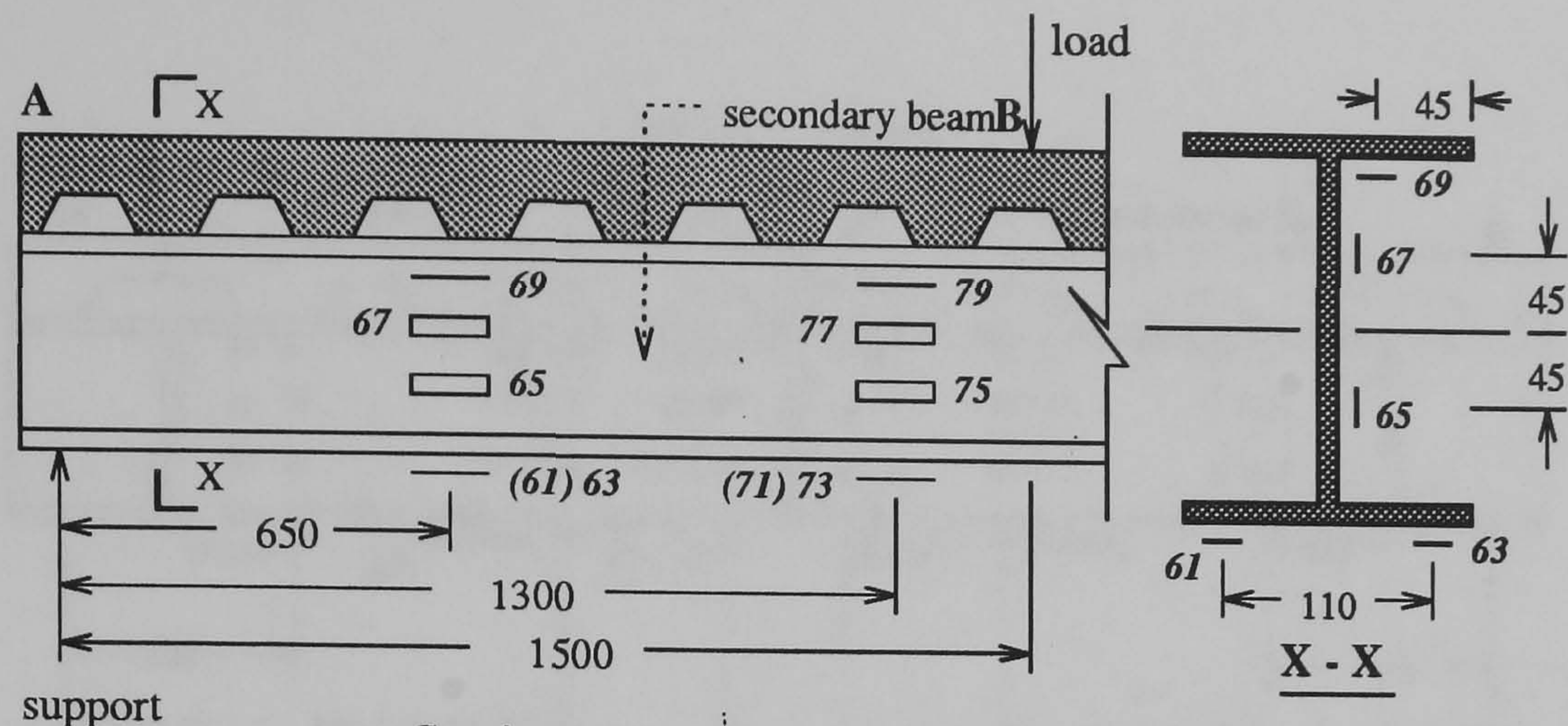
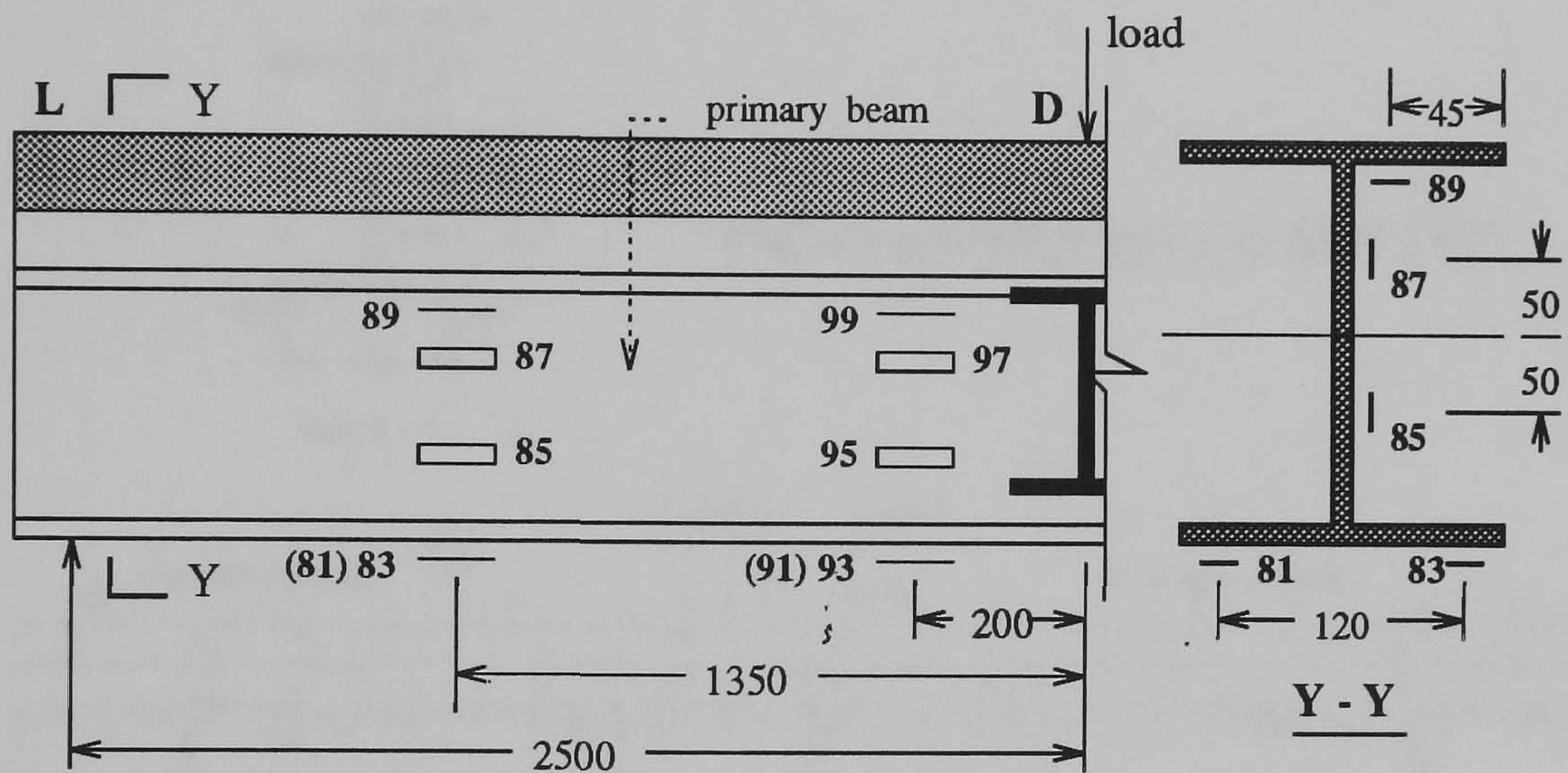


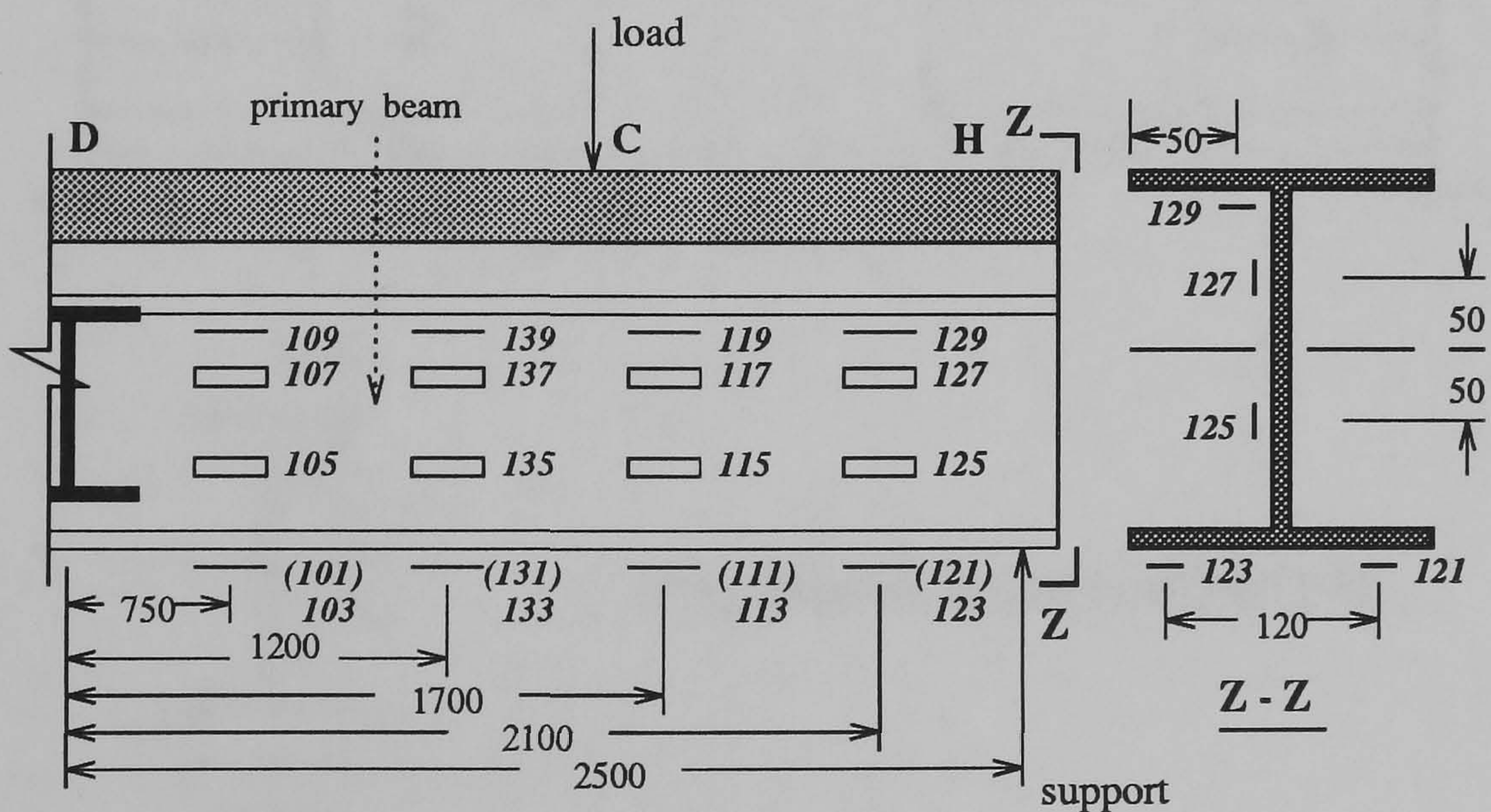
Figure 7.23: Calibration of 100-mm LVDT



Strain gauges on steel beam for test TR1T

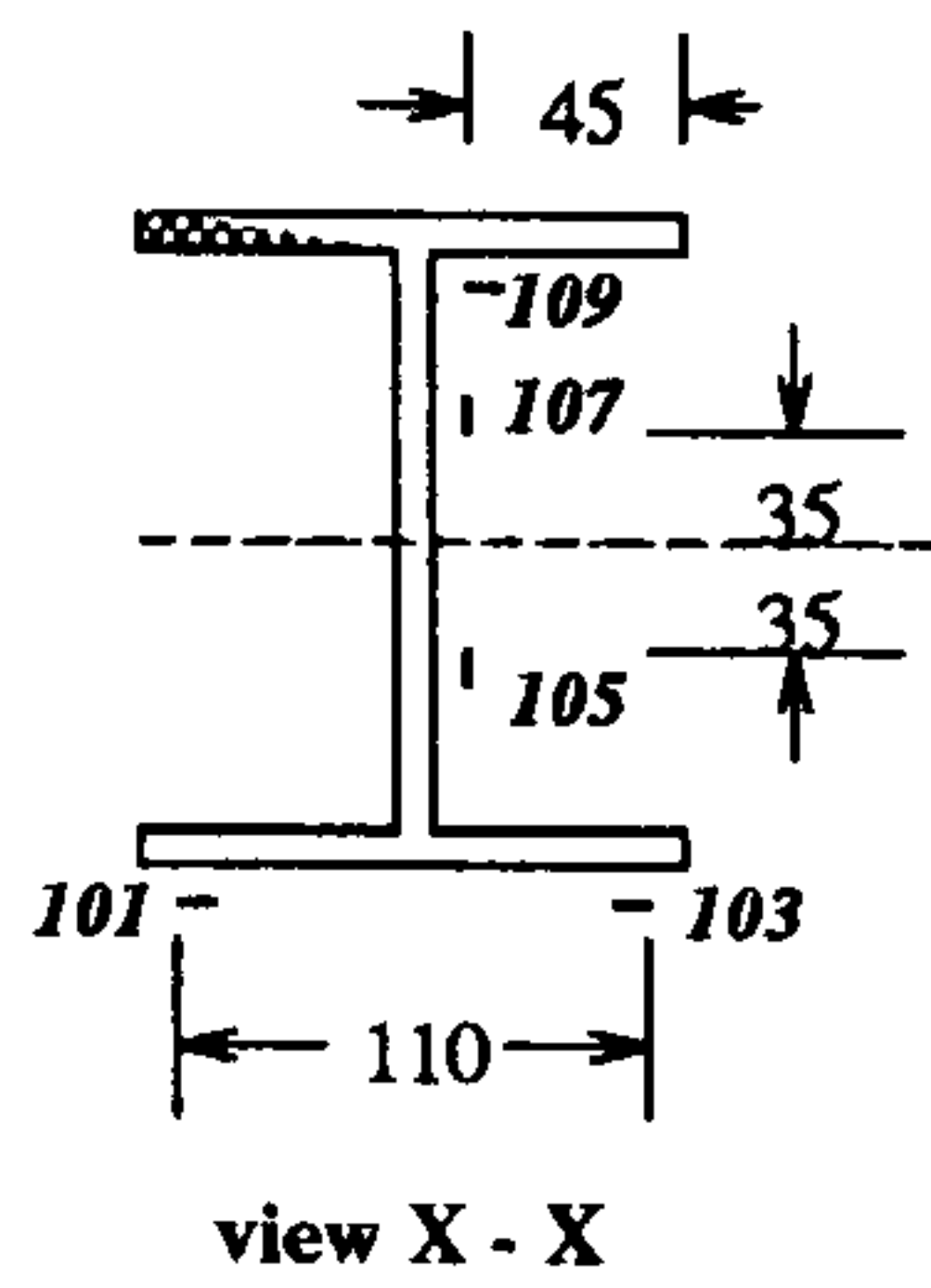
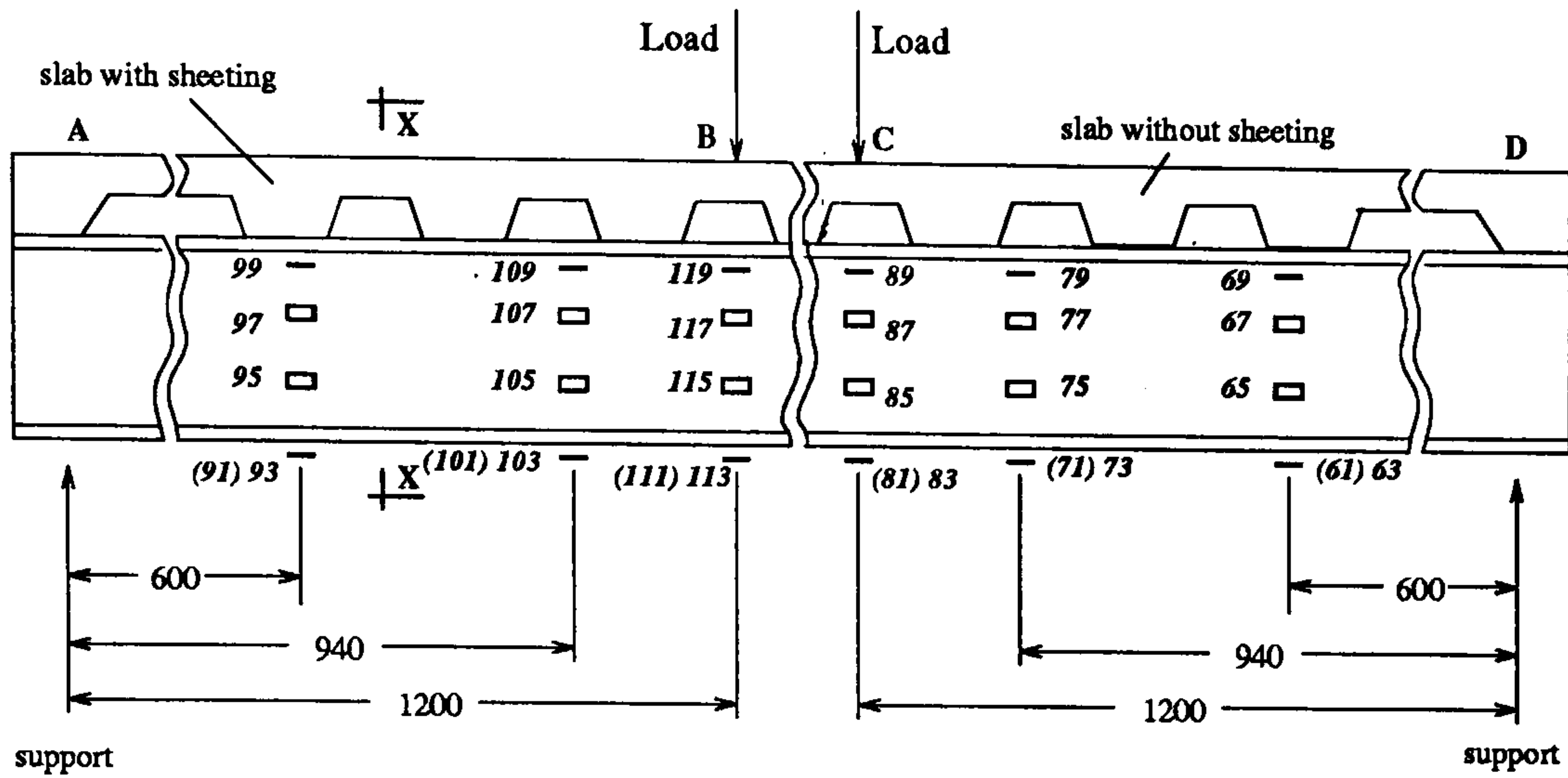


Strain gauges on steel beam for test TR1P1

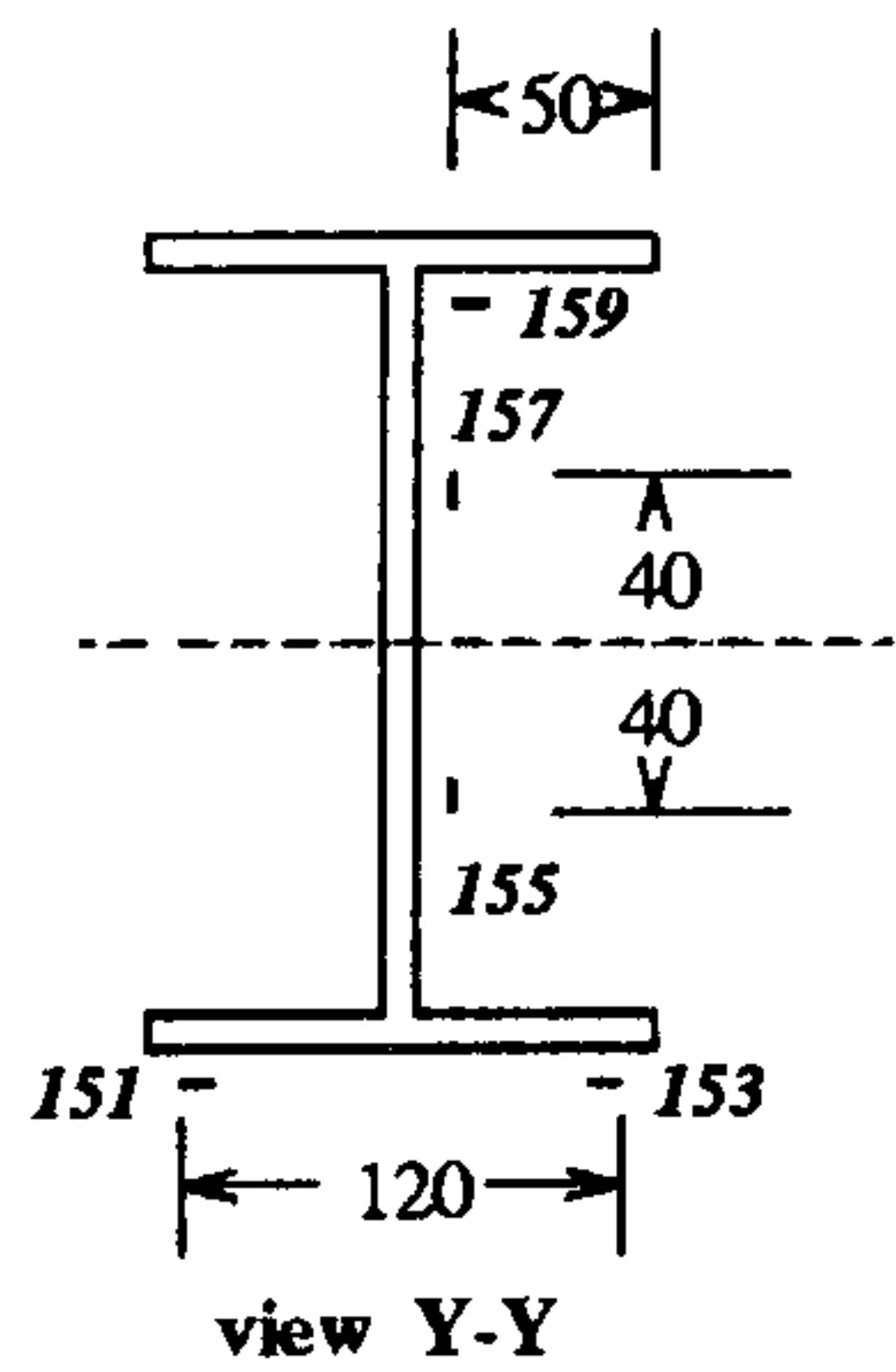
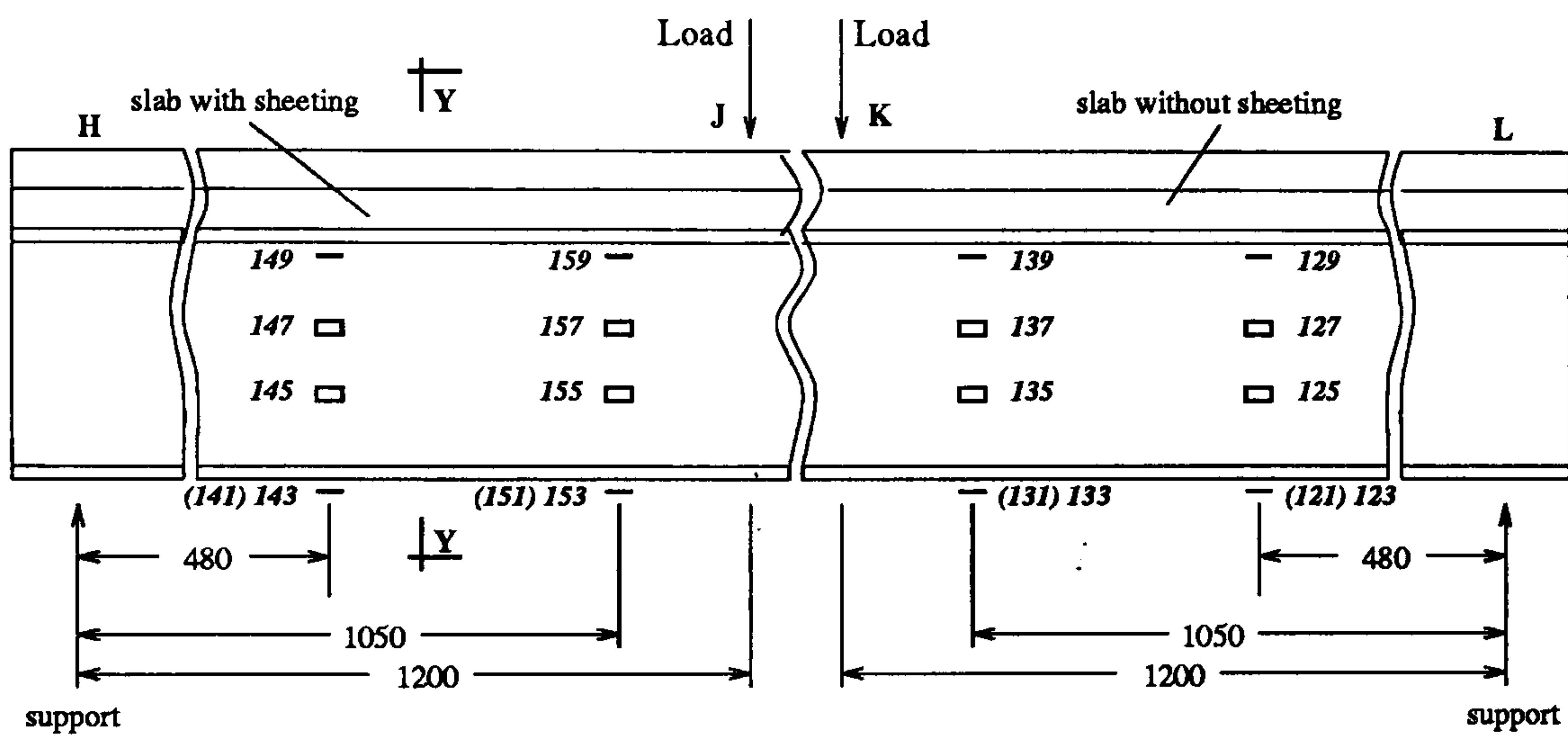


Strain gauges on steel beam for test TR1P2

Figure 7.24: Strain gauges in specimen TR1



Strain gauges on steel beam in specimen TR2T



Strain gauges on steel beam in specimen TR2P

Figure 7.25: Strain gauges in specimens TR2T & TR2P

Chapter 8

Testing procedure and results

In this chapter, conducting of the tests and the results obtained are reported. The discussions about the test results are made in Chapter 9.

8.1 Loading procedure, failure appearance and deformation

An electronic data-logger controlled by a personal computer was used in all tests to record the test information, including the applied load, deflexion, slip and readings from the strain gauges.

From simple beam theories [1,9], the ultimate loads for flexural failure can be calculated with respect to the geometry of the specimens and the measured strengths of materials. In order to make comparison later, the results from these calculations, ignoring self-weight of the specimens and taking the effective width as one quarter of the span, are presented in Tables 8.2 and 8.1. The maximum loads obtained in tests are also shown in Table 8.2.

The tests were carried out as follows.

Table 8.1: Predicted bending resistances

| | ¹ $M_{el,R}$ (kN-m) | ² F_{el} (kN) | ³ $M_{pp,R}$ (kN-m) | ⁴ F_{cp} (kN) | ⁵ $M_{pl,R}$ (kN-m) | ⁶ F_{cf} (kN) |
|-------------------|-----------------------------------|-------------------------------|-----------------------------------|-------------------------------|-----------------------------------|-------------------------------|
| TR1T | 162 | 630 | 209 | 905 | 225 | 1102 |
| TR1P1 (load at D) | 228 | 759 | - | - | 318 | 1378 |
| TR1P1 (load at F) | | | | | | |
| TR1P2 | 228 | 759 | 241 | 587 | 318 | 1378 |
| TR2T1 | | | | | | |
| TR2T2 | 158 | 637 | 173 | 612 | 210 | 1102 |
| TR2P1 | | | | | | |
| TR2P2 | 219 | 738 | - | - | 291 | 1378 |

- ¹ bending resistance at the first yielding of the steel beam, assuming full shear connection
- ² the force in concrete slab corresponding to $M_{el,R}$
- ³ ultimate bending resistance at plastic state, considering partial shear connection
- ⁴ the force in concrete slab corresponding to $M_{pp,R}$
- ⁵ the ultimate bending resistance at plastic state, assuming full shear connection
- ⁶ the force in concrete slab corresponding to $M_{pl,R}$

Table 8.2: The ultimate loads from bending theories and tests

| Test No. | ¹ $P_{el,R}$ (kN) | ² $P_{pp,R}$ (kN) | ³ $P_{pl,R}$ (kN) | ⁴ $P_{e,max}$ (kN) |
|--------------------|------------------------------|------------------------------|------------------------------|-------------------------------|
| TR1T | 173 | 223 | 240 | 300 |
| ⁵ TR1P1 | load at D | - | 254 | 235 |
| | load at F | 285 | 398 | 330 |
| TR1P2 | 285 | 301 | 398 | 385 |
| TR2T1 | 172 | 189 | 229 | 215 |
| TR2T2 | 172 | 189 | 229 | 186 |
| TR2P1 | 239 | - | 317 | 320 |
| TR2P2 | 239 | - | 317 | 300 |

- ¹ the load found from $M_{el,R}$
- ² the load found from $M_{pp,R}$
- ³ the load found from $M_{pl,R}$
- ⁴ the maximum load obtained from tests
- ⁵ $P_{e,max}$ reported here does not include the secondary load, as planned in section 7.1.1, at point G.

8.1.1 Tests on specimen TR1

Test TR1T As introduced in section 7.1, the load in this test was applied on point B (see Figure 7.1). The measured deflexion of this point is shown in Figure 8.1. In the first stage, the load was increased up to 160 kN in increments of 15 kN. Because the calculated elastic limit load $P_{el,R}$, as shown in Table 8.2, was being reached, the loading increment was then changed into 5 kN. Eventually, the load reached 300 kN and the failure occurred when a hole just under the loading plate was punched.

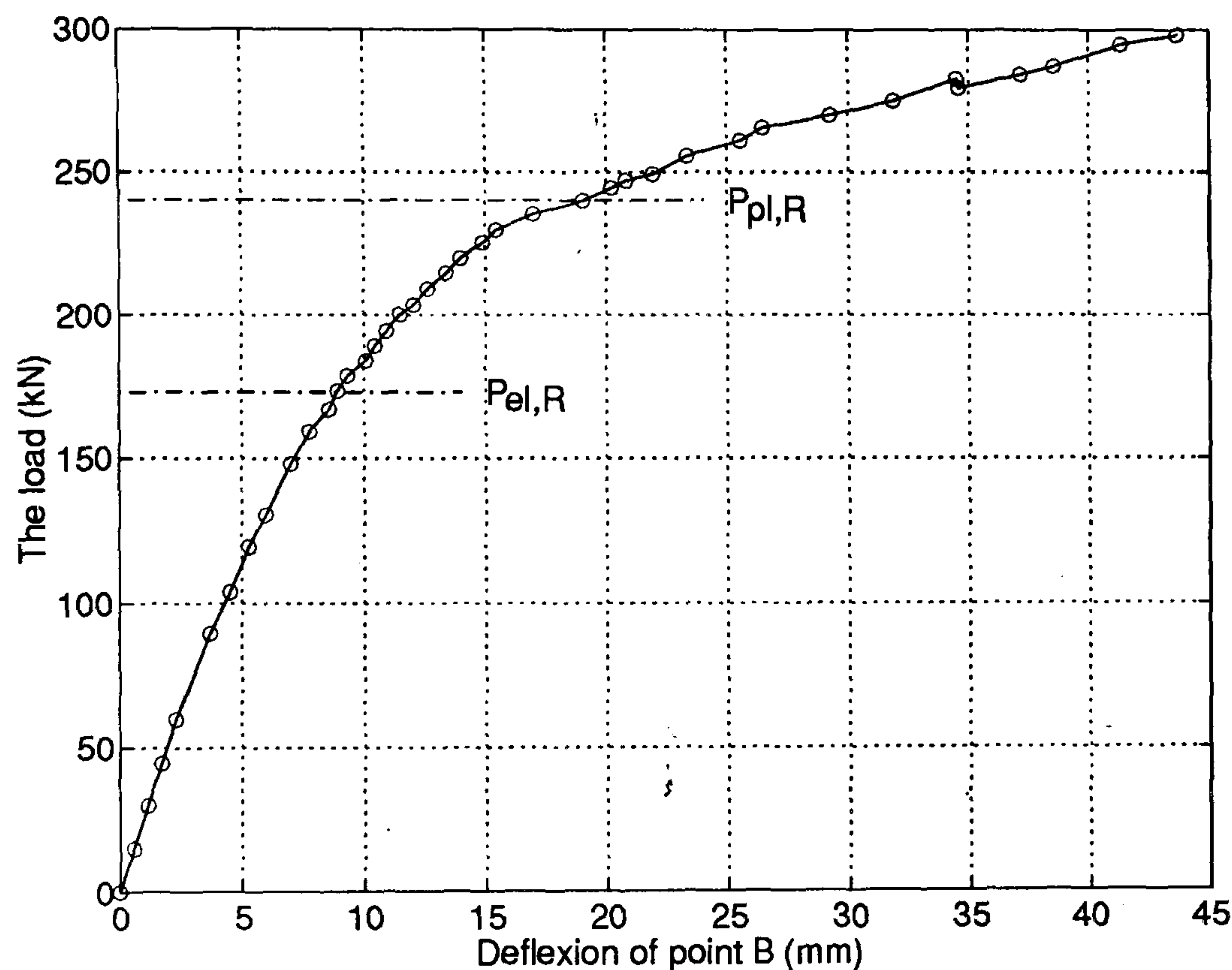


Figure 8.1: Deflexion of loaded point in TR1T

Test TR1P1 As notified in in section 7.1, a 35 kN load had been applied at point G in advance and was maintained throughout test TR1P1. The main load was applied at point D, as planned in Figure 7.1. However, as the main load was increased to 235 kN, the deflexion of the loaded point D had reached 40 mm. At this load level, it was also found that the primary steel beam under the main load had yielded over more than two-thirds of its depth, but no sign of any shear failure in the specimen appeared, which implied that the bending failure would

failure in the specimen appeared, which implied that the bending failure would have occurred if loading at D had been continued. Therefore, the main load was moved towards end L by 1 m and the loading point was changed into E, as shown in Figure 7.1. The load on this point was applied up to 270 kN and the specimen still gave no sign of shear failure. In order to avoid bending failure, the main load was again moved, and the loading point was therefore set at F (see Figure 7.1). The maximum value of the load at F eventually reached 330 kN. At this load, the test region of specimen was failed due to a hole under the loading plate being punched. Corresponding to loading at point F, the deflexion of this loaded point and slip at the tested end L, as marked in Figure 7.1, were obtained as shown in Figures 8.2 and 8.3.

During this test, the specimen withstood some unloading and reloading procedures. However, it is noted here that, for all the tests including TR1P1, the parts of any test curve measured before unloading and after reloading (if any) have smooth continuation, therefore, all the measurements made for unloading and reloading (if any) in any of the tests are not shown and discussed.

Test TR1P2 In this test, the secondary load at G was removed, so only point C as marked in Figure 7.1 was loaded. Measured deflexion of the loaded point and slip at the tested end are shown in Figures 8.2 and 8.3. Figure 8.4 presents a general view of the specimen in this test. The load was steadily increased from zero to 320 kN in increment of 20 kN. Because the load was approaching $P_{pl,R}$ (see Table 8.2), the load increment was then changed to 10 kN. When the load passed 360 kN, the increment was further reduced to 5 kN. The maximum load achieved was 385 kN. and, as Test TR1P1, the specimen in this test was failed when a hole was punched on the concrete slab under the loading.

8.1.2 Tests on specimens TR2T and TR2P

Test TR2T1 A concentrated load was applied at point B, as indicated in Figure 7.2. The measured deflexion of the loaded point and slip at the tested end are

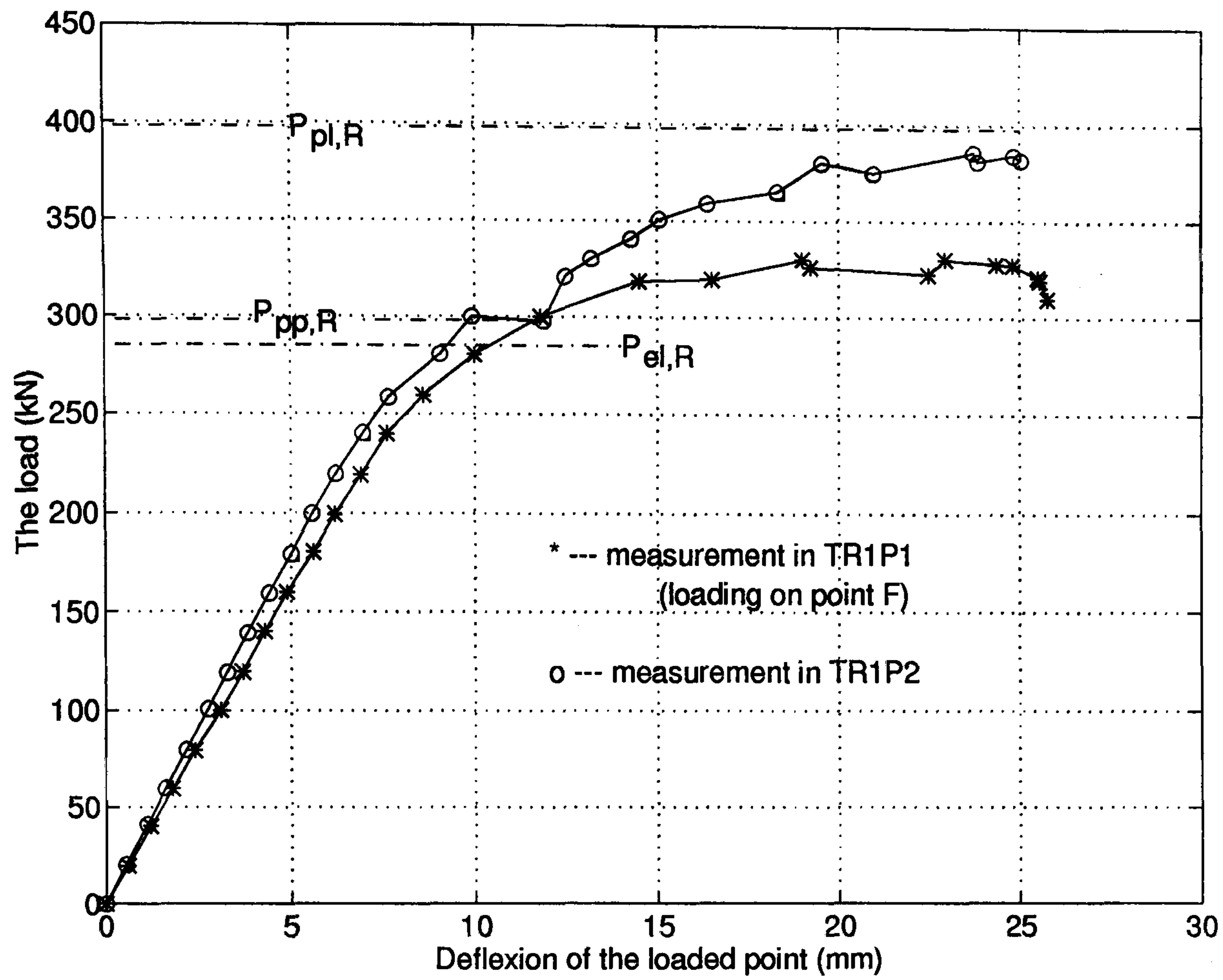


Figure 8.2: Deflexion of loaded points in TR1P1 & TR1P2

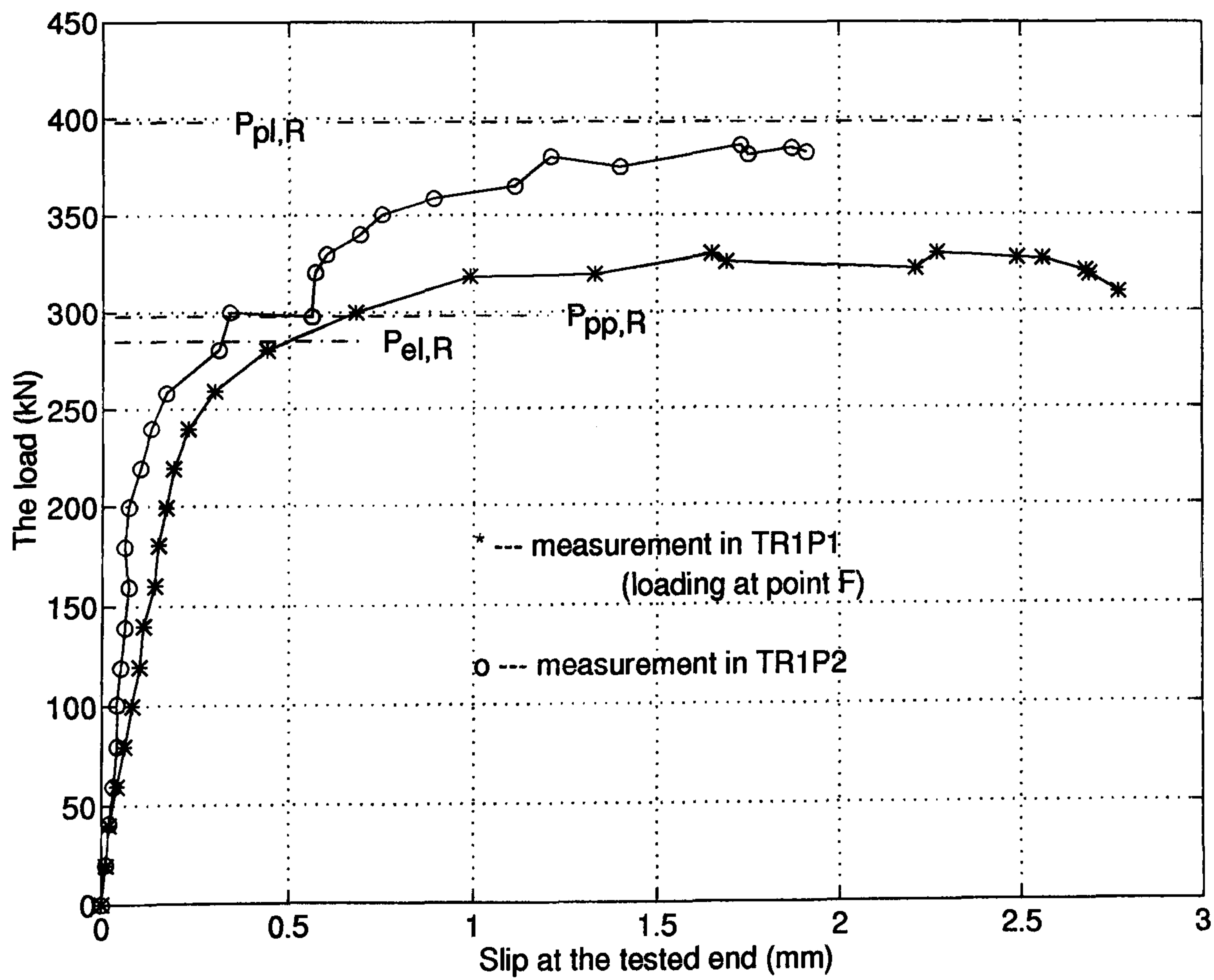


Figure 8.3: Slip at the tested ends in TR1P1 & TR1P2

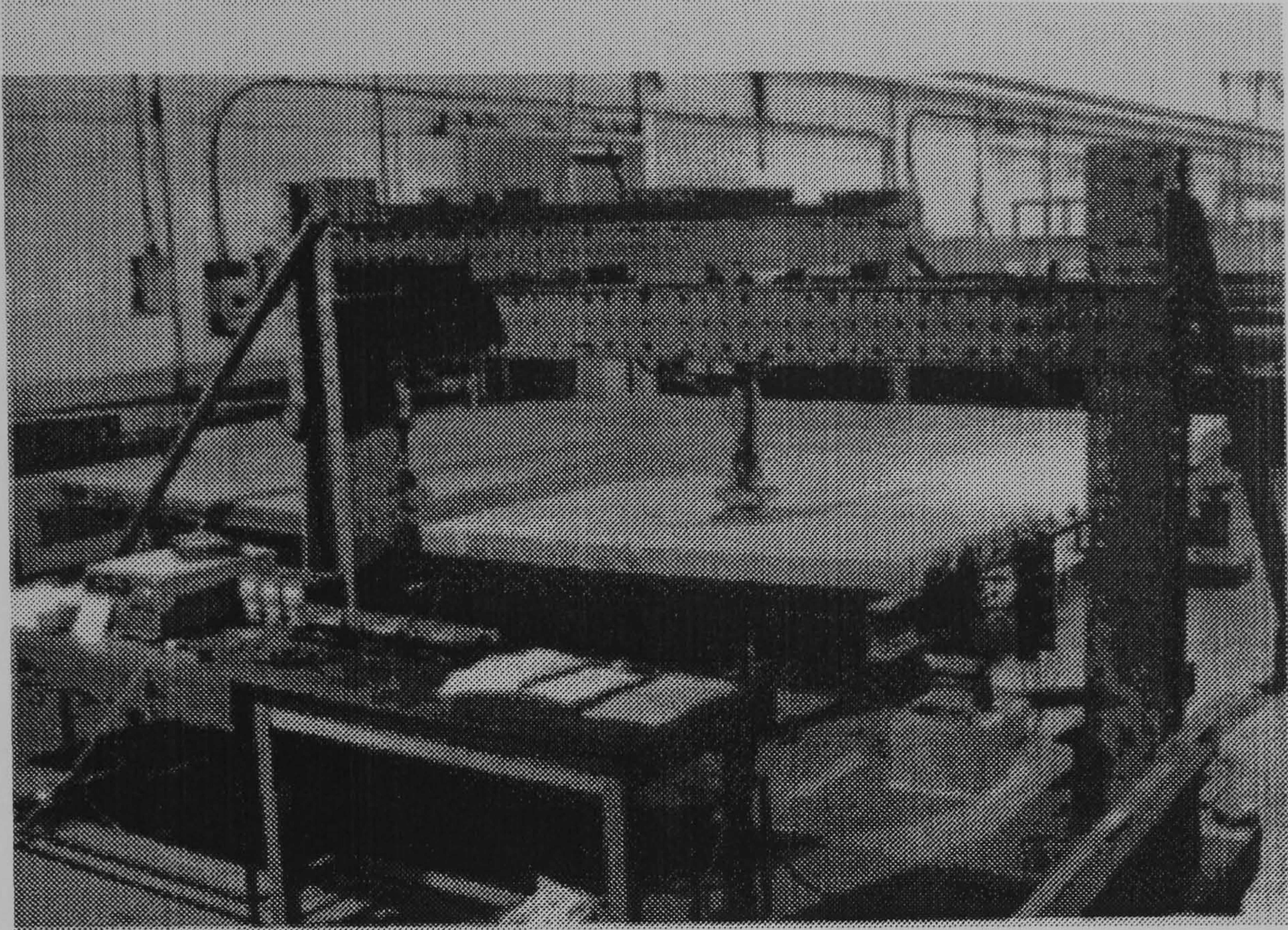


Figure 8.4: Specimen TR1 in Test TR1P2

presented in Figures 8.5 and 8.6, respectively. At the beginning of this test, the load was increased to 140 kN at intervals of 20 kN. Since, as given in Table 8.2, the calculated elastic limit load $P_{el,R}$ was being approached and cracks in concrete started to appear, the load was then increased in steps of 10 kN. After $P = 180$ kN, the load increment was decreased to 5 kN. When load reached 205 kN, it was found that the longitudinal crack occurred in region BC (Figure 7.2) had almost extended into region CD. In order to avoid test TR2T2 being possibly affected by such crack, it was decided to take the load off and to carry out test TR2T2 next. When test TR2T1 was started again, the load was increased from zero to 160 kN in step of 20 kN. Then the load increment was reduced to 10 kN and the load was applied up to 200 kN. Finally, the load was applied up to 215 kN in increments of 5 kN. The maximum slip at the end of the test was measured as about 6 mm. It appeared that the failure in this test occurred when the shear connection lost the strength.

Test TR2T2 As planned in Figure 7.2, this test applied load at point C. The

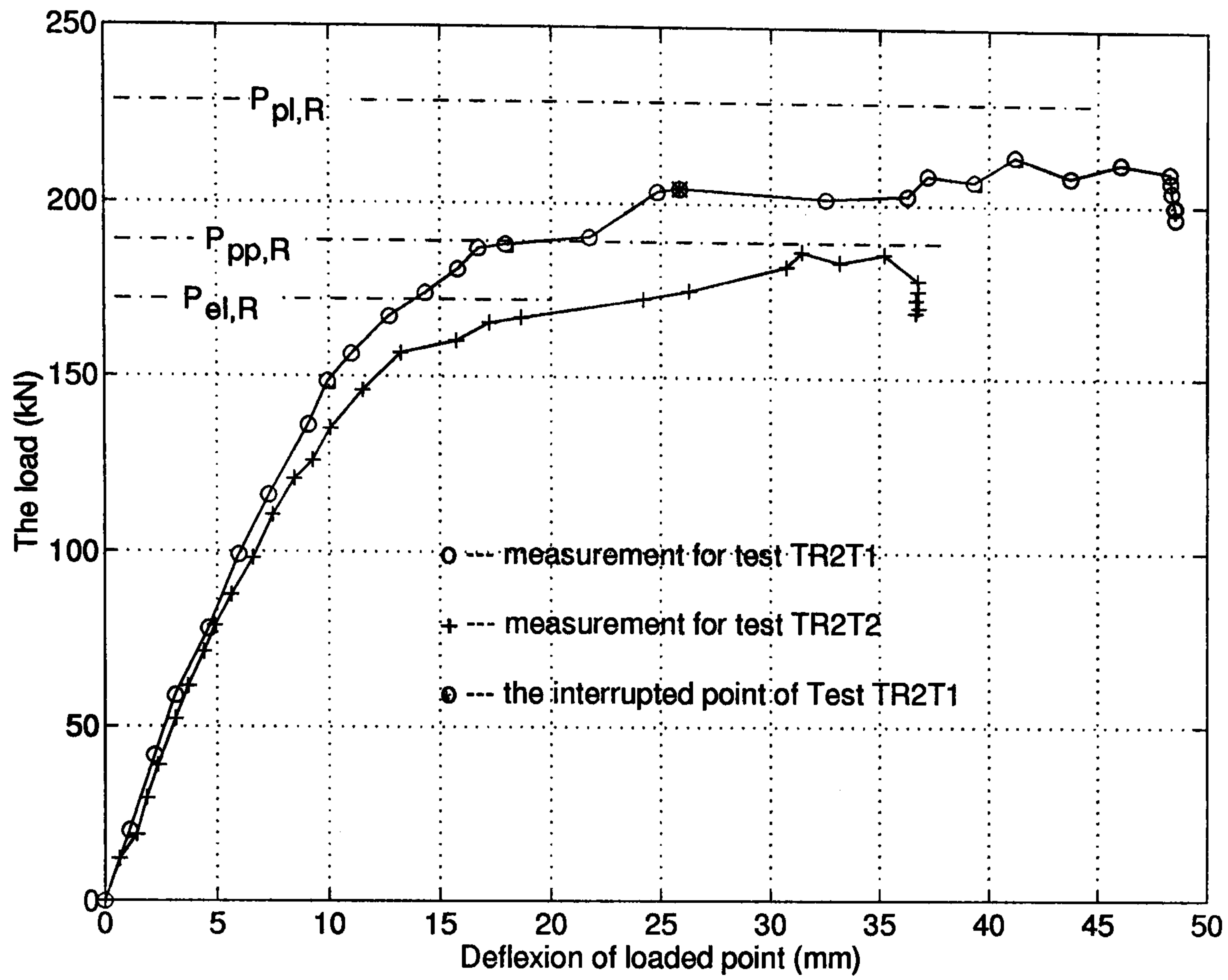


Figure 8.5: Deflexion of loaded points in TR2T

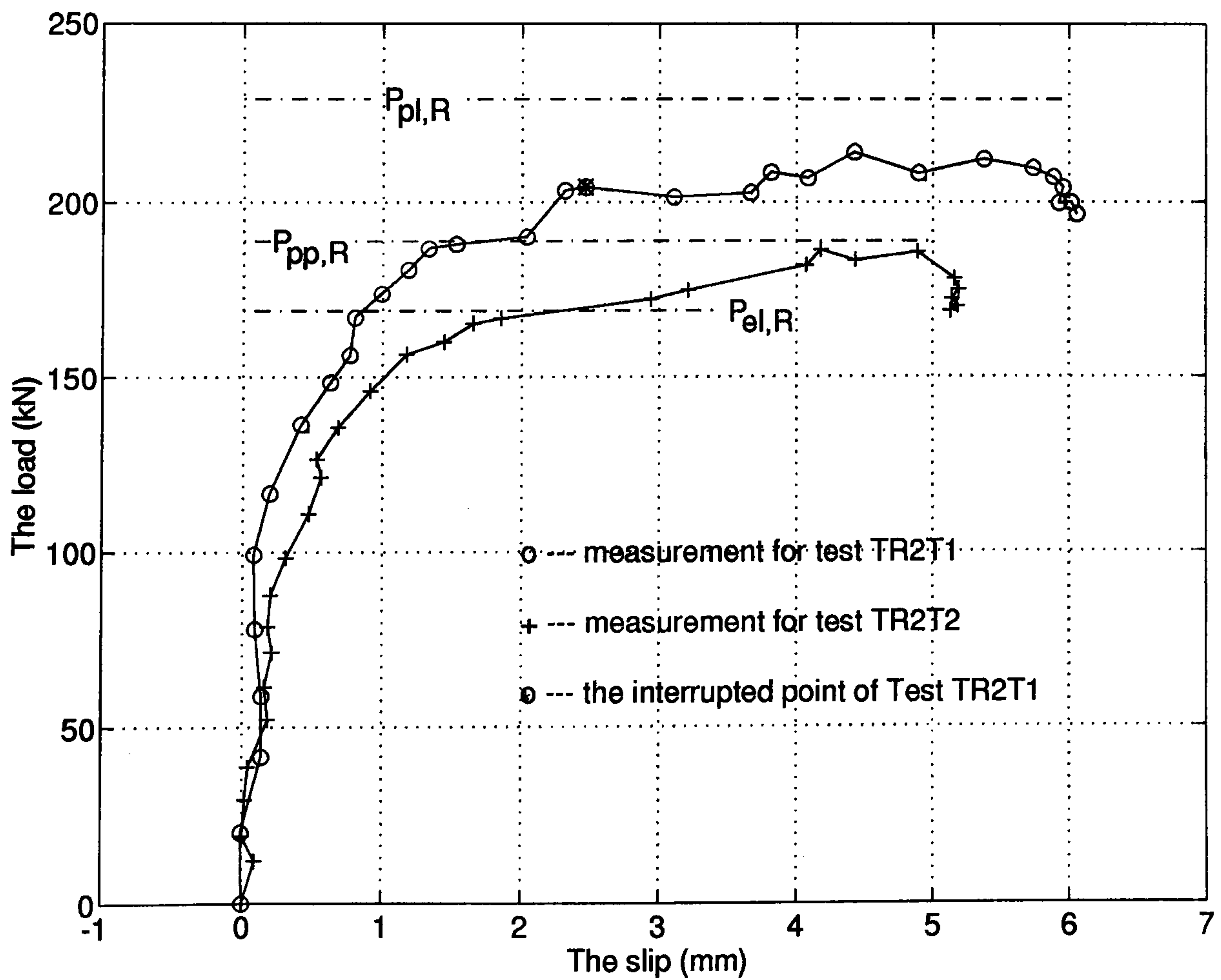


Figure 8.6: Slips at the tested ends in TR2T

deflexion and slip were measured as given in Figures 8.5 and 8.6, respectively. The load was increased to 160 kN by 10 kN at each step. The increment of load was then reduced to 5 kN until the end of the test. The maximum load was measured as 186 kN. As the failure approached, wide diagonal cracks were found on the bottom surface of the concrete slab, developing from the roots of the shear connectors. The slip at end D was measured at the maximum load as about 5 mm. The test was terminated as the failure of the shear connection in test region took place.

Test TR2P1 For this test, Figures 8.7 and 8.8 show the deflexion of loaded point and slip at the tested end, respectively. With reference to Figure 7.3, the loaded point was at J. The initial load increment was 30 kN which was kept until $P = 120\text{kN}$. Then the increment was decreased to 10 kN which was kept to $P = 280\text{kN}$. Before the load reached the maximum value, $P_{\text{max}} = 320\text{ kN}$, the load increment was 5 kN. At failure stage, within test region HJ (see Figure 7.3), a pair of wide longitudinal cracks in concrete emerged quite suddenly, in the concrete part without rib and slightly beyond the critical surface of longitudinal shear as shown in Figure 1.2(a), which was immediately followed by severe damage of the concrete slab. The load-carrying capacity of the specimen was then quickly collapsed. In the stage close to failure (i.e. $P = 295 \sim 300\text{ kN}$), the measurements from strain gauges suggested that the steel beam under the load was yielded in tension over about 65% of its depth.

Test TR2P2 The loaded point was changed from J to K. Figure 8.9 presents a general view of beam TR2P under loading in test TR2P2. At the beginning, the load increment was taken as 20 kN until $P = 120\text{kN}$. Afterwards, the increment was reduced to 10 kN which was kept towards end of the test. The maximum load appeared as 300 kN. The deflexion and slip in this test were measured as shown in Figures 8.7 and 8.8. At the failure stage, the diagonal cracks occurred in region KL widely opened and the concrete just above the steel beam along this region was crushed. In stage close to failure (i.e. $P = 270 \sim 275\text{ kN}$), the steel

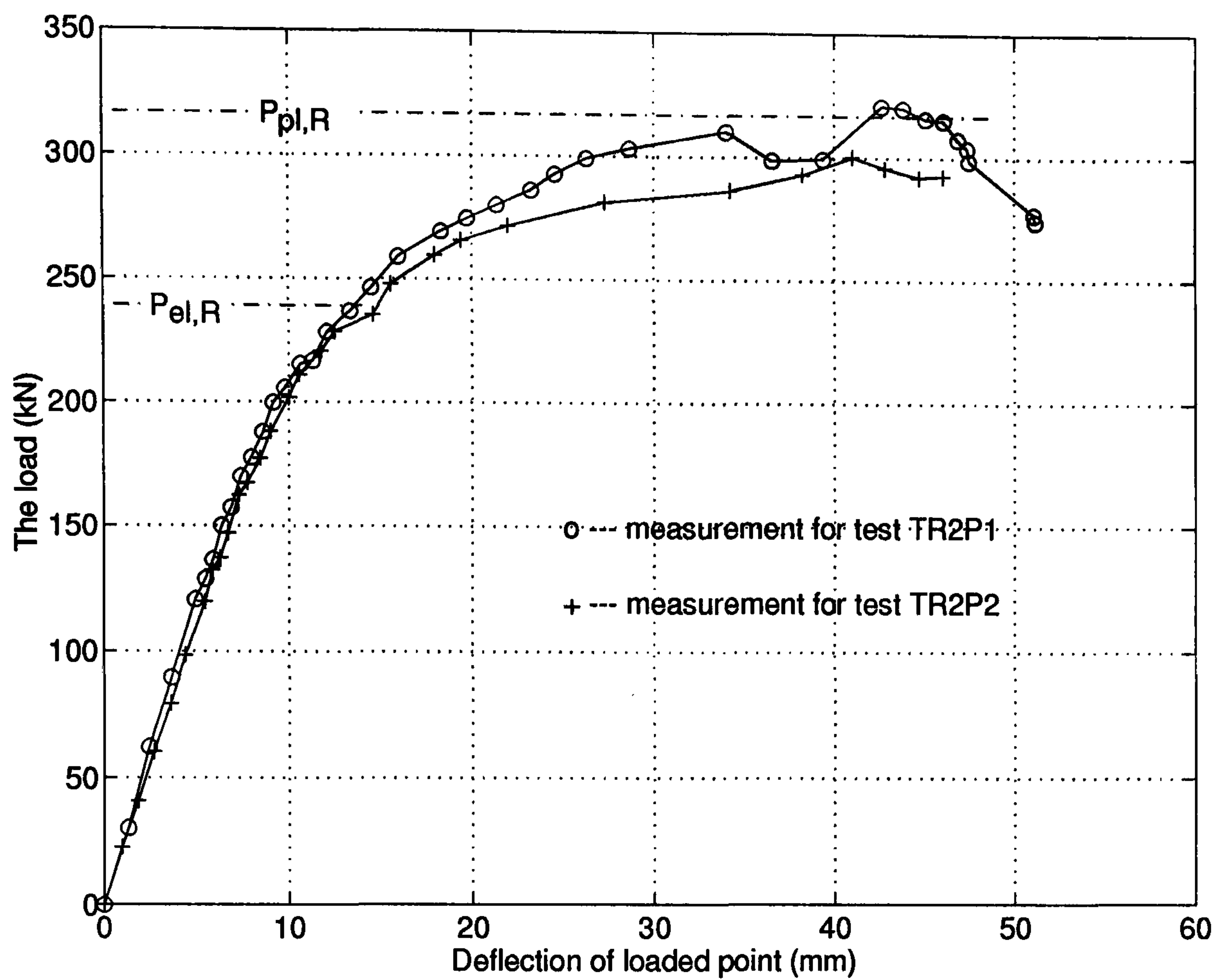


Figure 8.7: Deflexions of loaded point in TR2P

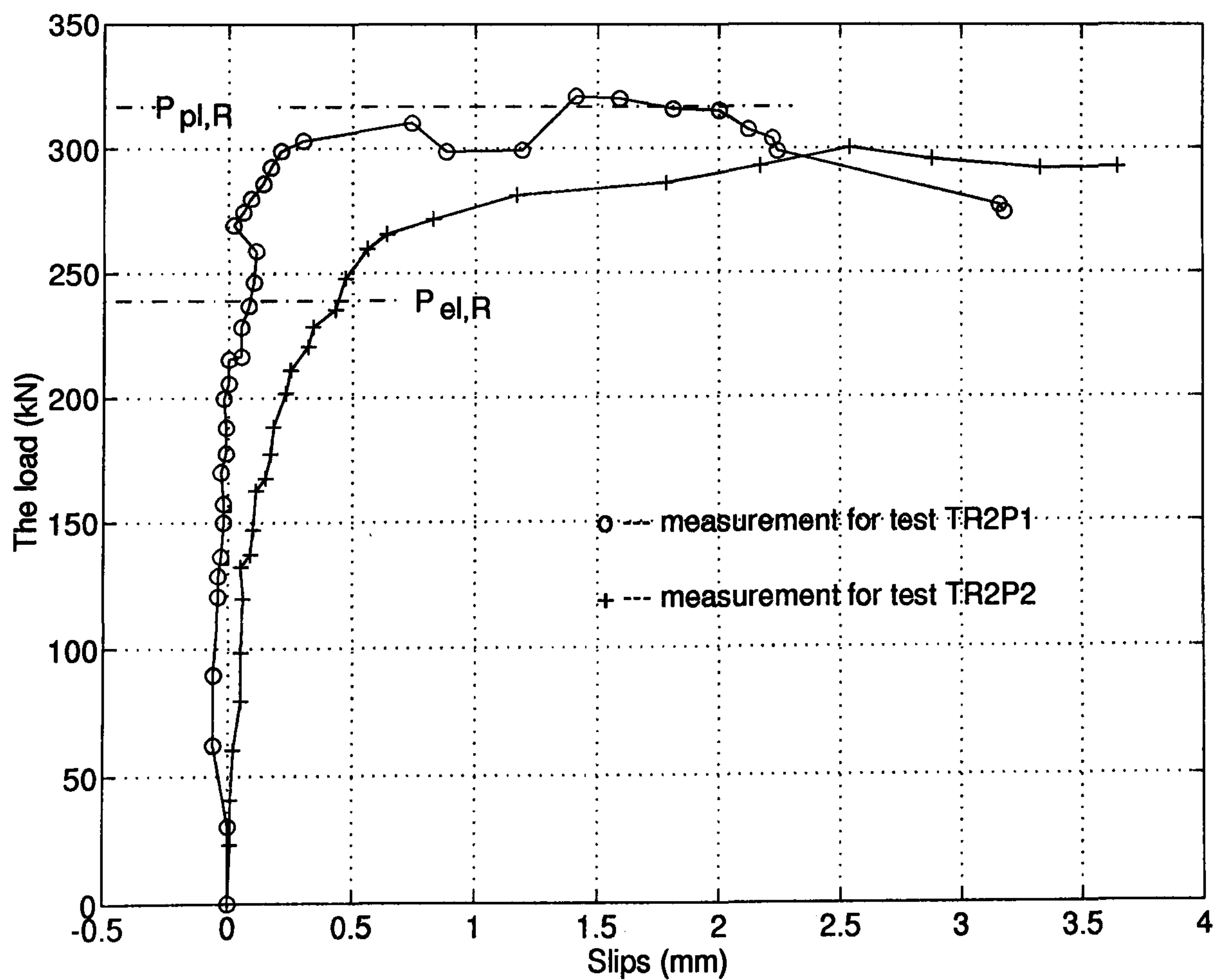


Figure 8.8: Slips at the tested ends in TR2P

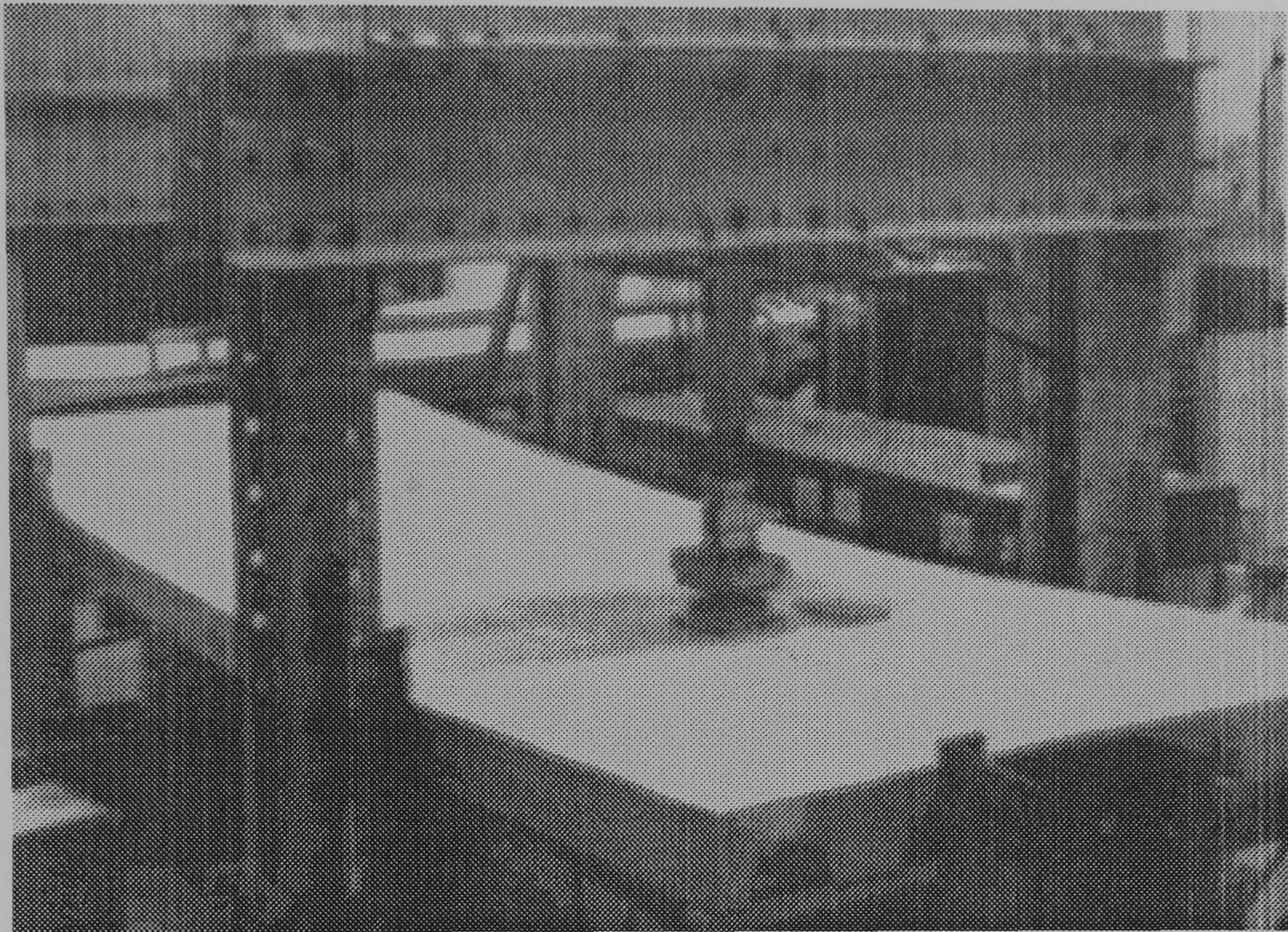


Figure 8.9: Beam TR2P under loading in test TR2P2

beam under the load was yielded in tension over about 50% of its depth.

8.2 Observation of cracks

Most of the cracks that appeared on top of the concrete slab developed diagonally. Figures 8.10 to 8.16 show the cracks in each test. It was found in tests that the concrete part near the support in tested region was always cracked at first.

The first crack in test TR1T was found at load 180 kN. When the load on B was up to 230 ~ 235 kN, a pair of diagonal cracks spread symmetrically from end A and appeared quite noticeable, as can be seen from Figure 8.10. As the load increased, these diagonal cracks became wider and eventually exceeded 0.5 mm. Besides these prominent cracks, more small cracks were also observed during the test.

For test TR1P1, because a small load ($P = 35\text{kN}$) was applied at point G in advance, the longitudinal cracks along the primary steel beam had occurred

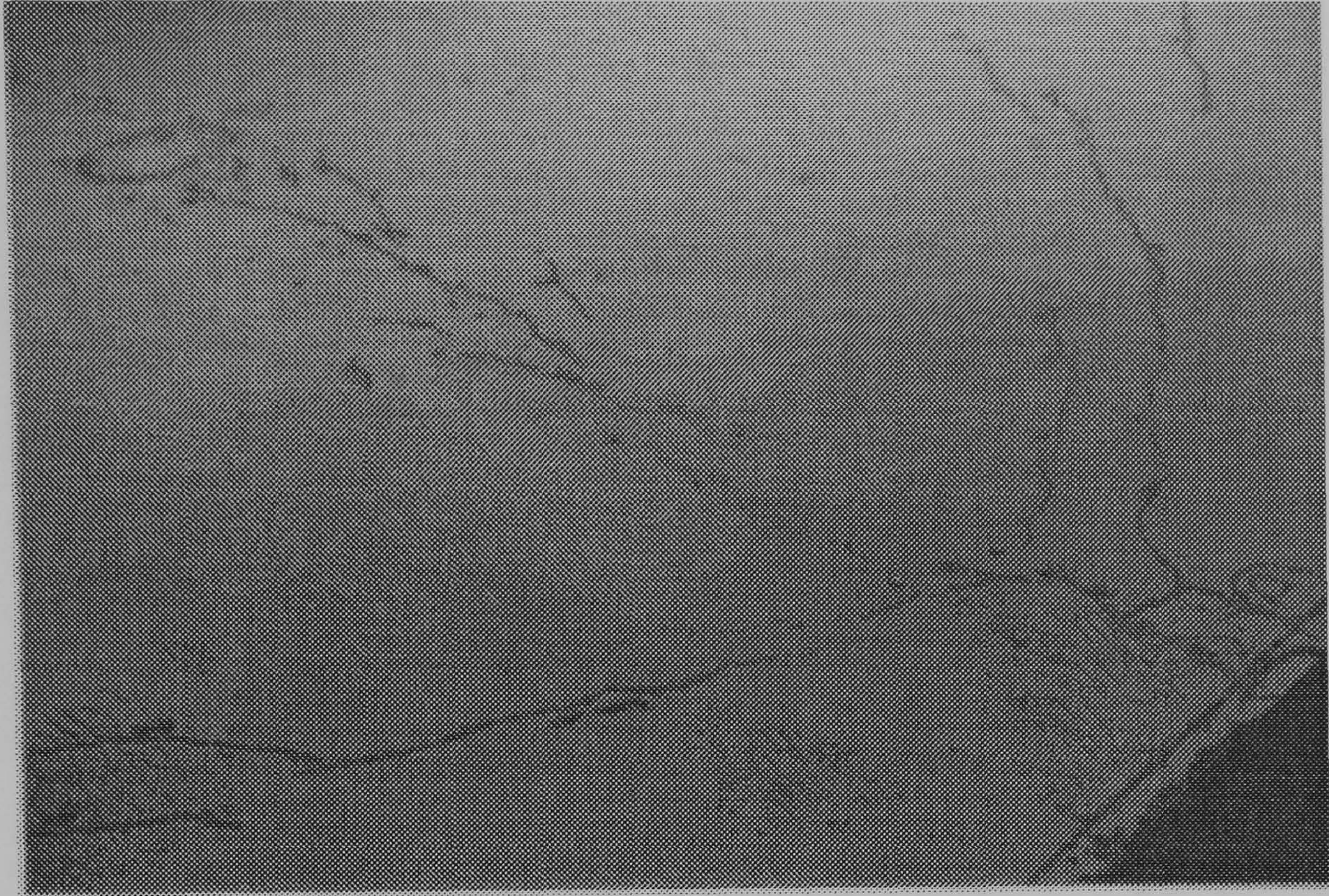


Figure 8.10: Crack pattern in test TR1T

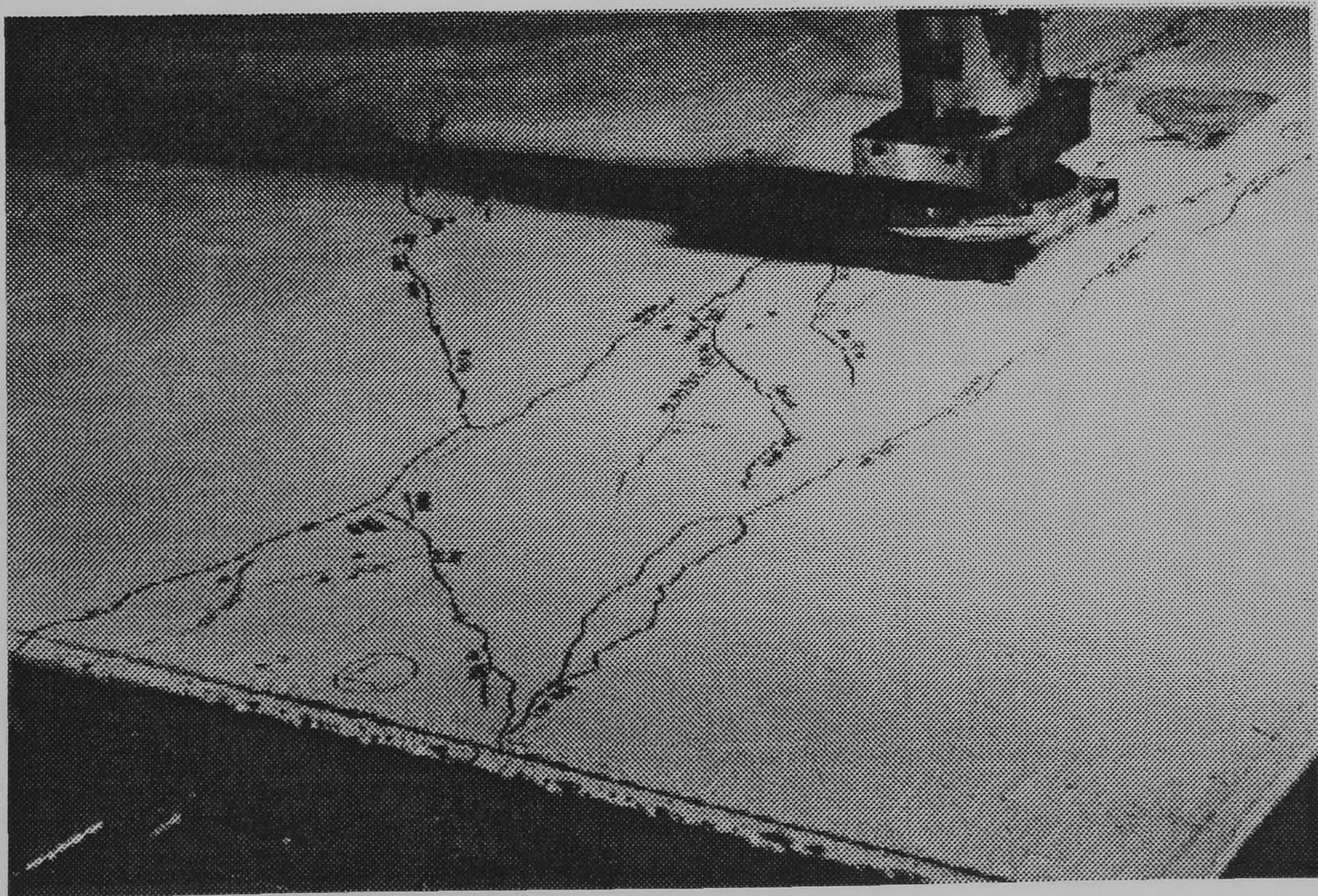


Figure 8.11: Crack pattern in test TR1P1



Figure 8.12: Crack pattern in test TR1P2

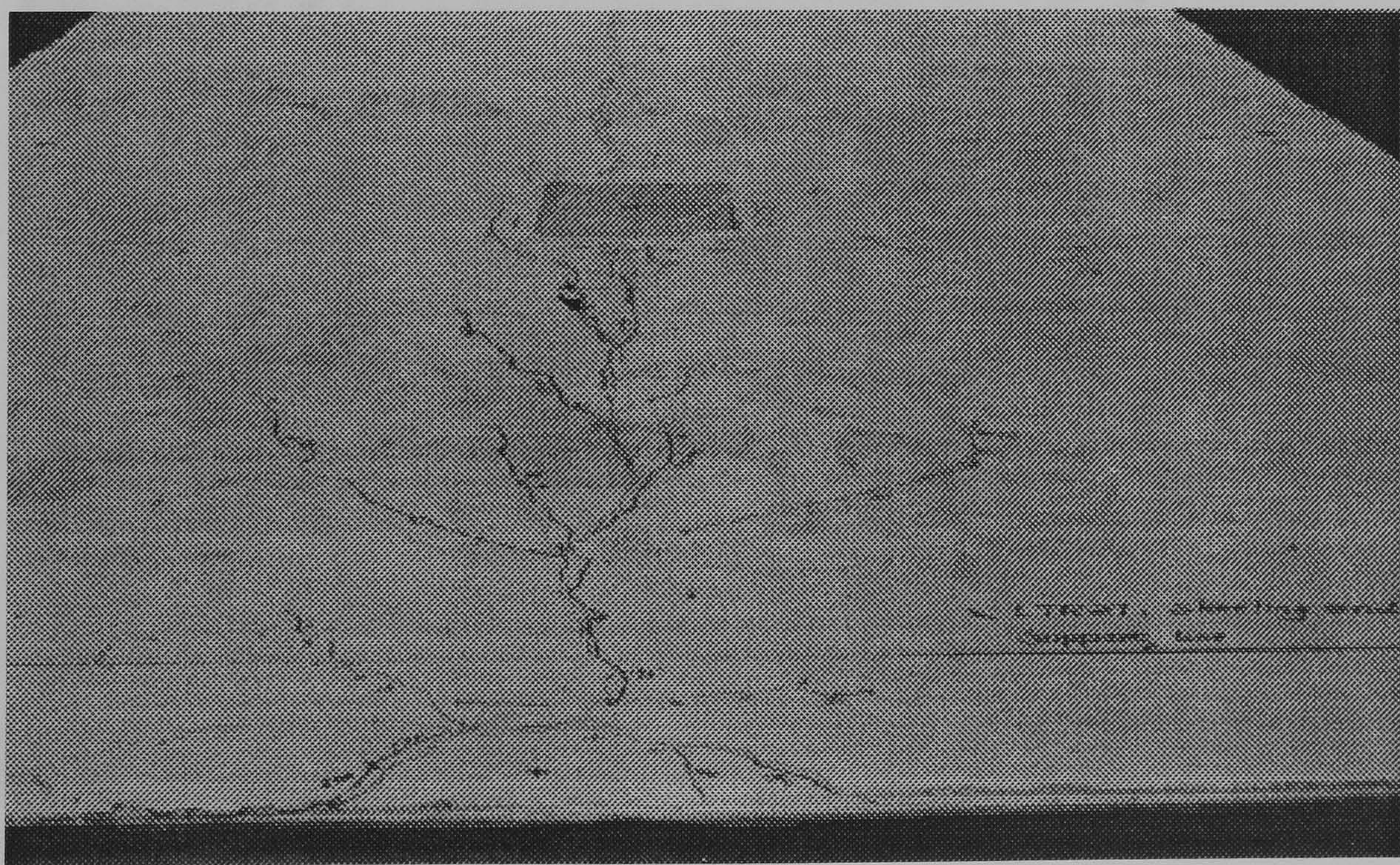


Figure 8.13: Crack pattern in test TR2T1

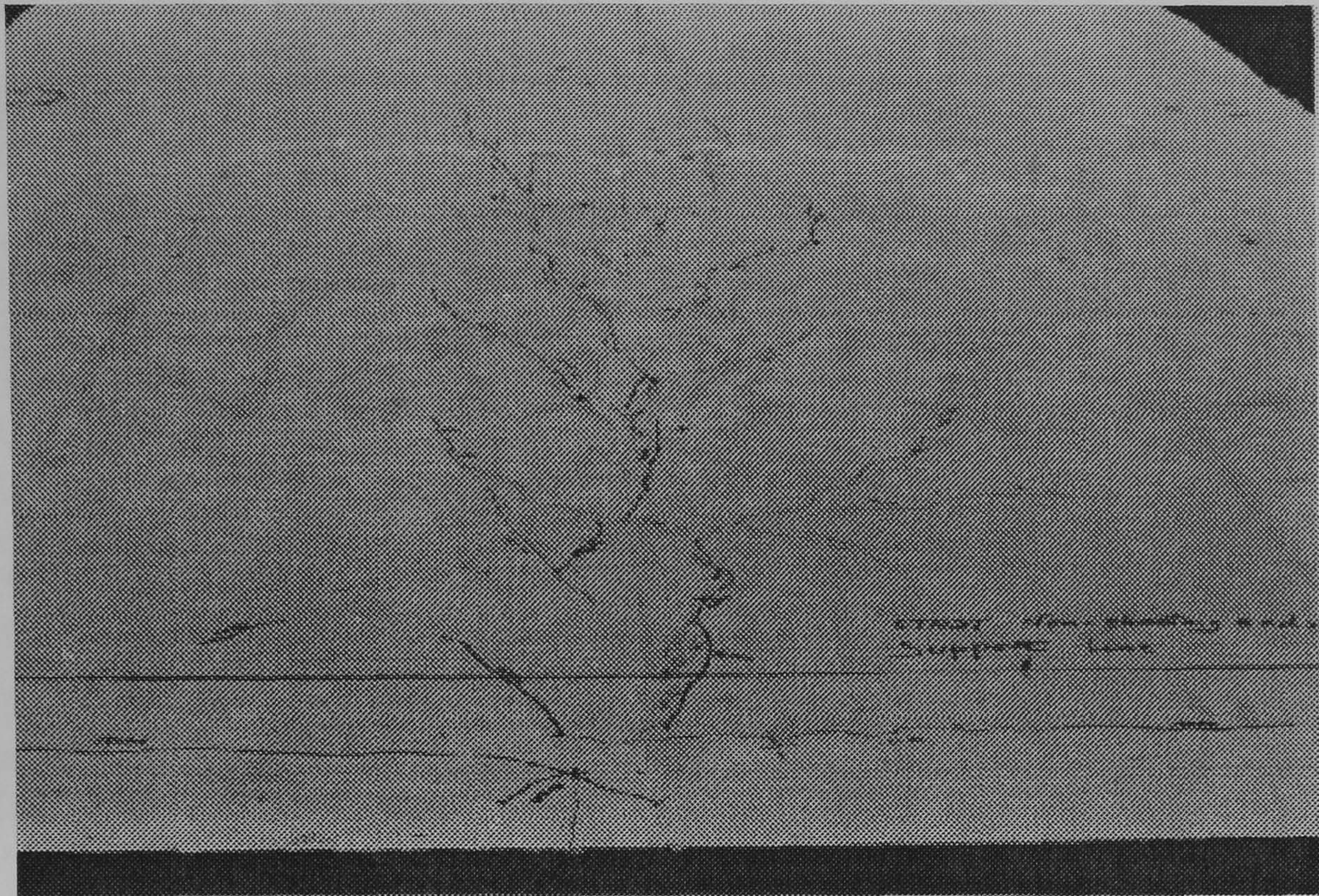


Figure 8.14: Crack pattern in test TR2T2

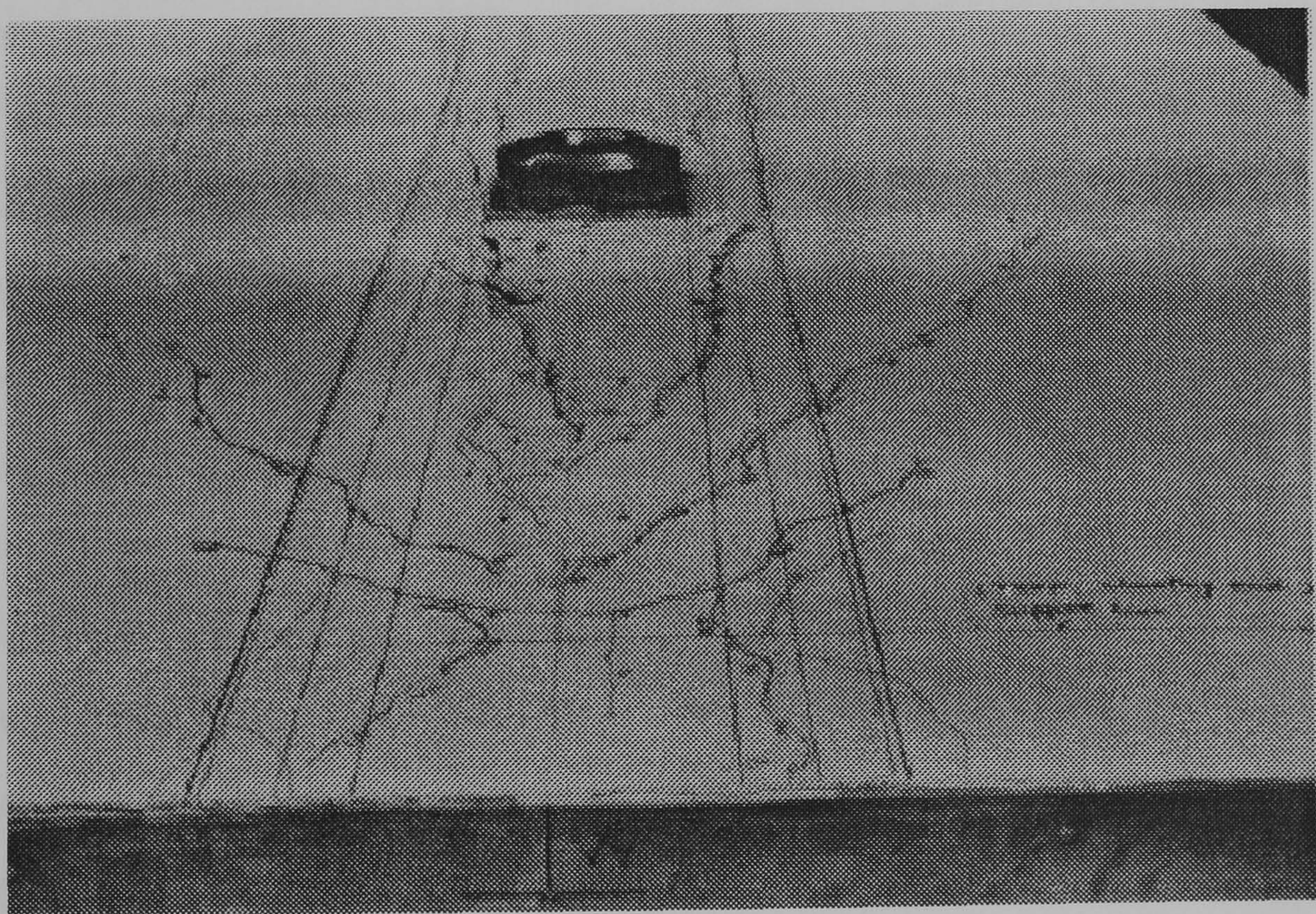


Figure 8.15: Crack pattern in test TR2P1

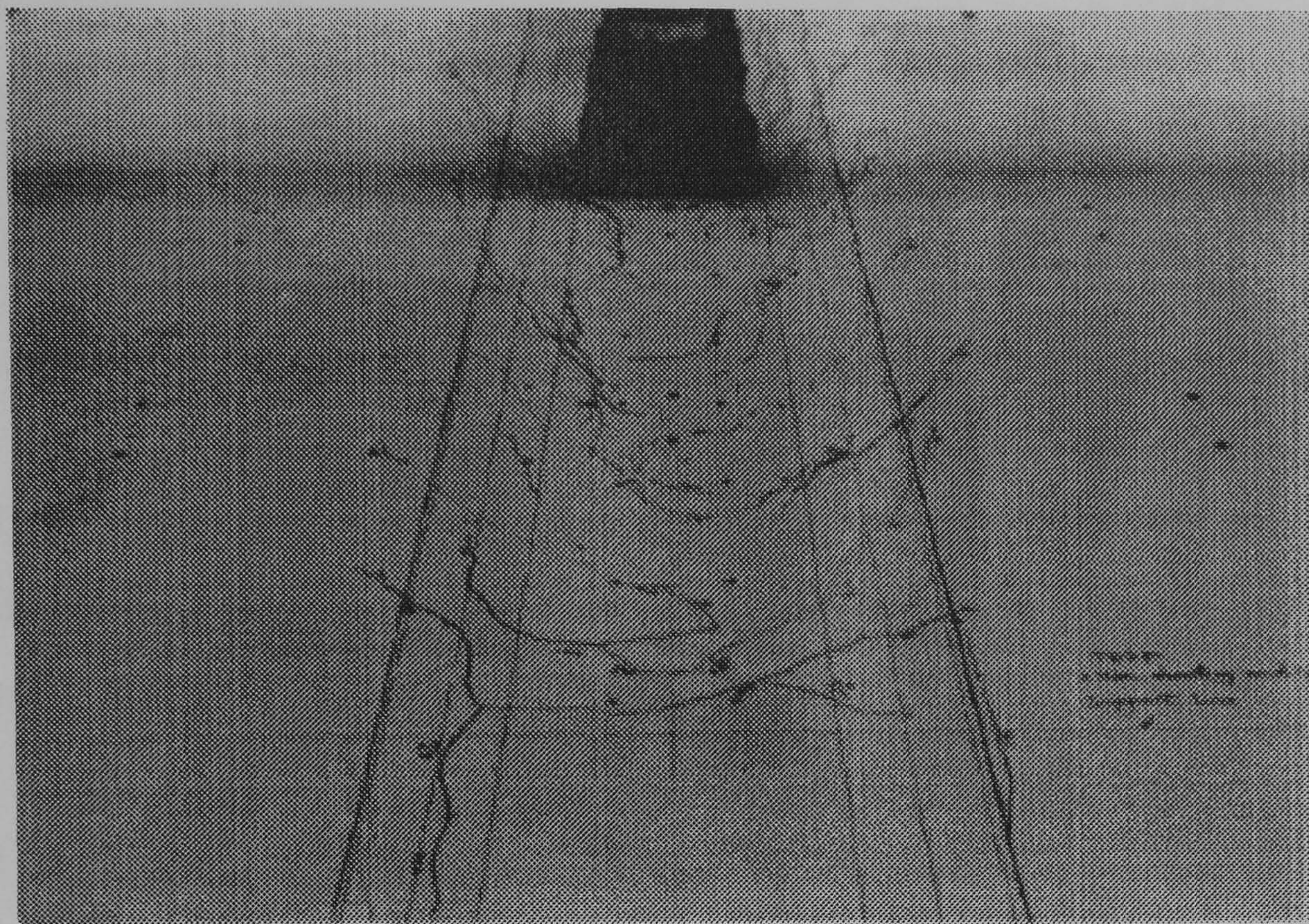


Figure 8.16: Crack pattern in test TR2P2.

before the main load was applied. This longitudinal crack extended towards both ends, H and L, (Figure 7.1). When the specimen was under load 165 kN at point D, a single diagonal crack was found at end L. Compared with the other cracks which emerged later, this crack developed outstandingly in the following stages of test TR1P1, as can be seen in Figure 8.11. At the final stage of loading at F, the width of this crack reached about 1mm.

When specimen TR1 was loaded to 230 kN at D in test TR1P1, a diagonal crack was also found at end H. During test TR1P2, this crack developed into the main diagonal crack, and width of this crack was about 1 mm at end of test TR1P2.

The earliest concrete cracks in tests TR2T1 and TR2T2 were found when loads reached 140 kN and 110 kN, respectively. These cracks emerged diagonally. According to the observation, the initial cracks in test TR2P1 on beam TR2P appeared when the load reached 180 kN and also developed diagonally. In fact, as shown in Figures 8.13 to 8.16, most of the cracks obtained on beams TR2T and TR2P extended diagonally and fairly symmetrically. In late stage of test

Table 8.3: Average width of longitudinal crack in test TR2P1

| load (kN) | | 220 | 240 | 260 | 280 | 300 | 320 |
|---------------------|-----------------------------|------|------|------|------|------|------|
| crack width (mm) | in region with A142 mesh | 0.30 | 0.45 | 0.55 | 0.68 | 0.65 | 0.70 |
| | in region without mesh | 0.23 | 0.31 | 0.50 | 0.72 | 1.18 | 1.87 |

TR2P1 ($P \approx 310$ kN), the diagonal cracks were even found in region KL for test TR2P2 (Figure 7.3).

Besides the diagonal cracks on beams TR2T and TR2P, when the load was raised to 190 kN in test TR2T1, a longitudinal crack just above the studs appeared in region BC (Figure 7.2) and quickly developed towards point C. The width of this crack was considerable but was not measured. In test TR2P1, at the load of 220 kN, a longitudinal crack emerged also in region JK (Figure 7.3) and developed towards the point K. The position of this crack was about the critical surface of longitudinal shear as typified in Figure 1.2(a). Table 8.3 gives the average measured width of this longitudinal crack.

In tests TR2T2 and TR2P2, where no sheeting was used in the tested region, it was found that many cracks occurred so that the whole thickness of concrete slab was directly penetrated. For tests TR2T1 and TR2P1, the same observation cannot be made because of the covering of profiled sheeting. However, in test TR2T1, the diagonal cracks closed up when the load was taken off when $P = 205$ kN, so it may be considered that the region around the diagonal cracks remained in elastic state. Therefore the direct penetration by cracks through the whole thickness of concrete slab may not have occurred in tests TR2T1 and TR2P1.

8.3 The forces in steel beams

According to measurements from the strain gauges on the steel beams and the measured properties of steel beams, as reported in Section 7.3, the tensile force on the cross-section of steel beam under the loaded point can be found.

In order to make convenient application, the steel force measured in each test is recorded here in terms of $f_a = F_a/l_m$, where F_a is the measured steel force and l_m is the distance from the section with the strain gauges used to measure the steel force to the nearest support.

Figure 8.17 shows the steel force f_a in test TR1T, found from the strain gauges No. 71 - 79 which were positioned as shown in Figure 7.24.

Figure 8.18 shows the steel forces f_a in tests TR1P1 and TR1P2, found from the strain gauges No. 81 - 89 and No. 111 - 119 (see Figure 7.24), respectively. The discovery of f_a from strain gauges No. 81 - 89 will be presented in Section 9.3. In Figure 8.18, the curves marked by "x" and "o" are those for test TR1P1 with the measured steel force excluding and including the *strain* caused by the secondary load at point G (see Figure 7.1), respectively.

Figure 8.19 shows the steel forces f_a in tests TR2T1 and TR2T2, found from the strain gauges No. 101 - 109 and 71 - 79 (see Figure 7.25), respectively.

Figure 8.20 shows the steel forces f_a in tests TR2P1 and TR2P2, found from the strain gauges No. 151 - 159 and 131 - 139 (see Figure 7.25), respectively.

It is considered that, in the final test stages, as the concrete was failed, the composite function of the specimens diminished, so the bending moment in steel beams would increase and, as shown by most curves in Figures 8.18 to 8.20, the resultant force in the steel beam would reduce.

Table 8.4 presents the maximum steel force $f_{a,max}$ measured for each of the tests.

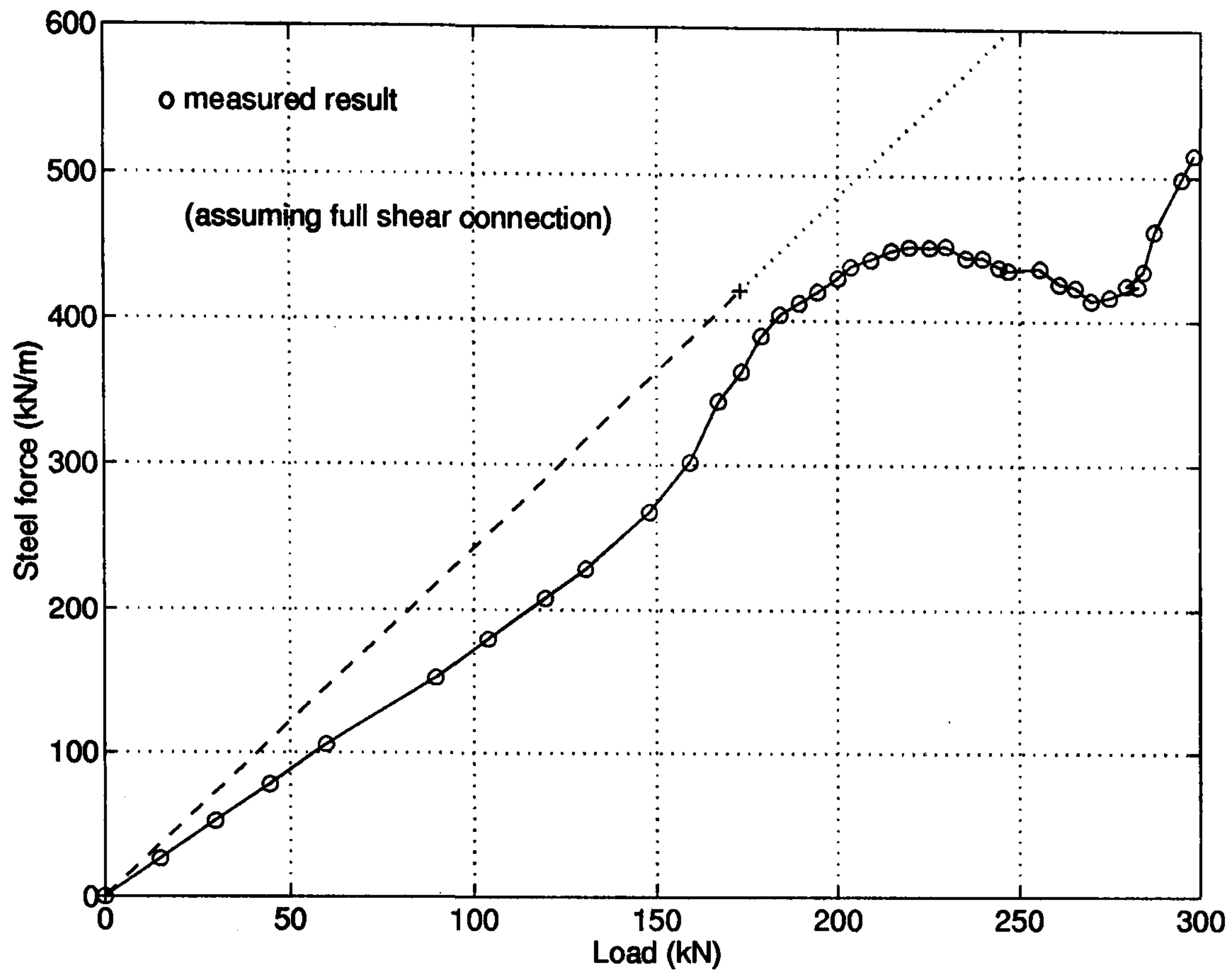


Figure 8.17: Steel force measured in test TR1T

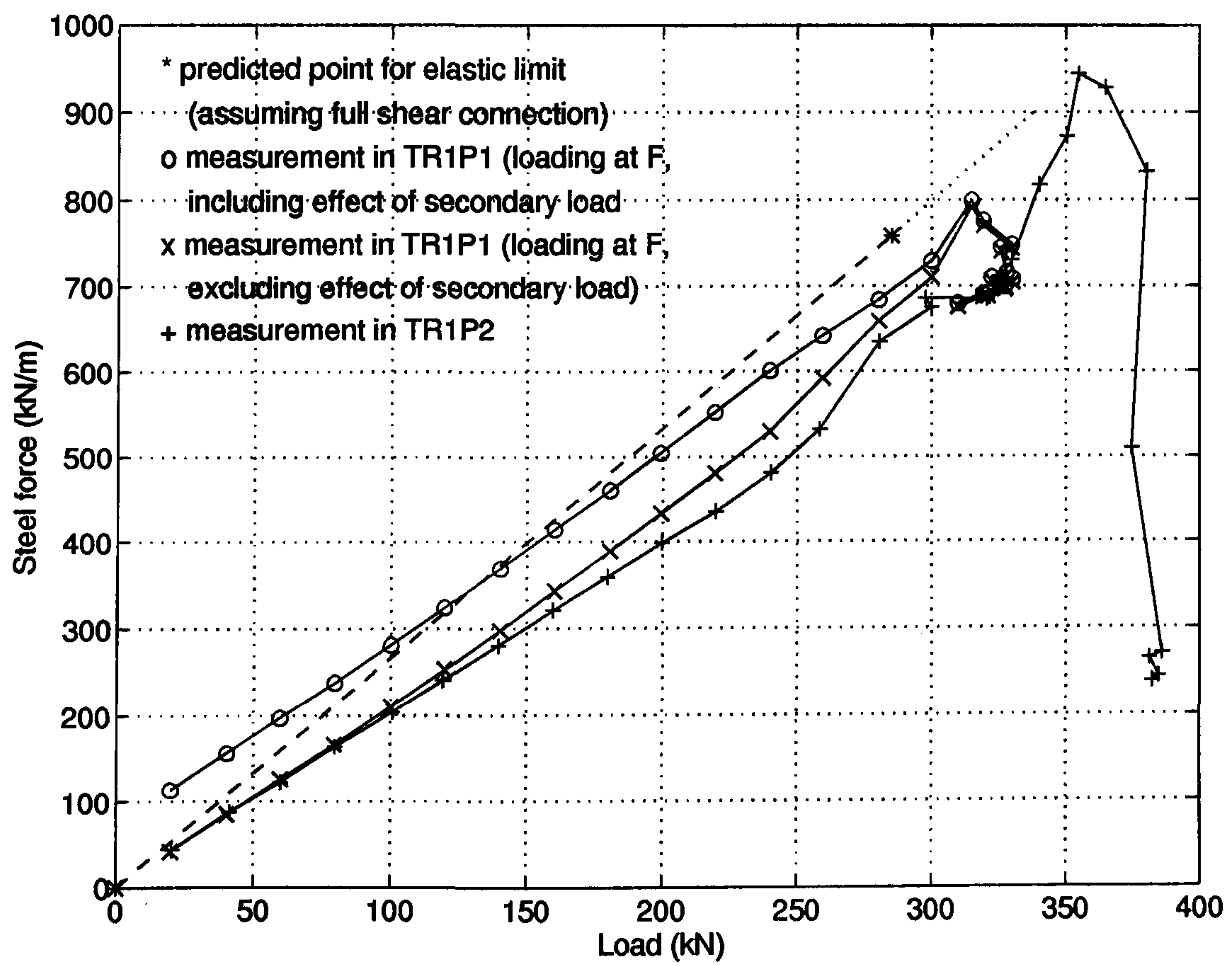


Figure 8.18: Steel force measured in tests TR1P1 & TR1P2

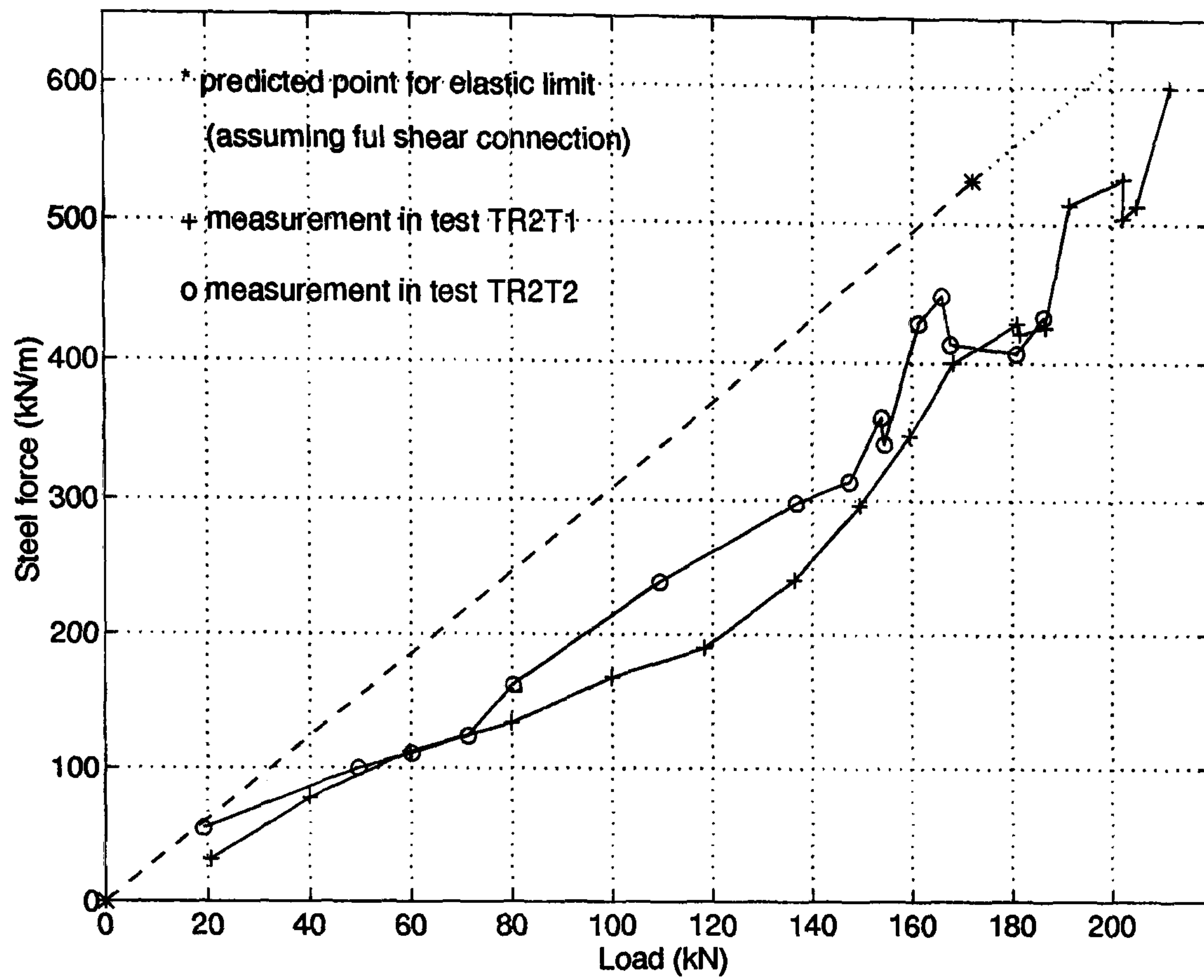


Figure 8.19: Steel force measured in tests TR2T1 & TR2T2

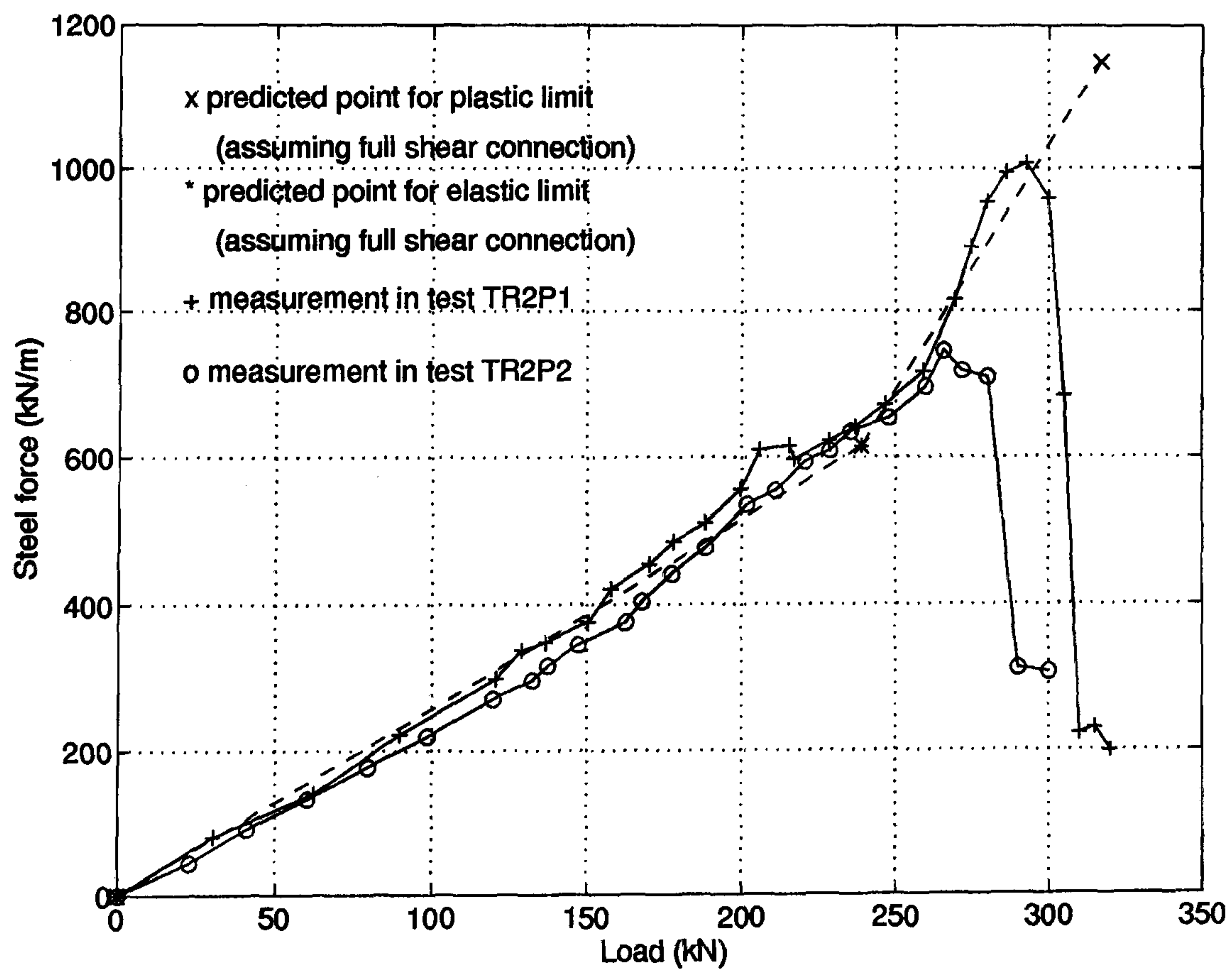


Figure 8.20: Steel force measured in tests TR2P1 & TR2P2

Table 8.4: The maximum steel force obtained from tests

| Test | $f_{a,\max}$ (kN/m) | l_m (m) | ¹ P_{fm} (kN) | ² l (m) |
|--------------------|---------------------|-----------|----------------------------|----------------------|
| TR1T | 515 | 1.30 | 300 | 1.50 |
| ³ TR1P1 | 800 | 1.15 | 315 | 1.00 |
| TR1P2 | 945 | 0.80 | 355 | 1.00 |
| TR2T1 | 601 | 0.94 | 215 | 1.20 |
| TR2T2 | 449 | 0.94 | 170 | 1.20 |
| TR2P1 | 1007 | 1.05 | 295 | 1.20 |
| TR2P2 | 746 | 1.05 | 270 | 1.20 |

- ¹ the load corresponding to $f_{a,\max}$;
- ² the distance from loaded point to the nearest support, i.e. the shear span as defined in Figure 6.1;
- ³ the test with loading at point F (see Figure 7.1), effect of the secondary load being included.

Chapter 9

Analysis of test results and design recommendations

Based on the results from tests in this study, the behaviour of composite beams in longitudinal shear and the effect of profiled sheeting were analyzed. With respect to the experimental measurements, the theory for longitudinal shear resistance presented in Chapter 6 was examined. As a result, design recommendations for longitudinal shear resistance were developed. This chapter presents such analysis and the suggestions for practical design work.

9.1 The cracking load

Figures 8.10 to 8.16 show that diagonal cracks were prominent in every test, which implied that the behaviour of the specimens in each test was considerably affected by the longitudinal shear.

Apart from tests TR1P1 and TR1P2 which were conducted after the longitudinal crack along the steel beam had been made by the secondary load, the test observations suggested that, when composite beam was mainly subjected to longitudinal shear, the concrete would crack first near the end of beam and the cracks would develop diagonally.

Since the concrete has only a small strength in tension, it is evident that, before cracking, the tensile stress in concrete slab is small. Therefore, the analysis of the cracking behaviour of a concrete slab under longitudinal shear may be simplified by ignoring the effects of the reinforcement and profiled sheeting and the normal stress σ_c on concrete, as caused by the in-plane bending shown in Figure 6.1. Thus, before the concrete cracks, the stress state in concrete along the critical longitudinal surface may be assumed to be as shown in Figure 9.1, where $\sigma_{c,b}$ stands for the normal stress in concrete due to bending moment M as shown in Figure 1.1(a) and τ_{ck} is the shear stress on the longitudinal surface.

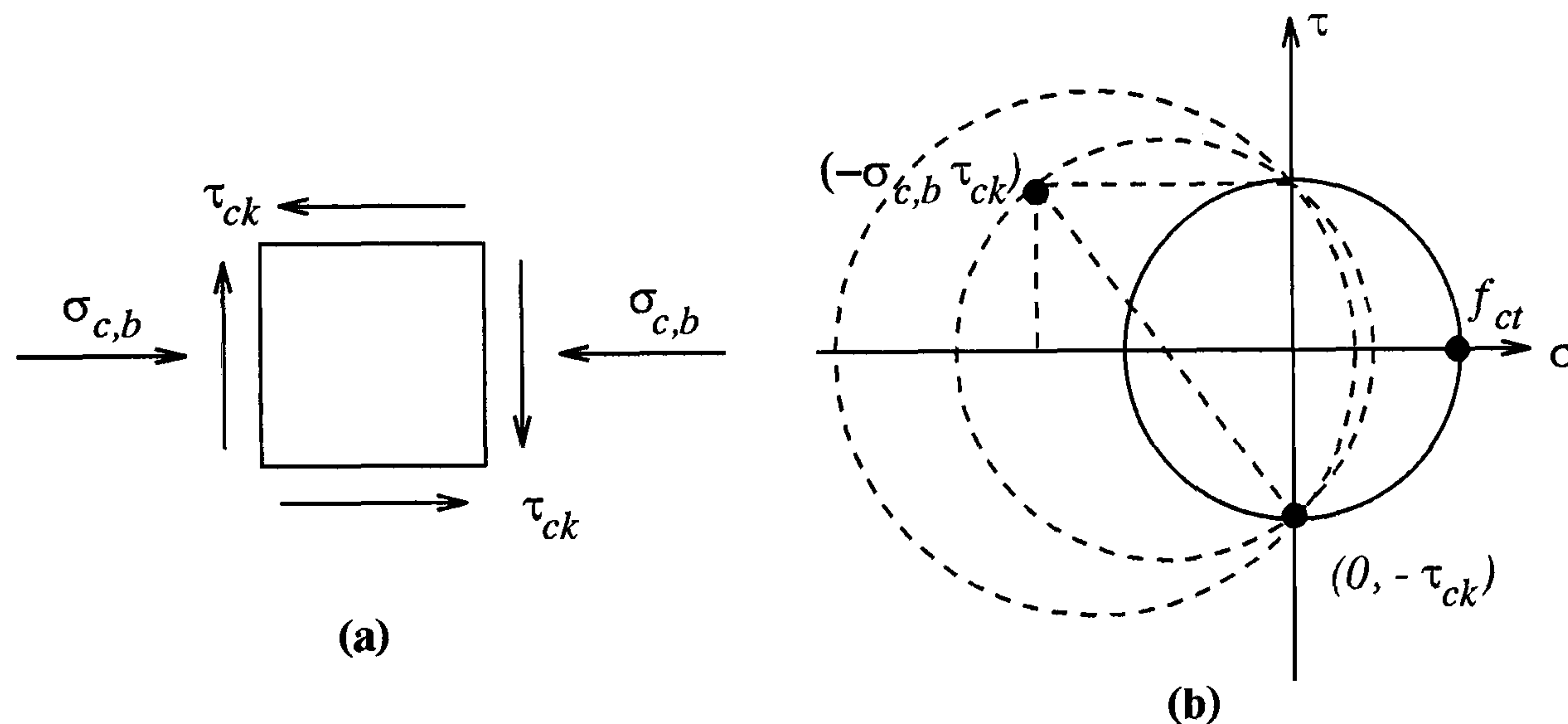


Figure 9.1: Stress state in uncracked concrete

Since there is no bending moment at the end of a simply supported beam, the stress state in concrete may be considered as pure shear, i.e. $\sigma_{c,b} = 0$. It can therefore be inferred from Figure 9.1(b) that the maximum tensile stress would occur towards the end of the beam, so the first crack should occur there, as observed in the tests.

It is considered that the occurrence of the first crack corresponds to the condition that the principal tensile stress in concrete reaches its tensile strength f_{ct} . According to Figure 9.1, this condition is

$$\tau_{ck} = f_{ct} \quad (9.1)$$

Assuming that the shear stress τ_{ck} is uniformly distributed on the longitudinal

surface, the longitudinal shear force at occurrence of the initial cracks, $F_{lg,ck}$, then appears:

$$F_{lg,ck} = lA_{cv}f_{ct} \quad (9.2)$$

where l is the shear span and A_{cv} represents the concrete area as defined after equations (6.1) and (6.2). For the part of a composite beam shown in Figure 9.2, F_{lg} , the normal force on area ABCD, may be related to the total bending force F_c on the slab as follows,

$$F_{lg} = \frac{F_c (b_{eff} - b_s)}{b_{eff} \cdot 2} \quad (9.3)$$

where b_{eff} is the effective width and b_s is distance between the two critical longitudinal surfaces, as shown in Figure 9.2.

Therefore, the bending force on the concrete slab corresponding to the occurrence of the initial crack, denoted F_{ck} , can be deduced from equations (9.2), (9.3) and (6.21). Taking $n = 0.15$ as assumed in Chapter 6, it yields

$$F_{ck} = lA_{cv}f_{ct} \left(2 + \frac{b_s}{0.3l} \right) \quad (9.4)$$

Taking advantage of the bending resistances given in Tables 8.1 and 8.2, linear interpolation may be used to estimate the load corresponding to the initial shear crack in the tests, P_{ck} , i.e.

- if $F_{el} \leq F_{cp}$ (in case of full shear connection, let F_{cf} replace F_{cp}), then

$$P_{ck} = \begin{cases} P_{el,R} \frac{F_{ck}}{F_{el}} & (0 < F_{ck} \leq F_{el}) \\ P_{el,R} + (P_{pp,R} - P_{el,R}) \frac{F_{ck} - F_{el}}{F_{cp} - F_{el}} & (F_{el} < F_{ck} \leq F_{cp}) \end{cases} \quad (9.5)$$

- if $F_{el} > F_{cp}$, then

$$P_{ck} = P_{pp,R} \frac{F_{ck}}{F_{cp}} \quad (0 < F_{ck} \leq F_{cp}) \quad (9.6)$$

No endeavour has been made to study P_{ck} if F_{ck} from equation (9.4) appears greater than F_{cp} , as if $F_{ck} > F_{cp}$, the composite beams should be so strong in

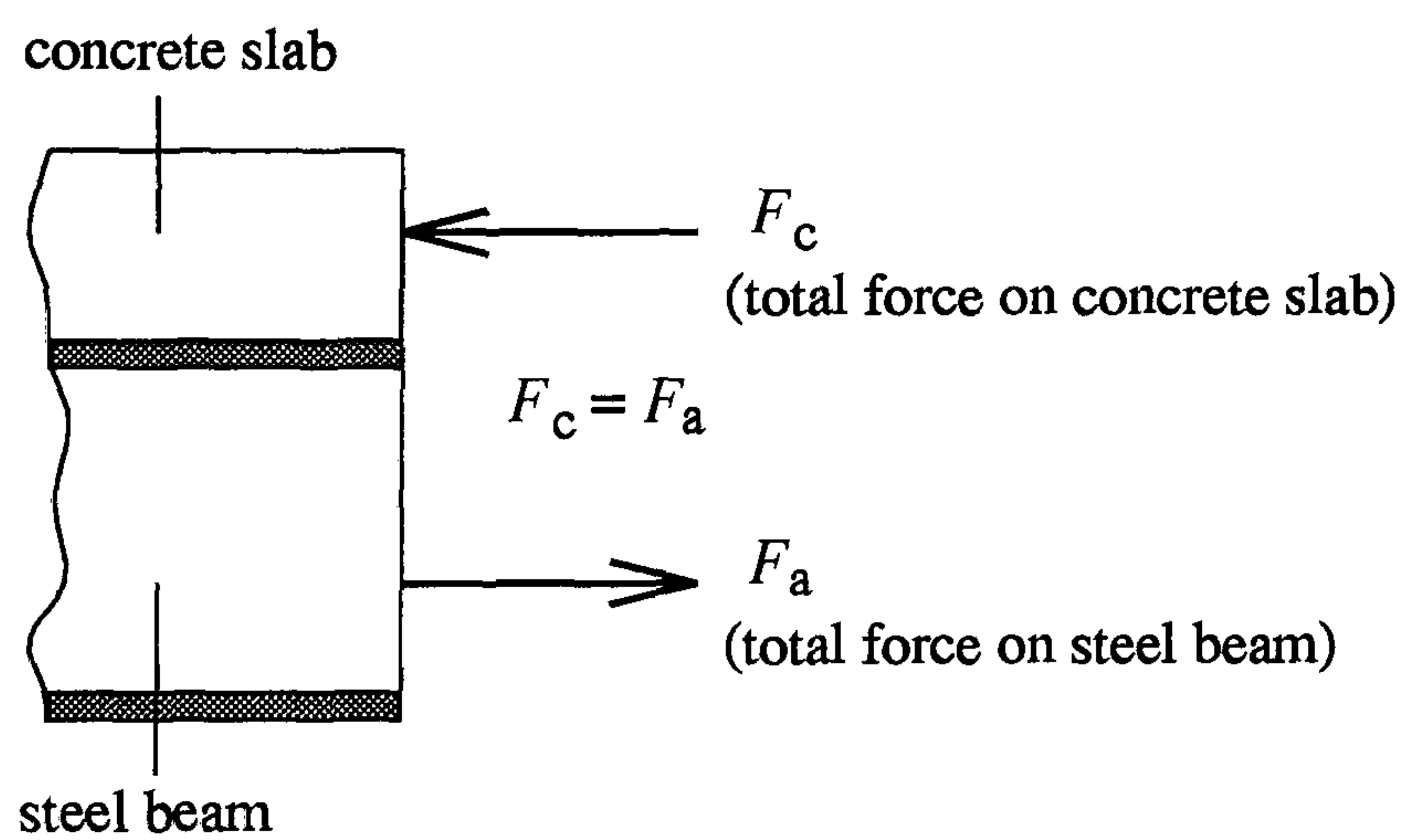
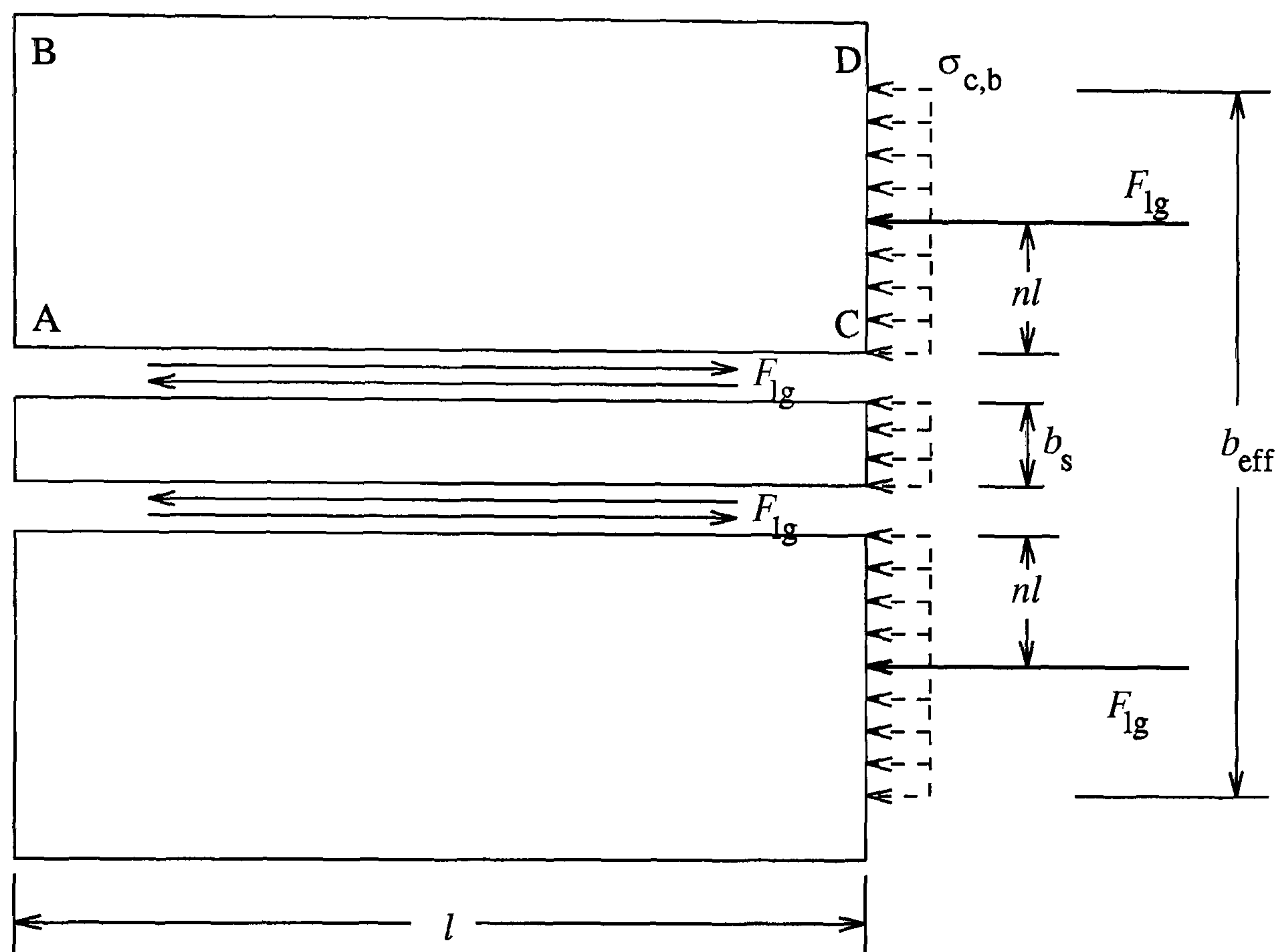


Figure 9.2: Longitudinal shear force and bending force in concrete

Table 9.1: Load at initial shear crack

| | TR1T | TR2T1 | TR2T2 | TR2P1 |
|------------------------------|--------------|-------|-------|-------|
| ¹ F_{ck} (kN) | 1154 | 584 | 584 | 490 |
| P_{ck} (kN) | $> P_{pp,R}$ | 180 | 180 | 159 |
| ² F_{ck} (kN) | 758 | 361 | 361 | 490 |
| P_{ck} (kN) | 196 | 111 | 111 | 159 |
| ³ $P_{ck,e}$ (kN) | 180 | 140 | 110 | 180 |

- ¹ calculation from A_{cv} including the rib area;
- ² calculation from A_{cv} excluding the rib area;
- ³ the load applied at which the concrete crack was first observed in the test.

longitudinal shear that the shear cracking would not be expected before flexural failure occurs.

Table 9.1 gives the predicted results from equations (9.4) to (9.6) and the test results. Tests TR1P1, TR1P2 and TR2P2 are not listed in Table 9.1, as before these tests started, the cracks had been caused by the previous test (for TR2P2) or by transverse hogging bending applied in advance (for TR1P1 and TR1P2).

In calculating F_{ck} for the specimens, the measured concrete strengths were used and A_{cv} was taken from the potential failure surface of longitudinal shear as shown in Figure 9.3.

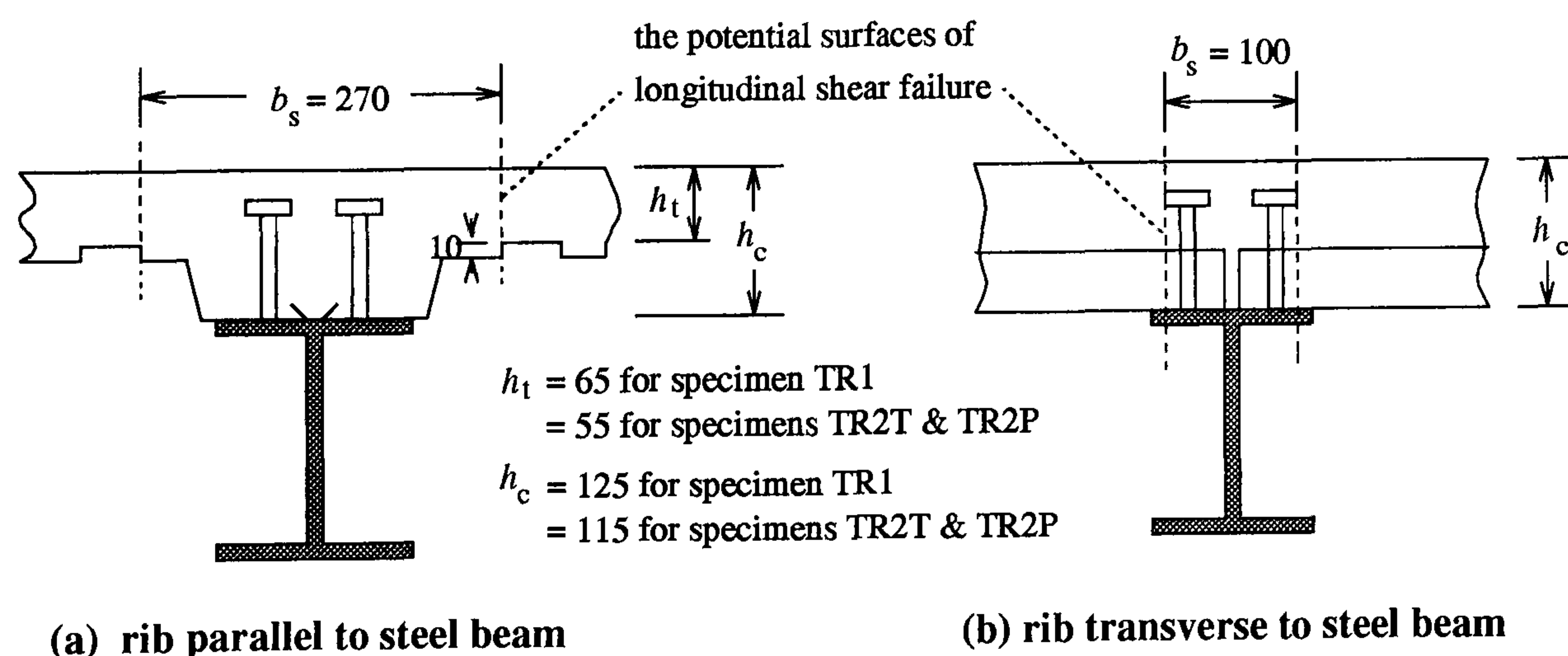


Figure 9.3: Failure surfaces of longitudinal shear considered for the tests

Comparing the predictions of P_{ck} with different A_{cv} as shown in Table 9.1, it seems more acceptable that, in finding F_{ck} or P_{ck} , the rib area should be excluded

from A_{cv} .

Ignoring the rib effect, Table 9.1 suggests that equations (9.4) to (9.6) can be used to estimate the load corresponding to the first crack in concrete due to longitudinal shear, if

- (1) the beam is originally uncracked;
- (2) the beam is subjected to a concentrated load.

It is noted that, in deriving F_{ck} as shown in equation (9.4), uniform distribution of shear stress along the shear span has been assumed. When longitudinal shear significantly affects the behaviour of composite beams, as occurred in beams TR2T or TR2P, the performance of the beam may be assumed to remain fairly elastic before the shear crack occurs. Thus, this assumption is appropriate for a beam subjected to a concentrated load, for which, from the elastic theory [15], the shear force per unit length developed along a longitudinal surface of the beam flange is constant. To estimate F_{ck} for the other load cases, it is reasonable to assume that distribution of shear stress along the shear span to be same as that of the vertical shear force. However, before making extensive application of this conclusion, it would be better to carry out further tests for other load arrangements, such as uniform load.

9.2 Performance and failure of the specimens in tests

As reported in Section 8.1, the behaviour of specimens at failure appeared to be not consistent in all the tests. The basic performance of the specimens for each test is recognized as follows.

9.2.1 TR2T1 and TR2T2 (shear connection failure)

According to measured deformations of specimen TR2T, as shown in Figures 8.5 and 8.6, the beam seemed to be not performing as one with full shear connection. From Table 8.2, it can be seen that the normal force on concrete slab (and the steel beam) F_{cp} , as determined from the actual strength of the shear connection, is smaller than the elastic force F_{el} calculated for full shear connection; consequently, when the load reached $P_{el,R}$ in the tests, slip at the tested end had become quite noticeable (about 0.9mm in TR2T1 and 2mm in TR2T2), as shown in Figure 8.6. Therefore, as implied in Figures 8.5 and 8.6, partial shear connection appears to have had a significant influence on the behaviour. Moreover, it is to be expected that, due to the considerable slip, the elastic calculation based on full shear connection would over-estimate the force developed in the steel beam (and the concrete slab), which was confirmed by measurement of the steel force in tests, as shown in Figure 8.19. So, it can be concluded that specimen TR2T behaved in tests as a composite beam with partial shear connection.

Figure 8.6 shows that large slip occurred at the loaded end in the final stage of test TR2T1. Actually, when failure occurred, no significant damage was observed in concrete. Although some diagonal cracks had appeared, the width of these cracks remained small; as mentioned in Section 8.2, these cracks were able to close up, on unloading just before failure occurred. Furthermore, the predicted $P_{pp,R}$ had been exceeded in this test, as shown in Table 8.3. Therefore, it was judged that the failure of the shear connection, instead of longitudinal shear failure, occurred in test TR2T1.

Since the maximum load obtained in test TR2T1 was even higher than that in TR2T2 (see Table 8.3), the contribution to longitudinal shear resistance from the transverse sheeting in TR2T1 is believed not less than that of A98 mesh in TR2T2. So, for longitudinal shear, the transverse sheeting performed like transverse reinforcement, as assumed in assumption (2) in Section 6.2.1.

As shown in Figure 8.6, large slip also occurred in test TR2T2. At failure,

wide diagonal cracks were found on the bottom surface of the concrete slab, developing from the roots of the shear connectors; but, except for some diagonal cracks similar to those found in TR2T1, concrete on top of the slab was not impaired. Therefore, considering further that the maximum load in this test had almost reached the predicted $P_{pp,R}$ (see Table 8.3), it can be concluded that, as in test TR2T1, the failure of the shear connection was achieved in test TR2T2.

From tests TR2T1 and TR2T2, it is concluded that, where sheeting is transverse to the steel beam, longitudinal shear failure will not normally govern the ultimate resistance of composite beams. This is because, if the shear span is short (say about a quarter of the beam span), the corrugations of the sheets will limit the number of shear connectors and the shear connection will fail before the longitudinal shear resistance in the same shear span is fully developed, while for long shear spans (say half of the beam span), the flexural failure will normally occur first.

In Section 8.2, it has been reported that, at a late stage of test TR2T1 ($P = 190$ kN), a longitudinal crack in concrete was formed in region BC as shown in Figure 7.2. Since the position of the crack was just over the studs and no reinforcement was supplied in the specimen except in the test region for TR2T2, this longitudinal crack was probably caused by the longitudinal splitting [1]. Since in test TR2T1 the maximum load was 14% higher than the predicted $P_{pp,R}$ as given in Table 8.3, this splitting may not have weakened the beam. However, the occurrence of such a crack implies that transverse reinforcement should not be omitted completely from a composite beam; the provisions for minimum transverse reinforcement given in the design code[1] should normally be followed.

9.2.2 TR2P1 and TR2P2 (longitudinal shear failure)

Although the maximum load obtained in test TR2P1 just reached the predicted load for the ultimate plastic bending resistance $P_{pl,R}$, as shown in Figure 8.7, the

measurements from strain gauges did not show the occurrence of full yielding over the full depth of the steel beam, either in test TR2P1 or TR2P2. Therefore, it is believed that flexure failure did not occur in these two tests.

It was noticed in test TR2P1 that the concrete in test region HJ (as marked in Figure 7.3) did not crack longitudinally until the failure stage was reached. According to the appearance of the failure in test TR2P1, described in Section 8.1, a pair of wide longitudinal cracks occurred at the final stage near the expected weak surface of longitudinal shear, as marked in Figure 9.3(a), in test region HJ. The occurrence of this pair of cracks was almost immediately followed by a reduction in the load-carrying capacity of the specimen. For test TR2P1, there was no reinforcement in the test region HJ and, due to corrugation of the sheets, little transverse strength would be expected from such parallel sheeting, (as indicated in assumption (3) in Section 6.2.1), so, the failure behaviour shows that, for a composite beam with light or no transverse reinforcement, the tensile strength of concrete, as considered in assumption (4) in Section 6.2.1, did contribute significantly to the resistance to transverse tension from in-plane bending. Thus, for such a beam with parallel sheeting and no transverse reinforcement, it is to be expected that the failure of concrete in tension would directly lead to breakdown of longitudinal shear resistance in the beam. So, it is concluded that a longitudinal shear failure occurred in test TR2P1.

Compared with test TR2P1, more diagonal cracks appeared in test TR2P2. According to the observation reported in Section 8.2, when the tested part of specimen failed, the diagonal cracks in the test region opened widely, and then, at the root of some cracks, concrete on the top surface of the slab was crushed. The wide cracks implied that the mesh in the tested part had yielded. Therefore, it is inferred that, in this test, the behaviour of beam TR2P in longitudinal shear was fairly close to that predicted by the truss analogy for longitudinal shear resistance in composite beams [1,7]. Accordingly, it was concluded that the failure in this test was also in longitudinal shear.

As shown in Figures 8.8, considerable slips were obtained for both tests TR2P1 and TR2P2. However, unlike tests TR2T1 and TR2T2, concrete along the shorter shear span in these two tests was severely damaged when failure occurred, as shown in Figures 8.15 and 8.16. The probable cause for such damage is longitudinal shear. So, it is thought that in these two tests, breakdown of shear connection might also occur eventually, but only after longitudinal shear failure.

According to the tests interpreted above, failure in longitudinal shear appears in two patterns:

- (1) the tensile stress from in-plane bending causes a longitudinal crack in the concrete on the critical surface of longitudinal shear failure, and then the longitudinal shear resistance on this cracked surface is lost; the critical surface of longitudinal shear failure may be taken as that typified in Figures 9.3 or 1.2, depending on the sheets used;
- (2) the concrete between the diagonal cracks and the transverse reinforcement behave like struts and ties of truss [1,7], respectively; the failure can be caused by yielding of transverse reinforcement and failure of the profiled sheeting, possibly followed by failure in concrete such as local crushing at the root of a strut.

Pattern 2 is more likely to occur in a concrete slab without sheeting, as, according to the crack observation reported in Section 8.2, the slab may be penetrated by the diagonal cracks, which would make concrete work like separated struts of a truss. For the concrete slab with profiled sheeting, the truss mechanism may not be formed, because the penetration of the diagonal cracks through the whole slab thickness may be prevented by the sheeting, as reported in Section 8.2.

An unexpected consequence in TR2P1 was that, as reported in Section 8.2, the concrete slab in region JK (as marked in Figure 7.3) was longitudinally cracked in the middle of the test (when the load reached about 220 kN). The possible reason for this cracking may still be the in-plane bending. According to the de-

sign of beam TR2P as shown in Figure 7.3, within length HK, only the region within one metre from point J was covered by mesh A142. Thus, the development of the crack width (see Table 8.4) again gave the impression that, as stated in assumptions (2) and (3) in Section 6.2.1, when sheeting runs parallel to steel beam, it should not be considered to provide resistance to the transverse tension due to in-plane bending. Based on this analysis, it is concluded that, if the parallel sheeting can contribute to the longitudinal shear resistance, the contribution should be from its resistance to the direct longitudinal shear, as stated in assumption (3) in Section 6.2.1.

Although the concrete was unexpectedly cracked in region JK in test TR2P1 the behaviours of the beam as shown in Figures 8.7, 8.8 and 8.20 seemed not to be significantly affected by such cracks. It is therefore considered that control of such cracks may be more important for the serviceability of the structure. Using the measured strengths of materials (Section 7.3) and specimen geometry reported in Section 7.2, the minimum reinforcement required to control cracks may be assessed according to Eurocode 4 (clause 5.3.3(2) and 5.3.4(1))[1]. The calculation shows that, for beam TR2P,

- (1) if no limits to crack width are specified, the minimum reinforcement is $139 \text{ mm}^2/\text{m}$, where the thickness of the concrete flange (clause 5.3.3(2) in Eurocode 4 [1]) was taken as 55 mm, as shown in Figure 9.3;
- (2) if the crack width is to be limited to 0.3 mm, taking the reinforcement stress as 450 N/mm^2 (clause 5.3.4(1) in Eurocode 4 [1]) and the thickness of the concrete flange as 55 mm, the reinforcement area required may be up to $185 \text{ mm}^2/\text{m}$ or more.

It can be noticed from Table 8.3 that the width of the longitudinal crack in region without mesh was developed considerably faster than that in the region with A142 mesh ($A_e = 142 \text{ mm}^2/\text{m}$). Therefore, it is concluded that, as stated in Eurocode 4[1], in controlling cracks in concrete of a composite beam for serviceability, the effect of profiled sheeting should be ignored and the minimum amount

of transverse reinforcement required by the code provisions should be supplied.

9.2.3 TR1T, TR1P1 and TR1P2 (punching shear failure)

It has been indicated in Section 8.2 that the failure in each of tests TR1T, TR1P1 and TR1P2 was caused by a hole punched under the loading point. The punching shear failure that occurred in each of these tests would not necessarily occur in practice, where such heavy point loads do not occur.

As presented in Section 7.2, specimen TR1 for tests TR1T, TR1P1 and TR1P2 was a slab grillage. Since the strength of the concrete ($f_{cu} = 33 \sim 37 \text{ N/mm}^2$) was considerably higher than the specification made for ordering ($f_{cu} = 20 \text{ N/mm}^2$) (see Section 7.3), the slab was too strong and could sustain high load and, therefore, large deformation due to yielding of steel occurred. However, under the test condition, the large deformation made specimen TR1 perform as a plate with nonlinear two-way action. Therefore, on one hand, specimen TR1 appeared very strong; as a result, only local failure (punching shear) was achieved in the tests; on the other hand, the behaviour of this specimen in the later stage of each test became over complicated, in relation to the objective of the test.

In test TR1T (loading at B as shown in Figure 7.1), as the deflexion increased, the steel channels along edges Q-H and T-L, began to share the load with the tested part, since they were connected to the concrete slab, as shown in Figure 7.9. This may be why no sign of flexural failure appeared, even when the load was considerably higher than predicted $P_{pl,R}$, as shown in Figure 8.1; and the force in the secondary steel beam calculated from the elastic state with full shear connection was higher than the measured results, as shown in Figure 8.17.

For tests TR1P1 with load at point F, (Figure 7.1), and TR1P2, both the deflexion-load curve and the slip-load curve, as shown in Figures 8.2 and 8.3, suggested that the ultimate bending resistance with full shear connection was not reached. In fact, calculations from simple beam theory [1,9,16], as presented in Table 8.2, show that the specimen may have performed in a way similar to a

beam with partial shear connection. However, before load reached $P_{e1,R}$, as shown in Figure 8.3, the slip at the test was not very significant, so the estimation of steel force based on full shear connection, within the elastic limit, fairly close to the measured value, as shown in Figure 8.18.

From Figures 8.2 and 8.3, it can be seen that higher load-carrying capacity appeared in test TR1P2 than in TR1P1. The reasons for this are possibly as follows:

- the load plotted in Figures 8.2 and 8.3 for test TR1P1 was only the main load on point F (Figure 7.1); in fact, before the main load was applied for TR1P1, the specimen had been subjected to a secondary load ($P = 35$ kN) at point G; so compared with the case of the same conditions but no such a secondary load (test TR1P2), the maximum value of the main load in TR1P1 should be obtained as smaller than that in TR1P2;
- the loading position was changed several times in test TR1P1, as reported in Section 8.1, thus the test region LD as marked in Figure 7.1 may be weakened a little by repeated loading and unloading.

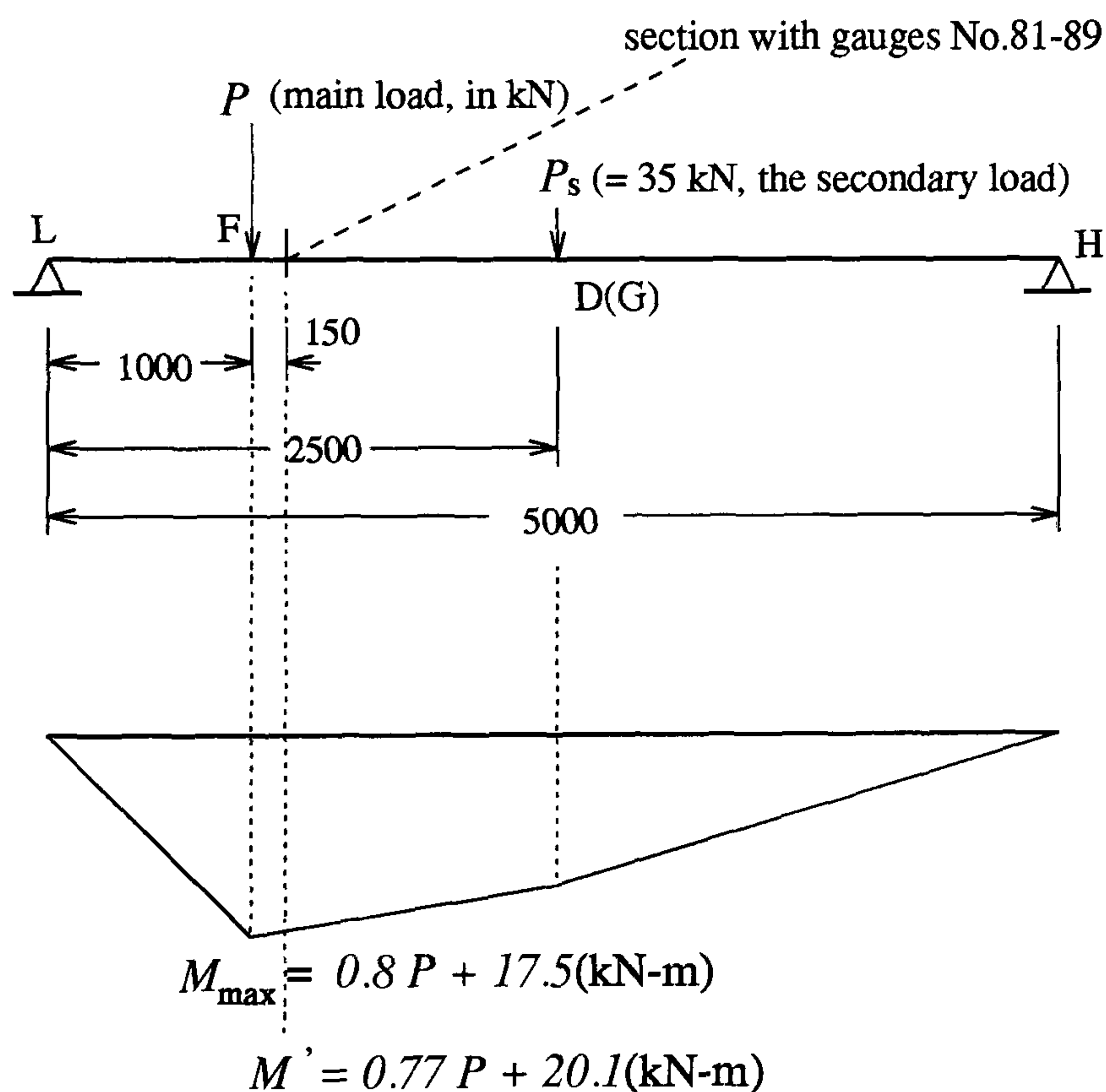
It should be noted that, from the available test results, it was not possible to see clearly the effect on the behaviour of the specimen of the pre-existing longitudinal crack which was caused by the secondary load at point G. This is because, on one hand, no corresponding test without such a crack was conducted; on the other hand, as indicated above, the specimen performed in the late test stage like a two-dimensional plate with large deformation, which made the situation too complicated to reveal a clear picture about the performance of the specimen.

However, from measurement of the steel forces (Figure 8.18) and observation of development of the crack patterns in tests TR1P1 and TR1P2, it seems that application of such secondary load has no significant influence on behaviour of the specimens in longitudinal shear.

9.3 Longitudinal shear resistances of the specimens

The longitudinal shear resistance developed in the specimens may be studied from the measured steel force in each test as presented in Figures 8.17 to 8.20 and Table 8.4.

It should be noted that, in test TR1P1, as the main load eventually was moved to point F (see Figure 7.1), no strain gauges were available within the tested shear span (region LF); in order to take advantage of strain gauges No. 81 - 89 (see Figure 7.24) to obtain the steel force developed within the shear span LF, the assumption had to be made that variation of the steel force was proportional to that of the external bending moment. Thus, f_a for test TR1P1 may be found as described in Figure 9.4.



Let F be the steel force on section F,
 F' be the steel force on the section
 with strain gauges No.81-89;

then, F is estimated from F' as

$$F = \frac{0.8P + 17.5}{0.77P + 20.1} F' \quad (a)$$

When $P > 65$ kN, it may be further
 simplified that

$$F = 0.8/0.77 F' \quad (b)$$

since the difference between (a) & (b)
 is then smaller than 5%.

So the steel force, f_a , in LF is obtained
 as

$$f_a = 1.039F' \quad (\text{kN/m}) \quad (c)$$

Figure 9.4: Finding steel force for test TR1P1

According to the test observations, the critical surfaces of longitudinal shear failure for ribs parallel or transverse to the steel beam may be taken as those in

Figures 9.3(a) or 9.3(b), respectively. Therefore, applying the theory established in Chapter 6, the longitudinal shear resistance of the specimens in each test can be calculated.

Either the formulae proposed by Eurocode 4, as shown in equations (6.1) and (6.2), or those developed in Chapter 6, as shown in equations (6.22) and (6.43), directly give the longitudinal shear resistances on the critical surfaces as shown in Figure 9.3. In tests, only the force developed in the steel beam, rather than the shear force on such longitudinal surfaces, could be measured. Therefore, in order to make comparison between the theoretical predictions and the test results, the steel force which corresponds to the longitudinal shear resistances on the critical surfaces of longitudinal shear failure should be predicted as well.

In Section 9.1, the relationship between shear force on the longitudinal surface, F_{lg} , and the total bending force on the concrete slab, F_c has been established by equation (9.3). Thus, from the equilibrium as shown in Figure 9.2, the steel force F_a should be equal to the concrete force F_c , and it can be immediately obtained from equation (9.3) that

$$F_c = F_a = 2F_{lg} \frac{b_{eff}}{b_{eff} - b_s} \quad (9.7)$$

Applying equation (6.21) with $n = 0.15$, F_a and F_c may be obtained as follows,

$$F_c = F_a = F_{lg} \left(2 + \frac{b_s}{0.3l} \right) \quad (9.8)$$

Therefore, if the longitudinal shear resistance v_R for the considered longitudinal surface is determined with respect to the theory, such as equation (6.22), then, within the shear span l , the corresponding force developed in steel beam may be assessed in terms of $f_{lg,a} = F_a/l$, i.e.,

$$f_{lg,a} = v_R \left(2 + \frac{b_s}{0.3l} \right) \quad (9.9)$$

As the longitudinal shear resistance v_R can be calculated by equations (6.1) or (6.2), or (6.22) or (6.46), and the corresponding steel force can then be estimated

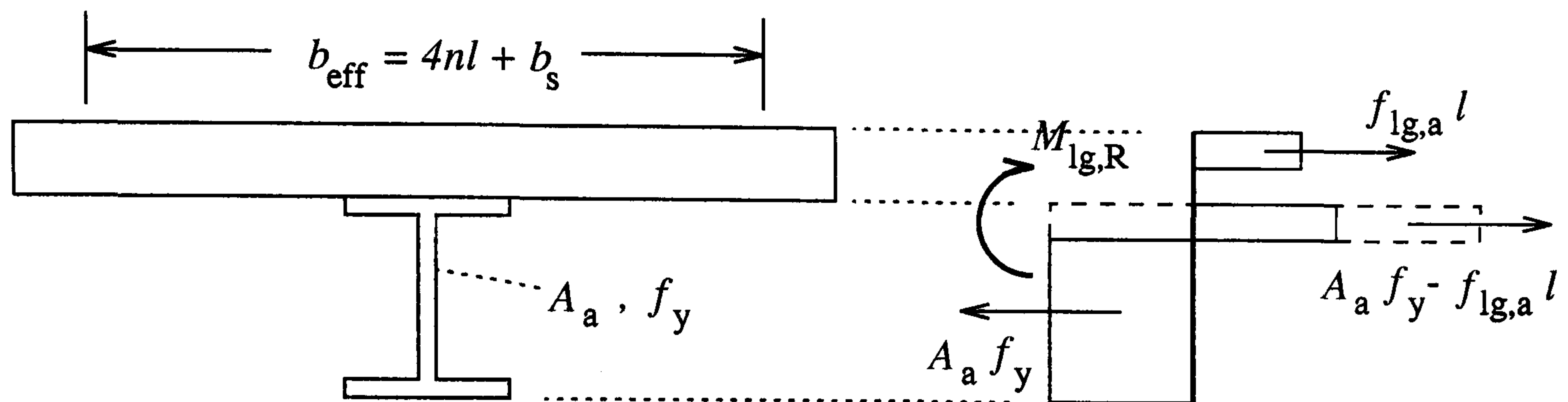
by equation (9.9), the examination of the theories for longitudinal shear resistance may be made by comparing the calculated values of $f_{lg,a}$ with the maximum steel force measured in each test, $f_{a,max}$, reported in Table 8.4.

According to the layout of specimens as shown in Figures 7.1 to 7.3 and the material strengths reported in Section 8.3, the theoretical resistances in longitudinal shear of the specimens for each test were calculated. Table 9.2 presents the results of such calculations, where $f_{a,max}$ given in Table 8.4 are also shown. In the calculations:

- the effect of the beneficial length, as discussed in Section 6.2.3, has been considered, so $\lambda\beta \neq 0$;
- in finding the contribution to v_R from the sheeting which was parallel to steel beam, the shear bond stress via the embossments on the sheet web to the concrete, f_b , as shown in Figure 6.8, was assumed as 0.5N/mm^2 , according to the span-load tables given in [14];
- the weld diameter ϕ_{do} as used in equations (6.48) and (6.51) was taken as $1.1d$, where $d(= 19\text{ mm})$ was the diameter of stud shank.

The ultimate load $P_{lg,R}$, based on the predicted longitudinal shear resistance, was also determined for each test, as shown in Table 9.3, where the maximum loads obtained in tests, $P_{e,max}$, are also listed. In calculating $P_{lg,R}$, the bending moment $M_{lg,R}$ corresponding to v_R was calculated from the rectangular-stress-block analysis [16], as shown in Figure 9.5.

The calculations from equations (6.22) and (6.43), as shown in Table 9.2, suggest that the longitudinal shear resistance of specimens for all the tests is governed by failure of profiled sheeting and transverse reinforcement, rather than crushing of the concrete. This is considered reasonable because, on one hand, no failure was initially caused by crushing of the concrete struts (see Section 6.3.1) in any test; and on the other hand, in the specimens, only light transverse reinforcement (at most A142) was used.



Here, n is taken as 0.15.

Figure 9.5: Bending moment at longitudinal shear failure

Table 9.2: Longitudinal shear resistance in each test

| in unit of kN/m | v_R from Sections 6.2 & 6.3 | | | | | | v_R from Eurocode 4 | | | | test value $f_{a,\text{max}}$ |
|-----------------------|-------------------------------|-------------------|--------------|----------------|-------|-------------------|-----------------------|-------------------|-------------|-------------------|----------------------------------|
| | by eq.(6.43) | | by eq.(6.22) | | | | by eq.(6.2) | | by eq.(6.1) | | |
| | v_R | $f_{\text{lg,a}}$ | $*\lambda l$ | $\lambda\beta$ | v_R | $f_{\text{lg,a}}$ | v_R | $f_{\text{lg,a}}$ | v_R | $f_{\text{lg,a}}$ | |
| TR2T1 | 374 | 852 | 275 | 0.23 | 281 | 640 | 236 | 538 | 192 | 437 | 601 |
| TR2T2 | 344 | 784 | 225 | 0.24 | 284 | 646 | 202 | 461 | 193 | 440 | 449 |
| TR2P1 | 441 | 1212 | 368 | 0.22 | 348 | 958 | 220 | 605 | 93 | 256 | 1007 |
| TR2P2 | 374 | 1028 | 275 | 0.23 | 218 | 600 | 220 | 605 | 152 | 418 | 746 |
| TR1T | 613 | 1362 | 168 | 0.11 | 425 | 944 | 370 | 822 | 322 | 715 | 515 |
| TR1P1 | 687 | 1994 | 336 | 0.25 | 405 | 1174 | 385 | 1116 | 201 | 583 | 800 |
| TR1P2 | 687 | 1994 | 329 | 0.25 | 438 | 1270 | 385 | 1116 | 227 | 658 | 945 |

* this is the determined beneficial length x_0 (see Figure 6.1), in unit of mm.

Table 9.3: Failure load from longitudinal shear resistance

| | $P_{lg,R}$ (kN) | | $P_{e,max}$ (kN) |
|-------|---------------------------------------|-------------------------------------|---------------------|
| | v_R from eq.(6.22) (Section 6.2) | v_R from eq.(6.1) (Eurocode 4) | |
| TR2T1 | 195 | 175 | 215 |
| TR2T2 | 195 | 176 | 186 |
| TR2P1 | 292 | 218 | 320 |
| TR2P2 | 263 | 242 | 300 |
| TR1T | *240 | 237 | 300 |
| TR1P1 | 364 | 297 | 330 |
| TR1P2 | 373 | 307 | 385 |

* The failure load was taken as the ultimate load $P_{pl,R}$ at which the plastic ultimate bending moment would be reached, this is because, in this case, $f_{lg,a}l > A_a f_y$, so the longitudinal shear resistance was determined to be so strong that the failure due to longitudinal shear would not occur.

According to the performance of the specimens discussed in the last section, longitudinal shear failure occurred only in tests TR2P1 and TR2P2, so the longitudinal shear resistance on the longitudinal surface shown in Figure 9.3(a) may have been fully developed only in these two tests. As shown in Table 9.2, the measured maximum steel force $f_{a,max}$ in tests TR2P1 and TR2P2 suggest that the theoretical model established in Chapter 6 with consideration of the beneficial length can quite satisfactorily predict the longitudinal shear resistance.

For comparison, the predictions of longitudinal shear resistances based on Eurocode 4 are also listed in Tables 9.2 and 9.3. One can see that, compared with the test results, Eurocode 4 [1] may be over-conservative.

The tests on where the profiled sheeting was parallel to the steel beam strongly suggested that the code method under-estimates the longitudinal shear resistances. In fact, from the current version of Eurocode 4[1], no contribution from profiled sheeting to the longitudinal shear resistance should be considered if the sheeting is parallel to the steel beam. However, according to the interpretation of the performance of beam TR2P given in the last section, the test results shown

in Tables 9.2 and 9.3 lead to the conclusion that the parallel sheeting, associated with the resistances from the concrete and transverse reinforcement to the transverse tension, can exert resistance directly in longitudinal shear. As studied in Section 6.2, equation (6.22) has included the effect of parallel sheeting on the direct resistance to longitudinal shear, from which the calculation of v_R can agree well with $f_{a,\max}$ in test TR2P1 whose failure occurred in longitudinal shear. Therefore, it is concluded that, the contribution of the parallel sheeting to the longitudinal shear resistance should not totally be ignored.

For sheeting transverse to the steel beam, the tests did not achieve the ultimate shear resistances, so it is still not clear from the test results to what extent the sheeting contribution as given by equation (6.48) can be increased. However, comparing test result from TR2T1 (TR1T was severely affected by the two-way action, so it is not considered here) with the predictions, the contribution from transverse sheeting to v_R can prudently be estimated from equation (6.48).

Compared with the code formula, equation (6.1), the predictions from equation (6.22) include a higher contribution from concrete to the longitudinal shear resistance. In fact, the conservatism in the code formula exposed by the tests imply that a higher contribution from the concrete can be assumed. According to calculation and test results of TR2P1, TR2P2 and even TR2T1, as shown in Table 9.2 and 9.3, it is considered that $0.8A_{cv}f_{ct}$ for the concrete contribution, as given in equation (6.22), is more suitable than $0.625A_{cv}f_{ct}$ given in the code formula (equation (6.1)).

Although no longitudinal shear failure was initially caused by concrete crushing and, therefore, direct investigation could not be made for the longitudinal shear resistances governed by strength of the concrete struts, as determined by equation (6.2) or (6.43), the measured maximum steel force $f_{a,\max}$ from tests TR2P1, TR2P2 and even TR2T1 show that the code prediction based on equation (6.2) can be increased further. Therefore, according to what was analyzed in Section 6.3 and the test results on beams TR2T and TR2P, equation (6.43) is

recommended to determine v_R controlled by the longitudinal shear failure due to crushing in concrete struts.

9.4 The recommendations for design

In finding longitudinal shear resistance in a flange portion of composite beam in Chapter 6, the effect of the beneficial length x_0 was studied by taking a concentrated load into account, as shown in Figure 6.1. It should be realized that the consideration of the effect from x_0 on longitudinal shear resistance, as accounted in term of $\lambda\beta$ in equation (6.22), is only an exploration; although the results from a limited number of tests with longitudinal shear failures (TR2P1 and TR2P2) support such an idea, further study still needs to be taken. So, at the current stage, it would be appropriate to ignore the effect of x_0 when recommending the formulae for design practice.

If the possible beneficial length x_0 is not considered, then it can be seen that the ultimate state of longitudinal shear resistance, as shown in Figures 6.1 or 6.4, is idealized by plasticity in the materials. Therefore, if considering that, for different load arrangement, the same plasticity in materials would be achieved eventually, as recognized in plastic theory of bending resistance etc, then longitudinal shear resistance as determined here may be regarded as applicable to the various common loads, such as uniform and concentrated loads, and it may be expected that, in the ultimate stage, a composite beam subjected to such loads, may perform in the similar way to those tested in this study.

In Section 6.4, to determine the resistance developed in profiled sheets to direct longitudinal shear, v_{ps} , the effect of shear bond stress f_b was considered, as shown in equation (6.50) or (6.51). According to the load-span tables given in [14], f_b for the sheets used in this experimental work is assumed as 0.5 N/mm^2 , and, according to dimensions of the sheet shown in Figure 7.5, A_{eb} (the shear bond area per unit length along the beam span) may be taken as $54 \text{ mm}^2/\text{mm}$ for the

specimens. Thus, the shear bond stress would contribute 27 N/mm (27 kN/m) to the total longitudinal shear resistance; compared with the whole longitudinal shear resistance determined from equation (6.22) or (6.43), as shown in Table 9.2, this contribution appears to be not significant. So, considering that the design shear bond stress may not be explicitly available for various type of sheets in design codes, the effect of $f_b A_{eb}$ on v_{ps} may be neglected for simplicity.

Hence, according to Sections 6.4 and 6.5, a method of determining v_R for design purpose is presented as follows.

On the longitudinal surface of potential shear failure, the shear resistance is

$$v_R = 0.8f_{ct}A_{cv} + A_e f_s + v_p \quad (9.10)$$

or

$$v_R = 0.3f_c S_{cv} + 0.4v_{pc} \quad (9.11)$$

whichever is smaller.

In equations (9.10) and (9.11), A_{cv} and S_{cv} are the mean cross-sectional area per unit length of beam of the concrete shear surface under consideration, but A_{cv} includes the rib area, if any, while S_{cv} excludes the rib area; v_p and v_{pc} are the contribution of the sheeting, as given below; the other symbols have the same meanings as those used in equations (6.1) and (6.2). It should be also noted that, compared with equation (6.53) or (6.43), the factor 0.34 for the concrete term is simply taken as 0.3 in equation (9.11).

The contributions of profiled sheeting v_p and v_{pc} may be determined such that,

- (1) if profiled sheeting with ribs transverse to the beam is discontinuous across the top flange of the steel beam, and stud shear connectors are welded to the steel beam directly through the profiled sheets, then

$$v_p = (1 + a/\phi_{do})\phi_{do} t f_{yp} / s \quad (9.12)$$

$$\text{but } (1.0 + a/\phi_{do}) \leq 4.0$$

where the symbols used are as in equation (6.48);

- (2) if profiled sheeting with ribs transverse to the beam is continuous across the top flange of the steel beam, then

$$v_p = A_p f_{yp} \quad (9.13)$$

where the symbols are as in equation (6.45);

- (3) if profiled sheeting runs parallel to the span of steel beam, then

$$v_p = 3.15 \phi_{do} t f_{yp} / s \quad (9.14)$$

but $v_p \leq 0.16 S_{cv} f_c$.

- (4) In situations where profiled sheeting either transverse or parallel to the steel beam, v_{pc} is taken as v_p in (3) (see discussion in Section 6.3.3).

Apart from applying equations (9.10) to (9.14) to determine longitudinal shear resistance for design, it is suggested that the other design rules given in Eurocode 4 should be not altered. Therefore, for design in practical engineering,

- (1) the rules given in Eurocode 4 for minimum amount of transverse reinforcement apply;
- (2) the reduction factor η for strength of light-weight concrete, as given in Eurocode 4, should be applied to f_c and f_{ct} in equations (9.10) and (9.11), if light-weight concrete is used;
- (3) as in Eurocode 4, studs should be located such that $a \geq 2\phi_{do}$.

As discussed in Sections 9.2.1 and 9.2.2, performance of beams TR2T and TR2P showed that the minimum amount of transverse reinforcement should be retained in composite beams to prevent longitudinal splitting and to control development of crack width.

The test results were all from the specimens fabricated with normal weight concrete. However, according to the analysis given in Chapter 6, the influence of the concrete on longitudinal shear resistance may be regarded as from the

Table 9.4: Longitudinal shear resistance from design formulae (kN/m)

| | v_R from new design method | | v_R from Eurocode 4 | | test result | |
|-------|------------------------------|------------|-----------------------|------------|-------------|-----------------|
| | v_R | $f_{lg,a}$ | v_R | $f_{lg,a}$ | obtained | failure |
| | | | | | $f_{a,max}$ | type |
| TR2T1 | 229 | 522 | 192 | 437 | 601 | ¹ SC |
| TR2T2 | 230 | 524 | 193 | 440 | 449 | |
| TR2P1 | 259 | 712 | 93 | 256 | 1007 | ² LS |
| TR2P2 | 178 | 490 | 152 | 418 | 746 | |
| TR1T | 382 | 848 | 322 | 715 | 515 | |
| TR1P1 | 297 | 862 | 201 | 583 | 800 | ³ PS |
| TR1P2 | 323 | 936 | 227 | 658 | 945 | |

- ¹ shear connection failure
² longitudinal shear failure
³ punching shear failure

strength only, so it is concluded that equations (9.10) and (9.11) are applicable to composite beams with light-weight concrete, but the reduction factor η for f_c and f_{ct} as given in Eurocode 4 should be used.

As shown in Figures 7.1 to 7.3, in all the specimens, the distance between the centre of stud to the sheet edge, a , broke the rule that $a \geq 2\phi_{do}$, but the test results showed that this seemed not to influence the behaviour of the specimens significantly. However, in absence of a comprehensive investigation from both theory and experiment of this problem, it is considered that the practical design should still follow the code provision that $a \geq 2\phi_{do}$.

According to observations made in the tests, it is suggested that the longitudinal surface of potential shear failure should be taken as that shown in Figure 1.2 or 9.3, depending on the shape of sheets.

Using the design method given above and equation (9.9), the longitudinal shear resistances of the specimens tested and the corresponding forces $f_{lg,a}$ developed in steel beam have been re-calculated, as shown in Table 9.4.

According to the rules given in the new design method and Eurocode 4, for the tests listed in Table 9.4, equations (9.10) (new design method) and (6.1)

(Eurocode 4) are used in all the cases to calculate v_R .

Since, except for tests TR2P1 and TR2P2, no longitudinal shear failure was achieved in the tests and, therefore, the real longitudinal shear resistance in the tests except TR2P1 and TR2P2 was not fully developed, then it can be deduced from Table 9.4 that the new design formula, equation (9.10), still give a conservative prediction for the longitudinal shear resistance. However, since the number of tests was limited, prudence would be still needed in taking advantage of this study.

From the push-off tests, Hofeck et al [2] found that, on cracked surfaces in reinforced concrete, the shear strength was a combination of cohesion and friction effects, with an upper limit to shear strength of $0.3f_c$ or 10.3N/mm^2 (whichever was smaller). Sen [4] further pointed out from Hofeck's tests that, in applying the "friction-cohesion" model, as shown by equation (6.3) or (6.4), to determine the shear strength of reinforced concrete on a cracked interface, the upper limit of the reinforcement strength may be taken as

$$A_e f_s / A_{cv} \leq \min\{0.3f_c, 10.3\text{N/mm}^2\} \quad (9.15)$$

The new design rules, as given by equations (9.10) and (9.11)) have a condition that $0.8f_{ct}A_{cv} + A_e f_s + v_p$ may not exceed $0.3f_c S_{cv} + 0.4v_{pc}$.

Assuming that $f_{ct} \approx 0.125f_c (= 0.1f_{cu})$, then for composite beams with solid slabs ($v_p = v_{pc} = 0$ and $S_{cv} = A_{cv}$), condition (9.15) gives $A_e f_s \leq 0.2A_{cv}f_c$. Furthermore, as f_c rarely exceeds 50N/mm^2 [1], then $A_e f_s / A_{cv}$ as controlled by condition (9.15) would be not exceed 10N/mm^2 . Thus, comparing these results with condition (9.15), it follows that equation (9.11) should provide a reasonable upper limit for the prediction of longitudinal shear resistance.

Compared with the formulae of Eurocode 4 (Equations (6.1) and (6.2)), the new recommendations make the following improvements:

- (1) the contribution from concrete tensile strength to longitudinal shear resistance is increased from $0.625A_{cv}f_{ct}$ to $0.8A_{cv}f_{ct}$, as shown in equations (6.1)

- and (9.10);
- (2) the resistance of concrete to crushing is increased from $0.2A_{cv}f_c$ to $0.3A_{cv}f_c$, as shown in equations (6.2) and (9.11);
 - (3) the contribution from sheeting parallel to the steel beam to longitudinal shear resistance (which is ignored by the code) is considered, determined by equation(9.14);
 - (4) the contribution of profiled sheeting to the longitudinal shear resistance governed by concrete crushing is $0.4v_{pc}$ (v_{pc} is determined from equation (9.14) for both parallel and transverse sheeting), instead of $v_p/\sqrt{3}$, as shown in equation (6.2), which is for transverse sheeting only, with v_p determined from equations (9.12) or (9.13).

The new design method (equations (9.10) and (9.11)) and Eurocode 4 formulae (equations (6.1) and (6.2)) are now compared graphically.

The more concerned case for the transverse sheeting in design may normally be that it is discontinuous over the steel beam. When sheeting is discontinuous over the steel beam but fixed to it by welded studs, the contribution of the sheeting v_p in equation (9.10) is found from equation (9.12); according to the condition attached for using equation (9.12), v_p in design will not be determined greater than $4.0\phi_{do}tf_{yp}/s$; and the other hand, the design rule gives that $a \geq 2\phi_{do}$, so, in design, v_p will usually be determined not smaller than $3.0\phi_{do}tf_{yp}/s$. Compared these values with v_{pc} used in equation (9.11), which is found from equation (9.14) (see statements after (9.11)), it can be assumed that, for the transverse sheeting discontinuous over the steel beam, the values of v_p and v_{pc} will be fairly close to each other. Furthermore, in the design method recommended above, v_{pc} would be determined as equal to v_p when sheeting runs parallel to steel beam.

Therefore, the simplification that $v_{pc} = v_p$ is made in presenting the design curves.

For sheeting transverse to the steel beam, the design formulae are as in Figure

9.6, where the conditions are further specified as: (1) $f_{ct} = 0.1f_{cu} = 0.1(f_c/0.8)$; (2) $S_{cv}/A_{cv} = 0.7$. In Figure 9.6, the following symbols are employed:

$$u = \frac{A_e f_s}{A_{cv} f_c} \quad v = \frac{v_R}{A_{cv} f_c} \quad w = \frac{v_p}{A_{cv} f_c}$$

For sheeting parallel to the beam, the longitudinal surface of potential shear failure is usually that beyond the rib area (see Figure 9.3(a)), so S_{cv} can always be assumed to be equal to A_{cv} . Therefore, taking $f_{ct} = 0.1(f_c/0.8)$ and using the same symbols as in Figure 9.6, the design curves are given in Figure 9.7.

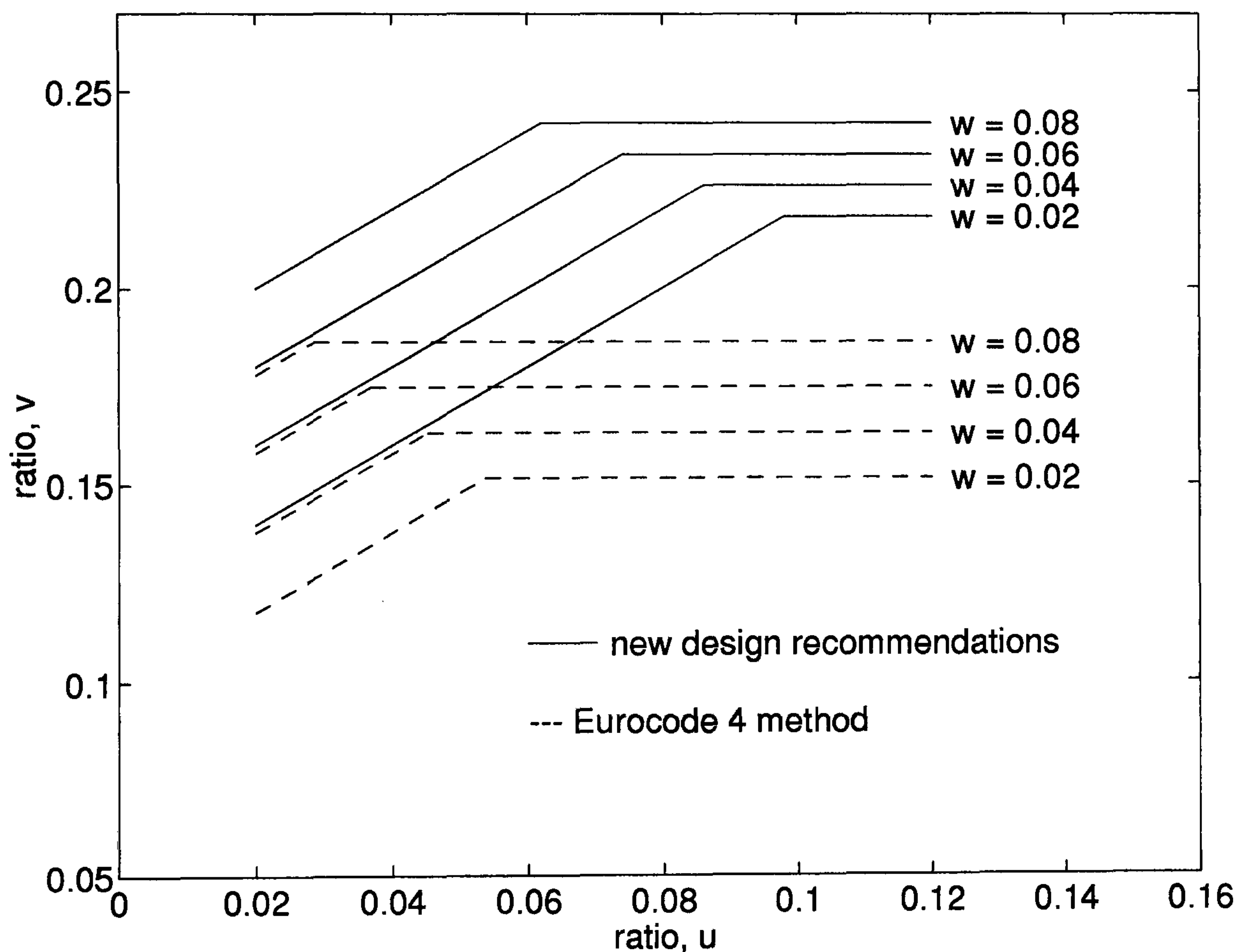


Figure 9.6: Design curve of longitudinal shear resistance (transverse sheeting)

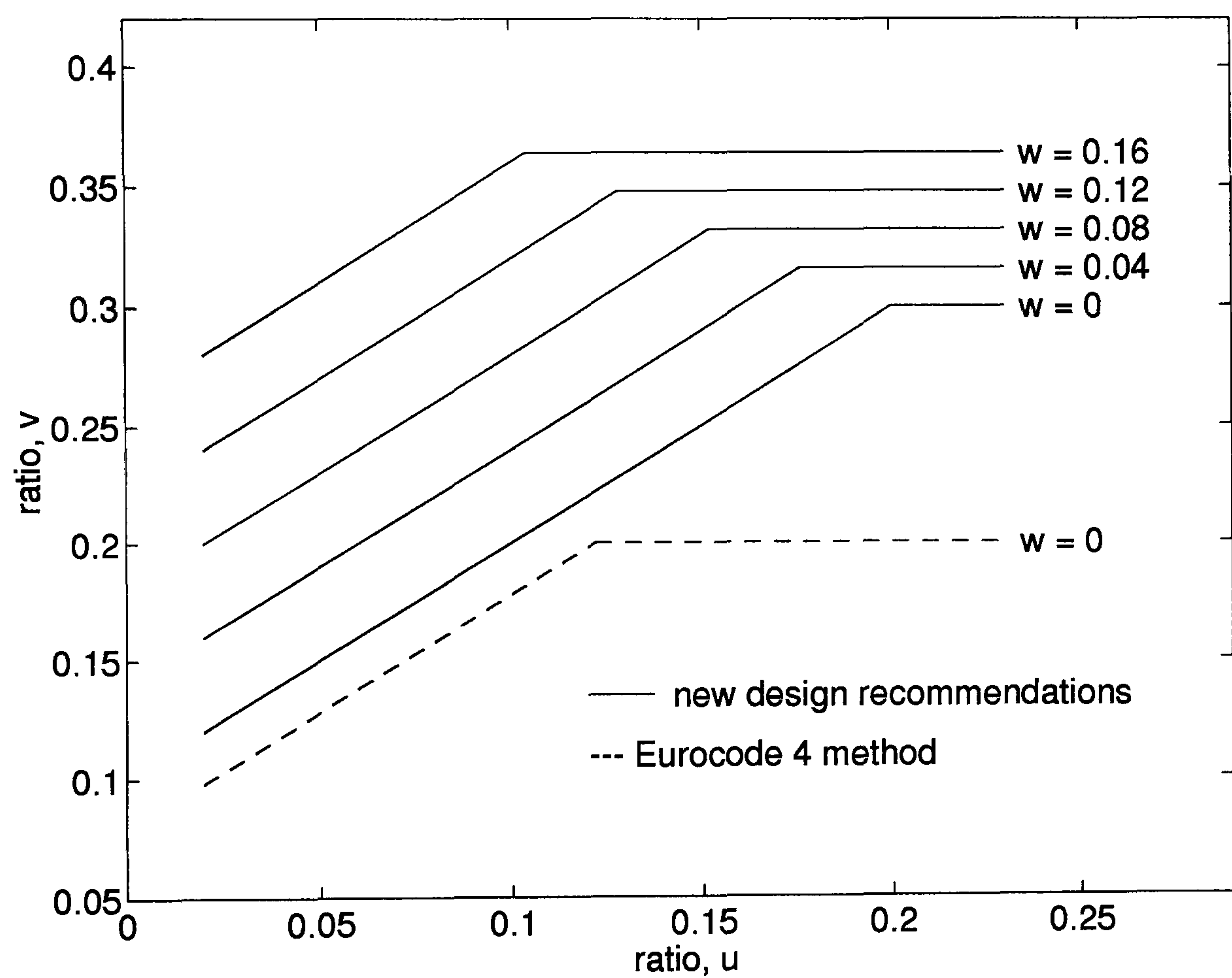


Figure 9.7: Design curve of longitudinal shear resistance (parallel sheeting, or without sheeting)

Chapter 10

Conclusions for resistances of composite beams to longitudinal shear

A study has been carried out to investigate the behaviour in longitudinal shear of composite beams with and without profiled sheeting. A model has been established for the effect of profiled sheeting, from which the longitudinal shear resistances of the flange portion of a composite beam may be determined for the two conditions: (1) failure (yielding) of transverse reinforcement and profiled sheeting; (2) crushing of the concrete struts. In addition to the theoretical analysis, seven tests were conducted on one composite slab grillage and two isolated composite beams. Eurocode 4 was taken in this study as the base for the comparisons and improvements. The study is considered to be applicable to the common situations in composite beams within the scope of the code [1]. The conclusions from this study are as follows.

1. Two patterns of longitudinal shear failure in composite beams have been found from the tests: (1) the tensile stress from in-plane bending causes a longitudinal crack in concrete on the critical surface of longitudinal shear failure, and then the longitudinal shear resistance on this cracked surface

is lost; (2) the concrete between the diagonal cracks and the transverse reinforcement behave like struts and ties of a truss, respectively; the failure can be caused by yielding of transverse reinforcement and failure of profiled sheeting. Pattern 2 is more likely to occur in a composite beam without sheeting.

2. As the corrugation of the sheeting would limit number of the shear connectors that can be used, for the situation of sheeting transverse to the steel beam, longitudinal shear failure does not normally occur prior to failure of the shear connection or failure in bending.
3. The minimum amount of transverse reinforcement required by Eurocode 4 should be provided to prevent longitudinal splitting and control the development of crack width.
4. In predicting the longitudinal shear resistance in composite beams, the formulae adopted by Eurocode 4 [1] seem over-conservative, especially the neglect of the effect of the profiled sheeting when it runs parallel to steel beam and is attached to it by welded studs.
5. Where sheeting runs transverse to the beam and is continuous over the top flange of the steel beam, or is discontinuous but fixed to the steel beam by studs welded through directly, its effect on longitudinal shear resistance may usually be considered to be the same as that of transverse reinforcement, as treated in the code [1].
6. Where sheeting runs parallel to the beam and is fixed to steel beam by studs welded through directly, its effect on longitudinal shear resistance should be considered, as the sheets can develop significant resistance to direct longitudinal shear.
7. For design, the longitudinal shear resistance on longitudinal surfaces of potential shear failure of composite beams may be determined with the formulae developed in this study, as given by equations (9.10) to (9.14).

8. The longitudinal surface of potential shear failure can be taken as that shown in Figure 1.2(b) if sheeting is transverse to the steel beam, and that shown in Figure 1.2(a) or 9.3(a) if sheeting is parallel to the steel beam, depending on the shape of the profile of the sheeting.
9. If a concentrated load is applied to a composite beam which is originally uncracked, the first concrete crack caused by longitudinal shear is normally formed near the support of beam and then develops diagonally, and the load value corresponding to this crack may be estimated by equations (9.4) to (9.6).
10. For beams subjected to a concentrated load, this study also explored the possible situation that the transverse shear force Q (see Figure 6.1) on the cross-section with the maximum bending moment M_{\max} was not zero; according to the theoretical analysis, taking such a condition into account, resistance to longitudinal shear in the shear span considered is increased. Compared with the test results, it seemed that such an favourable effect can be considered; however, to apply this idea generally, further study is needed.

Bibliography

- [1] Eurocode No.4: Design of composite steel and concrete structures, Part 1.1 — General Rules and Rules for Buildings, 1993.
- [2] Hofeck, J.A., Ibrahim, I.O. and Mattock, A. H. : “Shear transfer in reinforced concrete”, ACI Journal, Vol.66, February 1969, pp. 119 - 128.
- [3] Regan, P.E. and Placas, A.: “Limit-state design for shear in rectangular and T beam”, Magazine of Concrete Research: Vol.22, No.73, December 1970, pp. 170 - 208.
- [4] Sen, H.K and Chapman, J.C. “Longitudinal shear in simply-supported composite beam”, Research Report, Engineering Structures Laboratories, Imperial College of Science and Technology, London, March, 1971.
- [5] Morley, C.T. and Rajendran, S.: “The strength and effective width of reinforced concrete flanges”, Proc. Instn Civ. Engrs, Part 2, 59, March 1975, pp.103 - 122.
- [6] BS5400: Steel, concrete and composite bridges — Part 3: Design of steel bridges, 1982.
- [7] Johnson, R.P. and Anderson, D. “Designers’ handbook to Eurocode 4”, Part 1.1: Design of composite steel and concrete structures, Thomas Telford, London, 1993.
- [8] Eurocode No.2: Design of concrete structures, Part 1.1 — General Rules and Rules for Buildings, 1989.

- [9] Lawson, R.M.: "Design of composite slabs and beams with steel decking", SCI publication 055, The Steel Construction Institute, 1989.
- [10] Nielsen, M.P., Baræstrup, M.W., Jensen, B.C. and Bach, F.: "Concrete plasticity: beam shear - shear in joints - punching shear", Specialpublikation udgivet af Dansk Selskab for Bygningsstatik. Lyngby, Oktober 1978.
- [11] Johnson, R.P.: "Longitudinal shear strength of composite beams", ACI Journal, Vol.67, June 1970, pp. 464-466.
- [12] Johnson, R.P.: "Transverse reinforcement in composite beams for buildings", Structural Engineer, Vol.49, May 1971, Page 239.
- [13] Johnson, R.P.: "Design of composite bridge beams for longitudinal shear", Paper for the Conference on Developments in Bridge Design and Construction, University College, Cardiff, 29th March - 2nd April 1971.
- [14] Design manual of composite steel deck floors: "The modern approach for composite floors", The Alphlok Group: Capital Valley Industrial Estate, Rhymney, Gwent NP2 5XX, 1992.
- [15] Timoshenko, S.P. and Gere, J.M.: "Mechanics of materials", Van Nostrand Reinhold Company, New York, 1972.
- [16] Johnson, R.P. and Molenstra, N.: "Partial shear connection in composite beams for buildings", Proceeding of Institution of Civil Engineers, Part 2, Vol.91, December 1991, pp.679-704.
- [17] Birkeland, P.W. and Birkeland, H.W.: "Connections in precast concrete construction", ACI Journal, Proceedings Vol.63, No.3, March 1966, pp.345-368.
- [18] Mast, R.F.: "Auxiliary reinforcement in concrete connections", Proceedings, ASCE, Vol.94, ST6, June 1968, pp. 1485-1504.
- [19] Mattock, A.H. and Hawkins, N.M.: "Shear transfer in reinforced concrete - recent research", Journal of Prestressed Concrete Institute, Vol.17, No.2,

- March 1972, pp.55-75.
- [20] Crisinel, M.: "Partial-interaction analysis of composite beams with profiled sheeting and non-welded shear connectors", *Journal of Construction Steel Research*, Vol.15, 1990, pp.65-98.
- [21] Grant, J.A., Fisher, J.W. and Slutter, R.G.: "Composite beams with formed steel deck", *Engineering Journal of American Institute of Steel Construction*, First Quarter, 1977, pp.24-43.
- [22] Madsen, H.O., Kernk, S. and Lind, N.C.: "Methods of structural safety", Prentice-Hall, Inc., Englewood Cliffs, New Jersey 07632, 1986.
- [23] Cornell, C.A.: "Some thoughts on "maximum probable loads" and "structural safety insurance", *Memorandum*, Department of Civil Engineering, Massachusetts Institute of Technology, to Members of ASCE Structural Safety Committee, March 1967.
- [24] Cornell, C.A.: "A probability-based structural code", *Journal of the American Concrete Institute*, Vol.66, No.12, 1969, pp. 974-985.
- [25] Hasofer, A.M. and Lind, N.C.: "Exact and invariant second-moment code Format", *Journal of Engineering Mechanics Division, ASCE*, Vol.100, No.EM1, February, 1974, pp.111-121.
- [26] Ang, A.H-S. and Cornell, C.A.: "Reliability bases of structural safety and design", *Journal of Structural Division, ASCE*, Vol.100, No.ST9, September, 1974, pp.1755-1769.
- [27] Ellingwood, B.R. and Ang, A.H-S.: "Probablistic evaluation of design criteria", *Journal of Structural Division, ASCE*, Vol.100, No.ST9, September 1974, pp.1771-1788.
- [28] Bavindra, M.K., Lind, N.C. and Siu, W.: "Illustrations of reliability-based design", *Journal of Structural Division, ASCE*, Vol.100, No.ST9, September, 1974, pp.1789-1811.

-
- [29] Siu, W.W.C., Rarimi, S.R. and Lind, N.C.: "Practical approach to code calibration", *Journal of Structural Division, ASCE*, Vol.101, No.ST7, July, 1975, pp.1469-1480.
- [30] Allen, D.E.: "Limit states design – a probabilistic study", *Canadian Journal of Civil Engineering*, Vol.2, No.36, 1975, pp.36-49.
- [31] Vrouwenvelder, A.C.W.M. and Siemes, A.J.M.: "Probabilistic calibration procedure for the derivation of partial safety factors for the Netherlands building codes", *Heron*, Vol.32, N0.4, 1987, pp.9-29.
- [32] Nordic Committee on Building Regulation (NKB): "Guilelines for loading and safety regulations for structural design", NKB Report No.55E, June 1987.
- [33] Bijlaard, F.S.K, Sedlacek, G. and Stark, J.W.B.: "Procedure for the determination of design resistance from tests", Report BI-87-112, TNO Institute, Delft, Movember 1988.
- [34] Kersken-Bradley, M., Maier, W. and Vrouwenvelder, A.: "Estimation of structural properties by testing for use in limit state design", Working document of Joint Committee on Structural safety, November 1990.
- [35] Stark, J.W.B. and van Hove, B.W.E.M.: "Statistical analysis of push-out tests on stud connectors in composite steel and concrete structures", Report BI-89-007, TNO Institute, Delft, March 1989.
- [36] Stark, J.W.B. and van Hove, B.W.E.M.: "Statistical analysis of push-out tests on stud connectors in Composite Steel and Concrete Structures", Report BI-91-163, Parts 1,2 and 3, TNO Institute, Delft, September 1991.
- [37] Kennedy, J.B. and Neville, A.M.: "Basic statistical methods for engineers and sceintists", Third edition, Harper and Row, Publishers, New York, 1986.
- [38] Guenther, W.C.: "Sampling inspection in statistical quality control", Charles Griffin, London, 1977.

-
- [39] Resniff, G.J. and Lieberman, G.J.: "Tables of the non-central t -distribution", Stanford University Press, U.S.A., 1957.
- [40] Johnson, R.P. and Huang, D.J.: "Calibration of safety factors γ_M for steel and concrete composite beams in bending", a paper to be published in the Structures and Buildings Journal of ICE Proceedings in 1994.
- [41] Thomas, D.A.B.: "The behaviour of composite beams with profiled steel sheeting and shot-fired shear connection", M.Sc thesis, Salford University, 1989.
- [42] Teraszkiewicz, J.S.: "Static and fatigue behaviour of simply supported and continuous composite beams of steel and concrete", Ph.D thesis, Imperial College, London, September 1967.
- [43] Balakrishnan, B.E.: "The behaviour of composite steel and concrete beams with welded stud shear connectors", Ph.D thesis, Imperial College, London, March 1967.
- [44] Barnard, R.P. and Johnson, R.P.: "Plastic behaviour of continuous composite beams", Proceedings of Institution of Civil Engineers, Vol.32, October 1965, pp.180-197.
- [45] Barnard, R.P. and Johnson, R.P.: "Ultimate strength of composite beams", Proceedings of Institution of Civil Engineers, Vol.32, October, 1965, pp.162 - 179.
- [46] Barnard, R.P.: "A series of tests on simply supported composite beams", Journal of American Concrete Institute, Vol.62, April 1965, pp.443 - 455.
- [47] Hope-Gill, M.C. and Johnson, R.P.: "Tests on three 3-span composite beams", Proceedings of Institution of Civil Engineers, Part 2, Vol.61, June 1976, pp.367-381.
- [48] Vasseghi, A.: "Strength and behaviour of composite plate girders under shear and bending moments", Ph.D thesis, University of Texas at Austin, U.S.A., May 1989.

- [49] Garcia, I., and Daniels, J.H. Research Reports on Project No.359, Friz Engineering laboratory, Lehigh University, U.S.A. 1971.
- [50] Hamada, S. and Longworth, J. "Buckling of composite beams in negative bending", ASCE Proceedings, Vol.100, ST11, November 1974, pp.2205-2222.
- [51] Grant, J.A., Fisher, J.W. and Slutter, R.G.: "Composite beams with formed steel deck", Engineering Journal of American Institute of Steel Construction, Vol.14, No.1 1977, pp.24 - 43.
- [52] Hawkins, N.M. and Roderick, J.W.: "The behaviour of composite beams", Civil Engineering Transactions of Institution of Engineers, Australia, 1976, pp.102 - 108.
- [53] Seek, W.G., Fisher, J.W. and Slutter, R.G.: "Tests of lightweight composite beams with metal decking", Research Report (unpublished). Fritz Engineering laboratory, Lehigh University, U.S.A., November 1970.
- [54] Robinson, H.: "Multiple stud shear connections in deep ribbed metal deck", Canadian Journal of Civil Engineering, Vol.15, 1988, pp.553 - 569.
- [55] Helmut Bode und Roland Künzel: "Zur Anwendung der Durchschweißtechnik im Verbundbau", Bauingenieurwesen - Stahlbau - Postfach 30 49 - D - 6750 Kaiserslautern, Universität Kaiserslautern, March 1991.
- [56] R.M. Lawson, K.F. Chung and A.M. Price: "Tests on composite beams with large web openings", The Structural Engineer, Vol.70, No.1, 7th January 1992, pp. 1-7.
- [57] H.D.Wright and R.W.Francis: "Test on composite beams with low level of shear connection", The Structural Engineer, Vol.68, No.15, August 1990, pp.293-298.
- [58] Johnson, R.P. and Huang, D.J.: "Partial safety factor γ_M for composite beams in bending, found from test data", Research Report CE38, Department of Engineering, University of Warwick, February 1992,.

-
- [59] Johnson, R.P. and Huang, D.J.: "Reliability analysis for composite beams with ductile partial shear connection", Research Report CE40, Department of Engineering, University of Warwick, March 1992.
- [60] Huang, D.J. and Johnson, R.P.: "Reliability analysis for composite beams with non-ductile partial shear connection", Research Report CE42, Department of Engineering, University of Warwick, March 1993.
- [61] Johnson, R.P.: "Composite structures of steel and concrete", Vol.1, Crosby Lockwood Staples, 1975.
- [62] Johnson, R.P.: "Coefficients of variation of areas of flanges and webs of rolled steel I and H sections", Research Report CE43, Department of Engineering, University of Warwick, January 1993.
- [63] Document of Department of Transport: "Design of composite bridges — Use of BS 5400: Part 5: 1979 for development of transport structures", Department of Transport, St Christopher House, London SE1 0TE, December 1987.

Appendix A

Non-central t-distribution and fractile-factors

It has been shown in Sections 2.2.2 and 2.3 that the design fractile-factor k_d should be found from equation (2.32) or, more generally, (2.57). The factor k_b there should be determined with respect to the number of test specimens included in the group considered.

As discussed in Section 2.2.2, k_b is used for V_δ only (see (2.32) or (2.57)) and, therefore, can be regarded as only depending on the relative variation of the real resistance to the theoretical model, while such variation does not associate with the uncertainties of the basic variables. So, in determining factors k_b , the uncertainties of the basic variables are ignored and the theoretical resistance r_t is simply regarded as its mean value $g_R(\bar{X})$. Accordingly, from assumption (5) in Section 2.2.1, it can be further assumed here that $b = r/r_t = r/g_R(\bar{X})$ follows a log-normal distribution, or

$$y = \ln \frac{r}{g_R(\bar{X})} \quad (\text{A.1})$$

follows a normal distribution with unknown mean μ_y and standard deviation σ_y .

Based on a group of n test specimens, the estimators of μ_y and σ_y , denoted by \bar{y} and s_y , can be found as follows,

$$\bar{y} = \frac{1}{n} \sum_{i=1}^n y_i \quad (\text{A.2})$$

$$s_y = \sqrt{\frac{1}{n-1} \sum_{i=1}^n (y_i - \bar{y})^2} \quad (\text{A.3})$$

where $y_i = \ln(r_{ei}/r_{ti})$ is the i th observation of y from the test result of specimen i with $i = 1, \dots, n$.

From (A.2), (A.3) and the properties of a log-normal distribution [37], an alternative way, rather than equations (2.25) and (2.26), for estimating the mean correction \bar{b} and coefficient of variation V_δ can be given as

$$\bar{b} = \exp(\bar{y} + 0.5s_y^2) \quad (\text{A.4})$$

$$V_\delta = \sqrt{\exp(s_y^2) - 1} \quad (\text{A.5})$$

It should be noted that, usually, the estimators of \bar{b} and V_δ based on (2.25) and (2.26) may not be fully consistent with those from (A.2) to (A.5) unless $r_{e1}/r_{t1} = \dots = r_{en}/r_{tn}$. However, when V_δ calculated from (2.26) appears sufficiently small ($V_\delta = 0$ means $r_{e1}/r_{t1} = \dots = r_{en}/r_{tn}$), the estimators obtained from (A.2) to (A.5) may be assumed to be the same as those from (2.25) and (2.26). For bending resistances of composite beams to which $V_\delta \leq 0.1$ is obtained based on (2.26)(see Chapter 4), the calculation can show that the differences between the results from (2.25) to (2.26) and (A.2) to (A.5) are less than 4% and 0.1% for V_δ and \bar{b} , respectively, and, therefore, can be ignored.

Setting k_b as the fractile-factor for the design resistance r_b (subscript b denotes that the analysis does not consider the randomness in the basic variables), then it is obtained that

$$r_b = \bar{b}g_R(\bar{X})\exp(-k_b s_y - 0.5s_y^2) \quad (\text{A.6})$$

Since y defined in (A.1) follows a normal distribution and its mean and standard deviation have been estimated as \bar{y} and s_y , respectively, the probability P_f

that the resistance is smaller than r_b can be assessed as follows,

$$P\{r < r_b\} = P_f = P\{y < \bar{y} - k_b s_y\} \quad (\text{A.7})$$

where, $P\{\dots\}$ represents the probability of event \dots .

However, in estimating \bar{y} and s_y , the number of test specimens in the group considered is usually limited, so the determination of the failure probability P_f from equation (A.7) should be made by imposing a confidence level ϵ , such that [38],

$$P\{P\{r < r_b\} \leq P_f\} = \epsilon \quad (\text{A.8})$$

From equation (A.7), it yields

$$P_f = P\left\{\frac{y - \mu_y}{\sigma_y} < \frac{\bar{y} - k_b s_y - \mu_y}{\sigma_y}\right\} \quad (\text{A.9})$$

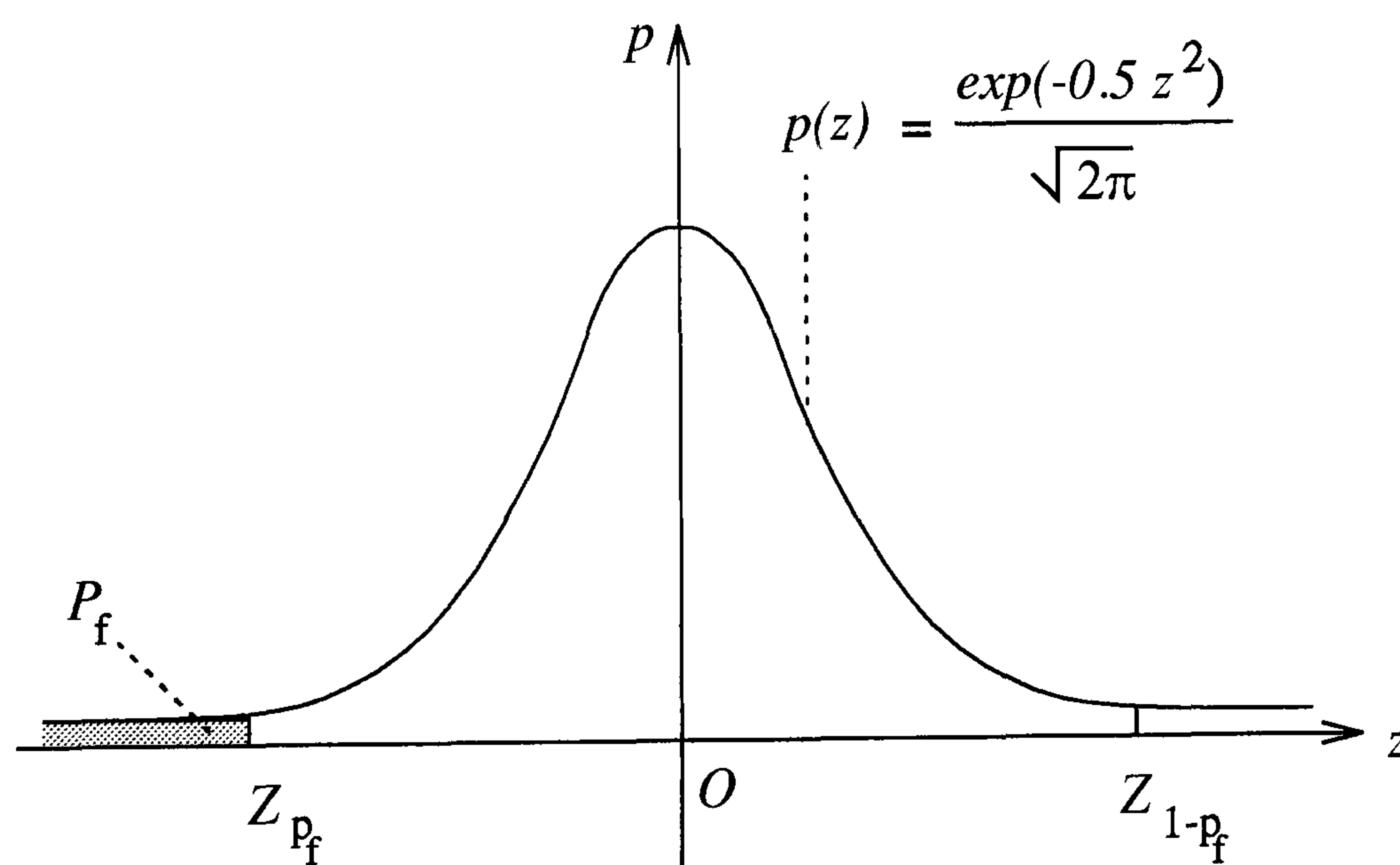


Figure A.1: Fractile-factor and probability of the standard normal distribution

Obviously, $Z = (y - \mu_y)/\sigma_y$ follows the standard normal distribution. So equation (A.9) can determine a fractile-factor $Z = Z_{P_f} = -Z_{1-P_f}$ when P_f is specified or vice versa, as shown in Figure A.1. According to the theory about the sample inspection [37,38], it can further be obtained from (A.7) and (A.9) that

$$P\{r < r_b\} \leq P_f \Leftrightarrow \frac{\bar{Y} - k_b S_Y - \mu_y}{\sigma_y} \leq -Z_{1-P_f} \quad (\text{A.10})$$

where

$$\bar{Y} = \frac{1}{n} \sum_{i=1}^n Y_i \quad (\text{A.11})$$

$$S_Y = \sqrt{\frac{1}{n-1} \sum_{i=1}^n (Y_i - \bar{Y})^2} \quad (\text{A.12})$$

and Y_i ($i = 1, \dots, n$) is the random variable corresponding to observation y_i of y , having the same distribution as y .

With respect to the equivalent condition shown in (A.10), the confidence level ϵ given in (A.8) can be turned into

$$\epsilon = P\{P\{r < r_b\} \leq P_f\} = P\left\{\frac{\bar{Y} - k_b S_Y - \mu_y}{\sigma_y} \leq -Z_{1-P_f}\right\} \quad (\text{A.13})$$

Therefore, the following relationship can further be derived from equation (A.13):

$$P\{t \leq \sqrt{n}k_b\} = \epsilon \quad (\text{A.14})$$

where

$$t = \frac{\sqrt{n}(\bar{Y} - \mu_y)/\sigma_y + \sqrt{n}Z_{1-P_f}}{S_Y/\sigma_y} \quad (\text{A.15})$$

follows the non-central t -distribution with $n - 1$ degrees of freedom and non-central parameter $\sqrt{n}Z_{1-P_f}$ [38,39]. The comprehensive study of the non-central t -distribution has been carried out, as described in Reference [39].

As shown in Figure A.1, Z_{1-P_f} is related to the failure probability P_f through the standard normal distribution. Therefore, from a non-central t -distribution, the fractile-factor k_b can be related to the confidence level ϵ , group size n and the failure probability P_f , such that

$$\begin{cases} P_f = 1 - \int_{-\infty}^{Z_{1-P_f}} \exp(-0.5z^2) dz / \sqrt{2\pi} \\ \epsilon = \int_{-\infty}^{\sqrt{n}k_b} p_{nt}(n-1, \sqrt{n}Z_{1-P_f}, t) dt \end{cases} \quad (\text{A.16})$$

where, $p_{nt}(n-1, \sqrt{n}Z_{1-P_f}, t)$ denotes the probability density of the non-central

Table A.1: Factor k_b with $P_f = 0.12\%$ at $\epsilon = 0.75$

| | | | | | | | | | | |
|-------|------|------|------|------|------|----------|------|------|------|------|
| n | 2 | 3 | 4 | 5 | 6 | 7 | 8 | 9 | 10 | 11 |
| k_b | 9.52 | 5.72 | 4.83 | 4.44 | 4.20 | 4.05 | 3.95 | 3.86 | 3.80 | 3.74 |
| n | 12 | 13 | 14 | 15 | 16 | 17 | 18 | 19 | 20 | 21 |
| k_b | 3.70 | 3.66 | 3.63 | 3.60 | 3.58 | 3.55 | 3.54 | 3.52 | 3.51 | 3.49 |
| n | 22 | 23 | 24 | 25 | 26 | 27 | 28 | 29 | 30 | 31 |
| k_b | 3.47 | 3.46 | 3.45 | 3.44 | 3.44 | 3.43 | 3.43 | 3.42 | 3.42 | 3.41 |
| n | 32 | 33 | 34 | 35 | 36 | 37 | 38 | 39 | 40 | 41 |
| k_b | 3.40 | 3.40 | 3.39 | 3.39 | 3.38 | 3.38 | 3.37 | 3.36 | 3.36 | 3.35 |
| n | 42 | 43 | 44 | 45 | 46 | 47 | 48 | 49 | 50 | 51 |
| k_b | 3.35 | 3.34 | 3.33 | 3.33 | 3.32 | 3.32 | 3.31 | 3.31 | 3.30 | 3.30 |
| n | 52 | 53 | 54 | 55 | ... | ∞ | | | | |
| k_b | 3.30 | 3.29 | 3.29 | 3.29 | ... | 3.04 | | | | |

variable t , whose details can be found in Reference [39].

With reference to the instruction given in [33], for the design resistance, the failure probability P_f and the confidence level imposed on it ϵ may be taken as 0.12% and 0.75, respectively. Thus, from the tabulated data in References [33, 39], the fractile factor k_b , as used in equation (2.32), can be determined according to equation (A.16) and group size n . Table A.1 shows these results.

Appendix B

Coefficients of variations of the basic variables

In finding the coefficient of variation V_{R_t} for equation (2.27), the values of the coefficients of variations of the basic variables, as denoted by V_{X_i} ($i = 1, \dots, J$) in Section 2.2.2, need to be known in advance. Since the present analysis for reliability in the structural resistances are intended to be applicable to practice, V_{X_i} ($i = 1, \dots, J$) are required to be those found in practice, not in laboratories where test specimens are made.

As is well known, methods of testing materials, curing procedures for concrete, and tolerances on structural steel can vary from country to country. The geometric tolerances on concrete members may even vary from site to site. Commonly, the coefficients of variation of geometric dimensions tend to decrease as size increases. Therefore, the coefficients of variation for the basic variables may actually not appear consistent in all cases, and the use of a single value for V_{X_i} ($i = 1, \dots, J$) in this study should be regarded as an approximation.

As indicated in [40], reported data of this subject are, inevitably, not comprehensive. The coefficients of variation referred in this study adopt the values given in Table B.1, which are assumed according to References [31,33,35,36], particularly [31] which are based on the most extensive study of this problem known

Table B.1: Coefficients of variation of basic variables

| Variables | | Coefficients of variation |
|--|-----------|---------------------------|
| yield strength of steel | f_y | $V_{f_y} = 0.08$ |
| Young's modulus of steel | E_a | $V_{E_a} = 0.04$ |
| compressive strength of concrete | f_c | $V_{f_c} = 0.15$ |
| Young's modulus of concrete | E_c | $V_{E_c} = 0.10$ |
| yield strength of reinforcement | f_s | $V_{f_s} = 0.10$ |
| tensile force in longitudinal reinforcement | $A_s f_s$ | $V_{A_s f_s} = 0.10$ |
| ultimate tensile strength of studs | f_u | $f_u = 0.08$ |
| all linear dimensions of a steel cross-section | | 0.04 |
| area of a steel cross-section | A_a | $V_{A_a} = 0.04$ |
| plastic modulus of a steel cross-section | W_a | $V_{W_a} = 0.04$ |
| inertial moment of a steel cross-section | I_a | $V_{I_a} = 0.04$ |
| breadth of concrete slab | b_c | $V_{b_c} = 0.008$ |
| depth of concrete slab | h_c | $V_{h_c} = 0.04$ |
| position of reinforcement | h_s | $V_{h_s} = 0.10$ |
| diameter of shank of welded stud | d | $V_d = 0.04$ |

to the author.

Appendix C

Coefficients of variation of resistance functions for composite beams

In this thesis, the reliability analysis of bending resistances is given to the beams represented by four groups defined in Section 3.1.2. For beams in group A (sagging bending with plastic neutral axis in the concrete slab), the resistance function has been shown in equation (3.2), and the coefficient of variation, V_{Rt} , is formulated in (3.3) to (3.5). The relevant formulae for the other groups are now given.

In the following presentation, the coefficients of variation for basic variables (see Appendix A), A_a , f_y etc. are denoted V_{A_a} , V_{f_y} etc., and the superscript bars stand for mean values.

C.1 Hogging bending with plastic neutral axis in steel web (group B)

As shown in Figure C.1, the resistance function is developed as [1,61],

$$r_t = g_R(\underline{X}) = W_a f_y + A_s f_s \left(h_s + h_{na} - \frac{A_s f_s}{4t_w f_y} \right) \quad (\text{C.1})$$

where W_a is the plastic section modulus of the steel section, h_{na} is the depth of plastic neutral axis of the steel section alone, and the other notations are defined in Figure C.1. It is noted that h_{na} is not necessarily equal to the distance from the top surface of top steel flange to the centre of area of the steel section, h_g .

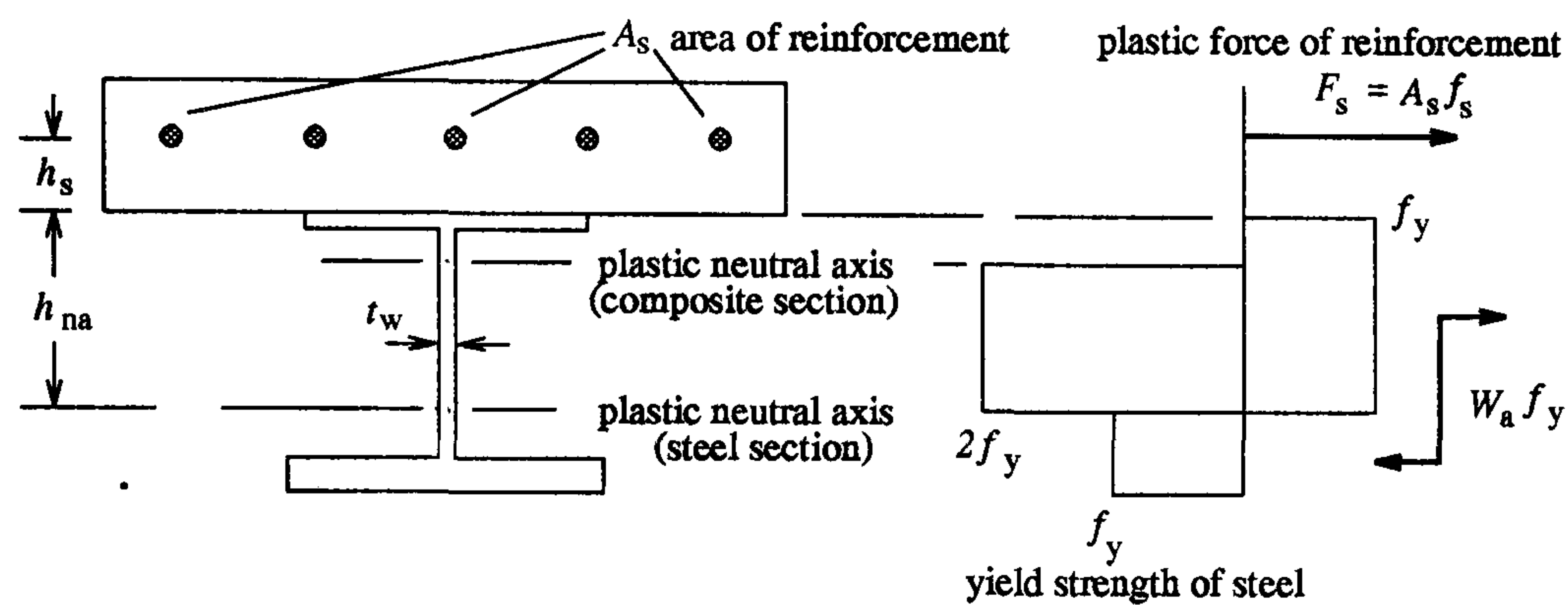


Figure C.1: Hogging bending of composite beams in full shear connection, plastic neutral axis in steel web

Applying equation (2.28) to the resistance function (C.1), it yields

$$V_{rt} = \frac{\{(\bar{r}_1 \bar{r}_2 V_{r1})^2 + [(\bar{r}_1 \bar{r}_2 - \bar{r}_6) V_{r2}]^2 + [(\bar{r}_3 \bar{r}_4 + 2\bar{r}_6) V_{r3}]^2 + (\bar{r}_3 \bar{r}_4 V_{r4})^2 + (\bar{r}_6 V_{r5})^2\}^{\frac{1}{2}}}{\bar{r}_1 \bar{r}_2 + \bar{r}_3 \bar{r}_4 + \bar{r}_3^2 \bar{r}_5 / \bar{r}_2} \quad (\text{C.2})$$

where

$$\left. \begin{aligned} \bar{r}_1 &= \bar{W}_a & V_{r1} &= V_{W_a} \\ \bar{r}_2 &= \bar{f}_y & V_{r2} &= V_{f_y} \\ \bar{r}_3 &= \bar{A}_s \bar{f}_s & V_{r3} &= \sqrt{V_{A_s}^2 + V_{f_s}^2} \\ \bar{r}_4 &= \bar{h}_s + \bar{h}_{na} & V_{r4} &= \sqrt{V_{h_s}^2 \bar{h}_s^2 + V_{h_{na}}^2 \bar{h}_{na}^2} / (\bar{h}_s + \bar{h}_{na}) \\ \bar{r}_5 &= -1/(4\bar{t}_w) & V_{r5} &= V_{t_w} \end{aligned} \right\} \quad (\text{C.3})$$

and

$$\bar{r}_6 = \bar{r}_3^2 \bar{r}_5 / \bar{r}_2 \quad (\text{C.4})$$

C.2 More bending situations of composite beams with full shear connection

Apart from the beams represented by the groups A and B, the coefficients of variation, V_{r_t} , for the other cases of plastic bending of composite beams with full shear connection are also formulated, and are presented below.

C.2.1 Sagging bending with plastic neutral axis in the steel top flange

The plastic stress distribution is shown in Figure C.2, and, accordingly, the resistance function is [61],

$$r_t = g_R(\underline{X}) = A_a f_y h_g + 0.425 b_c h_c^2 f_c - \frac{(A_a f_y - 0.85 b_c h_c f_c)^2}{4 b_f f_y} \quad (\text{C.5})$$

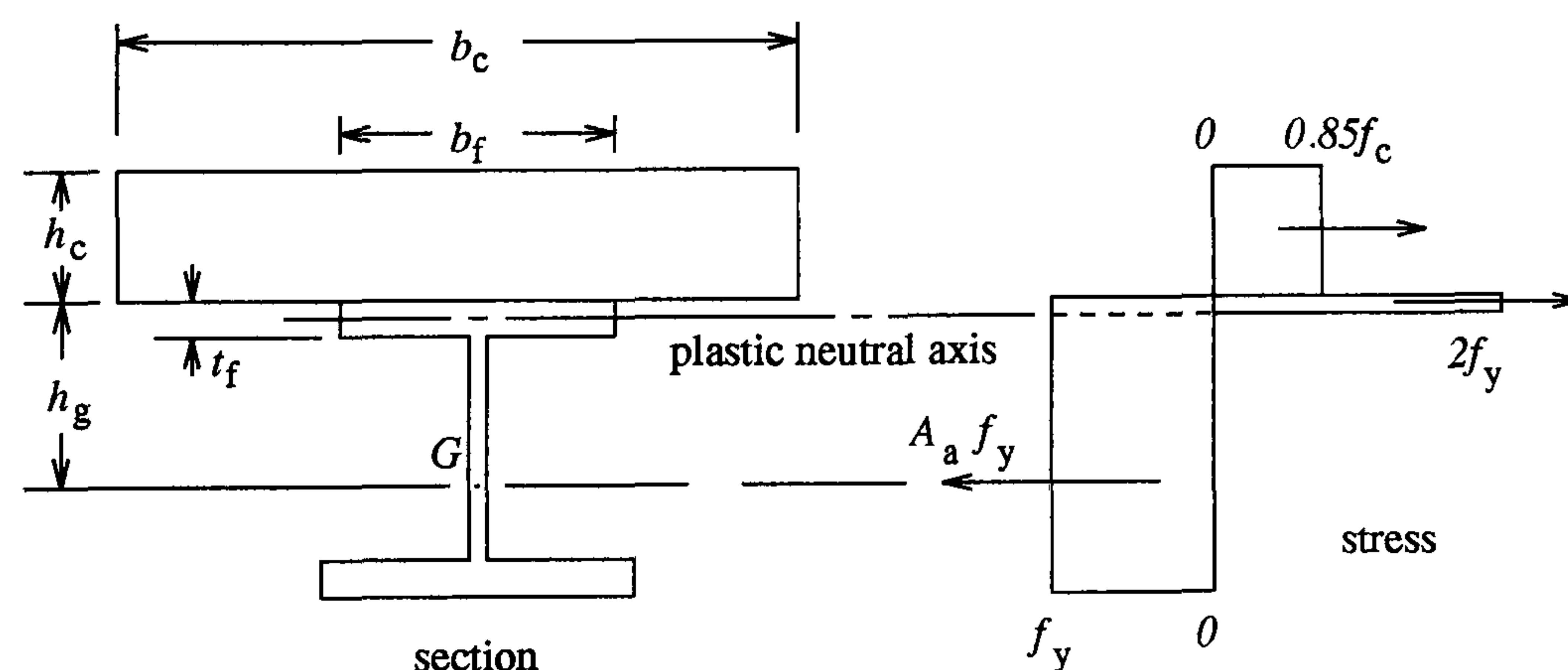


Figure C.2: Sagging bending of composite beams with full shear connection, plastic neutral axis in top steel flange

Usually, the thickness of steel flange, t_f , is much smaller than the dimension h_g , which makes the last term of equation (C.5) negligible, so, the resistance function may normally be simplified to

$$r_t = g_R(\underline{X}) = A_a f_y h_g + 0.425 b_c h_c^2 f_c \quad (\text{C.6})$$

According to (C.6), coefficient of variation of r_t can be given as

$$V_{r_t} = \frac{\sqrt{\bar{r}_1^2 V_{r_1}^2 + \bar{r}_2^2 V_{r_2}^2}}{\bar{r}_1 + \bar{r}_2} \quad (\text{C.7})$$

where

$$\left. \begin{aligned} \bar{r}_1 &= \bar{A}_a \bar{f}_y \bar{h}_g & V_{r_1} &= \sqrt{V_{A_a}^2 + V_{f_y}^2 + V_{h_g}^2} \\ \bar{r}_2 &= 0.425 \bar{b}_c \bar{h}_c^2 \bar{f}_c & V_{r_2} &= \sqrt{V_{b_c}^2 + 4V_{h_c}^2 + V_{f_c}^2} \end{aligned} \right\} \quad (\text{C.8})$$

C.2.2 Sagging bending with plastic neutral axis in steel web

As shown in Figure C.3, the resistance function is [61]:

$$r_t = g_R(\underline{X}) = W_a f_y + 0.85 b_c h_c f_c \left(\frac{h_c}{2} + h_{na} - \frac{0.85 b_c h_c f_c}{4 t_w f_y} \right) \quad (\text{C.9})$$

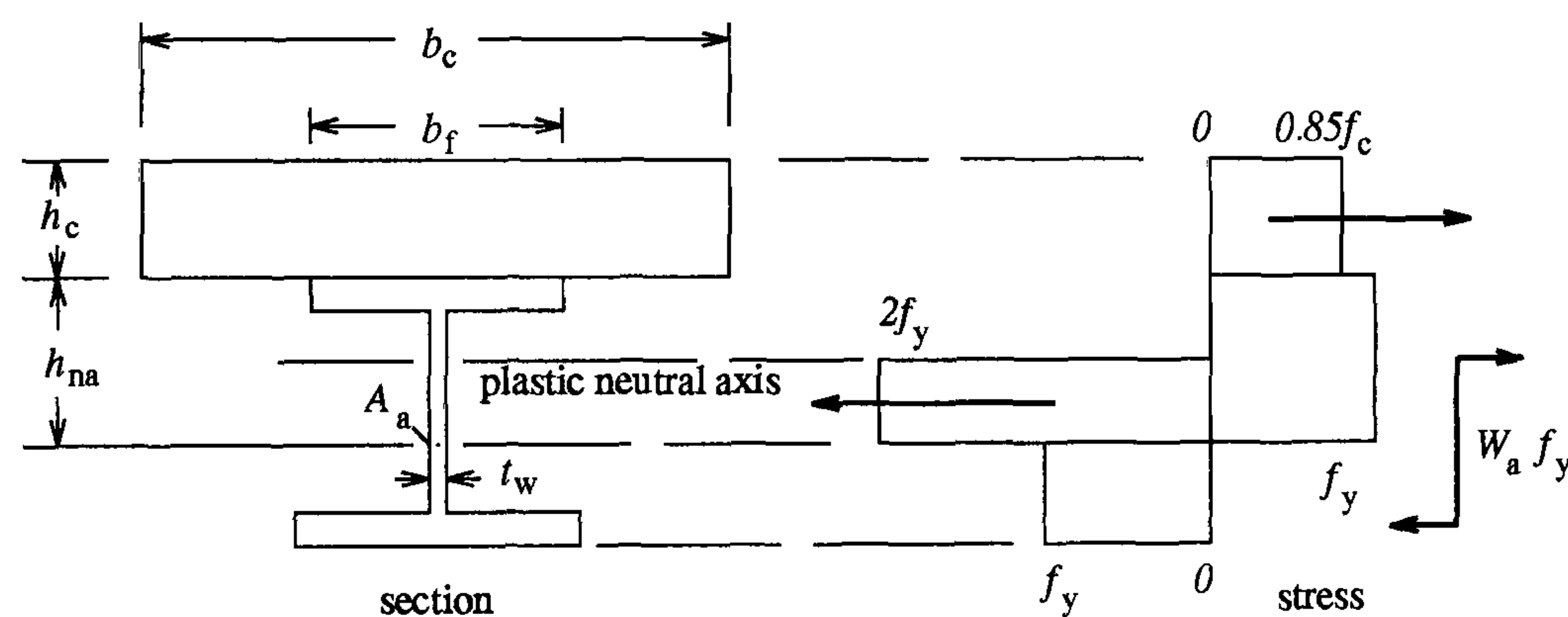


Figure C.3: Sagging bending of composite beams with full shear connection, plastic neutral axis in steel web

From equation (2.28), V_{r_t} for the resistance function (C.9) can be determined as

$$\begin{aligned} V_{r_t} &= [(\bar{r}_1 \bar{r}_2)^2 V_{r_1}^2 + (\bar{r}_1 \bar{r}_2 - \bar{r}_8)^2 V_{r_2}^2 + (0.5 \bar{r}_3 \bar{r}_4^2 + \bar{r}_7 + 2 \bar{r}_8)^2 V_{r_3}^2 \\ &\quad + (\bar{r}_3 \bar{r}_4^2 + \bar{r}_7 + 2 \bar{r}_8)^2 V_{r_4}^2 + \bar{r}_7^2 V_{r_5}^2 \\ &\quad + \bar{r}_8^2 V_{r_6}^2]^{\frac{1}{2}} / [\bar{r}_1 \bar{r}_2 + \bar{r}_3 \bar{r}_4 (0.5 \bar{r}_4 + \bar{r}_5 + \bar{r}_3 \bar{r}_4 \bar{r}_6 / \bar{r}_2)] \end{aligned} \quad (\text{C.10})$$

where

$$\left. \begin{aligned}
 \bar{r}_1 &= \bar{W}_a & V_{r1} &= V_{W_a} \\
 \bar{r}_2 &= \bar{f}_y & V_{r2} &= V_{f_y} \\
 \bar{r}_3 &= 0.85\bar{b}_c\bar{f}_c & V_{r3} &= \sqrt{V_{b_c}^2 + V_{f_c}^2} \\
 \bar{r}_4 &= \bar{h}_c & V_{r4} &= V_{h_c} \\
 \bar{r}_5 &= \bar{h}_{na} & V_{r5} &= V_{h_{na}} \\
 \bar{r}_6 &= -0.25\bar{t}_w & V_{r6} &= V_{t_w}
 \end{aligned} \right\} \quad (C.11)$$

and

$$\left. \begin{aligned}
 \bar{r}_7 &= \bar{r}_3\bar{r}_4\bar{r}_5 \\
 \bar{r}_8 &= \bar{r}_3^2\bar{r}_4^2\bar{r}_6/\bar{r}_2
 \end{aligned} \right\} \quad (C.12)$$

C.2.3 Hogging bending with plastic neutral axis in the steel top flange

Figure C.4 shows the stress distribution for the plastic hogging bending concerned here. According to simple plastic theory [61], the resistance function can be written as

$$r_t = g_R(\underline{X}) = A_a f_y h_g + A_s f_s h_s - \frac{(A_a f_y - A_s f_s)^2}{4 f_y b_f} \quad (C.13)$$

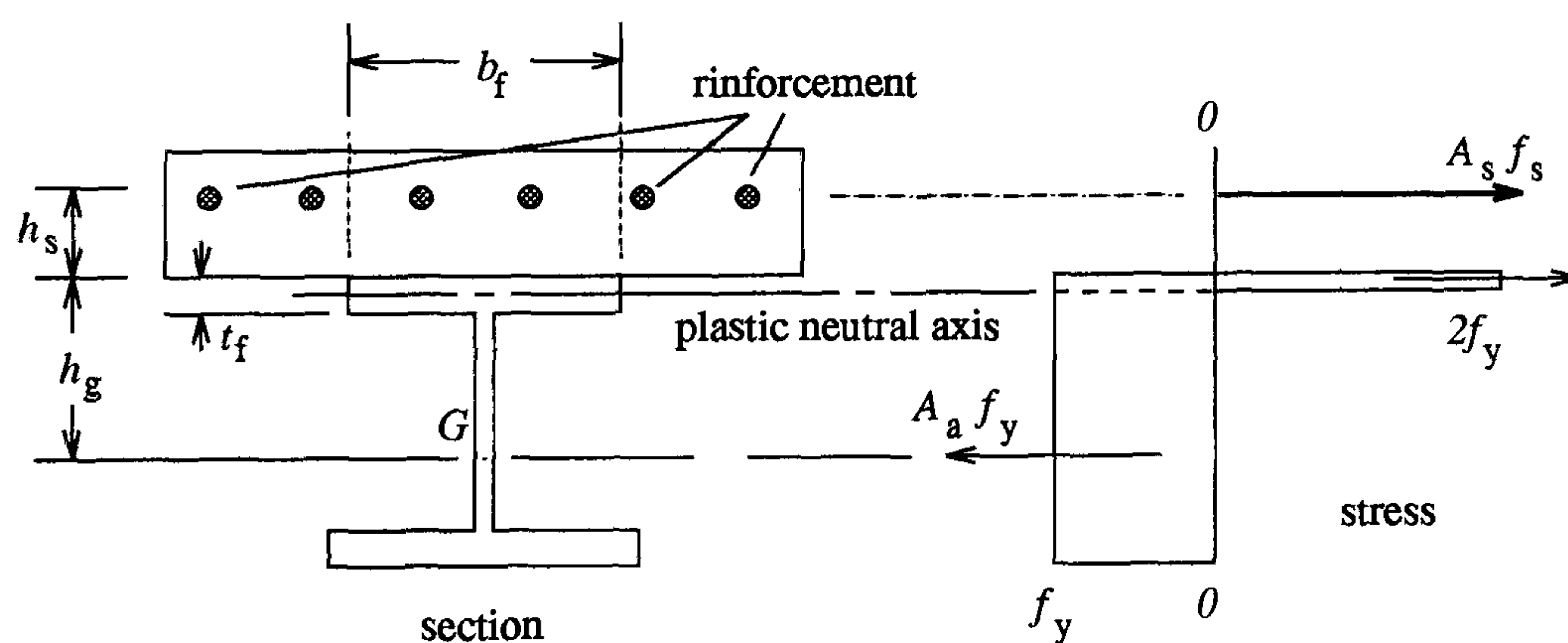


Figure C.4: Hogging bending of composite beams with full shear connection, plastic neutral axis in steel top flange

Compared with dimensions h_g , the thickness of steel flange, t_f , is normally so small that the last term in the resistance function can be neglected. Therefore,

(C.13) may be simplified as

$$r_t = g_R(\underline{X}) = A_a f_y h_g + A_s f_s h_s \quad (\text{C.14})$$

which gives

$$V_{r_t} = \frac{\sqrt{\bar{r}_1^2 V_{r_1}^2 + \bar{r}_2^2 V_{r_2}^2}}{\bar{r}_1 + \bar{r}_2} \quad (\text{C.15})$$

where

$$\left. \begin{aligned} \bar{r}_1 &= \bar{A}_a \bar{f}_y \bar{h}_g & V_{r_1} &= \sqrt{V_{A_a}^2 + V_{f_y}^2 + V_{h_g}^2} \\ \bar{r}_2 &= \bar{A}_s \bar{f}_s \bar{h}_s & V_{r_2} &= \sqrt{V_{A_s}^2 + V_{f_s}^2 + V_{h_s}^2} \end{aligned} \right\} \quad (\text{C.16})$$

C.3 Beams with ductile partial shear connection (group C)

As shown in Figure 3.3, two theoretical models, equilibrium method and linear interpolation, for plastic bending resistances of beams represented by group C have been used in practice [1,16]. The resistance functions from these models and the coefficients of variation of the theoretical resistances are now given.

C.3.1 Equilibrium method (second neutral axis in the steel top flange)

According to the plastic theory [1,16], there are two neutral axes in the composite section, the first neutral axis within concrete slab and the second in the steel section.

When the second neutral axis lies in the steel top flange, as shown in Figure 3.3, the equilibrium conditions lead to the theoretical resistance as

$$r_t = g_R(\underline{X}) = A_a f_y h_g + N P_R \left(h_c - \frac{N P_R}{1.7 b_c f_c} \right) - \frac{(A_a f_y - N P_R)^2}{4 b_f f_y} \quad (\text{C.17})$$

where, P_R for this study is given by equation (3.12).

Therefore, using equation (2.28), the coefficient of variation V_{r_t} for this resis-

tance function can be obtained as follows,

$$V_{Rt} = \frac{\sqrt{Q_{A_a}^2 + Q_{f_y}^2 + Q_d^2 + Q_{h_g}^2 + Q_{E_c}^2 + Q_{f_c}^2 + Q_{h_c}^2 + Q_{b_c}^2 + Q_{b_f}^2}}{1 + z_1 z_3 (1 - 0.5 z_2) - z_4 (1 - z_1)^2} \quad (C.18)$$

where

$$\left. \begin{aligned} \bar{P}_R &= 0.29 \alpha k d^2 \sqrt{\bar{E}_c \bar{f}_c} \\ z_1 &= (N \bar{P}_R) / (\bar{A}_a \bar{f}_y) \\ z_2 &= (N \bar{P}_R) / (0.85 \bar{f}_c \bar{b}_c \bar{h}_c) \\ z_3 &= \bar{h}_c / \bar{h}_g \\ z_4 &= \bar{A}_a / (4 \bar{b}_f \bar{h}_g) \end{aligned} \right\} \quad (C.19)$$

and

$$\left. \begin{aligned} Q_{A_a} &= [1 - 2z_4(1 - z_1)] V_{A_a} \\ Q_{f_y} &= [1 - z_4(1 - z_1^2)] V_{f_y} \\ Q_d &= 2z_1 [z_3(1 - z_2) + 2z_4(1 - z_1)] V_d \\ Q_{h_g} &= V_{h_g} \\ Q_{E_c} &= z_1 [z_3(1 - z_2)/2 + z_4(1 - z_1)] V_{E_c} \\ Q_{f_c} &= z_1 [z_3/2 + z_4(1 - z_1)] V_{f_c} \\ Q_{h_c} &= z_1 z_3 V_{h_c} \\ Q_{b_c} &= (z_1 z_2 z_3 / 2) V_{b_c} \\ Q_{b_f} &= z_4 (1 - z_1)^2 V_{b_f} \end{aligned} \right\} \quad (C.20)$$

C.3.2 Equilibrium method (second neutral axis in steel web)

When the second neutral axis is in the steel web, as shown in Figure C.5, the resistance function based on the equilibrium method can be written

$$r_t = g_R(\underline{X}) = W_a f_y + N P_R (h_{na} + h_c) - N P_R \left(\frac{N P_R}{4 t_w f_y} + \frac{N P_R}{1.7 b_c f_c} \right) \quad (C.21)$$

where, P_R is given by equation (3.12) and W_a is the plastic modulus of the steel

section.

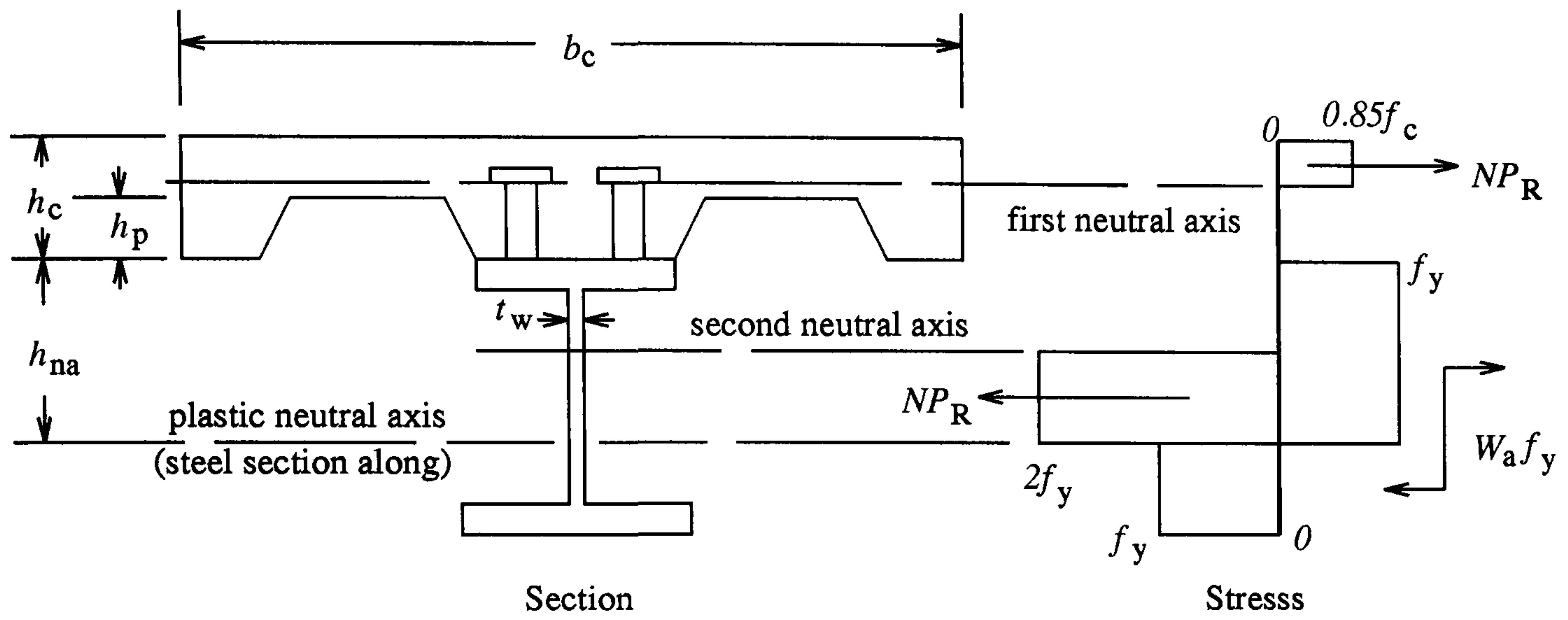


Figure C.5: Sagging bending of composite beams with ductile partial shear connection, second neutral axis in steel web

Applying equation (2.28), it yields

$$V_{Rt} = \frac{\sqrt{Q_{W_a}^2 + Q_{f_y}^2 + Q_{h_{na}}^2 + Q_{E_c}^2 + Q_{f_c}^2 + Q_{h_c}^2 + Q_d^2 + Q_{b_c}^2 + Q_{t_w}^2}}{1 + 2z_1(1 + z_3 - z_4 - z_2z_3/2)} \quad (C.22)$$

where, \bar{P}_R and z_2 are given in equation (C.19), and

$$\left. \begin{aligned} Q_{W_a} &= V_{W_a} \\ Q_{f_y} &= (1 + 2z_1z_4)V_{f_y} \\ Q_{h_{na}} &= 2z_1V_{h_{na}} \\ Q_{E_c} &= z_1(1 + z_3 - 2z_4 - z_2z_3)V_{E_c} \\ Q_{f_c} &= z_1(1 + z_3 - 2z_4)V_{f_c} \\ Q_{h_c} &= 2z_1z_3V_{h_c} \\ Q_d &= 4z_1(1 + z_3 - 2z_4 - z_2z_3)V_d \\ Q_{b_c} &= z_1z_2z_3V_{b_c} \\ Q_{t_w} &= 2z_1z_4V_{t_w} \end{aligned} \right\} \quad (C.23)$$

with

$$\left. \begin{aligned} z_1 &= (N\bar{P}_R\bar{h}_{na})/(2\bar{W}_a\bar{f}_y) \\ z_3 &= \bar{h}_c/\bar{h}_{na} \\ z_4 &= (N\bar{P}_R)/(4\bar{t}_w\bar{h}_{na}\bar{f}_y) \end{aligned} \right\} \quad (\text{C.24})$$

C.3.3 Linear interpolation (plastic neutral axis for $M_{pl,R}$ in concrete slab)

According to Eurocode 4 [1], a more conservative method, linear interpolation, may be used to predict the plastic bending resistances for beams with ductile shear connection. This method can be presented by the straight line AC in Figure 3.3. Hence, the resistance function based on the linear interpolation method can be generally expressed as

$$r_t = g_R(\underline{X}) = M_{apl} + \frac{N}{N_f}(M_{pl,R} - M_{apl}) \quad (\text{C.25})$$

where

$M_{pl,R}$ is the plastic bending resistance predicted by assuming full shear connection;

N_f is the number of shear connectors required in the shear span to fulfill the full shear connection, given by equation (3.10);

N is the number of shear connectors provided;

M_{apl} is the plastic bending resistance of the steel beam alone, to be determined as

$$M_{apl} = W_a f_y \quad (\text{C.26})$$

When the neutral axis for $M_{pl,R}$ lies in the concrete slab, $M_{pl,R}$ is given by equation (3.2), and, from equation (3.10),

$$\frac{N}{N_f} = \frac{N P_R}{A_a f_y} \quad (\text{C.27})$$

Therefore, equation (C.25) becomes

$$r_t = g_R(\underline{X}) = W_a f_y + N P_R \left(h_g + h_c - \frac{A_a f_y}{1.7 b_c f_c} - \frac{W_a}{A_a} \right) \quad (\text{C.28})$$

With respect to P_R given by (3.2), the coefficient of variation V_{r_t} for equation (C.28) is derived as follows,

$$V_{r_t} = \frac{\sqrt{Q_{W_a}^2 + Q_{f_y}^2 + Q_{A_a}^2 + Q_{h_g}^2 + Q_{h_c}^2 + Q_d^2 + Q_{E_c}^2 + Q_{f_c}^2 + Q_{b_c}^2}}{1 + v_1 [2z_1(1 + z_3) - v_2 z_1 z_3(1 - z_4) - 1]} \quad (\text{C.29})$$

where,

$$\left. \begin{aligned} Q_{W_a} &= (1 - v_1) V_{W_a} \\ Q_{A_a} &= v_1 [1 - v_2 z_1 z_3 (1 - z_4)] V_{A_a} \\ Q_{f_y} &= [1 - v_1 v_2 z_1 z_3 (1 - z_4)] V_{f_y} \\ Q_{h_g} &= 2v_1 z_1 V_{h_g} \\ Q_{h_c} &= 2v_1 z_1 z_3 V_{h_c} \\ Q_d &= 2v_1 [2z_1(1 + z_3) - v_2 z_1 z_3(1 - z_4) - 1] V_d \\ Q_{E_c} &= 0.5v_1 [2z_1(1 + z_3) - v_2 z_1 z_3(1 - z_4) - 1] V_{E_c} \\ Q_{f_c} &= 0.5v_1 [2z_1(1 + z_3) + v_2 z_1 z_3(1 - z_4) - 1] V_{f_c} \\ Q_{b_c} &= v_1 v_2 z_1 z_3 (1 - z_4) V_{b_c} \end{aligned} \right\} \quad (\text{C.30})$$

$$\left. \begin{aligned} v_1 &= (N \bar{P}_R) / (\bar{A}_a \bar{f}_y) \\ v_2 &= (\bar{A}_a \bar{f}_y) / [0.85 \bar{b}_c (\bar{h}_c - \bar{h}_p) \bar{f}_c] \\ z_1 &= (\bar{A}_a \bar{h}_g) / (2\bar{W}_a) \\ z_3 &= \bar{h}_c / \bar{h}_g \\ z_4 &= \bar{h}_p / \bar{h}_c \end{aligned} \right\} \quad (\text{C.31})$$

In the above equations, \bar{P}_R is still given by (C.19).

C.3.4 Linear interpolation (plastic neutral axis for $M_{pl,R}$ in the top steel flange)

In this case, the degree of shear connection N/N_f should be given by

$$\frac{N}{N_f} = \frac{NP_R}{0.85b_c(h_c - h_p)f_c} \quad (\text{C.32})$$

and $M_{pl,R}$ is determined from equation (C.5). So the resistance function (C.25) is specified here as

$$r_t = g_R(\underline{X}) = W_a f_y + \frac{NP_R}{0.85b_c(h_c - h_p)f_c} [A_a f_y h_g + 0.425b_c f_c (h_c^2 - h_p^2)] - \frac{[A_a f_y - 0.85b_c f_c (h_c - h_p)]^2}{4b_f f_y} \quad (\text{C.33})$$

Expressing P_R by equation (3.12), V_{rt} for resistance function (C.33) can be found out as

$$V_{rt} = \frac{\sqrt{Q_{W_a}^2 + Q_{A_a}^2 + Q_{f_y}^2 + Q_{h_g}^2 + Q_d^2 + Q_{E_c}^2 + Q_{f_c}^2 + Q_{b_c}^2 + Q_{h_c}^2 + Q_{b_f}^2}}{1 + v_1[2z_1 + v_2 z_1 z_3 (1 + z_4) - z_1 z_2 (1 - v_2)^2 - 1]} \quad (\text{C.34})$$

where

$$\left. \begin{aligned} Q_{W_a} &= (1 - v_1)V_{W_a} \\ Q_{A_a} &= 2z_1 v_1 [1 - z_2 (1 - v_2)]V_{A_a} \\ Q_{f_y} &= \{1 + v_1[2z_1 - z_1 z_2 (1 - v_2^2) - 1]\}V_{f_y} \\ Q_{h_g} &= 2v_1 z_1 V_{h_g} \\ Q_d &= 2v_1 [2z_1 + v_2 z_1 z_3 (1 + z_4) - z_1 z_2 (1 - v_2)^2 - 1]V_d \\ Q_{E_c} &= 0.5v_1 [2z_1 + v_2 z_1 z_3 (1 + z_4) - z_1 z_2 (1 - v_2)^2 - 1]V_{E_c} \\ Q_{f_c} &= 0.5v_1 [v_2 z_1 z_3 (1 + z_4) - 2z_1 + 1 + z_1 z_2 (1 + 2v_2 - 3v_2^2)]V_{f_c} \\ Q_{b_c} &= v_1 [z_1 z_2 (1 - v_2)^2 + 2z_1 z_2 v_2 (1 - v_2) - 2z_1 + 1]V_{b_c} \\ Q_{h_c} &= v_1 \{z_1 z_3 v_2 + [z_1 z_2 (1 - v_2^2) + 1 - 2z_1] / (1 - z_4)\}V_{h_c} \\ Q_{b_f} &= v_1 z_1 z_2 (1 - v_2)^2 V_{b_f} \end{aligned} \right\} \quad (\text{C.35})$$

$$\left. \begin{aligned} v_1 &= (NP_R) / [0.85\bar{b}_c(\bar{h}_c - \bar{h}_p)\bar{f}_c] \\ v_2 &= [(0.85\bar{b}_c(\bar{h}_c - \bar{h}_p)\bar{f}_c) / (\bar{A}_a \bar{f}_y)] \\ z_2 &= \bar{A}_a / (2\bar{b}_f \bar{h}_g) \end{aligned} \right\} \quad (\text{C.36})$$

and \bar{P}_R is determined from (C.19); z_1 , z_3 and z_4 are same as those in equation (C.31).

C.3.5 Linear interpolation (plastic neutral axis for $M_{pl,R}$ in steel web)

In this situation, the degree of shear connection is determined by equation (C.32), and $M_{pl,R}$ from equation (C.9). Then, the resistance function (C.25) becomes

$$r_t = g_R(\underline{X}) = W_a f_y + N P_R \left[\frac{h_c + h_p}{2} + h_{na} - \frac{0.85 b_c (h_c - h_p) f_c}{4 t_w f_y} \right] \quad (C.37)$$

Letting P_R be given by equation (3.12), it can be derived that

$$V_{rt} = \frac{\sqrt{Q_{W_a}^2 + Q_{f_y}^2 + Q_{f_c}^2 + Q_d^2 + Q_{E_c}^2 + Q_{h_c}^2 + Q_{b_c}^2 + Q_{h_{na}}^2 + Q_{t_w}^2}}{1 + v_1 v_2 z_1 [2 + z_3 (1 + z_4) - z_2 v_2]} \quad (C.38)$$

where

$$\left. \begin{aligned} Q_{W_a} &= V_{W_a} \\ Q_{f_y} &= (1 + v_1 v_2^2 z_1 z_2) V_{f_y} \\ Q_d &= 2 v_1 v_2 z_1 [2 + z_3 (1 + z_4) - v_2 z_2] V_d \\ Q_{E_c} &= 0.5 v_1 v_2 z_1 [2 + z_3 (1 + z_4) - v_2 z_2] V_{E_c} \\ Q_{f_c} &= 0.5 v_1 v_2 z_1 [2 + z_3 (1 + z_4) - 3 v_2 z_2] V_{f_c} \\ Q_{h_c} &= v_1 v_2 z_1 [z_3 - v_2 z_2 / (1 - z_4)] V_{h_c} \\ Q_{b_c} &= -v_1 v_2^2 z_1 z_2 V_{b_c} \\ Q_{t_w} &= v_1 v_2^2 z_1 z_2 V_{t_w} \\ Q_{h_{na}} &= 2 v_1 v_2 z_1 V_{h_{na}} \end{aligned} \right\} \quad (C.39)$$

$$\left. \begin{aligned} z_1 &= (\bar{A}_a \bar{h}_{na}) / (2 \bar{W}_a) \\ z_2 &= \bar{A}_a / (2 \bar{t}_w \bar{h}_{na}) \\ z_3 &= \bar{h}_c / \bar{h}_{na} \end{aligned} \right\} \quad (C.40)$$

and \bar{P}_R is given by (C.19); v_1 and v_2 are defined in (C.36), and z_4 in (C.31).

Appendix D

Computer programs of safety calibration for composite beams

According to the theories presented in Chapters 2 and 3, the computer programs for the calculations relevant to the calibrations have been written. They are all in Sun FORTRAN (FORTRAN 77 on SUN Unix machines) and now explained.

D.1 Program for composite beams with full shear connection

D.1.1 Scope of program

This program, named *sacb*, is developed to determine partial safety factors for design plastic bending resistances of composite beams with full shear connection, i.e. for beams represented by test groups A and B (see Section 3.1.2). At present, *sacb* can deal with following cases:

- (1) sagging bending with the plastic neutral axis in the concrete slab;
- (2) hogging bending with the plastic neutral axis in the steel web, where the steel beam can have either a symmetric section or a symmetric section attached by a plate to the bottom flange, as shown in Figure D.1.

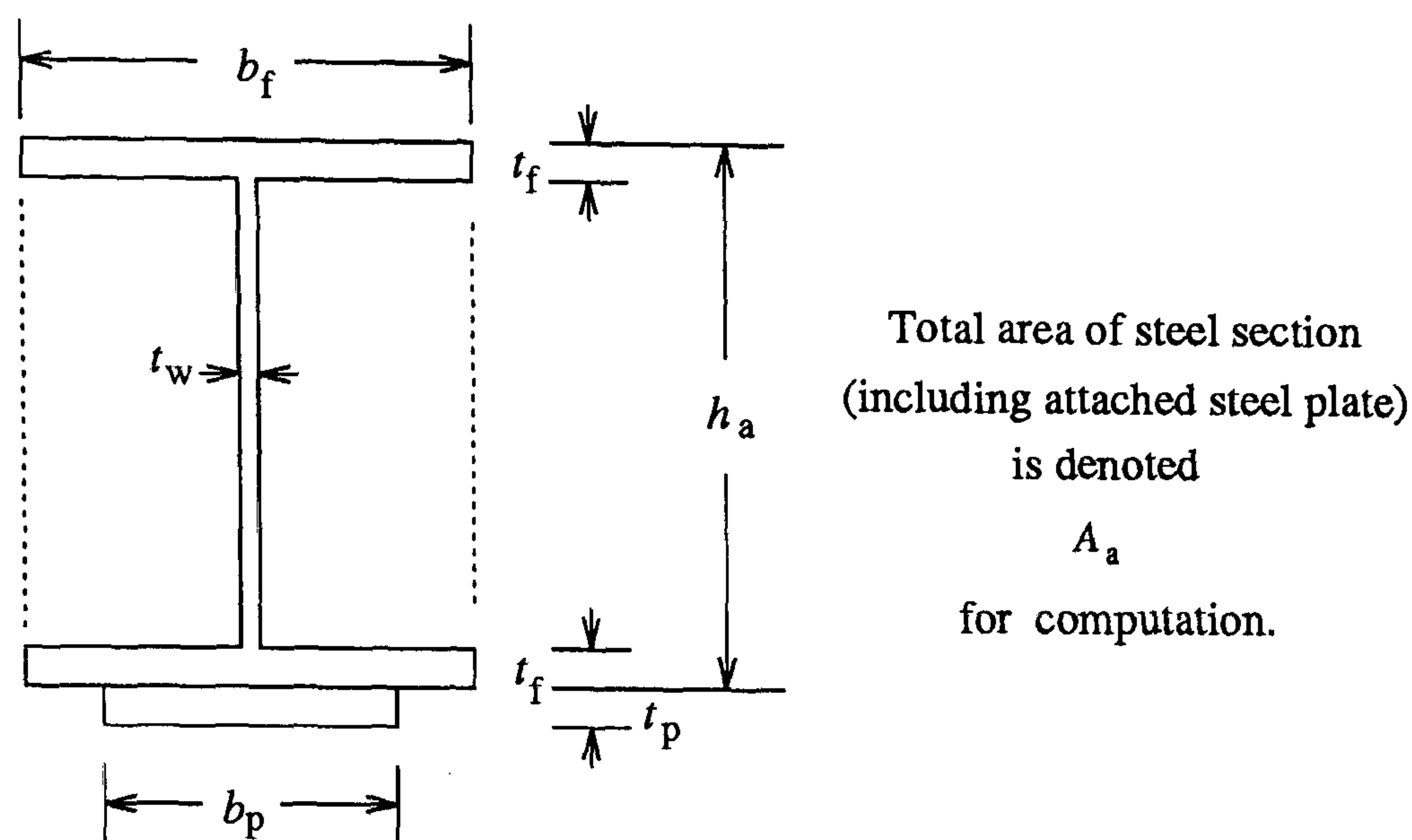


Figure D.1: Steel section considered by program *sacb* for hogging bending

The main outputs of *sacb* include:

- (1) the test corrections, \bar{b} and v_δ , and the correlation coefficient of real (experimental) resistances and the theoretical resistances, ρ (as defined by equation (2.20));
- (2) coefficients of variation of the resistance, v_{r_t} , v_r , $\sigma_{\ln r_t}$ and $\sigma_{\ln r}$ for each beam sample from the test group;
- (3) mean theoretical resistance, \bar{r}_t and the target design resistance r_d for each of the beam samples;
- (4) target design fractile-factor, k_d , (corresponding to $P_f = 0.0012$), and safety factors, γ_{md} , γ_a , γ_c or γ_s for each of the beam samples.

As required by equations (2.20), (2.25) and (2.26), to determine \bar{b} , v_δ and ρ , from a group of n_n specimens, the values of both r_{ei} and r_{ti} for specimen i ($i = 1, \dots, n_n$) should be known by program *sacb*. So to complete the calibration, some ready-made packages need to be used to find r_{ti} for each of the specimens. In the calibration which has been done, the ready-made program *EP-PCB1* (R.P. Johnson, made in 1984 and revised in 1990) has been used. For using of *EP-PCB1*, Johnson has written two notes, which, together with the source program

of *EPPCB1* and its input data file *csdat* for each specimen are given at the end of this appendix.

To run program *sacb*, type the following command in UNIX system:

```
[%] sacb <return>
```

where, [%] represents the prompt sign given by UNIX system, <return> means pressing return-key on the keyboard.

Once *sacb* starts, the user can follow the prompts shown on the screen to type in date and fractile-factor of characteristic steel strength, k_{as} . As the programs are designed based on the concepts given in Chapters 2 and 3, k_{as} should be taken not greater than 3.04 (see Section 2.2.3); in the calculations which have been done, $k_{as} = 2.00$ is used.

For convenience in computation, Table (A.1) has been established in the program.

D.1.2 Function of subroutines

Similar to most Fortran programs, *sacb* consists of several subroutines. Their functions are listed below.

1. Subroutine *cmce*(nn, cmv, cvoe, cc) — calculate \bar{b} , V_δ and ρ .
2. Subroutine *fcvs*(n, conb, cvoe, rtm, rtn) — find the coefficients of variation for the beam samples, V_{rt} , V_r and σ_{lrr} , and the resistance based on the γ_{mp} -altered strengths of materials (see equation(2.45)).
3. Subroutine *dsis*(n, cvoe, skd) — determine the design fractile-factor, k_d , corresponding to failure probability $P_f = 0.0012$, for the samples;
4. Subroutine *esfs*(n, rd, rtn, conb, sk) — evaluate the safety factors for the samples.

D.1.3 Definition of main variables

The main simple variables are defined in *sacb* as follows,

| | |
|-----------------|--|
| nn | the number of specimens used for calculating \bar{b} , v_δ and ρ ; |
| n | the number of beam samples to be analyzed; |
| $cmv, cvoe, cc$ | \bar{b} , V_δ and ρ respectively; |
| vaa, vw, vfy | v_{A_a} , V_{W_a} and v_{f_y} , respectively; |
| lds | coefficient of variation of linear dimension of steel section; |
| vhc, vbc, vfc | v_{h_c} , v_{b_c} and v_{f_c} , respectively; |
| var, vhr, vfr | v_{A_s} , v_{h_s} and v_{f_s} , respectively. |

The main arrays in *sacb* are as follows,

| | |
|-----------------------------|--|
| $es(1) \dots es(nn)$ | experimental bending resistances of the specimens, r_{ei} ($i = 1, \dots, nn$); |
| $ts(1) \dots ts(nn)$ | theoretical bending resistances of the specimens, r_{ti} , ($i = 1, \dots, nn$); |
| $bnum(1) \dots bnum(n)$ | (character array, length = 10) names of beam samples; |
| $bds(1,1) \dots bds(n,1)$ | \bar{A}_a of beam samples (sagging); |
| $bds(1,2) \dots bds(n,2)$ | \bar{f}_y of beam samples (sagging); |
| $bds(1,3) \dots bds(n,3)$ | \bar{h}_g of beam samples (sagging); |
| $bds(1,4) \dots bds(n,4)$ | \bar{h}_c of beam samples (sagging); |
| $bds(1,5) \dots bds(n,5)$ | \bar{b}_c of beam samples (sagging); |
| $bds(1,6) \dots bds(n,6)$ | \bar{f}_c of beam samples (sagging); |
| $bds(1,7) \dots bds(n,7)$ | \bar{t}_w of beam samples (sagging); |
| $bds(1,8) \dots bds(n,8)$ | \bar{t}_f of beam samples (sagging); |
| $bds(1,9) \dots bds(n,9)$ | \bar{b}_f of beam samples (sagging); |
| $bds(1,10) \dots bds(n,10)$ | \bar{h}_p of beam samples (sagging); |

| | |
|--|---|
| $bdh(1,1) \dots bdh(n,1)$ | \bar{A}_r of beam samples (hogging); |
| $bdh(1,2) \dots bdh(n,2)$ | \bar{f}_y of beam samples (hogging); |
| $bdh(1,3) \dots bdh(n,3)$ | \bar{h}_a of beam samples (hogging); |
| $bdh(1,4) \dots bdh(n,4)$ | \bar{f}_s of beam samples (hogging); |
| $bdh(1,5) \dots bdh(n,5)$ | \bar{h}_s of beam samples (hogging); |
| $bdh(1,6) \dots bdh(n,6)$ | \bar{b}_f of beam samples (hogging); |
| $bdh(1,7) \dots bdh(n,7)$ | \bar{t}_w of beam samples (hogging); |
| $bdh(1,8) \dots bdh(n,8)$ | \bar{t}_f of beam samples (hogging); |
| $bdh(1,9) \dots bdh(n,9)$ | \bar{A}_a of beam samples (hogging); |
| $bdh(1,10) \dots bdh(n,10)$ | \bar{b}_p of beam samples (hogging); |
| $bdh(1,11) \dots bdh(n,11)$ | \bar{t}_p of beam samples (hogging); |
| $rd(i), rtm(i)$ ($i = 1, \dots, n$) | the target design resistance, r_d , and mean resistance, \bar{r}_t , of beam sample i , respectively; |
| $bata(1) \dots bata(n)$ | k_d of beam samples. |
| $cov(i,1), \dots, cov(i,4)$ ($i = 1, \dots, n$) | $v_{r_t}, \sqrt{\ln(1 + v_{r_t}^2)}, v_r$ and σ_{lnr} for beam sample i , respectively; |
| $gamma(i,1), gamma(i,2), gamma(i,3)$ ($i = 1, \dots, n$) | γ_{md}, γ_a and γ_c (for sagging) or γ_s (for hogging) of beam sample i , respectively; |

The maximum dimension of arrays in *sacb* is currently fixed as 55.

D.1.4 The layout of input file and output file

The input datafile in *sacb* is defined with name, *inod*, and the output file, *outoc*. The format of datafile *inod* for sagging bending is only very slightly different from that for hogging bending. These are as follows.

inod for sagging bending (beams in group A)

$nn, n, vaa, vfy, vds, vhc, vfc, cbc$

$bnum(1)$

$bds(1,1), bds(1,2), \dots bds(1,10)$

\vdots

$bnum(n)$

$bds(n,1), bds(n,2), \dots bds(n,10)$

$es(1), es(2), es(3), \dots es(nn)$

$ts(1), ts(2), ts(3), \dots ts(nn)$

$inod$ for hogging bending (beams in group B)

h

$nn, n, vw, vfy, vds, vfr, var, vhr, vaa$

$bnum(1)$

$bdh(1,1), bdh(1,2), \dots bdh(1,11)$

\vdots

$bnum(n)$

$bdh(n,1), bdh(n,2), \dots bdh(n,11)$

$es(1), es(2), es(3), \dots es(nn)$

$ts(1), ts(2), ts(3), \dots ts(nn)$

In above, the first entry s (for sagging) or h (for hogging) are not the variable names but just the characters. The units for data input to $es(i)$ and $ts(i)$ can be kN-m, and for the rest, the units based on N and mm should be used.

The output file is *outoc*, and it is quite self-explanatory. So only the notations for designating the entities of the tables in *outoc* are explained here.

- Under the title “*The measured resistance < KN-m >*”:
 - *Experimental result* — r_{ei} for each beam specimen;
 - *Theoretical result* — r_{ti} for each beam specimen;
 - *Ratio of expe. to theo.* — r_{ei}/r_{ti} ;
- Under the title “*The analyzed resistance < KN-m >*”:

- *Theoretical mean* — \bar{r}_t for beam samples;
 - *Design* — r_d for beam samples;
 - *Strength-altering* — r_t calculated from f_{yk}/γ_{ma} and f_{ck}/γ_{mc} OR f_{sk}/γ_{ms} , for beam samples;
- Under the title “*The relevant c.v. of bending resistance*”:
 - *Theory* — V_{rt} ;
 - *Log-theory* — $\sqrt{\ln(1 + V_{rt}^2)}$;
 - *Reality* — $V_r (= \sqrt{V_{rt}^2 + V_\delta^2})$;
 - *Log-reality* — σ_{lnr} ;
 - Under the title “*The safety factors and indices*”:
 - *Safety index* — k_d ((found according to $P_f = 0.0012$));
 - *S.F-model* — γ_{md} (from k_d);
 - *S.F-steel* — γ_a (from γ_{md});
 - *S.F-concrete* — γ_c (from γ_{md});
 - *S.F-reinforcement* — γ_s (from γ_{md});
 - Under the title “*Beam Data (N, mm)*”:
 - $A_r, f_y, h_a, f_r, h_r, b_a, t_w, t_f, A_a, h_g, h_c, b_c, f_c$ — $\bar{A}_s, \bar{f}_y, \bar{h}_a, \bar{f}_s, \bar{h}_s, \bar{b}_f, \bar{t}_w, \bar{t}_f, \bar{A}_a, \bar{h}_g, \bar{h}_c, \bar{b}_c$ and \bar{f}_c , respectively.

D.2 Program for beams with ductile partial shear connection

D.2.1 Scope of program

The program is developed to analyse reliability of bending resistances of beams with ductile partial shear connection (beams in group C, see Section 3.1.2.), and

consists of two independent packages, one named *ctc* and the other *crb*.

Currently, all the test specimens collected in group C are of the steel beams with symmetrical sections, therefore, the program is coded only for the situation in which the steel section is symmetrical about both axes.

To implement the computation by this program, the packages *ctc* and *crb* need to be executed jointly. In the UNIX system, a supervision package, named *rcc*, should be created to run *ctc* and *crb*. This supervision package has been coded by C-Shell Scripts and will be given later. As a result, to run *ctc* and *crb* properly, only the following command needs to be issued to Unix:

```
[%] sh rcc <return>
```

During running of the program, the prompts shown on the screen are very easy to follow, and no further explanation is needed.

From a run, the program will give the calibration results for the two models, equilibrium method and linear interpolation (see Figure 3.3). These results include

- theoretical resistance, r_{ti} , and experimental resistance, r_{ei} , of each specimen;
- the actual degree of shear connection and the lowest degree for ductile shear connection required by Eurocode 4 [1] for each specimen;
- the test corrections, \bar{b} and v_{δ} , and correlation coefficient of test and theory, ρ ;
- V_{rt} and V_r for each beam sample;
- the safety factors, γ_{md} , γ_a , γ_c and γ_v for each of the beam samples, determined from the design fractile-factor corresponding to $P_f = 0.0012$;
- for each beam sample, the design fractile-factors under two prescribed conditions: (1) $\gamma_a = 1.10$, $\gamma_c = 1.25$ and $\gamma_v = 1.25$; (2) $\gamma_a = 1.05$, $\gamma_c = 1.25$ and $\gamma_v = 1.25$;
- correspondingly, the failure probabilities under two prescribed conditions: (1) $\gamma_a = 1.10$, $\gamma_c = 1.25$ and $\gamma_v = 1.25$; (2) $\gamma_a = 1.05$, $\gamma_c = 1.25$ and

$$\gamma_v = 1.25.$$

D.2.2 Supervision package *rcc*

The supervision package, *rcc*, is as follows,

```
cp inodp0 inodp1
ctc
cat add >> inodp1
crb
cat outodp1 >> outodp
rm inodp1 outodp1 add
```

Datafile *inodp0* is originally created by the user, as explained later. To run the program, this file is first of all copied onto another temporary file, *inodp1*, which can then be recognized by package *crb*. Package *ctc* obtains the input data from the file named *inodp* which does not appear in *rcc*. Like *inodp0*, *inodp* needs to be established by the user.

After running, package *ctc* determines the parameters, \bar{b} , V_δ and ρ and the number of eligible specimens (i.e. the specimens with ductile shear connection). All these results are sent into a file named *add* which is then catenated to *inodp1* for package *crb*.

The results from *crb* are all stored in the temporary file, *outodp1*, and this file is finally appended to file *outodp* which is in advance created by *ctc* for holding the results from running of that package. Thus, to see the results of calibration, the user needs only to read *outodp*.

Since all the information has been held in files, *inodp0*, *inodp* and *outodp*, the files, *inodp1*, *add* and *outodp1*, become superfluous and are therefore removed from the directory.

D.2.3 Package *ctc*

The functions of this package include calculation of the theoretical resistance, r_{ti} , of each specimen, the degrees of shear connection and the test correction \bar{b} , V_δ and correlation coefficient ρ . Using this program, the user himself does not need to decide if a specimen has ductile or non-ductile shear connection; the program will make the classification according to Eurocode 4 [1].

The following subroutines are contained in the package.

1. Subroutine *cfr*(*nn, arg*) — calculates the theoretical resistance r_{ti} , the actual degree and the lowest degree required for ductile shear connection for the test specimens;
2. Subroutine *cmce*(*n, cmv, cvoe, cc, es, ts*) — calculates \bar{b} , V_δ and ρ .
3. Subroutine *bren*(*ts, es, re, rl, bdh, cps, bnum, nn, cmv, cc, cvoe, cmvl, cvoel, ccl*) — call subroutine *cmce* to calculate \bar{b} , V_δ and ρ for test groups with ductile and non-ductile partial shear connectors, respectively, and output all the calculated results.

The main simple variables in the program are defined as follows,

- | | |
|------------------|--|
| <i>nn</i> | total number of the test specimens; |
| <i>kn</i> | number of test specimens with non-ductile shear connection; |
| <i>jn</i> | number of test specimens with ductile shear connection; |
| <i>csc</i> | a control parameter; if r_{ei}/r_{ti} is smaller than it, the information of the specimen is considered as suspect and excluded from the analysis by the program; in the current analysis, the value of this variable is taken as 0.6; |
| <i>arg</i> | factor for determining the strength of a shear connector, P_R ; according to Eurocode 4 [1], this factor is to be taken as 0.29; |
| <i>cmv, cmvl</i> | \bar{b} for equilibrium method and linear interpolation, respectively; |

cvoe, *cvoel* V_s for equilibrium method and linear interpolation, respectively;
cc, *ccl* ρ for equilibrium method and linear interpolation, respectively.

The main arrays employed by *ctc* are explained below. It should be noted that the values of basic variables or the calculation results stored in these arrays are those achieved in accordance with assumption (3) in Section 2.2.1.

- *es(i)* — experimental resistance, r_{ei} , of specimen i , size = 100×1 .
- *ts(i)* — theoretical resistance, r_{ti} , of specimen i , size = 100×1 , this array is only used in subroutine *cmce*.
- *re(100,3)*, used for equilibrium method:
 - re(i,1)* — r_{ti} of specimen i .
 - re(i,2)* — depth of the second neutral axis of specimen i , measured from the top of steel section.
 - re(i,3)* — depth of the first neutral axis of specimen i .
- *rl(100,5)*:
 - rl(i,1)* — r_{ti} of specimen i by linear interpolation;
 - rl(i,2)* — actual degree of shear connection of specimen i ;
 - rl(i,3)* — depth of the neutral axis of specimen i , assuming full shear connection;
 - rl(i,4)* — ultimate plastic bending moment of specimen i , assuming full shear connection;
 - rl(i,5)* — bending resistance of steel beam alone, $W_a f_y$, of specimen i .
- *cps(100,9)*:
 - cps(i,1)* — b_c of specimen i ;
 - cps(i,2)* — h_c of specimen i ;
 - cps(i,3)* — h_p of specimen i ;
 - cps(i,4)* — b_0 of specimen i ;
 - cps(i,5)* — cylinder strength of concrete, f_c , of specimen i ;

$cps(i,6)$ — concrete density, W_c , of specimen i , in kN/m^3 ;

$cps(i,7)$ — span of specimen i , in metres.

$cps(i,8)$ — the lowest required degree for ductile shear connection for specimen i ;

$cps(i,9)$ — Young's modulus of concrete, E_c , of specimen i .

- $bdh(100,9)$:

$bdh(i,1)$ — d of studs or, when G is input to $bnum(i,2)$, the given ratio of shear connection in specimen i ;

$bdh(i,2)$ — f_y of specimen i ;

$bdh(i,3)$ — h_a of specimen i ;

$bdh(i,4)$ — stud strength, f_u , of specimen i ;

$bdh(i,5)$ — overall height of stud, h , of specimen i ;

$bdh(i,6)$ — b_f of specimen i ;

$bdh(i,7)$ — t_w of specimen i ;

$bdh(i,8)$ — t_f of specimen i ;

$bdh(i,9)$ — A_a , of specimen i .

- $bnum(100,3)$ (character array, string length = 10):

$bnum(i,1)$ — reference name of specimen i .

$bnum(i,2)$ — sheeting direction of specimen i , to be input: T if transverse, P if parallel, S if solid slab, G if ratio of shear connection is given directly;

$bnum(i,3)$ — the indicator of potential failure mode of shear connection in specimen i : *stud* if studs dominant or *concrete* if concrete dominant.

- $ns(100,2)$:

$ns(i,1)$ — total number of shear studs in the shear span specimen i ;

$ns(i,2)$ — number of studs per rib, N_p , of specimen i ; when the specimen is constructed with ribs transverse to the beam span, and, in the shear span, has N_{r1} ribs with one stud and N_{r2} with two studs, the input value of N_p

should be¹

$$N_p = \frac{(N_{r1} + 2N_{r2})^2}{(N_{r1} + \sqrt{2}N_{r2})^2} \quad (\text{D.1})$$

If specimen i has a solid slab or the parallel ribs, $ns(i, 2)$ is not used in the program, so it can be assigned any value.

The program also employs two more families of arrays. These arrays have the same significance as those introduced above, and they are defined in the program by simply adding one more character to, or changing the last character of the name of above arrays, i.e. adding “f” or changing the last character into “f” for beams with non-ductile shear connection, while “w” for ductile shear connectors. Thus, for example, $ref(100,3)$ and $rew(100,3)$ would have the same significance as $re(100,3)$, but $ref(100,3)$ is specially for specimens with non-ductile shear connectors only, while $rew(100,3)$ for ductile shear connectors only.

D.2.4 Package *crb*

Based on the results from ctc , \bar{b} , V_δ , etc., this program can, in theory, carry out the reliability analysis for any beam population. However, as the estimators of ctc , \bar{b} and V_δ , are only from a limited number of test specimens generally, the populations of beams to be calculated are usually restricted within those represented by the samples from the test specimens processed by ctc .

As for ctc , the users do not need to check whether or not the beam samples are with ductile shear connection. The program will exclude the samples whose

¹According to Eurocode 4 [1] (see equation (3.15)), if assuming the strength of one shear connector as P_R , then, for a transverse rib with two studs, the total strength of the shear connectors in this rib would be $\sqrt{2}P_R$. Therefore, for beams with transverse ribs, if there are N_{r1} ribs with one stud and N_{r2} with two studs in the shear span, then the total longitudinal shear resistance in the shear span should be

$$F_c = N_{r1}P_R + N_{r2}(\sqrt{2}P_R) = (N_{r1} + 2N_{r2})\frac{P_R}{\sqrt{N_p}}$$

where, $N_{r1} + 2N_{r2}$ is the total number of studs in the shear span and N_p is the average number of studs per rib, as given in equation (D.1). By such a conversion, equation (3.15) can be consistently used by the program.

degrees of shear connection are lower than a critical value specified by Eurocode 4 [1].

Apart from Table (A.1), two more ready-made tables are established in this package, which are

- (1) the table of standard normal distribution such that

$$P_p = 1 - P_f = \int_{-\infty}^{Z_{1-P_f}} \frac{1}{\sqrt{2\pi}} e^{-\frac{t^2}{2}} dt \quad (\text{D.2})$$

- (2) the table of non-central t -distribution with fractile-factor K ² against the probability P_f determined by Z_{1-P_f} from equation (D.2) at $\epsilon = 75\%$ ³.

This package is made for obtaining the partial safety factors, at target safety level $P_f = 0.0012$, and, inversely, the failure probabilities under two prescribed conditions: (1) $\gamma_a = 1.10$, $\gamma_c = 1.25$ and $\gamma_v = 1.25$; (2) $\gamma_a = 1.05$, $\gamma_c = 1.25$ and $\gamma_v = 1.25$.

Five subroutines and two function subprograms are included in *crb*.

- Subroutine *cfr(nn, arg)* — applies the equilibrium method and linear interpolation to calculate the mean theoretical resistances for each beam sample from the test group, using mean value of the basic variables.
- Subroutine *sfed(j, skd, bdhw, bnuw, rew, zw)* — conducts calibration for the beam samples with respect to the equilibrium method including finding V_{rt} and V_r , determining partial safety factors, γ_a , γ_c and γ_v , at target safety level $P_f = 0.0012$.

²The relationship between the K and the concerned fractile-factor k_b in the reliability analysis is $K = \sqrt{\frac{n}{n-1}} k_b$, where n is the number of test results used.

³According to Appendix A, it can be shown that Z_{1-P_f} is just $k_{d,\infty}$ in equation (2.57) and related to K at $\epsilon = 75\%$ as follows,

$$P\left\{\frac{t}{\sqrt{n-1}} \leq K\right\} = 0.75$$

where, t , as defined in equation (A.15), is the non-central t -distribution variable.

- Subroutine *sfld* (*j*, *skd*, *bdhw*, *bnuw*, *rew*, *zw*) — the same as *sfed* (*j*, *skd*, *bdhw*, *bnuw*, *rew*, *zw*) but based on linear interpolation.
- Subroutine *sfp* (*pf*, *er*, *df*, *vt*, *vd*, *n*, *bnu*, *el*, *sf*) — calculates the failure probability P_f underlying the design resistance with given partial safety factors.
- Subroutine *fmi*(*rr*, *da*, *fc*, *hg*, *hc*, *hp*, *tw*, *bf*, *bma*, *fs*, *ty*, *ra*, *rc*, *ru*) — calculates the bending resistance for the beam samples with linear interpolation, using the factored strengths of material and shear connectors, e.g. using γ_{mp} -altered strengths (see equation (2.45)).
- Function *pnt* (*x*, *n*) — determines P_f from k_b , according to the non-central *t*-distribution.
- Function *psn* (*p*) — obtains Z_{1-P_f} (i.e. $k_{d,\infty}$) from P_f , according to the standard normal distribution.

Many arrays in the package are defined in the same way as those in *ctc*. These arrays are listed as follows,

- *re*(100,3), *rew*(100,3), *ref*(100,3);
- *rl*(100,5), *rlw*(100,5), *rlf*(100,5);
- *cps*(100,9), *cpsw*(100,9), *cpsf*(100,9);
- *bdh*(100,9), *bdhw*(100,9), *bdhf*(100,9);
- *bnum*(100,3), *bnuw*(100,9), *bnuv*(100,9);
- *ns*(100,2).

These arrays are used in *crb* in the same way as in package *ctc*, except that

- (1) the entity for each element of these arrays is now for a beam sample, rather than a beam specimen;

- (2) the information stored in an element of these arrays, in concept, is that obtained from the mean values of basic variables of the beam samples, rather than the measured or intended values from a test specimen.

The other main arrays used in *crb* are as follows.

- $gaw(100,3)$, $galw(100,3)$ (for the equilibrium method and linear interpolation, respectively)
 $gaw(i,1)$, $galw(i,1)$ — the design fractile-factor corresponding to the target probability of failure $P_f = 0.0012$ for sample i ;
 $gaw(i,2)$, $galw(i,2)$ — the design fractile-factor of sample i , corresponding to $\gamma_a = 1.10$, $\gamma_c = 1.25$ and $\gamma_v = 1.25$;
 $gaw(i,3)$, $galw(i,3)$ — the design fractile-factor of sample i , corresponding to $\gamma_a = 1.05$, $\gamma_c = 1.25$ and $\gamma_v = 1.25$;
- $sfw(100,4)$, $sflw(100,4)$ (for the equilibrium method and linear interpolation, respectively)
 $sfw(i,1)$, $sflw(i,1)$ — model factor, γ_{md} , of sample i ;
 $sfw(i,2)$, $sflw(i,2)$ — γ_a of sample i ;
 $sfw(i,3)$, $sflw(i,3)$ — γ_c of sample i ;
 $sfw(i,4)$, $sflw(i,4)$ — γ_v of sample i ;
- $vrw(100,3)$, $vrlw(100,3)$ (for the equilibrium method and linear interpolation, respectively)
 $vrw(i,1)$, $vrlw(i,1)$ — V_{Rt} of sample i ;
 $vrw(i,2)$, $vrlw(i,2)$ — V_R of sample i ;
 $vrw(i,3)$, $vrlw(i,3)$ — σ_{lnr} of sample i .
- $pfw(100,3,2)$, $pflw(100,3,2)$ (for the equilibrium method and linear interpolation, respectively)
 $pfw(i,1,1)$, $pflw(i,1,1)$ — the target failure probability for sample i (0.0012 is assigned to these elements in the program);
 $pfw(i,1,2)$, $pflw(i,1,2)$ — the difference between $P_f = 0.0012$ and the found

failure probability, if the found probability appears lower than 0.0012⁴;

$pfw(i,2,1)$, $pflw(i,2,1)$ — the failure probability for sample i , corresponding to $\gamma_a = 1.10$, $\gamma_c = 1.25$ and $\gamma_v = 1.25$;

$pfw(i,2,2)$, $pflw(i,2,2)$ — remaining relative error after the final iteration for determining P_f under condition: $\gamma_a = 1.10$, $\gamma_c = 1.25$ and $\gamma_v = 1.25$;

$pfw(i,3,1)$, $pflw(i,3,1)$ — the failure probability for sample i , corresponding to $\gamma_a = 1.05$, $\gamma_c = 1.25$ and $\gamma_v = 1.25$;

$pfw(i,3,2)$, $pflw(i,3,2)$ — remaining relative error after the final iteration for determining P_f under condition: $\gamma_a = 1.05$, $\gamma_c = 1.25$ and $\gamma_v = 1.25$;

The main simple variables in *crb* are listed below,

- bd , ccd , cvd — \bar{b} , ρ and V_δ , respectively, used for beams with ductile shear connectors and applicable for calibration to the equilibrium method;
- bdl , $ccd1$, $cvdl$ — \bar{b} , ρ and V_δ , respectively, used for beams with ductile shear connectors and applicable to calibration for the linear interpolation model;
- bn , ccn , cvn — same as bd , ccd , cvd but obtained from the test specimens with non-ductile shear connectors;
- bnl , $ccnl$, $cvnl$ — same as bdl , $ccd1$, $cvdl$ but obtained from the test specimens with non-ductile shear connectors;
- nn — total number of the beam samples to be analysed;
- arg — as explained for *ctc*;
- vfy , vfc , vec , vf_u , vd , vhc , vbc , vwa , vaa , vhg , vba , vtw — V_{fy} , V_{fc} , V_{Ec} , V_{fu} , V_d , V_{hc} , V_{bc} , V_{W_a} , V_{A_a} , V_{hg} ⁵, V_{bf} and V_{tw} , respectively.

⁴For sample i , if the design fractile-factor corresponding to the given safety factors appears higher than the factor corresponding to $P_f = 0.0012$, then the failure probability to be obtained would be lower than 0.0012. This means that, with the given safety factors, sufficient reliability underlying the design resistance must have been obtained. In this case, the program simply assumes the failure probability as $P_f = 0.0012$. So, in fact, elements $pfw(i,1,2)$ and $pflw(i,1,2)$ always hold zero and are not used.

⁵Where necessary, the program takes $V_{h_{na}}$ same as as V_{hg} .

D.2.5 Input datafiles for *ctc* and *crb*

There are two datafiles to be created by the users: *inodp* for *ctc* and *inodp0* for *crb*. The layout of *inodp* may be shown below:

```

nn, csc, arg
bnum(1,1)
bnum(1,2)
bdh(1,1), bdh(1,2), bdh(1,3), bdh(1,4), bdh(1,5), bdh(1,6), bdh(1,7), bdh(1,8),
bdh(1,9)
cps(1,1), cps(1,2), cps(1,3), cps(1,4), cps(1,5), cps(1,6), cps(1,7)
cps(1,9)
ns(1,1), ns(1,2)
...
bnum(nn,1)
bnum(nn,2)
bdh(nn,1), bdh(nn,2), bdh(nn,3), bdh(nn,4), bdh(nn,5), bdh(nn,6), bdh(nn,7),
bdh(nn,8), bdh(nn,9)
cps(nn,1), cps(nn,2), cps(nn,3), cps(nn,4), cps(nn,5), cps(nn,6), cps(nn,7),
cps(nn,9)
ns(nn,1), ns(nn,2)
es(1), ..., es(nn)

```

The layout of datafile *inodp0* is as follows.

```

vfy, vfc, vec, vfu, vd, vhc, vbc, vwa, vaa, vhg, vba, vtw
nn, arg
bnum(1,1)
bnum(1,2)
bdh(1,1), bdh(1,2), bdh(1,3), bdh(1,4), bdh(1,5), bdh(1,6), bdh(1,7), bdh(1,8),
bdh(1,9)
cps(1,1), cps(1,2), cps(1,3), cps(1,4), cps(1,5), cps(1,6), cps(1,7)

```


cps(1,9)
ns(1,1), ns(1,2)
 ...
bnum(nn,1)
bnum(nn,2)
bdh(nn,1), bdh(nn,2), bdh(nn,3), bdh(nn,4), bdh(nn,5), bdh(nn,6), bdh(nn,7),
bdh(nn,8), bdh(nn,9)
cps(nn,1), cps(nn,2), cps(nn,3), cps(nn,4), cps(nn,5), cps(nn,6), cps(nn,7),
cps(nn,9)
ns(nn,1), ns(nn,2)

In setting these files, the following points should be noticed:

- (1) the input data are all in units based on N and mm except W_c (to *cps(i,6)*), L (to *cps(i,7)*) and r_{ei} (to *es(i)*); W_c , L and r_{ei} are input in units of kN/m^3 , m and kN-m, respectively;
- (2) the current version of the programs are only developed to do the calibration based on the strength of shear connection given by equation (3.12), so, to use the programs properly, the user can input f_u (to *bdh(i,4)*) a large value, say 1000000.0N/mm^2 ;
- (3) according to Eurocode 4 [1], *arg* should be taken as 0.29.
- (4) for a test specimen or a beam sample, if E_c (to *cps(i,9)*) is unknown but f_c (to *cps(i,5)*) is known, *cps(i,9)* should be assigned 0 in the datafiles, thus, the program will estimate E_c according to equation (3.16).

D.2.6 Output file after running *ctc* and *crb*

The results obtained after running *ctc* and *crb* are recorded in output file *outodp*. This output file is basically self-explanatory. The following is the explanation of the notations used to designate the table entities in *outodp*.

- Under table titles, “*Results of beams with the non-ductile connection*” and “*Results of beams with the ductile connection*”:
 - *Beam name* — name of beam specimens;
 - *SC ratio* — the actual degree of shear connection of beam specimens;
 - *LBSCR* — the lowest degree of ductile shear connection for beam specimens required by Eurocode 4 [1];
 - *M by inter* — r_{ti} from linear interpolation method for each beam specimen, (2.25) and (2.26));
 - *M by equi* — r_{ti} from equilibrium method for each beam specimen;
 - *M by test* — r_{ei} for beam specimen i ;
 - $(3)/(1)$ — r_{ei}/r_{ti} for each beam specimen, where r_{ti} found from the linear interpolation;
 - $(3)/(2)$ — r_{ei}/r_{ti} each beam specimen, where r_{ti} found from the equilibrium method;
 - X_c, X_a — depths of the first neutral axis (measured from top of concrete slab) and the depth of the second neutral axis (measured from steel top flange), respectively, for beam specimens, found from the equilibrium method;
 - M_f, M_a — theoretical plastic bending resistances of composite section (assuming full shear connection) and steel beam alone, respectively, for beam specimens;
 - $P.N.A._{(M_f)}$ — depth of the neutral axis corresponding to M_f ;
 - t_f, h_c-h_p, h_c+t_f — intended or measured values of $t_f, h_c - h_p$ and $h_c + t_f$, respectively, for beam specimens;
- Under the table title “*The coefficients of variation*”:
 - $V_{rt}, V_r, Log.V_r$ — V_{rt}, V_r and σ_{lnr} , respectively, for beam samples;

- Under the table title “*The Partial Safety Factors*”:
 - *Model factor* — γ_{md} (found according to $P_f = 0.0012$) for beam samples;
 - *Steel S.F* — γ_a (from γ_{md}) for beam samples;
 - *Concrete S.F* — γ_c (from γ_{md}) for beam samples;
 - *Connector S.F* — γ_v (from γ_{md}) for beam samples;
- Under the table title “*The safety fractile-factor on resistance side*”:
 - *Presumed value* — k_d determined from $P_f = 0.0012$ for beam samples;
 - $rc,ru=1.25 \quad ry=1.10$ — k_d for beam samples, determined from $\gamma_c = 1.25$, $\gamma_v = 1.25$ and $\gamma_a = 1.10$;
 - $rc,ru=1.25 \quad ry=1.05$ — k_d for beam samples, determined from $\gamma_c = 1.25$, $\gamma_v = 1.25$ and $\gamma_a = 1.05$;
- Under the table title “*The failure probability with the given safety factors*”:
 - *Presumed value* — required failure probability for design (being regarded as $P_f = 0.0012$); the values in the brackets are data stored in element $pfw(i,1,2)$ or $pflw(i,1,2)$, which, as explained in Section D.2.4, can be ignored;
 - $rc,ru=1.25 \quad ry=1.10$ — failure probability underlying the design resistance under the condition: $\gamma_c = 1.25$, $\gamma_v = 1.25$ and $\gamma_a = 1.10$; the values in the brackets are the remaining relative errors after the final iteration (see Section 3.3);
 - $rc,ru=1.25 \quad ry=1.10$ — failure probability underlying the design resistance under the condition: $\gamma_c = 1.25$, $\gamma_v = 1.25$ and $\gamma_a = 1.05$; the values in the brackets are the remaining relative errors after the final iteration.

D.3 Program for beams with non-ductile partial shear connection

D.3.1 Scope of program

This program also consists of two independent packages. One is named *ntc* and the other *nrb*. These two packages were developed to make calibration for design bending resistances of beams with non-ductile shear connection. The relevant theory has been presented in Section 3.2.3.

Because all the relevant beam specimens collected so far have symmetric steel sections and are simply supported, the program, at present, is only developed to be applicable to simply supported composite beams with symmetrical steel sections.

To implement the calibration, *ntc* and *nrb* should be used jointly. For this purpose, a control program, *rcn*, has been written in C-Shell Scripts in UNIX system, which is shown below.

```
ntc
cat add.nrb >> temp
nrb
cat outonc >> outodn
rm outonc
```

Datafile *add.nrb* is originally created by the user. File *outonc* is created by *ntc* for storing the results calculated, which, after running *nrb*, is catenated to the output file of *nrb*, *outodn*. So all the results can be available in *outodn*, and, therefore, *outonc* can be removed from the directory.

So, using *rcn*, *ntc* and *nrb* can be run properly by simply issuing the following command to UNIX system:

```
[%] sh rcn <return>
```

During running, the program will show three sets of results about the test

specimens. The results include test group size n , \bar{b} , V_δ and ρ . Three different ways are adopted to obtain these results: (1) using assumptions (4) of Section 3.2.3 but with the resistance function restricted to that for propped construction only; (2) using the assumption but the resistance function being restricted to that for unpropped construction only; (3) using assumptions (3) and (4) in Section 3.2.3. The user can choose one set of the results for further calibration by typing in one of the following letters:

- m — using n , \bar{b} , V_δ and ρ based on (3);
- p — using n , \bar{b} , V_δ and ρ based on (1);
- u — using n , \bar{b} , V_δ and ρ based on (2);

According to Section 3.2.3, for calibration for beams with non-ductile shear connectors, m should be chosen.

The functions of *ntc* are as follows.

- Calculate the theoretical resistances, r_{ti} , for each specimen, based on the models for propped construction and unpropped construction.
- Determine \bar{b} , V_δ and ρ , and size of test group, n , in the different ways explained above.

The main functions of *nrb* are as follows.

- Determine V_{rt} and V_r for the beam samples.
- With respect to $P_f = 0.0012$, find safety factors γ_a , γ_c and γ_v for the beam samples.

D.3.2 Subroutines and variables in *ntc* and *nrb*

It has been designed that the calculations in *ntc* are carried out for the beam specimens, and, therefore (as considered in assumption (3) in Section 2.2.1), the measured values or intended values (not for material strengths) of basic variables of the specimens should be used, while for calculations made in *nrb*, the processed

objectives are the beam samples, so the mean values of basic variables for the samples should be used.

Several subroutines are developed in *ntc* and *nrb*, whose functions are noted below.

Subroutines in *ntc*

- *Subroutine cfpu*(*nn, arg, k, kp, ku, kmax*) — uses the models based on propped and unpropped construction to calculate the theoretical resistances r_{ti} for each beam specimen;
- *Subroutine elrdu*(*i, bmelrd, fel, sigmaa, fc, bmsd*) — determines $M_{eI,R}$ for test specimens, considering unpropped construction;
- *Subroutine elrdp*(*i, bmelrd, fel, sigmaa*) — determines $M_{eI,R}$ for beam specimens, considering propped construction;
- *Subroutine cmce*(*n, cmv, cc, es, ts*) — determines \bar{b} , V_{δ} and ρ .

Subroutines in *nrb*

- *Subroutine cfpu*(*nn, arg, si*) — uses the models based on propped and unpropped construction to calculate the mean theoretical resistances for each beam sample;
- *Subroutine elrdu*(*i, bmelrd, fel, sigmaa, fc, bmsd*) — determines $M_{eI,R}$ for beam samples, considering unpropped construction;
- *Subroutine elrdp*(*i, bmelrd, fel, sigmaa*) — determines $M_{eI,R}$ for beam samples, considering propped construction;

Many variables and functions dealt with in both *ntc* and *nrb* are the same. Therefore, in packages *ntc* and *nrb*, the arrays representing the same basic variables or the same functions are defined with the same names. The user may only need to know that, as indicated above, these arrays in *ntc* are used to store the measured or intended values of basic variables for every beam specimen and the results found from these values; while for *nrb*, they are used to store the mean

values of basic variables for beam samples and the results from these mean values.

Thus, the main arrays in *ntc* and *nrb* can be explained together as follows.

- *cps(100,9)*:

cps(i,1) — b_c for specimen i or sample i ;

cps(i,2) — h_c for specimen i or sample i ;

cps(i,3) — h_p for specimen i or sample i ;

cps(i,4) — b_0 for specimen i or sample i ;

cps(i,5) — cylinder strength of concrete, f_c , for specimen i or sample i ;

cps(i,6) — the density of the concrete, for specimen i or sample i ;

cps(i,7) — beam span, in metres, for specimen i or sample i ;

cps(i,8) — the required lowest degree of ductile shear connection for specimen i or sample i ;

cps(i,9) — Young's modulus of concrete, E_c , for specimen i or sample i .

- *bdh(100,11)*:

bdh(i,1) — d of studs or, when G is input to *bnum(i,2)* (for *ntc* only), the given ratio of shear connection in specimen i or sample i ;

bdh(i,2) — yield strength of steel, f_y , for specimen i or sample i ;

bdh(i,3) — h_a for specimen i or sample i ;

bdh(i,4) — stud strength, f_u , for specimen i or sample i ;

bdh(i,5) — h for specimen i or sample i ;

bdh(i,6) — b_f for specimen i or sample i ;

bdh(i,7) — t_w for specimen i or sample i ;

bdh(i,8) — t_f for specimen i or sample i ;

bdh(i,9) — area of steel section, A_a , for specimen i or sample i ;

bdh(i,10) — Young's modulus of the steel, E_a , for specimen i or sample i ;

bdh(i,11) — second moment of steel area, I_a , for specimen i or sample i .

- *rp(100,3)* and *ru(100,3)*:

rp(i,1), *ru(i,1)* — $M_{el,R}$ by assuming propped and unpropped construction, respectively, for specimen i or sample i ;

$rp(i,2)$, $ru(i,2)$ — F_{el} by assuming propped and unpropped construction, respectively, for specimen i or sample i ;

$rp(i,3)$, $ru(i,3)$ — r_t by assuming propped and unpropped construction, respectively, for specimen i or sample i .

- $rc(100,5)$:

$rc(i,1)$ — $M_{a,s}$ for specimen i or sample i ;

$rc(i,2)$ — F_c for specimen i or sample i ;

$rc(i,3)$ — N/N_f for specimen i or sample i ;

$rc(i,4)$ — $M_{pl,R}$ for specimen i or sample i ;

$rc(i,5)$ — M_{apl} for specimen i or sample i .

- $sfp(100,4)$ and $sfu(100,4)$:

$sfp(i,1)$, $sfu(i,1)$ — γ_{md} for sample i with respect to propped and unpropped construction, respectively;

$sfp(i,2)$, $sfu(i,2)$ — γ_a for sample i with respect to propped and unpropped construction, respectively;

$sfp(i,3)$, $sfu(i,3)$ — γ_c for sample i with respect to propped and unpropped construction, respectively;

$sfp(i,4)$, $sfu(i,4)$ — γ_u for beam sample i with respect to propped and unpropped construction, respectively.

- $vrp(100,3)$, $vru(100,3)$:

$vrp(i,1)$, $vru(i,1)$ — V_{rt} of sample i for propped and unpropped construction, respectively;

$vrp(i,2)$, $vru(i,2)$ — V_r of sample i for propped and unpropped construction, respectively;

$vrp(i,3)$, $vru(i,3)$ — σ_{lnr} of sample i for propped and unpropped construction, respectively.

- $ffp(100,3)$, $ffu(100,3)$:

$ffp(i,1)$, $ffu(i,1)$ — k_d of sample i (corresponding to $P_f = 0.0012$), for

- propped and unpropped construction, respectively;
 $ffp(i,2)$, $ffu(i,2)$, $ffp(i,3)$, $ffu(i,3)$ — not being used.
- $es(100)$:
 $es(i)$ — experimental value of the bending resistance, r_{ei} , for specimen i .
 - $bnum(100,3)$ (character array, string length = 10):
 $bnum(i,1)$ — the reference name of specimen i or sample i .
 $bnum(i,2)$ — sheeting direction of specimen i or sample i : T if transverse;
 P if parallel; S if solid slab, G (for ntc only) if ratio of shear connection is
given directly;
 $bnum(i,3)$ — the indicator of potential failure of shear connection in spec-
imen i or sample i : $stud$ if studs dominant; $concrete$ if concrete dominant.
 - $ns(100,2)$:
 $ns(i,1)$ — number of shear studs of specimen i or sample i ; $ns(i,2)$ —
number of studs per rib, N_p , of specimen i or sample i ; when the ribs run
transverse to the beam span, and the specimen contains N_{r1} ribs with one
stud and N_{r2} two studs, N_p is determined from equation (D.1);
 - $cvb(1), \dots, cvb(11)$ — V_d , V_{fy} , V_{ha} , V_{fu} , V_h^6 , V_{bf} , V_{tw} , V_{tf} , V_{Aa} , V_{Ea} , V_{Ia} ,
respectively;
 - $cvc(1), \dots, cvc(9)$ — V_{bc} , V_{hc} , V_{hp}^7 , V_{b0}^8 , V_{fc} , V_{Wc}^9 , V_L^{10} , V_{CR}^{11} , V_{Ec} , respec-
tively.

The main simple variables in ntc and nrb are defined as follows.

- nn — total number of specimens plus samples;

⁶coefficient of variation of h

⁷coefficient of variation of h_p

⁸coefficient of variation of b_0

⁹coefficient of variation of W_c

¹⁰coefficient of variation of L

¹¹the coefficient of variation of the required lowest degree of ductile shear connection; this is set only for convenience in computation and is assigned as zero during running of the program.

- *arg* — the factor for determining the strength of shear connector P_R , to be taken as 0.29 [1];
- *ip* — number of specimens whose r_{ti} based on propped construction appears greater than the M_{apl} (for convenience, the group of these specimens is named D_p here);
- *cmvp*, *cvoep*, *ccp* — \bar{b} , V_δ and ρ from group D_p , respectively; the r_{ti} is calculated using the model for propped construction;
- *iu* — number of specimens whose r_{ti} based on unpropped construction appears greater than the M_{apl} (for convenience, the group of these specimens is named D_u here);
- *cmvu*, *cvoeu*, *ccu* — \bar{b} , V_δ and ρ from group D_u , respectively; the r_{ti} is calculated using the model for unpropped construction;
- *imax*, *cmvmax*, *cvoemax*, *ccmax* — number of test specimens in group D, \bar{b} , V_δ and ρ , respectively; the determination of these parameters is in accordance with assumptions (3) and (4) in Section 3.2.3;
- *ri* — the increment ratio of basic variables to evaluate the derivatives of theoretical resistance for obtaining V_{ri} ; this will be chosen by the user (a value between 0.001 to 0.005 is recommended).

D.3.3 Input files of *ntc* and *nrb*

There are two datafiles to be made by the user: *inodn* and *add.nrb*.

The layout of file *inodn* is shown as follows.

```
nn, csc, arg,
bnum(i,1), bnum(i,2)
bdh(1,1), ..., bdh(1,11)
cps(1,1), ..., cps(1,7)
cps(1,9)
```



```

ns(1,1), ns(1,2)
es(1)
... bnum(nn,1), bnum(nn,2)
bdh(nn,1), ..., bdh(nn,11)
cps(nn,1), ..., cps(nn,7)
cps(nn,9)
ns(nn,1), ns(nn,2)
es(nn)

and file add.nrb

arg, ri
cvb(1), ..., cvb(11)
cvc(1), ..., cvc(9)

```

In creating these files, it should be particularly pointed out that

- (1) as explained above, nn stands for the total number of beams to be analysed, including test specimens and the samples, so file *inodn* actually contains the relevant data for both test specimens and the samples formed thereby, but the value of $es(i)$ (which represents the experimental value of resistances) for the beam samples should be given as zero. Thus, the program will not take the samples into account in determining the size of test group and the parameters, \bar{b} , V_δ and ρ ;
- (2) the users need not select by themselves the test specimens and samples according to assumption (4) in Section 3.2.3. The program will do it;
- (3) the user himself does not need to decide if a specimen or sample has ductile or non-ductile shear connection; the program will do it according to Eurocode 4 [1];
- (4) as indicated above, the value for $cvc(8)$ (corresponding to V_{CR}) should be taken as zero; furthermore, if h , h_p , b_0 , W_c and L are assumed as determi-

nate (as considered in Section 3.2.2 and 3.2.3), then the values for $cvc(5)$, $cvc(3)$, $cvc(4)$, $cvc(6)$ and $cvc(7)$ should be given as zero as well.

Besides the above points, the notes for datafiles, $indop$ and $inodp0$, (see Section D.2.5) should be also applied here.

D.3.4 Output file of ntc and nrb

The final results provided by ntc and nrb are recorded into a file named $outodn$.

Like output files for the other programs, the information in $outodn$ is presented in form of tables, and is basically self-explanatory. If the names of specimens and samples are defined with different names, then the user can easily recognize the results obtained for the specimens or the samples.

The notations for designating the tables entities in $outodn$ are now explained.

- Under the table title “*Results of beams with the non-ductile connection*”
 - SC ratio and $LBSCR$ — as explained for output file $outodp$ (Section D.2.6);
 - $Mapl, Rd$ — M_{apl} of test specimens;
 - M (*unpr.*) — r_{ti} for test specimen, found by assuming unpropped construction;
 - M (*prop.*) — r_{ti} for test specimens, found by assuming propped construction;
 - M (*maxi.*) — r_{ti} for test specimens, in accordance with assumption (3) in Section 3.2.3;
 - M *by test* — r_{ei} for test specimens;
 - (1)/(2) — $M_{apl,i}/r_{ti}$ for each test specimens (where $M_{apl,i}$ is the M_{apl} for specimen i);
 - (3)/(2) — r_{ei}/r_{ti} for test specimens;

- F_c , Me/M_f — F_c and $r_{ei}/M_{pl,R}$ for test specimens, respectively;
- $Me_{l,p}$, $F_c/F_{el,p}$, M_p/M_f — $Me_{l,R}$, F_c/F_{el} and $r_{ti}/M_{pl,R}$ for test specimens, respectively, where the calculation is made assuming propped construction;
- $Me_{l,u}$, $F_c/F_{el,u}$, M_u/M_f — $Me_{l,R}$, F_c/F_{el} and $r_{ti}/M_{pl,R}$ for test specimens, respectively, where the calculation is made assuming unpropped construction;
- Under the table title “*The coefficients of variation and safety indices*”:
 - kd , V_{rt} , V_r , $Log.V_r$ — k_d corresponding to $P_f = 0.0012$, V_{r_t} , V_r and σ_{lnr} , respectively;
- Under the table title “*The Partial Safety Factors*”:
 - *Model factor*, *Steel S.F*, *Concrete S.F* and *Connector S.F* — as explained for file *outodp* (see Section D.2.6)

D.4 Using *ctc* and *crb* for beams with non-ductile shear connection

As introduced in Section D.2, according to data of beam specimens in input file *inodp*, package *ctc* will classify the beams into groups with ductile and non-ductile shear connection, and then calculate the parameters, \bar{b} , V_δ and ρ , for these two groups, using the equilibrium method and linear interpolation, respectively.

Similarly, the beams samples dealt with in package *crb* are also classified into two groups: one with ductile shear connection and the other with non-ductile shear connection. As designed, package *crb* carries out the further calibration for beams with ductile shear connection (group C), using the relevant values of \bar{b} and V_δ , and the group size n .

However, for the beam specimens with non-ductile shear connection, the group size n and the test corrections, \bar{b} , V_δ and ρ , found in *ctc* will be also read into *crb*.

Therefore, *crb* can be easily applied to calibrate the safety of using the equilibrium method and linear interpolation to beams with non-ductile shear connection (group D). The only modification is to switch over the test corrections, \bar{b} and V_{δ} , the group size n and the mean values of basic variables for beam samples with ductile and non-ductile connectors.

Such a modified package for beams in group D is named *crn*; it uses the same input file as *crb*, *inodp0* (see Section D.2.5). To implement the calibration, user may run *ctc* and *crn* jointly. On UNIX system, same as running *ctc* and *crb* jointly (see Section D.2.2), a simple supervision package in C-Shell Scripts can be made as follows,

```
cp inodp0 inodp1
ctc
cat add >> inodp1
crn
cat outodp1 >> outodp
rm outodp1 add inodp1
```

The results obtained are stored in the file with the same name (*outodp*) as that for results from running *ctc* and *crb*), to which the explanation has been given in Section D.2.6.

D.5 Use of program *EPPCB1*, source programs and input data files

In the following parts, the note for using program *EPPCB1* (the note and the program are all written by R.P. Johnson), as well as all the other relevant computer files, is given. The documents are listed in the following sequence:

- (1) notes of using *EPPCB1*

- (2) source program of *EPPCB1*, *EPPCB1.f*;
- (3) input datafile *csdat* for each test specimen;
- (4) source program of *sacb*, *sacb.f*;
- (5) input datafile, *inod*, for beams in sagging bending;
- (6) input datafile, *inod*, for beams in hogging bending;
- (7) source programs of *ctc* and *crb*, *ctc.f* and *crb.f*;
- (8) source program of *crn*, *crn.f*;
- (9) input datafiles, *inodp* and *inodp0*;
- (10) source programs of *ntc* and *nrb*, *ntc.f* and *nrb.f*;
- (11) input datafiles, *inodn* and *add.nrb*.

Computer Program EPPCB, "Elastic and plastic properties of a composite beam"

1. History and Availability

The program was prepared by R.P. Johnson in April 1984, from programs ELPCS and PLPCS, for use from a terminal. It is in FORTRAN, and is stored on RPJ's file esrpj/comp/eppcb on the SUN (eagle).

2. Scope and Options

Only one composite cross section is analysed in each run, but up to three values of the modular ratio can be specified. The design yield stresses in the steel tension flange, web, compression flange, reinforcement in tension, and reinforcement in compression may all be different.

Provision is made for a concrete cross section of two rectangles (slab and haunch), for reinforcement in the slab (but not in the haunch) at two levels, for an I-section steel plate girder or rolled section, and for up to two extra steel bottom-flange plates.

Table 1 : Names of Variables

| Property | Section | structural steel only | unreinforced composite | cracked unreinforced composite | cracked reinforced, hogging |
|---------------------------------|---------|-----------------------|------------------------|--------------------------------|-----------------------------|
| Depth of n.a. below top of slab | | YNS | YNU | YN | YNC |
| Area of cross section | | AS | AU | ACU | AC |
| Second moment of area | | IS | IU | I | IC |
| Section moduli: | | | | | |
| top (slab or reinforcement) | | - | ZTUC* | ZTC* | ZTHR† |
| top of steel section | | ZTS | ZTUS | ZT | ZTHS |
| bottom of steel section | | ZBS | ZBU | ZB | ZBH |
| Shear factor $A\bar{y}/I$ | | - | AYU | AYC | AYCH |

*In 'concrete' units.

†In 'reinforcement' units.

The elastic properties given in Table 1 are always calculated, for each value of the modular ratio, plus the limiting elastic moments BMHE and BMSE, the corresponding stresses, and the flange and web slendernesses SLFL and SLWEB. For no options, input NCAL = 0, NOPT = 0.

Further calculations for the primary (isostatic) effects of temperature and shrinkage modified by creep (TSC) are done in accordance with the Bridge Code (BS 5400) when the integer NCAL is input as 1, 2, or 3, as follows.

NCAL = 1. Analysis for temperature distributions Type 1 ("positive") and Type 2 ("reversed") of Clause 5.4.5 of BS 5400 : Part 2.

NCAL = 2. Analysis for uniform longitudinal shrinkage of the concrete slab (and haunch, if any).

NCAL = 3. Analyses as for NCAL = 1 and NCAL = 2.

Details of these analyses are given in Section 8 of this Note. If TSC analyses are not required, NCAL = 0 must be input. A flowchart for NCAL ≠ 0 is given on page 8.

NOPT = 1. Calculation of plastic moments of resistance BMS and BMH and neutral axis depths YP and YPH, the hogging moment with the web excluded, BMHR, and the flange and web slendernesses in hogging bending, SLFL and SLPWEB.

The influence of a lateral buckling stress SLB lower than the yield stress SYF is shown by output of BMPLH (which is BMHR for SLB = SYF) and the ratio SLBRAT, which is SLB/SYF.

The shape factor SHPFS is the ratio of BMS to BMSE for the first modular ratio input. The shape factor SHPFH is the ratio of BMPLH to BMHE.

NOPT = 2. This is as NOPT = 1 with additional output of VD and VR, corresponding to shear strengths V_D and V_R in BS 5400: Part 3, and the safety ratio R, defined in section 10.

3. Properties of materials

ES = Young's modulus for structural steel.

ER = Young's modulus for reinforcement

AE(M) = Modular ratio (E_s/E_c), with $M = 1, \dots, MR$ and $MR \neq 3$. When

TSC calculations are done, AE(1) must be the ratio for short-term loading (used in temperature calculations) and AE(2) must be a ratio for long-term loading, as it is used in the shrinkage calculations. The value AE(3), if input, is not used in the TSC part of the program. Additional properties input only when NCAL ≠ 0 are explained in Section 7.

SYF = Yield stress for steel flange plates

SYW = Yield stress for steel web plate

SLB = Limiting stress for steel compression flange subject to lateral buckling

SRT = Yield stress for steel reinforcement in tension

SRC = Yield stress for steel reinforcement in compression

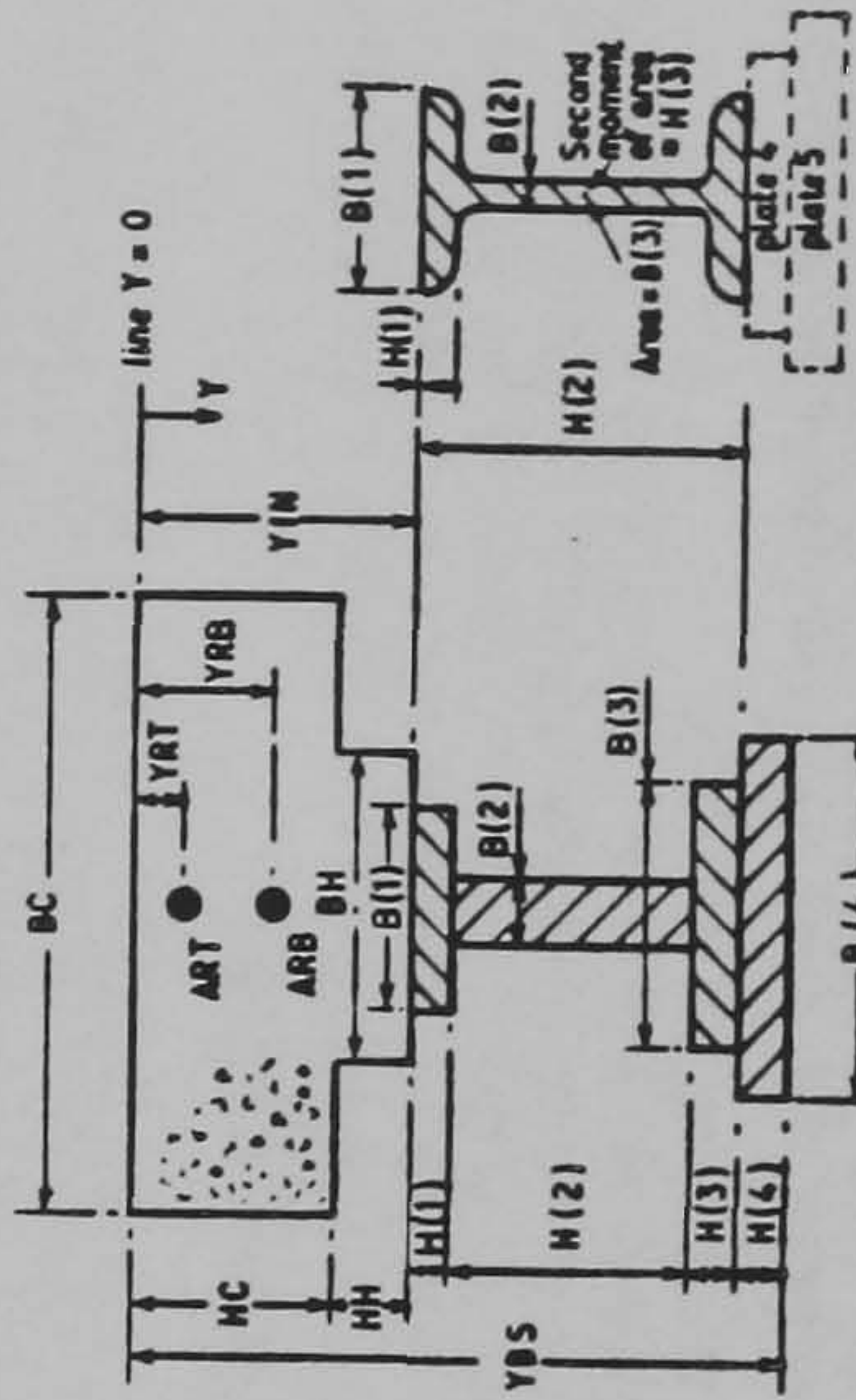
SCC = Limiting compressive stress in concrete (normally $0.4 f_{cu}$)

TAU = Design stress in shear for steel web (τ_k in BS 5400: Part 3)

TAUR = Reduced value of TAU, used for calculating V_R to §9.9.3.1 of Part 3.

4. Assumptions on the geometry of the cross section

4.1 The dimensions of the steel section are defined by arrays B(N) and H(N) where N has the value 3, 4, or 5. A plate girder is treated as three rectangular areas



(a) Plate girder (NRS = 0, N = 4)
(b) Alternative for plates 1 to 3 (NRS = 1, N = 3)

Fig. 1 Dimensions of cross section

of steel. The concrete and structural steel together comprise $N + 2$ rectangular areas. Simpler sections can be treated by input of zeros, but non-zero dimensions must be input for the slab and at least one of steel plates 1 to 3.

The rectangular areas must be arranged, in direction of increasing Y, in the sequence shown in Fig. 1, and each must share a common boundary ($Y = \text{constant}$) with the next one. Figure 1 shows the notation for input data. The dimensions YIN and YBS are computed by the program.

4.2 Where a rolled I-section is present, its six relevant properties are input in place of the dimensions of plates 1 to 3, as shown in Fig. 1. The program makes no assumptions about taper of flanges or root radii. It replaces the rolled section by three plates. It retains the correct overall dimensions, web thickness, and total area, and calculates a new thickness for the flange plates that satisfies these conditions. It also retains the correct second moment of area, IS, which differs slightly from a value calculated from the dimensions of the three plates.

The constant NRS (Number of Rolled Sections) is input as 0 or 1. The constant N (Number of plates) is input as 3, 4 or 5; for this purpose a rolled section is treated as 3 plates. The computed array Y(N) gives the Y-coordinate of the centroid of each rectangular plate.

4.3 When the elastic neutral axis lies within the haunch, its level is calculated by an approximate method that assumes that the area of the haunch is much less than that of the slab.

4.4 Reinforcement areas ART and ARB are assumed to be on the same side of the neutral axis and are lumped together at their common centroid.

5. Conventions of sign.

All properties of materials are input as positive numbers, except shrinkage strain. At output, sagging bending moments and tensile force, stress, and strain are positive. The section moduli are consistent with that: positive for points below the neutral axis and negative for points above it.

6. Units

All input and output is in NEWTON and MILLIMETRE units, except that:

(a) When NCAL = 0, any consistent units can be used for ES and ER since only their ratio is used.

(b) All output values of I and Z are given as $10^{-6}I$ (mm^4), and $10^{-6}Z$ (mm^3) so that $M = fZ$ can be used with M in kNm and f in N/mm^2 .

(c) All output values of $A\bar{y}/I$ are in m^{-1} units so that $q = V\bar{A}\bar{y}/I$ can be used with V in kN and q in kN/m .

(d) All bending moments are in kNm and all forces in kN, for both input and output. Curvature is in km^{-1} units.

Output formats for the results in Table 1 are of type F13.n, where n (the number of decimal places) is 1 for neutral axis depths, 0 for areas, 2 for $10^{-6}I$, 4 for $10^{-6}Z$, and 5 for $A\bar{y}/I$.

7. Input of data, on file CSDAT

Free format is used, but the data must be input in distinct lines corresponding to the READ statements in the program, and in the correct sequence. Real variables must have a decimal point or an exponent (e.g. 200E3). Integer variables must not have either of these. In this program, integer variables begin with J to N inclusive; IS, IU, etc. are real variables.

Runs are identified by the integer constant NB (Number of Beam), not exceeding 16380.

The input lines and sequence are:

For all NCAL and NOPT

NB, ES, ER, MR, NCAL, NOPT

AE()

BC, HC, BH, HH

ART, YRT, ARB, YRB, NRS, N

B(1), H(1), B(2), H(2)

SYF, SYW, SLB, SRT, SRC, SCC

For NCAL = 1 and NCAL = 3 only

BTC, BTS, T1, T2

For NCAL = 2 and NCAL = 3 only

EPS

For NOPT = 2 only

TAU, TAUR, GMB, CMV, BM, V

7.1 Reinforcement in the slab. If there is only one layer, input ARB = YRB = 0. In the elastic analyses, reinforcement is included only in the "cracked reinforced hogging" section. If there is none, input ART = YRT = 0 as well, and give ER (which must be specified) the same value as ES. ZTHR will still be output, and will relate to non-existent steel at level $Y = 0$.

In the plastic analysis for sagging bending, slab reinforcement is assumed to be in compression at stress SRC - SCC (to allow for the displaced concrete). If no reinforcement is to be included, input SRC with the value SCC. If AR is the area of reinforcement in hogging bending (= ART + ARB) and k.AR is the area in sagging bending (assumed to be in proportion to ART and ARB), input SRC with the value

$$\text{SRC}(\text{new}) = (1-k) \cdot \text{SCC} + k \cdot \text{SRC}(\text{old})$$

7.2 Use for non-composite steel section. If there is no concrete slab, input NCAL = 0, MR = 1, AE(1) = 1., BC = 0., HC = 0.. The section moduli ZTUC and ZTC will still be output, and will have the same value as ZTS.

7.3 Composite plate. If the structural steel section consists of one plate only, for elastic analysis input NCAL = 0, NOPT = 0, NRS = 0, N = 3, B(1) = H(1) = B(2) = H(2) = 0 .. Calculations for the cracked reinforced section under hogging moment will neglect the small area of concrete in compression below the neutral axis, so results for A, I, Z, and $A\bar{y}/I$ will be a little too low. The TSC part of the program has not been checked for composite plates.

For plastic analysis, input NOPT = 1, NRS = 0, N = 3, B(2) = H(2) = B(3) = H(3) = 0., SYW = 0.. The program will run only if the neutral axis lies within the plate; the yield stress of the plate should be input as SYF and as SLC. Option NOPT = 2 is not available.

8. Notes on the TSC calculations

The method and sign convention are as given in Appendix D of "Composite structures of steel and concrete, Vol. 2: Bridges" by R.P. Johnson and R.J. Buckby, Granada Publishing, 1979; except that no distinction is made between the effective breadth and the actual breadth of the slab. It is suggested that BC should be input as the effective breadth at quarter-span for u.-d. load, (given in BS 5400: Part 5).

All the calculations are done for the uncracked unreinforced cross section, using results YNU, AU, and IU (Table 1), computed for the appropriate modular ratio.

8.1 Input data

BTC and BTS are the coefficients of thermal expansion of concrete and steel. Both are normally input as 12E-6.

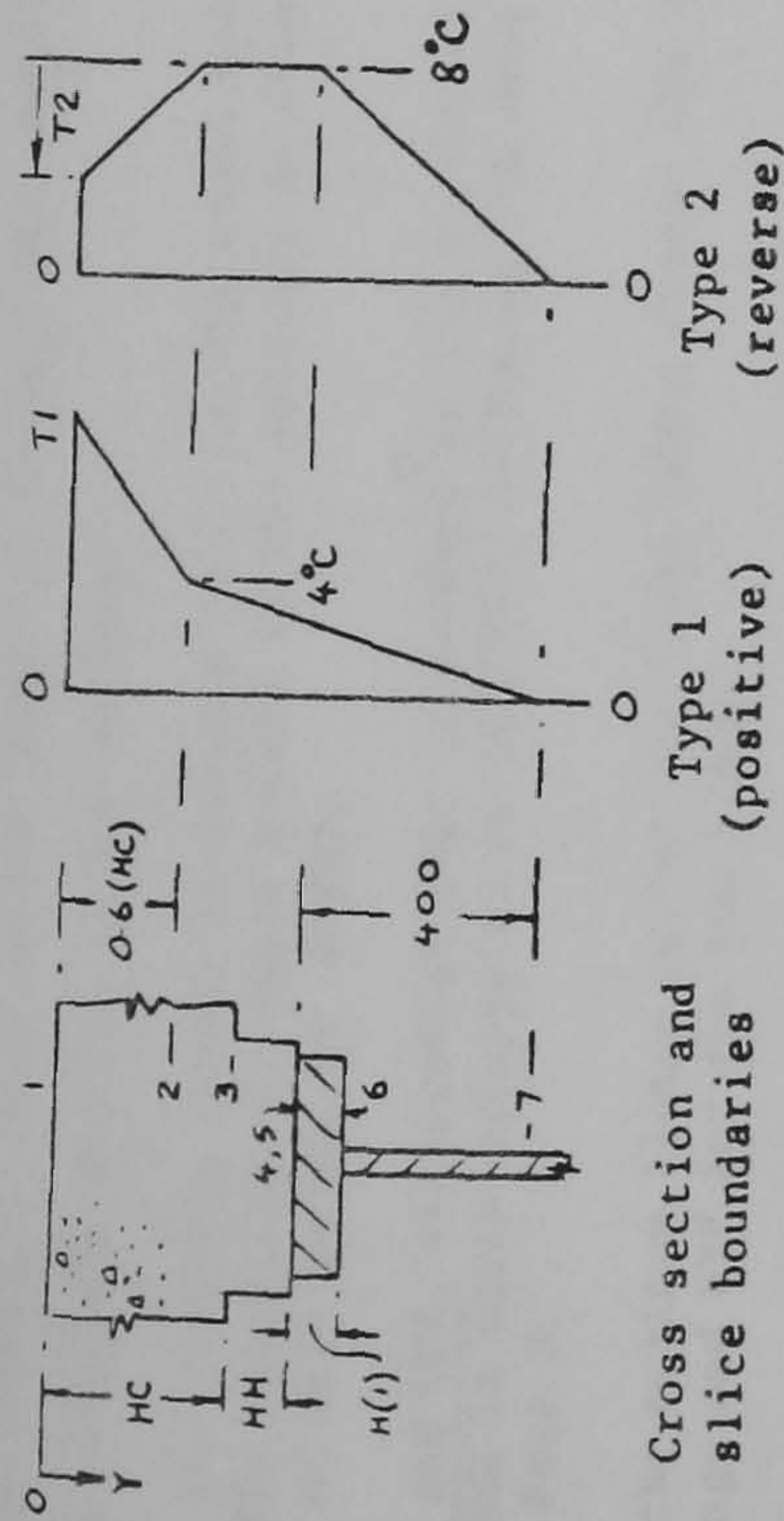


Fig. 2 Temperature differences to BS 5400: Part 2

T1 and T2 are the temperature differences at the top surface of the concrete slab specified in Clause 5.4.5 of BS 5400: Part 2 for the cross section analysed. These and the other (fixed) temperatures specified for Temperature Differences Type 1 and Type 2 are shown in Fig. 2. All Type 2 temperatures are taken (in the program) as 8°C higher than those given in BS 5400, so that no temperature movement need be considered in the lower part of the composite cross section. (Uniform change of temperature of course has no influence on the results calculated). Even so, T2 must be input as defined in BS 5400, and so is always negative (e.g. -4.0).

EPS is the free shrinkage strain and is always negative (e.g., -200E-6).

8.2 Output of TSC results

Each output listing begins with NCAL, NTYP, and M, which together show which type of calculation has been done, (Table 2). NCAL is explained in Section 3; NTYP is a counter used in the program; and M indicates that modular ratio AE(M) has been used.

Table 2

| NCAL | NTYP | M | Meaning |
|--------|--------|---|--------------------------------|
| 1 or 3 | -1 | 1 | Temperature difference, Type 1 |
| 1 or 3 | 0 | 1 | Temperature difference, Type 2 |
| 2 or 3 | 0 or 1 | 2 | Shrinkage |

FBAR is \bar{F} in Eq. (D.11) of Vol. 2, positive when tensile.

QCON is Q in Eq. (D.16) of Vol. 2, the longitudinal force in the concrete, positive when tensile.

MBAR is \bar{M} in Eq. (D.11) of Vol. 2, positive when sagging.

CURV is the curvature of the member in km^{-1} units, positive when sagging.

The upper part of the cross section is divided into six slices (Fig. 2) which relate to the temperature distributions. [Note: it is not clear in the

Code whether 0.6 (HC) should be 0.6 (HC + HH).] Coordinates YI(1) to YI(7) define the boundaries of these slices, and the same numbers 1 to 7 indicate levels at which stresses are calculated: FC1 to FC4 are stresses in concrete levels 4 and 5 are at the concrete-steel interface.

9. Design philosophy

The program does not introduce any partial safety factors (except in the calculation of R, see section 9.1). The elastic properties are relevant to both Serviceability and Ultimate limit states (SLS and ULS).

For strengths in bending, the user must adjust the stresses input and/or the strengths output, depending on the purpose of the calculation. Some examples follow.

9.1 For calculation strictly in accordance with BD 5400: Part 3. The Code gives design strengths in the form (e.g.)

$$M_D = Z_{pe} \sigma_{lc} / \gamma_m \gamma_{f3}$$

with $\gamma_m = 1.05$ for vertical shear and for sagging bending,

$\gamma_m = 1.2$ for hogging bending, and

$\gamma_{f3} = 1.1$ always.

Stresses for structural steel should be input as the unfactored values defined in Part 3. For reinforcement Part 5 gives $\gamma_m = 1.15$, so SRT should be taken as 1.2/1.15 times the characteristic yield strength. If account is to be taken of reinforcement in compression in computing BMS, SRC should be input as 0.72 times SRT (§6.5.4.3 of Part 4). See also section 7.1.

For concrete in compression, the stress $0.4f_{cu}$ includes γ_m for concrete. As $\gamma_m = 1.05$ is applied to the moment of resistance, SCC should be input as $0.42f_{cu}$.

The output values of BMS, VD, and VR should be divided by 1.155 ($-\gamma_m \gamma_{f3}$) to obtain design values, and the output BMB and BMBR should be divided by 1.32. Option NOPT = 2 does this automatically when calculating R, if GMB is input as 1.32 and GMV as 1.155.

9.2 Calculation using γ_m for structural steel. Assuming that there is no γ_m to be applied to the bending strengths, no γ_{f3} , and no lateral buckling, input all bending strengths for steel as f_y / γ_m and $SCC = 0.4f_{cu}$.

9.3 For calculation related to laboratory tests. Input steel stresses as the appropriate yield or buckling values, and SCC as the expected mean compressive stress at crushing (e.g., $0.7f_{cu}$). Input GMB = GMV = 1.0. The output values then need no adjustment.

10. The safety ratio, R

This enables the strength of a section in combined negative bending and vertical shear to be checked in relation to known design actions BM and V. When NOPT = 2, the program constructs the failure envelope in M-V space defined by §9.9.3.1 of BS 5400: Part 3, and computes R, which is the factor by which both BM and V would have to be divided for the point (BM, V) to lie on the failure envelope. Provision is made for possible input values BM = 0.0 or V = 0.0.

11. Assumptions made in calculating bending strengths

Only propped construction is considered.

For BMHE, the limiting stress is assumed to be in the bottom flange, top flange, or reinforcement. Following §9.8.3 of BS 5400: Part 3, the limiting compressive stress is taken as the lesser of $(D/2y_t) \cdot SLB$ and SYF, on the assumption that the section is non-compact.

For BMSE, the limiting stress is assumed to be in the steel bottom or top flange. The resulting top-fibre stress in the concrete is output as FC, and the ratio of this to SCC as FCRAT.

For BMPLH and BMH, the neutral axis is assumed to lie in the steel top flange or web. BMH is BMPLH multiplied by SLB/SYF, following the Note to §9.9.1.2 of BS 5400 : Part 3.

For BMHR, the maximum flange forces are found using stress SLB for the bottom flange and SYF for the top flange.

For BMS, the plastic neutral axis may lie in the slab or haunch, or steel top flange or web.

12. Shape factors

The factor for sagging bending, SHPFS, is the ratio of BMS to BMSE when the modular ratio has the first of the values input. The factor for hogging bending, SHPFH, is the ratio of BMPLH to BMHE.

13. Slenderness ratios

These are calculated in the form used in BS 5400 : Part 3; i.e., that

$$(\text{Breadth/thickness}) \cdot (f_y/355)^{1/2} \cdot n,$$

where n is a numerical value. They relate to hogging bending only.

SLFL is the ratio of flange outstand to thickness.

SLWEB is the ratio of depth of web in compression to its thickness, using elastic theory and neglecting concrete. It is not given if the whole of the web is in compression.

SLPWEB is similar, but uses the plastic neutral axis, which is assumed to lie within the web.

The output also gives the relevant slenderness limits of BS 5400 : Part 3.

14. Sequence of Output, on file EPOUT (See page 9.)

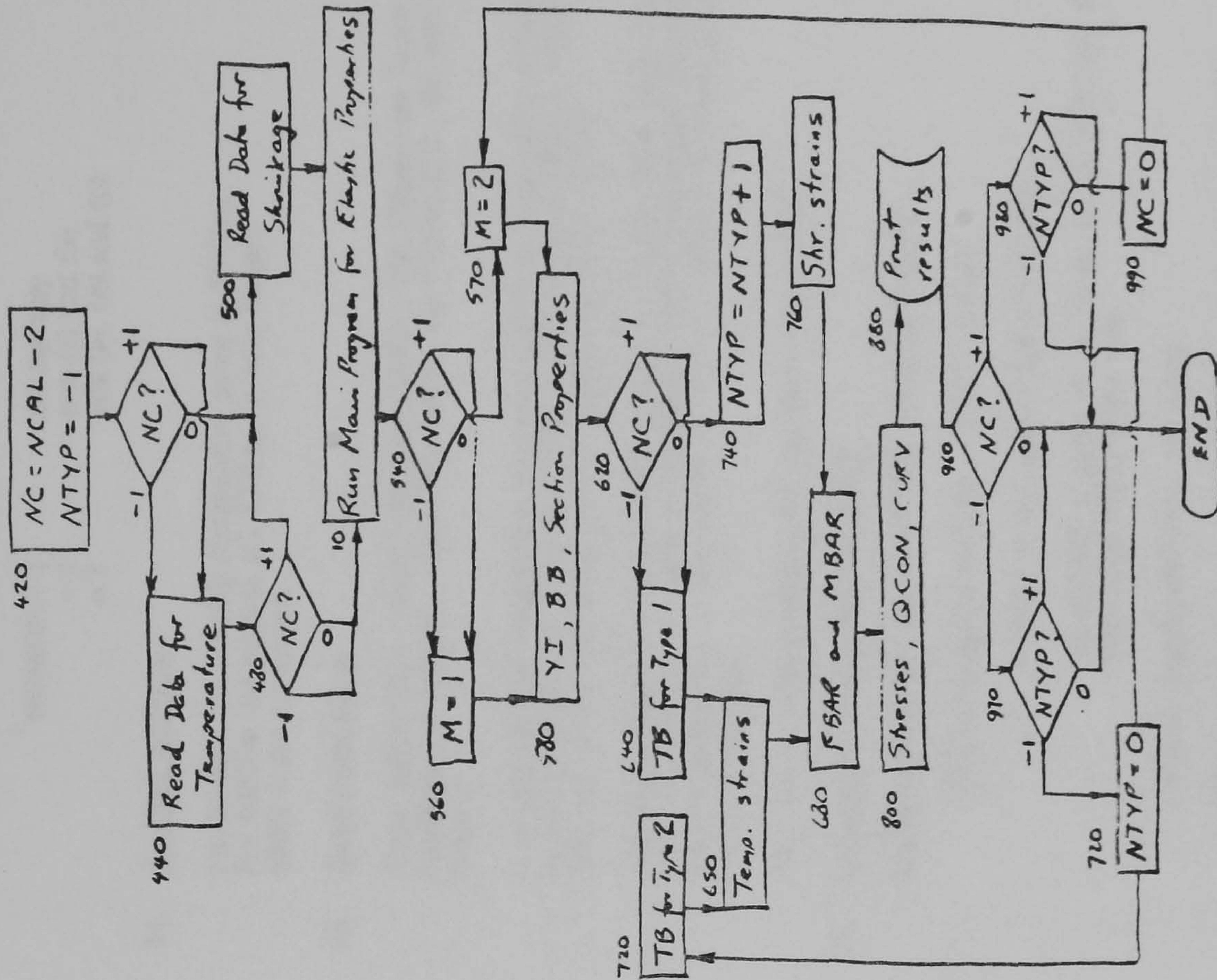
- (a) Repeat of input data.
- (b) Elastic hogging bending: - BMHE; then stresses FBH, FTHS, FTHR; then D2YT - Slendernesses SLFL, SLWEB
- (c) Modular ratio, then Table 1, then elastic sagging bending: BMSE; stresses FB, FT, FC; ratio FCRAT. Then results for the next modular ratio, etc.
- (d) If NCAL > 0, the TSC results as in section 8.2.
- (e) Plastic sagging bending: BMS, YP, SHPFS
- (f) Plastic hogging bending: BMPLH, YPH, SHPFH, SLBRAT
BMH, BMHR
CITY CTRAMP

(g) Input data for NOPT = 2.

(h) Shear strength and safety ratio: VD, VR, R.

Outputs (e) and (f) occur only when NOPT > 0, and outputs (g) and (h) only when NOPT = 2.

15. Flowchart for TSC calculations



12th April 1984

RPJ

Computer Program EPPCB1.f. "Elastic and plastic properties of a composite beam"

This note sets out the changes from the program EPPCB. The note of April 1984 on EPPCB should be read first. Its paragraph numbers are used here.

2. Scope and options

The values NCAL = 0, NOPT = 1 are written into the program.

3. Properties of materials

For concrete, Young's modulus (EC) is input, in place of AE(M). For all elastic calculations, AE = ES/EC. There is no provision for a lateral buckling stress SLB. In place of SCC, FCYL (cylinder strength of concrete) is input, and SCC is always taken as $0.85f_c/\gamma_c$. Shear is not considered.

4. Geometry of section

The clear depth of the web (d in EC4) is input as HWEBCL. This must allow for fillets in rolled sections and welds in welded sections. Reinforcement areas ART and ARB are not lumped together.

7. Input of data on file CSDAT

Runs are identified by the name of the beam, BNUM, (alphanumeric up to 20 characters). The input lines and sequence are :

BNUM
ES, ER, EC
BC, HC, BH, HH, ART, YRT, ARB, YRB, NRS, N
B(1), H(1), ..., B(N), H(N)
HWEBCL
SYF, SYW, SRTT, SRTB, SRC, FCYL
NGMOP (see para.9 below)

Measured or mean values should be input, NOT characteristic or specified values.

7.1 Slab reinforcement

In plastic analysis for sagging bending, the bottom layer of slab reinforcement is ignored. If ART is incorrect for the top layer, allow for this by altering SRC.

7.2 & 7.3 Non-composite sections, composite plates

Do not use the program for these.

9. Design philosophy

All calculations of plastic properties are based on design strengths f_y/γ_a , $0.85f_c/\gamma_c$, f_s/γ_s , etc.

Three sets of γ values are written into the program :

| | γ_a | γ_c | γ_s |
|-----|------------|------------|------------|
| (a) | 1.0 | 1.0 | 1.0 |
| (b) | 1.0 | 1.5 | 1.15 |
| (c) | 1.1 | 1.5 | 1.15 |

The outputs are determined by the input NGMOP, thus :

| | |
|-----------|-----------------------|
| NGMOP = 1 | set (a) only |
| = 2 | sets (a) and (b) |
| = 3 | sets (a), (b) and (c) |

11. Bending strengths

For BMHE, the limiting compressive stress is SYF/γ_a . For BMHR, the stresses are SYF/γ_a in both flanges. BMH is not computed.

13. Slenderness ratios

These follow EC4 : Part 1 (October 1990). The Classes are listed as continuous functions, not integers. Thus, for a value $1.0 < \text{value} \leq 2$, the web or flange is in Class 2.

It is assumed that slenderness zero corresponds to Class zero. Linear interpolation is used between this point and Class 1, and between Class 1 and 2. Values > 2 using the plastic neutral axis are extrapolations of the 1-2 line.

All values using the elastic neutral axis lie on the line from the origin to the point defined in EC4 as the class 3/4 interface. Thus a web with a slenderness around 2 (on this basis) may or may not be in Class 2, because that is determined using the plastic neutral axis.

The "hole-in-web" procedure has not been programmed.

14. Sequence of output (file EPPROUT)

Generally as in the note on EPPCB, except as follows :

(b) Elastic hogging bending : - D2YT omitted

- C/TEPS is c/t_e as in Table 4.1 of EC4

- ALD/TEPS is $\alpha d/t_e$ as in Table 4.2 of EC4, but for an elastic stress distribution in the web.

(c) Plastic sagging bending : no change

(f) Plastic hogging bending : - BMPLH, YPH, SHPFH, BMHR

- C/TEPS and Class of flange copied from (b) above

- ALD/TEPS as in (b), but for plastic stress distribution

- If flange in class 1 or 2 and web in class 3, applicability of "hole-in-web" method is stated.


```

C ** EPPCB1.f
C FINDS ELASTIC AND PLASTIC PROPERTIES OF A COMPOSITE BEAM
C IN ACCORDANCE WITH THE OCTOBER 1985 DRAFT OF EC4:PART 1, USING 3 SETS
C OF VALUES OF GAMMA-M, FOR THE ULTIMATE LIMIT STATE.
C IT IS BASED ON EPPCB, AS AT 30 NOV. 1990. ITS SUBROUTINE PLCS1 IS
C BASED ON PLCS IN EPPCB.
C There is provision for only one modular ratio, based on EC as
C input. The following are not considered: unproped construction,
C lateral buckling, TSC effects, vertical shear, M-V interaction,
C haunches within profiled sheeting, shear lag, the hole-in-web method,
C partial shear connection.
C In sagging bending, compressive stress in the top layer of
C reinforcement is allowed for, but not in the second layer. In hogging
C bending, both layers are effective.
C
C * REVISED 9 APR 84. ZRAT ADDED 18 JUL 85. AR CORRECTED IN PLCS,
C * 11 NOV 85.
C * Converted to SUN UNIX by AJH 8/8/90. Last revised 13 Dec. 1990.
C
C IMPLICIT REAL(I)
C DIMENSION B(5),H(5),Y(5),A(5),GM(3,3)
C CHARACTER*60 BNUM
C COMMON B,H,Y,A
C OPEN(1,FILE='csdat')
C OPEN(2,FILE='eppout')
C
C INPUT OF DATA
C READ(1,*) (A,I) BNUM
C WRITE(2,320) BNUM
C320 FORMAT (' DATA FOR BEAM NO. ',A60,/)
C READ(1,*) ES,ER,EC
C WRITE(2,330) ES,ER,EC
C330 FORMAT (' ES=',F8.0,3X,'ER=',F8.0,3X,'EC=',F8.0)
C NCAL=0
C NOPT=1
C AE=ES/EC
C WRITE(2,340) AE
C340 FORMAT (' MODULAR RATIO',3X,F7.3)
C READ(1,*) BC,HC,BH,HH,ART,YRT,ARB,YRB,NRS,N
C WRITE(2,360) BC,HC,BH,HH
C360 FORMAT (' CONCRETE SLAB',4F10.1, )
C WRITE(2,370) ART,YRT,ARB,YRB,NRS,N
C370 FORMAT (' REINFORCEMENT',4F10.1,3X,'NRS=',I1,3X,'N=',I1,/)
C READ(1,*) (B(J),H(J),J=1,N)
C WRITE(2,380) (B(J),H(J),J=1,N)
C380 FORMAT (' RSJ OR PLATE, B AND H',2F14.1, )
C READ(1,*) HWEBCL
C WRITE(2,382) HWEBCL
C382 FORMAT (' CLEAR DEPTH OF WEB=',F7.1)
C READ(1,*) SYF,SYW,SRTT,SRTB,SRC,FCYL
C WRITE(2,390) SYF,SYW,SRTT,SRTB,SRC,FCYL
C390 FORMAT (' SYF=',F5.1,' SYW=',F5.1,3X,'SRTT=',F6.1,3X,'SRTB=',F6.1
C +',F5.1,2X,'SRC=',F5.1,3X,'FCYL=',F5.1)
C READ(1,*) NGMOP
C WRITE(2,392) NGMOP
C392 FORMAT (' NGMOP=',I2,/)
C
C * VALUES OF GAMMA M
C394 GM(1,1) = 1.0
C GM(1,2) = 1.0
C GM(1,3) = 1.0
C GM(2,1) = 1.0
C GM(2,2) = 1.5
C GM(2,3) = 1.15
C GM(3,1) = 1.1

```

```

C GM(3,2) = 1.5
C GM(3,3) = 1.15
C ** STEEL SECTION ONLY
C10 YIN = HC+HH
C20 NRT = NRS+1
C GO TO (40,30),NRT
C
C * ROLLED SECTION REPLACED BY THREE PLATES
C30 ISR = H(3)
C YNS = YIN+H(2)/2
C YBS = YIN+H(2)
C HRS=H(2)
C H(1)=(B(3)-H(2)*B(2))/(2*(B(1)-B(2)))
C H(3)=H(1)
C B(3)=B(1)
C H(2)=H(2)-2*H(1)
C WRITE(2,35) H(1), H(2)
C35 FORMAT (' * The steel section is rolled, where',/,
C +',
C H(1)=H(3)=',F4.1,', H(2)=',F6.1,',/,/)
C
C * 3 TO 5 PLATES
C40 AS = 0
C DO 50 J = 1,N
C A(J) = H(J)*B(J)
C AS = AS+A(J)
C50 CONTINUE
C Y(1) = YIN+H(1)/2
C DO 60 J = 2,N
C Y(J) = Y(J-1)+(H(J-1)+H(J))/2
C60 CONTINUE
C FMA = 0
C DO 70 J = 1,N
C FMA = FMA+A(J)*Y(J)
C70 CONTINUE
C YNS = FMA/AS
C YBS = Y(N)+H(N)/2
C IS = 0
C DO 80 J = 1,N
C IS = IS+A(J)*H(J)**2/12+A(J)*(Y(J)-YNS)**2
C80 CONTINUE
C IF (N-NRS-2) 135,85,135
C85 IS=ISR
C
C * SECTION MODULI
C135 ZTS = - IS/(YNS-YIN)/1.E06
C ZBS = IS/(YBS-YNS)/1.E06
C
C ** CRACKED REINFORCED SECTION, HOGGING
C140 ARTT = ART*ER/ES
C ARBT = ARB*ER/ES
C AC = AS+ARTT+ARBT
C YNC = (AS*YNS+ARTT*YRT+ARBT*YRB)/AC
C IC = IS+AS*(YNS-YNC)**2+ARTT*(YNC-YRT)**2+ARBT*(YNC-YRB)**2
C ZTHR = -IC*(ES/ER)/(YNC-YIN)/1.E06
C ZBHS = IC/(YBS-YNC)/1.E06
C AR = ARTT + ARBT
C IF (AR) 143,143,145
C143 YBAR=0
C GO TO 147
C145 YBAR = (ARTT*(YIN-YRT)+ARBT*(YIN-YRB))/AR
C147 AYCH = AR*YBAR*1000/IC
C
C ** UNCRACKED UNREINFORCED SECTION
C YH = HC+HH/2

```



```

ACT = BC*HC/AE
AHT = BH*HH/AE
AU = AS+ACT+AHT
YNU = (AS*YNS+ACT*HC/2+AHT*YH)/AU
IU = IS+AS*(YNS-YNU)**2+(ACT*HC*HC+AHT*HH*HH)/12+ACT*
1 (YNU-HC/2)**2+AHT*(YNU-YH)**2
* SECTION MODULI AND AY/I
160 ZTUC = -IU*AE/YNU/1.E06
ZTUS = IU/(YIN-YNU)/1.E06
ZBU = IU/(YBS-YNU)/1.E06
IF (YNU-HC-HH) 162,162,163
162 AYU = AS*(YNS-YNU)*1000/IU
163 ACE = ACT+AHT
YBAR=(ACT*(YNU-HC/2)+AHT*(YNU-HC-HH/2))/ACE
AYU = ACE*YBAR*1000/IU
C
C
C
** CRACKED UNREINFORCED SECTION
170 IF (YNU-YIN) 190,180,180
180 YN = YNU
ACU=AU
I=IU
ZTC=ZTUC
ZT=ZTUS
ZB=ZBU
AYC=AYU
GO TO 240
190 IF (YNU-HC) 220,220,200
200 IF (AS*(YNS-HC)-ACT*HC/2) 220,220,210
C
C
* NEUTRAL AXIS IN HAUNCH
210 YN = (AS*YNS+ACT*HC/2+BH*(HH/2)*(HC+HH/4)/AE)/(ACT+AS
1 +BH*(HH/2)/AE)
ACU = AS+ACT*(YN-HC)*BH/AE
I = IS+AS*(YNS-YN)**2+ACT*HC**2/12+ACT*(YN-HC/2)**2
1 +BH*(YN-HC)**3/3/AE
GO TO 230
C
C
* NEUTRAL AXIS IN SLAB
220 C1 = AE*AS/BC
C2 = SQRT(C1**2+2*C1*YNS)
YN = C2-C1
ACU = AS+BC*YIN/AE
I = IS+AS*(YNS-YN)**2+BC*YIN**3/3/AE
C
C
* SECTION MODULI AND AY/I
230 ZTC = -I*AE/YN/1.E06
ZT = I/(YIN-YN)/1.E06
ZB = I/(YBS-YN)/1.E06
AYC = AS*(YNS-YN)*1000/I
C
C
* SCALING OF I
240 ISS = IS/1.E06
I = I/1.E06
ICS = IC/1.E06
IU = IU/1.E06
C
C
** OUTPUT OF RESULTS
WRITE (2,270)
270 FORMAT (27X,'STEEL',4X,'UNCRACKED',6X,'CRACKED',6X,'HOGGING',/)
WRITE (2,280)YNS,YNU,YN,INC,AS,AU,ACU,AC
280 FORMAT (' NEUTRAL AXIS',6X,4F13.1,/, ' A,STEEL UNITS',5X,4F13.0,/)
WRITE (2,290)ISS,IU,ICS
290 FORMAT (' I(E-6),STEEL UNITS',4F13.2,/)
WRITE (2,300)ZTUC,ZTC,ZTHR

```

```

300 FORMAT (' Z(E-6),SLAB OR RFT',13X,3F13.4)
WRITE (2,303)ZTS,ZTUS,ZT,ZTHS,ZBS,ZBU,ZB,ZBH
303 FORMAT (' Z(E-6),TOP FLANGE',1X,4F13.4,/, ' Z(E-6),BOT FLANGE',1X,
1 4F13.4,/)
WRITE (2,304) AYU,AYC,AYCH
304 FORMAT (' SHEAR FACTOR AY/I,M** (-1) UNITS',3F13.5,/)
WRITE (2,305)
305 FORMAT (' NOTE: ALL RESULTS IN MM UNITS EXCEPT WHERE NOTED',)
C
C
** LOOP FOR GAMMA-M
DO 1150 JG=1,NGMOP
GMA = GM(JG,1)
GMC = GM(JG,2)
GMR = GM(JG,3)
SRCD = SRC/GMR
SYFD = SYF/GMA
SYWD = SYW/GMA
SRTTD = SRTT/GMR
SRTBD = SRTB/GMR
SCCD = 0.85*FCYL/GMC
C
C
* ELASTIC RESISTANCE, HOGGING BENDING, PROPPED
2170 BMHE=-ZBH*SYFD
BMHET=-ABS(ZTHS*SYFD)
BMHER=ZTHR*SRTTD
IF (BMHET-BMHE) 2190,2190,2180
2180 BMHE=BMHET
2190 IF (BMHER-BMHE) 2210,2210,2200
2200 BMHE=BMHER
2210 FBH=BMHE/ZBH
FTHS=BMHE/ZTHS
FTHR=BMHE/ZTHR
WRITE (2,2213) GMA,GMC,GMR
2213 FORMAT (///,10X,'RESULTS FOR GMA=',F5.2,' GMC=',F5.2,' GMR=',
+ F5.2)
WRITE (2,2215)
2215 FORMAT (//,'.HOGGING BENDING OF SLENDER SECTION.....',/)
WRITE (2,2220) BMHE,FBH,FTHS,FTHR
2220 FORMAT (' BMHE=',F8.2,4X,'FBH=',F6.1,1X,'FTHS=',F6.1,1X,
1 'FTHR=',F6.1)
C
C
* SLENDERNESSES (ELASTIC N.A.) TO EC4 (OCT 1990)
BFBR=B(3)
BFTH=H(3)
IF (N-3) 2261,2261,2230
2230 DO 2260 J=4,N
IF (B(J)-BFBR) 2250,2250,2240
2240 BFBR=B(J)
2250 BFTH=BFTH+H(J)
2260 CONTINUE
2261 EPSFL = SQRT(235/SYF)
EPSWB = SQRT(235/SYW)
C
* BOTTOM FLANGE
IF (NRS) 2267,2267,2262
2262 CTEE = BFBR/(2*BFTH*EPSFL)
IF (CTEE-11) 2263,2263,2266
2263 IF (CTEE-10) 2264,2264,2265
2264 CLFL = CTEE/10
GO TO 3271
2265 CLFL = CTEE-9
GO TO 3271
2266 CLFL = (CTEE-3)/4
GO TO 3271
2267 WELD = (H(2)-HWEBCL)/2
CTEE = (BFBR-B(2)-2*WELD)/(2*BFTH*EPSFL)
IF (CTEE-10) 2268,2268,2271

```



```

2268 IF (CTEE-9) 2269,2269,2270
2269 CLFL = CTEE/9
GO TO 3271
2270 CLFL = CTEE-8
GO TO 3271
2271 CLFL = (CTEE-2)/4
C * CLASS IS THE NEAREST INTEGER GTE THE VALUE GIVEN
C * WEB
3271 DWEBC = YIN+H(1)+(H(2)+HWEBCL)/2-YNC
WRITE (2,3272) DWEBC
3272 FORMAT (' DWEBC=',F7.1)
IF (DWEBC.LE.0) GO TO 3273
PSI = -(HWEBCL-DWEBC)/DWEBC
ALPHA = 1/(1-PSI)
IF (PSI-1) 2273,2273,2274
2273 DTEREQ = 62*EPSWB*(1-PSI)*SQRT(-PSI)
GO TO 2275
2274 DTEREQ = 42*EPSWB/(0.67+0.33*PSI)
2275 DTEE = HWEBCL/B(2)/EPSWB
CLWEB = 3*DTEE/DTEREQ
ALDTEE = ALPHA*DTEE
WRITE (2,2280) CTEE,CLFL,ALDTEE,CLWEB,PSI,DTEREQ
2280 FORMAT (' FLANGE: C/TEPS=',F6.1,5X,'CLASS=',F5.2,/, ' WEB:
+ALD/TEPS=',F6.1,5X,'CLASS=',F5.2,5X,'PSI=',F7.3,3X,'DTEREQ=',
+ ,F6.1)
WRITE (2,2282)
2282 FORMAT (5X,'NOTE: the "web class" is three times the ratio of',
+ x,'actual to required',/,5X,'slenderness at the Class 3/4',
+ x,'boundary, so a value 3.1 (e.g.) means Class 4.')
C * RESISTANCE IN SAGGING BENDING, PROPPED, SYF GOVERNS
C
3273 BMSEB=ZB*SYFD
BMSET=ABS(ZT*SYFD)
IF (BMSEB-BMSET) 2320,2320,2330
2320 BMSE=BMSEB
GO TO 2340
2330 BMSE=BMSET
2340 FB=BMSE/ZB
FT=BMSE/ZT
FC=BMSE/ZTC
FCRAT=-FC/SCCD
WRITE (2,2345)
2345 FORMAT (' .SAGGING BENDING OF SLENDER SECTION.....',/)
2350 FORMAT (' BMSE=',F8.2,5X,'FB=',F6.1,3X,'FT=',F6.1,3X,'FC=',F6.1,
1 2X,'FCRAT=',F6.3)
2360 BMSEM=BMSE
C ** PLASTIC SECTION PROPERTIES
C
1140 CALL PLCS1(BC,HC,BH,HH,ART,YRT,ARB,YRB,NRT,N,SYFD,SYWD,SRTTD,
+ SRTBD,SRCD,SCCD,BNUM,NOPT,BMSEM,BMHE,YIN,HRS,CTEE,CLFL,ZBH,
+ HWEBCL,EPSFL,EPSWB)
1150 CONTINUE
C
CLOSE (1)
CLOSE (2)
C
STOP
END
C
SUBROUTINE PLCS1(BC,HC,BH,HH,ART,YRT,ARB,YRB,NRT,N,SYFD,SYWD,
+ SRTTD,SRTBD,SRCD,SCCD,BNUM,NOPT,BMSEM,BMHE,YIN,HRS,CTEE,CLFL
+ ,ZBH,HWEBCL,EPSFL,EPSWB)
C ** PLCS1 FINDS PLASTIC PROPERTIES FOR A COMPOSITE SECTION

```

```

C according to EC4:Part 1, October 1990
C
DIMENSION B(5),H(5),Y(5),A(5)
COMMON B,H,Y,A
CHARACTER*60 BNUM
C * LONGITUDINAL FORCES
AR=ART+ARB
780 FTF=B(1)*H(1)*SYFD
FW=B(2)*H(2)*SYWD
A(3)=B(3)*H(3)
FBF=A(3)*SYFD
800 FRC=ART*(SRCD-SCCD)
C * Force in bottom reinforcement neglected, for sagging bending
FS=BC*HC*SCCD
FH=BH*HH*SCCD
820 FRTT=ART*SRTTD
FRTB = ARB*SRTBD
FRT = FRTT+FRTB
WRITE (2,825) FS,FRC,FRT,FH,FTF,FW,FBF
825 FORMAT (' FS=',E10.3,' FRC=',E10.3,' FRT=',E10.3,'
+ E10.3,/, ' FTF=',E10.3,' FW=',E10.3,' FBF=',E10.3)
C * EXTRA PLATES MERGED WITH BOTTOM FLANGE
80 NN=N-2
GO TO (110,90,90),NN
90 FMA=A(3)*Y(3)
ABOT=A(3)
DO 100 J=4,N
A(J)=B(J)*H(J)
A(3)=A(3)+A(J)
Y(J)=Y(J-1)+(H(J-1)+H(J))/2
FMA=FMA+A(J)*Y(J)
Y(3)=FMA/A(3)
100 CONTINUE
FBF=FBF*A(3)/ABOT
110 FSTL=FTF+FW+FBF
C ** SAGGING MOMENTS OF RESISTANCE
C * NA IN SLAB
115 BMPT=FBF*Y(3)+FW*Y(2)-FRC*YRT
IF (FSTL-FRC-FS) 120,120,130
120 YP=(FSTL-FRC)/SCCD/BC
BMS=BMPT+FTF*Y(1)-YP*SCCD*BC*YP/2
GO TO 180
C * NA IN HAUNCH
130 IF (FSTL-FRC-FS-FH) 140,140,150
140 FPH=FSTL-FRC-FS
YP=FPH/SCCD/BH + HC
BMS=BMPT+FTF*Y(1)-FS*HC/2-FPH*(HC+YP)/2
GO TO 180
C * NA IN TOP FLANGE
150 FORCE=(FSTL+FH+FS+FRC)/2
BMSTL=BMPT+FRC*YRT+FTF*Y(1)
BMCON=FRC*YRT+FS*HC/2+FH*(HC+HH/2)
IF (FW+FBF-FORCE) 160,160,170
160 FPTF=FORCE-FRC-FS-FH
YP=YIN+FPTF/B(1)/SYFD
BMS=BMSTL-BMCON-FPTF*(YP+YIN)
GO TO 180
C * NA IN WEB
170 FPW=FORCE-FRC-FS-FH-FTF
YP=YIN+H(1)+FPW/B(2)/SYWD
BMS=BMSTL-BMCON-FPW*(YP+YIN+H(1))-2*FTF*Y(1)
180 BMS=BMS/1.E06
SHFFS=BMS/BMSEM

```



```

C
C ** HOGGING MOMENTS OF RESISTANCE
185 FORCE=(FSTL+FRT)/2
C BMPH=FBF*Y(3)+FW*Y(2)-FRTT*YRT-FRTB*YRB+FTF*Y(1)
C * NA IN TOP FLANGE
190 IF (FW+FBF-FORCE) 190,190,200
C FPF=FORCE-FRT
C YPH=YIN+FPF/B(1)/SYFD
C BMLH=(BMPH-FPF*(YPH+YIN))
C GO TO 220
C * NA IN WEB
200 IF (FBF-FORCE) 210,210,220
210 FPW=FORCE-FRT-FTF
C YPH=YIN+H(1)+FPW/B(2)/SYWD
220 BMLH=(BMPH-2*FTF*Y(1)-FPW*(YPH+YIN+h(1)))
C SHPFH=BMLH/BMHE
C WRITE (2,222)
222 FORMAT (/,', BENDING STRENGTHS OF COMPACT SECTION.....',/)
C
C * WEB EXCLUDED
C FLTT=FRT+FTF
C BMHR=FLTT*Y(3)-FRTT*YRT-FRTB*YRB-FTF*Y(1)
C FBFC=FBF
C IF (FLTT-FBFC) 240,240,230
230 BMHR=BMHR*FBFC/FLTT
240 BMHR=-BMHR/1.E06
C
C * SLENDERNESS OF WEB (PLASTIC N.A.) TO EC4
C DWBEC = YIN+H(1)+H(2)+HWEBCL)/2-YPH
C ALPHA = DWBEC/HWEBCL
C DTE = HWEBCL/B(2)/EPSWB
C ALDTE = ALPHA*DTE
C IF (ALPHA-0.5) 242,242,248
242 IF (ALDTE-36) 244,244,246
244 CLWEB = ALDTE/36
C GO TO 253
246 CLWEB = (ALDTE-30.5)/5.5
C GO TO 253
248 DTEREQ = 396/(13*ALPHA-1)
C IF (DTE-DTEREQ) 250,250,252
250 CLWEB = DTE/DTEREQ
C GO TO 253
252 CLWEB = (DTE*(13*ALPHA-1)-336)/60
C
C * OUTPUT FOR NOPT=1
253 WRITE (2,255) BMS,YP,SHPFH
255 FORMAT (' BMS=',F10.2,' kNm YP=',F7.1,' SHPFH=',F6.3)
C WRITE (2,257) BMLH,YPH,SHPFH,BMHR
257 FORMAT (/,', BMLH=',F10.2,' kNm YPH=',F7.1,' SHPFH=',F6.3,
+ ', BMHR=',F10.2,' kNm')
C WRITE (2,260) CTEE,CLFL,ALDTE,CLWEB
260 FORMAT (' FLANGE: C/TEPS=',F6.1,5X,' CLASS=',F5.2,/,', WEB:
+ ALD/TEPS=',F6.1,5X,' CLASS=',F5.2)
C IF (CLWEB-2) 480,480,262
262 IF (CLFL-2) 264,264,480
264 WRITE (2,265)
265 FORMAT (' Hole in web procedure applicable, unless class of web',
+ ',X', (elastic n.a.) exceeds 3.0')
C GO TO 480
C
C ** SHEAR RESISTANCE
280 READ (1,*) TAU,TAUR,GMB,GMV,BM,V
C WRITE (2,285) TAU,TAUR,GMB,GMV,BM,V
285 FORMAT (/,', TAU=',F5.1,' TAUR=',F5.1,' GMB=',F5.3,' GMV=',F5.3,
1 ' BM=',F10.3,' V=',F9.3,/)

```

```

290 GO TO (300,310),NRT
300 DW=H(2)
C GO TO 320
310 DW=HRS
320 VD=TAUR*B(2)*DW/10**3
C VR=TAUR*B(2)*DW/10**3
C ** SAFETY RATIO, HOGGING BENDING
330 DMH=ABS (BMH/GMB)
C DMHR=ABS (BMHR/GMB)
C DVD=VD/GMV
C DVR=VR/GMV
335 IF (BM) 350,340,350
340 R=V/DVD
C GO TO 460
350 BM=ABS (BM)
C VOM=V/BM
360 IF (VOM-DVR/2/DMH) 360,360,370
C R=BM/DMH
C GO TO 460
370 IF (VOM-DVR/DMHR) 380,380,390
380 R=(2*V*(DMH-DMHR)+BM*DVR)/DVR/(2*DMH-DMHR)
C GO TO 460
390 IF (VOM-2*DVD/DMHR) 400,400,340
400 R=(2*BM*(DVD-DVR)+V*DMHR)/DMHR/(2*DVD-DVR)
C
C * OUTPUT FOR NOPT=2
C WRITE (2,450)
450 FORMAT (/,', SHEAR STRENGTH OF COMPACT SECTION')
460 WRITE (2,470) VD,VR,R
470 FORMAT(' VD=',F10.2,' KN VR=',F10.2,' KN SAFETY RATIO=',F7.3)
480 RETURN
C END

```


The following are the input data files, csdat, for the test specimens in sagging bending used for calibration.

```

BEAM NO 1 (THOMAS)
210.00 200.00 19.10
1499.0 76.0 114.5 51.0 198.0 23.0 0.0 51.0 1 3
123.5 10.7 7.2 303.8 4750.0 71620000.0
264.6
308.00 308.00 529.00 0.00 22.99 27.04
1
*****
BEAM NO.1
210.00 200.00 31.03
610.0 60.0 0.0 445.4 20.0 148.4 35.0 1 3
76.2 9.6 5.8 152.0 2271.0 8737000.0
112.0
301.9 301.9 315.95 315.95 40.5 47.6
1
*****
BEAM NO.2
210.00 200.00 33.38
610.0 60.0 0.0 445.4 20.0 148.4 35.0 1 3
76.2 9.6 5.8 152.0 2271.0 8737000.0
112.0
330.2 330.2 315.95 315.95 31.94 37.58
1
*****
A1
210.00 200.00 29.80
1219.0 152.0 0.0 1797.0 25.0 1797.0 25.0 1 3
152.4 17.8 11.0 304.8 8387.1 131850000.0
280.0
233.00 233.00 400.00 400.00 18.7 22.0
1
*****
A2
210.00 200.00 27.03
1219.0 152.0 0.0 198.0 25.0 198.0 127.0 1 3
152.4 17.8 11.0 304.8 8387.1 131850000.0
260.0
234.00 234.20 400.00 400.00 22.9 26.9
1
*****
A3
210.00 200.00 18.97
1219.0 152.0 0.0 198.0 25.0 198.0 127.0 1 3
152.4 17.8 11.0 304.8 8387.1 131850000.0
260.0
277.1 277.1 400.00 400.00 15.6 18.3
1
*****
A4
210.00 200.00 20.97
1219.0 152.0 0.0 198.0 25.0 198.0 127.0 1 3
152.4 17.8 11.0 304.8 8387.1 131850000.0
260.0
278.4 278.4 400.00 400.00 17.0 20.0
1

```

```

*****
A5
210.00 200.00 28.48
1219.0 152.0 0.0 198.0 25.0 198.0 127.0 1 3
152.4 17.8 11.0 304.8 8387.1 131850000.0
260.0
260.8 260.8 400.00 400.00 21.1 24.8
1
*****
C1
210.00 200.00 31.17
1219.0 152.0 0.0 198.0 25.0 198.0 127.0 1 3
152.4 17.8 11.0 304.8 8387.1 131850000.0
260.0
252.8 252.8 400.00 400.00 21.1 24.8
1
*****
D1
210.00 200.00 27.86
1219.0 152.0 0.0 198.0 25.0 198.0 127.0 1 3
152.4 17.8 11.0 304.8 8387.1 131850000.0
260.0
266.4 266.4 400.00 400.00 16.6 19.5
1
*****
F1
210.00 200.00 30.90
1219.0 152.0 0.0 198.0 25.0 198.0 127.0 1 3
152.4 17.8 11.0 304.8 8387.1 131850000.0
260.0
274.3 274.3 400.00 400.00 18.6 21.9
1
*****
T1
210.00 200.00 30.34
1219.0 152.0 0.0 1797.0 25.0 1797.0 127.0 1 3
152.4 17.8 11.0 304.8 8387.1 131850000.0
260.0
233.2 233.2 400.00 400.00 16.2 19.1
1
*****
B1
210.00 200.00 30.48
1219.0 152.0 0.0 198.0 25.0 198.0 127.0 1 3
152.4 17.8 11.0 304.8 8387.1 131850000.0
260.0
229.2 229.2 400.00 400.00 26.3 30.9
1
*****
E1
210.00 200.00 33.59
1219.0 152.0 0.0 198.0 25.0 198.0 127.0 1 3
152.4 17.8 11.0 304.8 8387.1 131850000.0
260.0
268.5 268.5 400.00 400.00 27.8 32.7
1
*****
U1

```



```

210.00 200.00 34.48
1219.0 152.0 0.0 198.0 25.0 198.0 127.0 1 3
152.4 17.8 11.0 8397.1 131850000.0
260.0
268.2 268.2 400.00 22.4 26.3
1
*****
U2 210.00 200.00 29.31
1219.0 152.0 0.0 198.0 25.0 198.0 127.0 1 3
152.4 17.8 11.0 8387.1 131850000.0
260.0
225.9 225.9 400.00 25.6 30.1
1
*****
U3 210.00 200.00 40.34
1219.0 152.0 0.0 198.0 25.0 198.0 127.0 1 3
152.4 17.8 11.0 8387.1 131850000.0
260.0
231.3 231.3 400.00 22.7 26.7
1
*****
CB2 210.00 200.00 34.48
305.0 76.0 0.0 190.0 25.4 31.7 50.8 1 3
44.5 8.3 4.6 1232.3 2801000.0
89.4
286.2 286.2 427.57 20.52 24.14
1
*****
CB4 210.00 200.00 34.48
305.0 76.0 0.0 190.0 25.4 31.7 50.8 1 3
44.5 8.3 4.6 1232.3 2801000.0
89.4
286.2 286.2 427.57 18.76 22.07
1
*****
SS1 210.00 200.00 30.00
254.0 127.0 0.0 0.0 25.0 0.0 102.0 1 3
133.8 9.6 6.3 206.8 3800.0 28870000.0
172.3
220.00 220.0 400.00 34.68 40.80
1
*****
SS2 210.00 200.00 30.00
305.0 127.0 0.0 0.0 25.0 0.0 102.0 1 3
133.8 9.6 6.3 206.8 3800.0 28870000.0
192.0
249.00 249.00 400.00 36.04 42.40
1
*****
SS3 210.00 200.00 30.00
406.0 127.0 0.0 0.0 25.0 0.0 102.0 1 3
133.8 9.6 6.3 206.8 3800.0 28870000.0

```

```

192.0
303.00 303.00 400.00 26.52 31.20
1
*****
SS6 210.00 200.00 30.00
616.0 127.0 0.0 0.0 25.0 0.0 102.0 1 3
133.8 9.6 6.3 206.8 3800.0 28870000.0
192.0
304.00 304.00 400.00 26.52 31.20
1
*****
CB10 210.00 200.00 30.00
915.0 76.0 0.0 679.0 25.0 314.0 52.0 1 3
133.8 9.6 6.3 206.8 3800.0 28870000.0
172.0
276.00 276.00 504.00 25.0 29.4
1
*****
CB12 210.00 200.00 30.00
1220.0 102.0 0.0 904.0 26.0 113.0 76.0 1 3
133.8 9.6 6.3 206.8 3800.0 28870000.0
172.0
267.00 267.00 504.00 25.2 29.7
1
*****
GIRDER 2 210.00 200.00 29.65
1193.8 190.5 0.0 506.7 25.0 507.7 165.5 0 3
254.0 12.7 6.4 1016.0 406.4 25.5
1016.0
338.2 338.2 404.80 33.4 39.3
1
*****
GIRDER 3 210.00 200.00 34.48
1168.4 165.1 0.0 1520.1 82.6 0.0 140.1 0 3
203.2 15.9 5.0 812.8 406.4 19.1
812.8
364.5 364.5 1669.00 0.00 43.4 51.0
1

```

The following are the input data files, csdat, for the test specimens in hogging bending used for calibration. The specimens in samples H5 to H14 (see Table 4.2 in the thesis) are not calculated by EPPCBI, because the reported theoretical resistances [50] have been used for the analysis.

```

BEAM NO.1
210.00 200.00 31.03
610.0 60.0 0.0 445.4 20.0 148.4 35.0 1 3
76.2 9.6 5.8 152.0 2271.0 8737000.0
112.0
301.9 301.9 315.95 315.95 40.5 47.6
1

```

BEAM NO.2
 210.00 200.00 33.38
 610.0 60.0 0.0 0.0 445.4 20.0 148.4 35.0 1 3
 76.2 9.6 5.8 152.0 2271.0 8737000.0
 112.0
 330.2 330.2 315.95 315.95 31.94 37.58
 1

CB2
 210.00 200.00 34.48
 305.0 76.0 0.0 0.0 190.0 25.4 31.7 50.8 1 3
 44.5 8.3 4.6 120.7 1232.3 2801000.0
 89.4
 286.2 286.2 427.57 427.57 20.52 24.14
 1

CB4
 210.00 200.00 34.48
 305.0 76.0 0.0 0.0 190.0 25.4 31.7 50.8 1 3
 44.5 8.3 4.6 120.7 1232.3 2801000.0
 89.4
 286.2 286.2 427.57 427.57 18.76 22.07
 1

SC-3S
 210.00 200.00 23.93
 1524.0 152.0 0.0 0.0 1419.4 37.2 0.0 127.0 1 3
 212.5 14.0 10.3 532.3 11274.0 518360000.0
 490.0
 240.0 240.0 310.30 310.30 26.86 31.60
 1

SC-4S
 210.00 200.00 27.17
 1524.0 152.0 0.0 0.0 2419.4 52.3 0.0 127.0 1 3
 209.7 14.0 10.5 533.0 11376.0 523230016.0
 490.0
 240.0 240.0 310.30 310.30 23.72 27.90
 1

GIRDER 3
 210.00 200.00 34.48
 1168.4 165.1 0.0 0.0 1520.1 82.6 0.0 140.1 0 3
 203.2 15.9 6.4 812.8 406.4 34.9
 812.8
 363.1 363.1 1669.00 0.00 43.4 51.0
 1


```

67 write (4,67)
   format (3x,'Experimental result',6x,'Theoretical result',6x,
+ 'Ratio of expe. to theo.',/)
68 write (4,68) (es(i), ts(i), es(i)/ts(i), i=1,nn)
   format (9x,f7.2,17x,f7.2,21x,f6.4)
   write (4,1)
   write (4,69) nn
69 format (3x,'In this analysis',x,i3,' specimens are used.')
```

```

70 write (4,40) cmv
   write (4,41) cvoe
   write (4,42) cc
   write (4,1)
   write (4,70)
70 format (16x,'-----The analyzed resistance <KN-m>-----',/)
   write (4,75)
75 format (20x,'Theoretical mean',8x,'Design',8x,'Strength-altering'
+ ',')
   do 85 i=1,n
     rtm(i)=rtm(i)/1000000
     rd(i)=rd(i)/1000000
     rtn(i)=rtn(i)/1000000
     write (4,80) bnum(i), rtm(i), rd(i), rtn(i)
     format (5x,a,9x,f8.3,10x,f8.3,11x,f8.3)
80 continue
85 write (4,95)
95 format (/16x,'-----The relevant c.v. of bending resistance-----',/)
   write (4,100)
100 format (22x,'Theory',6x,'Log-theory',6x,'Reality',6x,'Log-reality'
+ ',')
   do 110 i=1,n
     write (4,105) bnum(i), (cov(i,j), j=1,4)
105 format (6x,a,6x,f5.3,9x,f5.3,10x,f5.3,10x,f5.3)
110 continue
   write (4,1)
   write (4,115)
115 format (/16x,'-----The safety factors and indices-----',/)
   write (4,120) mate
120 format (16x,'Safety index',3x,'S.F--model',4x,'S.F--steel',4x,
+ ',S.F--',a,/)
   abat=0.0
   amod=0.0
   vbat=0.0
   vmod=0.0
   do 130 i=1,n
     abat=abat+bata(i)/real(n)
     amod=amod+gamma(i,1)/real(n)
     write (4,125) bnum(i), bata(i), (gamma(i,j), j=1,3)
125 format (2x,a,8x,f5.3,9x,f5.3,9x,f5.3,10x,f5.3)
130 continue
   do 141 i=1,n
     vbat=vbat+(bata(i)/abat-1.0)**2/real(n-1)
     vmod=vmod+(gamma(i,1)/amod-1.0)**2/real(n-1)
141 continue
   vbat=sqrt(vbat)
   vmod=sqrt(vmod)
   write (4,143) abat,vbat
143 format (/3x,'The mean of design fractor, kd, is ',f5.3,
+ ', and the c.v of kd is ',f5.3,')
   write (4,144) amod,vmod
144 format (3x,'The mean of model factor, rmd, is ',f5.3,
+ ', and the c.v of rmd is ',f5.3,')
   write (4,131) sk
131 format (3x,'The parameter, ks, for characteristic',
+ ', strength of steel is ',x,f4.2,')
   write (4,38)
   write (4,132)

```

```

132 format (/16x,'-----Beam Data (N, mm)-----',/)
   if (comb.NE.'s'.and.comb.NE.'S') then
     write (4,133)
133 format (15x,'Ar',5x,'fy',5x,'ha',5x,'fr',5x,'ba',5x,'tw',
+ 5x,'tf',5x,'Aa',/)
   do 135 i=1,n
     write (4,134) bnum(i), (bdh(i,j), j=1,9)
134 format (a,2x,f6.1,x,f6.1,x,f6.1,x,f6.1,2x,f5.1,2x,f5.1,2x,f5.1,3x,f4.1,
+ 3x,f4.1,2x,f7.1)
135 continue
   else
     write (4,136)
136 format (18x,'Aa',8x,'fy',8x,'hg',8x,'hc',9x,'bc',8x,'fc',/)
     do 138 i=1,n
       write (4,137) bnum(i), (bds(i,j), j=1,6)
137 format (3x,a,3x,f7.1,4x,f5.1,5x,f5.1,5x,f5.1,5x,f6.1,5x,f4.1)
138 continue
   end if
   if (comb.EQ.'s'.OR.comb.EQ.'S') then
     write (4,139) vaa, vfy, vds, vhc, vfc, vbc
139 format (/3x,'Vaa=',f5.3,2x,'Vfy=',f5.3,2x,'Vds=',f5.3,2x,'Vhc=',
+ f5.3,2x,'Vfc=',f5.3,2x,'Vbc=',f5.3)
   else
     write (4,140) vw, vfy, vds, vfr, var, vhr, vaa
140 format (/x,'Vw=',f5.3,2x,'Vfy=',f5.3,2x,'Vds=',f5.3,2x,'Vfr=',
+ f5.3,2x,'Var=',f5.3,2x,'Vhr=',f5.3,2x,'Vaa=',f5.3)
   end if
   write (6,1)
   write (6,142)
142 format (3x,'SACB has fulfilled the analysis. Please open "Outoc" to
+ look at the results.',/)
   write (6,145)
145 format (/30x,'SEE YOU NEXT TIME !',/////////)
   c
   close(2)
   close(4)
   c
   stop
   end
   c
   subroutine cmce(n,cmv,cvoe,cc)
   dimension es(55), ts(55)
   common /et/ es, ts
   cmv=0
   cvoe=0
   em=0
   tm=0
   etm=0
   se=0
   st=0
   do 5 i=1,n
     cmv = cmv+es(i)/ts(i)/n
     em = em+es(i)/n
     tm = tm+ts(i)/n
     etm = etm+es(i)*ts(i)/n
   continue
5   do 10 i=1,n
     cvoe = cvoe+(es(i)/ts(i)-cmv)**2
     se = se+(es(i)-em)**2
     st = st+(ts(i)-tm)**2
   continue
10  cvoe = sqrt(cvoe/(n-1))/cmv
     se = sqrt(se/(n-1))
     st = sqrt(st/(n-1))
     cc = (etm-em*tm)*n/(n-1)/se/st
   return

```



```

c
end
subroutine fcvs(n, conb, cvoe, rtm, rtn)
dimension bds(55,10), bdh(55,11), cov(55,4), rtm(n), rtn(n)
character conb
common /bd/ bds, bdh
common /co/ cov
common vfc, vfr, vfy, vaa, vds, vhc, vbc, var, vhr, vw
-----Define the resistance formulas and some functions-----
smpc(r1,r2,r3,r4)=r1*(r2+r3+r1*r4)
hmpw(r1,r2,r3,r4,r5)=r1*r2+r3*r4+r3*r3*r5/r2
hmpf(r1,r2,r3,r4,r5,r6)=r1*r2+r4+r3*r5-(r1*r2-r3)**2*r6/r2
dl(v)=sqrt(log(1+v*v))
fm(v)=exp(3.04*v+0.5*v*v)
rsq(u,v)=sqrt(u*u+v*v)
-----Calculate the material-strength factor for steel-----
dyl=dl(vfy)
fmy=fm(dyl)
wk = (2.0*d1(0.08)+0.5*d1(0.08)**2 - 0.5*dyl*dyl)/dyl
fmy = exp((1.04+wk)*dyl+0.5*dyl*dyl)
-----Analyze the sagging cases-----
if (conb.NE.'s'.AND.conb.NE.'S') goto 10
dcl=dl(vfc)
fmc=fm(dcl)
vr1=rsq(vaa,vfy)
vr4=rsq(vfc,vbc)
do 5 i=1,n
r1=bds(i,1)*bds(i,2)
r2=bds(i,3)
r3=bds(i,4)
r4=-1/(1.7*bds(i,5)*bds(i,6))
rtm(i)=-1
rtn(i)=-1
c
Excluding the sample with p.n.a of composite section within the
steel section
c
if (-2*r1*r4.GT.(r3-bds(i,10))) then
write(6,4) i, -2*r1*r4, r3-bds(i,10)
format(x,'For sample ',i2,', yc = ',f7.2,' (mm) > ',
+ , hc - hp = ', f7.2,' (mm).')
write(6,12)
stop
end if
c
rtm(i)=smpc(r1,r2,r3,r4)
cov(i,1)=((r2+r3+2*r1*r4)*vr1)**2+(r2*vds)**2+(r3*vhc)**2
cov(i,1)=sqrt(cov(i,1)+(r1*r4*vr4)**2)*r1/rtm(i)
cov(i,2)=dl(cov(i,1))
cov(i,3)=rsq(cov(i,1),cvoe)
cov(i,4)=dl(cov(i,3))
r1=r1/fmy
r4=r4*fmc
rtn(i)=smpc(r1,r2,r3,r4)
hce = bds(i,4) - bds(i,10)
fyd = bds(i,2)/fmy
fcd = bds(i,6)/fmc
c

```

```

if(abs(r1*r4**2).GT.hce) then
ya = (bds(i,1)*fyd - 0.85*bds(i,5)*hce*fcd)/2.0/fyd/bds(i,9)
yx = 0.0
x0 = 0.0
xd = 0.0
if(ya.GT.bds(i,8)) then
x0 = (0.5*bds(i,1) - bds(i,9)*bds(i,8))/bds(i,7)
xd = 0.85*fcd*bds(i,5)*hce/2.0/fyd/bds(i,7)
yx = (x0 - xd)/2.0 + bds(i,8)
ya = bds(i,8)
end if
rtn(i) = 0.425*bds(i,5)*fcd*(bds(i,4)**2 - bds(i,10)**2)
rtn(i) = rtn(i) - yx*(x0-xd)*bds(i,7)*2*fyd
rtn(i) = rtn(i) + bds(i,1)*fyd*bds(i,3) - ya**2*fyd*bds(i,9)
end if
5 continue
return
c
-----Analyze the hogging cases-----
drl=dl(vfr)
fmr=fm(drl)
vr3=rsq(var,vfr)
do 15 i=1,n
hg = bdh(i,10)*bdh(i,11)*(bdh(i,3)+bdh(i,11))/bdh(i,9)/2.0
hg = hg + bdh(i,3)/2.0
hna = bdh(i,10)*bdh(i,11)/2.0/bdh(i,7) + bdh(i,3)/2.0
c
Excluding the sample with p.n.a of steel beam alone within the bottom
steel flange
c
if (hna.GT.(bdh(i,3)-bdh(i,8))) then
write(6,11) i, hna, bdh(i,3)-bdh(i,8)
format(x,'For sample ',i2,', hna = ',f7.2,' (mm) > ',
+ , ha - tf = ', f7.2,' (mm).')
write(6,12)
format(x,'The beam of such type has not been considered,
+ , so please exclude sample ',i2,' and run the program again.')
stop
end if
c
wa1 = bdh(i,6)*bdh(i,8)*(hna-bdh(i,8)/2.0)
wa2 = bdh(i,7)*(hna-bdh(i,8))**2/2.0
wa3 = bdh(i,7)*(bdh(i,3)-bdh(i,8)-hna)**2/2.0
wa4 = bdh(i,6)*bdh(i,8)*(bdh(i,3)-hna-bdh(i,8)/2.0)
wa5 = bdh(i,10)*bdh(i,11)*(bdh(i,11)/2.0+bdh(i,3)-hna)
r1 = wa1 + wa2 + wa3 + wa4 + wa5
r2=bdh(i,2)
r3=bdh(i,1)*bdh(i,4)
r4=hna + bdh(i,5)
r5=-0.25/bdh(i,7)
rtm(i)=-1
rtn(i)=-1
rw= 2.0*(hna - bdh(i,8))*bdh(i,7)*bdh(i,2)
c
if (rw.GE.r3) then
vr4=rsq(vds*hna,vhr*bdh(i,5))/r4
rtm(i)=hmpw(r1,r2,r3,r4,r5)
cov(i,1)=(r1*r2*vw)**2+(r1*r2-r3*r3*r5/r2)*vfy)**2
cov(i,1)=cov(i,1)+(r3*r4+2*r3*r3*r5/r2)*vr3)**2+(r3*r4*vr4)**2
cov(i,1)=sqrt(cov(i,1)+(r3*r3*r5/r2*vds)**2)/rtm(i)
else
c
Excluding the sample with p.n.a of composite section within the
steel top flange
c

```



```

14 write(6,14) i
format(x,'Sample ',i2,' has the p.n.a in steel top flange.')
write(6,12)
stop
c
end if
c
cov(i,2)=dl(cov(i,1))
cov(i,3)=rsq(cov(i,1),cvoe)
cov(i,4)=dl(cov(i,3))
c
r2=r2/fmy
r3=r3/fmr
rw=rw/fmy
if(rw.GE.r3) then
r1 = wa1 + wa2 + wa3 + wa4 + wa5
r4=hna + bdh(i,5)
r5=-0.25/bdh(i,7)
rtn(i) = hmpw(r1,r2,r3,r4,r5)
else
r1=bdh(i,9)
r4=bg
r5=bdh(i,5)
r6=0.25/bdh(i,6)
rtn(i)=hmpf(r1,r2,r3,r4,r5,r6)
end if
c
15 continue
return
end
c
subroutine dsis(n,cvoe,skd)
dimension cov(55,4), bata(55)
common /co/ cov
common /si/ bata
do 5 i=1,n
bata(i)=(3.04*cov(i,1)**2+skd*cvoe**2)/cov(i,3)**2
5 continue
return
end
c
subroutine ddr(n,cmv,rd,rtm)
dimension cov(55,4), bata(55), rd(n), rtm(n)
common /si/ bata
common /co/ cov
do 5 i=1,n
rd(i)=cmv*rtm(i)/exp(bata(i)*cov(i,4)+0.5*cov(i,4)**2)
5 continue
return
end
c
subroutine esfs(n,rd,rtn,comb,sk)
dimension rd(n), rtn(n), gamma(55,3)
character comb
common /sf/ gamma
common vfc, vfr, vfy
dcrl=sqrt(log(1+vfc**2))
if (comb.NE.'s'.AND.comb.NE.'s') dcrl=sqrt(log(1+vfr**2))
c
sks = 3.04 - sk
c
sks=1.04
c
fmcr=exp(1.40*dcrl)
dyl=sqrt(log(1+vfy**2))
fmy=exp(sks*dyl)

```

```

do 5 i=1,n
gamma(i,1)=rtn(i)/rd(i)
gamma(i,2)=gamma(i,1)*fmy
gamma(i,3)=gamma(i,1)*fmcr
5 continue
return
end

```


^s
 27, 14, 0.04, 0.08, 0.04, 0.04, 0.15, 0.008
 Beam 1
 4750.0, 308.0, 151.9, 127.0, 1500.0, 27.0, 7.2, 10.7, 123.5, 51.0
 Beam No.1
 2271.0, 316.0, 76.0, 60.0, 610.0, 48.0, 5.8, 9.6, 76.2, 0.0
 Beam No.2
 2271.0, 316.0, 76.0, 60.0, 610.0, 38.0, 5.8, 9.6, 76.2, 0.0
 A.T1C1D1F1
 8387.0, 253.0, 152.4, 152.0, 1219.0, 22.1, 11.0, 17.8, 152.4, 0.0
 B1E1U1-3
 8387.0, 253.0, 152.4, 152.0, 1219.0, 30.1, 11.0, 17.8, 152.4, 0.0
 CB2.4
 1232.3, 286.2, 60.4, 76.0, 305.0, 24.2, 4.6, 8.3, 44.5, 0.0
 SS1
 3800.0, 269.2, 103.4, 127.0, 254.0, 41.0, 6.3, 9.6, 133.8, 0.0
 SS2
 3800.0, 269.2, 103.4, 127.0, 305.0, 43.0, 6.3, 9.6, 133.8, 0.0
 SS3
 3800.0, 269.2, 103.4, 127.0, 406.0, 32.0, 6.3, 9.6, 133.8, 0.0
 SS6
 3800.0, 269.2, 103.4, 127.0, 616.0, 32.0, 6.3, 9.6, 133.8, 0.0
 CB10
 3800.0, 281.8, 103.4, 76.0, 915.0, 29.6, 6.3, 9.6, 133.8, 0.0
 CB12
 3800.0, 281.8, 103.4, 102.0, 1220.0, 29.6, 6.3, 9.6, 133.8, 0.0
 Girder 2
 20050.8, 336.0, 706.0, 190.5, 1194.0, 41.0, 6.4, 12.7, 254.0, 0.0
 Girder 3
 14894.6, 336.0, 549.2, 165.1, 1168.4, 51.0, 4.8, 15.9, 203.2, 0.0
 435.0, 87.0, 92.0, 578.0, 604.9, 604.9, 696.3, 638.5, 655.3
 601.6, 612.9, 697.3, 653.3, 604.9, 699.6, 695.6, 680.5, 46.9
 40.0, 188.7, 200.0, 216.9, 232.8, 199.0, 205.0, 6019.8, 3618.1
 377.0, 83.7, 87.6, 511.1, 528.5, 565.0, 579.2, 572.3, 527.5
 557.9, 556.6, 610.7, 583.7, 498.7, 592.5, 519.2, 522.5, 38.2
 37.2, 152.9, 177.3, 203.7, 225.3, 164.1, 191.7, 5517.7, 3615.4

h
21, 14, 0.04, 0.08, 0.04, 0.10, 0.00, 0.10, 0.04
Beam No1-2
593.8, 316.0, 152.0, 316.0, 36.3, 76.2, 5.8, 9.6, 2271.0, 0.00, 0.00
CB1-4
221.7, 286.2, 120.7, 427.6, 47.0, 44.5, 4.6, 8.3, 1232.3, 0.00, 0.00
SC-3S
1419.4, 240.0, 532.7, 310.3, 114.8, 211.1, 10.4, 14.0, 11325.0, 0.00, 0.00
SC-4S
2419.4, 240.0, 532.7, 310.3, 99.7, 211.1, 10.4, 14.0, 11325.0, 0.00, 0.00
HA4A
774.2, 319.3, 304.8, 329.1, 38.1, 101.6, 6.11, 6.67, 3859.4, 76.2, 9.5
HA256
1600.0, 319.5, 304.8, 329.1, 38.1, 101.6, 6.11, 6.67, 3859.4, 76.2, 9.5
HA11
761.3, 296.0, 310.9, 373.3, 50.8, 166.6, 7.8, 13.7, 6832.2, 0.00, 0.00
HA12
1264.5, 296.0, 310.9, 373.3, 50.8, 166.6, 7.8, 13.7, 6832.2, 0.00, 0.00
HA131617
1600.0, 296.0, 310.9, 373.3, 50.8, 166.6, 7.8, 13.7, 6832.2, 0.00, 0.00
HA22
516.1, 302.9, 307.1, 340.9, 50.8, 165.6, 6.7, 11.8, 5883.9, 0.00, 0.00
HA23
1200.0, 302.9, 307.1, 340.9, 50.8, 165.6, 6.7, 11.8, 5883.9, 0.00, 0.00
HA24
1600.0, 302.9, 307.1, 340.9, 50.8, 165.6, 6.7, 11.8, 5883.9, 0.00, 0.00
HA32
516.1, 350.9, 303.5, 340.9, 50.8, 165.1, 6.1, 10.2, 5141.9, 0.00, 0.00
HA33
1032.3, 350.9, 303.5, 340.9, 50.8, 165.1, 6.1, 10.2, 5141.9, 0.00, 0.00
73.9, 78.9, 31.2, 30.6, 697.8, 778.3, 217.0, 238.7,
239.1, 244.1, 375.2, 388.7, 393.2, 391.0, 388.7, 323.2,
337.9, 340.1, 271.2, 291.5, 4293.5
56.0, 60.1, 24.1, 24.1, 683.3, 757.6, 185.0, 224.0,
224.0, 224.0, 280.2, 305.0, 313.0, 313.0, 313.0, 253.9,
280.8, 285.0, 240.9, 266.1, 4110.4


```

c   if (cps(i,6).LT.23.52) e1 = cps(i,6)/23.52
c   if (cps(i,9).NE.0.0) then
c     prdc = arlfa*arg*bdh(i,1)**2*sqrt(cps(i,9)*cps(i,5))
c   else
c     prdc = arg*el*arlfa*bdh(i,1)**2*exp(2.0*log(cps(i,5))/3.0)
c     prdc = 97.4679*prdc
c   end if
c   fs = prdc*beta*ns(i,1)
c   bnum(i,3)='(concrete)'
c   if (prdc.gt.prds) then
c     fs = prds*beta*ns(i,1)
c   bnum(i,3)='(stud)'
c   end if
c   if (fs.gt.min(fc,fa)) fs = min(fc,fa)
c   rl(i,5) = bdh(i,2)*wa(bdh(i,3),bdh(i,6),bdh(i,8),bdh(i,7))
c   rl(i,2) = fs/min(fc,fa)
c   re(i,3) = fs/(0.85*cps(i,1)*cps(i,5))
c   re(i,2) = (fa-fs)/(2*bdh(i,6)*bdh(i,2))
c
c ----Set up the lowest ratio of ductile shear connection (6.1.4(2) EC4)----
c
c   cps(i,8)=0.25+0.03*cps(i,7)
c   if(cps(i,7).LE.5.0) cps(i,8) = 0.4
c   if(cps(i,7).GT.25.0) cps(i,8) = 1.0
c
c ----If calculation leads to tf<Xa<tf+0.5 mm, then Xa=tf is assumed----
c
c   if(re(i,2).GT.bdh(i,8)) then
c     if(re(i,2)-bdh(i,8).LT.0.5) re(i,2) = bdh(i,8)
c   end if
c
c ----Evaluate bending resistance under the partial shear connection----
c
c   if (re(i,2).gt.bdh(i,8)) then
c     dw = fs/bdh(i,7)/bdh(i,2)/2
c     re(i,2) = bdh(i,3)/2-dw
c     cm = cps(i,2)+(bdh(i,3)-dw-re(i,3))/2
c     re(i,1) = rl(i,5)+fs*cm
c     z(i,1) = fs*bdh(i,3)/rl(i,5)/4.0
c     z(i,4) = fs/bdh(i,7)/bdh(i,3)/bdh(i,2)/2.0
c   else
c     re(i,1) = (cps(i,2)+(bdh(i,3)-re(i,3))/2)*fa
c     re(i,1) = re(i,1)-(fa-fs)*(cps(i,2)+(re(i,2)-re(i,3))/2)
c     z(i,1) = fs/fa
c     z(i,4) = bdh(i,9)/bdh(i,6)/bdh(i,3)/2.0
c   end if
c   z(i,2) = (1.0 - cps(i,3)/cps(i,2))*fs/fc
c   z(i,3) = cps(i,2)*2.0/bdh(i,3)
c   if (fc-fa) 5, 10, 10
c
c ----Evaluate bending resistance of section with full shear connection----
c
c   xa = (fa-fc)/(2*bdh(i,6)*bdh(i,2))
c   if (xa.le.bdh(i,8)) then
c     rl(i,4) = fa*(cps(i,3)+cps(i,2)+bdh(i,3))/2
c     rl(i,4) = rl(i,4)-(fa-fc)*(xa+cps(i,3)+cps(i,2))/2
c     rl(i,3) = xa+cps(i,2)
c   else
c     dw = fc/bdh(i,2)/bdh(i,7)/2.0
c     cm = (cps(i,2)+cps(i,3)+bdh(i,3)-dw)/2
c     rl(i,4) = rl(i,5)+fc*cm
c     rl(i,3) = cps(i,2)+bdh(i,3)/2-dw
c   end if
c   goto 15
c   rl(i,3) = fa/(0.85*cps(i,1)*cps(i,5))

```

10

```

c   rl(i,4) = fa*(bdh(i,3)-rl(i,3))/2+cps(i,2)
c --Estimate bending resistance with partial SC by linear interpolation--
c
c   15   rl(i,1) = (1-rl(i,2))*rl(i,5)+rl(i,2)*rl(i,4)
c -----
c
c   20   continue
c       return
c       end
c
c -----Calculate the test correction such as c.v. of observed errors-----
c
c   subroutine cmce(n,cmv,cvoe,cc,es,ts)
c   dimension es(n), ts(n)
c   cmv=0
c   cvoe=0
c   em=0
c   tm=0
c   etm=0
c   se=0
c   st=0
c   do 5 i=1,n
c     cmv = cmv+es(i)/ts(i)/n
c     em = em+es(i)/n
c     tm = tm+ts(i)/n
c     etm = etm+es(i)*ts(i)/n
c   continue
c   do 10 i=1,n
c     cvoe = cvoe+(es(i)/ts(i)-cmv)**2
c     se = se+(es(i)-em)**2
c     st = st+(ts(i)-tm)**2
c   continue
c   cvoe = sqrt(cvoe/(n-1))/cmv
c   se = sqrt(se/(n-1))
c   st = sqrt(st/(n-1))
c   cc = (etm-em*tm)*n/(n-1)/se/st
c   return
c   end

```

5

10


```

data (cn(17,i),i=1,10)/3.699,3.366,3.184,2.802,2.375,
+ 2.131,1.857,1.589,1.310,0.901/
data (cn(18,i),i=1,10)/3.675,3.344,3.163,2.784,2.359,
+ 2.117,1.844,1.578,1.300,0.894/
data (cn(19,i),i=1,10)/3.653,3.324,3.144,2.767,2.344,
+ 2.104,1.833,1.568,1.291,0.887/
data (cn(20,i),i=1,10)/3.633,3.306,3.127,2.752,2.331,
+ 2.092,1.822,1.558,1.282,0.880/
data (cn(21,i),i=1,10)/3.615,3.290,3.111,2.738,2.319,
+ 2.081,1.812,1.550,1.275,0.874/
data (cn(22,i),i=1,10)/3.599,3.274,3.097,2.725,2.308,
+ 2.070,1.803,1.542,1.268,0.868/
data (cn(23,i),i=1,10)/3.584,3.260,3.084,2.713,2.298,
+ 2.061,1.795,1.534,1.261,0.863/
data (cn(24,i),i=1,10)/3.569,3.248,3.072,2.702,2.288,
+ 2.053,1.787,1.527,1.256,0.859/
data (cn(25,i),i=1,10)/3.558,3.237,3.062,2.693,2.280,
+ 2.046,1.781,1.522,1.251,0.855/
data (cn(26,i),i=1,10)/3.547,3.227,3.052,2.684,2.273,
+ 2.039,1.775,1.516,1.246,0.851/
data (cn(27,i),i=1,10)/3.535,3.216,3.042,2.676,2.264,
+ 2.032,1.768,1.511,1.241,0.847/
data (cn(28,i),i=1,10)/3.524,3.206,3.032,2.667,2.258,
+ 2.025,1.762,1.505,1.236,0.843/
data (cn(29,i),i=1,10)/3.513,3.195,3.022,2.658,2.250,
+ 2.018,1.756,1.500,1.231,0.839/
data (cn(30,i),i=1,10)/3.505,3.187,3.015,2.652,2.244,
+ 2.013,1.751,1.496,1.227,0.836/
data (cn(31,i),i=1,10)/3.496,3.180,3.008,2.645,2.239,
+ 2.008,1.747,1.492,1.224,0.833/
data (cn(32,i),i=1,10)/3.488,3.172,3.000,2.639,2.233,
+ 2.002,1.742,1.487,1.220,0.830/
data (cn(33,i),i=1,10)/3.479,3.165,2.993,2.632,2.228,
+ 1.997,1.738,1.483,1.217,0.827/
data (cn(34,i),i=1,10)/3.471,3.157,2.986,2.626,2.222,
+ 1.992,1.733,1.479,1.213,0.824/
data (cn(35,i),i=1,10)/3.464,3.151,2.980,2.621,2.218,
+ 1.988,1.729,1.476,1.210,0.822/
data (cn(36,i),i=1,10)/3.458,3.145,2.975,2.616,2.213,
+ 1.984,1.726,1.473,1.207,0.820/
data (cn(37,i),i=1,10)/3.451,3.139,2.969,2.611,2.209,
+ 1.980,1.722,1.469,1.205,0.817/
data (cn(38,i),i=1,10)/3.445,3.133,2.964,2.606,2.204,
+ 1.976,1.719,1.466,1.202,0.815/
data (cn(39,i),i=1,10)/3.438,3.127,2.958,2.601,2.200,
+ 1.972,1.715,1.463,1.199,0.813/
data (cn(40,i),i=1,10)/3.433,3.122,2.953,2.597,2.197,
+ 1.969,1.712,1.461,1.197,0.811/
data (cn(41,i),i=1,10)/3.428,3.118,2.949,2.593,2.193,
+ 1.966,1.709,1.458,1.195,0.809/
data (cn(42,i),i=1,10)/3.423,3.113,2.944,2.589,2.190,
+ 1.962,1.707,1.456,1.192,0.808/
data (cn(43,i),i=1,10)/3.418,3.109,2.940,2.585,2.186,
+ 1.959,1.704,1.453,1.190,0.806/
data (cn(44,i),i=1,10)/3.413,3.104,2.935,2.581,2.183,
+ 1.956,1.701,1.451,1.188,0.804/
data (cn(45,i),i=1,10)/3.409,3.100,2.931,2.578,2.180,
+ 1.953,1.699,1.449,1.186,0.802/
data (cn(46,i),i=1,10)/3.405,3.096,2.928,2.574,2.177,
+ 1.951,1.696,1.447,1.184,0.801/
data (cn(47,i),i=1,10)/3.400,3.093,2.924,2.571,2.174,
+ 1.948,1.694,1.444,1.183,0.799/
data (cn(48,i),i=1,10)/3.396,3.089,2.921,2.567,2.171,
+ 1.946,1.691,1.442,1.181,0.798/
data (cn(49,i),i=1,10)/3.392,3.085,2.917,2.564,2.168,
+ 1.943,1.689,1.440,1.179,0.796/

```

```

data (cn(50,i),i=1,10)/3.334,3.030,2.865,2.517,2.126,
+ 1.905,1.654,1.409,1.150,0.772/
data (cn(51,i),i=1,10)/3.275,2.975,2.812,2.470,2.085,
+ 1.868,1.619,1.378,1.121,0.748/
data (cn(52,i),i=1,10)/3.217,2.920,2.760,2.424,2.043,
+ 1.830,1.585,1.347,1.093,0.723/
data (cn(53,i),i=1,10)/3.158,2.865,2.707,2.377,2.001,
+ 1.793,1.550,1.316,1.064,0.699/
data (cn(54,i),i=1,10)/3.100,2.810,2.655,2.330,1.960,
+ 1.755,1.515,1.285,1.035,0.675/
open (2, file='inodp1')
open (3, file='trail')
open (4, file='outodp1')
write (4,5)
format (/15x,'- - - - -')
5 -----Input the initial data-----
c
c
c
read (2,*) vfy,vfc,vec,vfu,vd,vhc,vbc,vwa,vaa,vhg,vba,vtw
read (2,*) nn, arg
do 30 i=1,nn
read (2,'(a)') (bnum(i,j), j=1,2)
read (2,*) (bdh(i,j), j=1,9)
read (2,*) (cps(i,j), j=1,7)
read (2,*) (cps(i,9))
read (2,*) (ns(i,j), j=1,2)
30 continue
read (2,*) bd,cvd,ccd,bdl,cvdl,ccd1,bn,cvn,ccn,bnl,cvn1,ccn1
read (2,*) kn,jn
c
c
c -----Calculate Flexure Resistance-----
c (The resistance is calculated here by the method for beams with
c ductile connections, but the ratio of shear connection would be
c valid for both ductile and non-ductile cases)
c
c call cfr (nn,arg)
c
c ---Classify the groups with ductile and non-ductile shear connection---
c (This classification is based on the ratio of shear connection worked
c out from the Subroutine "cfr")
k=0
j=0
do 34 i= 1,nn
if (rl(i,2) .LT. 0.99) then
if (rl(i,2) .LT. cps(i,8)) then
k = k+1
do 31 ki = 1,9
bdhf(k,ki) = bdh(i,ki)
cpsf(k,ki) = cps(i,ki)
if (ki.LE.5) rlf(k,ki) = rl(i,ki)
if (ki.LE.4) zlf(k,ki) = z(i,ki)
if (ki.LE.3) rlf(k,ki) = re(i,ki)
if (ki.LE.3) bnuf(k,ki) = bnum(i,ki)
31 continue
else
j=j+1
do 32 ji = 1,9
bdhw(j,ji) = bdh(i,ji)
cpsw(j,ji) = cps(i,ji)
if (ji.LE.5) rlw(j,ji) = rl(i,ji)
if (ji.LE.4) zw(j,ji) = z(i,ji)
if (ji.LE.3) rew(j,ji) = re(i,ji)
if (ji.LE.3) bnuw(j,ji) = bnum(i,ji)
32 continue
end if

```



```

else
  write (4,33) bnum(i,1), rl(i,2)
  format (6x, 'The S.C. ratio of beam ', a,x, 'is ', f5.3)
end if
34 continue
write (4,18)
18 format (/6x, '[NOTE] Safety analysis excludes any full S.C. case')
write (4,115)
115 format (15x, '-----')
write (4,120)
120 format (/12x,
+ 'The calibration for beams with ductile connectors')
write (4,125)
125 format (/15x, '-----')
c
c -----Develop calibration for beams with the ductile shear connection-----
c
c skd = 3.04
if (jn.LE.55) skd = kd(jn-1)
call sfed(j, skd, bdhw, cpsw, bnuw, rew, rlw, zw)
call sfld(j, skd, bdhw, cpsw, bnuw, rlw, zlw)
c
c ---Evaluate the failure probability according to the fracture-factors---
c
equ = '(Equilib.)'
lin = '(Li. int.)'
sf1 = 'ra = 1.10'
sf2 = 'ra = 1.05'
do 50 i=1, j
  pfw(i,1,1)=0.0012
  pfw(i,1,2)=0.0000
  pfw(i,2,1)=0.0012
  pfw(i,2,2)=0.0000
  pfw(i,3,1)=0.0012
  pfw(i,3,2)=0.0000
  pfw(i,1,1)=0.0012
  pfw(i,1,2)=0.0000
  pfw(i,2,1)=0.0012
  pfw(i,2,2)=0.0000
  pfw(i,3,1)=0.0012
  pfw(i,3,2)=0.0000
  if (gaw(i,2).LT.gaw(i,1))
    + call sfp(pfw(i,2,1), pfw(i,2,2), gaw(i,2), virw(i,1), cvd, jn,
    + bnuw(i,1), equ, sf1)
    if (gaw(i,3).LT.gaw(i,1))
    + call sfp(pfw(i,3,1), pfw(i,3,2), gaw(i,3), virw(i,1), cvd, jn,
    + bnuw(i,1), equ, sf2)
    if (galw(i,2).LT.galw(i,1))
    + call sfp(pfw(i,2,1), pfw(i,2,2), galw(i,2), vrlw(i,1), cvdl, jn,
    + bnuw(i,1), lin, sf1)
    if (galw(i,3).LT.galw(i,1))
    + call sfp(pfw(i,3,1), pfw(i,3,2), galw(i,3), vrlw(i,1), cvdl, jn,
    + bnuw(i,1), lin, sf2)
c
c 50 continue
c
c ---Print out the failure probability based on the given safety factors---
c
c
write (4,55)
55 format (/3x, '-----',
+ 'The failure probability with the given safety factors',
+ '-----')
write (4,56)
56 format (26x, '(Equilibrium method)', /)

```

```

write (4,60)
60 format (19x, 'Presumed', l2x, 'rc, ru=1.25', l11x, 'rc, ru=1.25')
write (4,61)
61 format (20x, 'value', l5x, 'ry=1.10', l4x, 'ry=1.05', /)
do 70 i = 1, j
  write (4,65) bnuw(i,1), pfw(i,1,1), pfw(i,1,2), pfw(i,2,1),
+ pfw(i,2,2), pfw(i,3,1), pfw(i,3,2)
+
65 format (a, 3x, 3(f9.5, '(, f7.5, ', ', 3x))
70 continue
write (4,55)
write (4,75)
75 format (24x, '(Linear interpolation)', /)
write (4,60)
do 80 i = 1, j
  write (4,65) bnuw(i,1), pfw(i,1,1), pfw(i,1,2), pfw(i,2,1),
+ pfw(i,2,2), pfw(i,3,1), pfw(i,3,2)
+
80 continue
c
close(2)
close(3)
close(4)
close(7)
c
stop
end
c
c ---Calculating the resistances, with assuming the shear connection to be
c always ductile, and determining the ratio of shear connection by EC4---
c
subroutine cfr (nn, arg)
dimension bdh(100,9), cps(100,9), re(100,3), rl(100,5), z(100,4)
real ns(100,2)
character bnum (100,3)*10
common /bc/ bdh, cps
common /el/ re, rl
common /nsc/ ns
common /ps/ z
common /bn/ bnum
sd(h, hp, b0) = b0*(h-hp)/hp**2
wa(ha, ba, tf, tw) = (ba*ha*ha - (ba-tw)*(ha-2*tf)**2)/4
do 20 i=1, nn
  fc = 0.85*cps(i,1)*cps(i,5)*(cps(i,2)-cps(i,3))
  fa = bdh(i,2)*bdh(i,9)
  if (bnum(i,2).eq.'g'.or.bnum(i,2).eq.'G') then
    fs = bdh(i,1)*min(fc, fa)
    goto 3
  end if
  beta = 1.0
  if (bnum(i,2).eq.'S'.or.bnum(i,2).eq.'s') goto 1
  if (bnum(i,2).eq.'T'.or.bnum(i,2).eq.'t') then
    if (ns(i,2).gt.2.0) ns(i,2) = 2.0
    beta = 0.7*sd(bdh(i,5), cps(i,3), cps(i,4))/sqrt(ns(i,2))
  else
    beta = 0.6*sd(bdh(i,5), cps(i,3), cps(i,4))
  end if
  if (beta.gt.1.0) beta = 1.0
  prds = 0.62832*bdh(i,4)*bdh(i,1)**2
  arlfa = 0.2*(bdh(i,5)/bdh(i,1)+1)
  if (arlfa.gt.1.0) arlfa = 1.0
c
c ----- Working out if it is a lightweight concrete -----
c
e1 = 1.0
if (cps(i,6).LT.23.52) e1 = cps(i,6)/23.52

```



```

qfy = vfy*(1.0+2.0*zw(i,1))*zw(i,4)
qhna = 2.0*vhg*zw(i,1)
qec = vec*zw(i,1)*(1.0+zw(i,3)-2.0*zw(i,4)-zw(i,2))*zw(i,3)
qfc = vfc*zw(i,1)*(1.0+zw(i,3)-2.0*zw(i,4))
qhc = 2.0*zw(i,1)*zw(i,3)*vhc
qd = zw(i,1)*(1.0+zw(i,3)-2.0*zw(i,4)-zw(i,2))*zw(i,3)
qd = qd*4.0*vvd
qbc = zw(i,1)*zw(i,2)*zw(i,3)*vbc
qtw = 2.0*vvtw*zw(i,1)*zw(i,4)
vrw(i,1) = qwa**2+qfy**2+qd**2+qhna**2+qec**2+qfc**2+qhc**2
vrw(i,1) = sqrt(vrw(i,1)+qbc**2+qtw**2)/rm
xap(i) = '(Xa>tf)'
rm = rm*rlw(i,5)
end if
vrw(i,2) = sqrt(cvd**2 + vrw(i,1)**2)
vrw(i,3) = oln(vrw(i,2))

zws1 = zw(i,1)
zws4 = zw(i,4)
afh = bdhw(i,2)*bdhw(i,9)*bdhw(i,3)/2.0

fc = 0.85*cpsw(i,1)*cpsw(i,5)*(cpsw(i,2)-cpsw(i,3))
fa = bdhw(i,9)*bdhw(i,2)
fs = rlw(i,2)*min(fc,fa)

fns = fs/pc
fnc = fc/pfc
fan = fa/pfy
if (fns.GT.min(fan,fcn)) fns = min(fan,fcn)
yan = (fan-fns)/(2.0*bdhw(i,6)*bdhw(i,2)/pfy)
if (yan - bdhw(i,8).LT.0) then
  zw(i,1) = fs/fa
  zw(i,4) = bdhw(i,9)/bdhw(i,6)/bdhw(i,3)/2.0
  rn = 1.0/pfy + zw(i,1)*zw(i,3)*(1.0-0.5*zw(i,2))*pfc/pc/pc
  rn = (rn - pfy*zw(i,4))*(pc/pfy-zw(i,1))*2/pc/pc)*afh
else
  zw(i,1) = fs*bdhw(i,3)/rlw(i,5)/4.0
  zw(i,4) = fs/bdhw(i,7)/bdhw(i,3)/bdhw(i,2)/2.0
  rn = zw(i,1)*(zw(i,4)+zw(i,2))*zw(i,3)*pfc/pfy/2.0)*pfy/pc/pc
  rn = (1.0/pfy + 2.0*zw(i,1)*(1.0+zw(i,3))/pc - 2.0*rn)*rlw(i,5)
end if

fcd = fc/rc
fsd = fs/ru
fad1 = fa/rfy1
if (fsd.GT.min(fad1,fcd)) fsd = min(fad1,fcd)
yad1 = (fad1-fsd)/(2.0*bdhw(i,6)*bdhw(i,2)/rfy1)
if (yad1 - bdhw(i,8).LT.0) then
  zw(i,1) = fs/fa
  zw(i,4) = bdhw(i,9)/bdhw(i,6)/bdhw(i,3)/2.0
  rd1 = 1.0/rfy1 + zw(i,1)*zw(i,3)*(1.0-0.5*zw(i,2))*rc/ru/ru
  rd1 = (rd1 - rfy1*zw(i,4))*(ru/rfy1-zw(i,1))*2/ru/ru)*afh
else
  zw(i,1) = fs*bdhw(i,3)/rlw(i,5)/4.0
  zw(i,4) = fs/bdhw(i,7)/bdhw(i,3)/bdhw(i,2)/2.0
  rd1 = zw(i,1)*(zw(i,4)+zw(i,2))*zw(i,3)*rc/rfy1/2.0)*rfy1/ru/ru
  rd1 = 1.0/rfy1 + 2.0*zw(i,1)*(1.0+zw(i,3))/ru - 2.0*rd1
  rd1 = rd1*rlw(i,5)
end if

fsd = fs/ru
fad2 = fa/rfy2
if (fsd.GT.min(fad2,fcd)) fsd = min(fad2,fcd)
yad2 = (fad2-fsd)/(2.0*bdhw(i,6)*bdhw(i,2)/rfy2)
if (yad2 - bdhw(i,8).LT.0) then
  zw(i,1) = fs/fa

```

c

c

c

c

c

```

zw(i,4) = bdhw(i,9)/bdhw(i,6)/bdhw(i,3)/2.0
rd2 = 1.0/rfy2 + zw(i,1)*zw(i,3)*(1.0-0.5*zw(i,2))*rc/ru/ru
rd2 = (rd2 - rfy2*zw(i,4))*(ru/rfy2-zw(i,1))*2/ru/ru)*afh
else
  zw(i,1) = fs*bdhw(i,3)/rlw(i,5)/4.0
  zw(i,4) = fs/bdhw(i,7)/bdhw(i,3)/bdhw(i,2)/2.0
  rd2 = zw(i,1)*(zw(i,4)+zw(i,2))*zw(i,3)*rc/rfy2/2.0)*rfy2/ru/ru
  rd2 = 1.0/rfy2 + 2.0*zw(i,1)*(1.0+zw(i,3))/ru - 2.0*rd2
  rd2 = rd2*rlw(i,5)
end if

zws1 = zw(i,1)
zws4 = zw(i,4)

gaw(i,1) = (3.04*vrw(i,1)**2 + skd*cvd**2) / vrw(i,2)**2
gaw(i,2) = log(bd*rm/rd1)/vrw(i,3) - 0.5*vrw(i,3)
gaw(i,3) = log(bd*rm/rd2)/vrw(i,3) - 0.5*vrw(i,3)
sfw(i,1) = rn*exp(gaw(i,1))*vrw(i,3)+0.5*vrw(i,3)**2)/rm/bd
sfw(i,2) = sfw(i,1)*exp((akd-aks)*oln(vfy))
sfw(i,3) = sfw(i,1)*exp((3.04-1.64)*oln(vfc))
sfw(i,4) = sfw(i,1)*1.25
continue

ekp = 0.0
ek1 = 0.0
ek2 = 0.0
vkp = 0.0
vk1 = 0.0
vk2 = 0.0
era = 0.0
erc = 0.0
eru = 0.0
vra = 0.0
vrc = 0.0
vru = 0.0
do 6 i=1,j
  ekp = ekp + gaw(i,1)/j
  ek1 = ek1 + gaw(i,2)/j
  ek2 = ek2 + gaw(i,3)/j
  era = era + sfw(i,2)/j
  erc = erc + sfw(i,3)/j
  eru = eru + sfw(i,4)/j
6 continue

vkp = vkp + (gaw(i,1)-ekp)**2/(j-1)
vk1 = vk1 + (gaw(i,2)-ek1)**2/(j-1)
vk2 = vk2 + (gaw(i,3)-ek2)**2/(j-1)
vra = vra + (sfw(i,2)-era)**2/(j-1)
vrc = vrc + (sfw(i,3)-erc)**2/(j-1)
vru = vru + (sfw(i,4)-eru)**2/(j-1)
7 continue

vkp = sqrt(vkp)
vk1 = sqrt(vk1)
vk2 = sqrt(vk2)
vra = sqrt(vra)
vrc = sqrt(vrc)
vru = sqrt(vru)

c -----Output calibration results for beams with the ductile connections-----
c
c
10 write (4,10)
format (//,
+ 'The calibration results for beams with ducile shear connection',
+ ' (EQUILIBRIUM)',
write (4,15)
format (//23x,'The coefficients of variation')
write (4,20)

```

c

c

5

6

7

c

c

c


```
5  continue
10  continue
15  continue
C
20  write (6,20)
   format(x,'Abnormal stop occurred! Please check file trail.dp')
   stop
C
C  end
C
C  ----- Find out factored reisistance with linear interpolation -----
C
C  subroutine fmi(rr,fa,fc,hg,hc,hp,tw,bf,fy,bma,fs,tf,ra,rc,ru)
C
C  fy = fy/ra
C  fss = fs/ru
C  faa = fa/ra
C  fcc = fc/rc
C  bmaa = bma/ra
C
C  yc = faa*(hc-hp)/fcc
   if (yc.LE.(hc - hp)) then
     bpl = faa*(hg+hc-yc/2.0)
   else
     ya = (faa-fcc)/2.0/fyy/bf
     if (ya.LE.tf) then
       bpl = faa*hg+fcc*(hc+hp)/2.0-(faa-fcc)**2/4.0/bf/fyy
     else
       bpl = bmaa + fcc*(hg+0.5*(hc+hp)-fcc/4.0/tw/fyy)
     end if
   end if
C
C  rsc = fss/min(faa,fcc)
   rr = bmaa + rsc*(bpl - bmaa)
C
C  return
C  end
```



```

C This package continues serving the safety analysis of composite
C beams but for the beams with non-ductile connectors. However,
C the calculations performed in this package are all based on the
C design mode for beams in ductile shear connection as classified in
C accordance with EC4 of 1991. Therefore, this program is mainly
C copied from crb.f. The program-making is started on 17th July 1992
C and the last version is updated to 5th November 1993.

```

```

C Program CRN

```

```

C dimension re(100,3), rl(100,5)
C dimension cps(100,9), bdh(100,9), z(100,4)
C dimension ref(100,3), rlf(100,5)
C dimension cpsf(100,9), bdhf(100,9), zf(100,4)
C dimension rew(100,3), rlw(100,5)
C dimension cpsw(100,9), bdhw(100,9), zw(100,4)
C dimension gaw(100,3), sfw(100,4), vrw(100,3)
C dimension zlw(100,5), galw(100,3), sflw(100,4), vrlw(100,3)
C real pfw(100,3,2), pflw(100,3,2)
C real sn(5,10,10), cn(54,10), tn(10)
C real ns(100,2), kd(54)

```

```

C character bnum(100,3)*10, bnuf(100,3)*10, bnuw(100,3)*10
C character equ*10, lin*10, sfl*15, sf2*15

```

```

C common /nsc/ ns
C common /bc/ bdh, cps
C common /ps/ z
C common /bn/ bnum

```

```

C common /el/ re, rl
C common /vr/ vrw, vrlw
C common /sf/ sfw, sflw
C common /ga/ gaw, galw
C common /table/ sn, tn, cn

```

```

C common /bcv/ bdc, ccd, bdl, cvdl, cvdl, bn, cvn, ccn, bnl, cvnl, ccnl
C common vfy, vfc, vec, vfu, vd, vhc, vbc, vva, vaa, vhg, vba, vtw
C data (kd(i), i=1, 6)/9.52, 5.72, 4.83, 4.44, 4.20, 4.05/
C data (kd(i), i=7, 12)/3.95, 3.86, 3.80, 3.74, 3.70, 3.66/
C data (kd(i), i=13, 18)/3.63, 3.60, 3.58, 3.55, 3.54, 3.52/
C data (kd(i), i=19, 24)/3.51, 3.49, 3.47, 3.46, 3.45, 3.44/
C data (kd(i), i=25, 30)/3.44, 3.43, 3.43, 3.42, 3.42, 3.41/
C data (kd(i), i=31, 36)/3.40, 3.40, 3.39, 3.39, 3.38, 3.38/
C data (kd(i), i=37, 42)/3.37, 3.36, 3.36, 3.35, 3.35, 3.34/
C data (kd(i), i=43, 48)/3.33, 3.33, 3.32, 3.32, 3.31, 3.31/
C data (kd(i), i=49, 54)/3.30, 3.30, 3.30, 3.29, 3.29, 3.29/

```

```

C data ((sn(1, i1, i2), i2=1, 10), i1=1, 10)/0.5000, 0.5040, 0.5080, 0.5120,
+ 0.5160, 0.5199, 0.5239, 0.5279, 0.5319, 0.5359, 0.5398, 0.5438, 0.5478,
+ 0.5517, 0.5557, 0.5596, 0.5636, 0.5675, 0.5714, 0.5753, 0.5793, 0.5832,
+ 0.5871, 0.5910, 0.5948, 0.5987, 0.6026, 0.6064, 0.6103, 0.6141, 0.6179,
+ 0.6217, 0.6255, 0.6293, 0.6331, 0.6368, 0.6406, 0.6443, 0.6480, 0.6517,
+ 0.6554, 0.6591, 0.6628, 0.6664, 0.6700, 0.6736, 0.6772, 0.6808, 0.6844,
+ 0.6879, 0.6915, 0.6950, 0.6985, 0.7019, 0.7054, 0.7088, 0.7123, 0.7157,
+ 0.7190, 0.7224, 0.7257, 0.7291, 0.7324, 0.7357, 0.7389, 0.7422, 0.7454,
+ 0.7486, 0.7517, 0.7549, 0.7580, 0.7611, 0.7642, 0.7673, 0.7703, 0.7734,
+ 0.7764, 0.7794, 0.7823, 0.7852, 0.7881, 0.7910, 0.7939, 0.7967, 0.7995,
+ 0.8023, 0.8051, 0.8078, 0.8106, 0.8133, 0.8159, 0.8186, 0.8212, 0.8238,
+ 0.8264, 0.8289, 0.8315, 0.8340, 0.8365, 0.8389/

```

```

C data ((sn(2, i1, i2), i2=1, 10), i1=1, 10)/0.8413, 0.8438, 0.8461, 0.8485,
+ 0.8508, 0.8531, 0.8554, 0.8577, 0.8599, 0.8621, 0.8643, 0.8665, 0.8686,
+ 0.8708, 0.8729, 0.8749, 0.8770, 0.8790, 0.8810, 0.8830, 0.8849, 0.8869,
+ 0.8888, 0.8907, 0.8925, 0.8944, 0.8962, 0.8980, 0.8997, 0.9015, 0.9032,
+ 0.9049, 0.9066, 0.9082, 0.9099, 0.9115, 0.9131, 0.9147, 0.9162, 0.9177,
+ 0.9192, 0.9207, 0.9222, 0.9236, 0.9251, 0.9265, 0.9279, 0.9292, 0.9306,
+ 0.9319, 0.9332, 0.9345, 0.9357, 0.9370, 0.9382, 0.9394, 0.9406, 0.9418,
+ 0.9430, 0.9441, 0.9452, 0.9463, 0.9474, 0.9485, 0.9495, 0.9505, 0.9515,
+ 0.9525, 0.9535, 0.9545, 0.9554, 0.9564, 0.9573, 0.9582, 0.9591, 0.9599,
+ 0.9608, 0.9616, 0.9625, 0.9633, 0.9641, 0.9649, 0.9656, 0.9664, 0.9671,
+ 0.9678, 0.9686, 0.9693, 0.9700, 0.9706, 0.9713, 0.9719, 0.9726, 0.9732,

```

```

+ 0.9738, 0.9744, 0.9750, 0.9756, 0.9762, 0.9767, 0.9773, 0.9778, 0.9783, 0.9788,
C data ((sn(3, i1, i2), i2=1, 10), i1=1, 10)/0.9773, 0.9778, 0.9783, 0.9788,
+ 0.9793, 0.9798, 0.9803, 0.9808, 0.9812, 0.9817, 0.9821, 0.9826, 0.9830,
+ 0.9834, 0.9838, 0.9842, 0.9846, 0.9850, 0.9854, 0.9857, 0.9861, 0.9865,
+ 0.9868, 0.9871, 0.9875, 0.9878, 0.9881, 0.9884, 0.9887, 0.9890, 0.9893,
+ 0.9896, 0.9898, 0.9901, 0.9904, 0.9906, 0.9909, 0.9911, 0.9913, 0.9916,
+ 0.9918, 0.9920, 0.9922, 0.9925, 0.9927, 0.9929, 0.9931, 0.9932, 0.9934,
+ 0.9936, 0.9938, 0.9940, 0.9941, 0.9943, 0.9945, 0.9946, 0.9948, 0.9949,
+ 0.9951, 0.9952, 0.9953, 0.9955, 0.9956, 0.9957, 0.9959, 0.9960, 0.9961,
+ 0.9962, 0.9963, 0.9964, 0.9965, 0.9966, 0.9967, 0.9968, 0.9969, 0.9970,
+ 0.9971, 0.9972, 0.9973, 0.9974, 0.9975, 0.9976, 0.9977, 0.9978, 0.9979,
+ 0.9980, 0.9981, 0.9982, 0.9983, 0.9984, 0.9985, 0.9986, 0.9987, 0.9988,
+ 0.9989, 0.9990, 0.9991, 0.9992, 0.9993, 0.9994, 0.9995, 0.9996, 0.9997,
+ 0.9998, 0.9999, 1.0000, 1.0001, 1.0002, 1.0003, 1.0004, 1.0005, 1.0006,
+ 0.99946, 0.99948, 0.99950, 0.99952, 0.99953, 0.99954, 0.99955, 0.99956,
+ 0.99957, 0.99958, 0.99959, 0.99960, 0.99961, 0.99962, 0.99963, 0.99964, 0.99965, 0.99966, 0.99967,
+ 0.99968, 0.99969, 0.99970, 0.99971, 0.99972, 0.99973, 0.99974, 0.99975, 0.99976, 0.99977,
+ 0.99978, 0.99979, 0.99980, 0.99981, 0.99982, 0.99983, 0.99984, 0.99985, 0.99986,
+ 0.99987, 0.99988, 0.99989, 0.99990, 0.99991, 0.99992, 0.99993, 0.99994, 0.99995,
+ 0.99996, 0.99997, 0.99998, 0.99999, 1.00000, 1.00001, 1.00002, 1.00003, 1.00004,
+ 0.999972, 0.999973, 0.999974, 0.999975, 0.999976, 0.999977, 0.999978,
+ 0.999979, 0.999980, 0.999981, 0.999982, 0.999983, 0.999984, 0.999985, 0.999986,
+ 0.999987, 0.999988, 0.999989, 0.999990, 0.999991, 0.999992, 0.999993,
+ 0.999994, 0.999995, 0.999996, 0.999997, 0.999998, 0.999999, 1.000000,
+ 0.9999972, 0.9999973, 0.9999974, 0.9999975, 0.9999976, 0.9999977, 0.9999978,
+ 0.9999979, 0.9999980, 0.9999981, 0.9999982, 0.9999983, 0.9999984, 0.9999985,
+ 0.9999986, 0.9999987, 0.9999988, 0.9999989, 0.9999990, 0.9999991, 0.9999992,
+ 0.9999993, 0.9999994, 0.9999995, 0.9999996, 0.9999997, 0.9999998, 0.9999999,
+ 1.0000000, 0.99999972, 0.99999973, 0.99999974, 0.99999975, 0.99999976,
+ 0.99999977, 0.99999978, 0.99999979, 0.99999980, 0.99999981, 0.99999982,
+ 0.99999983, 0.99999984, 0.99999985, 0.99999986, 0.99999987, 0.99999988,
+ 0.99999989, 0.99999990, 0.99999991, 0.99999992, 0.99999993, 0.99999994,
+ 0.99999995, 0.99999996, 0.99999997, 0.99999998, 0.99999999, 1.00000000,
+ 0.999999972, 0.999999973, 0.999999974, 0.999999975, 0.999999976, 0.999999977,
+ 0.999999978, 0.999999979, 0.999999980, 0.999999981, 0.999999982, 0.999999983,
+ 0.999999984, 0.999999985, 0.999999986, 0.999999987, 0.999999988, 0.999999989,
+ 0.999999990, 0.999999991, 0.999999992, 0.999999993, 0.999999994, 0.999999995,
+ 0.999999996, 0.999999997, 0.999999998, 0.999999999, 1.000000000,
+ 0.999999972, 0.999999973, 0.999999974, 0.999999975, 0.999999976, 0.999999977,
+ 0.999999978, 0.999999979, 0.999999980, 0.999999981, 0.999999982, 0.999999983,
+ 0.999999984, 0.999999985, 0.999999986, 0.999999987, 0.999999988, 0.999999989,
+ 0.999999990, 0.999999991, 0.999999992, 0.999999993, 0.999999994, 0.999999995,
+ 0.999999996, 0.999999997, 0.999999998, 0.999999999, 1.000000000,
+ 0.999999972, 0.999999973, 0.999999974, 0.999999975, 0.999999976, 0.999999977,
+ 0.999999978, 0.999999979, 0.999999980, 0.999999981, 0.999999982, 0.999999983,
+ 0.999999984, 0.999999985, 0.999999986, 0.999999987, 0.999999988, 0.999999989,
+ 0.999999990, 0.999999991, 0.999999992, 0.999999993, 0.999999994, 0.999999995,
+ 0.999999996, 0.999999997, 0.999999998, 0.999999999, 1.000000000,
+ 0.999999972, 0.999999973, 0.999999974, 0.999999975, 0.999999976, 0.999999977,
+ 0.999999978, 0.999999979, 0.999999980, 0.999999981, 0.999999982, 0.999999983,
+ 0.999999984, 0.999999985, 0.999999986, 0.999999987, 0.999999988, 0.999999989,
+ 0.999999990, 0.999999991, 0.999999992, 0.999999993, 0.999999994, 0.999999995,
+ 0.999999996, 0.999999997, 0.999999998, 0.999999999, 1.000000000,
+ 0.999999972, 0.999999973, 0.999999974, 0.999999975, 0.999999976, 0.999999977,
+ 0.999999978, 0.999999979, 0.999999980, 0.999999981, 0.999999982, 0.999999983,
+ 0.999999984, 0.999999985, 0.999999986, 0.999999987, 0.999999988, 0.999999989,
+ 0.999999990, 0.999999991, 0.999999992, 0.999999993, 0.999999994, 0.999999995,
+ 0.999999996, 0.999999997, 0.999999998, 0.999999999, 1.000000000,
+ 0.999999972, 0.999999973, 0.999999974, 0.999999975, 0.999999976, 0.999999977,
+ 0.999999978, 0.999999979, 0.999999980, 0.999999981, 0.999999982, 0.999999983,
+ 0.999999984, 0.999999985, 0.999999986, 0.999999987, 0.999999988, 0.999999989,
+ 0.999999990, 0.999999991, 0.999999992, 0.999999993, 0.999999994, 0.999999995,
+ 0.999999996, 0.999999997, 0.999999998, 0.999999999, 1.000000000,
+ 0.999999972, 0.999999973, 0.999999974, 0.999999975, 0.999999976, 0.999999977,
+ 0.999999978, 0.999999979, 0.999999980, 0.999999981, 0.999999982, 0.999999983,
+ 0.999999984, 0.999999985, 0.999999986, 0.999999987, 0.999999988, 0.999999989,
+ 0.999999990, 0.999999991, 0.999999992, 0.999999993, 0.999999994, 0.999999995,
+ 0.999999996, 0.999999997, 0.999999998, 0.999999999, 1.000000000,
+ 0.999999972, 0.999999973, 0.999999974, 0.999999975, 0.999999976, 0.999999977,
+ 0.999999978, 0.999999979, 0.999999980, 0.999999981, 0.999999982, 0.999999983,
+ 0.999999984, 0.999999985, 0.999999986, 0.999999987, 0.999999988, 0.999999989,
+ 0.999999990, 0.999999991, 0.999999992, 0.999999993, 0.999999994, 0.999999995,
+ 0.999999996, 0.999999997, 0.999999998, 0.999999999, 1.000000000,
+ 0.999999972, 0.999999973, 0.999999974, 0.999999975, 0.999999976, 0.999999977,
+ 0.999999978, 0.999999979, 0.999999980, 0.999999981, 0.999999982, 0.999999983,
+ 0.999999984, 0.999999985, 0.999999986, 0.999999987, 0.999999988, 0.999999989,
+ 0.999999990, 0.999999991, 0.999999992, 0.999999993, 0.999999994, 0.999999995,
+ 0.999999996, 0.999999997, 0.999999998, 0.999999999, 1.000000000,
+ 0.999999972, 0.999999973, 0.999999974, 0.999999975, 0.999999976, 0.999999977,
+ 0.999999978, 0.999999979, 0.999999980, 0.999999981, 0.999999982, 0.999999983,
+ 0.999999984, 0.999999985, 0.999999986, 0.999999987, 0.999999988, 0.999999989,
+ 0.999999990, 0.999999991, 0.999999992, 0.999999993, 0.999999994, 0.999999995,
+ 0.999999996, 0.999999997, 0.999999998, 0.999999999, 1.000000000,
+ 0.999999972, 0.999999973, 0.999999974, 0.999999975, 0.999999976, 0.999999977,
+ 0.999999978, 0.999999979, 0.999999980, 0.999999981, 0.999999982, 0.999999983,
+ 0.999999984, 0.999999985, 0.999999986, 0.999999987, 0.999999988, 0.999999989,
+ 0.999999990, 0.999999991, 0.999999992, 0.999999993, 0.999999994, 0.999999995,
+ 0.999999996, 0.999999997, 0.999999998, 0.999999999, 1.000000000,
+ 0.999999972, 0.999999973, 0.999999974, 0.999999975, 0.999999976, 0.999999977,
+ 0.999999978, 0.999999979, 0.999999980, 0.999999981, 0.999999982, 0.999999983,
+ 0.999999984, 0.999999985, 0.999999986, 0.999999987, 0.999999988, 0.999999989,
+ 0.999999990, 0.999999991, 0.999999992, 0.999999993, 0.999999994, 0.999999995,
+ 0.999999996, 0.999999997, 0.999999998, 0.999999999, 1.000000000,
+ 0.999999972, 0.999999973, 0.999999974, 0.999999975, 0.999999976, 0.999999977,
+ 0.999999978, 0.999999979, 0.999999980, 0.999999981, 0.999999982, 0.999999983,
+ 0.999999984, 0.999999985, 0.999999986, 0.999999987, 0.999999988, 0.999999989,
+ 0.999999990, 0.999999991, 0.999999992, 0.999999993, 0.999999994, 0.999999995,
+ 0.999999996, 0.999999997, 0.999999998, 0.999999999, 1.000000000,
+ 0.999999972, 0.999999973, 0.999999974, 0.999999975, 0.999999976, 0.999999977,
+ 0.999999978, 0.999999979, 0.999999980, 0.999999981, 0.999999982, 0.999999983,
+ 0.999999984, 0.999999985, 0.999999986, 0.999999987, 0.999999988, 0.999999989,
+ 0.999999990, 0.999999991, 0.999999992, 0.999999993, 0.999999994, 0.999999995,
+ 0.999999996, 0.999999997, 0.999999998, 0.999999999, 1.000000000,
+ 0.999999972, 0.999999973, 0.999999974, 0.999999975, 0.999999976, 0.999999977,
+ 0.999999978, 0.999999979, 0.999999980, 0.999999981, 0.999999982, 0.999999983,
+ 0.999999984, 0.999999985, 0.999999986, 0.999999987, 0.999999988, 0.999999989,
+ 0.999999990, 0.999999991, 0.999999992, 0.999999993, 0.999999994, 0.999999995,
+ 0.999999996, 0.999999997, 0.999999998, 0.999999999, 1.000000000,
+ 0.999999972, 0.999999973, 0.999999974, 0.999999975, 0.999999976, 0.999999977,
+ 0.999999978, 0.999999979, 0.999999980, 0.999999981, 0.999999982, 0.999999983,
+ 0.999999984, 0.999999985, 0.999999986, 0.999999987, 0.999999988, 0.999999989,
+ 0.999999990, 0.999999991, 0.999999992, 0.999999993, 0.999999994, 0.999999995,
+ 0.999999996, 0.999999997, 0.999999998, 0.999999999, 1.000000000,
+ 0.999999972, 0.999999973, 0.999999974, 0.999999975, 0.999999976, 0.999999977,
+ 0.999999978, 0.999999979, 0.999999980, 0.999999981, 0.999999982, 0.999999983,
+ 0.999999984, 0.999999985, 0.999999986, 0.999999987, 0.999999988, 0.999999989,
+ 0.999999990, 0.999999991, 0.999999992, 0.999999993, 0.999999994, 0.999999995,
+ 0.999999996, 0.999999997, 0.999999998, 0.999999999, 1.0000000
```



```

fs = prdc*beta*ns(i,1)
bnum(i,3) = ' (concrete)
if (prdc.gt.prds) then
  fs = prds*beta*ns(i,1)
  bnum(i,3) = ' (stud)
end if
3  if (fs.gt.min(fc,fa)) fs = min(fc,fa)
    rl(i,5) = bdh(i,2)*wa(bdh(i,3),bdh(i,6),bdh(i,8),bdh(i,7))
    rl(i,2) = fs/min(fc,fa)
    re(i,3) = fs/0.85*cps(i,1)*cps(i,5))
    re(i,2) = (fa-fs)/(2*bdh(i,6)*bdh(i,2))

c  ---Set up the lowest ratio of ductile shear connection (6.1.4(2) EC4)---
c
c  cps(i,8)=0.25+0.03*cps(i,7)
  if(cps(i,7).LE.5.0) cps(i,8) = 0.4
  if(cps(i,7).GT.25.0) cps(i,8) = 1.0

c  -----If calculation leads to tf<Xa<tf+0.5 mm, then Xa=tf is assumed-----
c
c  if(re(i,2).GT.bdh(i,8)) then
  if(re(i,2)-bdh(i,8).LT.0.5) re(i,2) = bdh(i,8)
  end if

c  -----Evaluate bending resistance under the partial shear connection-----
c
c  if (re(i,2).gt.bdh(i,8)) then
  dw = fs/bdh(i,7)/bdh(i,2)/2
  re(i,2) = bdh(i,3)/2-dw
  cm = cps(i,2)+(bdh(i,3)-dw-re(i,3))/2
  re(i,1) = rl(i,5)+fs*cm
  z(i,1) = fs*bdh(i,3)/rl(i,5)/4.0
  z(i,4) = fs/bdh(i,7)/bdh(i,3)/bdh(i,2)/2.0
  else
  re(i,1) = (cps(i,2)+(bdh(i,3)-re(i,3))/2)*fa
  re(i,1) = re(i,1)-(fa-fs)*(cps(i,2)+(re(i,2)-re(i,3))/2)
  z(i,1) = fs/fa
  z(i,4) = bdh(i,9)/bdh(i,6)/bdh(i,3)/2.0
  end if
  z(i,2) = (1.0 - cps(i,3)/cps(i,2))*fs/fc
  z(i,3) = cps(i,2)*2.0/bdh(i,3)
  if (fc-fa) 5, 10, 10

c  -----Evaluate bending resistance of section with full shear connection-----
c
c
c  5  xa = (fa-fc)/(2*bdh(i,6)*bdh(i,2))
    if (xa.le.bdh(i,8)) then
      rl(i,4) = fa*(cps(i,3)+cps(i,2)+bdh(i,3))/2
      rl(i,4) = rl(i,4)-(fa-fc)*(xa+cps(i,3)+cps(i,2))/2
      rl(i,3) = xa+cps(i,2)
    else
      dw = fc/bdh(i,2)/bdh(i,7)/2.0
      cm = (cps(i,2)+cps(i,3)+bdh(i,3)-dw)/2
      rl(i,4) = rl(i,5)+fc*cm
      rl(i,3) = cps(i,2)+bdh(i,3)/2-dw
    end if
    goto 15
  10  rl(i,3) = fa/(0.85*cps(i,1)*cps(i,5))
      rl(i,4) = fa*(bdh(i,3)-rl(i,3))/2+cps(i,2))

c  --Estimate bending resistance with partial SC by linear interpolation--
c
c  15  rl(i,1) = (1-rl(i,2))*rl(i,5)+rl(i,2)*rl(i,4)
c  -----
c

```

```

20  continue
    return
    end
c
c  -----Analysis of safety of the beams with partial shear
c  connection, in conjunction with the equilibrium method-----
c
c  subroutine sfed(j, skd, bdhw, cpsw, bnuw, rew, rlw, zw)
  dimension bdhw(100,9),rew(100,3),zw(100,4),vrv(100,3),vrlw(100,3)
  dimension gaw(100,3),sflw(100,4),galw(100,3),sflw(100,4),rlw(100,5)
  dimension cpsw(100,9)
  character bnuw(100,3)*10, xap(100)*7
  common /vr/ vrv, vrlw
  common /sf/ sflw, sflw
  common /ga/ gaw, galw
  common /bcv/ bd,cvd,ccd,bdl,cvdl,ccd1,bn,cvn,ccn,bnl,cvnl,ccnl
  common vfy, vfc, vec, vfu, vd, vhc, vbc, vwa, vaa, vhg, vba, vtv
  oln(x) = sqrt(log(1.0 + x*x))

c  aks=(2.00*oln(0.08)+0.5*oln(0.08)**2-0.5*oln(vfy)**2)/oln(vfy)
c
c  aks = 2.0
  akd=1.04 + aks

c
c  pfy = exp(akd*oln(vfy) + 0.5*oln(vfy)**2)
  pfc = exp(3.04*oln(vfc) + 0.5*oln(vfc)**2)
  pec = exp(3.04*oln(vec) + 0.5*oln(vec)**2)
  pc = 1.25*sqrt(exp(1.64*oln(vfc) + 0.5*oln(vfc)**2))

c
c  rfy1 = 1.1*exp(aks*oln(vfy) + 0.5*oln(vfy)**2)
  rfy2 = 1.05*exp(aks*oln(vfy) + 0.5*oln(vfy)**2)
  rc = 1.25*exp(1.64*oln(vfc) + 0.5*oln(vfc)**2)
  ru = 1.25*sqrt(exp(1.64*oln(vfc) + 0.5*oln(vfc)**2))

c
c  do 5 i = 1,j
  if(rew(i,2).LE.bdhw(i,8)) then
    rm=zw(i,1)*zw(i,3)*(1.0-0.5*zw(i,2))-zw(i,4)*(1.0-zw(i,1))**2
    rm = rm + 1.0
    qaa = vaa*(1.0-2.0*zw(i,4)*(1.0-zw(i,1)))
    qfy = vfy*(1.0-zw(i,4)*(1.0-zw(i,1))**2)
    qd = zw(i,3)*(1.0-zw(i,2))+2.0*zw(i,4)*(1.0-zw(i,1))
    qd = qd*2.0*vd*zw(i,1)
    qhg = vhg
    qec = (1.0-zw(i,2))*zw(i,3)/2.0+zw(i,4)*(1.0-zw(i,1))
    qec = vec*zw(i,1)*qec
    qfc = vfc*zw(i,1)*(zw(i,3)/2.0+zw(i,4)*(1.0-zw(i,1)))
    qhc = vhc*zw(i,1)*zw(i,3)
    qbc = vbc*zw(i,1)*zw(i,2)*zw(i,3)/2.0
    qba = vba*zw(i,4)*(1.0-zw(i,1))**2
    vrv(i,1) = qaa**2+qfy**2+qd**2+qhg**2+qec**2+qfc**2+qhc**2
    vrv(i,1) = sqrt(vrv(i,1)+qbc**2+qba**2)/rm
    xap(i) = ' (Xa<tf)
    rm = rm*bdhw(i,2)*bdhw(i,9)*bdhw(i,3)/2.0
  else
    rm = 2.0*zw(i,1)*(1.0+zw(i,3)-zw(i,4)-zw(i,2)*zw(i,3)/2.0)
    rm = rm + 1.0
    qwa = vwa
    qfy = vfy*(1.0+2.0*zw(i,1)*zw(i,4))
    qhna = 2.0*vhg*zw(i,1)
    qec = vec*zw(i,1)*(1.0+zw(i,3)-2.0*zw(i,4)-zw(i,2)*zw(i,3))
    qfc = vfc*zw(i,1)*(1.0+zw(i,3)-2.0*zw(i,4))
    qhc = 2.0*zw(i,1)*zw(i,3)*vhc
    qd = zw(i,1)*(1.0+zw(i,3)-2.0*zw(i,4)-zw(i,2)*zw(i,3))
    qd = qd*4.0*vd

```



```

+ 'The Partial Safety Factors'
+ '-----'
write (4,40)
format (20x,'Model factor',4x,'Steel S.F',4x,'Concrete S.F',4x,
+ 'Connector S.F',/)
do 50 i=1,j
write (4,45) bnuw(i,1), xap(i), (sfw(i,k),k=1,4)
format (a,x,a,6x,f5.3,9x,f5.3,9x,f5.3,12x,f5.3)
continue
write (4,51) era,erc,eru
format (/9x,'AVERAGE VALUE',16x,f5.3,9x,f5.3,12x,f5.3)
write (4,52) via,vic,vru
format (12x,'SCATTER',19x,f5.3,9x,f5.3,12x,f5.3)
format (/2x,'-----',)
+ 'The safety fracture-factor on resistance side',
+ '-----'
write (4,55)
write (4,60)
format (25x,'Presumed',8x,'rc,ru=1.25',8x,
+ 'rc,ru=1.25',)
write (4,61)
format (26x,'value',11x,'ry=1.10',12x,'ry=1.05',/)
do 70 i = 1,j
write (4,65) bnuw(i,1), xap(i), (gaw(i,k),k=1,3)
format (a,3x,a,6x,f5.3,12x,f5.3,14x,f5.3)
continue
write (4,75) ekp,ek1,ek2
format (/6x,'AVERAGE VALUE',7x,f5.3,12x,f5.3,14x,f5.3)
write (4,80) vkp,vk1,vk2
format (9x,'SCATTER',10x,f5.3,12x,f5.3,14x,f5.3)
return
end
c
c
c
c
c
c
-----Analysis of safety of the beams with the partial shear
connection, in conjunction with the linear interpolation-----
subroutine sfld (j, skd, bdhw, cpsw, bnuw, rlw, zlw)
dimension bdhw(100,9), rlw(100,3), zlw(100,5), vrw(100,3)
dimension vrlw(100,3), cpsw(100,9)
dimension gaw(100,3), sfw(100,4), galw(100,3), sflw(100,4)
character bnuw(100,3)*10, xap(100)*13
common /vr/ vrw, vrlw
common /sf/ sfw, sflw
common /ga/ gaw, galw
common /bcv/ bd,cvd,ccd,ddl,cvdl,cvdl,ccdl,bn,cvn,ccn,bnl,cvnl,ccnl
common vfy, vfc, vec, vfu, vd, vhc, vbc, vva, vaa, vhg, vba, vtw
oln(x) = sqrt(log(1.0 + x*x))
aks=(2.00*oln(0.08)+0.5*oln(0.08)**2-0.5*oln(vfy)**2)/oln(vfy)
aks = 2.0
akd = 1.04 + aks
c
pfy = exp(akd*oln(vfy) + 0.5*oln(vfy)**2)
pfc = exp(3.04*oln(vfc) + 0.5*oln(vfc)**2)
pec = exp(3.04*oln(vec) + 0.5*oln(vec)**2)
pc = 1.25*sqrt(exp(1.64*oln(vfc) + 0.5*oln(vfc)**2))
c
rfy1 = 1.1*exp(aks*oln(vfy) + 0.5*oln(vfy)**2)
rfy2 = 1.05*exp(aks*oln(vfy) + 0.5*oln(vfy)**2)
rc = 1.25*exp(1.64*oln(vfc) + 0.5*oln(vfc)**2)
ru = 1.25*sqrt(exp(1.64*oln(vfc) + 0.5*oln(vfc)**2))
do 5 i = 1,j

```

```

zlw(i,1) = bdhw(i,9)*bdhw(i,3)*bdhw(i,2)/4.0/rlw(i,5)
zlw(i,3) = cpsw(i,2)*2.0/bdhw(i,3)
zlw(i,4) = cpsw(i,3)/cpsw(i,2)
fc = 0.85*cpsw(i,1)*cpsw(i,5)*cpsw(i,2)-cpsw(i,3)
fa = bdhw(i,9)*bdhw(i,2)
c
if (rlw(i,3).LE.(cpsw(i,2)-cpsw(i,3))) then
zlw(i,5) = fa/fa
qwa = (1.0-rlw(i,2))*vva
qaa = rlw(i,2)*(1.0-zlw(i,1)*zlw(i,3))*(1.0-zlw(i,4))*zlw(i,5)
qaa = qaa*vaa
qfy = (qaa/vaa-rlw(i,2)+1.0)*vfy
qhg = 2.0*rlw(i,2)*zlw(i,1)*vhg
qhc = qhg*zlw(i,3)*vhc/vhg
qd = 2.0+2.0*zlw(i,3)-zlw(i,5)*zlw(i,3)*(1.0-zlw(i,4))
qd = 2.0*rlw(i,2)*(qd*zlw(i,1)-1.0)*vd
qec = qd*vec/vd/4.0
qfc = 2.0+2.0*zlw(i,3)+zlw(i,5)*zlw(i,3)*(1.0-zlw(i,4))
qfc = rlw(i,2)*(qfc*zlw(i,1)-1.0)*vfc/2.0
qbc = rlw(i,2)*zlw(i,5)*zlw(i,1)*zlw(i,3)*(1.0-zlw(i,4))*vbc
rm = 2.0+2.0*zlw(i,3)-zlw(i,5)*zlw(i,3)*(1.0-zlw(i,4))
rm = rlw(i,2)*(zlw(i,1)*rm-1.0)+1.0
vrlw(i,1) = qwa**2+qaa**2+qfy**2+qhg**2+qhc**2+qec**2
vrlw(i,1) = sqrt(vrlw(i,1)+qbc**2+qfc**2)/rm
xap(i) = '( Yc<hc-hp )'
rm = rm*rlw(i,5)
else
if (rlw(i,3).LE.(cpsw(i,2)+bdhw(i,8))) then
zlw(i,5) = fc/fa
zlw(i,2) = bdhw(i,9)/bdhw(i,6)/bdhw(i,3)
qaa = (1.0-rlw(i,2))*vva
qaa = 2.0*zlw(i,1)*rlw(i,2)*(1.0-zlw(i,2))*(1.0-zlw(i,5))*vaa
qfy = zlw(i,1)*(2.0-zlw(i,2))*(1.0-zlw(i,5)**2)-1.0
qfy = (1.0+rlw(i,2)*qfy)*vfy
qhg = 2.0*zlw(i,1)*rlw(i,2)*vhg
qd = zlw(i,1)*(2.0+zlw(i,3)*(1.0+zlw(i,4))*zlw(i,5))
qd = 2.0*rlw(i,2)*(qd-zlw(i,1)*zlw(i,2))*(1.0-zlw(i,5)**2-1.0)
qd = qd*vd
qec = qd*vec/vd/4.0
qfc = zlw(i,1)*(zlw(i,3)*(1.0+zlw(i,4))*zlw(i,5)-2.0)
qfc = qfc+zlw(i,1)*zlw(i,2)*(1.0+2.0*zlw(i,5)-3.0*zlw(i,5)**2)
qfc = rlw(i,2)*(qfc+1.0)*vfc/2.0
qbc = zlw(i,1)*(zlw(i,2)*(1.0-zlw(i,5)**2-2.0)+1.0)
qbc = qbc+2.0*zlw(i,1)*zlw(i,2)*zlw(i,5)*(1.0-zlw(i,5))
qbc = rlw(i,2)*qbc*vbc
qhc = zlw(i,1)*zlw(i,2)*(1.0-zlw(i,5)**2)+1.0-2.0*zlw(i,1)
qhc = zlw(i,1)*zlw(i,3)*zlw(i,5)+qhc/(1.0-zlw(i,4))
qhc = qhc*rlw(i,2)*vhc
qba = zlw(i,1)*zlw(i,2)*rlw(i,2)*(1.0-zlw(i,5)**2*vba
rm = zlw(i,1)*(2.0+zlw(i,5)*zlw(i,3)*(1.0+zlw(i,4))-1.0)
rm = 1.0+rlw(i,2)*(rm-zlw(i,2)*zlw(i,1)*(1.0-zlw(i,5)**2)
vrlw(i,1) = qwa**2+qaa**2+qfy**2+qhg**2+qhc**2+qec**2
vrlw(i,1) = sqrt(vrlw(i,1)+qbc**2+qba**2)/rm
xap(i) = '(hc<Yc<hc+tf)'
rm = rm*rlw(i,5)
else
zlw(i,2) = bdhw(i,9)/bdhw(i,3)/bdhw(i,7)
zlw(i,5) = fc/fa
qwa = vva
qfy = (1.0+rlw(i,2)*zlw(i,5)**2*zlw(i,1)*zlw(i,2))*vfy
qd = 2.0+zlw(i,3)*(1.0+zlw(i,4))-zlw(i,5)*zlw(i,2)
qd = 2.0*rlw(i,2)*zlw(i,1)*zlw(i,5)*qd*vd
qec = qd*vec/4.0/vd
qfc = 2.0+zlw(i,3)*(1.0+zlw(i,4))-3.0*zlw(i,5)*zlw(i,2)
qfc = zlw(i,5)*rlw(i,2)*zlw(i,1)*qfc*vfc/2.0
qhc = zlw(i,3)-zlw(i,2)*zlw(i,5)/(1.0-zlw(i,4))

```



```

i2 = int(10*(ddf-1))
i3 = int(10*(10*(ddf-1)-i2))
pf = 1 - sn(i1+1,i2+1,i3+1)
return
5  pf0 = 0.0012
   skd = 3.04
   tkd = (ddf*vr**2-sk*dvt**2)/dvd**2
   dn = n
c
   write (3,50) bnu,el
   format (/25x,a,x,a)
   write (3,55) sf
   format (28x,a)
   write (3,100) n,vi,dvt,dvd,ddf
100 format (/3x,'n=',i3,' vr=',f7.5,3x,' dvt=',f7.5,3x,
+ ' dvd=',f7.5,3x,' ddf=',f7.5)
c
   pf = pnt(sqrt(dn/(dn-1))*tkd,n)
c
   write (3,150) pf0,skd
150 format(3x,'Initial trail:',f5x,'pf0=',f7.5,3x,'skd=',f7.5)
   write (3,200) pf,sqrt(dn/(dn-1))*tkd
200 format(22x,'pf =',f7.5,3x,'x =',f7.5)
c
   limit = 1
10  if (abs((pf-pf0)/pf).LT.0.001) goto 15
   pf0 = (pf+pf0)/2.0
   skd = psn(1.0-pf0)
c
   write (3,300) limit,pf0,skd
300 format (6x,'Trail ',i2,4x,'pf0=',f8.5,3x,'skd=',f8.5)
c
   tkd = (ddf*vr**2-sk*dvt**2)/dvd**2
   pf = pnt(sqrt(dn/(dn-1))*tkd,n)
c
   write (3,250) pf,sqrt(dn/(dn-1))*tkd
250 format (18x,'pf =',f8.5,3x,'x =',f8.5)
c
   limit = limit + 1
   if(limit.LT.60) goto 10
15  er = abs(pf-pf0)/pf
   pf = (pf+pf0)/2.0
c
   write (3,400) limit,pf,er
400 format (2x,'Iteration time:',i3,5x,'Pf=',f7.5,5x,'Error=',f7.5)
c
return
end
c
c ----Find out the failure probability from non-central t-distribution----
(The confidence level is 75%)
c
real function pnt(x,n)
real sn(5,10,10), cn(54,10), tn(10)
real x
common/table/ sn,tn,cn
c
check the abnormal situations
c
if (x.LT.cn(n-1,10)) then
write (6,1) x, cn(n-1,10)
write (3,1) x, cn(n-1,10)
format ('Note: here occurs: x=',f6.3,'< the min.cn=',f6.3)
1  write (6,3)
   pnt = 0.25

```

```

goto 10
end if
if (x.GT.cn(n-1,1)) then
write (6,2) x, cn(n-1,1)
write (3,2) x, cn(n-1,1)
format ('Note: here occurs: x=',f6.3,'> the max.cn=',f6.3)
2  write (6,3)
   pnt = 0.001
   goto 10
end if
format ('Please check the trace file: trail.np')
c
ix=0
ix=ix+1
5  if (x.LE.cn(n-1,ix)) goto 5
   pi = (x-cn(n-1,ix))/(cn(n-1,ix-1)-cn(n-1,ix))
   pnt = tn(ix)+pi*(tn(ix-1)-tn(ix))
10 return
end
c
c ----Find out fratile-factor based on standard normal ditribution-----
c
real function psn(p)
real sn(5,10,10), cn(54,10), tn(10)
real x, p, p0
common/table/ sn,tn,cn
c
check the abnormal situations
c
if (p.LT.sn(1,1,1)) then
write (6,1) p, sn(1,1,1)
write (3,1) p, sn(1,1,1)
format ('Note: here occurs: p=',f10.7,'< sn=',f10.7)
1  write (6,3)
   psn = 0.0
   return
end if
if (p.GT.sn(5,10,10)) then
write (6,2) p, sn(5,10,10)
write (3,2) p, sn(5,10,10)
format ('Note: here occurs: p=',f10.7,'> sn=',f10.7)
2  write (6,3)
   psn = 4.99
   return
end if
format ('Please check the trace file: trail.np')
c
p0 = sn(1,1,1)
do 15 kp=1,5
do 10 ip=1,10
do 5 jp=1,10
if (p.LE.sn(kp,ip,jp)) then
x = kp-1+real(ip-1)/10.0+real(jp-1)/100.0
psn = x-0.01*(sn(kp,ip,jp)-p)/(sn(kp,ip,jp)-p0)
return
else
p0 = sn(kp,ip,jp)
end if
5  continue
10 continue
15 continue
c
write (6,20)
format(x,'Abnormal stop occurred! Please check file trail.np')
stop

```



```
c
end
c
c ----- Find out factored reisistance with linear interpolation -----
c
c subroutine fmi(rr,fa,fc,hg,hc,hp,tw,bf,fy,bma,fs,tf,ra,rc,ru)
c
c   fyy = fy/ra
c   fss = fs/ru
c   faa = fa/ra
c   fcc = fc/rc
c   bmaa = bma/ra
c
c   yc = faa*(hc-hp)/fcc
c   if(yc.LE.(hc - hp)) then
c     bpl = faa*(hg+hc-yc/2.0)
c   else
c     ya = (faa-fcc)/2.0/fyy/bf
c     if(ya.LE.tf) then
c       bpl = faa*hg+fcc*(hc+hp)/2.0-(faa-fcc)**2/4.0/bf/fyy
c     else
c       bpl = bmaa + fcc*(hg+0.5*(hc+hp)-fcc/4.0/tw/fyy)
c     end if
c   end if
c
c   rsc = fss/min(faa,fcc)
c   rr = bmaa + rsc*(bpl - bmaa)
c
c
c
return
end
```


| | | | | |
|-------------------------|--|---|---|-----|
| 14, 1_ Robinson T | 359.8, 403.0, 1000000.0, 116.0, 177.0, 7.5, 10.9, 6717.6 | 2440.0, 141.0, 76.0, 21.3, 23.52, 9.144 | 19.0, 19.1, 2440.0, 141.0, 76.0, 21.9, 177.0, 7.5, 10.9, 6717.6 | 0.0 |
| 8, 2_ Robinson T | 359.8, 403.0, 1000000.0, 116.0, 177.0, 7.5, 10.9, 6717.6 | 2440.0, 141.0, 76.0, 21.3, 23.52, 9.144 | 19.0, 19.1, 2440.0, 141.0, 76.0, 21.9, 177.0, 7.5, 10.9, 6717.6 | 0.0 |
| 10, 70-4 T | 359.8, 403.0, 1000000.0, 116.0, 177.0, 7.5, 10.9, 6717.6 | 2440.0, 141.0, 76.0, 21.3, 23.52, 9.144 | 19.0, 19.1, 2440.0, 141.0, 76.0, 21.9, 177.0, 7.5, 10.9, 6717.6 | 0.0 |
| 19.1, 1778.0, 0.0 | 282.1, 398.5, 1000000.0, 76.2, 139.7, 6.4, 8.8, 4954.8 | 101.6, 38.1, 54.1, 21.9, 17.8, 9.144 | 282.1, 398.5, 1000000.0, 76.2, 139.7, 6.4, 8.8, 4954.8 | 0.0 |
| 14, 66-11(42) T | 342.1, 206.0, 1000000.0, 76.2, 102.0, 6.2, 8.0, 2864.5 | 101.6, 38.1, 57.2, 22.9, 22.8, 6.096 | 342.1, 206.0, 1000000.0, 76.2, 102.0, 6.2, 8.0, 2864.5 | 0.0 |
| 19.1, 1117.6, 0.0 | 318.6, 206.0, 1000000.0, 76.2, 102.0, 6.2, 8.0, 2864.5 | 101.6, 38.1, 57.2, 22.5, 22.8, 6.096 | 318.6, 206.0, 1000000.0, 76.2, 102.0, 6.2, 8.0, 2864.5 | 0.0 |
| 5, 66-11(B) T | 338.6, 311.5, 1000000.0, 76.2, 145.7, 6.8, 10.2, 4558.1 | 101.6, 38.1, 57.2, 23.9, 22.7, 6.096 | 338.6, 311.5, 1000000.0, 76.2, 145.7, 6.8, 10.2, 4558.1 | 0.0 |
| 19.1, 1117.6, 0.0 | 271.0, 351.5, 1000000.0, 76.2, 170.9, 6.9, 9.8, 5709.7 | 101.6, 38.1, 57.2, 27.8, 22.8, 6.096 | 271.0, 351.5, 1000000.0, 76.2, 170.9, 6.9, 9.8, 5709.7 | 0.0 |
| 13, 64-15(H1) T | 286.2, 310.4, 1000000.0, 76.2, 171.1, 6.0, 9.7, 4935.5 | 101.6, 38.1, 114.3, 26.6, 18.1, 4.572 | 286.2, 310.4, 1000000.0, 76.2, 171.1, 6.0, 9.7, 4935.5 | 0.0 |
| 12, 64-15(E1) T | 254.1, 310.4, 1000000.0, 76.2, 171.1, 6.0, 9.7, 5125.3 | 101.6, 38.1, 114.3, 27.7, 18.1, 4.572 | 254.1, 310.4, 1000000.0, 76.2, 171.1, 6.0, 9.7, 5125.3 | 0.0 |
| 13, 64-15(E2) T | 257.2, 310.4, 1000000.0, 76.2, 171.1, 6.0, 9.7, 5125.3 | 101.6, 38.1, 114.3, 34.6, 18.0, 4.572 | 257.2, 310.4, 1000000.0, 76.2, 171.1, 6.0, 9.7, 5125.3 | 0.0 |
| 16, 67-38 T | 274.8, 351.5, 1000000.0, 88.9, 170.9, 6.9, 9.8, 5709.7 | 120.7, 44.5, 152.4, 21.4, 18.0, 7.315 | 274.8, 351.5, 1000000.0, 88.9, 170.9, 6.9, 9.8, 5709.7 | 0.0 |

| | | | | |
|--|--|---------------------------------------|--|-----|
| 10, 71(EPIC) T | 246.9, 310.4, 1000000.0, 101.6, 164.8, 5.8, 9.7, 4935.5 | 133.4, 50.8, 21.3, 17.0, 4.572 | 246.9, 310.4, 1000000.0, 101.6, 164.8, 5.8, 9.7, 4935.5 | 0.0 |
| 11, 72-12(75) T | 404.5, 309.6, 1000000.0, 114.3, 254.3, 9.1, 16.3, 10967.7 | 158.2, 76.2, 28.0, 18.0, 7.62 | 404.5, 309.6, 1000000.0, 114.3, 254.3, 9.1, 16.3, 10967.7 | 0.0 |
| 14, 73(RF) T | 264.1, 351.5, 1000000.0, 139.7, 170.9, 6.9, 9.8, 5709.7 | 158.8, 76.2, 101.6, 17.0, 7.62 | 264.1, 351.5, 1000000.0, 139.7, 170.9, 6.9, 9.8, 5709.7 | 0.0 |
| 16, 67-11(B1) T | 269.3, 310.4, 1000000.0, 127.0, 171.1, 6.0, 9.7, 5125.3 | 139.7, 76.2, 103.1, 18.0, 4.572 | 269.3, 310.4, 1000000.0, 127.0, 171.1, 6.0, 9.7, 5125.3 | 0.0 |
| 19.1, 1219.2, 14964.91 8, 67-11(B2) T | 269.3, 310.4, 1000000.0, 127.0, 171.1, 6.0, 9.7, 5125.3 | 139.7, 76.2, 103.1, 18.0, 4.572 | 269.3, 310.4, 1000000.0, 127.0, 171.1, 6.0, 9.7, 5125.3 | 0.0 |
| 19.1, 1219.2, 14964.91 8, 68-4(1) T | 263.8, 351.5, 1000000.0, 76.2, 170.9, 6.9, 9.8, 5709.7 | 101.6, 38.1, 57.1, 18.0, 6.096 | 263.8, 351.5, 1000000.0, 76.2, 170.9, 6.9, 9.8, 5709.7 | 0.0 |
| 19.1, 1193.8, 17861.35 13, 68-5(2) T | 317.6, 396.8, 1000000.0, 76.2, 139.7, 6.4, 9.5, 4935.5 | 101.6, 38.1, 57.1, 17.0, 9.114 | 317.6, 396.8, 1000000.0, 76.2, 139.7, 6.4, 9.5, 4935.5 | 0.0 |
| 14, 69-1(3) T | 259.0, 351.5, 1000000.0, 76.2, 170.9, 6.9, 9.8, 5709.7 | 101.6, 38.1, 57.1, 18.0, 6.096 | 259.0, 351.5, 1000000.0, 76.2, 170.9, 6.9, 9.8, 5709.7 | 0.0 |
| 12, 70-31(A) T | 251.7, 351.5, 1000000.0, 76.2, 170.9, 6.9, 9.8, 5709.7 | 101.6, 38.1, 57.1, 18.0, 5.791 | 251.7, 351.5, 1000000.0, 76.2, 170.9, 6.9, 9.8, 5709.7 | 0.0 |
| 19.1, 1219.2, 16344.17 18, 70-31(D) T | 251.7, 351.5, 1000000.0, 76.2, 170.9, 6.9, 9.8, 5709.7 | 101.6, 38.1, 57.1, 18.0, 5.791 | 251.7, 351.5, 1000000.0, 76.2, 170.9, 6.9, 9.8, 5709.7 | 0.0 |
| 12.7, 1219.2, 16344.17 23, 70-31(C) T | 251.7, 351.5, 1000000.0, 76.2, 170.9, 6.9, 9.8, 5709.7 | 101.6, 38.1, 57.1, 18.0, 5.791 | 251.7, 351.5, 1000000.0, 76.2, 170.9, 6.9, 9.8, 5709.7 | 0.0 |
| 19.1, 1828.8, 16344.17 T | 241.0, 463.3, 1000000.0, 127.0, 191.9, 10.5, 17.7, 11354.8 | 152.4, 76.2, 143.0, 22.8, 18.0, 10.82 | 241.0, 463.3, 1000000.0, 127.0, 191.9, 10.5, 17.7, 11354.8 | 0.0 |

| | | | | | | | | | |
|------------|--------|--------|------------|--------|--------|-------|-------|---------|--|
| 0.0 | | | | | | | | | |
| 10, | 1 | | | | | | | | |
| 70-4 | | | | | | | | | |
| T | | | | | | | | | |
| 19.1, | 282.1, | 398.5, | 1000000.0, | 76.2, | 139.7, | 6.4, | 8.8, | 4954.8 | |
| 1778.0, | 101.6, | 38.1, | 54.1, | 21.9, | 17.8, | 9.144 | | | |
| 0.0 | | | | | | | | | |
| 14, | 1 | | | | | | | | |
| 66-11 (42) | | | | | | | | | |
| T | | | | | | | | | |
| 19.1, | 342.1, | 206.0, | 1000000.0, | 76.2, | 102.0, | 6.2, | 8.0, | 2864.5 | |
| 1117.6, | 101.6, | 38.1, | 57.2, | 22.9, | 22.8, | 6.096 | | | |
| 0.0 | | | | | | | | | |
| 4, | 1 | | | | | | | | |
| 66-11 (56) | | | | | | | | | |
| T | | | | | | | | | |
| 19.1, | 318.6, | 206.0, | 1000000.0, | 76.2, | 102.0, | 6.2, | 8.0, | 2864.5 | |
| 1117.6, | 101.6, | 38.1, | 57.2, | 22.5, | 22.8, | 6.096 | | | |
| 0.0 | | | | | | | | | |
| 5, | 1 | | | | | | | | |
| 66-11 (W) | | | | | | | | | |
| T | | | | | | | | | |
| 19.1, | 271.0, | 351.5, | 1000000.0, | 76.2, | 170.9, | 6.9, | 9.8, | 5709.7 | |
| 1193.8, | 101.6, | 38.1, | 57.2, | 27.8, | 22.8, | 6.096 | | | |
| 0.0 | | | | | | | | | |
| 13, | 1 | | | | | | | | |
| 64-15 (H1) | | | | | | | | | |
| T | | | | | | | | | |
| 19.1, | 286.2, | 310.4, | 1000000.0, | 76.2, | 171.1, | 6.0, | 9.7, | 4935.5 | |
| 1219.2, | 101.6, | 38.1, | 114.3, | 26.6, | 18.1, | 4.572 | | | |
| 0.0 | | | | | | | | | |
| 12, | 1 | | | | | | | | |
| 64-15 (E1) | | | | | | | | | |
| T | | | | | | | | | |
| 19.1, | 254.1, | 310.4, | 1000000.0, | 76.2, | 171.1, | 6.0, | 9.7, | 5125.3 | |
| 1219.2, | 101.6, | 38.1, | 114.3, | 27.7, | 18.1, | 4.572 | | | |
| 0.0 | | | | | | | | | |
| 13, | 1.49 | | | | | | | | |
| 64-15 (E2) | | | | | | | | | |
| T | | | | | | | | | |
| 19.1, | 257.2, | 310.4, | 1000000.0, | 76.2, | 171.1, | 6.0, | 9.7, | 5125.3 | |
| 1219.2, | 101.6, | 38.1, | 114.3, | 34.6, | 18.0, | 4.572 | | | |
| 0.0 | | | | | | | | | |
| 16, | 2 | | | | | | | | |
| 67-38 | | | | | | | | | |
| T | | | | | | | | | |
| 19.1, | 274.8, | 351.5, | 1000000.0, | 88.9, | 170.9, | 6.9, | 9.8, | 5709.7 | |
| 1473.2, | 120.7, | 44.5, | 152.4, | 21.4, | 18.0, | 7.315 | | | |
| 0.0 | | | | | | | | | |
| 10, | 2 | | | | | | | | |
| 71 (EPIC) | | | | | | | | | |
| T | | | | | | | | | |
| 19.1, | 246.9, | 310.4, | 1000000.0, | 101.6, | 164.8, | 5.8, | 9.7, | 4935.5 | |
| 1524.0, | 133.4, | 50.8, | 127.0, | 21.3, | 17.0, | 4.572 | | | |
| 0.0 | | | | | | | | | |
| 11, | 1 | | | | | | | | |
| 72-12 (75) | | | | | | | | | |
| T | | | | | | | | | |
| 19.1, | 404.5, | 309.6, | 1000000.0, | 114.3, | 254.3, | 9.1, | 16.3, | 10967.7 | |
| 1828.8, | 158.2, | 76.2, | 184.2, | 28.0, | 18.0, | 7.62 | | | |
| 0.0 | | | | | | | | | |
| 14, | 2 | | | | | | | | |
| 73 (RF) | | | | | | | | | |
| T | | | | | | | | | |
| 19.1, | 264.1, | 351.5, | 1000000.0, | 139.7, | 170.9, | 6.9, | 9.8, | 5709.7 | |
| 2438.4, | 158.8, | 76.2, | 101.6, | 32.7, | 17.0, | 7.62 | | | |

| | | | | | | | | | |
|----------------|--------|--------|------------|--------|--------|-------|-------|---------|--|
| 0.0 | | | | | | | | | |
| 16, | 2 | | | | | | | | |
| 67-11 (B1, B2) | | | | | | | | | |
| T | | | | | | | | | |
| 19.1, | 269.3, | 310.4, | 1000000.0, | 127.0, | 171.1, | 6.0, | 9.7, | 5125.3 | |
| 1219.2, | 139.7, | 76.2, | 103.1, | 32.07, | 18.0, | 4.572 | | | |
| 14964.91 | | | | | | | | | |
| 8, | 2 | | | | | | | | |
| 68-4 (1) | | | | | | | | | |
| T | | | | | | | | | |
| 19.1, | 263.8, | 351.5, | 1000000.0, | 76.2, | 170.9, | 6.9, | 9.8, | 5709.7 | |
| 1193.8, | 101.6, | 38.1, | 57.1, | 29.7, | 18.0, | 6.096 | | | |
| 17861.35 | | | | | | | | | |
| 13, | 1 | | | | | | | | |
| 68-5 (2) | | | | | | | | | |
| T | | | | | | | | | |
| 19.1, | 317.6, | 396.8, | 1000000.0, | 76.2, | 139.7, | 6.4, | 9.5, | 4935.5 | |
| 1155.7, | 101.6, | 38.1, | 57.1, | 23.5, | 17.0, | 9.114 | | | |
| 17123.45 | | | | | | | | | |
| 14, | 1 | | | | | | | | |
| 69-1 (3) | | | | | | | | | |
| T | | | | | | | | | |
| 19.1, | 259.0, | 351.5, | 1000000.0, | 76.2, | 170.9, | 6.9, | 9.8, | 5709.7 | |
| 1193.8, | 101.6, | 38.1, | 57.1, | 31.7, | 18.0, | 6.096 | | | |
| 15378.69 | | | | | | | | | |
| 12, | 1 | | | | | | | | |
| 70-31 (A) | | | | | | | | | |
| T | | | | | | | | | |
| 19.1, | 251.7, | 351.5, | 1000000.0, | 76.2, | 170.9, | 6.9, | 9.8, | 5709.7 | |
| 1219.2, | 101.6, | 38.1, | 57.1, | 22.8, | 18.0, | 5.791 | | | |
| 16344.17 | | | | | | | | | |
| 18, | 1.43 | | | | | | | | |
| 70-31 (D) | | | | | | | | | |
| T | | | | | | | | | |
| 12.7, | 251.7, | 351.5, | 1000000.0, | 76.2, | 170.9, | 6.9, | 9.8, | 5709.7 | |
| 1219.2, | 101.6, | 38.1, | 57.1, | 22.8, | 18.0, | 5.791 | | | |
| 16344.17 | | | | | | | | | |
| 23, | 1.68 | | | | | | | | |
| 70-31 (C) | | | | | | | | | |
| T | | | | | | | | | |
| 19.1, | 241.0, | 463.3, | 1000000.0, | 127.0, | 191.9, | 10.5, | 17.7, | 11354.8 | |
| 1828.8, | 152.4, | 76.2, | 143.0, | 22.8, | 18.0, | 10.82 | | | |
| 16344.17 | | | | | | | | | |
| 18, | 1.09 | | | | | | | | |
| 69-2 (HR) | | | | | | | | | |
| T | | | | | | | | | |
| 19.1, | 263.1, | 258.3, | 1000000.0, | 127.8, | 139.5, | 5.8, | 9.1, | 3996.8 | |
| 1270.0, | 157.5, | 76.2, | 66.8, | 33.1, | 23.0, | 6.401 | | | |
| 24068.00 | | | | | | | | | |
| 6, | 1 | | | | | | | | |
| 67-36 (CU3) | | | | | | | | | |
| T | | | | | | | | | |
| 15.9, | 251.0, | 310.4, | 1000000.0, | 63.5, | 171.1, | 6.0, | 9.7, | 5125.3 | |
| 1587.5, | 88.9, | 38.1, | 57.2, | 22.1, | 23.0, | 7.315 | | | |
| 0.0 | | | | | | | | | |
| 18, | 1.23 | | | | | | | | |
| 65-19 BS12 | | | | | | | | | |
| T | | | | | | | | | |
| 19.1, | 266.5, | 310.4, | 1000000.0, | 76.2, | 171.1, | 6.1, | 9.7, | 5125.3 | |
| 1219.2, | 101.6, | 33.3, | 57.1, | 27.6, | 23.0, | 4.572 | | | |
| 0.0 | | | | | | | | | |
| 14, | 1 | | | | | | | | |
| 65-19 BS11 | | | | | | | | | |
| T | | | | | | | | | |
| 19.1, | 267.6, | 310.4, | 1000000.0, | 76.2, | 171.1, | 6.1, | 9.7, | 5125.3 | |
| 1219.2, | 101.6, | 22.4, | 44.5, | 27.6, | 23.0, | 4.572 | | | |


```

0.0
14, 1
67-36 (CU2)
T
15.6, 279.3, 310.4, 1000000.0, 63.5, 171.1, 6.1, 9.7, 5125.3
1587.5, 88.9, 38.1, 92.2, 29.0, 23.0, 7.315
0.0
18, 1
67-36 (CUI)
T
15.6, 279.3, 310.4, 1000000.0, 63.5, 171.1, 6.1, 9.7, 5125.3
1587.5, 88.9, 38.1, 127.0, 29.0, 23.0, 7.315
0.0
18, 1.32
TEX-<1,6>
T
19.1, 259.1, 413.0, 1000000.0, 114.3, 179.6, 9.7, 16.0, 9483.9
2438.4, 158.8, 76.2, 152.4, 22.8, 16.5, 9.754
0.0
26, 2
TEX-<2,8>
T
19.1, 275.33, 413.0, 1000000.0, 139.7, 179.6, 9.7, 16.0, 9483.9
2438.4, 158.8, 76.2, 152.4, 27.07, 16.5, 9.754
0.0
26, 2
TEX-3
T
19.1, 250.0, 413.0, 1000000.0, 152.4, 179.6, 9.7, 16.0, 9483.9
2438.4, 158.8, 76.2, 152.4, 26.2, 17.0, 9.754
0.0
26, 2
TEX-<4,5,7>
T
19.1, 260.9, 413.0, 1000000.0, 127.0, 179.6, 9.7, 16.0, 9483.9
2438.4, 158.8, 76.2, 152.4, 25.03, 16.3, 9.754
0.0
26, 2
IR-76<1,2>
T
19.1, 265.2, 409.7, 1000000.0, 127.0, 178.7, 8.8, 14.4, 8580.6
2413.0, 139.7, 76.2, 184.2, 30.73, 23.0, 9.754
0.0
12, 2
RFHHR<1,2>
T
19.1, 270.9, 409.7, 1000000.0, 127.0, 178.7, 8.8, 14.4, 8580.6
2413.0, 139.7, 76.2, 152.4, 30.28, 22.75, 9.754
0.0
12, 2
72-12 (80)
T
19.1, 244.8, 307.8, 1000000.0, 114.3, 304.8, 9.9, 15.4, 12322.6
1828.8, 177.8, 76.2, 184.2, 26.6, 18.0, 7.62
0.0
21, 2
75-16
T
19.1, 312.1, 406.7, 1000000.0, 114.3, 177.7, 7.7, 12.8, 7612.9
2209.8, 127.0, 76.2, 152.4, 22.7, 23.0, 9.144
0.0
12, 1
175-75
T
19.1, 265.5, 598.7, 1000000.0, 127.0, 177.9, 10.0, 12.8, 10451.6
2616.2, 158.8, 76.2, 184.2, 27.9, 18.0, 10.638

```

```

0.0
18, 1.68
174-75
T
19.1, 250.0, 603.0, 1000000.0, 177.8, 175.9, 10.7, 15.0, 11552.5
2616.2, 228.6, 76.2, 184.2, 29.3, 23.0, 10.638
0.0
22, 2
16-76
T
19.1, 286.2, 524.8, 1000000.0, 124.5, 165.1, 8.9, 11.4, 8387.1
2400.3, 139.7, 76.2, 171.5, 23.9, 23.0, 12.192
0.0
20, 2
BS<1,2>
T
19.0, 454.8, 360.0, 1000000.0, 100.0, 170.0, 8.0, 12.7, 7270.0
1500.0, 130.0, 51.0, 114.5, 35.3, 23.0, 7.7775
0.0
13, 1
1S (Warwi.)
T
19.0, 327.0, 528.3, 1000000.0, 100.0, 208.7, 9.6, 13.2, 10400.0
2500.0, 120.0, 60.0, 150.0, 34.6, 23.0, 10.0
0.0
17, 1
1 (Cardiff)
T
19.0, 297.0, 312.7, 1E6, 100.0, 102.4, 6.6, 10.8, 4180.0
2000.0, 125.0, 50.0, 150.0, 33.6, 19.5, 8.0
24300
5, 1
2 (Cardiff)
T
19.0, 325.0, 312.7, 1E6, 100.0, 102.4, 6.6, 10.8, 4180.0
2000.0, 125.0, 50.0, 150.0, 35.2, 19.5, 8.0
19300
3, 1
3 (Cardiff)
T
19.0, 307.0, 312.7, 1E6, 100.0, 102.4, 6.6, 10.8, 4180.0
2000.0, 125.0, 50.0, 150.0, 32.0, 19.5, 8.0
20300
4, 1
4 (Cardiff)
T
19.0, 317.0, 312.7, 1E6, 100.0, 102.4, 6.6, 10.8, 4180.0
2000.0, 125.0, 50.0, 150.0, 32.0, 19.5, 8.0
24000
2, 1

```



```

c This package serves the safety analysis of composite beams with
c non-ductile shear connectors, the flexure resistance of such beams
c can be hereby evaluated, in accordance with EC4 of 1991. This program
c is also designed to find out the concerned test corrections. The
c program-making was started in 12th July 1992, and the last version
c is updated to 30th July 1992.
c
c Program NTC
c
c dimension es(100), bdh(100,11), cps(100,9), ni(100)
c dimension rc(100,5), esf(100), np(100), nmax(100)
c dimension tsu(100), ru(100,3), nu(100)
c dimension tsp(100), rp(100,3), rtmax(100)
c real ns(100,2)
c character bnum(100,3)*10
c character date*8, conb, form*3, b*10
c
c common /nik/ ni, np, nu, nmax
c common /nsc/ ns
c common /bc/ bdh, cps
c common /bn/ bnum
c common /puc/ rp, ru, rc, rtmax
c
c open (2, file = 'inodn')
c open (3, file = 'temp')
c open (4, file = 'outodn')
c
c write (6,5)
c format (/2x,'This program can be used to calculate the', x,
+ 'flexure resistance of',/2x,'composite beams with non-ductile',
+ x, 'shear connection.')
c
c write (6,10)
c format (/2x,'Does this program make you happy?'/2x,'If yes', x,
+ 'press RETURN key to continue, otherwise enter N to stop.', /)
c read (5,'(a)') conb
c if (conb.NE.'n'.AND.conb.NE.'N') goto 21
c stop
c
c write (6,25)
c format (/14x,'Please input current date in form of "***/**/****".',/)
c read (5,'(a)') date
c write (4,27)
c format (/2x,'The calculation of test correction for beams with ',
+ 'non-ductile connectors')
c write (4,28) date
c format (/33x,a,/)
c
c read (2,*) nn, arg
c do 30 i=1,nn
c read (2,'(a)') (bnum(i,j), j=1,2)
c read (2,*) (bdh(i,j), j=1,11)
c read (2,*) (cps(i,j), j=1,7)
c read (2,*) cps(i,9)
c read (2,*) (ns(i,j), j=1,2)
c read (2,*) es(i)
c continue
c
c call ccpu (nn, arg, k, kp, ku, kmax)
c
c write (3,52) kmax
c format (i3)
c do 105 i = 1, kmax
c jm = nmax(i)
c write (3,53) (bnum(ni(jm),j), j = 1, 3)
c format(a)
c write (3,50) (bdh(ni(jm),j), j = 1, 11)
c format (f14.3)

```

```

c
c write (3,50) (cps(ni(jm),j), j = 1, 9)
c write (3,70) ns(ni(jm),1), ns(ni(jm),2)
c format (2f12.2)
c write (3,71) rp(jm,1), rp(jm,2), rp(jm,3)
c format (3e14.4)
c write (3,71) ru(jm,1), ru(jm,2), ru(jm,3)
c write (3,72) rc(jm,1), rc(jm,2), rc(jm,3), rc(jm,4), rc(jm,5)
c format (5e14.4)
c 105 continue
c
c write (4,15) nn, k
c format (/3x,'The number of beams checked is',i3,';', ' and',
+ ' there are',i3,' beams with non-ductile connectors.')
```

```

c write (4,16) arg
c format (/,' (Shear Connection Factor = ',f4.2,')')
```

```

c write (4,17)
c format (//,' The following beams are excluded, as Map1,Rd > M :')
```

```

c write (4,18)
c format (/2x,'(1) for propped construction',/)
```

```

c write (4,155)
c write (4,160)
c do 20 i = 1,k
c do 19 j = 1,kp
c if (i.eq.np(j)) goto 20
c continue
c rlk = rc(i,5)/1000000.
c rek = rp(i,3)/1000000.
c ral = rlk/rek
c rae = es(ni(i))/rek
c form = '(c)'
```

```

c if (bnum(ni(i),3).EQ.'(stud)') form = '(s)'
```

```

c b = bnum(ni(i),1)
c rld = cps(ni(i),8)
c write (4,165) b,rc(i,3),form,rld,rlk,rek,es(ni(i)),ral,rae
c 20 continue
c
c write (4,118)
c 118 format (/2x,'(2) for unpropped construction',/)
```

```

c write (4,255)
c write (4,260)
c do 120 i = 1,k
c do 119 j = 1,ku
c if (i.eq.nu(j)) goto 120
c continue
c rlk = rc(i,5)/1000000.
c rek = ru(i,3)/1000000.
c ral = rlk/rek
c rae = es(ni(i))/rek
c form = '(c)'
```

```

c if (bnum(ni(i),3).EQ.'(stud)') form = '(s)'
```

```

c b = bnum(ni(i),1)
c rld = cps(ni(i),8)
c write (4,165) b,rc(i,3),form,rld,rlk,rek,es(ni(i)),ral,rae
c 120 continue
c
c write (4,44) 'Results of beams with the non-ductile connection'
```

```

c format (//,'* * * * *',a,' * * * * *')
```

```

c write (4,45) '(Assuming propped construction)'
```

```

c format (22x,a,/)
c
c ip = 0.0
c do 35 i = 1, kp
c if (es(ni(np(i))).eq.0.0) goto 35
c ip = ip + 1
c esf(ip) = es(ni(np(i)))

```



```

35  tsp(ip) = rp(np(i),3)/1000000.0
    continue
    call cmce (ip,cmvp, cvoep, ccp, esf, tsp)
    write (4,155)
155  format ('Beam name',3x,'SC ratio',2x,'LBSCR',2x,' Map1,Rd ',2x,
+ 'M (prop.)',2x,'M by test',3x,'(1)/(2)',x,'(3)/(2)')
    write (4,160)
160  format (33x,'(1)',8x,'(2)',8x,'(3)',/)
    do 170 i = 1, kp
    if (es(ni(np(i))).eq.0.0) goto 170
    rlk = rc(np(i),5)/1000000.
    rek = rp(np(i),3)/1000000.
    ral = rlk/rek
    rae = es(ni(np(i)))/rek
    form = '(c)'
    if (bnum(ni(np(i)),3).EQ.(stud)) form = '(s)'
    b = bnum(ni(np(i)),1)
    rld = cps(ni(np(i)),8)
165  write (4,165) b,rc(np(i),3),form,rld,rlk,rek,esf(i),ral,rae
+ f5.3)
170  continue
    write (4,75) ip
75  Format (/3x,'In the analysis based on propped construction,
+ ,x,i3,x,'specimens are used;')
    write (4,90) cmvp
    write (4,95) cvoep
    write (4,100) ccp
c
    iu = 0
    do 36 i = 1, ku
    if(es(ni(nu(i))).eq.0.0) goto 36
    iu = iu + 1
    esf(iu) = es(ni(nu(i)))
    tsu(iu) = ru(nu(i),3)/1000000.0
36  continue
    call cmce (iu,cmvu, cvoeu, ccu, esf, tsu)
c
    write (4,244) 'Results of beams with the non-ductile connection'
244  format (/'*** * * * * ,a, * * * * *')
    write (4,245) '(Assuming unpropped construction)'
245  format (21x,a,/)
    write (4,255)
255  format ('Beam name',3x,'SC ratio',2x,'LBSCR',2x,' Map1,Rd ',2x,
+ 'M (unpr.)',2x,'M by test',3x,'(1)/(2)',x,'(3)/(2)')
    write (4,260)
260  format (33x,'(1)',8x,'(2)',8x,'(3)',/)
    do 270 i = 1, ku
    if (es(ni(nu(i))).eq.0.0) goto 270
    rlk = rc(nu(i),5)/1000000.
    rek = ru(nu(i),3)/1000000.
    ral = rlk/rek
    rae = es(ni(nu(i)))/rek
    form = '(c)'
    if (bnum(ni(nu(i)),3).EQ.(stud)) form = '(s)'
    b = bnum(ni(nu(i)),1)
    rld = cps(ni(nu(i)),8)
    write (4,165) b,rc(nu(i),3),form,rld,rlk,rek,esf(i),ral,rae
270  continue
    write (4,85) iu
85  format (/3x,'In the analysis based on unpropped construction,
+ ,x,i3,x,'specimens are used;')
    write (4,90) cmvu
    write (4,95) cvoeu
    write (4,100) ccu

```

```

c
90  format (3x,'the mean value correction is ',f5.3,')
95  format (3x,'the c.v of observing error terms is ',f5.3,')
100  format (3x,'the correlation coefficient of test and thereoy is ',
+ f8.6,')
c
    imax = 0
    do 335 i = 1, kmax
    if (es(ni(nmax(i))).eq.0.0) goto 335
    imax = imax + 1
    esf(imax) = es(ni(nmax(i)))
    tsp(imax) = rtmax(i)/1000000.0
335  continue
    call cmce (imax,cmvmax, cvoemax, ccmax, esf, tsp)
c
    write (4,44) 'Results of beams with the non-ductile connection'
    write (4,445) '(Adopting maximum theoretical resistances)'
445  format (18x,a,/)
c
    write (4,455)
455  format ('Beam name',3x,'SC ratio',2x,'LBSCR',2x,' Map1,Rd ',2x,
+ 'M (maxi.)',2x,'M by test',3x,'(1)/(2)',x,'(3)/(2)')
    do 470 i = 1, kmax
    if (es(ni(nmax(i))).eq.0.0) goto 470
    rlk = rc(nmax(i),5)/1000000.
    rek = rtmax(i)/1000000.
    ral = rlk/rek
    rae = es(ni(nmax(i)))/rek
    form = '(c)'
    if (bnum(ni(nmax(i)),3).EQ.(stud)) form = '(s)'
    b = bnum(ni(nmax(i)),1)
    rld = cps(ni(nmax(i)),8)
    write (4,165) b,rc(nmax(i),3),form,rld,rlk,rek,esf(i),ral,rae
470  continue
c
    write (4,375) imax
375  Format (/3x,'In the analysis based on maximum theoretical values,
+ ,x,i3,x,'specimens are used;')
    write (4,90) cmvmax
    write (4,95) cvoemax
    write (4,100) ccmax
c
    write (4,106)
106  format (/'/'/'Beam name',4x,'Fc',5x,'Mel,p',3x,'Mel,u',2x,
+ 'Fc/Fel,p',2x,'Fc/Fel,u',2x,'Me/Mf',3x,'Mu/Mf',3x,'Mp/Mf',/)
    do 125 i = 1,k
    Fc = rc(i,2)/1000.
    Bmelp = rp(i,1)/1000000.
    Bmelu = ru(i,1)/1000000.
    Rfcep = rc(i,2)/rp(i,2)
    Rfceu = rc(i,2)/ru(i,2)
    RMeMf = es(ni(i))/rc(i,4)*1000000.0
    RMpMf = ru(i,3)/rc(i,4)
    RMpMf = rp(i,3)/rc(i,4)
    b = bnum(ni(i),1)
    write (4,102) b,Fc,Bmelp,Bmelu,Rfcep,Rfceu,RMeMf,RMpMf
102  format (a,x,f6.1,2x,f6.1,2x,f6.1,3x,f5.3,5x,f5.3,4x,f5.3,3x,
+ f5.3, 3x,f5.3)
125  continue
c
    write (3,91) ip, cmvp, cvoep, ccp
91  format (i3,3f10.4)
    write (3,91) iu, cmvu, cvoeu, ccu
    write (3,91) imax, cmvmax, cvoemax, ccmax
c
    close(2)

```



```

c close(3)
c close(4)
c stop
c end
c
c Subroutine cfpu(nn, arg, k, kp, ku, kmax)
c
c dimension bdh(100,11), cps(100,9), ni(100), rc(100,5)
c dimension ru(100,3), np(100), nmax(100)
c dimension rp(100,3), nu(100), rtmax(100)
c real ns(100,2)
c character bnum(100,3)*10
c
c common /nik/ ni, np, nu, nmax
c common /bc/ bdh, cps
c common /nsc/ ns
c common /bn/ bnum
c common /puc/ rp, ru, rc, rtmax
c
c Bmsd1(Fc, Fel, Bmel, Bmasd) = Fc*(Bmel-Bmasd)/Fel+Bmasd
c Bmsd2(Fc, Fel, Fcf, Bmrd, Bmel) = (Fc-Fel)*(Bmrd-Bmel)/(Fcf-Fel)+Bmel
c wa(ha,ba,tf,tw) = (ba*ha*ha-(ba-tw)*(ha-2*tf)**2)/4
c sd(h,hp,b0) = b0*(h-hp)/hp**2
c
c k = 0
c kp = 0
c ku = 0
c do 10 i=1,nn
c
c *****Determine Fc, N/Nf and Ma,sd *****
c
c Fc = 0.85*cps(i,1)*cps(i,5)*(cps(i,2)-cps(i,3))
c Fa = bdh(i,2)*bdh(i,9)
c if (bnum(i,2).eq.'g'.or.bnum(i,2).eq.'G') then
c   Fs = bdh(i,1)*min(fc,fa)
c   el = 1.0
c   if (cps(i,6).LT.23.52) el = (cps(i,6)/23.52)**2
c   if (cps(i,9).eq.0.0) cps(i,9) = el*9500*exp(log(cps(i,5))/3.0)
c   goto 3
c end if
c beta = 1.0
c if (bnum(i,2).eq.'s'.or.bnum(i,2).eq.'S') goto 5
c if (bnum(i,2).eq.'T'.or.bnum(i,2).eq.'t') then
c   if (ns(i,2).gt.2.0) ns(i,2) = 2.0
c   beta = 0.7*sd(bdh(i,5),cps(i,3),cps(i,4))/sqrt(ns(i,2))
c else
c   beta = 0.6*sd(bdh(i,5),cps(i,3),cps(i,4))
c end if
c if (beta.gt.1.0) beta = 1.0
c prds = 0.62832*bdh(i,4)*bdh(i,1)**2
c arlfa = 0.2*(bdh(i,5)/bdh(i,1)+1)
c if (arlfa.gt.1.0) arlfa = 1.0
c el = 1.0
c if (cps(i,6).LT.23.52) el = (cps(i,6)/23.52)**2
c if (cps(i,9).eq.0.0) cps(i,9) = el*9500*exp(log(cps(i,5))/3.0)
c prdc = arlfa*arg*bdh(i,1)**2*sqrt(cps(i,9)*cps(i,5))
c Fs = prdc*beta*ns(i,1)
c bnum(i,3) = 'concrete'
c if (prdc.gt.prds) then
c   Fs = prds*beta*ns(i,1)
c   bnum(i,3) = 'stud'
c end if
c cps(i,8) = 0.25+0.03*cps(i,7)

```

```

c if (cps(i,7).LE.5.0) cps(i,8) = 0.4
c if (cps(i,7).GT.25.0) cps(i,8) = 1.0
c
c if (cps(i,8).LE.Fs/min(Fc,Fa)) goto 10
c
c k = k+1
c ni(k) = i
c rc(k,2) = Fs
c rc(k,3) = Fs/min(Fc,Fa)
c qwc = (cps(i,2)-cps(i,3)/2.0)*cps(i,6)*cps(i,1)/1000000.0
c rc(k,1) = 1000000.0*cps(i,7)**2*qwc/8.0
c sigmaa = rc(k,1)*bdh(i,3)/bdh(i,11)/2.0
c
c *****Determine Mrd *****
c
c if (Fc.GE.Fa) then
c   Yc = Fa/cps(i,5)/cps(i,1)/0.85
c   rc(k,4) = Fa*(bdh(i,3)/2.0 - Yc/2.0 + cps(i,2))
c else
c   if (Fa-Fc.GT.2.0*bdh(i,6)*bdh(i,8)*bdh(i,2)) then
c     dw = Fc/2.0/bdh(i,2)/bdh(i,7)
c     rc(k,4) = bdh(i,2)*wa(bdh(i,3),bdh(i,6),bdh(i,8),bdh(i,7))
c     rc(k,4) = Fc*(cps(i,3)+cps(i,2)+bdh(i,3)-dw)/2.0 + rc(k,4)
c
c     write(6,11) bnum(i,1)
c     format(/x,'Warning: the neutral axis for plastic bending ',
c           'resistance with full shear connection of beam ',a,' is in ',
c           'steel web, please check from file outodn if this resistance ',
c           'is used to determine the resistance wanted --- if it is ',
c           'then it is suggested to exclude this beam, as the program ',
c           'has not been developed well to deal with this unusual case.',/)
c
c   else
c     Xa = (Fa-Fc)/bdh(i,6)/bdh(i,2)/2.0
c     rc(k,4) = Fc*(cps(i,2)+cps(i,3)+bdh(i,3))/2.0
c     rc(k,4) = (Fa-Fc)*(bdh(i,3)-Xa)/2.0 + rc(k,4)
c   end if
c end if
c
c *****Determine Mel,rd *****
c
c call elrdp(i, rp(k,1), rp(k,2), 0.0)
c call elrdp(i, ru(k,1), ru(k,2), sigmaa, rc(k,2), rc(k,1))
c
c *****Determine Msd (propped) *****
c
c if (rc(k,2).LT.rp(k,2)) then
c   rp(k,3) = Bmsd1(rc(k,2), rp(k,2), rp(k,1), 0.0)
c else
c   rp(k,3) = Bmsd2(rc(k,2), rp(k,2), min(Fc,Fa), rc(k,4), rp(k,1))
c end if
c
c *****Determine Msd (unpropped) *****
c
c if (rc(k,2).LT.ru(k,2)) then
c   ru(k,3) = Bmsd1(rc(k,2), ru(k,2), ru(k,1), rc(k,1))
c else
c   ru(k,3) = Bmsd2(rc(k,2), ru(k,2), min(Fc,Fa), rc(k,4), ru(k,1))
c end if
c rc(k,5) = bdh(i,2)*wa(bdh(i,3),bdh(i,6),bdh(i,8),bdh(i,7))
c if (rc(k,5).gt.rp(k,3)) goto 12
c kp = kp + 1
c np(kp) = k
c ku = ku + 1
c nu(ku) = k

```



```

10 continue
c
kmax = 0
do 9 i = 1, k
  if (ru(i,3).LT.rp(i,3)) then
    if (rc(i,5).LE.rp(i,3)) then
      kmax = kmax + 1
      nmax(kmax) = i
      rtmax(kmax) = rp(i,3)
    end if
  else
    if (rc(i,5).LE.ru(i,3)) then
      kmax = kmax + 1
      nmax(kmax) = i
      rtmax(kmax) = ru(i,3)
    end if
  end if
end if
9 continue
c
return
end
c
Subroutine elrdu(i, Bmelrd, Fel, sigmaa)
real Ie
dimension bdh(100,11), cps(100,9)
common /bc/ bdh, cps
ae = bdh(i,10)/cps(i,9)
r = bdh(i,9)/cps(i,1)/(cps(i,2)-cps(i,3))
Ye = (cps(i,2)-cps(i,3))/2.0+ae*r*(bdh(i,3)/2.0+cps(i,2))
Ye = Ye/(1+ae*r)
Ie = bdh(i,11)+cps(i,1)*(cps(i,2)-cps(i,3))**3/ae/12.0
Ie = Ie+bdh(i,9)*(bdh(i,3)+cps(i,2)+cps(i,3))**2/(1+ae*r)/4.0
fy = bdh(i,2) - sigmaa
Bmelc = ae*0.85*cps(i,5)*Ie/Ye
Bmela = fy*Ie/(cps(i,2)+bdh(i,3)-Ye)
Bmelrd = min(Bmelc,Bmela)
Fel = Bmelrd*(Ye-(cps(i,2)-cps(i,3))/2.0)/ae/Ie
Fel = Fel*cps(i,1)*(cps(i,2)-cps(i,3))
c
return
end
c
Subroutine elrdu(i, Bmelrd, Fel, sigmaa, Fc, Bmsd)
dimension bdh(100,11), cps(100,9)
real Ie
common /bc/ bdh, cps
ae = bdh(i,10)/cps(i,9)
r = bdh(i,9)/cps(i,1)/(cps(i,2)-cps(i,3))
Ye = (cps(i,2)-cps(i,3))/2.0+ae*r*(bdh(i,3)/2.0+cps(i,2))
Ye = Ye/(1+ae*r)
Ie = bdh(i,11)+cps(i,1)*(cps(i,2)-cps(i,3))**3/ae/12.0
Ie = Ie+bdh(i,9)*(bdh(i,3)+cps(i,2)+cps(i,3))**2/(1+ae*r)/4.0
fy = bdh(i,2) - sigmaa
Bmelc = ae*0.85*cps(i,5)*Ie/Ye
Bmela = fy*Ie/(cps(i,2)+bdh(i,3)-Ye)
Bmelrd = min(Bmelc,Bmela)
Fel = Bmelrd*(Ye-(cps(i,2)-cps(i,3))/2.0)/ae/Ie
Fel = Fel*cps(i,1)*(cps(i,2)-cps(i,3))
c
return
end
c
Subroutine elrdu(i, Bmelrd, Fel, sigmaa, Fc, Bmsd)
dimension bdh(100,11), cps(100,9)
real Ie
common /bc/ bdh, cps
ae = bdh(i,10)/cps(i,9)
r = bdh(i,9)/cps(i,1)/(cps(i,2)-cps(i,3))
Ye = (cps(i,2)-cps(i,3))/2.0+ae*r*(bdh(i,3)/2.0+cps(i,2))
Ye = Ye/(1+ae*r)
Ie = bdh(i,11)+cps(i,1)*(cps(i,2)-cps(i,3))**3/ae/12.0
Ie = Ie+bdh(i,9)*(bdh(i,3)+cps(i,2)+cps(i,3))**2/(1+ae*r)/4.0
hn = cps(i,2) - cps(i,3)
if (Ye.LT.hn) then
  Bmc = Ie*Fc/(bdh(i,3)/2.0+cps(i,2)-Ye)/bdh(i,9)
else
  Bmc = ae*Fc*Ie/(Ye-hn/2.0)/Ac

```

```

end if
Ze = bdh(i,3) + cps(i,2) - Ye
fca = Bmc*Ze/Ie
fy = bdh(i,2)
if (Ie*bdh(i,2)/Ze.GT.ae*Ie*0.85*cps(i,5)/Ye) then
  fy=ae*0.85*cps(i,5)*Ze/Ye
end if
Bmelrd = (Bmc+Bmsd)*fy/(sigmaa+fca)
Fel = Fc*fy/(sigmaa+fca)
c
return
end
c
Subroutine cmce(n, cmv, cvoe, cc, es, ts)
dimension es(n), ts(n)
cmv=0
cvoe=0
em=0
tm=0
etm=0
se=0
st=0
do 5 i=1,n
  cmv = cmv+es(i)/ts(i)/n
  em = em+es(i)/n
  tm = tm+ts(i)/n
  etm = etm+es(i)*ts(i)/n
5 continue
do 10 i=1,n
  cvoe = cvoe+(es(i)/ts(i)-cmv)**2
  se = se+(es(i)-em)**2
  st = st+(ts(i)-tm)**2
10 continue
cvoe = sqrt(cvoe/(n-1))/cmv
se = sqrt(se/(n-1))
st = sqrt(st/(n-1))
cc = (etm-em*tm)*n/(n-1)/se/st
return
end

```



```

C This program should be used in conjunction with the program, ntc,
C to assess the safety factors for the design of composite beams
C with non-ductile shear connectors. The design model is that as
C proposed in Eurocode 4 (1991). The program-making is started on
C 28/07/92. The last version is updated to 14/11/93.
C
C Program Nrb

```

```

C dimension bdh(100,11), cps(100,9), stl(11), cnr(9), cvb(11)
C dimension rc(100,5), rp(100,3), ru(100,3), c(5), p(3), u(3)
C dimension vrp(100,3), vru(100,3), ffp(100,3), ffu(100,3)
C dimension sfp(100,4), sfu(100,4), cvc(9)
C real ns(100,2), kd(54)
C character bnum(100,3)*10, case

```

```

C common /nsc/ ns
C common /bc/ bdh, cps
C common /bn/ bnum
C common /puc/ rp, ru, rc

```

```

C oln(x) = sqrt(log(1.0 + x*x))

```

```

C data (kd(i),i=1,6)/9.52,5.72,4.83,4.44,4.20,4.05/
C data (kd(i),i=7,12)/3.95,3.86,3.80,3.74,3.70,3.66/
C data (kd(i),i=13,18)/3.63,3.60,3.58,3.55,3.54,3.52/
C data (kd(i),i=19,24)/3.51,3.49,3.47,3.46,3.45,3.44/
C data (kd(i),i=25,30)/3.44,3.43,3.43,3.42,3.42,3.41/
C data (kd(i),i=31,36)/3.40,3.40,3.39,3.39,3.38,3.38/
C data (kd(i),i=37,42)/3.37,3.36,3.36,3.36,3.35,3.34/
C data (kd(i),i=43,48)/3.33,3.33,3.32,3.32,3.31,3.31/
C data (kd(i),i=49,54)/3.30,3.30,3.30,3.29,3.29,3.29/

```

```

C open (3, file = 'temp')
C open (4, file = 'outonc')
C open (2, file = 'check.nrb')

```

```

C write (6,5)
C format(/,The following data are found for calibrating the ',
C + 'reliabilities of beams with non-ductile connectors...',//)

```

```

C read (3,*) nn
C do 10 i = 1, nn
C   read (3,(a*)) (bnum(i,j), j = 1,3)
C   read (3,*) (bdh(i,j), j = 1,11)
C   read (3,*) (cps(i,j), j = 1,9)
C   read (3,*) (ns(i,j), j = 1,2)
C   read (3,*) (rp(i,j), j = 1,3)
C   read (3,*) (ru(i,j), j = 1,3)
C   read (3,*) (rc(i,j), j = 1,5)

```

```

10 continue
C read (3,*) ip, cmvp, cvoep, ccp
C read (3,*) iu, cmvu, cvoeu, ccu
C read (3,*) imax, cmvmax, cvoemax, ccmax
C read (3,*) arg, ri
C read (3,*) (cvc(j), j = 1,11)
C read (3,*) (cvc(j), j = 1,9)

```

```

C write (6,15) ip, cmvp, cvoep, ccp
C format(x,'Propped construction:',5x,'ip=',i3,4x,'cmvp=',
C + f5.3,4x,'cvoep=',f5.3,4x,'ccp=',f5.3)
C write (6,20) iu, cmvu, cvoeu, ccu
C format(x,'Unpropped construction: iu=',i3,4x,'cmvu=',f5.3,
C + 4x,'cvoeu=',f5.3,4x,'ccu=',f5.3)
C write (6,25) imax, cmvmax, cvoemax, ccmax
C format(x,'Maximum rt:',l3x,'imax=',i3,2x,'cmvmax=',f5.3,2x,

```

```

C + 'cvoemax=',f5.3,2x,'ccmax=',f5.3)
C write (6,35)
C format (/x,'Please make a choice: m <= Maximum rt>',/,23x,
C + 'p <= Propped construction>',/,23x,
C + 'u <= Unpropped construction>')

```

```

C read (5,(a*)) case
C if (case.eq.'m'.or.case.eq.'M') then

```

```

C   nd = imax
C   cv = cvoemax
C   cm = cmvmax
C   cc = ccmax
C   goto 40
C end if

```

```

C if (case.eq.'p'.or.case.eq.'P') then

```

```

C   nd = ip
C   cv = cvoep
C   cm = cmvp
C   cc = ccp
C   goto 40
C end if
C if (case.eq.'u'.or.case.eq.'U') then

```

```

C   nd = iu
C   cv = cvoeu
C   cm = cmvu
C   cc = ccu
C   goto 40
C end if
C goto 30

```

```

C 40 si = 1.0
C call cfpu (nn,arg,si)

```

```

C do 80 i = 1,nn

```

```

C   write (2,600) bnum(i,1), rp(i,3), ru(i,3)
C   format (/2x,a,2f20.4,/)

```

```

C   do 800 ii = 1,nn
C     write (2,600) bnum(ii,1), rp(ii,3), ru(ii,3)
C     continue
C     write (2,700)
C     format (/)

```

```

C   do 45 j = 1,11
C     stl(j) = bdh(i,j)
C     if (j.LE.9) cnr(j) = cps(i,j)
C     if (j.LE.3) then
C       p(j) = rp(i,j)
C       u(j) = ru(i,j)
C     end if
C     if (j.LE.5) c(j) = rc(i,j)
C     continue

```

```

C   sip = 1.0
C   if (c(2).LT.p(2)) sip = -1.0
C   siu = 1.0
C   if (c(2).LT.u(2)) siu = -1.0
C   si = sip
C   if (sip.eq.siu) goto 50
C   if (abs(c(2)-p(2)).GT.abs(c(2)-u(2))) si = siu

```

```

C 50 vrp(i,1) = 0.0
C   vru(i,1) = 0.0
C   do 55 j = 1,11
C     bdh(i,j) = bdh(i,j)*(1.0+si*ri)
C     call cfpu (nn,arg,si)

```



```

c   vrp(i,1)=vrp(i,1)+((rp(i,3)-p(3))*cvb(j)/si/ri/p(3))**2
    vru(i,1)=vru(i,1)+((ru(i,3)-u(3))*cvb(j)/si/ri/u(3))**2
+   vvv = sqrt(vrp(i,1))
    uuu = sqrt(vru(i,1))
    write(2,500) i,j, rp(i,3)/1000000, p(3)/1000000,
    ru(i,3)/1000000, u(3)/1000000, vvv, uuu, si, ri
500  format(x,' ',i2,' ',i2,' ',4f9.3,2f7.4,x,f4.1,x,f6.4)
c   bdh(i,j) = stl(j)
55  continue
    do 60 j = 1,9
      cps(i,j) = cps(i,j)*(1.0+si*ri)
      call cfpv(nn, arg, si)
      vrp(i,1)=vrp(i,1)+((rp(i,3)-p(3))*cvc(j)/si/ri/p(3))**2
      vru(i,1)=vru(i,1)+((ru(i,3)-u(3))*cvc(j)/si/ri/u(3))**2
c   vvv = sqrt(vrp(i,1))
    uuu = sqrt(vru(i,1))
    write(2,500) i,j, rp(i,3)/1000000, p(3)/1000000,
+   ru(i,3)/1000000, u(3)/1000000, vvv, uuu, si, ri
c   cps(i,j) = cnr(j)
60  continue
c   vrp(i,2) = sqrt(vrp(i,1) + cv**2)
    vru(i,2) = sqrt(vru(i,1) + cv**2)
    vrp(i,3) = oln(vrp(i,2))
    vru(i,3) = oln(vru(i,2))
    vrp(i,1) = sqrt(vrp(i,1))
    vru(i,1) = sqrt(vru(i,1))
c   ff = 3.04
    if (nd.lt.56) ff = kd(nd-1)
    ffp(i,1) = (ff*cv**2 + 3.04*vrp(i,1)**2)/vrp(i,2)**2
    ffu(i,1) = (ff*cv**2 + 3.04*vru(i,1)**2)/vru(i,2)**2
c   cvfy = oln(cvb(2))
c   wk = (2.00*oln(0.08)+0.5*oln(0.08)**2-0.5*cvfy**2)/cvfy
c   ranm = exp(3.04*cvfy+0.5*cvfy**2)
    cvfc = oln(cvc(5))
    rcnm = exp(3.04*cvfc+0.5*cvfc**2)
    cvfu = oln(cvb(4))
    runm = exp(3.04*cvfu+0.5*cvfu**2)
    cvec = oln(cvc(9))
    renm = 1.25**2*exp(1.64*cvfc+0.5*cvfc**2)/rcnm
c   write(2,900) bdh(i,2), stl(2), bdh(i,4), stl(4), bdh(i,10),
+   stl(10)
c   format(/x,6f13.2)
c   write(2,900) cps(i,5), cnr(5), cps(i,9), cnr(9)
c   bdh(i,2) = bdh(i,2)/ranm
    bdh(i,4) = bdh(i,4)/runm
    bdh(i,10) = bdh(i,10)/renm
    cps(i,5) = cps(i,5)/rcnm
    cps(i,9) = cps(i,9)/renm
c   write(2,900) bdh(i,2), stl(2), bdh(i,4), stl(4), bdh(i,10),
+   stl(10)
c   write(2,900) cps(i,5), cnr(5), cps(i,9), cnr(9)
c   si = 0.0

```

```

c   call cfpv(nn, arg, si)
    sfp(i,1) = rp(i,3)*exp(ffp(i,1)*vrp(i,3)+0.5*vrp(i,3)**2)/cm/p(3)
    sfp(i,2) = sfp(i,1)*exp(1.04*cvfy)
    sfp(i,3) = sfp(i,1)*exp(1.4*cvfc)
    sfp(i,4) = sfp(i,1)*1.25
    tp = exp(ffp(i,1)*vrp(i,3)+0.5*vrp(i,3)**2)
    write(2,64) rp(i,3), p(3), tp
    format(2x,'rn (propped) =',f12.1,2x,'rm (propped) =',f12.1,
+   2x,'tp =',f5.3)
c   tu = exp(-ffu(i,1)*vru(i,3)-0.5*vru(i,3)**2)
    ite = 0
    rmd0 = 3.0
    rmdo = 0.5
    rmd = (rmd0+rmdo)/2.0
    bdh(i,2) = stl(2)/(ranm*rmd)
    bdh(i,4) = stl(4)/(runm*rmd)
    bdh(i,10) = stl(10)/(renm*rmd)
    cps(i,5) = cnr(5)/(rcnm*rmd)
    cps(i,9) = cnr(9)/(renm*rmd)
    call cfpv(nn, arg, si)
    if (abs(ru(i,3)/(tu*cm*u(3))-1.0).le.0.0001) goto 70
    if (ru(i,3)/(tu*cm*u(3)).lt.1.0) then
      rmd0 = rmd
    else
      rmdo = rmd
    end if
    write(2,66) rmd, tu, cm, u(3), ru(i,3)
+   format(3x,'rmd=',f6.4,' tu=',f6.3,' cm=',f6.3,' u=',f12.1,
    ite = ite + 1
    if (ite.le.30) goto 65
70  sfu(i,1) = rmd
    sfu(i,2) = rmd*exp(1.04*cvfy)
    sfu(i,3) = rmd*exp(1.4*cvfc)
    sfu(i,4) = rmd*1.25
c   do 75 j = 1,11
    bdh(i,j) = stl(j)
    if (j.le.9) cps(i,j) = cnr(j)
    if (j.le.3) then
      rp(i,j) = p(j)
      ru(i,j) = u(j)
    end if
75  continue
c   rpa = 0.0
    rpc = 0.0
    rpu = 0.0
    vpa = 0.0
    vpc = 0.0
    vpu = 0.0
    rua = 0.0
    ruc = 0.0
    ruu = 0.0
    vua = 0.0
    vuc = 0.0
    vuu = 0.0
    do 81 i = 1,nn
      rpa = rpa + sfp(i,2)/nn
      rpc = rpc + sfp(i,3)/nn
      rpu = rpu + sfp(i,4)/nn
      rua = rua + sfu(i,2)/nn
      ruc = ruc + sfu(i,3)/nn

```



```

      rc(i,4) = Fc*(cps(i,2)+cps(i,3)+bdh(i,3))/2.0
      rc(i,4) = (Fa-Fc)*(bdh(i,3)-Xa)/2.0 + rc(i,4)
    end if
  end if
C
C ***** Determine Mel,rd *****
C
C call elrdp(i,rc(i,1),rp(i,2),0.0)
C call elrdu(i,ru(i,1),ru(i,2),sigma,rc(i,2),rc(i,1))
C
C ***** Determine Msd (propped) *****
C
C if (rc(i,2).LT.rc(i,2)) then
  rp(i,3) = Bmsd1(rc(i,2),rp(i,2),rp(i,1),0.0)
else
  rp(i,3) = Bmsd2(rc(i,2),rp(i,2),min(Fc,Fa),rc(i,4),rp(i,1))
end if
C
C ***** Determine Msd (unpropped) *****
C
C if (rc(i,2).LT.ru(i,2)) then
  ru(i,3) = Bmsd1(rc(i,2),ru(i,2),ru(i,1),rc(i,1))
else
  ru(i,3) = Bmsd2(rc(i,2),ru(i,2),min(Fc,Fa),rc(i,4),ru(i,1))
end if
  rc(i,5) = bdh(i,2)*wa(bdh(i,3),bdh(i,6),bdh(i,8),bdh(i,7))
10 continue
C
C return
C end
C
C subroutine elrdp(i, Bmelrd, Fel, sigma)
C
C real Ie
C dimension bdh(100,11), cps(100,9)
C
C common /bc/ bdh, cps
C
C ae = bdh(i,10)/cps(i,9)
C r = bdh(i,9)/cps(i,1)/(cps(i,2)-cps(i,3))
C Ye = (cps(i,2)-cps(i,3))/2.0+ae*r*(bdh(i,3)/2.0+cps(i,2))
C Ye = Ye/(1+ae*r)
C Ie = bdh(i,11)+cps(i,1)*(cps(i,2)-cps(i,3))*3/ae/12.0
C Ie = Ie+bdh(i,9)*(bdh(i,3)+cps(i,2)+cps(i,3))*2/(1+ae*r)/4.0
C fy = bdh(i,2) - sigma
C Bmelc = ae*0.85*cps(i,5)*Ie/Ye
C Bmela = fy*Ie/(cps(i,2)+bdh(i,3)-Ye)
C Bmelrd = min(Bmelc,Bmela)
C Fel = Bmelrd*(Ye-(cps(i,2)-cps(i,3))/2.0)/ae/Ie
C Fel = Fel*cps(i,1)*(cps(i,2)-cps(i,3))
C
C return
C end
C
C subroutine elrdu(i, Bmelrd, Fel, sigma, Fc, Bmsd)
C
C dimension bdh(100,11), cps(100,9)
C real Ie
C
C common /bc/ bdh, cps
C
C ae = bdh(i,10)/cps(i,9)
C r = bdh(i,9)/cps(i,1)/(cps(i,2)-cps(i,3))
C Ye = (cps(i,2)-cps(i,3))/2.0+ae*r*(bdh(i,3)/2.0+cps(i,2))

```

```

Ye = Ye/(1+ae*r)
Ie = bdh(i,11)+cps(i,1)*(cps(i,2)-cps(i,3))*3/ae/12.0
Ie = Ie+bdh(i,9)*(bdh(i,3)+cps(i,2)+cps(i,3))*2/(1+ae*r)/4.0
Ac = cps(i,1)*(cps(i,2)-cps(i,3))
hn = cps(i,2) - cps(i,3)
if (ye.LT.hn) then
  Bmc = Ie*Fc/(bdh(i,3)/2.0+cps(i,2)-Ye)/bdh(i,9)
else
  Bmc = ae*Fc*Ie/(Ye-hn/2.0)/Ac
end if
Ze = bdh(i,3) + cps(i,2) - Ye
fca = Bmc*Ze/Ie
fy = bdh(i,2)
if (Ie*bdh(i,2)/Ze.GT.ae*Ie*0.85*cps(i,5)/Ye) then
  fy=ae*0.85*cps(i,5)*Ze/Ye
end if
Bmelrd = (Bmc+Bmsd)*fy/(sigma+fca)
Fel = Fc*fy/(sigma+fca)
C
C return
C end

```


85, 0.29
IA1R
T
19.1, 495.5, 406.7, 1E6, 76.2, 177.7, 7.75, 12.8, 7612.9, 2.1E5, 2.156E8
1828.8, 101.6, 38.0, 57.0, 23.9, 18.0, 7.315
13999.44
24, 1.75
826.6
IA2
T
19.1, 411.0, 406.7, 1E6, 88.9, 177.7, 7.75, 12.8, 7612.9, 2.1E5, 2.156E8
2032.0, 114.0, 51.0, 76.0, 25.6, 18.5, 7.315
14964.91
24, 1.75
705.0
IA3R
T
19.1, 461.4, 406.7, 1E6, 114.3, 177.7, 7.75, 12.8, 7612.9, 2.1E5, 2.156E8
2438.4, 139.7, 76.0, 114.0, 22.4, 18.1, 9.754
13723.59
26, 2
788.3
IA5R
T
19.1, 463.4, 409.7, 1E6, 76.2, 178.7, 8.76, 14.4, 8580.6, 2.1E5, 2.439E8
1828.8, 101.6, 38.0, 76.0, 25.6, 18.5, 6.096
14964.91
18, 1.83
1026.2
IA6R
T
19.1, 461.0, 409.7, 1E6, 88.9, 178.7, 8.76, 14.4, 8580.6, 2.1E5, 2.439E8
2032.0, 114.3, 50.8, 101.6, 34.0, 19.8, 7.315
17378.61
20, 2
945.5
IA7
T
19.1, 445.2, 406.7, 1E6, 114.3, 177.7, 7.75, 12.8, 7612.9, 2.1E5, 2.156E8
2438.4, 139.7, 76.0, 152.0, 29.0, 18.8, 9.754
15792.47
18, 1.68
698.8
IB1
T
19.1, 231.4, 403.2, 1E6, 114.3, 215.9, 11.1, 15.8, 10993.5, 2.1E5, 3.155E8
2438.4, 139.7, 76.0, 114.0, 25.9, 19.3, 9.754
12482.26
25, 1.94
650.3
IB2
T
19.1, 262.8, 403.2, 1E6, 76.2, 215.9, 11.1, 15.8, 10993.5, 2.1E5, 3.155E8
1828.8, 101.6, 38.0, 76.0, 33.3, 18.1, 7.315
14895.95
19, 1.92
682.5
IC1
T
19.1, 414.1, 406.7, 1E6, 76.2, 177.7, 7.75, 12.8, 7612.9, 2.1E5, 2.156E8
1828.8, 101.6, 38.0, 57.0, 30.0, 18.3, 7.315
17171.72
11, 1
690.1
IC2A
T

19.1, 459.3, 406.7, 1E6, 114.3, 177.7, 7.75, 12.8, 7612.9, 2.1E5, 2.156E8
2438.4, 139.7, 76.0, 114.0, 28.5, 17.8, 9.754
0.0
9, 1.32
710.9
IC2B
T
19.1, 466.5, 406.7, 1E6, 114.3, 177.7, 7.75, 12.8, 7612.9, 2.1E5, 2.156E8
2438.4, 139.7, 76.0, 114.0, 27.5, 17.8, 9.754
0.0
12, 1.75
728.5
IC3
T
19.1, 496.2, 406.7, 1E6, 88.9, 177.7, 7.75, 12.8, 7612.9, 2.1E5, 2.156E8
2032.0, 114.3, 51.0, 102.0, 33.4, 18.5, 7.315
17240.68
8, 1
782.8
IC4
T
19.1, 459.0, 409.7, 1E6, 114.3, 178.7, 8.8, 14.4, 8580.6, 2.1E5, 2.439E8
2438.4, 139.7, 76.0, 152.0, 22.4, 18.7, 9.754
14413.21
14, 2
841.7
ID1
T
19.1, 492.4, 406.7, 1E6, 76.2, 177.7, 7.75, 12.8, 7612.9, 2.1E5, 2.156E8
1828.8, 101.6, 38.0, 57.0, 23.9, 18.0, 7.315
13999.43
24, 1.75
813.3
ID2
T
19.1, 400.0, 406.7, 1E6, 76.2, 177.7, 7.75, 12.8, 7612.9, 2.1E5, 2.156E8
1828.8, 101.6, 38.0, 57.0, 31.8, 18.1, 7.315
14964.91
24, 1.75
698.4
ID3
T
19.1, 458.0, 409.7, 1E6, 114.3, 178.7, 8.8, 14.4, 8580.6, 2.1E5, 2.439E8
2438.4, 139.7, 76.0, 152.0, 27.3, 19.1, 9.754
15171.80
18, 1.68
846.1
ID4
T
19.1, 458.6, 406.7, 1E6, 114.3, 177.7, 7.8, 12.8, 7612.9, 2.1E5, 2.156E8
2438.4, 139.7, 76.0, 152.0, 33.4, 19.6, 9.754
17792.39
18, 1.68
717.7
A1_Hawkins
S
20.0, 296.0, 254.0, 454.0, 76.0, 114.3, 7.62, 12.8, 4741.9, 2.1E5, 0.509E8
1830.0, 102.0, 0.0, 0.0, 27.9, 23.52, 5.19
28300.0
10, 2
264.7
A2_Hawkins
S
20.0, 297.0, 254.0, 500.0, 76.0, 114.3, 7.62, 12.8, 4741.9, 2.1E5, 0.509E8
1830.0, 102.0, 0.0, 0.0, 30.1, 23.52, 5.19
27600.0

10, 2
 276.8
 A3_Hawkins
 S
 20.0, 296.0, 254.0, 454.0, 76.0, 114.3, 7.62, 12.8, 4741.9, 2.1E5, 0.509E8
 1830.0, 102.0, 0.0, 0.0, 32.3, 18.0, 5.19
 15200.0
 10, 2
 257.8
 A4_Hawkins
 S
 20.0, 350.0, 254.0, 430.0, 76.0, 114.3, 7.62, 12.8, 4741.9, 2.1E5, 0.509E8
 1830.0, 102.0, 0.0, 0.0, 20.3, 23.52, 5.19
 22800.0
 14, 2
 285.5
 A5_Hawkins
 S
 20.0, 351.0, 254.0, 496.0, 76.0, 114.3, 7.62, 12.8, 4741.9, 2.1E5, 0.509E8
 1830.0, 102.0, 0.0, 0.0, 30.5, 23.52, 5.19
 26900.0
 14, 2
 314.9
 1_Robinson
 T
 19.0, 359.8, 403.0, 1E6, 116.0, 177.0, 7.5, 10.9, 6717.6, 2.1E5, 1.830E8
 2440.0, 141.0, 76.0, 181.5, 21.3, 23.52, 9.144
 0.0
 8, 1
 538.5
 2_Robinson
 T
 19.0, 359.8, 403.0, 1E6, 116.0, 177.0, 7.5, 10.9, 6717.6, 2.1E5, 1.830E8
 2440.0, 141.0, 76.0, 152.5, 21.9, 23.52, 9.144
 0.0
 10, 1
 537.6
 70-4
 T
 19.1, 282.1, 398.5, 1E6, 76.2, 139.7, 6.4, 8.8, 4954.8, 2.1E5, 1.253E8
 1778.0, 101.6, 38.1, 54.1, 21.9, 17.8, 9.144
 0.0
 14, 1
 361.2
 66-11(42)
 T
 19.1, 342.1, 206.0, 1E6, 76.2, 102.0, 6.2, 8.0, 2864.5, 2.1E5, 0.200E8
 1117.6, 101.6, 38.1, 57.2, 22.9, 22.8, 6.096
 0.0
 4, 1
 139.0
 66-11(56)
 T
 19.1, 318.6, 206.0, 1E6, 76.2, 102.0, 6.2, 8.0, 2864.5, 2.1E5, 0.200E8
 1117.6, 101.6, 38.1, 57.2, 22.5, 22.8, 6.096
 0.0
 5, 1
 147.4
 66-11(B)
 T
 19.1, 338.6, 311.5, 1E6, 76.2, 145.7, 6.8, 10.2, 4558.1, 2.1E5, 0.708E8
 1117.6, 101.6, 38.1, 57.2, 23.9, 22.7, 6.096
 0.0
 9, 1
 173.3
 66-11(W)

T
 19.1, 271.0, 351.5, 1E6, 76.2, 170.9, 6.9, 9.8, 5709.7, 2.1E5, 1.211E8
 1193.8, 101.6, 38.1, 57.2, 27.8, 22.8, 6.096
 0.0
 13, 1
 382.0
 64-15(H1)
 T
 19.1, 286.2, 310.4, 1E6, 76.2, 171.1, 6.0, 9.7, 4935.5, 2.1E5, 0.882E8
 1219.2, 101.6, 38.1, 114.3, 26.6, 18.1, 4.572
 0.0
 12, 1
 330.6
 64-15(E1)
 T
 19.1, 254.1, 310.4, 1E6, 76.2, 171.1, 6.0, 9.7, 5125.3, 2.1E5, 0.882E8
 1219.2, 101.6, 38.1, 114.3, 27.7, 18.1, 4.572
 0.0
 13, 1.49
 322.8
 64-15(E2)
 T
 19.1, 257.2, 310.4, 1E6, 76.2, 171.1, 6.0, 9.7, 5125.3, 2.1E5, 0.882E8
 1219.2, 101.6, 38.1, 114.3, 34.6, 18.0, 4.572
 0.0
 16, 2
 330.0
 67-38
 T
 19.1, 274.8, 351.5, 1E6, 88.9, 170.9, 6.9, 9.8, 5709.7, 2.1E5, 1.211E8
 1473.2, 120.7, 44.5, 152.4, 21.4, 18.0, 7.315
 0.0
 10, 2
 410.8
 71(EPIC)
 T
 19.1, 246.9, 310.4, 1E6, 101.6, 164.8, 5.8, 9.7, 4935.5, 2.1E5, 0.882E8
 1524.0, 133.4, 50.8, 127.0, 21.3, 17.0, 4.572
 0.0
 11, 1
 327.1
 72-12(75)
 T
 19.1, 404.5, 309.6, 1E6, 114.3, 254.3, 9.1, 16.3, 10967.7, 2.1E5, 1.977E8
 1828.8, 158.2, 76.2, 184.2, 28.0, 18.0, 7.62
 0.0
 14, 2
 716.1
 73(RF)
 T
 19.1, 264.1, 351.5, 1E6, 139.7, 170.9, 6.9, 9.8, 5709.7, 2.1E5, 1.211E8
 2438.4, 158.8, 76.2, 101.6, 32.7, 17.0, 7.62
 0.0
 16, 2
 415.1
 67-11(B1)
 T
 19.1, 269.3, 310.4, 1E6, 127.0, 171.1, 6.0, 9.7, 5125.3, 2.1E5, 0.882E8
 1219.2, 139.7, 76.2, 103.1, 30.3, 18.0, 4.572
 14964.91
 8, 2
 252.3
 67-11(B2)
 T
 19.1, 269.3, 310.4, 1E6, 127.0, 171.1, 6.0, 9.7, 5125.3, 2.1E5, 0.882E8
 1219.2, 139.7, 76.2, 103.1, 33.8, 18.0, 4.572

14964.91
 8, 2
 246.6
 68-4(1)
 T
 19.1, 263.8, 351.5, 1E6, 76.2, 170.9, 6.9, 9.8, 5709.7, 2.1E5, 1.241E8
 1193.8, 101.6, 38.1, 57.1, 29.7, 18.0, 6.096
 17861.35
 13, 1
 328.5
 68-5(2)
 T
 19.1, 317.6, 396.8, 1E6, 76.2, 139.7, 6.4, 9.5, 4935.5, 2.1E5, 1.241E8
 1155.7, 101.6, 38.1, 57.1, 23.5, 17.0, 9.114
 17123.45
 14, 1
 384.7
 69-1(3)
 T
 19.1, 259.0, 351.5, 1E6, 76.2, 170.9, 6.9, 9.8, 5709.7, 2.1E5, 2.899E8
 1193.8, 101.6, 38.1, 57.1, 31.7, 18.0, 6.096
 15378.69
 12, 1
 341.6
 70-31(A)
 T
 19.1, 251.7, 351.5, 1E6, 76.2, 170.9, 6.9, 9.8, 5709.7, 2.1E5, 1.241E8
 1219.2, 101.6, 38.1, 57.1, 22.8, 18.0, 5.791
 16344.17
 18, 1.43
 357.6
 70-31(D)
 T
 12.7, 251.7, 351.5, 1E6, 76.2, 170.9, 6.9, 9.8, 5709.7, 2.1E5, 1.241E8
 1219.2, 101.6, 38.1, 57.1, 22.8, 18.0, 5.791
 16344.17
 23, 1.68
 342.7
 70-31(C)
 T
 19.1, 241.0, 463.3, 1E6, 127.0, 191.9, 10.5, 17.7, 11354.8, 2.1E5, 4.096E8
 1828.8, 152.4, 76.2, 143.0, 22.8, 18.0, 10.82
 16344.17
 18, 1.09
 846.6
 69-2(HR)
 T
 19.1, 263.1, 258.3, 1E6, 127.8, 139.5, 5.8, 9.1, 3996.8, 2.1E5, 0.469E8
 1270.0, 157.5, 76.2, 66.8, 33.1, 23.0, 6.401
 24068.00
 6, 1
 175.8
 67-36(CU3)
 T
 15.9, 251.0, 310.4, 1E6, 63.5, 171.1, 6.0, 9.7, 5125.3, 2.1E5, 0.882E8
 1587.5, 88.9, 38.1, 57.2, 22.1, 23.0, 7.315
 0.0
 18, 1.23
 270.0
 65-19 BS12
 T
 19.1, 266.5, 310.4, 1E6, 76.2, 171.1, 6.1, 9.7, 5125.3, 2.1E5, 0.882E8
 1219.2, 101.6, 33.3, 57.1, 27.6, 23.0, 4.572
 0.0
 14, 1
 299.5

65-19 BS11
 T
 19.1, 267.6, 310.4, 1E6, 76.2, 171.1, 6.1, 9.7, 5125.3, 2.1E5, 0.882E8
 1219.2, 101.6, 22.4, 44.5, 27.6, 23.0, 4.572
 0.0
 14, 1
 310.2
 67-36(CU2)
 T
 15.6, 279.3, 310.4, 1E6, 63.5, 171.1, 6.1, 9.7, 5125.3, 2.1E5, 0.882E8
 1587.5, 88.9, 38.1, 92.2, 29.0, 23.0, 7.315
 0.0
 18, 1
 317.1
 67-36(CU1)
 T
 15.6, 249.0, 310.4, 1E6, 63.5, 171.1, 6.1, 9.7, 5125.3, 2.1E5, 0.882E8
 1587.5, 88.9, 38.1, 127.0, 29.7, 23.0, 7.315
 0.0
 1.32
 339.9
 TEX-1
 T
 19.1, 258.3, 413.0, 1E6, 114.3, 179.6, 9.7, 16.0, 9483.9, 2.1E5, 2.743E8
 2438.4, 158.8, 76.2, 152.4, 20.7, 17.0, 9.754
 0.0
 2
 26, 2
 677.2
 TEX-2
 T
 19.1, 278.95, 413.0, 1E6, 139.7, 179.6, 9.7, 16.0, 9483.9, 2.1E5, 2.743E8
 2438.4, 158.8, 76.2, 152.4, 26.21, 17.0, 9.754
 0.0
 26, 2
 899.1
 TEX-3
 T
 19.1, 250.0, 413.0, 1E6, 152.4, 179.6, 9.7, 16.0, 9483.9, 2.1E5, 2.743E8
 2438.4, 158.8, 76.2, 152.4, 26.2, 17.0, 9.754
 0.0
 2
 26, 2
 859.8
 TEX-4
 T
 19.1, 251.0, 413.0, 1E6, 127.0, 179.6, 9.7, 16.0, 9483.9, 2.1E5, 2.743E8
 2438.4, 158.8, 76.2, 152.4, 24.1, 16.0, 9.754
 0.0
 2
 26, 2
 752.1
 TEX-5
 T
 19.1, 260.3, 413.0, 1E6, 127.0, 179.6, 9.7, 16.0, 9483.9, 2.1E5, 2.743E8
 2438.4, 158.8, 76.2, 152.4, 24.1, 16.0, 9.754
 0.0
 2
 26, 2
 790.1
 TEX-6
 T
 19.1, 260.0, 413.0, 1E6, 114.0, 179.6, 9.7, 16.0, 9483.9, 2.1E5, 2.743E8
 2438.4, 158.8, 76.2, 152.4, 24.8, 16.0, 9.754
 0.0
 2
 26, 2
 724.9
 TEX-7
 T
 19.1, 271.4, 413.0, 1E6, 127.0, 179.6, 9.7, 16.0, 9483.9, 2.1E5, 2.743E8

2438.4, 158.8, 76.2, 152.4, 26.9, 17.0, 9.754
 0.0
 26, 2
 819.6
 TEX-8
 T
 19.1, 271.71, 413.0, 1E6, 139.7, 179.6, 9.7, 16.0, 9483.9, 2.1E5, 2.743E8
 2438.4, 158.8, 76.2, 152.4, 27.93, 16.0, 9.754
 0.0
 26, 2
 867.5
 HHR-1-76
 T
 19.1, 273.4, 409.7, 1E6, 127.0, 178.7, 8.8, 14.4, 8580.6, 2.1E5, 2.439E8
 2413.0, 139.7, 76.2, 152.4, 29.4, 23.0, 9.754
 0.0
 12, 2
 592.6
 IR-1-76
 T
 19.1, 264.1, 409.7, 1E6, 127.0, 178.7, 8.8, 14.4, 8580.6, 2.1E5, 2.439E8
 2413.0, 139.7, 76.2, 184.2, 28.8, 23.0, 9.754
 0.0
 12, 2
 645.2
 HHR-2-76
 T
 19.1, 269.3, 409.7, 1E6, 127.0, 178.7, 8.8, 14.4, 8580.6, 2.1E5, 2.439E8
 2413.0, 139.7, 76.2, 152.4, 31.7, 23.0, 9.754
 0.0
 12, 2
 590.3
 IR-2-76
 T
 19.1, 266.2, 409.7, 1E6, 127.0, 178.7, 8.8, 14.4, 8580.6, 2.1E5, 2.439E8
 2413.0, 139.7, 76.2, 184.2, 32.6, 23.0, 9.754
 0.0
 12, 2
 638.5
 RF-1-76
 T
 19.1, 272.4, 409.7, 1E6, 127.0, 178.7, 8.8, 14.4, 8580.6, 2.1E5, 2.439E8
 2413.0, 139.7, 76.2, 152.4, 30.3, 23.0, 9.754
 0.0
 12, 2
 606.3
 RF-2-76
 T
 19.1, 268.3, 409.7, 1E6, 127.0, 178.7, 8.8, 14.4, 8580.6, 2.1E5, 2.439E8
 2413.0, 139.7, 76.2, 152.4, 29.7, 22.0, 9.754
 0.0
 12, 2
 610.9
 72-12(80)
 T
 19.1, 244.8, 307.8, 1E6, 114.3, 304.8, 9.9, 15.4, 12322.6, 2.1E5, 2.219E8
 1828.8, 177.8, 76.2, 184.2, 26.6, 18.0, 7.62
 0.0
 21, 2
 574.0
 75-16
 T
 19.1, 312.1, 406.7, 1E6, 114.3, 177.7, 7.7, 12.8, 7612.9, 2.1E5, 2.156E8
 2209.8, 127.0, 76.2, 152.4, 22.7, 23.0, 9.144
 0.0
 12, 1

547.7
 175-75
 T
 19.1, 265.5, 598.7, 1E6, 127.0, 177.9, 10.0, 12.8, 10451.6, 2.1E5, 5.619E8
 2616.2, 158.8, 76.2, 184.2, 27.9, 18.0, 10.638
 0.0
 18, 1.68
 1071.8
 174-75
 T
 19.1, 250.0, 603.0, 1E6, 177.8, 175.9, 10.7, 15.0, 11552.5, 2.1E5, 6.348E8
 2616.2, 228.6, 76.2, 184.2, 29.3, 23.0, 10.638
 0.0
 28, 2
 1469.5
 16-76
 T
 19.1, 286.2, 524.8, 1E6, 124.5, 165.1, 8.9, 11.4, 8387.1, 2.1E5, 3.509E8
 2400.3, 139.7, 76.2, 171.5, 23.9, 23.0, 12.192
 0.0
 20, 2
 931.8
 BS1
 T
 19.0, 461.5, 360.0, 1E6, 100.0, 170.0, 8.0, 12.7, 7270.0, 2.1E5, 1.627E8
 1500.0, 130.0, 51.0, 114.5, 31.5, 23.0, 7.7775
 0.0
 13, 1
 710.4
 BS2
 T
 19.0, 448.0, 360.0, 1E6, 100.0, 170.0, 8.0, 12.7, 7270.0, 2.1E5, 1.627E8
 1500.0, 130.0, 51.0, 114.5, 39.1, 23.0, 7.7775
 0.0
 13, 1
 715.5
 IS(Warwi.)
 T
 19.0, 327.0, 528.3, 1E6, 100.0, 208.7, 9.6, 13.2, 10400.0, 2.1E5, 4.749E8
 2500.0, 120.0, 60.0, 150.0, 34.6, 23.0, 10.0
 0.0
 17, 1
 1011.0
 1(Cardiff)
 T
 19.0, 297.0, 312.7, 1E6, 100.0, 102.4, 6.6, 10.8, 4180.0, 2.07E5, 0.649E8
 2000.0, 125.0, 50.0, 150.0, 33.6, 19.5, 8.0
 24300
 5, 1
 254.4
 2(Cardiff)
 T
 19.0, 325.0, 312.7, 1E6, 100.0, 102.4, 6.6, 10.8, 4180.0, 2.04E5, 0.649E8
 2000.0, 125.0, 50.0, 150.0, 35.2, 19.5, 8.0
 19300
 3, 1
 214.4
 3(Cardiff)
 T
 19.0, 307.0, 312.7, 1E6, 100.0, 102.4, 6.6, 10.8, 4180.0, 1.99E5, 0.649E8
 2000.0, 125.0, 50.0, 150.0, 32.0, 19.5, 8.0
 20300
 4, 1
 238.4
 4(Cardiff)
 T


```

19.0, 317.0, 312.7, 1E6, 100.0, 102.4, 6.6, 10.8, 4180.0, 2.01E5, 0.649E8
2000.0, 125.0, 50.0, 150.0, 32.0, 19.5, 8.0
24000
2, 1
184.4
A<1,2>
S
20.0, 323.5, 254.0, 454.0, 76.0, 114.3, 7.62, 12.8, 4741.9, 2.1E5, 0.509E8
1830.0, 102.0, 0.0, 0.0, 27.2, 23.52, 5.19
26400.0
10, 2
0.0
A<4,5>
S
20.0, 323.5, 254.0, 454.0, 76.0, 114.3, 7.62, 12.8, 4741.9, 2.1E5, 0.509E8
1830.0, 102.0, 0.0, 0.0, 27.2, 23.52, 5.19
26400.0
14, 2
0.0
67-11<B1,B2>
T
19.1, 269.3, 310.4, 1000000.0, 127.0, 171.1, 6.0, 9.7, 5125.3, 2.1E5, 0.882E8
1219.2, 139.7, 76.2, 103.1, 32.07, 18.0, 4.572
14964.91
8, 2
0.0
TEX-<1,6>
T
19.1, 259.1, 413.0, 1000000.0, 114.3, 179.6, 9.7, 16.0, 9483.9, 2.1E5, 2.743E8
2438.4, 158.8, 76.2, 152.4, 22.8, 16.5, 9.754
0.0
26, 2
0.0
TEX-<2,8>
T
19.1, 275.33, 413.0, 1000000.0, 139.7, 179.6, 9.7, 16.0, 9483.9, 2.1E5, 2.743E8
2438.4, 158.8, 76.2, 152.4, 27.07, 16.5, 9.754
0.0
26, 2
0.0
TEX-<4,5,7>
T
19.1, 260.9, 413.0, 1000000.0, 127.0, 179.6, 9.7, 16.0, 9483.9, 2.1E5, 2.743E8
2438.4, 158.8, 76.2, 152.4, 25.06, 16.3, 9.754
0.0
26, 2
0.0
IR-76<1,2>
T
19.1, 265.2, 409.7, 1000000.0, 127.0, 178.7, 8.8, 14.4, 8580.6, 2.1E5, 2.439E8
2413.0, 139.7, 76.2, 184.2, 30.73, 23.0, 9.754
0.0
12, 2
0.0
RFHHR<1,2>
T
19.1, 270.9, 409.7, 1000000.0, 127.0, 178.7, 8.8, 14.4, 8580.6, 2.1E5, 2.439E8
2413.0, 139.7, 76.2, 152.4, 30.28, 22.75, 9.754
0.0
12, 2
0.0
BS<1,2>
T
19.0, 454.8, 360.0, 1000000.0, 100.0, 170.0, 8.0, 12.7, 7270.0, 2.1E5, 1.627E8
1500.0, 130.0, 51.0, 114.5, 35.3, 23.0, 7.7775
0.0

```

```

13,
0.0
1

```


10, 2
 276.8
 A3_Hawkins
 S
 20.0, 296.0, 254.0, 454.0, 76.0, 114.3, 7.62, 12.8, 4741.9, 2.1E5, 0.509E8
 1830.0, 102.0, 0.0, 0.0, 32.3, 18.0, 5.19
 15200.0
 10, 2
 257.8
 A4_Hawkins
 S
 20.0, 350.0, 254.0, 430.0, 76.0, 114.3, 7.62, 12.8, 4741.9, 2.1E5, 0.509E8
 1830.0, 102.0, 0.0, 0.0, 20.3, 23.52, 5.19
 22800.0
 14, 2
 285.5
 A5_Hawkins
 S
 20.0, 351.0, 254.0, 496.0, 76.0, 114.3, 7.62, 12.8, 4741.9, 2.1E5, 0.509E8
 1830.0, 102.0, 0.0, 0.0, 30.5, 23.52, 5.19
 26900.0
 14, 2
 314.9
 1_Robinson
 T
 19.0, 359.8, 403.0, 1E6, 116.0, 177.0, 7.5, 10.9, 6717.6, 2.1E5, 1.830E8
 2440.0, 141.0, 76.0, 181.5, 21.3, 23.52, 9.144
 0.0
 8, 1
 538.5
 2_Robinson
 T
 19.0, 359.8, 403.0, 1E6, 116.0, 177.0, 7.5, 10.9, 6717.6, 2.1E5, 1.830E8
 2440.0, 141.0, 76.0, 152.5, 21.9, 23.52, 9.144
 0.0
 10, 1
 537.6
 70-4
 T
 19.1, 282.1, 398.5, 1E6, 76.2, 139.7, 6.4, 8.8, 4954.8, 2.1E5, 1.253E8
 1778.0, 101.6, 38.1, 54.1, 21.9, 17.8, 9.144
 0.0
 14, 1
 361.2
 66-11(42)
 T
 19.1, 342.1, 206.0, 1E6, 76.2, 102.0, 6.2, 8.0, 2864.5, 2.1E5, 0.200E8
 1117.6, 101.6, 38.1, 57.2, 22.9, 22.8, 6.096
 0.0
 4, 1
 139.0
 66-11(56)
 T
 19.1, 318.6, 206.0, 1E6, 76.2, 102.0, 6.2, 8.0, 2864.5, 2.1E5, 0.200E8
 1117.6, 101.6, 38.1, 57.2, 22.5, 22.8, 6.096
 0.0
 5, 1
 147.4
 66-11(B)
 T
 19.1, 338.6, 311.5, 1E6, 76.2, 145.7, 6.8, 10.2, 4558.1, 2.1E5, 0.708E8
 1117.6, 101.6, 38.1, 57.2, 23.9, 22.7, 6.096
 0.0
 9, 1
 173.3
 66-11(W)

T
 19.1, 271.0, 351.5, 1E6, 76.2, 170.9, 6.9, 9.8, 5709.7, 2.1E5, 1.211E8
 1193.8, 101.6, 38.1, 57.2, 27.8, 22.8, 6.096
 0.0
 13, 1
 382.0
 64-15(H1)
 T
 19.1, 286.2, 310.4, 1E6, 76.2, 171.1, 6.0, 9.7, 4935.5, 2.1E5, 0.882E8
 1219.2, 101.6, 38.1, 114.3, 26.6, 18.1, 4.572
 0.0
 12, 1
 330.6
 64-15(E1)
 T
 19.1, 254.1, 310.4, 1E6, 76.2, 171.1, 6.0, 9.7, 5125.3, 2.1E5, 0.882E8
 1219.2, 101.6, 38.1, 114.3, 27.7, 18.1, 4.572
 0.0
 13, 1.49
 322.8
 64-15(E2)
 T
 19.1, 257.2, 310.4, 1E6, 76.2, 171.1, 6.0, 9.7, 5125.3, 2.1E5, 0.882E8
 1219.2, 101.6, 38.1, 114.3, 34.6, 18.0, 4.572
 0.0
 16, 2
 330.0
 67-38
 T
 19.1, 274.8, 351.5, 1E6, 88.9, 170.9, 6.9, 9.8, 5709.7, 2.1E5, 1.211E8
 1473.2, 120.7, 44.5, 152.4, 21.4, 18.0, 7.315
 0.0
 10, 2
 410.8
 71(EPIC)
 T
 19.1, 246.9, 310.4, 1E6, 101.6, 164.8, 5.8, 9.7, 4935.5, 2.1E5, 0.882E8
 1524.0, 133.4, 50.8, 127.0, 21.3, 17.0, 4.572
 0.0
 11, 1
 327.1
 72-12(75)
 T
 19.1, 404.5, 309.6, 1E6, 114.3, 254.3, 9.1, 16.3, 10967.7, 2.1E5, 1.977E8
 1828.8, 158.2, 76.2, 184.2, 28.0, 18.0, 7.62
 0.0
 14, 2
 716.1
 73(RF)
 T
 19.1, 264.1, 351.5, 1E6, 139.7, 170.9, 6.9, 9.8, 5709.7, 2.1E5, 1.211E8
 2438.4, 158.8, 76.2, 101.6, 32.7, 17.0, 7.62
 0.0
 16, 2
 415.1
 67-11(B1)
 T
 19.1, 269.3, 310.4, 1E6, 127.0, 171.1, 6.0, 9.7, 5125.3, 2.1E5, 0.882E8
 1219.2, 139.7, 76.2, 103.1, 30.3, 18.0, 4.572
 14964.91
 8, 2
 252.3
 67-11(B2)
 T
 19.1, 269.3, 310.4, 1E6, 127.0, 171.1, 6.0, 9.7, 5125.3, 2.1E5, 0.882E8
 1219.2, 139.7, 76.2, 103.1, 33.8, 18.0, 4.572

14964.91
 8, 2
 246.6
 68-4(1)
 T
 19.1, 263.8, 351.5, 1E6, 76.2, 170.9, 6.9, 9.8, 5709.7, 2.1E5, 1.241E8
 1193.8, 101.6, 38.1, 57.1, 29.7, 18.0, 6.096
 17861.35
 13, 1
 328.5
 68-5(2)
 T
 19.1, 317.6, 396.8, 1E6, 76.2, 139.7, 6.4, 9.5, 4935.5, 2.1E5, 1.241E8
 1155.7, 101.6, 38.1, 57.1, 23.5, 17.0, 9.114
 17123.45
 14, 1
 384.7
 69-1(3)
 T
 19.1, 259.0, 351.5, 1E6, 76.2, 170.9, 6.9, 9.8, 5709.7, 2.1E5, 2.899E8
 1193.8, 101.6, 38.1, 57.1, 31.7, 18.0, 6.096
 15378.69
 12, 1
 341.6
 70-31(A)
 T
 19.1, 251.7, 351.5, 1E6, 76.2, 170.9, 6.9, 9.8, 5709.7, 2.1E5, 1.241E8
 1219.2, 101.6, 38.1, 57.1, 22.8, 18.0, 5.791
 16344.17
 18, 1.43
 357.6
 70-31(D)
 T
 12.7, 251.7, 351.5, 1E6, 76.2, 170.9, 6.9, 9.8, 5709.7, 2.1E5, 1.241E8
 1219.2, 101.6, 38.1, 57.1, 22.8, 18.0, 5.791
 16344.17
 23, 1.68
 342.7
 70-31(C)
 T
 19.1, 241.0, 463.3, 1E6, 127.0, 191.9, 10.5, 17.7, 11354.8, 2.1E5, 4.096E8
 1828.8, 152.4, 76.2, 143.0, 22.8, 18.0, 10.82
 16344.17
 18, 1.09
 846.6
 69-2(HR)
 T
 19.1, 263.1, 258.3, 1E6, 127.8, 139.5, 5.8, 9.1, 3996.8, 2.1E5, 0.469E8
 1270.0, 157.5, 76.2, 66.8, 33.1, 23.0, 6.401
 24068.00
 6, 1
 175.8
 67-36(CU3)
 T
 15.9, 251.0, 310.4, 1E6, 63.5, 171.1, 6.0, 9.7, 5125.3, 2.1E5, 0.882E8
 1587.5, 88.9, 38.1, 57.2, 22.1, 23.0, 7.315
 0.0
 18, 1.23
 270.0
 65-19 BS12
 T
 19.1, 266.5, 310.4, 1E6, 76.2, 171.1, 6.1, 9.7, 5125.3, 2.1E5, 0.882E8
 1219.2, 101.6, 33.3, 57.1, 27.6, 23.0, 4.572
 0.0
 14, 1
 299.5

65-19 BS11
 T
 19.1, 267.6, 310.4, 1E6, 76.2, 171.1, 6.1, 9.7, 5125.3, 2.1E5, 0.882E8
 1219.2, 101.6, 22.4, 44.5, 27.6, 23.0, 4.572
 0.0
 14, 1
 310.2
 67-36(CU2)
 T
 15.6, 279.3, 310.4, 1E6, 63.5, 171.1, 6.1, 9.7, 5125.3, 2.1E5, 0.882E8
 1587.5, 88.9, 38.1, 92.2, 29.0, 23.0, 7.315
 0.0
 18, 1
 317.1
 67-36(CU1)
 T
 15.6, 249.0, 310.4, 1E6, 63.5, 171.1, 6.1, 9.7, 5125.3, 2.1E5, 0.882E8
 1587.5, 88.9, 38.1, 127.0, 29.7, 23.0, 7.315
 0.0
 1.32
 339.9
 TEX-1
 T
 19.1, 258.3, 413.0, 1E6, 114.3, 179.6, 9.7, 16.0, 9483.9, 2.1E5, 2.743E8
 2438.4, 158.8, 76.2, 152.4, 20.7, 17.0, 9.754
 0.0
 2
 677.2
 TEX-2
 T
 19.1, 278.95, 413.0, 1E6, 139.7, 179.6, 9.7, 16.0, 9483.9, 2.1E5, 2.743E8
 2438.4, 158.8, 76.2, 152.4, 26.21, 17.0, 9.754
 0.0
 2
 899.1
 TEX-3
 T
 19.1, 250.0, 413.0, 1E6, 152.4, 179.6, 9.7, 16.0, 9483.9, 2.1E5, 2.743E8
 2438.4, 158.8, 76.2, 152.4, 26.2, 17.0, 9.754
 0.0
 2
 859.8
 TEX-4
 T
 19.1, 251.0, 413.0, 1E6, 127.0, 179.6, 9.7, 16.0, 9483.9, 2.1E5, 2.743E8
 2438.4, 158.8, 76.2, 152.4, 24.1, 16.0, 9.754
 0.0
 2
 752.1
 TEX-5
 T
 19.1, 260.3, 413.0, 1E6, 127.0, 179.6, 9.7, 16.0, 9483.9, 2.1E5, 2.743E8
 2438.4, 158.8, 76.2, 152.4, 24.1, 16.0, 9.754
 0.0
 2
 790.1
 TEX-6
 T
 19.1, 260.0, 413.0, 1E6, 114.0, 179.6, 9.7, 16.0, 9483.9, 2.1E5, 2.743E8
 2438.4, 158.8, 76.2, 152.4, 24.8, 16.0, 9.754
 0.0
 2
 724.9
 TEX-7
 T
 19.1, 271.4, 413.0, 1E6, 127.0, 179.6, 9.7, 16.0, 9483.9, 2.1E5, 2.743E8

2438.4, 158.8, 76.2, 152.4, 26.9, 17.0, 9.754
0.0
26, 2
819.6
TEX-8
T
19.1, 271.71, 413.0, 1E6, 139.7, 179.6, 9.7, 16.0, 9483.9, 2.1E5, 2.743E8
2438.4, 158.8, 76.2, 152.4, 27.93, 16.0, 9.754
0.0
26, 2
867.5
HHR-1-76
T
19.1, 273.4, 409.7, 1E6, 127.0, 178.7, 8.8, 14.4, 8580.6, 2.1E5, 2.439E8
2413.0, 139.7, 76.2, 152.4, 29.4, 23.0, 9.754
0.0
12, 2
592.6
IR-1-76
T
19.1, 264.1, 409.7, 1E6, 127.0, 178.7, 8.8, 14.4, 8580.6, 2.1E5, 2.439E8
2413.0, 139.7, 76.2, 184.2, 28.8, 23.0, 9.754
0.0
12, 2
645.2
HHR-2-76
T
19.1, 269.3, 409.7, 1E6, 127.0, 178.7, 8.8, 14.4, 8580.6, 2.1E5, 2.439E8
2413.0, 139.7, 76.2, 152.4, 31.7, 23.0, 9.754
0.0
12, 2
590.3
IR-2-76
T
19.1, 266.2, 409.7, 1E6, 127.0, 178.7, 8.8, 14.4, 8580.6, 2.1E5, 2.439E8
2413.0, 139.7, 76.2, 184.2, 32.6, 23.0, 9.754
0.0
12, 2
638.5
RF-1-76
T
19.1, 272.4, 409.7, 1E6, 127.0, 178.7, 8.8, 14.4, 8580.6, 2.1E5, 2.439E8
2413.0, 139.7, 76.2, 152.4, 30.3, 23.0, 9.754
0.0
12, 2
606.3
RF-2-76
T
19.1, 268.3, 409.7, 1E6, 127.0, 178.7, 8.8, 14.4, 8580.6, 2.1E5, 2.439E8
2413.0, 139.7, 76.2, 152.4, 29.7, 22.0, 9.754
0.0
12, 2
610.9
72-12(80)
T
19.1, 244.8, 307.8, 1E6, 114.3, 304.8, 9.9, 15.4, 12322.6, 2.1E5, 2.219E8
1828.8, 177.8, 76.2, 184.2, 26.6, 18.0, 7.62
0.0
21, 2
574.0
75-16
T
19.1, 312.1, 406.7, 1E6, 114.3, 177.7, 7.7, 12.8, 7612.9, 2.1E5, 2.156E8
2209.8, 127.0, 76.2, 152.4, 22.7, 23.0, 9.144
0.0
12, 1

547.7
175-75
T
19.1, 265.5, 598.7, 1E6, 127.0, 177.9, 10.0, 12.8, 10451.6, 2.1E5, 5.619E8
2616.2, 158.8, 76.2, 184.2, 27.9, 18.0, 10.638
0.0
18, 1.68
1071.8
174-75
T
19.1, 250.0, 603.0, 1E6, 177.8, 175.9, 10.7, 15.0, 11552.5, 2.1E5, 6.348E8
2616.2, 228.6, 76.2, 184.2, 29.3, 23.0, 10.638
0.0
28, 2
1469.5
16-76
T
19.1, 286.2, 524.8, 1E6, 124.5, 165.1, 8.9, 11.4, 8387.1, 2.1E5, 3.509E8
2400.3, 139.7, 76.2, 171.5, 23.9, 23.0, 12.192
0.0
20, 2
931.8
BS1
T
19.0, 461.5, 360.0, 1E6, 100.0, 170.0, 8.0, 12.7, 7270.0, 2.1E5, 1.627E8
1500.0, 130.0, 51.0, 114.5, 23.0, 7.7775
0.0
13, 1
710.4
BS2
T
19.0, 448.0, 360.0, 1E6, 100.0, 170.0, 8.0, 12.7, 7270.0, 2.1E5, 1.627E8
1500.0, 130.0, 51.0, 114.5, 23.0, 7.7775
0.0
13, 1
715.5
1S(Warwi.)
T
19.0, 327.0, 528.3, 1E6, 100.0, 208.7, 9.6, 13.2, 10400.0, 2.1E5, 4.749E8
2500.0, 120.0, 60.0, 150.0, 34.6, 23.0, 10.0
0.0
17, 1
1011.0
1(Cardiff)
T
19.0, 297.0, 312.7, 1E6, 100.0, 102.4, 6.6, 10.8, 4180.0, 2.07E5, 0.649E8
2000.0, 125.0, 50.0, 150.0, 33.6, 19.5, 8.0
24300
5, 1
254.4
2(Cardiff)
T
19.0, 325.0, 312.7, 1E6, 100.0, 102.4, 6.6, 10.8, 4180.0, 2.04E5, 0.649E8
2000.0, 125.0, 50.0, 150.0, 35.2, 19.5, 8.0
19300
3, 1
214.4
3(Cardiff)
T
19.0, 307.0, 312.7, 1E6, 100.0, 102.4, 6.6, 10.8, 4180.0, 1.99E5, 0.649E8
2000.0, 125.0, 50.0, 150.0, 32.0, 19.5, 8.0
20300
4, 1
238.4
4(Cardiff)
T


```

19.0, 317.0, 312.7, 1E6, 100.0, 102.4, 6.6, 10.8, 4180.0, 2.01E5, 0.649E8
2000.0, 125.0, 50.0, 150.0, 32.0, 19.5, 8.0
24000
2, 1
184.4
A<1,2>
S
20.0, 323.5, 254.0, 454.0, 76.0, 114.3, 7.62, 12.8, 4741.9, 2.1E5, 0.509E8
1830.0, 102.0, 0.0, 0.0, 27.2, 23.52, 5.19
26400.0
10, 2
0.0
A<4,5>
S
20.0, 323.5, 254.0, 454.0, 76.0, 114.3, 7.62, 12.8, 4741.9, 2.1E5, 0.509E8
1830.0, 102.0, 0.0, 0.0, 27.2, 23.52, 5.19
26400.0
14, 2
0.0
67-11<B1,B2>
T
19.1, 269.3, 310.4, 1000000.0, 127.0, 171.1, 6.0, 9.7, 5125.3, 2.1E5, 0.882E8
1219.2, 139.7, 76.2, 103.1, 32.07, 18.0, 4.572
14964.91
8, 2
0.0
TEX-<1,6>
T
19.1, 259.1, 413.0, 1000000.0, 114.3, 179.6, 9.7, 16.0, 9483.9, 2.1E5, 2.743E8
2438.4, 158.8, 76.2, 152.4, 22.8, 16.5, 9.754
0.0
26, 2
0.0
TEX-<2,8>
T
19.1, 275.33, 413.0, 1000000.0, 139.7, 179.6, 9.7, 16.0, 9483.9, 2.1E5, 2.743E8
2438.4, 158.8, 76.2, 152.4, 27.07, 16.5, 9.754
0.0
26, 2
0.0
TEX-<4,5,7>
T
19.1, 260.9, 413.0, 1000000.0, 127.0, 179.6, 9.7, 16.0, 9483.9, 2.1E5, 2.743E8
2438.4, 158.8, 76.2, 152.4, 25.06, 16.3, 9.754
0.0
26, 2
0.0
IR-76<1,2>
T
19.1, 265.2, 409.7, 1000000.0, 127.0, 178.7, 8.8, 14.4, 8580.6, 2.1E5, 2.439E8
2413.0, 139.7, 76.2, 184.2, 30.73, 23.0, 9.754
0.0
12, 2
0.0
RFHHR<1,2>
T
19.1, 270.9, 409.7, 1000000.0, 127.0, 178.7, 8.8, 14.4, 8580.6, 2.1E5, 2.439E8
2413.0, 139.7, 76.2, 152.4, 30.28, 22.75, 9.754
0.0
12, 2
0.0
BS<1,2>
T
19.0, 454.8, 360.0, 1000000.0, 100.0, 170.0, 8.0, 12.7, 7270.0, 2.1E5, 1.627E8
1500.0, 130.0, 51.0, 114.5, 35.3, 23.0, 7.7775
0.0

```

```

13, 1
0.0

```


0.29, 0.001
0.04, 0.08, 0.04, 0.08, 0.00, 0.04, 0.04, 0.04, 0.04, 0.04, 0.04, 0.04
0.008, 0.04, 0.00, 0.00, 0.15, 0.00, 0.00, 0.00, 0.00, 0.10